



PHD

Electrochemical studies of mass and heat transfer in a simulated fouling deposit

Alderman, Neil John

Award date:
1986

Awarding institution:
University of Bath

[Link to publication](#)

Alternative formats

If you require this document in an alternative format, please contact:
openaccess@bath.ac.uk

Copyright of this thesis rests with the author. Access is subject to the above licence, if given. If no licence is specified above, original content in this thesis is licensed under the terms of the Creative Commons Attribution-NonCommercial 4.0 International (CC BY-NC-ND 4.0) Licence (<https://creativecommons.org/licenses/by-nc-nd/4.0/>). Any third-party copyright material present remains the property of its respective owner(s) and is licensed under its existing terms.

Take down policy

If you consider content within Bath's Research Portal to be in breach of UK law, please contact: openaccess@bath.ac.uk with the details. Your claim will be investigated and, where appropriate, the item will be removed from public view as soon as possible.

ELECTROCHEMICAL STUDIES OF MASS AND HEAT TRANSFER
IN A SIMULATED FOULING DEPOSIT

submitted by Neil John Alderman, B.Sc.
for the degree of Ph.D
of the University of Bath
1986

COPYRIGHT

Attention is drawn to the fact that copyright of this thesis rest with its author. This copy of the thesis has been supplied on condition that anyone who consults it is understood to recognise that its copyright rests with its author and that no quotation from the thesis and no information derived from it may be published without the prior consent of the author.

This thesis may be made available for consultation within the University Library and may be photocopied or lent to other libraries for the purposes of consultation.

Neil J Alderman

UMI Number: U601938

All rights reserved

INFORMATION TO ALL USERS

The quality of this reproduction is dependent upon the quality of the copy submitted.

In the unlikely event that the author did not send a complete manuscript and there are missing pages, these will be noted. Also, if material had to be removed, a note will indicate the deletion.



UMI U601938

Published by ProQuest LLC 2013. Copyright in the Dissertation held by the Author.
Microform Edition © ProQuest LLC.

All rights reserved. This work is protected against
unauthorized copying under Title 17, United States Code.



ProQuest LLC
789 East Eisenhower Parkway
P.O. Box 1346
Ann Arbor, MI 48106-1346

To Mum
and
in the memory of Dad
for their love and support

ACKNOWLEDGEMENTS

I wish to express my sincere gratitude to those people who have given me assistance and encouragement throughout this course of study. In particular, I would like to thank:

Dr B.D.Crittenden, my supervisor, for his guidance and help which was so assiduously given throughout the course. I am also indebted to him for his helpful remarks and criticisms made during the preparation of this thesis.

Professor W.J.Thomas for providing me with the opportunity to carry out this research project at the School of Chemical Engineering, University of Bath.

The Science and Engineering Research Council for the award of a research studentship and the funding of this project.

Mr T.B.Walton for procuring the equipment required for this study.

The Inter-Schools workshop team for the fabrication of the experimental apparatus.

Mr A.D.Lockett and Mr J.Bishop for their advice on electrical matters associated with the experimental apparatus.

The Material Science Department for allowing me to use their surface preparation facilities.

Mr T.Carter, School of Engineering, for his assistance with the surface texture measurements on the nickel cathode.

Mr H.R.Perrott, Centre of Electron Optic Studies, for obtaining the electron micrograph of the nickel cathode given in this thesis.

The University Photographic Department for the preparation of the photographs in this thesis.

My mother for her assistance in the typing of this thesis.

Permission to reproduce the following copyright material is gratefully acknowledged.

AMERICAN CHEMICAL SOCIETY

Ind. Eng. Chem. Fundam., 7(1), 59-65, 1968. Figure 1.3
(Hasson,D. et al) Figure 6.

AMERICAN SOCIETY OF MECHANICAL ENGINEERS

ASME Paper 71-WA/HT-45 (Haller,K.J. et al) Figure 8. Figure 1.12

HTD, 17, 1-15, 1981 (Characklis,W.G. et al) Figure 21. Figure 1.17

BLACKWELL SCIENTIFIC PUBLICATIONS LTD

J. Appl. Chem., 19, 222-226, 1969. (Taylor, W.F.) Figures 1.21 & 1.22
Figures 3 & 4.

CANADIAN SOCIETY FOR CHEMICAL ENGINEERING

Can. J. Chem. Eng., 55, 272-278, June 1977 Figure 1.24
(Morse,R.W. and Knudsen,J.) Figure 6.

HEMISPHERE PUBLISHING CORPORATION

Proc. 6th Int. Conf. on Heat Transfer, Toronto, Figure 1.15
7-11 August 1978, 4, 373-378, (Bott,T.R and Gudmundsson,J.S.) Figure 1.

Proc. 6th Int. Conf. on Heat Transfer, Toronto, Figure 1.16
7-11 August 1978, 6, 235-253, (Epstein,N.) Figure 2.

Proc. 6th Int. Conf. on Heat Transfer, Toronto, Figure 1.4
7-11 August 1978, 6, 391-396, (Hasson,D.) Figure 5.

Proc. Int. Conf. on Fouling of Heat Transfer Figures 1.8 & 1.9
Equipment, Troy, 13-17 August 1979 pp 251-291
(Characklis,W.G.) Figures 8 & 9.

NATIONAL ASSOCIATION OF CORROSION ENGINEERS

Corrosion (Houston), 37(2), 70-76, Feb 1981. Figures 2.7 - 2.11
(Wolfson,S.L. and Hartt, W.H.) Figures 5,6,7,9 & 11.

PERGAMON PRESS LTD

Int. J. Heat Mass Transfer, 16, 443-460, 1973. Figures 2.4 - 2.6
(Galloway,T.R.) Figures 6-8.

J. Aerosol Sci., 9, 445-461, 1978. (Beal,S.K.) Figures 1.18 & 1.19
Figures 5 & 7

SCRIPTA TECHNICA LTD

Heat Transfer Jpn. Res., 10(1) 23-26, 1981. Figures 1.13 & 1.14
(Ishikawa, H. et al) Figures 3 & 15.

THE ELECTROCHEMICAL SOCIETY

J. Electrochem. Soc., 118(7), 1070-1078, 1971 Figure A4.1
(Selman, J.R. and Newman,J.) Figure 8.

THE INSTITUTE OF ENERGY

J. Inst. Fuel, 42, 412-419, 1969. (Boow,J. and Goard,P.R.C.) Figure 4.

Figure 1.10

THE SOCIETY OF CHEMICAL ENGINEERS, JAPAN

J. Chem. Eng Jpn, 15(2), 98-104, 1982. (Hiraoka,S. et al) Figure 4.

Figure A4.2

UNITED KINGDOM ATOMIC ENERGY AUTHORITY

Biotechnology and Bioengineering, 24(1), 153-164, 1982 (Duddridge, J.E. et al) Figure 3.

Figure 1.23

VERLAG CHEMIE GmbH

Dechema. Mongr., 65, 109-129, 1971 (Liddle, C.J.) Figure 2.

Figure 1.5

WATER POLLUTION CONTROL FEDERATION

J. Water Pollut. Control Fed., 45, 2302-2320, 1973 (Hoehn, R.C. and Ray, A.D.) Figures 12,19 & 20.

Figures 1.6 & 1.7

SUMMARY

The well known limiting diffusion current technique for the $K_3Fe(CN)_6$ - $K_4Fe(CN)_6$ - NaOH system was used to study the effect of deposit characteristics on mass and heat transfer rates in a simple mixing cell. The simulated fouling deposit consisted of spherical glass spherical particles resting randomly on the nickel cathode base to the mixing cell.

Mass transfer results were expressed in terms of the Gilliland-Sherwood correlation

$$Sh = a Re^b Sc^{\frac{1}{3}}$$

where a and b for $0 \leq d_p \leq 12mm$ and $0 \leq n_1 \leq 7$ were found to be

$$a = 1.0330 \exp\{-7.7799 n_1^{0.1122} (e^{-0.2672d_p} - e^{-4.0086d_p})\}$$

$$b = 0.5644 + 1.0081(e^{-0.2924d_p} - e^{-3.1486d_p})$$

where d_p = particle diameter

n_1 = number of layers

The corresponding heat transfer results were expressed in the form of

$$Nu = a Re^b Pr^{\frac{1}{3}}$$

where a and b were found to be

$$a \approx 1.0330 \left[\frac{Pr}{Sc} \right]^{\frac{1}{3}} \exp\{-7.7799 n_1^{0.1122} (e^{-0.2672d_p} - e^{-4.0086d_p})\}$$

$$b = 0.5644 + 1.0081(e^{-0.2924d_p} - e^{-3.1486d_p})$$

The presence of the particles on the cathode has two effects on transfer rates. Firstly, the resistances to mass and heat transfer through the deposit increase with increasing number of layers. Secondly, the presence of particles, large with respect to the surface roughness of the unfouled surface, reduce the resistance to mass and heat transfer through the fluid film at the fluid-deposit interface. At relatively high Reynolds numbers, the latter effect can predominate to such an extent that the overall resistance

to transfer can become less than that of the unfouled surface.

CONTENTS

	Page
ACKNOWLEDGEMENTS	i
SUMMARY	iv
CONTENTS	vi
NOMENCLATURE	x
INTRODUCTION	1
CHAPTER 1 FOULING OF HEAT TRANSFER SURFACES	4
1.1 Definition	4
1.2 Classification	4
1.3 Terminology	5
1.4 Design	5
1.5 Measurement	9
1.5.1 Characterisation of deposit accumulation	9
1.5.2 Measurement of deposit accumulation	10
1.5.3 Fouling curves	12
1.5.4 Fouling models	15
1.6 Deposit characterisation	17
1.6.1 Deposit thickness	20
1.6.2 Deposit mass	23
1.6.3 Deposit morphology	25
1.6.4 Deposit physical properties	29
1.6.4.1 Deposit density	29
1.6.4.2 Deposit thermal conductivity	31
1.6.4.3 Deposit porosity	38
1.6.4.4 Deposit roughness	42
1.6.4.5 Deposit adhesion	46
1.6.4.6. Deposit strength	58
1.6.5 Deposit chemical analysis	62
1.6.6 Deposit microbiological analysis	65
CHAPTER 2 THE ELECTROCHEMICAL METHOD	68
2.1 The limiting diffusion current technique	68
2.1.1 Fundamentals	68

2.1.2 Model electrochemical reactions	75
2.1.3 Applications	78
2.2 Previous work	78
CHAPTER 3 EXPERIMENTAL APPARATUS AND PROCEDURE	85
3.1 Model fouling system	85
3.1.1 Electrochemical system	85
3.1.1.1 Density	89
3.1.1.2 Kinematic viscosity	89
3.1.1.3 Diffusivity	91
3.1.1.4 Thermal conductivity	93
3.1.1.5 Heat capacity	96
3.1.1.6 $\Delta\rho_m$	99
3.1.1.7 $\Delta\rho_h$	101
3.1.2 Simulated fouling deposit	101
3.2 Experimental apparatus	101
3.2.1 Mixing cell	101
3.2.2 Electrical circuit	108
3.3 Experimental procedure	108
3.3.1 Preparation of the electrolytic solution	109
3.3.2 Preparation of the electrodes	109
3.3.3 Assembly of the electrolytic mixing cell	115
3.3.4 Data acquisition	118
3.3.4.1 Determination of the current-potential plot as a function of the impeller rotational speed	118
3.3.4.2 Determination of the limiting current as a function of the impeller rotational speed	118
CHAPTER 4 EXPERIMENTAL RESULTS AND OBSERVATIONS	121
4.1 Mass transfer studies	121
4.1.1 Mass transfer in the electrolytic mixing cell without the presence of glass spherical particles on the cathode	121
4.1.1.1 Free convection mass transfer	124
4.1.1.2 Forced convection mass transfer	130
4.1.2 Mass transfer in the electrolytic mixing cell with the presence of glass spherical particles on the cathode	132
4.2 Mass and heat transfer studies	144
4.2.1 Mass and heat transfer in the electrolytic mixing cell without the presence of the glass spherical particles on the cathode	144
4.2.1.1 Free convection mass and heat transfer	154

4.2.1.2 Forced convection mass and heat transfer	166
4.2.2 Mass and heat transfer in the electrolytic mixing cell with the presence of glass spherical particles on the cathode	173
CHAPTER 5 DISCUSSION OF RESULTS	190
CHAPTER 6 CONCLUSIONS	198
REFERENCES	199
APPENDICES	236
A1 Electrolytic solution density data	236
A2 Electrolytic solution kinematic viscosity data	237
A3 The basis of the ionic densification coefficients evaluated by Selman and Newman for the $K_3Fe(CN)_6 - K_4Fe(CN)_6 - KOH/NaOH$ system	238
A4 The various methods that have used to evaluate Δc_j for the $K_3Fe(CN)_6 - K_4Fe(CN)_6 - KOH/NaOH$ system	240
A5 Titrimetric analysis for the electrolytic solution	254
A6 Experimental data	256
A6.1 Current-potential data as a function of the impeller rotational speed for the electrolytic mixing cell without the presence of glass spherical particles	256
A6.2 Reproducibility data for the current-potential curve determined at an impeller rotational speed of 34.8 ± 2.8 rpm in the electrolytic mixing cell without the presence of glass spherical particles on the cathode	260
A6.3 Mass transfer data for the electrolytic mixing cell without the presence of glass spherical particles on the cathode	264
A6.4 Current-potential data as a function of the impeller rotational speed for the electrolytic mixing cell with the presence of 1 layer of 3mm glass spherical particles on the cathode	276
A6.5 $I_L - N$ data for the electrolytic mixing cell with the presence of 1 layer of 3mm glass spherical particles on the cathode	279
A6.6 Mass transfer data for the electrolytic mixing cell with the presence of one or more layers of glass spherical particles on the cathode	280
A6.7 The effect of the cathode surface temperature upon the current-potential data at an impeller speed of 37.5 ± 2.2 rpm for the electrolytic mixing cell without the presence of glass spherical particles on the cathode where $\Delta T = 0$	356

A6.8	Mass and heat transfer data for the electrolytic mixing cell without the presence of glass spherical particles on the heated cathode	358
A6.9	Mass and heat transfer data for the electrolytic mixing cell with the presence of one or more layers of glass spherical particles on the heated cathode	376
A7	Program listings	397
A7.1	A listing of the program 'MASS'	397
A7.2	A listing of the program 'MAHE'	399
A8	The basis of the equation for the simulated fouling deposit thickness	404
A9	The basis of the equation for the tortuosity of the simulated fouling deposit	406

NOMENCLATURE

a	Constant
α	Empirical constant representing the probability of the presence of weak planes in the deposit layer
α_i	Coefficients for equations 3.7 and 3.8
A	Area of electrode surface
A_a	Area of adhesion
A	Area of heat transfer surface
A_1	Surface area of the neoprene gasket
A_2	Surface area of the central nickel rod
A_3	Surface area of the nickel plate
A_4	Surface area of the Sindanyo base plate accessory
b	Constant
$b_{j,k}$	Coefficients for equation 3.7
c	Constant
c_b	Bulk concentration of fouling species
c_p	Specific heat capacity at constant pressure
c_b	Bulk ion concentration
c_j	Concentration of species j
c_{jb}	Concentration of species j in the bulk solution
c_{js}	Concentration of species j at the electrode surface
c_s	Surface ion concentration
c_R	Concentration of limiting reactant R
c_{Rb}	Concentration of limiting reactant R in the bulk solution
c_{Rs}	Concentration of limiting reactant R at the electrode surface
C_j	Dimensionless concentration of species j
C_R	Dimensionless concentration of limiting reactant R
d	Electrode diameter
d_i	Impeller diameter
d_p	Particle diameter
d_{pore}	Average pore diameter of the fouling deposit
d_v	Diameter of the agitated vessel
d_1	Diameter of the central nickel rod

d_2	Diameter of the Sindanyo base plate accessory
d_3	Inner diameter of the neoprene gasket
d_4	Diameter of the nickel plate
d	Tube diameter
d_i	Inside tube diameter
D	Diffusivity of reacting species in the bulk
D_j	Diffusivity of species j
D_F	Diffusivity of reacting species in the fouling deposit
D_R	Diffusivity of limiting reactant R
e	Roughness height
e^-	Symbol for electron
E	Activation energy
f	Dimensionless stream function
f_1	Function
f_2	Function
f_1^*	Function
f_2^*	Function
f	Friction factor
F	Faraday's constant
F_a	Van der Waals attractive force between a particle and a surface
F_r	Electrical double layer repulsive force between a particle and a surface
F_t	Total interaction force between a particle and a surface
F_T	Correction factor based on the geometry of the heat exchanger to give the true mean temperature difference
F_s	Frossling number
g	Gravitational acceleration
Gr_h	Grashof number for heat transfer
Gr_m	Grashof number for mass transfer
GR_h	Combined Grashof number for heat transfer defined by equation 4.18
GR_m	Combined Grashof number for mass transfer defined by equation 4.16
h	Heat transfer coefficient
h_a	Heat transfer coefficient for free convection from a surface to air
h_f	Heat transfer coefficient for the fluid phase

h	Separation distance between a particle and a surface
i	Current density
I	Current
I_h	Heater current
I_L	Limiting current
I	Ionic strength
k	Mass transfer coefficient
k_d	Deposition coefficient
k_j	Mass transfer coefficient for species j
k	Thermal conductivity of the bulk solution
k_{eff}	Effective thermal conductivity of the fouling deposit
k_f	Thermal conductivity of the fluid phase
k_p	Thermal conductivity of the particulate phase
k_F	Thermal conductivity of the fouling deposit
k_{H_2O}	Thermal conductivity of water
k_1	Thermal conductivity of neoprene
k_2	Thermal conductivity of nickel
k_3	Thermal conductivity of Sindanyo
K	Overall mass transfer coefficient
l	Characteristic length
l'	Path length of the fouling deposit
l'_{close}	Path length of a close packed bed of spheres
l'_{open}	Path length of an open packed bed of spheres
l_b	Impeller blade length
l	A/p
L	Tube length
LMTD	Overall logarithmic mean temperature difference
m	Mass of fouling deposit
m	Mass of electrolytic solution
m_j	Mass of species j in the electrolytic solution
M	Mass of fouling deposit per unit area of heat transfer surface
M_j	Symbol for the chemical formula of species j
M_j	Mass fraction of species j in the electrolytic solution
n	Number of electrons transferred in the electrochemical reaction

n_1	Number of layers
n_B	Number of baffles in the agitated vessel
N	Flux
N_j	Flux of species j
Nu	Nusselt number
N	Impeller rotational speed
N_f	Impeller rotational speed at which fluidisation begins to occur
p	Perimeter of cathode
P	Pressure
Pr	Prandtl number
q	Heat transfer rate
q_b	Heat transfer rate into the electrolytic solution
q_f	Heat transfer rate into the fluid phase
q_p	Heat transfer rate into the particulate phase
q_L	Total heat loss from the electrolytic mixing cell
q_{L1}	Heat loss through the neoprene gasket
q_{L2}	Heat loss through the central nickel rod
q_{L3}	Heat loss through the Sindanyo base plate and accessories
q_{L4}	Heat loss from the Sindanyo base plate and accessories to air by free convection
q_{L5}	Heat loss from the central nickel rod to air by free convection
r	Concentration ratio for supporting electrolyte
r_a	Concentration ratio for anodic reaction
r_c	Concentration ratio for cathodic reaction
r	Radial distance from the centre of the cathode
R	Universal gas constant
R_h	Heater resistance
R_i	Heat transfer resistance inside the wall
R_o	Heat transfer resistance outside the wall
R_w	Heat transfer resistance of the wall
R_B	Deposit bond resistance
R_F	Fouling resistance
R_F^*	Asymptotic fouling resistance
R_{Fi}	Fouling resistance inside the wall

R_{Fo}	Fouling resistance outside the wall
Re	Reynolds number
Re_c	Critical Reynolds number
R_a	Average peak to valley height
R_m	Maximum peak to valley height
s	Roughness spacing
s_j	Stoichiometric coefficient of species j
s_R	Stoichiometric coefficient of limiting reactant R
s_j	Number of molecules or ions of species j reacting at the electrode when one Faraday flows through the electrochemical cell
s_R	Number of molecules or ions of limiting reactant R reacting at the electrode when one Faraday flows through the electrochemical cell
S	Sticking probability
S^+	Dimensionless stopping distance
Sc	Schmidt number
Sh	Sherwood number
t_j	Transference number of species j
t_R	Transference number of limiting reactant R
t	Tortuosity of the fouling deposit
T	Temperature
T_a	Ambient temperature
T_b	Bulk fluid temperature
T_{bi}	Inside bulk fluid temperature
T_{bo}	Outside bulk fluid temperature
T_c	Critical temperature
T_f	Mean film temperature
T_i	Interfacial temperature
T_{ii}	Inside interfacial temperature
T_{io}	Outside interfacial temperature
T_s	Surface temperature
T_{si}	Inside surface temperature
T_{so}	Outside surface temperature
T_w	Wall temperature
T^*	Reduced temperature

$T_i(z)$	Chebyshev polynomial of the i th degree with z normalised in the range $-1 \leq z \leq 1$
u_j	Mobility of species j
u_R	Mobility of limiting reactant R
U	Overall heat transfer coefficient
U_0	Overall heat transfer coefficient at time zero
U_C	Overall heat transfer coefficient for a clean surface
U_F	Overall heat transfer coefficient for a fouled surface
v	Bulk fluid velocity
v_s	Velocity of the particles normal to the surface
v_x	Velocity component parallel to the electrode
v_y	Velocity component perpendicular to the electrode
V	Volume of the electrolytic solution
V_f	Volume of the fluid phase
V_p	Volume of the particulate phase
V_i	Viscosity ratio, μ/μ_s
w_b	Impeller blade width
w_B	Baffle width
x	Distance in the x -direction
x_1	Thickness of the neoprene gasket
x_2	Length of the central nickel rod
x_3	Thickness of the Sindanyo base plate as shown in Figure 4.21
x_4	Thickness of the Sindanyo base plate accessory
x	Fouling deposit thickness
x_{close}	Thickness of a close packed bed of spheres
x_{open}	Thickness of an open packed bed of spheres
X	$k_d _{S=S}/k_d _{S=1}$
y	Distance in the y -direction
y_{cd}	Vertical distance between the cathode and the horizontal diaphragm
y_{fl}	Free liquid distance in the direction normal to the cathode
z_j	Charge number of species j
z_R	Charge number of limiting reactant R
z_i	Height of impeller from the base of the agitated vessel
z_l	Height of liquid in the agitated vessel

α	Fraction of the total deposit thickness that can be represented by the parallel arrangement of particles and pores with respect to the direction of heat flow
$\bar{\alpha}$	Overall densification coefficient
α_j	Densification coefficient of species j
α_R	Densification coefficient of limiting reactant R
β	Coefficient representing the rate of approach to R_F^*
γ_C	Critical surface tension for wetting
γ_{LS}	Interfacial tension between the liquid and the substrate surface
γ_{PL}	Interfacial tension between the particles and the liquid
γ_{PS}	Interfacial tension between the particles and the substrate surface
Γ	Stream function defined by equation A4.27
δ	Diffusion layer thickness
δ_N	Nernst diffusion layer thickness
Δ_a	Average of rms value of the slope of the roughness profile throughout its length
Δc_j	Concentration difference of species j between the bulk and the electrode surface
Δc_R	Concentration difference of limiting reactant R between the bulk and the electrode surface
ΔF	Net surface free energy resulting from adhesion
ΔL	Tube sectional length
ΔP	Pressure drop
ΔT	Temperature difference between the cathode surface and the bulk solution
$\Delta \rho_h$	Density difference between the bulk solution and the electrode surface required for the evaluation of Gr_h
$\Delta \rho_m$	Density difference between the bulk solution and the electrode surface required for the evaluation of Gr_m
ϵ	Porosity of the fouling deposit
ϵ_s	Equivalent sand grain roughness
ζ	Dimensionless distance from electrode surface defined by equation A4.26
η	Dimensionless distance from electrode surface defined by equation A4.41

θ	Time
θ_c	Time constant of the fouling transient
θ_e	Efflux time
θ_D	Delay time
i	Intensity of turbulence
κ	First order rate constant for the process of overcoming the surface energy barrier between the particles and the surface
λ_a	Average wavelength
λ_j	Mobility of species j
Λ	Stream function defined by equation A4.42
μ	Viscosity of the electrolytic solution
μ_s	Viscosity of the electrolytic solution at the surface
ν	Kinematic viscosity of the electrolytic solution in the bulk
ν_s	Kinematic viscosity of the electrolytic solution at the electrode surface
ξ	Dimensionless fouling deposit thickness
ρ	Density of the electrolytic solution
ρ_c	Critical density
ρ_p	Particle density
ρ_F	Density of the fouling deposit
ρ^*	Reduced density
σ_j	Coefficient that is characteristic of species j for use in equation 3.6
τ	Fluid shear stress at the surface
T	Dimensionless electrostatic potential
ϕ	Contact angle
Φ	Electrostatic potential
Φ_d	Deposition rate
Φ_r	Removal rate
χ	Ratio of thermal conductivity of the fluid phase and thermal conductivity of the particulate phase
ψ	Fractional volume of the particulate phase
Ψ	A function of deposit structure

INTRODUCTION

Fouling, although widely recognised as a serious constraint in the design and operation of heat transfer equipment, remains one of the least understood phenomena encountered in industry today⁽¹⁻⁴⁾. Fouling of heat transfer equipment occurs in most chemical and process industries⁽⁵⁻⁷⁾, including oil refineries, pulp and paper manufacturing, polymer and fibre production, desalination, food processing and power generation. In a heat transfer survey conducted by Sabersky⁽⁸⁾, fouling was considered 'by many to be the single most unknown factor in the design of heat exchangers'.

Fouling of heat transfer equipment can cause a reduction in thermal and hydrodynamic performance, an increased energy consumption, an additional maintenance and cleaning cost and a partial or total loss in production. In addition, the extra surface area allowed for fouling in the original design of heat transfer equipment will incur an extra capital cost. Excess surface area of 30-40%, equivalent to an capital cost of 25%, is probably a typical average^(9,10).

The overall cost of fouling of heat transfer surfaces in the United Kingdom based on 1979 prices was estimated by Thackery⁽⁹⁾ to be £300-500M per year, ie. equivalent to 0.5% of the UK Gross National Product. Scaled up to 1980 prices, this figure becomes £500-1000M per year. Van Nostrand, Leach and Haluska⁽¹¹⁾ of Exxon Chemical Co. have estimated the total cost of fouling for a hypothetical, typical 100,000 Bbl/SD refinery in the United States to be \$9.9M per year. By extrapolating this figure proportionally, the fouling related expenses for all US refineries was estimated at about \$1400M per year and for worldwide non-communist refineries at about \$4400M per year.

Despite the accumulation of the fouling literature in recent years, fouling appears to be a topic that eludes generalisation⁽¹²⁾. This lack of understanding almost reflects the complex nature of the phenomena by which fouling occurs in industrial equipment. The wide range of process streams and operating conditions present in industry tends to make most fouling situations unique thus rendering a general analysis of the problem difficult⁽¹³⁾.

Fouling is an extremely complex phenomenon. Fundamentally, fouling may be characterised as a combined, unsteady state, momentum, mass and heat transfer

problem. In certain fouling situations, additional knowledge of chemical kinetics, solubility data and corrosion principles may also be required⁽¹⁴⁾. There is also strong evidence from the available fouling data that the overall fouling process consists of a number of sub-processes^(12,15-17). These are

1. Processes in the bulk of the fluid
2. Transport to the deposit-fluid interface
3. Attachment/formation reaction at the deposit-fluid interface
4. Removal of the fouling deposit
5. Transport from the deposit-fluid interface

Epstein⁽¹⁵⁻¹⁷⁾ stressed that some of the sub-processes may not be applicable in certain fouling situations.

Much of the fouling research undertaken has been focussed on the elucidation of models that would attempt to describe the overall fouling process of fouling on heat transfer surfaces. Most of the fouling models found in the literature are based on the observation made by Kern and Seaton^(18,19). They proposed the net overall rate of fouling at any time θ is the difference between the two simultaneous opposing rates, a deposition rate ϕ_d and a removal rate ϕ_r . The models differ essentially on the functional dependence of the operating variables on ϕ_d and ϕ_r . Unfortunately, due to the complexity of the fouling process, all of these models are highly simplified, semi-analytical and only have a limited applicability. Clearly, these models do reflect the lack of understanding of the fundamental laws which govern the overall fouling process.

The need for a general fouling model that will be of use to designers and operators of heat transfer equipment has been strongly emphasized^(12,20,21). To date, two general fouling models^(21,22) have been reported in the fouling literature. Unfortunately for both models, considerable experimentation on the crucial fundamental aspects of the model is required before the model can be used in the design and operation of heat transfer equipment.

It was suggested that all future investigations of fouling should be based on a 'process analysis' of the overall fouling process. This approach, originally proposed by Characklis^(23,24) for a complex microbial fouling system, involves the breaking down of the overall fouling process into a number of sub-processes and establishing the fundamentals which lie behind

each of the sub-processes. It was generally felt that this approach will ameliorate our understanding of the overall fouling process.

The research needs for the 'process analysis' approach have been summarised by Somerscales⁽¹²⁾. A strong emphasis was placed on the need for a better understanding of the influence of the fouling deposit characteristics on the overall fouling process. It is the aim of this study to investigate the effect of deposit characteristics on heat transfer and the influence of the deposit interface on fluid flow.

As industrial fouling deposits are difficult to quantify in terms of well-defined deposit characteristics, it was decided to simulate the fouling deposit in this study. Of the various options listed by Epstein⁽²⁵⁾ for monitoring fouling in small scale rigs, the electrochemical method was selected for two reasons:

1. To date, only two papers^(26,27) on the use of the electrochemical method for monitoring fouling have been reported in the literature.
2. Using a model fouling system, the electrochemical method provides the most suitable method to study the effect of deposit characteristics on heat transfer and the influence of the deposit interface on fluid flow.

1. FOULING OF HEAT TRANSFER SURFACES

Several workers have reviewed fouling of heat transfer surfaces in general. Excellent reviews have been presented by Bott and Walker⁽²⁾ in 1971, Taborek et al⁽²⁸⁻³¹⁾ in 1972, Hopkins⁽³²⁾ and Walker⁽³³⁾ in 1973, Bott^(3,4) in 1975 and 1981, Gupta⁽³⁴⁾ in 1978, Epstein^(25,35) in 1978 and 1979, Somerscales⁽¹²⁾ in 1979, Knudsen^(7,36) in 1980 and 1984, Lund and Sandu⁽²⁰⁾, Pinherio⁽²²⁾, O'Callagan⁽³⁷⁾ and Collier⁽³⁸⁾ in 1981 and Knudsen and Roy⁽³⁹⁾ in 1982.

1.1 Definition

Fouling may generally be defined as the formation of undesirable solid material on a heat transfer surface which impedes the transfer of heat and increases the resistance to fluid flow⁽¹²⁾. This accumulation of deposits causes the thermal and hydrodynamic performance of heat transfer equipment to decline with time.

1.2 Classification

The generally favoured scheme for the classification of different types of fouling that can occur on heat transfer surfaces is the one based on the principal physical/chemical process that will give rise to the phenomenon. The six categories identified by Epstein^(15-17,25,35) are:

1. Precipitation fouling^(14,40-46) - the crystallisation from solution of dissolved substances onto the heat transfer surface.
2. Particulate fouling^(6,47-53) - the accumulation of finely divided solids suspended in the process fluid onto the heat transfer surface.
3. Chemical reaction fouling⁽⁵⁴⁻⁵⁹⁾ - the deposit formation at the heat transfer surface by chemical reactions in which the surface material itself is not a reactant.
4. Corrosion fouling^(60,61) - the accumulation of indigeneous corrosion products on the heat transfer surface.
5. Biological fouling^(23,24,62-66) - the attachment of macroorganisms and/or microorganisms on a heat transfer surface.

6. Solidification fouling^(67,68) - the freezing of a pure liquid or crystallisation from a multicomponent melt onto a subcooled surface.

1.3 Terminology

The various terms used in the literature as synonyms for fouling deposits are shown in Table 1.1.

1.4 Design

The effect of fouling on the design and operation of heat transfer equipment is expressed in the basic design equation for heat transfer:

$$q = U A F_T (\text{LMTD}) \quad 1.1$$

where q is the heat transfer rate, U is the overall heat transfer coefficient, A is the heat transfer area, LMTD is the overall logarithmic mean temperature difference based on inlet and outlet temperatures of both streams and F_T is a correction factor based on the geometry of the system to give the true mean temperature difference between the fluids.

The various resistances to heat transfer encountered as heat flows from a hot fluid to a cold fluid and the accompanying temperature differences are shown in Figure 1.1A for clean surfaces and Figure 1.1B for fouled surfaces. The resistances are in series. The overall heat transfer coefficient for clean and fouled surfaces, U_C and U_F , are respectively given by:

$$\frac{1}{U_C} = R_i + R_w + R_o \quad 1.2$$

$$\frac{1}{U_F} = R_i + R_{Fi} + R_w + R_{Fo} + R_o \quad 1.3$$

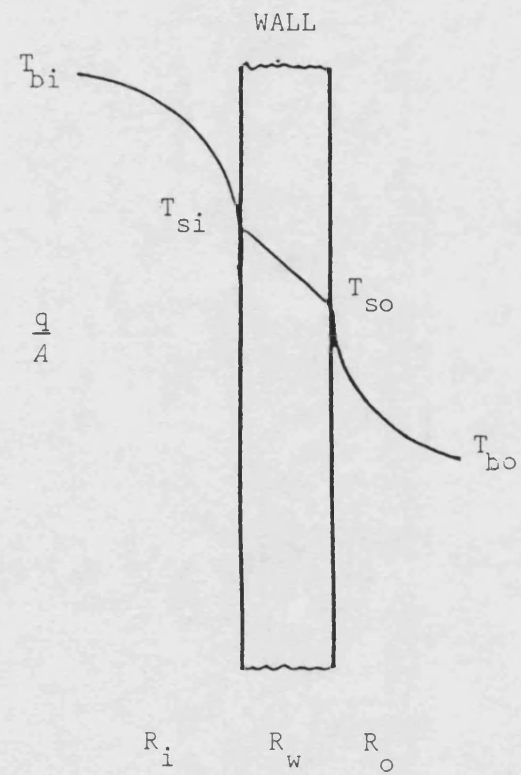
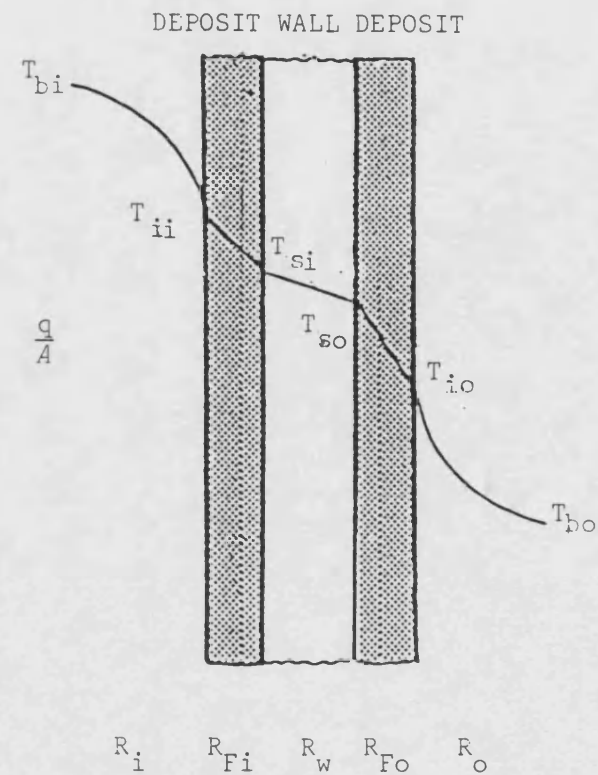
The heat transfer resistances inside and outside the wall, R_i and R_o , are obtained from design correlations. The heat transfer resistance of the wall, R_w , is obtained from the thermal conductivity of the wall material and its thickness. The fouling resistances inside and outside the wall, R_{Fi} and R_{Fo} , account for the fouling and roughness of the heat transfer surface.

If U_C and U_F are both known, the sum of R_{Fi} and R_{Fo} can be determined from equations 1.2 and 1.3.

$$R_{Fi} + R_{Fo} = \frac{1}{U_F} - \frac{1}{U_C} \quad 1.4$$

TABLE 1.1 TERMINOLOGY OF FOULING DEPOSITS⁽¹²⁾

CATEGORY	FOULING DEPOSIT	OCCURENCE/APPLICATION	INTERPRETATION
Precipitation	Scale	Evaporators and Boilers	Inorganic, crystalline and tenacious deposits, - formed by 1. inverse solubility salts on heated surfaces 2. normal solubility salts on sub-cooled surfaces.
	Sludge		Porous and loosely adherent deposits.
Particulate	Magnetite deposit	Fossil Fuel Fired and Nuclear Reactor Steam generators	Deposits of fine magnetite - formed elsewhere in reactor system and transported to the heat transfer surface.
	Crud		Deposits of corrosion products - formed elsewhere in reactor system and transported to the heat transfer surface.
	Ash, Slag	Coal Fired Boilers	Deposits of silica based minerals - formed in the fuel elsewhere in reactor system and transported to the heat transfer surface.
Chemical Reaction	Coke	Petroleum refining, petrochemical processing and gas turbine fuel handling systems	Carbonaceous tenacious deposit - formed by polymerised organic compounds.
	Soot		Carbonaceous, soft and loosely adherent deposits.
	Milkstone	Milk processing	Deposit derived from constituents of milk.
	Crud	Organic cooled Nuclear Reactors	Deposit formed from organic coolants.
Corrosion	Corrosion Scale	Heat transfer equipment exposed to natural water	Deposit of indigeneous corrosion products.
Biofouling	Fouling	Ship hulls and heat transfer equipment exposed to sea water	Growth of 1. macro- and micro- organisms 2. macro-organisms.
	Slime, mircobial fouling	Cooling water side of heat transfer equipment using natural water	Growth of micro-organisms.
Solidification	Ice deposit	Refrigeration units	Freezing of a single component liquid, e.g. water.
	Wax deposit		Crystallisation of a multicomponent melt on sub-cooled surfaces.

A. CLEANB. FOULEDFIGURE 1.1 HEAT TRANSFER RESISTANCES AND TEMPERATURE PROFILES

Equation 1.4 gives the physical significance of the average fouling resistance, R_F as R_{Fi} and R_{Fo} cannot be evaluated individually.

The fouling resistance of a heat transfer surface, R_F is dependent on several physical and economic factors. The physical factors which influence the extent of fouling in heat transfer equipment include^(13,69-72)

1. time
2. the velocity of a fluid over a surface
3. the wall temperature and the interfacial temperature between the fluid and the wall
4. the physical and chemical characteristics of the fouling fluid
5. the material and finish of the heat transfer surface
6. the geometry of the heat transfer equipment
7. the nature of the fouling deposit

The economic factors which enter in the determination of the permissible extent of fouling in heat transfer equipment include⁽⁶⁹⁾

1. the initial capital cost of a heat exchanger
2. the variation of the capital cost with the size of heat exchanger
3. the cost of wasted energy associated with the poorer performance of the heat exchanger
4. maintenance costs
5. the number of plant shutdowns for cleaning
6. cleaning costs
7. the loss of revenue during plant shutdown
8. depreciation, tax, net return of investment, etc.

Clearly, there is an optimum value for R_F to be used in a given heat exchanger design problem. TEMA⁽⁶⁹⁾ defines the optimum as 'The best design fouling resistance, chosen with all physical and economic factors properly evaluated, will result in a minimum cost based on the capital and operating costs of the heat transfer equipment'. Several methods for predicting the optimum economic performance of heat transfer equipment have been suggested⁽⁷³⁻⁷⁷⁾. All of these methods require reliable equations or operating data for the prediction of the fouling transient. Unfortunately, this information is rarely available.

The general practice for the specification of the fouling resistance in the design of heat transfer equipment is to 'throw in fouling factors' for R_{Fi} and R_{Fo} ⁽⁷⁸⁾ - fixed values obtained from

1. standard sources such as TEMA tables⁽⁶⁹⁾ or nomographs⁽⁷⁹⁻⁸²⁾
2. previous user experience
3. laboratory and field tests

The fouling resistances are usually of the order 0.0001 to 0.0018 m²/kW. In some cases, the fouling resistance may be the controlling resistance^(83,84).

Unfortunately, the information provided by the TEMA tables suffers from three serious disadvantages⁽¹²⁾, ie.

1. it does not recognise that fouling is a transient process.
2. it does not usefully relate to the design and operation of certain types of heat transfer equipment.
3. it is only available for a limited number of fluids.

Moreover, Bott and Walker⁽²⁾ have questioned the reliability and accuracy of these fixed values.

Until recently, there has been no demand for information more comprehensive than that provided by the TEMA tables. However, as a consequence of

1. the rapidly increasing costs of energy and of the materials used in the construction of heat transfer equipment since 1973
2. the gradual improvements in design procedures for estimating the inside and outside film heat transfer coefficients, h_i and h_o

there is an increasing awareness among designers, manufacturers and users alike for the need 'to reduce the ignorance factor associated with fouling'⁽³⁴⁾ in the design of heat transfer equipment.

1.5 Measurement

1.5.1 Characterisation of deposit accumulation

The amount of deposit accumulation on a heat transfer surface may be expressed as

1. mass per unit area of heat transfer surface, M
2. thickness, x
3. unit thermal fouling resistance, R_F

The three entities are inter-related differentially as

$$dM = \rho_F dx = \rho_F k_F dR_F$$

1.5

where ρ_F = density of fouling deposit

k_F = thermal conductivity of fouling deposit

The corresponding expressions for the rate of deposit accumulation at any time θ is given by

$$\frac{dM}{d\theta} = \rho_F \frac{dx}{d\theta} = \rho_F k_F \frac{dR_F}{d\theta} \quad 1.6$$

Depending on the relative values of ρ_F and k_F , it should be noted that two deposits with the same incremental increase in M may give rise to very different corresponding increases in R_F . A hard adherent non-porous deposit will typically have relatively high values of ρ_F and k_F while a soft loose porous deposit will have considerably lower values of ρ_F and k_F ⁽¹⁵⁻¹⁷⁾.

Assuming that ρ_F and k_F does not vary with x , integration of equation 1.5 yields

$$M = \rho_F x = \rho_F k_F R_F \quad 1.7$$

The assumption on which equation 1.7 is based is rarely met in practice. An example of this assumption being violated is given by the complex formation of deposits on a steam generator pipe reported by Meeter et al ⁽⁸⁵⁾. In such violations, ρ_F and k_F represent composite average values of the density and thermal conductivity respectively. However, for the rare cases where the variation of ρ_F and k_F with x is known, equation 1.5 can be integrated taking this variation into account.

1.5.2 Measurement of deposit accumulation

The ideal approach for obtaining fouling data is to monitor the performance of in-plant heat transfer equipment using the actual fluids ^(36,86). This is frequently accomplished ⁽⁸⁷⁻⁸⁹⁾ but much of the fouling data obtained is widely scattered and not particularly useful for the development of fouling models. The problems of obtaining fouling data from in-plant heat transfer equipment have been highlighted ^(86,87).

Due to the difficulties of carrying out controlled experiments on in-plant heat transfer equipment, several laboratory and field techniques were developed. Epstein ⁽²⁵⁾ summarised these techniques in terms of equipment geometry, the type of heating and the method of interpreting the results. This collation is reproduced in Table 1.2. Knudsen ⁽⁸⁶⁾ described several

TABLE 1.2 CHARACTERISTICS OF TECHNIQUES USED BY VARIOUS INVESTIGATORS TO STUDY FOULING ON HEAT TRANSFER SURFACES (25)

Geometry	Type of Heating	Interpretation
Inside of tube	Sensible fluid heating	Visually
Annulus	Condensing Vapour	Direct weighting
Sphere	Direct electrical heating	Pressure drop
Outside of U-tube	Indirect electrical heating	Thermally
Metallic strip or plate	Thermo-electric heating and cooling	Chemically
Stirred Cell	None	Microscopically
Wire		Radioactively
Wire Coil		Electrolytically
Shell side of model heat exchanger		
Helix		

experimental test sections that have been used by various investigators to carry out dynamic, often accelerated, fouling experiments under controlled conditions. The advantages and disadvantages for each test section were also discussed. A summary of the comparison of these test sections is given in Table 1.3.

Merry and Polley^(87,88) have pointed out there are conditions which must be satisfied before the fouling data obtained from laboratory or field techniques can be used in the design or performance analysis of industrial heat transfer equipment. These conditions are

1. The actual fluid to be handled by the industrial heat exchanger must be used in the laboratory or field tests.
2. The apparatus must be constructed of the same material as the industrial heat exchanger.
3. The thermal and hydrodynamic conditions must be representative of those present in the industrial heat exchanger.

These conditions indicate that many of the techniques outlined by Epstein⁽²⁵⁾ are invalid. The only suitable laboratory or field test for the simulation of tubeside/shellside fouling in industrial heat transfer equipment is the thermal monitoring of fouling inside tubes/over tube bundles or in a model exchanger.

However, the other techniques are useful for the evaluation of the fouling propensity of a fluid⁽⁸⁷⁾ and the determination of the nature of the fouling deposit⁽⁸⁶⁾.

1.5.3 Fouling Curves

The most common fouling curves found experimentally are shown in Figure 1.2. In principle, the net overall rate of fouling at any time θ can be expressed as the difference between the deposition rate ϕ_d and the removal rate ϕ_r ^(18,19). Curve A represents the linear mode which is indicative of either a constant ϕ_d with ϕ_r being negligible or $(\phi_d - \phi_r)$ is constant. This is generally characteristic of hard adherent non-porous deposits. Curve B illustrates the falling rate mode which results from either a decreasing ϕ_d with ϕ_r being constant or a decreasing ϕ_d and an increasing ϕ_r . Curve C represents the asymptotic mode which is characteristic of soft loose porous deposits which flake off easily due to the shearing action of the fluid

TABLE 1.3 COMPARISON OF TEST SECTIONS⁽⁸⁶⁾

FEATURE	TEST SECTION													
	1	2a	2b	2a	3	4			5			6	7	8
						T	A		T	A		T	A	
						H	C		H	C				
Visual observation possible during run	X						X		X	X		X	X	
Must be destroyed (or dis-assembled) to observe deposit		X	X	X	X	X		X	X			X	X	
Local heat flux easily determined	X						X							X
Local heat flux easily determined but losses to environment must be accounted for			X	X	X	X	X							
Local heat flux usually cannot be determined								X	X	X	X	X	X	X
Wall temperature can be determined	X	X	X	X	X	X	X	X	X	X	X	X	X	X
Surface temperature can be determined	X	X	X	X	X	X	X							X
Can be made from a wide variety of materials	X	X	X	X	X			X	X	X	X	X	X	X
Can be made from a limited number of materials						X	X							X
Can determine local fouling factor	X	X	X	X	X	X	X							X
Can determine only average fouling factor								X	X	X	X	X	X	X
Results can be extrapolated to circular tube conditions	X	X	X	X	X	X	X	X	X	X	X	X	X	?
Results can be extrapolated to complex geometries	?	?	?	?	?	?	?	?	?	?	?	?	?	?
Easy to control	X	X	X	X	X	X	X	X		X				X
Difficult to control									X		X	X	X	?
Stable operation during fouling test	X	X	X	X	X	X	X	X	X	X	X			?
Retains calibration	X	X	?	?	?	X	X	X	X	X	X	X	X	X
Low power requirement				X	X									X
High power requirement	X	X	X			X	X	X	X	X	X	X	X	X

- T - Fouling fluid flows in circular tube
 A - Fouling fluid flows in annular duct
 H - Heating fouling fluid
 C - Cooling fouling fluid
 1 - Annular geometry, indirect electric heating
 2a - Thin-walled tube, indirect electric heating
 2b - Thick-walled tube, indirect electric heating
 2c - Thick-walled tube, transient technique
 3 - Circular tube geometry, thermoelectric heating or cooling
 4 - Annular or circular tube geometry, direct electric heating
 5 - Annular or circular tube geometry, sensible heat of fluids
 6 - Annular or circular tube geometry, condensing vapor
 7 - Complex geometries
 8 - Electrically heated wires and coils

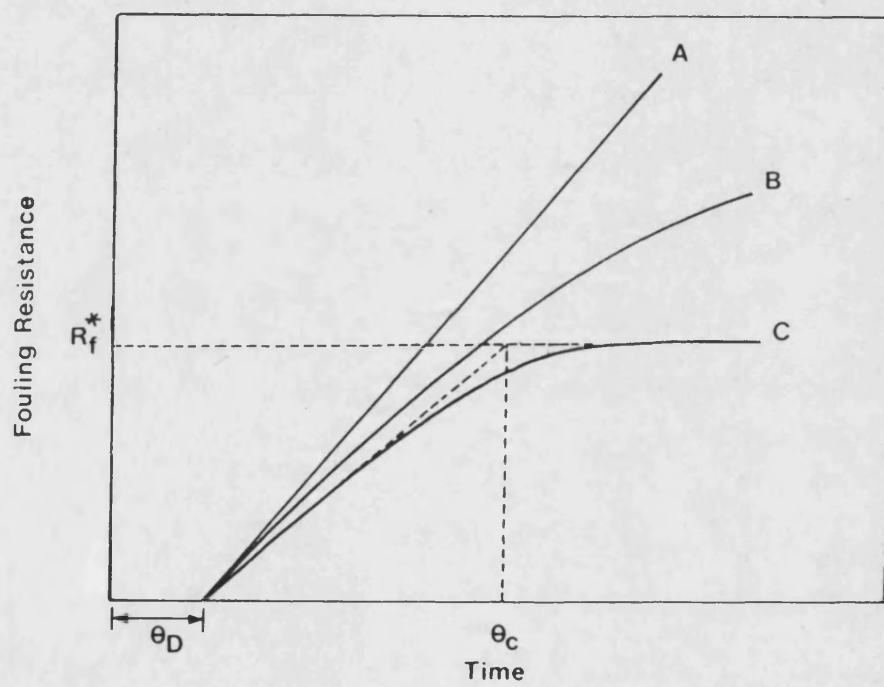


FIGURE 1.2 FOULING CURVES

flowing past the deposit. The asymptotic mode may be described by an exponential equation indicative of a constant ϕ_d and ϕ_r being directly proportional to R_F until $\phi_r = \phi_d$ at the asymptote.

Epstein⁽²⁵⁾ pointed out that the linear and falling rate modes may be the early events which if followed to completion would ultimately produce the asymptotic mode. This is especially true when there is scatter in the results.

In some fouling situations, an initiation period is required before deposition occurs on the heat transfer surface. This is represented by the delay time, θ_D in Figure 1.2. Values of θ_D are not predictable and appear to be random in nature or have a normal distribution about some mean value. θ_D have been observed to be somewhat longer for new surfaces than for cleaned surfaces.

Fouling curves of more complex shapes have been observed^(28,90,91). These curves can sometimes be broken down into one of the three above simpler modes.

1.5.4 Fouling models

The first attempt to describe fouling on a mathematical basis was made by Kern and Seaton^(18,19). They observed that the fouling resistance of several oil refinery heat exchangers appeared to increase asymptotically with time. They suggested that the fouling transient could be approximated by

$$R_F = R_F^* [1 - \exp(-\beta\theta)] \quad 1.8$$

where R_F and R_F^* are the fouling resistances at any time θ and at asymptotic conditions $\theta \rightarrow \infty$ respectively and β is a coefficient representing the rate of approach to R_F^* .

To explain the fouling transient, Kern and Seaton suggested by intuitive reasoning, that the net overall rate of fouling at any time θ is the result of two simultaneous opposing rates, a deposition rate ϕ_d and a removal rate ϕ_r :

$$\left. \frac{dR_F}{d\theta} \right|_{\theta=\theta} = \phi_d - \phi_r \quad 1.9$$

They also considered that ϕ_d is independent of time and ϕ_r is directly proportional to R_F :

$$\phi_d = \left. \frac{dR_F}{d\theta} \right|_{\theta=\theta} \quad 1.10$$

$$\phi_r = \beta R_F \quad 1.11$$

Under these conditions, the integration of equation 1.9 will yield equation 1.8 with $R_F^* = \frac{\phi d}{\beta}$. The time constant of the fouling transient θ_c is given by $\frac{1}{\beta}$. This represents the time it would take to reach R_F^* if fouling proceeded linearly at the initial fouling rate and also the mean residence time of an element of fouling deposit on a heat transfer surface⁽²⁵⁾. θ_c could be used to distinguish between the falling rate and asymptotic fouling transient⁽³⁷⁾.

Epstein⁽²⁵⁾ suggested that there is a conceptual problem over the possibility of removal co-existing with deposition at the heat transfer surface. For example, in the case of particulate fouling, how does a particle ever get deposited if it becomes subjected to removal as it approaches the heat transfer surface. There seems to be two possibilities for the removal process:

1. The removal of material already deposited on the surface^(18,19).
2. The suppression of the deposition process^(92,93).

Charlesworth⁽⁹⁴⁾ attributed the removal process to three mechanisms:

1. Dissolution - This occurs when the deposit formed at the heat transfer surface dissolves into the bulk fluid.
2. Spalling - This is due to the mechanical stresses set up in the fouling layer by temperature gradients. Loo and Bridgewater⁽⁹⁵⁾ have provided a mathematical basis for this removal mechanism.
3. Erosion - This is due to the shear stress acting at the deposit-fluid interface. The nature of the fouling deposit and the velocity of the fluid govern this removal mechanism. However, Cleaver and Yates⁽⁹⁶⁻⁹⁹⁾ have argued that shear is not capable of generating a sufficiently large 'lifting force' to dislodge particles from a surface. According to their theory, removal occurs as a result of randomly periodic and randomly distributed turbulent bursts. These bursts originate and cover less than 0.5% of the fouled surface at any instant. These bursts act as miniature tornadoes which have the ability to lift deposited material from the surface. The evolution of turbulent bursts away from the surface produces a 'back sweep' of the fluid back to the surface. Such movement could provide the basis of the deposition process. For a given deposit and fluid,

a minimum friction velocity is required before removal will occur.

The Kern-Seaton model constitutes the basis for most of the fouling models that have appeared in the literature. These fouling models have been reviewed in general^(2,3,5,6,14,20,25,29,33,44) and according to their particular fouling category^(6,42,47,54-57,62). These models differ essentially on the functional dependence of the operating variables on ϕ_d and ϕ_r . Unfortunately, due to the complexity of the fouling process, these models are highly simplified, semi-analytical and only have a limited applicability. None of these models incorporates all the variables likely to affect the overall fouling process. The models tend to only incorporate the transfer variables such as time, velocity, concentration and temperature. Other factors such as the nature and the condition of the heat transfer surface, the characteristics of the fouling fluid, the nature of the fouling deposit, the geometry of the heat transfer equipment, the variation of the properties of the fouling fluid due to process fluctuation and the simultaneous action of the different fouling mechanisms are ignored.

Attempts to elucidate general fouling models have been minimal. To date, two general models have been reported in the fouling literature. Pinherio⁽²²⁾ deduced a semi-analytical generalised model by recognising the similarities between the models proposed by Watkinson and Epstein^(100,101) and Gudmundsson⁽⁶⁾ for particulate fouling, Taborek et al⁽²⁹⁻³¹⁾ for crystallisation fouling and Crittenden and Kolaczowski⁽¹⁰²⁾ for chemical reaction fouling. Sandu and Lund⁽²¹⁾ derived a general fouling model from momentum, mass and heat transfer considerations.

1.6 Deposit characterisation

One of the research needs for the 'process analysis' approach that was summarised by Somerscales⁽¹²⁾ called for a better understanding of the influence of the deposit characteristics on the overall fouling process. To date, very few papers on deposit characterisation⁽¹⁰³⁻¹⁰⁶⁾ have been reported in the fouling literature. This can be attributed to the difficulties associated with the identification of the materials found in a typical fouling deposit and the removal of deposits from their substrates which may involve partial/total destruction of the heat transfer equipment⁽¹⁰⁷⁾. The problems concerning the isolation and characterisation of deposits have been

highlighted by Mansfield and Walters⁽¹⁰⁴⁾ for cooling water systems and Duddridge⁽¹⁰⁶⁾ for biofouling systems.

The type of deposit formed on a heat transfer surface is dependent on the nature of the feedstock and the conditions of the fouling environment⁽¹⁰⁸⁾. Nelson^(1,109) describes three types of deposits which are found in heat transfer equipment, namely

1. Hard deposits: Examples of this type of fouling deposit are scale, corrosion scale, rust and coke. The fouling resistance of these deposits increase almost linearly with time. Such deposits are tenacious and their removal can only be effected by
 - a. dry sandblasting
 - b. mechanical methods eg rodding, scraping, etc
 - c. chemical cleaning
2. Porous deposits: These deposits are essentially the same material but containing trapped fluid whose thermal conductivity is generally lower than that of the hard structure. The removal of these deposits is usually done by
 - a. wet sandblasting
 - b. chemical cleaning
3. Loose deposits: Examples of this type of fouling deposit are silt, mud, algae, powdered coke and soft carbonaceous material. The fouling resistance of these deposits is largely dependent on the properties of the trapped fluid. The removal of these deposits is usually accomplished by
 - a. wet sandblasting
 - b. mechanical methods eg rodding, scraping, etc
 - c. the use of a high fluid velocity

Fouling deposits are often complex and non-homogeneous. The complexity of the deposit is generally due to the strong interactions between two or more of the fouling categories identified by Epstein^(15-17,25,35). These interactions may cause mutually reinforcing (ie. synergistic) or weakening effects. Fouling deposits which are stratified in two or more layers have been observed in several fouling situations^(20,29,94,110-119).

Industrial fouling deposits are rarely described in detail. Cooling water deposits invariably consist of a complex mixture of the constituents listed in Table 1.4^(120,121). Many of the microorganisms found in cooling water

TABLE 1.4 NATURE OF COOLING WATER DEPOSITS⁽¹²¹⁾

COMMON TYPES OF SCALE	:	Calcium carbonate
		Calcium sulphate
		Calcium phosphate
		Magnesium salts
		Silica
		Iron oxide
COMMON FOULANTS	:	Mud/silt
		Sand
		Clay
		Corrosion products
		Organic matter
		Microbiological material
		Clarifier carryover
		Iron and/or aluminium phosphate
		Miscellaneous debris
		Process leaks e.g. oil
		Corrosion inhibitor

systems possess the ability to exude hydrated polymeric slimes⁽⁶⁶⁾. These slimes, which consist mainly of polysaccharides and polypeptides,

1. enable the microorganisms to adhere to the heat transfer surface
2. protect the microorganisms from physical and chemical attack
3. capture food (suspended organic matter) for the microorganisms
4. entrap the other constituents present in the cooling water

The main types of microorganisms likely to cause problems in cooling water systems are listed in Table 1.5. Refinery deposits consist of a mixture of inorganic salts, corrosion products, organic polymers and/or coke⁽¹²²⁻¹²⁴⁾. A survey carried out by Coggins⁽¹²⁵⁾ gives a summary of the nature of deposits found in gas-making units. This summary is shown in Table 1.6.

Data sheets for the characterisation of fouling deposits have been reported in the literature^(103,126). A full description of any fouling deposit would require knowledge of its

1. thickness
2. mass
3. morphology
4. physical properties
5. chemical analysis
6. microbiological analysis

Each of these deposit characteristics will be discussed in turn.

1.6.1 Deposit thickness

Information on the estimation of deposit thickness is limited in the fouling literature. Techniques used by various investigators for the direct measurement of deposit thickness include

1. the microscope⁽¹²⁷⁻¹³⁶⁾/travelling microscope^(137,138) focussing method
2. the conductance method^(106,136,139-143)
3. the use of a graduated probe⁽¹⁴⁴⁾
4. the use of a micrometer⁽¹⁴⁵⁻¹⁴⁷⁾

The main disadvantage of these methods is the need to dismantle the test section from the fouling experimental rig for the measurement of deposit thickness. From a practical viewpoint, it is more advantageous to estimate the deposit thickness from in-situ measurements of thickness-related variables such as the fouling resistance and the fluid frictional velocity than to

TABLE 1.5 MAIN TYPES OF HARMFUL MICRO-ORGANISMS FOUND IN
COOLING WATER DEPOSITS⁽¹²¹⁾

Bacteria Classification	Characteristics	Harmful Effects on Cooling Systems
Filamentous Type <i>Sulfur-depositing</i> <i>Iron-depositing</i> <i>Streptomyces</i>	Stringy, slippery, grey or gray-green	Fouling
Corrosive <i>Desulfovibrio</i> <i>Clostridium</i> (spore-forming)	Black, granular appearance; grow under slime, deposits	Metal corrosion; gas formation
Nonspore-Forming <i>Flavobacterium</i> <i>Alcaligenes</i> <i>Pseudomonas</i> <i>Achromobacter</i> <i>Aerobacter</i> <i>Mucoids</i>	Gelatinuous, floccu- lant substance resembling mucus; may be coloured	Fouling; gas formation; protection of corrosive bacteria
Spore-Forming <i>B. subtilis</i> <i>B. cereus</i> <i>B. megatherium</i> <i>B. mycoides</i>	Gelatinous; may be stringy; may be coloured	Fouling; protection of corrosive bacteria
Fungi, Spore- Forming Molds <i>Aspergillus</i> <i>Penicillium</i> <i>Trichoderma</i> <i>Cladosporium</i> <i>Mucor</i>	Stringy, fluffy or matted; normally colour- less but may be green	Fouling; wood decay; formation of corrosion cells
Fungi, Yeast-Type <i>Monillia</i> <i>Oospora</i> <i>Torula</i> <i>Endomyces</i> <i>Rhodotorula</i>	Leathery, rubbery or resembling mucus; coloured or colourless	Fouling; formation of corrosion cells
Algae <i>Chroococcus</i> <i>Oscillatoria</i> <i>Chlorococcum</i> <i>Ulothrix</i> <i>Navicula</i> <i>Fragilaria</i>	Loose; slimy or rubbery; green or blue-green; found only in sunlight	Fouling; protection of corrosive bacteria

TABLE 1.6 NATURE OF DEPOSITS IN GAS MAKING UNITS⁽¹²⁵⁾

	PREHEATERS	VAPORISERS	SUPERHEATERS
	%	%	%
Type of deposits:			
Hard, Brittle, Scaly	57	19	26
Massive, coke-like, spongy	17	7	-
Finely divided powder	17	9	36
Scaly + spongy	5	28	16
Spongy + powder	-	4	-
Powder + scaly	-	24	11
Scaly, spongy + powder	4	9	11
Frequency of deposits becoming serious:			
0 - 5 weeks	36	24	40
5 - 10 weeks	9	34	30
10 - 20 weeks	27	22	20
20 - 52 weeks	-	9	10
More than 52 weeks	28	11	-
TOTAL (Actual)	23	55	20

directly measure the deposit thickness. The various techniques that have used for the indirect measurement of deposit thickness are outlined in Table 1.2.

As fouling is a complex process involving deposition and removal, the variation in the local fouling deposit thicknesses can be quite considerable. This variation is clearly seen in Figure 1.3 for a typical 'uniform' CaCO_3 scale thickness profile across the heated section of an annular constant heat flux exchanger⁽¹⁴⁸⁾. A sevenfold variation has been reported for biofilms^(142,143). Clearly, the overall thickness of a fouling deposit can only be best represented by an average value.

The shape of the deposit thickness profile is strongly influenced by the tube wall temperature distribution of a heat exchanger. Uniform^(130,148) and non-uniform^(145,149-153) profiles across the heat exchanger have been reported in the literature. Hasson⁽¹⁴⁹⁾ found the Na_2SO_4 scale thickness profile across the heat exchanger to be dependent on whether the solution is circulated in a closed or an open circuit. This dependency is shown in Figure 1.4. Clearly, the closed circuit operation is characterised by relatively high local deposition rates in the downstream portion of the heated tube while the open circuit operation is characterised by relatively lower local deposition rates which increase almost linearly in the flow direction. The reasons for this marked difference are not clear. Eccentric scale⁽¹⁵⁴⁾, magnetite⁽¹³⁴⁾ and coke^(116,155) profiles due to the unequal circumferential tube wall temperature distribution have also been reported.

1.6.2 Deposit mass

The mass of the fouling deposit can be obtained directly by

1. weighing the test section before and after the experimental run on a dry^(104,156-167) or wet^(105,168) basis.
2. weighing the test section before and after cleaning at the end of the experimental run^(67,128,169-171).
3. measuring the change in mass of the test section periodically⁽¹⁷²⁾ or continuously⁽¹⁷³⁾ with time.

Alternatively, it may be more advantageous from a practical viewpoint to estimate the deposit mass from in-situ measurements of mass-related variables such as the fouling resistance. The various techniques that have been used for the indirect measurement of deposit mass are outlined in

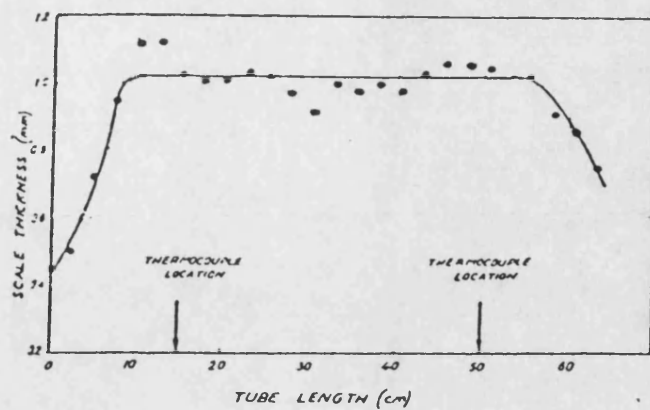


FIGURE 1.3 CaCO_3 SCALE THICKNESS PROFILE⁽¹⁴⁸⁾

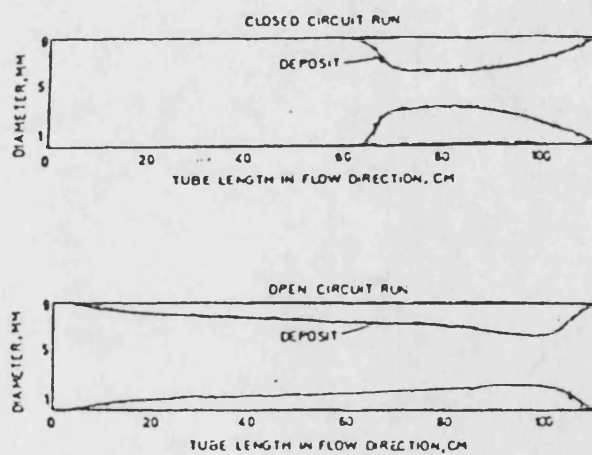


FIGURE 1.4 Na_2SO_4 SCALE PROFILES OBTAINED FROM CLOSED AND OPEN CIRCUIT RUNS⁽¹⁴⁹⁾

Table 1.2.

Alternative methods for expressing the deposit mass have been reported in the fouling literature. Taylor et al⁽¹⁷⁴⁻¹⁷⁷⁾ and Watt et al⁽¹⁷⁸⁾ measured the deposit mass in terms of the amount of carbon in the CO₂ formed by the reaction between the carbonaceous deposit and oxygen in a tube furnace and the conversion of any CO formed by the reaction. Duddridge⁽¹⁰⁶⁾ and Bryers and Characklis^(179,180) described the various methods that have been used for the determination of the amount of biofilm accumulation. A list of these methods is given in Table 1.7. Due to the lack of sensitivity and precision of the direct and indirect methods of mass measurement, the 'initial' phase of biofilm development can only be monitored by methods which measure the amount of a particular biofilm/cell constituent. However, any method of mass measurement can be used to monitor the 'growth' and 'plateau' phases of biofilm development.

1.6.3 Deposit morphology

Studies of the fouling deposit morphology have been carried out using

1. optical microscopy^(91,106,114,127,152,159,179-186)
(6,27-30,56,104-106,133,134,146,150,151,174,177,183-204)
2. scanning electron microscopy
3. transmission electron microscopy^(106,186,198)

The morphology of a fouling deposit can strongly influence the heat transfer rate^(104,181,200) and the residence time of the liquid in the boundary layer adjacent to the heat transfer surface⁽²⁰⁰⁾.

Few attempts have been made to correlate the deposit morphology with the operating variables of the fouling process. The deposit morphology is strongly dependent on temperature. Watkinson⁽¹⁵²⁾ observed that the CaCO₃ scale formed in a steam heated annular test section at relatively low temperatures was compact and rough while the CaCO₃ scale formed at higher temperatures consisted of a fluffy top layer and a consolidated powdery bottom layer. The electron micrographs obtained by Scott and Dawson⁽¹⁵¹⁾ revealed the CaCO₃ scale formed in an electrically heated annular test section at temperatures below 28°C is predominately calcite crystals while the CaCO₃ scale formed at temperatures above 40°C is predominately needle-like aragonite crystals. Several workers^(41,45,145,153,154,205,206) found the

TABLE 1.7 MEASUREMENT OF BIOFILM ACCUMULATION^(106, 179, 180)

A. DIRECT MEASUREMENT OF BIOFILM ACCUMULATION

Thickness
Mass

B. INDIRECT MEASUREMENT OF BIOFILM ACCUMULATION

Heat transfer resistance
Frictional resistance

C. MEASUREMENT OF BIOFILM CONSTITUENT

Chemical oxygen demand
Total organic matter
Total organic carbon
Total organic nitrogen
Total organic acids
Total polysaccharide
Total protein
Total nucleic acids
Total bacterial counts
Total viable cell bacterial counts

D. MEASUREMENT OF CELL CONSTITUENT

Adenosine triphosphate
DNA/RNA
Muramic acid
Poly-beta-hydroxybutyrate
Lipopolysaccharide

E. MICROSCOPIC SURVEILLANCE

crystal form of CaSO_4 scale in sea water distillation units to be dependent on the brine temperature and concentration. This dependency is clearly shown in the solubility diagram of CaSO_4 in sea water given in Figure 1.5.

In the operation of power stations with organic coolants, Bogdanov⁽¹²⁹⁾ noted that at the lower temperatures, the deposits were amorphous in nature while at the higher temperatures in the vapour phase, the deposits were transformed into a hard crust. Smith⁽²⁰⁷⁾ found the temperatures below the break point temperature, jet fuel deposits were powdery and relatively loosely adherent to the tube wall while at temperatures above the break point temperature, jet fuel deposits were hard and firmly adherent to the tube wall. Khater⁽⁵⁶⁾ observed that the deposits formed in a hydrocarbon vapouriser at relatively low temperatures were generally soft, spongy and light brown and consisted of a fine porous structure of near-spherical particles while the deposits formed at higher temperatures were hard, brittle and black and consisted of a filament and plate-like structure with few spherical particles. Kneil et al⁽²⁰⁸⁾ reports that the coke formed in a vapour phase thermal cracking furnace at extremely high temperatures consist of a filament-like structure.

Hermans⁽²⁰⁹⁾, in his study of milk fouling on heat transfer surfaces, observed that

1. at 50°C , the deposits were white and consisted of a hard sandpaper-like structure.
2. between 50°C and 100°C , the deposits were essentially the same as for 50°C with a soft, wool-like structure containing denatured proteins.
3. at 100°C , the deposits become harder and slightly discoloured due to the increase in the mineral content.
4. between 120°C and 150°C , the deposits were brown in appearance.

Frankenfeld and Taylor⁽¹⁷⁷⁾ studied the effect of the dissolved oxygen content on the morphology of jet fuel deposits. Their electron micrographs revealed the air-saturated fuel deposits consist of numerous near-spherical particles on a varnish-like background while the deoxygenated fuel deposits consist of few near-spherical particles on a varnish-like background. Braun⁽¹⁹⁹⁾ and Braun and Hausler⁽²⁰⁰⁾ found the morphology of refinery deposits to be strongly dependent on the nature and dissolved oxygen content of the feedstock.

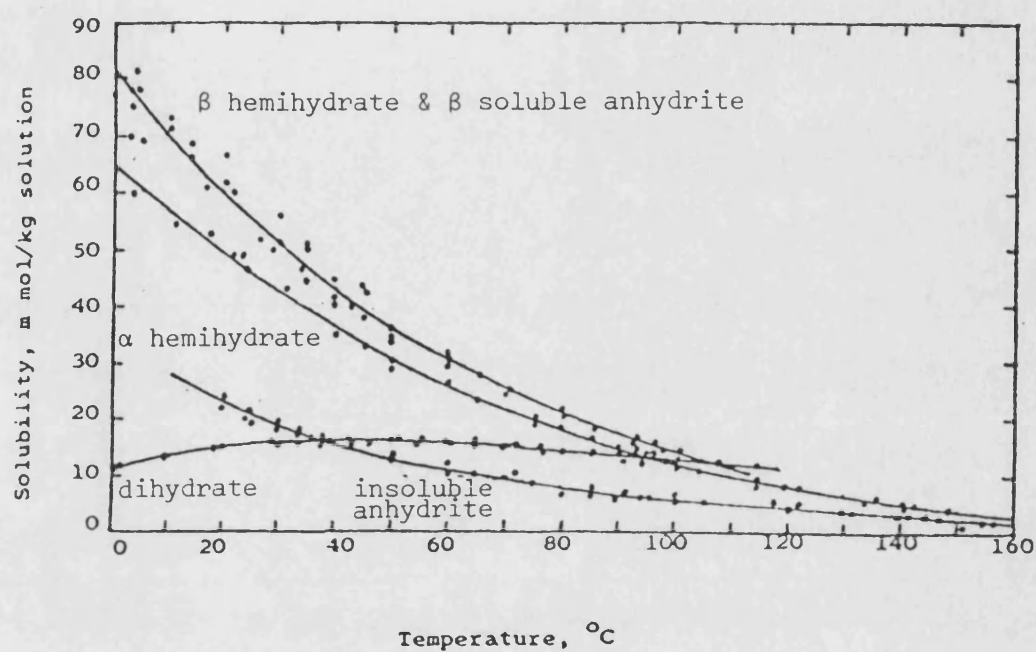


FIGURE 1.5 THE SOLUBILITY OF CALCIUM SULPHATE IN SEA WATER AS A FUNCTION OF TEMPERATURE⁽¹⁵⁴⁾

The addition of antifoulants to the fouling process can have a marked effect on the amount of deposit accumulation^(210,211) and the deposit morphology^(181,191,192,202,212). Generally, there are four types of antifoulant⁽²¹³⁻²¹⁵⁾:

1. Flocculants
2. Dispersants
3. Surfactants
4. Chelants

A variety of corrosion inhibitors, oxygen scavengers, antipolymerants and/or metal deactivators may also be included with the antifoulant^(210,211). Scanning electron micrographs which depict the effect of various antifoulants on the morphology of calcium carbonate and calcium phosphate scales have been presented by Harris and Marshall⁽¹⁹²⁾ and Thurston⁽¹⁹¹⁾ respectively. A set of micrographs given by Hodgson and Smith⁽¹⁸¹⁾ illustrate the transition from hard to soft scale in the presence of increasing concentrations of a particular chemical additive in sea water.

1.6.4 Deposit physical properties

1.6.4.1 Deposit density

Information on deposit density is limited in the fouling literature⁽¹²⁾. This is due to the difficulties in obtaining accurate in-situ measurements. In most fouling situations, the deposit density varies during the course of deposition⁽⁸⁶⁾. Clearly, the value of deposit density is highly dependent on the conditions existing at the time of measurement. The deposit density can be obtained ex-situ by

1. using a pycnometer⁽¹⁵²⁾.
2. measuring the mass of dry deposit and estimating the volume of wet deposit^(24,91,133,136,139,215).
3. measuring the mass per unit area and the average thickness of the deposit^(103,104,135,216).

A collation of the fragmentary data on deposit density is given in Table 1.8.

Mansfield⁽¹⁰³⁾ and Mansfield and Walters⁽¹⁰⁴⁾, in their study of cooling water fouling in an open recirculating system, found the density of cooling water deposits to be dependent on

TABLE 1.8 DEPOSIT DENSITY DATA

FOULING DEPOSIT	DENSITY (kg/m ³)	SOURCE
CaCO ₃ scale	2650-2790	Hasson ⁽²¹⁶⁾
	2600	Watkinson ⁽¹⁵²⁾
CaCO ₃ scale - aragonite	2760	Hasson et al ^(148, 217)
	2400-2500	Hasson and Perl ⁽²¹⁸⁾
CaSO ₄ scale	2700-3000	Hasson et al ⁽¹⁴⁵⁾
	2135	Liddle ⁽¹⁵⁴⁾
Sea water scale	500-1050	Little and Lavoie ⁽¹³³⁾
Magnetite deposits - $\epsilon = 0.7-0.9$, no chimneys, boiling	700-1600	Rooth et al ⁽¹³⁵⁾
Corrosion products - BWR	500-1600	Charlesworth ⁽⁹⁴⁾
Biofilms	20 - 105	Hoehn and Ray ⁽¹³⁹⁾
Biofilms - laminar flow conditions	30 - 100	Characklis et al ⁽¹³⁶⁾
Biofilms - turbulent flow conditions	5 - 50	Characklis et al ^(24, 136, 215)

1. the material of the heat transfer surface
2. the operating control of the recirculating system
3. the heating of the recirculating system

Their results are summarised in Table 1.9.

In biofouling, it has been observed that the density is strongly dependent on the

1. biofilm thickness⁽¹³⁹⁾
2. fluid velocity⁽²⁴⁾
3. glucose loading rate^(24,215)

Hoehn and Ray⁽¹³⁹⁾ measured the biofilm density as a function of thickness for approximately 100 samples. From their results shown in Figure 1.6, they concluded that the biofilm density with respect to thickness first increases rapidly to a maximum and then decreases sharply to an asymptote. To explain this variation, they postulated a sequence of events that occur during the development of the biofilm. These events are summarised in Figure 1.7. Characklis et al⁽²⁴⁾ observed the biofilm density increases with increasing fluid velocity. This dependency, illustrated in Figure 1.8, was thought to be caused by one of the following phenomena:

1. the selective attachment of only certain microbial species from the available population
 2. the microorganism response to environmental stress
 3. the fluid pressure forces 'squeeze' loosely bound water from the biofilm
- Characklis et al^(24,215) noted the biofilm density increases non-linearly with respect to glucose loading rate. This dependency is shown in Figure 1.9.

1.6.4.2 Deposit thermal conductivity

Due to the difficulties in obtaining accurate in-situ measurements, information on the deposit thermal conductivity is limited in the fouling literature⁽¹²⁾. In most fouling situations, the deposit thermal conductivity varies during the course of deposition⁽⁸⁶⁾. Thermal conductivity data for various fouling deposits is given in Table 1.10.

Attempts to estimate the effective thermal conductivity of porous deposits using theoretical models have been minimal. Cohen⁽²²⁶⁾ estimated the effective thermal conductivity of magnetite deposits in water cooled reactors using the Maxwell model:

TABLE 1.9 COOLING WATER DEPOSIT DENSITY DATA

		Flow Velocity (m/s)	Operating Time	Tube Material	Density (kg/m ³)	Standard Deviation	Number of Measure- ments	Reference
NO HEAT TRANSFER	Synergised chromate treatment/ Ryznar index control	0.3	2000 hrs.	Mild Steel	482	283	9	Mansfield ⁽¹⁰³⁾
				Stainless Steel	347	179	4	
				Alumbro	215	82	4	
				Polypropylene	321	257	9	
	Synergised chromate treatment	0.3	87 days	Mild Steel	507-1324	-	-	Mansfield and Walters ⁽¹⁰⁴⁾
				Stainless Steel	387- 773	-	-	
				PVC	100-184	-	-	
	Ryznar index control	0.3	87 days	Mild Steel	190-2220	-	-	Mansfield and Walters ⁽¹⁰⁴⁾
				Stainless Steel	137- 538	-	-	
				Alumbro	40- 141	-	-	
				PVC	30- 81	-	-	
WITH HEAT TRANSFER	Synergised chromate treatment	0.5	56 days	Mild Steel	902-2640	-	-	Mansfield and Walters ⁽¹⁰⁴⁾

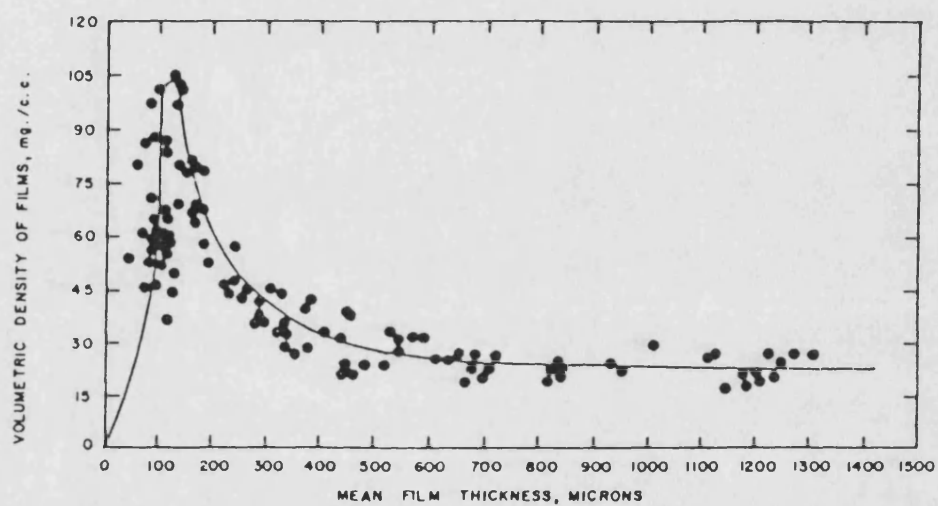
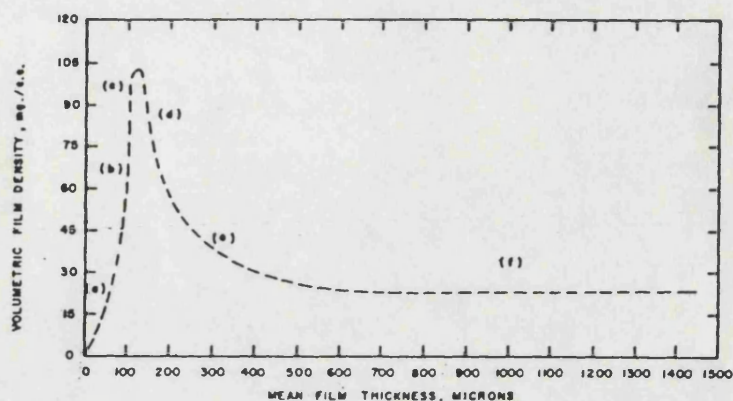
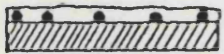

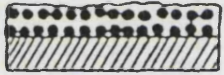
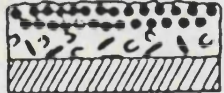
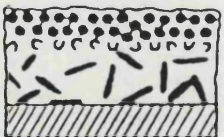
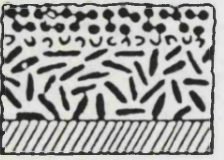



FIGURE 1.6 THE VARIATION OF BIOFILM DENSITY WITH THICKNESS⁽¹³⁹⁾

FIGURE 1.7 THE SEQUENCE OF EVENTS WHICH OCCUR DURING BIOFILM DEVELOPMENT POSTULATED BY HOEHN AND RAY⁽¹³⁹⁾ TO EXPLAIN THE VARIATION OF BIOFILM DENSITY WITH THICKNESS



- (a)  A low density gelatinuous matrix is formed on the substrate by the sparse microbial population.
- (b)  Microbial growth is accelerated and unimpeded by the lack of nutrient or oxygen. The biofilm density increases rapidly.
- (c)  Organisms in the lower layer begin to die when oxygen becomes limiting. Facultative organisms cease functionally aerobically and begin fermentation reactions. Conditions become suitable for growth of a few anaerobic organisms. The lysing of aerobic organisms provides nutrients that are consumed by the surviving organisms in the upper layer. This causes a sharp decrease in biofilm density.
- (d)  Facultative and anaerobic organisms begin to adjust to the new environmental conditions and are growing near/at maximum rates. The increased growth where organisms lived, died and were consumed causes the gradual deceleration of the rate of decrease in biofilm density.
- (e)  A steady state is achieved with respect to the death rate of aerobic organisms and the growth rate of facultative and anaerobic organisms. The biofilm density stabilizes.
- (f)  The steady state conditions persists until the food reserves at the substrate surface are depleted. When this occurs, the organisms near the substrate surface die and lyse. Due to the weakening of the structure of the biofilm, massive 'sloughing-off' of the biofilm will occur.
- (g)  The steady state conditions persists until the food reserves at the substrate surface are depleted. When this occurs, the organisms near the substrate surface die and lyse. Due to the weakening of the structure of the biofilm, massive 'sloughing-off' of the biofilm will occur.

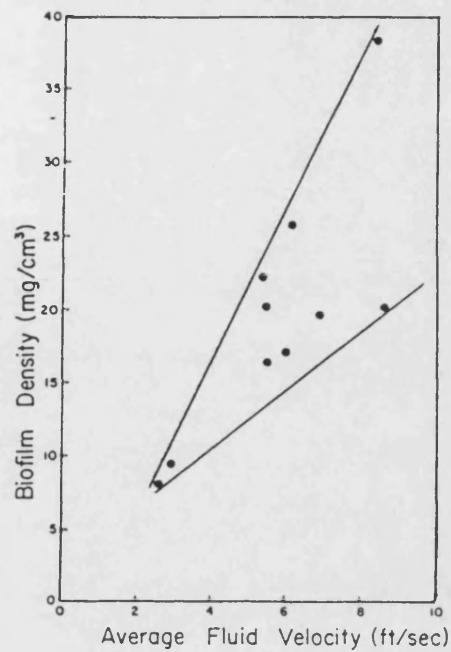


FIGURE 1.8 THE VARIATION OF BIOFILM DENSITY WITH AVERAGE FLUID VELOCITY⁽²⁴⁾.

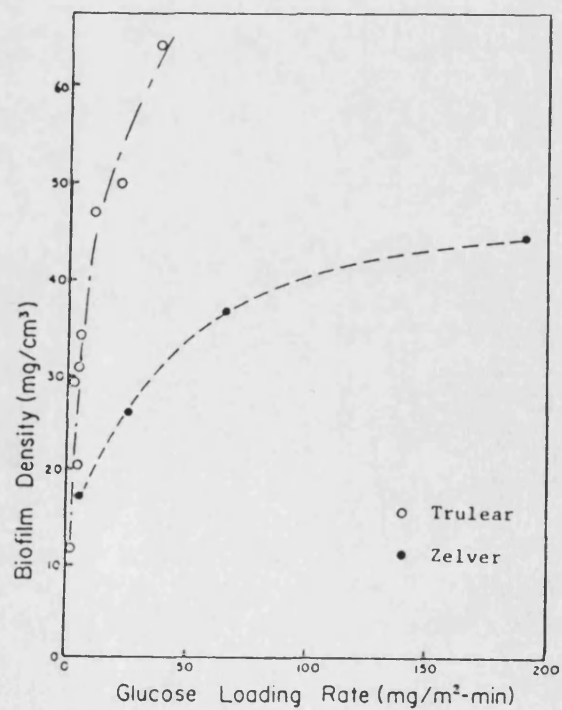


FIGURE 1.9 THE VARIATION OF BIOFILM DENSITY WITH GLUCOSE LOADING RATE⁽²⁴⁾.

TABLE 1.10 DEPOSIT THERMAL CONDUCTIVITY DATA

FOULING DEPOSIT	THERMAL CONDUCTIVITY (W/mk)	SOURCE
CaCO ₃ scale	1.50 - 2.27 1.70 - 4.60 2.26 - 2.93	Hasson ⁽²¹⁶⁾ Watkinson ⁽¹⁵²⁾ Characklis et al ⁽²¹⁵⁾
CaCO ₃ scale - porous	0.35	Capper ⁽²¹⁹⁾
CaCO ₃ scale - aragonite	1.69	Hasson et al ^(148,217)
CaSO ₄ scale	0.59 - 2.32 0.74 2.31	Capper ⁽²¹⁹⁾ Liddle ⁽¹⁵⁴⁾ Characklis et al ⁽²¹⁵⁾
Ca ₃ (PO ₄) ₂ scale	2.60	Characklis et al ⁽²¹⁵⁾
Cooling water deposits	1.38 - 3.22	Mansfield ⁽¹⁰³⁾
Coal ash deposits	0.02 - 1.93	Boow and Goard ⁽²²⁰⁾
Oil ash deposits	0.17 - 1.95 0.05 - 1.40	Neal and Northover ⁽²²¹⁾ Ivanov and Chudnovskaya ⁽²²²⁾
Magnetite deposits -		
$\epsilon \approx 0$, no chimneys, non boiling	5.1	Rassokhim et al ⁽²²³⁾
$\epsilon \approx 0$, 10 μ chimneys, non boiling	3.0 - 3.2	
$\epsilon \approx 0$, 10 μ chimneys, boiling	18.3 - 24.2	
$\epsilon \approx 0.38$, no chimneys, supercritical boiling	1.51 - 3.49	Ishikawa et al ⁽¹³⁴⁾
$\epsilon \approx 0.65$, no chimneys, supercritical boiling	1.3 - 2.6	Haller et al ⁽²²⁴⁾
$\epsilon \approx 0.7-0.77$, 5 μ chimneys, boiling	1.0 - 2.0	Macbeth et al ⁽¹⁴⁶⁾
$\epsilon \approx 0.7 - 0.9$, no chimneys, boiling	0.15 - 1.30	Rooth et al ⁽¹³⁵⁾
Corrosion products - BWR	0.69 - 0.84	Breden et al ⁽¹⁴⁷⁾
- LMFBR	0.07 - 0.29	Cohen and Efferding ⁽²²⁵⁾
Iron sulphide scale	1.25	Burrill ⁽¹⁵⁰⁾
Coke	0.29 - 0.86	Scarborough et al ⁽¹³⁰⁾
Gas oil deposits	0.28 - 1.06	Watkinson ⁽⁵⁾
Jet Fuel deposits	0.12	Watt et al ⁽¹⁷⁸⁾
Biofilms	0.52 - 0.71	Characklis et al ^(23,24,215)

$$k_{\text{eff}} = k_f \frac{1 + 2\chi - 2\psi(\chi-1)}{1 + 2\chi + \psi(\chi-1)} \quad 1.12$$

where χ is the ratio of the thermal conductivity of the fluid phase and the particulate phase, $\frac{k_f}{k_p}$ and ψ is the fractional volume of the particulate phase, $\frac{V_p}{V_f + V_p}$. For a magnetite deposit of 65% porosity in water, he computed k_{eff} to be 0.78 W/m K^(226,227). Cohen and Efferding⁽²²⁵⁾ found good agreement between the effective thermal conductivity data for crud deposits of 60-70% porosity and 50-75 μm thick in a model sodium heated steam generator and the effective thermal conductivity data computed from the Maxwell model. Haller et al⁽²²⁴⁾ estimated the effective thermal conductivity of magnetite deposits in once-through supercritical boilers using a parallel-series model:

$$k_{\text{eff}} = k_f \frac{\chi [1 - \psi (1 - \chi)]}{\alpha\chi + (1 - \gamma)[1 - \psi (1 - \chi)][\chi + \psi (1 - \chi)]} \quad 1.13$$

where α is the fraction of the total deposit thickness that can be represented by the parallel arrangement of particles and pores with respect to the direction of heat flow. For the following range of parameters:

Pressure	207-276 bar
Heat Flux	1.58×10^5 - 6.31×10^5 W/m ²
Fluid Temperature	282-393 °C
Porosity	0.65-0.75
Deposit mass/unit area of surface	0.064-0.306 kg/m ²

they correlated 110 data points with a standard deviation of 10.1%.

Measurements of the effective thermal conductivity of various porous deposits have been made

1. in-situ^(5,134,135,223-335)
2. ex-situ using a. the axial flow method^(138,146,220,222)
b. the radial flow method⁽²²²⁾

Further details on ex-situ thermal conductivity measurement methods can be found in an excellent monograph by Parrott and Stuckes⁽²²⁸⁾.

Boow and Goard⁽²²⁰⁾ measured the effective thermal conductivity as a function of temperature for ash deposits found in pulverised coal-fired boilers. As shown in Figure 1.10, they found the effective thermal

with temperature as a function of particle size while the effective thermal conductivity of sintered coal ashes increases rapidly and irreversibly with temperature.

Ivanov and Chudnovskaya⁽²²²⁾ investigated the variation of the effective thermal conductivity with temperature for each of the three layers which comprise the ash deposit in oil-fired boilers. As shown in Figure 1.11, they observed the effective thermal conductivity for the middle and bottom layers increase moderately with temperature while the effective thermal conductivity for the top layer increases sharply with temperature. The difference in the variation of the effective thermal conductivity with temperature for each layer was attributed to the difference in the porosity of each layer since that for pore sizes < 0.5 mm, the mode of heat transfer through the pores is by conduction whereas for pore sizes > 0.5 mm, the mode of heat transfer through the pores is by conduction, convection and radiation.

Haller et al⁽²²⁴⁾ and Ishikawa et al⁽¹³⁴⁾ measured the variation of the effective thermal conductivity with temperature for magnetite deposits found in supercritical boilers. As shown respectively in Figures 1.12 and 1.13, they found the effective thermal conductivity of the magnetite deposits decreases with increasing bulk fluid temperature.

1.6.4.3 Deposit porosity

Information on deposit porosity is sparse in the fouling literature. The deposit porosity is defined as the volume fraction of the pores in the deposit layer^(135,222). Ishikawa et al⁽¹³⁴⁾ reported two techniques for the measurement of the deposit porosity, namely:

1. the evaporation method
2. the electrolysis exfoliation method

For magnetite deposits in the range of 0.05 – 0.18 kg/m² and 0.22 – 0.43 kg/m², the porosities are respectively 0.70 – 0.77 ⁽¹⁴⁶⁾ and 0.65 – 0.75 ⁽²²⁴⁾. Ishikawa et al⁽¹³⁴⁾ measured the radial porosity distribution for magnetite deposits in supercritical boilers and found it to be strongly dependent on the tube wall radial temperature distribution. This dependency is shown in Figure 1.14.

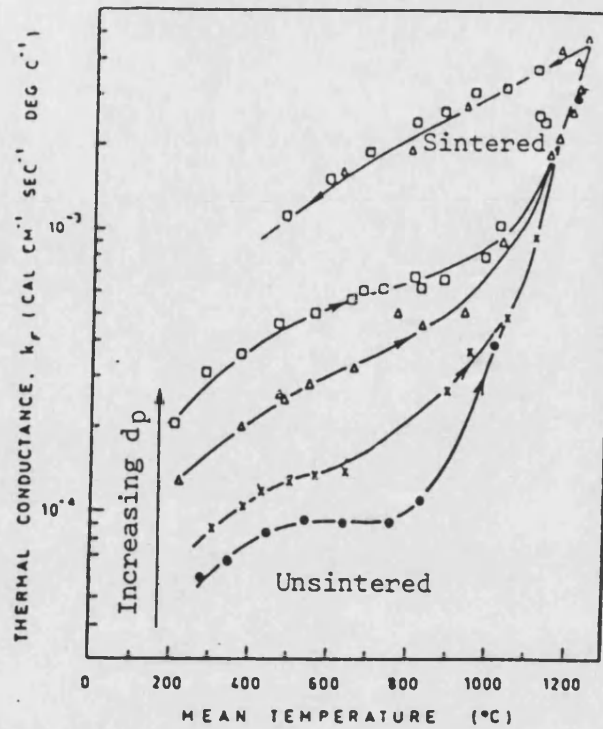


FIGURE 1.10 THE VARIATION OF EFFECTIVE THERMAL CONDUCTIVITY OF COAL ASH DEPOSITS WITH TEMPERATURE⁽²²⁰⁾

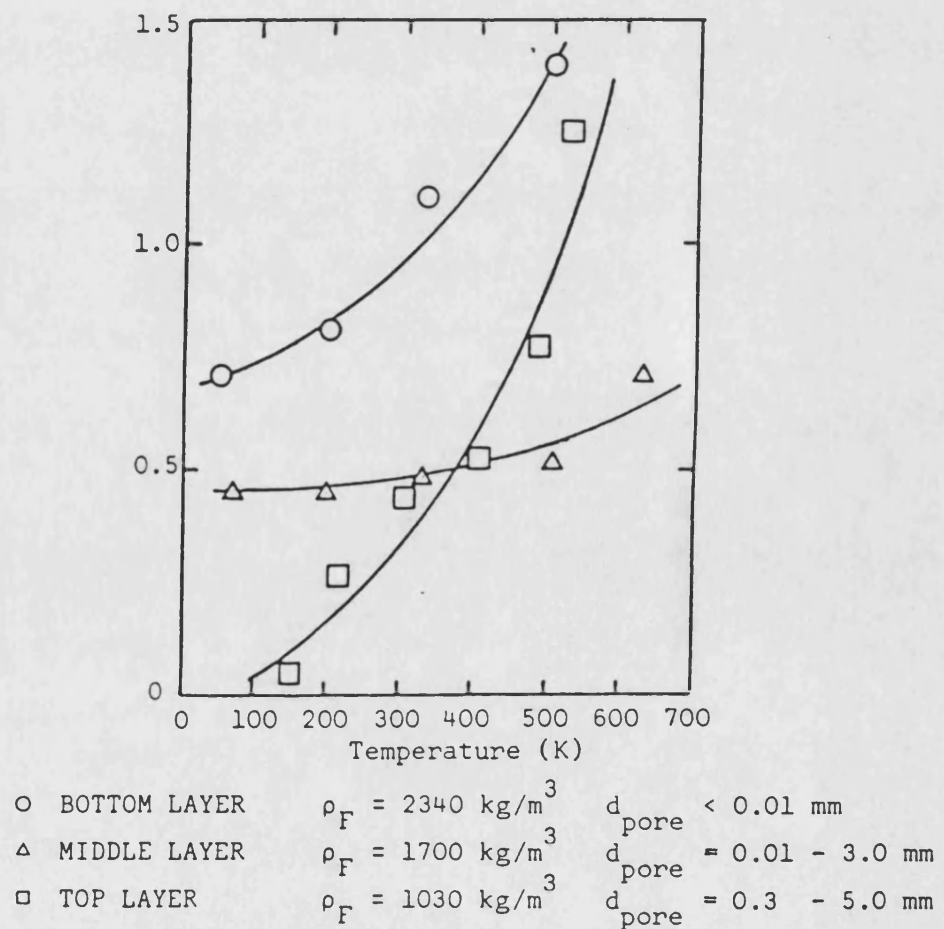


FIGURE 1.11 THE VARIATION OF EFFECTIVE THERMAL CONDUCTIVITY OF OIL ASH DEPOSIT WITH TEMPERATURE⁽²²²⁾

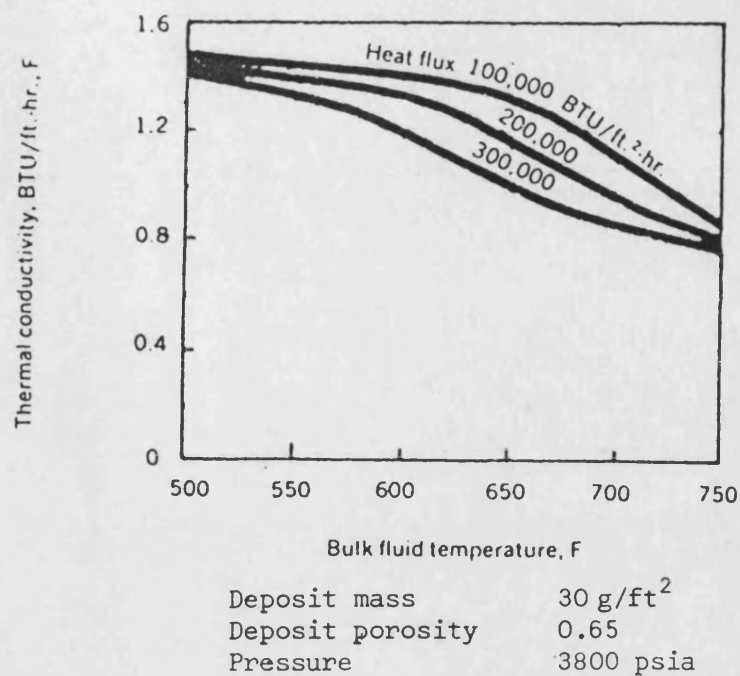


FIGURE 1.12 THE VARIATION OF EFFECTIVE THERMAL CONDUCTIVITY WITH TEMPERATURE FOR MAGNETITE DEPOSITS FOUND IN SUPERCRITICAL BOILERS⁽²²⁴⁾

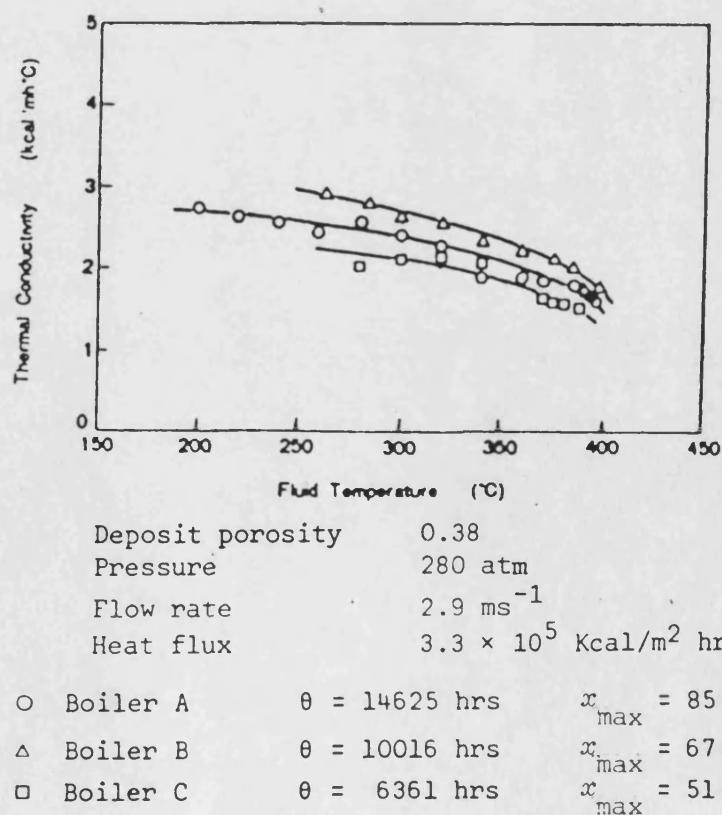


FIGURE 1.13 THE VARIATION OF EFFECTIVE THERMAL CONDUCTIVITY WITH TEMPERATURE FOR MAGNETITE DEPOSITS FOUND IN SUPERCRITICAL BOILERS⁽¹³⁴⁾

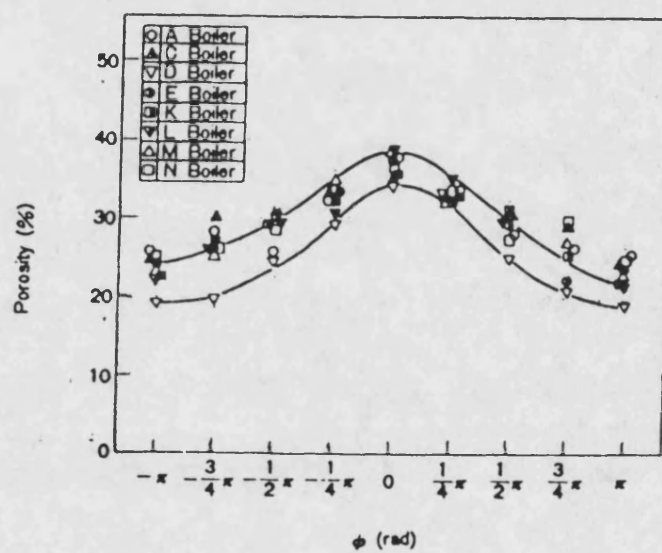


FIGURE 1.14 THE RADIAL POROSITY DISTRIBUTION FOR MAGNETITE DEPOSITS IN SUPERCRITICAL BOILERS⁽¹³⁴⁾.

1.6.4.4 Deposit roughness

Information on the deposit roughness is limited in the fouling literature. Order of magnitude measurements of the surface roughness have been made directly by means of

1. a profilometer^(127,229-235)
2. an optical microscope^(207,224,233-239)
3. a scanning electron microscope^(232,233,237,238)

Instead of measuring the surface roughness directly, several workers^(23-25,215,232,233,240) have carried out pressure drop measurements across the test section for various fluid flow rates in order to express the surface roughness in terms of an 'equivalent sand grain roughness'. This is either obtained either by comparing the computed friction factor-Reynolds number plot for the test section with the Moody⁽²⁴¹⁾ chart or from the empirical Colebrook-White⁽²⁴²⁾ equation:

$$\epsilon_s = \frac{d}{2} \left(10 \left[0.87 - \frac{1}{2\sqrt{f}} \right] - \frac{18.7}{\text{Re}\sqrt{f}} \right) \quad 1.14$$

where ϵ_s = equivalent sand grain roughness

d = tube diameter

f = friction factor

Re = Reynolds number

A collation of the surface roughness data for various fouling deposits is given in Table 1.11.

It has been long recognised by several workers that the surface roughness can have a significant effect on momentum, mass and heat transfer under turbulent flow conditions. The magnitude of this roughness effect is dependent on the ratio of roughness height to hydraulic diameter or to laminar sublayer thickness⁽²³³⁾. The increase or decrease in the transfer rate is mainly dependent on the nature of the surface roughness⁽²⁴³⁾, ie. the number per unit surface area, size, shape, orientation and distribution of the roughness elements.

In monitoring R_F as $\frac{1}{U} - \frac{1}{U_0}$, it is not uncommon to obtain deceptively low or even negative values of R_F during the initial stages of the fouling process^(25,35). This effect, clearly illustrated by the rippled silica fouling

TABLE 1.11 DEPOSIT ROUGHNESS DATA

	ROUGHNESS		θ	x (mm)	OPERATING CONDITIONS					ΔP (bar)	ΔL (m)	Re	f	MEASUREMENT TECHNIQUE	REFERENCE
	e (mm)	s (mm)			M (kg/m ²)	d_i (mm)	L (mm)	P (bar)	T (C)						
Fresh Water Scale	0.5 - 1.0	3.0 - 8.0	3 yrs	-	-	500	8000	-	-	Increase by 57%	178.1	-	-	Profilometer/Optical Microscope	Wiederhold ⁽²³⁴⁾
	0.5 - 4.0	4.0 - 16.0	18 yrs	1.5-12.0	-	1950	-	-	-	-	-	-	-	Optical Microscope	Geßner ⁽²³⁰⁾
Boiler Water Scale	0.025-0.04	0.20 - 0.35	-	-	-	-	-	-	384	-	-	-	-	Optical Microscope/Electon Microscope	Schoch et al ⁽²³⁶⁾
	0.02 - 0.04	0.18 - 0.30	12720 hrs	-	-	-	-	-	384	Increase by 70%	-	1.6×10^5	-	Optical Microscope/Electron Microscope	Richter et al ⁽²³⁸⁾
	0.045	0.35	-	-	-	-	-	-	-	-	-	-	-	Optical Microscope	Bott et al ⁽²³⁹⁾
	0.1	0.8	-	-	-	-	-	-	-	-	-	-	-	-	-
	0.0142	0.193	18 mths	-	0.013-0.051	15.75	0.65	268.6	-	-	-	-	-	-	-
	0.0165	0.201	18 mths	-	0.015-0.055	16.75	-	-	-	-	-	1.2×10^5 - 2.0×10^5	0.022 - 0.028	Optical Microscope	Haller et al ⁽²²⁴⁾
Sea Water Scale	1.08	4.73	5 yrs	5.0 - 7.0	-	6.0	-	-	-	0.365	2.692	1.39×10^5	0.0148	Optical Microscope	Bott et al ⁽²³⁹⁾
Geothermal Water Scale	0.123	0.81	2000 hrs	0.25-0.3	-	10.26	2	-	80	-	0.38	4.4×10^4	0.028	Optical Microscope	Bott et al ⁽²³⁹⁾
Jet Fuel Deposit	0.025-0.076		50 hrs	-	-	2.79	-	-	150	-	-	4.39×10^3	-	Optical Microscope	Smith ⁽²⁰⁷⁾
	< 0.025		> 50 hrs	-	-	2.79	-	-	150	-	-	4.39×10^3	-	-	-

data of Bott and Gudmundsson⁽²³⁹⁾ in Figure 1.15, results mainly from the increase in heat transfer coefficient, h due to the disturbance of the laminar sublayer by the deposit surface roughness⁽²⁰⁷⁾. This increase may override the increase in R_F to cause $\frac{1}{U}$ to be less than $\frac{1}{U_0}$. The negative value of R_F even at $\theta = 0$ arises from the violation of the assumption upon which $R_F = \frac{1}{U} - \frac{1}{U_0}$ is based^(25,35), that is there is no change in h due to fluid velocity changes accompanying the reduced flow area or surface roughness changes. However, the misleading result can be largely corrected for when the effect of roughness on h is included in the calculation of R_F . This is clearly shown in Figure 1.16 where Mayo-Abad⁽²⁴⁴⁾ recalculated the oil-gas and sand-water fouling data of Watkinson and Epstein^(100,101) which ignored the effect of roughness on h in the calculation of R_F .

Rankin and Adamson⁽¹²⁷⁾ reported the role of surface roughness on scale formation on various sea water evaporator surfaces. They observed an increase in the substrate surface roughness due to the rapid growth on the peaks followed by a decrease in this roughness due to the filling up the valleys. The process of 'roughness eradication' takes place rapidly when the constituents of a fouling fluid have dimensions comparable to the roughness dimensions^(20,59).

Bott⁽⁶²⁾ briefly outlined the effect of surface roughness on biofilm formation on various substrate surfaces. The presence of roughness elements on a surface can promote the retention of microbial particles by providing sites less affected by the flowing fluid for the establishment of microbial colonies. However, as the biofilm develops, the rough edges will be smoothed off, masking the topography of the substrate surface. Such a biofilm, however, is usually viscoelastic with a relatively high viscous modulus^(24,141), ie. flexible and capable of deformation or rippling under the influence of the flowing fluid. Clearly, this will affect biofilm stability and nutrient and product diffusion rates. Characklis et al^(23,24,215) reported the change in the equivalent sand grain roughness due to the biofilm development in a 1.27 cm I.D. tube at a given pressure drop. As shown in Figure 1.17, they observed that the equivalent sand grain roughness generally increases with increasing biofilm thickness.

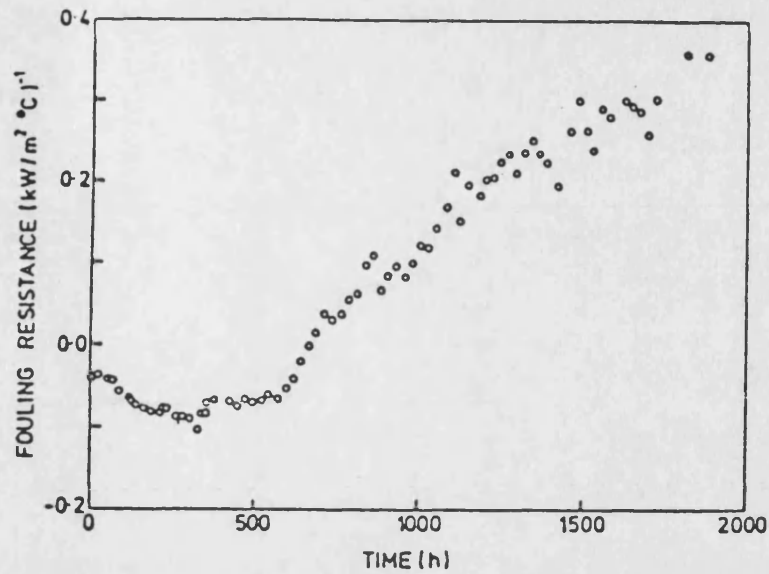


FIGURE 1.15 A TYPICAL FOULING CURVE FOR RIPPLED SILICA DEPOSITS⁽²³⁹⁾.

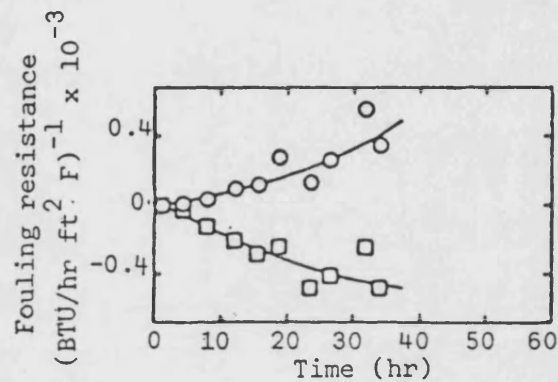


FIGURE 1.16 A COMPARISON BETWEEN WATKINSON-EPSTEIN'S DATA WHICH IGNORED THE EFFECT OF ROUGHNESS ON h IN THE CALCULATION OF R_F AND MAYO-ABAD'S DATA WHICH INCLUDED THE EFFECT OF ROUGHNESS ON h IN THE CALCULATION OF R_F ^(25,244).

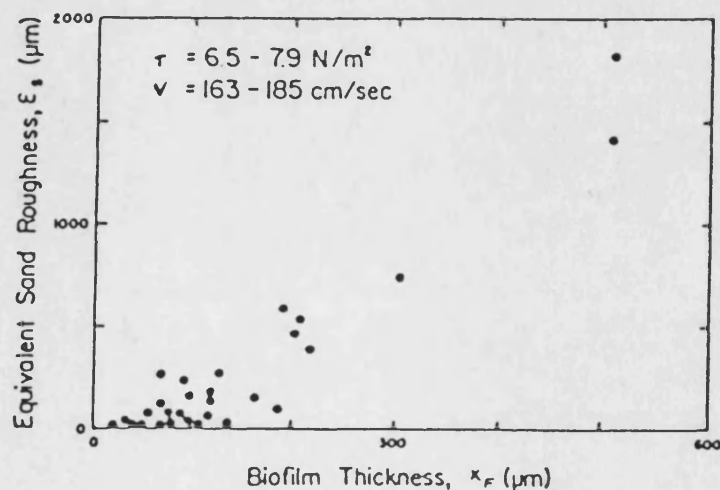


FIGURE 1.17 THE CHANGE IN THE EQUIVALENT SAND GRAIN ROUGHNESS DUE TO BIOFILM DEVELOPMENT IN A 1.27 cm TUBE AT A GIVEN PRESSURE DROP⁽²¹⁵⁾.

1.6.4.5 Deposit adhesion

Studies of deposit adhesion on heat transfer surfaces have been quite extensive in the fouling literature. The various bonding mechanisms between a fouling deposit and a heat transfer surface are summarised in Table 1.12^(245,246). Clearly, a prerequisite for deposit adhesion on heat transfer surfaces is that the attraction forces must be greater than the repulsion forces. Mathematical expressions of the adhesion force have been obtained for ideal particle/surface systems⁽²⁴⁵⁻²⁵⁰⁾. However, due to the complexity of the fouling process, the adhesion of a fouling deposit to a heat transfer surface can only at best be described conceptually. Taborek et al⁽²⁸⁻³¹⁾ defined the deposit bond resistance, R_b as the adhesive strength of the deposit per unit area at the plane of weakest adhesion. Based on limited observations, they speculated that:

1. R_b increases with the uniformity of the deposit structure.
2. R_b decreases with the deposit thickness due to the increase in the number of planes of weakness.
3. R_b is a function of the original surface characteristics if the deposit-surface adhesion is weaker than the deposit internal adhesion.

In mathematical terms,

$$R_b \propto \Psi \left[\frac{1}{x} \right]^a \quad 1.15$$

where Ψ is a function of the deposit structure and a is an empirical constant representing the probability of the presence of weak planes in the deposit layer.

Parkins^(251,252) defined the sticking probability, S as the probability that a particle sticks at the instant it reaches the surface. Epstein⁽³⁵⁾ listed three different approaches for the sticking probability:

1. Watkinson and Epstein⁽¹⁰¹⁾ defined S as the ratio of the adhesive forces (dependent on the surface temperature, T_s according to an Arrhenius-type relationship) binding a particle to the surface to the hydrodynamic forces (directly proportional to the average axial velocity in the laminar sublayer) on the particle at the instant it reaches the surface.

$$S \propto \frac{e^{-E/RT}}{v^2 f} \quad 1.16$$

TABLE 1.12 THE VARIOUS BONDING MECHANISMS BETWEEN A FOULING
DEPOSIT AND THE HEAT TRANSFER SURFACE^(245, 246)

1. LONG RANGE FORCES

Van der Waals forces
Electrostatic forces

2. SHORT RANGE FORCES

Chemical bonding i.e. ionic
 covalent
 hydrogen
Dipole interactions
Hydrophobic bonding

3. BRIDGING INTERACTIONS

Sintering
Liquid bridging
Polymer bridging

2. For the deposition of suspended particles on a surface, Beal⁽²⁵³⁻³⁵⁵⁾ defined the deposition coefficient, k_d as

$$k_d = \frac{1}{\frac{1}{k} + \frac{1}{Sv_s}} \quad 1.17$$

where k is the mass transfer coefficient and v_s is the velocity of the particles normal to the surface. He also defined X as

$$X = \frac{k_d|_{S=S}}{k_d|_{S=1}} \quad 1.18$$

where $k_d|_{S=S}$ is the measured value of k_d where S may be ≤ 1 and $k_d|_{S=1}$ is the computed value of k_d where $S=1$. Beal^(254,255) combined equations 1.17 and 1.18 to yield

$$S = \frac{kX}{k + v_s(1-X)} \quad 1.19$$

3. For the deposition of colloidal particles on a surface, several workers^(25,256-264) defined

$$\phi_d = \frac{c_b}{\frac{1}{k} + \frac{1}{\kappa}} \quad 1.20$$

where k is the mass transfer coefficient and κ is the first order rate constant for the process of overcoming the surface energy barrier between the particles and the surface. Epstein⁽³⁵⁾ compared equation 1.20 and equation 1.21

$$\phi_d = kc_bS \quad 1.21$$

to yield

$$S = \frac{\frac{1}{k}}{\frac{1}{k} + \frac{1}{\kappa}} \quad 1.22$$

Sufficient reliable data are still unavailable to establish S with any confidence by any of the three expressions⁽³⁵⁾. Using the deposition data experimentally obtained by Schmel⁽²⁶⁵⁻²⁶⁷⁾ for uranine-methylene blue particles suspended in air and by Watkinson⁽⁵⁾ for sand particles suspended in water, Beal^(254,255) correlated the sticking probability as a function of

dimensionless stopping distance, S^+ . This is shown respectively in Figures 1.18 and 1.19. He found the equation of the least squares line for Schmel's data to be

$$\begin{aligned} S &= 1 & S^+ &\leq 4.5 \\ S &= \left[\frac{4.5}{S^+} \right]^3 & S^+ &\geq 4.5 \end{aligned} \quad 1.23$$

and the equation of the least squares line for Watkinson's data to be

$$\begin{aligned} S &= 1 & S^+ &\leq 2.4 \\ S &= \left[\frac{2.4}{S^+} \right]^4 & S^+ &\geq 2.4 \end{aligned} \quad 1.24$$

Excellent reviews of the adhesion of microorganisms to surfaces have been presented by Corpe⁽¹⁸⁵⁾, Corpe and Winters⁽¹⁸⁶⁾, Lips and Jessup⁽²⁶⁸⁾, Marshall⁽²⁶⁹⁾, Rutter and Vincent⁽²⁷⁰⁾, Tadros⁽²⁷¹⁾, Rutter⁽²⁷²⁾, Norde⁽²⁷³⁾, Kent⁽⁶⁵⁾, Duddridge et al⁽²⁷⁴⁾ and Powell⁽²⁷⁵⁾. Factors that will determine whether or not an individual microorganism will become attached to a solid surface include⁽²⁷⁶⁾

1. the environment
2. the attachment mechanism

Two stages of microbial adhesion have been recognised⁽¹⁸⁷⁾: a reversible attachment stage followed by an irreversible attachment stage.

Microorganisms, especially bacteria, possess a net charge and because of their small size and low density, they may be considered as living colloid particles^(65,269). Some of their behaviour at surfaces may be explained by the classical DLVO colloid theory^(277,278). This states the total interaction force between a particle and a surface, F_T is the sum of the van der Waals attractive forces, F_a and the electrical double layer (electrostatic) repulsive forces, F_r . A typical total interaction force-separation distance plot is given in Figure 1.20. This clearly shows

1. a particle is able to approach the surface up to the point of 'secondary minimum' (typically 5-10 nm from the surface)
2. an energy barrier, representing a compression of the electrical double layers, must be overcome before a closer approach of the particle to the surface at the 'primary minimum' (typically 1 nm from the surface) can occur.

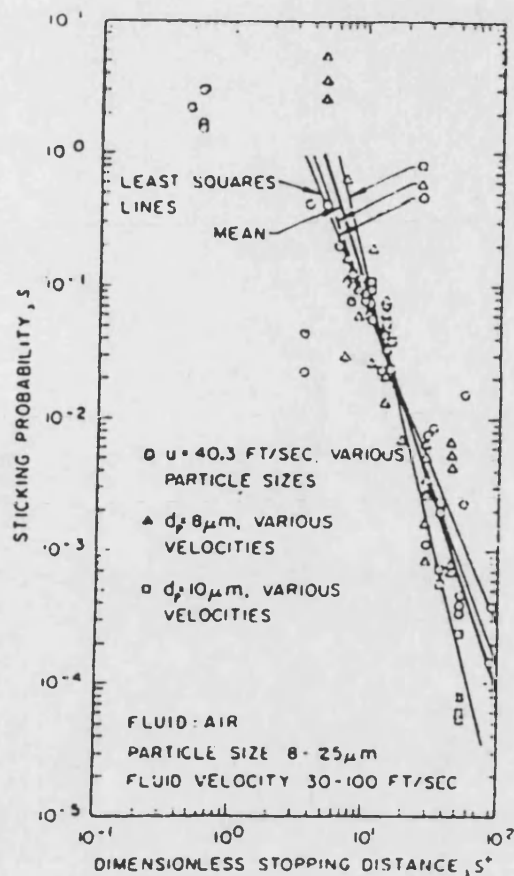


FIGURE 1.18 THE VARIATION OF STICKING PROBABILITY INFERRED FROM SEHMEL'S DATA WITH DIMENSIONLESS STOPPING DISTANCE (254,255)

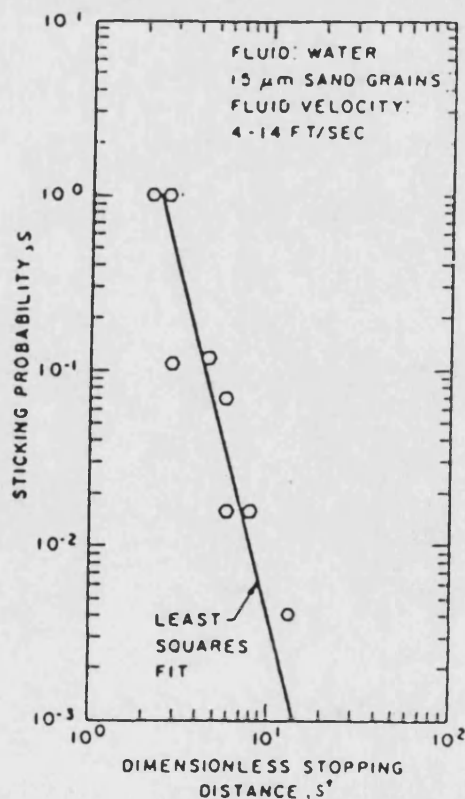


FIGURE 1.19 THE VARIATION OF STICKING PROBABILITY INFERRED FROM WATKINSON'S DATA WITH DIMENSIONLESS STOPPING DISTANCE (254,255)

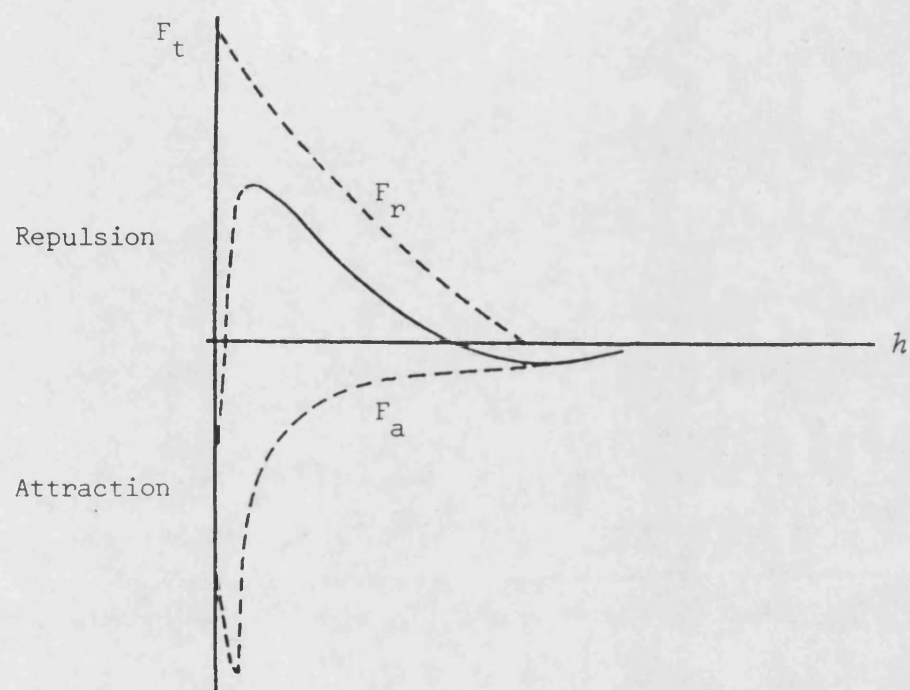


FIGURE 1.20 A TYPICAL TOTAL INTERACTION FORCE - SEPARATION DISTANCE PLOT.

It can be qualitatively concluded from the DLVO theory that

1. The reversible attachment stage refers to the weak physical attraction of microorganisms to a surface at the 'secondary minimum'.
2. The irreversible attachment stage refers to the firm adhesion of microorganisms to a surface at the 'primary minimum'. In order to overcome the energy barrier, some mechanism other than the physical interaction between the microorganism and the surface must be available to the microorganism. The bridging of the energy barrier is either due to
 - a. the microbial surface appendages such as flagella, pili & fimbriae, prosthecae
 - b. the extracellular polymeric slimes

The exact mechanism for polymer bridging is not yet fully understood^(65,269). Since various modes of attachment to surfaces are known, it might be assumed that a wide variety of bridging polymers is involved. The different forms that a bridging polymer can take up have been illustrated⁽²⁶⁹⁾.

It should be noted that the DLVO theory is insufficient to explain the microbial adhesion to surfaces quantitatively because^(65,270,271)

1. the microorganisms have surfaces over which different localised charges can occur
2. the microorganisms are complex and non-homogeneous
3. the microorganisms are irregular in shape
4. the microorganisms may change with time
5. the microorganisms may attach specifically with the surface

An alternative approach to describe the microbial adhesion to surfaces is that of surface 'wettability'^(279,280). As a result of the presence of a liquid film which wets both particle and substrate surface, a considerable capillary pressure develops; this provides a substantial adhesive force. The net surface free energy resulting from adhesion, ΔF is given by

$$\Delta F = (\gamma_{PS} - \gamma_{PL} - \gamma_{LS}) A_a \quad 1.25$$

where γ_{PS} = interfacial tension between the particle and the substrate surface

γ_{PL} = interfacial tension between the particle and the liquid

γ_{LS} = interfacial tension between the liquid and the substrate surface

A_a = area of adhesion

If ΔF is negative, adhesion takes place, whereas if ΔF is positive, adhesion is restrained. To evaluate ΔF , γ_{PS} , γ_{PL} and γ_{LS} must be determined. The most successful practical method is through contact angle measurements which can be used for establishing the critical surface tension of wetting of the substrate. In this method^(281,282), the surface tensions of a homologous series of liquids are plotted against the cosines of the corresponding contact angles of a drop of each liquid on a substrate. The resulting linear plot is then extrapolated to $\cos \phi = 1$ to obtain the critical surface tension for wetting, γ_C . If γ_C is high, adhesion occurs whereas if γ_C is low, adhesion is restrained. The minimum γ_C required for microbial adhesion to surfaces has been suggested to be 0.02-0.03 N/m²⁽²⁸³⁾.

Due to experimental difficulties, few attempts have only been made to measure deposit adhesion to heat transfer surfaces. Rankin and Adamson⁽¹²⁷⁾ used a balanced beam scrape adhesion tester to evaluate scale adhesion on various sea water evaporator surfaces. They expressed scale adhesion in terms of the beam loading required to break the scale from the surface. Visser^(249,250) briefly discussed the various techniques that have been used by several investigators to measure particle adhesion to surfaces. These techniques, listed in Table 1.13, mostly express particle adhesion in terms of the minimum force required to separate a particle from the surface. The various techniques that have been used by several investigators to measure microbial adhesion to surfaces was recently reviewed by Fowler and McKay⁽²⁸⁴⁾. A list of these techniques is given in Table 1.14.

Factors which influence deposit adhesion include

1. substrate surface roughness^(127,249,250,285)
2. 'particle' surface roughness^(249,250)
3. substrate material^(127,285)
4. substrate surface coating^(110,127,158,164,286)
5. temperature^(249,250)
6. surface shear stress^(274,287)

Rankin and Adamson⁽¹²⁷⁾ observed the adhesion of sea water scale to a 90-10 CuNi substrate to be a strong function of the substrate surface roughness. They found the beam loading required to break the scale from smooth surfaces (0.0508-0.1270 μm) was less than 5 kg whereas the scale did not break from

TABLE 1.13 MEASUREMENT OF PARTICLE ADHESION TO SURFACES^(249,250)

A. DIRECT MEASUREMENT METHODS

Centrifugal method

Vibration method

Pneumatic Adhesiometer

Gravity method

Electrostatic field method

Microbalance/Springbalance method

Pendulum method

Elastic deformation method

Jump method

B. INDIRECT MEASUREMENT METHODS

Aerodynamic/Hydrodynamic method

TABLE 1.14 MEASUREMENT OF MICROBIAL ADHESION TO SURFACES⁽²⁸⁴⁾

A. BIOFILM DETACHMENT METHODS

 'Adhesion number' tests

 'Critical force' tests

B. DYNAMIC MEASUREMENT METHODS

 Flocculation method

 Column penetration method

 Radial flow growth chamber

rough surfaces (1.016-1.270 μm) at maximum beam loading of 10 kg. Visser^(249,250) briefly discussed the influence of surface roughness on particle adhesion to surfaces. Experimental observations have shown that an increase in surface roughness leads to

1. a decrease in adhesion if substrate surface roughness dimensions < particle surface roughness dimensions
2. an increase in adhesion if substrate surface roughness dimensions = particle surface roughness dimensions

Masurovsky and Jordan⁽²⁸⁵⁾ investigated the effect of the substrate surface finish on the adhesion of milk to a stainless steel substrate. Table 1.15 lists their results for twelve different surface finishes. They found little difference between the finishes, the major divisions occurring between (i) ground and polished finishes, (ii) cold-rolled sheet finishes and (iii) vapour and sand blasted finishes.

Rankin and Adamson⁽¹²⁷⁾ found the adhesion of sea water scale to a metallic substrate to be a weak function of the substrate material. They observed the order of decreasing adhesion strength to be CuNi alloys and Monel; stainless steel; titanium. Masurovsky and Jordan⁽²⁸⁵⁾ studied extensively the adhesion of milk to various substrates used in the dairy industry. Their results revealed that the order of decreasing adhesion strength to be aluminium alloys; plastics; nickel alloys; stainless steel and copper alloys; glasses.

Rankin and Adamson⁽¹²⁷⁾ studied the effect of a thin polyfluorocarbon coating on a 90-10 CuNi substrate on seawater scale formation. They found the beam loading necessary to break the scale from uncoated surfaces to be five times that necessary to break the scale from coated surfaces. This was attributed to the large difference in the substrate surface energy between uncoated and coated surfaces. McAllister et al⁽¹¹⁰⁾ found the rate of river water scale formation to be identical for the following:

1. uncoated admiralty brass tube
2. admiralty brass tube coated with a baked-on coating of a silicone dispersion in a phenolic solution
3. admiralty brass tube coated with a baked-on coating of a phenolic solution

Palen and Westwater⁽¹⁵⁸⁾ studied the effect of a thin polyfluorocarbon coating on a flat aluminium heating strip on CaSO_4 scale formation under

TABLE 1.15 THE EFFECT OF SUBSTRATE SURFACE FINISH ON THE ADHESION
OF MILK TO A STAINLESS STEEL (TYPES 302 and 304)
SUBSTRATE⁽²⁸⁵⁾

TYPE OF SUBSTRATE SURFACE FINISH	SUBSTRATE SURFACE ROUGHNESS (μm)	NET COUNTS/MINUTE CAUSED BY BACTERIA REMAINING ON SURFACES AFTER CLEANING ^a	
No.8 (Mirror)	0.0127-0.0305	3 ^b	3 ^c
No.7 (High lustre polish)	0.0254-0.1270	3	3
Electropolish	0.1778-0.2286	3	4
240-grit finish	0.4318-0.5080	3	4
No.6 (Tampico brushed)	0.1270-0.2032	3	4
No.4 (Standard 'commercial')	0.2032-0.3048	4	4
No.3 (Rough polish)	0.2286-0.5334	4	5
Mill finish	0.2032-0.3302	4	10
2B (Bright cold rolled)	0.2032-0.5334	8	15
2D (Dull cold rolled)	0.127 -0.8128	11	19
Vapour blast	1.0668	12	19
Sand blast	3.556	21	26

a A measure of adhesion strength.

b Fouling of test substrates with an *Escherichia coli* suspension
in homogenised whole milk.

c Fouling of test substrates with a *Micrococcus pyrogenes* var. *aureus*
suspension in homogenised whole milk.

boiling conditions in a batch system. From their experimental observations, they found the surface coating deterred scale formation. This was also observed by Kos and Tao⁽²⁸⁶⁾ who compared the effect of uncoated and polyfluorocarbon coated tubes on CaSO_4 scale formation in an evaporator with a continuous feed system.

Taylor⁽¹⁶⁴⁾ studied the effect of various polymeric surface coatings on a titanium alloy substrate on jet fuel deposit formation. As shown in Figures 1.21 and 1.22, he found the surface coating did not eliminate the formation of deposits, but on the contrary, increased the amount of deposit formation at temperatures above 177°C . The relative rates of jet fuel deposit formation on five different coated titanium alloy substrates at 204°C and 0.21 bar is summarised in Table 1.16

Visser^(249,250) briefly discussed the influence of temperature on particle adhesion of surfaces. At elevated temperatures, particles may undergo sintering. This will cause an increase in the contact area thus an increase in adhesion.

Using the radial flow growth chamber, Duddridge et al^(274,287) investigated the effect of surface shear stress on the adhesion of *Pseudomonas Fluorescens* to a stainless steel substrate. Their experimental results given in Figure 1.23 revealed

1. the maximum level of attached bacteria occurred in regions of lowest surface shear stress, particularly less than $6-8 \text{ N/m}^2$.
2. the level of attached bacteria decreased markedly with increasing surface shear stress up to a 'critical' shear stress above which the decreasing rate of attachment levelled off, ie. between $6-8 \text{ N/m}^2$.
3. the attachment of bacteria was still noticeable at surface shear stresses up to 130 N/m^2 .

1.6.4.6 Deposit strength

Information on deposit strength is sparse in the fouling literature. The deposit strength, sometimes referred to as deposit toughness⁽⁷⁾, is used to characterise the structure of the fouling deposit. Factors which influence deposit strength include

1. the fluid velocity⁽²⁹⁾
2. the nature of the fouling deposit^(29,288)

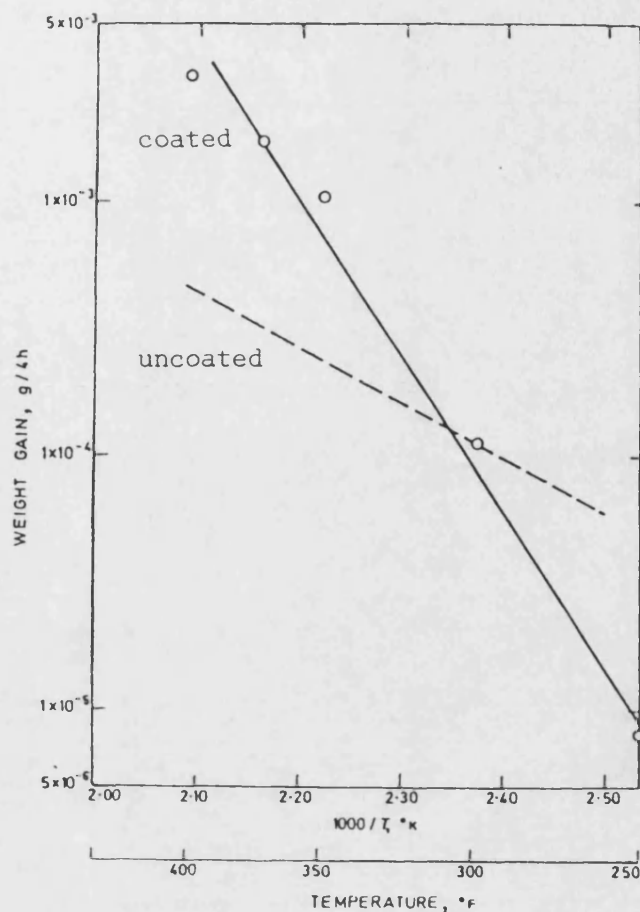


FIGURE 1.21 THE EFFECT OF A POLYIMIDE POLYMER COATING (COATING B) ON A TITANIUM ALLOY SUBSTRATE ON JET FUEL DEPOSIT FORMATION⁽¹⁶⁴⁾.

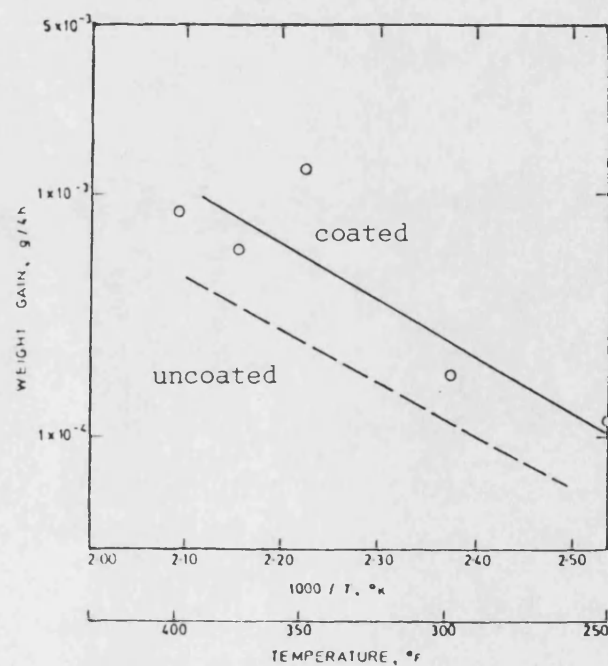
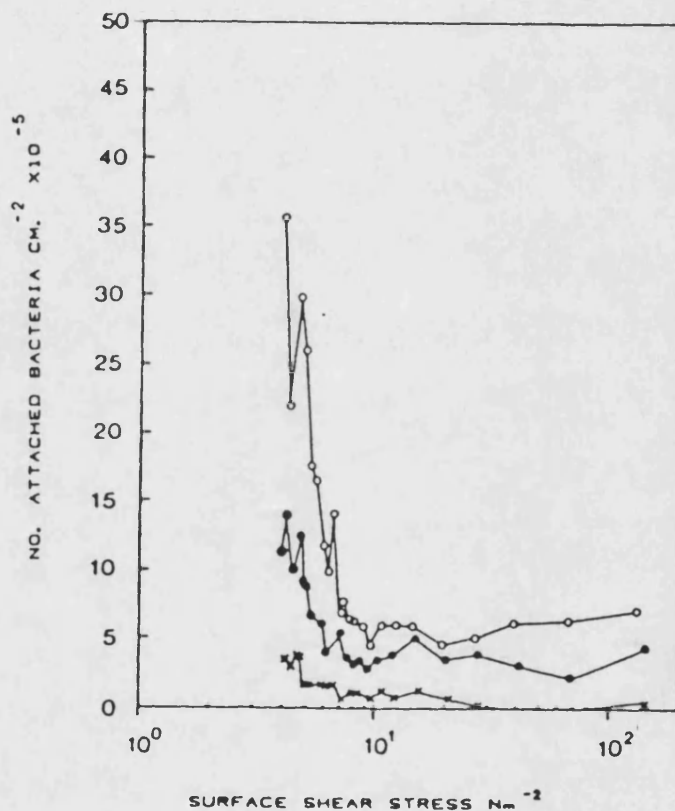


FIGURE 1.22 THE EFFECT OF A FLUOROCARBON POLYMER COATING (COATING E) ON A TITANIUM ALLOY SUBSTRATE ON JET FUEL DEPOSIT FORMATION⁽¹⁶⁴⁾.

TABLE 1.16 A SUMMARY OF THE EFFECT OF POLYMERIC SURFACE COATINGS
ON A TITANIUM ALLOY SUBSTRATE ON JET FUEL DEPOSIT
FORMATION⁽¹⁶⁴⁾

COATING	TYPE OF POLYMERIC SURFACE COATING	RELATIVE RATE OF DEPOSIT FORMATION ^a
A	Fluorocarbon	9.2
B	Polyimide	7.3
C	Silicone	2.7
D	Fluorosilicone	13.0
E	Fluorocarbon	1.9

^a Rate of deposit formation with coated Ti alloy substrate
relative to rate of deposit formation with uncoated Ti
alloy substrate at 204°C and 0.21 bar.



KEY

- x 18 hr exposure
- o 72 hr exposure
- 90 hr exposure

FIGURE 1.23 THE EFFECT OF SURFACE SHEAR STRESS ON THE ATTACHMENT OF *PSEUDOMONAS FLUORESCENS* TO STAINLESS STEEL (TYPE AISI 316) USING A SUSPENDED CELL CONCENTRATION OF $\approx 5 \times 10^7$ cells ml⁻¹ (274,287)

3. the addition of antifoulants⁽⁷⁾
4. the aging of the fouling deposit⁽¹⁵⁻¹⁷⁾

Taborek et al⁽²⁹⁾ observed the strength of cooling water deposits increases with increasing fluid velocity. This was attributed to the increase in the rate of removal of the particulate top layer from the crystalline bottom layer with increasing fluid velocity. They also noted the strength of cooling water deposits is a function of deposit purity. Using preliminary data, Morse and Knudsen⁽²⁸⁸⁾ plotted the time constant for various fouling transients as a function of non-CaCO₃ components of the cooling water deposit. As shown in Figure 1.24, they found the time constant approaches infinity as the scale composition becomes pure CaCO₃. In other words, since the time constant, θ_c is related to scale strength, Ψ according to the model proposed by Taborek et al⁽²⁹⁻³¹⁾ for the Kern-Seaton removal term:

$$\theta_c = \frac{1}{\beta} = \frac{\Psi}{c k_F \tau} \quad 1.26$$

the less pure scales are substantially weaker than the scale which is essentially pure CaCO₃. Knudsen⁽⁷⁾ reported that changes in the structure of cooling water deposits due to the addition of antifoulants may lead to a reduction in the scale strength. Epstein⁽¹⁵⁻¹⁷⁾ briefly discussed the aging of the fouling deposits on heat transfer surfaces. The aging processes may involve changes in the structure of the fouling deposit. Examples of such changes include

1. dehydration
2. chemical degradation eg. of hydrocarbon gums to coke
3. the slow poisoning of microorganisms by corrosion cations released from the heat transfer surface.

These changes may cause either an increase or decrease in deposit strength with time.

1.6.5 Deposit chemical analysis

Although details of deposit chemical analysis are widespread in the fouling literature, there is no information regarding the standard procedure for chemical analysis of fouling deposits. Most fouling deposits can be divided into one of three classes, namely⁽²⁸⁹⁾

1. inorganics

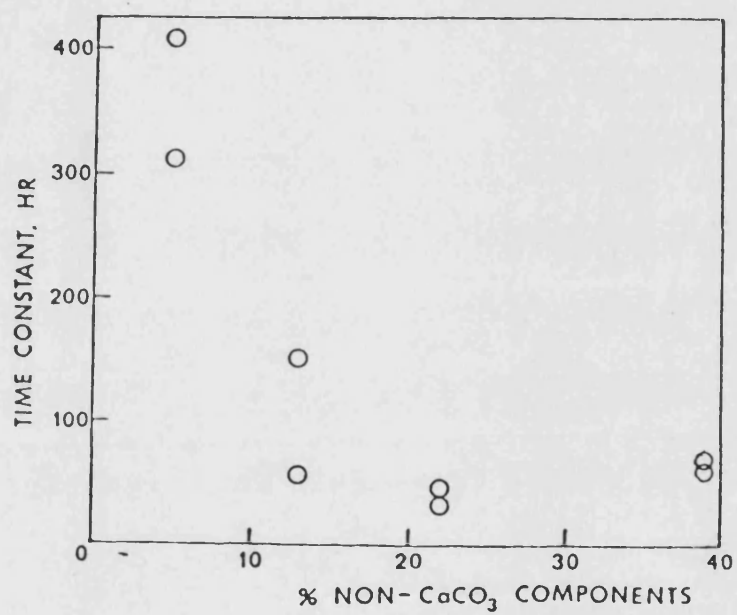


FIGURE 1.24 THE VARIATION OF THE TIME CONSTANT WITH THE NON-CaCO₃ COMPONENTS OF THE COOLING WATER DEPOSIT⁽²⁸⁸⁾.

2. organics

3. inorganics and organics

Basically, the deposit chemical analysis consist of three parts:

A. the determination of the relative amounts of inorganics, organics and water

The relative amount of water to inorganics and organics is estimated from the weight loss on drying the fouling deposit to a constant weight at 105°C (6,24,63,65,103,105,136,290-292). The loss at 105°C can consist of bound water, ie. free water, water in the microorganisms, some water of crystallisation⁽¹⁰⁵⁾.

The relative amount of organics to inorganics is estimated from the weight loss on heating the fouling deposit at 800°C or above (5,24,63,65,91,105,111,114,122,124-126,128,136,182,201,207,290,291,293-298).

The loss at 800°C or above can consist of organics, microorganisms, carbonate most water of crystallisation and if any, bound water^(105,291).

B. the inorganic analysis

There are essentially two parts to the inorganic analysis of fouling deposits, namely

1. the determination of the inorganic constituents in fouling deposits by

(5,6,24,45,49-52,63,65,91,100,103,105,108,110,111,
114,117,122,124-127,134,135,136,138,146,147,152,
157,160,165,170,171,174,175,177,182,201,207,216,

a. Gravimetric analysis 217,222,239,251,290-295,297-301)

b. X-ray analysis

Electron microprobe analysis (104,105,114,147,183,193,203,238,251,302)

X-ray fluorescence analysis (52,103,104,133,135,195,196,207,225)

X-ray photoelectron spectroscopy⁽¹¹²⁾

c. Atomic absorption spectroscopy^(127,301)

d. Emission spectroscopy^(114,128,159,225)

e. Flame spectroscopy⁽³⁰³⁾

2. the identification of the crystalline species in the fouling deposit

(20,52,59,103,104,111,114,126,127,135,145,
147,148,151,153,154,192,194,195,197,202,205,

by X-ray diffraction analysis 207,217,225,238,239,304,305)

C. the organic analysis

The organic analysis of fouling deposits may involve

1. the identification of the organic constituents in fouling deposits by
 - a. Infra red spectroscopy^(103,125,160,165,193,198,204,283,301,306)
 - b. NMR spectroscopy⁽¹²⁵⁾
 - c. Ultra violet spectroscopy⁽¹²⁵⁾
2. the determination of the biofilm constituent in fouling deposit in terms of
 - a. Chemical oxygen demand^(106,139,179,180)
 - b. Total organic matter^(106,307)
 - c. Total organic carbon^(133,139,179,180)
 - d. Total organic nitrogen^(106,307)
 - e. Total organic acids^(106,307)
 - f. Total polysaccharide^(106,179,180,307)
 - g. Total protein^(106,179,180,301)
 - h. Total nucleic acids^(179,180)

Chemical analyses of typical industrial fouling deposits are summarised in Table 1.17

1.6.6 Deposit microbiological analysis

The microbiological analysis of fouling deposits is essentially the identification and enumeration of organisms in fouling deposits by

1. Phase contrast microscopy⁽¹⁰⁶⁾
2. Fluorescence microscopy^(106,189,190)
3. Scanning electron microscopy^(106,189,190)
4. Transmission electron microscopy⁽¹⁰⁶⁾
5. Culture techniques^(106,189,203,285,307)

To date, there is only one paper reported in the fouling literature which gives the microbiological analysis of a fouling deposit. This paper is by Oberhofer and Fulks⁽¹⁰⁵⁾ who carried out a microbiological analysis on a typical cooling water deposit. Their results are summarised in Table 1.18.

TABLE 1.17 CHEMICAL ANALYSIS OF TYPICAL INDUSTRIAL FOULING DEPOSITS

[illegible]

TABLE 1.18 MICROBIOLOGICAL ANALYSIS OF A TYPICAL COOLING WATER DEPOSIT⁽¹⁰⁵⁾

Organism	Number of Organisms per gram of deposit
----------	---

Aerobic Slime Forming Bacteria

<i>Flavobacterium</i>	1,000,000
<i>Pseudomonas</i>	1,000,000
<i>B. subtilis</i>	500
<i>B. megatherium</i>	4,000
<i>B. mycoides</i>	300

Anaerobic Corrosive Bacteria

<i>Desulfovibrio</i>	5,000
<i>Clostridia</i>	3,000

Total Bacteria Count	40,000,000
----------------------	------------

Molds

<i>Fusarium</i>	2,000
<i>Aspergillus</i>	2,000

Blue Green Algae

<i>Oscillatoria</i>	Few
---------------------	-----

Green Algae

<i>Chlorococcus</i>	Moderate
<i>Scenedesmus</i>	Few
<i>Cyclotella</i>	Few

Diatoms

<i>Navicula</i>	Few
<i>Pinularia</i>	Many
<i>Synerda</i>	Few
<i>Melosira</i>	Few

2. THE ELECTROCHEMICAL METHOD

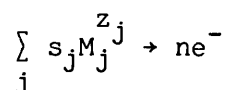
The electrochemical method for monitoring fouling utilises the limiting diffusion current technique (LDCT) for measuring mass transfer rates and, by analogy, heat and momentum transfer rates between a fluid and a solid surface. Excellent reviews on LDCT have been presented by Levich^(308,309) in 1942, 1944 and 1962, Agar⁽³¹⁰⁾ in 1947, Tobias et al⁽³¹¹⁾ in 1952, Ibl⁽³¹²⁾ in 1963, Newman⁽³¹³⁻³¹⁵⁾ in 1967, 1968 and 1973, Arvia and Marchiano⁽³¹⁶⁾, Mizushina⁽³¹⁷⁾ and Ravoo^(318,319) in 1971, Selman^(320,321) in 1971 and 1981, Landau^(322,323) in 1976 and 1981, Pickett⁽³²⁴⁾, Shemilt⁽³²⁵⁾ and Wragg⁽³²⁶⁾ in 1977, Selman and Tobias⁽³²⁷⁾ in 1978, Fahidy and Mohanta⁽³²⁸⁾ in 1980 and Poulson⁽³²⁹⁾ in 1982.

2.1 The limiting diffusion current technique

2.1.1 Fundamentals

In any electrochemical system, there are three consecutive steps⁽³⁰⁹⁾:

1. the transfer of the reactants from the bulk of the solution to the surface of the electrode.
2. the electrochemical reaction at the electrode



where s_j is the number of molecules or ions of species j participating in the transfer of n electrons to and from the electrode.

3. the transfer of the products from the surface of the electrode to the bulk of the solution or the deposition of the products on the surface of the electrode.

The rate of the electrochemical reaction is balanced, and sometimes limited, by the rate of mass transfer^(318,319).

The limiting diffusion current technique (LDCT) is based on driving an electrochemical reaction to its maximum possible rate when it becomes limited by mass transfer^(322,323). The basic features of LDCT can be highlighted by considering an electrochemical reaction at a cathode:

As the potential of the cathode is increased, the positive ions migrate from the bulk of the solution to the surface of the cathode where they are

consumed by the electrochemical reaction. Since the current is not exclusively carried by the discharging species, the ions are consumed much faster than they are supplied by migration. This causes a thin layer depleted of the reacting species to develop near the cathode. This layer, shown schematically in Figure 2.1, is known as the diffusion or mass transfer boundary layer. The balance of the reacting species must be supplied across this layer to the cathode by diffusion down the concentration gradient.

The movement of ionic species to the surface of the electrode is described by the ionic flux equation:

$$N_j = - D_j \nabla c_j - z_j u_j F c_j \nabla \Phi + c_j v \quad 2.1$$

where N_j = flux of species j

D_j = diffusivity of species j

c_j = concentration of species j

z_j = charge number of species j

u_j = mobility of species j

F = Faraday's constant

Φ = electrostatic potential

v = fluid velocity

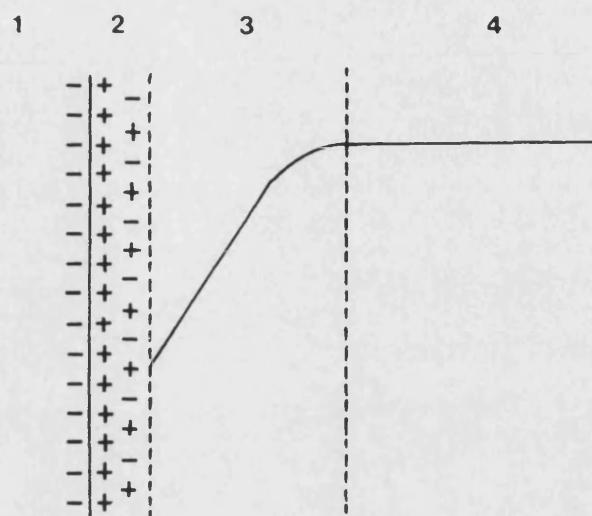
The three terms on the RHS of equation 2.1 represent, respectively, the contributions of

1. diffusion due to the concentration gradient
2. migration due to the electric field
3. convection due to the bulk motion of the fluid

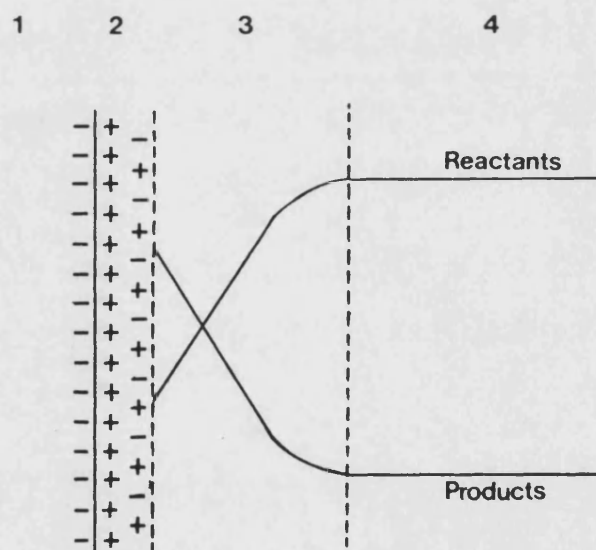
Since the current in the electrolytic solution is due to the movement of the ionic species, the current density, i is given by

$$i = F \sum_j z_j N_j \quad 2.2$$

In most electrochemical systems, the migration term in equation 2.1 is eliminated by the addition of a large excess of supporting (or indifferent) electrolyte to the electrolytic solution. If such electrolytes, which do not participate in the electrochemical reaction, exist in the electrolytic solution in relatively high concentrations and have high conductivity compared with the reacting species, there should be no sharp potential gradient near the electrode. Thus, $\nabla \Phi$ may be assumed to be zero rendering the



a. Deposition reaction



b. Redox reaction

KEY

- 1. ELECTRODE
- 2. DOUBLE LAYER
- 3. MASS TRANSFER BOUNDARY LAYER
- 4. BULK

FIGURE 2.1

TYPICAL CONCENTRATION PROFILES NEAR THE ELECTRODE-ELECTROLYTIC SOLUTION INTERFACE .

migration term negligible. Furthermore, the convection term in equation 2.1 is also rendered zero since in redox systems, the convection term vanishes due to no net convective flow to the electrode while in non-redox systems, the convection term is usually negligible due to the very small net convective flow to the electrode.

Consequently, the flux at the electrode is solely controlled by diffusion. Assuming the transfer of ions is unidirectional in the y-direction perpendicular to the surface of the electrode, the flux at the electrode is now expressed as

$$N_j = \frac{I}{z_j F A} = - D_j \left. \frac{\partial c_j}{\partial y} \right|_{y=0} \quad 2.3$$

where I = current

A = area of electrode surface

Since electrochemical reactions involving one species are only considered, the subscript j will henceforth be omitted. Thus, equation 2.3 becomes

$$N = \frac{I}{z F A} = - D \left. \frac{\partial c}{\partial y} \right|_{y=0} \quad 2.4$$

In order to determine the concentration gradient in the vicinity of the electrode, it is necessary to use a mass transfer boundary layer model in which

1. the mass transfer resistance is assumed to be localised in a quasi-stagnant layer adjacent to the double layer.
2. the double layer is assumed to be negligibly thin compared with the thickness of the mass transfer boundary layer.

A summary of the models are proposed by various workers is given in Figure 2.2.

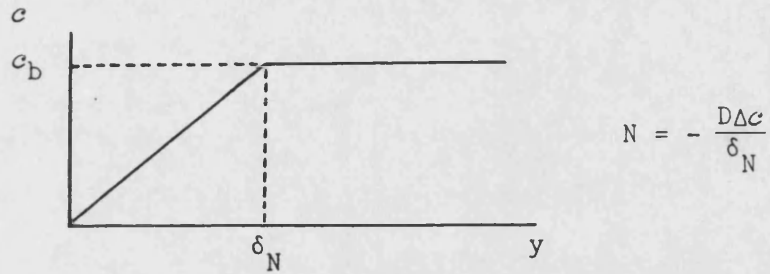
However, in most electrochemical systems, only the concentration difference between the bulk solution and the electrode surface is known. In such cases, it is more convenient to express the flux of the electrode in terms of a mass transfer coefficient.

$$N = \frac{I}{z F A} = k(c_b - c_s) \quad 2.5$$

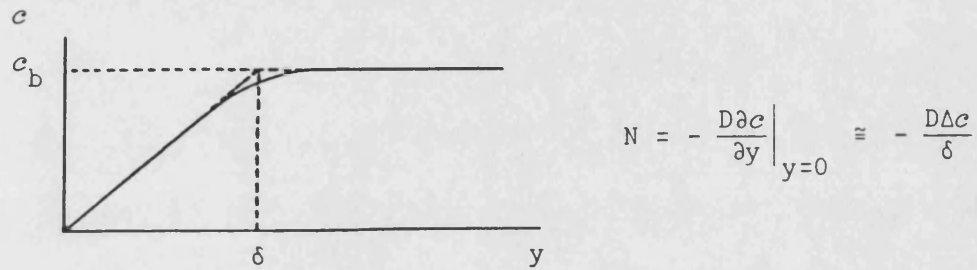
where k = mass transfer coefficient

FIGURE 2.2 A SUMMARY OF MASS TRANSFER BOUNDARY LAYER MODELS⁽³¹⁸⁾

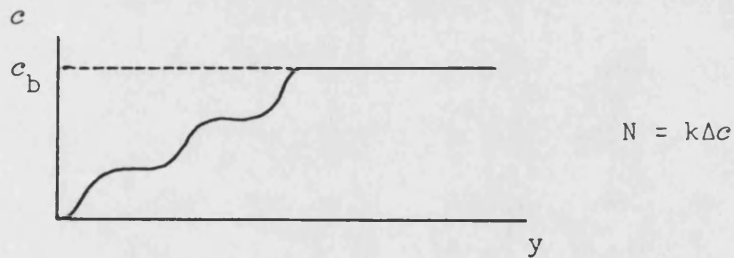
(a) NERNST STAGNANT DIFFUSION LAYER MODEL



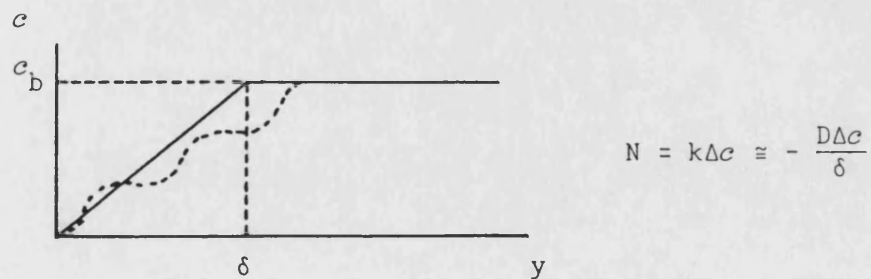
(b) CONCENTRATION BOUNDARY LAYER MODEL



(c) PHENOMENOLOGICAL MODEL



(d) EQUIVALENT BOUNDARY LAYER MODEL



c_b = bulk ion concentration

c_s = surface ion concentration

As the potential of the cathode is further increased, the ions are consumed faster by the electrochemical reaction causing the surface ion concentration to become lower and eventually zero. Correspondingly, the current increases exponentially to an asymptote of a constant value, ie. a limiting current. This is clearly shown in Figure 2.3 which illustrates a typical current-potential plot for a mass transfer controlled electrochemical system. At the limiting current, the electrochemical reaction proceeds at its maximum possible rate. Since the surface ion concentration is zero at the limiting current, equation 2.5 reduces to

$$N = \frac{I_L}{zFA} = k c_b \quad 2.6$$

where I_L = limiting current

A further increase of the potential over the limiting current plateau causes a steep increase in current due to the discharge by a secondary reaction such as hydrogen evolution on the cathode.

Since mass transfer coefficients can be readily and accurately calculated from the experimentally obtained limiting current plateau, LDCT provides a very convenient, easy to use and accurate method for mass transfer studies. Furthermore, the similarity with non-electrolytic mass and heat transfer make LDCT particularly apt for the investigation of analogous transfer processes. In view of this generality, it is convenient to introduce dimensionless variables for the correlation of the transfer characteristics.

The mass transfer coefficient obtained from equation 2.6 is usually expressed in terms of the Sherwood number, Sh:

$$Sh = \frac{k l}{D} = \frac{I_L l}{z F A D c_b} \quad 2.7$$

where l = characteristic length

The mass transfer correlation for systems with forced convection is of the form

$$Sh = f_1(Re, Sc) \quad 2.8$$

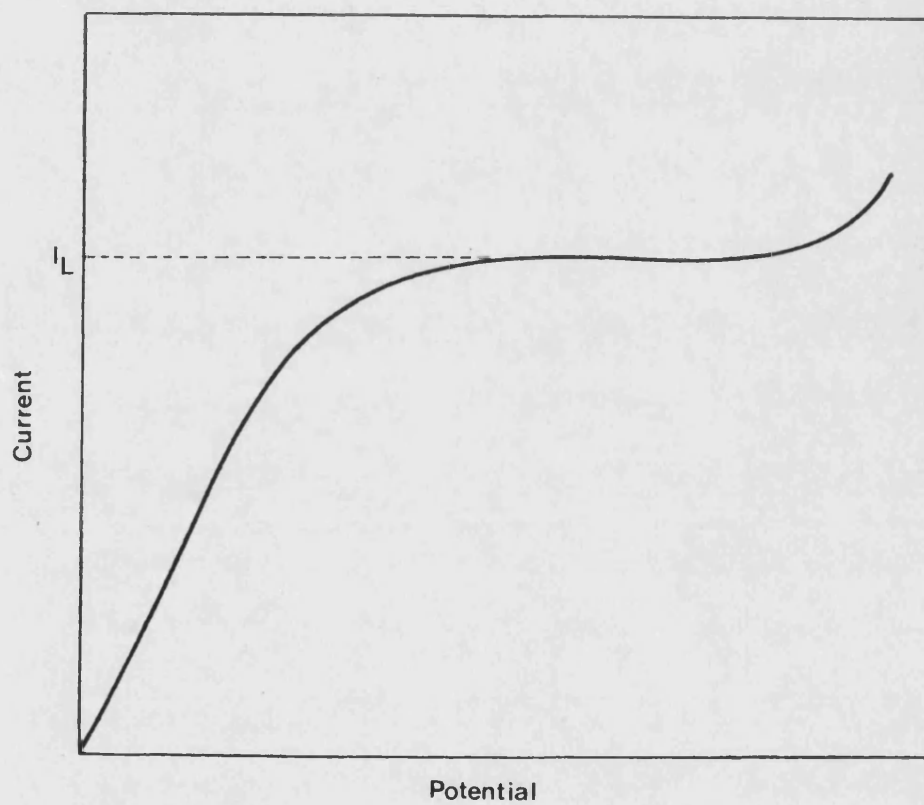


FIGURE 2.3 A TYPICAL CURRENT-POTENTIAL PLOT FOR A MASS TRANSFER CONTROLLED ELECTROCHEMICAL SYSTEM .

whereas the mass transfer correlation for systems with free convection is of the form

$$Sh = f_2(Gr_m, Sc) \quad 2.9$$

$$\text{where } Re = \frac{vl}{\nu} = \text{Reynolds number} \quad 2.10$$

$$Sc = \frac{\nu}{D} = \text{Schmidt number} \quad 2.11$$

$$Gr_m = \frac{gl^3}{\nu^2} \left[\frac{\Delta\rho}{\rho} \right]_m = \text{Grashof number for mass transfer} \quad 2.12$$

The corresponding heat transfer correlations are given by

$$Nu = f_1^*(Re, Pr) \quad 2.13$$

$$Nu = f_2^*(Gr, Pr) \quad 2.14$$

$$\text{where } Nu = \frac{hl}{k} = \text{Nusselt number} \quad 2.15$$

$$Pr = \frac{\mu c_p}{k} = \text{Prandtl number} \quad 2.16$$

$$Gr_h = \frac{gl^3}{\nu^2} \left[\frac{\Delta\rho}{\rho} \right]_h = \text{Grashof number for heat transfer} \quad 2.17$$

It is normal practice to assume a direct analogy between mass and heat transfer. However, some authors, in particular Ravoo⁽³¹⁸⁾ and Berger and Ziai⁽³³⁰⁾ have indicated the analogy should be treated with caution since for electrochemical systems, Sc usually is of the order 1000 to 10000 while for heat transfer systems, Pr is usually of the order 1 to 10.

2.1.2 Model electrochemical reactions

The electrochemical system to be employed for LDCT must satisfy the following requirements^(319,327):

1. Kinetically, the electrochemical reaction should be fast and unaccompanied by side reactions over a range of at least a few hundred millivolts in order to obtain a long and well-defined limiting current plateau.
2. During the course of measurement, the surface area of the working electrode should not become ill-defined by passivation or formation of rough deposits.

3. The experimental rig and the electrode material should be inert to the electrolytic solution.
4. The electrolytic solution should be chemically stable.
5. The physical properties of the electrolytic solution such as density, viscosity and diffusivity must be known as a function of composition and temperature.

Selman et al^(320,321,327) listed the electrochemical reactions most often used for LDCT. This collation is reproduced in Table 2.1. Of the electrochemical systems used, two in particular have attained wide popularity:

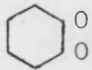
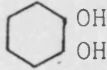
1. The cathodic deposition of copper by the reduction of Cu^{2+} ions.

The electrolytic solution is usually aqueous CuSO_4 heavily swamped with H_2SO_4 . The cathode material is usually copper. If the anode is also copper so that the reverse reaction takes place, the bulk Cu^{2+} concentration remains constant. The main disadvantage of this deposition reaction is that the electrode surface may, in some circumstances, become roughened to an intolerable degree. However, the advantages of the deposition reaction include the high solubility of CuSO_4 at room temperature and the large density difference between the bulk and the surface.

2. The cathodic reduction of ferricyanide ions to ferrocyanide ions at an inert electrode

The electrolytic solution is usually an equimolar mixture of potassium ferricyanide and potassium ferrocyanide in a supporting electrolyte of either KOH or NaOH. The electrode material is usually nickel or platinum. As the oxidation of ferrocyanide at the anode compensates for the reduction of ferricyanide at the cathode, the bulk concentration remains constant. Due to the sensitivity of nickel or platinum electrodes to deactivation through poisoning by free cyanide ions or by contaminants, the use of freshly prepared electrolytic solutions and carefully prepared electrodes is advisable. To maintain the stability of the electrolytic solution, the exclusion of light and dissolved gases is necessary. The main advantages of this redox reaction include the long and well-defined limiting current plateau and the unchanging nature of the electrode surface topography.

TABLE 2.1 MODEL REACTIONS USED IN ELECTROCHEMICAL MASS TRANSFER STUDIES^(320, 321, 327)

	Electrode material	Supporting electrolyte
Cathodic		
1. $\text{Cd}^{2+} + 2e \rightarrow \text{Cd}$	Cd(Hg)	None
2. $\text{Cu}^{2+} + 2e \rightarrow \text{Cu}$	Cu	H_2SO_4 None
3. $\text{Fe}(\text{CN})_6^{3-} + e \rightarrow \text{Fe}(\text{CN})_6^{4-}$	Ni, Pt	NaOH KOH
4. $\text{O}_2 + 2\text{H}_2\text{O} + 4e \rightarrow 4\text{OH}^-$	Pt, Ag	NaOH NaCl
5. $\text{I}_3^- + 2e \rightarrow 3\text{I}^-$	Pt	KI
6.  $+ 2\text{H}^+ + 2e \rightarrow$ 	Ag	Phosphate buffer
7. $\text{Fe}^{3+} + e \rightarrow \text{Fe}^{2+}$	Pt, Cu	H_2SO_4
8. $\text{Ag}^+ + e \rightarrow \text{Ag}$	Ag	HClO_4
9. $\text{Ce}^{4+} + e \rightarrow \text{Ce}^{3+}$	Pt, Cu	H_2SO_4
Anodic		
10. $\text{CuCl}_4^{3-} \rightarrow \text{CuCl}_4^{2-} + e$	Pt	CaCl_2
11. $\text{Fe}(\text{CN})_6^{4-} \rightarrow \text{Fe}(\text{CN})_6^{3-} + e$	Ni, Pt	NaOH KOH
12. $\text{Ce}^{3+} \rightarrow \text{Ce}^{4+} + e$	Pt	H_2SO_4

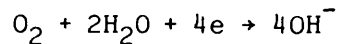
2.1.3 Applications

With suitable electrochemical reactions under carefully controlled conditions, many complex transfer problems can be effectively investigated using LDCT. Numerous cases of successful application have been reported in the literature^(312,317,320,324,326-329,331).

2.2 Previous work

To date, two papers on the use of the electrochemical method for monitoring fouling^(26,27) have been reported in the literature. The method was used in both papers for the investigation of the growth of calcereous deposits on cathodic steel surfaces in sea water. The mechanism of calcereous deposit formation can be described in two stages:

1. the reduction of dissolved oxygen in sea water at the cathode



2. the reaction between the hydroxyl ion and the metallic ions in sea water.

Galloway⁽²⁶⁾ monitored the growth of calcereous deposits on a spherical steel cathode in a batch sea water system by obtaining a series of current - potential curves as a function of time. His results, given typically in Figure 2.4, revealed that the limiting current decreases as the calcereous deposit accumulates with time. A typical limiting current current decay curve is shown in Figure 2.5. He developed a model that would predict the shape of the limiting current decay curves as a function of time, fluid and deposit properties and hydrodynamic variables.

Since the transport of oxygen from the bulk solution to the cathode surface involves two steps:

1. the diffusion of oxygen from the bulk solution to the deposit-solution interface.
2. the diffusion of oxygen through the deposit to the cathode

the rate of transport of oxygen is given by

$$N = \frac{c_b - c_s}{\frac{1}{k} + \frac{x}{D_F}} \quad 2.18$$

where D_F is the diffusivity of oxygen in the fouling deposit

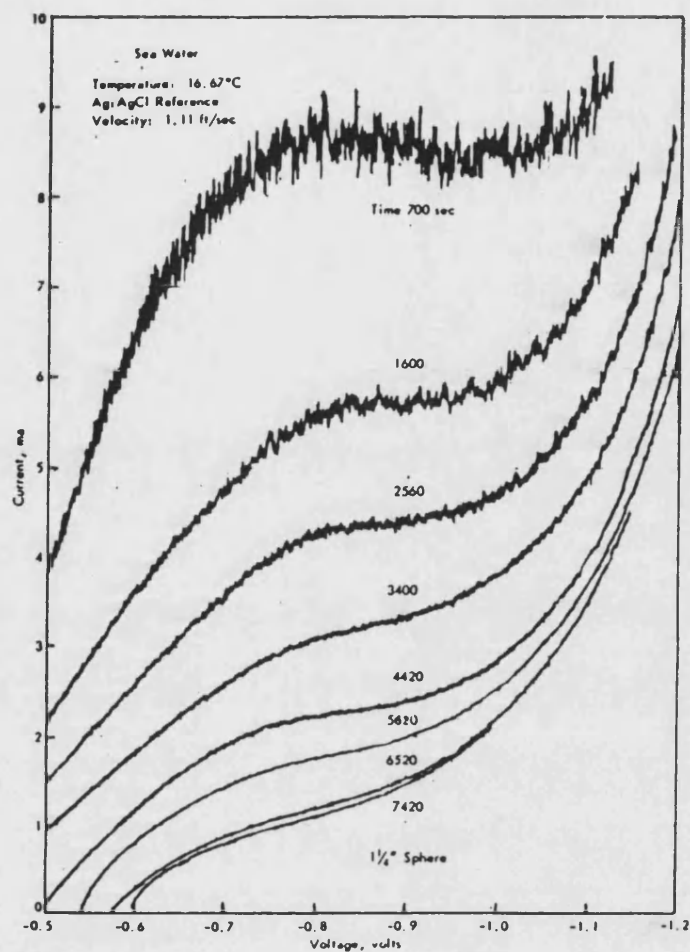


FIGURE 2.4 CURRENT-POTENTIAL CURVES AS A FUNCTION OF TIME⁽²⁶⁾.

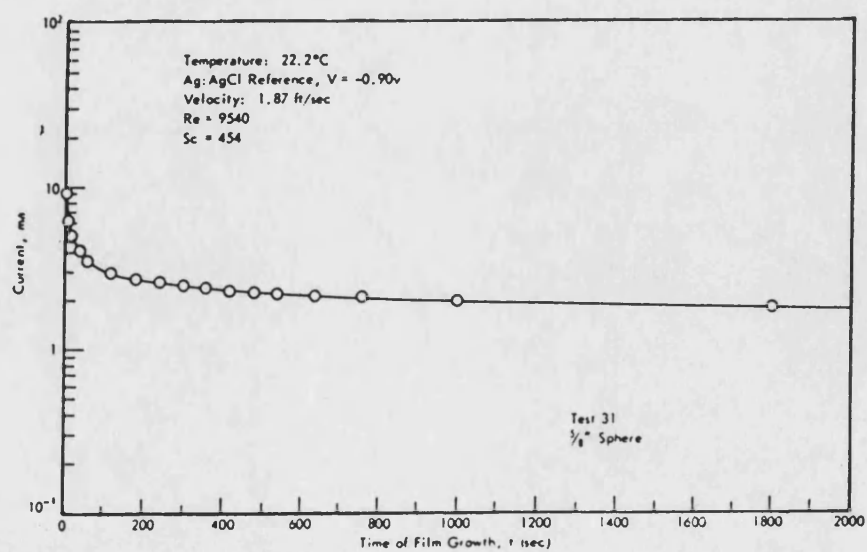


FIGURE 2.5 DECAY OF THE LIMITING CURRENT⁽²⁶⁾.

Noting the Sherwood number based on the diameter of a clean spherical electrode, d is given by

$$Sh = \frac{kd}{D} \quad 2.19$$

and the dimensionless deposit thickness, ξ is given by

$$\xi = \frac{x}{d} \quad 2.20$$

and assuming all the hydroxyl ions formed by oxygen reduction at the cathode react with either calcium or magnesium ions in sea water, ie. $c_s = 0$, equation 2.18 becomes

$$\frac{Nd}{Dc_b} = \frac{1}{\frac{1}{Sh} + \frac{D}{D_F} \xi} \quad 2.21$$

The rate of calcereous deposit accumulation is given by

$$N = \rho_F d \frac{d\xi}{d\theta} \quad 2.22$$

At steady state, the rate of transport of oxygen from the bulk solution to the cathode must equal the rate of calcereous deposit accumulation. Hence, from equations 2.21 and 2.22

$$\frac{\rho_F d^2}{Dc_b} \frac{d\xi}{d\theta} = \frac{1}{\frac{1}{Sh} + \frac{D}{D_F} \xi} \quad 2.23$$

With the initial condition of $\xi = 0$ at $\theta = 0$, integration of equation 2.23 yields

$$\xi = \sqrt{\frac{2D_F c_b}{\rho_F d^2} \theta + \left[\frac{D_F}{D Sh} \right]^2} - \frac{D_F}{D Sh} \quad 2.24$$

Substituting equations 2.2 and 2.24 for N and ξ respectively in equation 2.22 gives

$$\frac{I}{zFADc_b} = \frac{1}{\sqrt{\left[\frac{2D_F c_b}{\rho_F d^2} \right] \left[\frac{D_F}{D} \right] \theta + \left[\frac{1}{Sh} \right]^2}} \quad 2.25$$

Since Re , Sc , intensity of turbulence, i and kinematic viscosity ratio, $\frac{\nu_s}{\nu}$ can be determined, the average Sherwood number for a clean spherical cathode can be computed from Figure 2.6 as the average Frossling number, Fs is given by

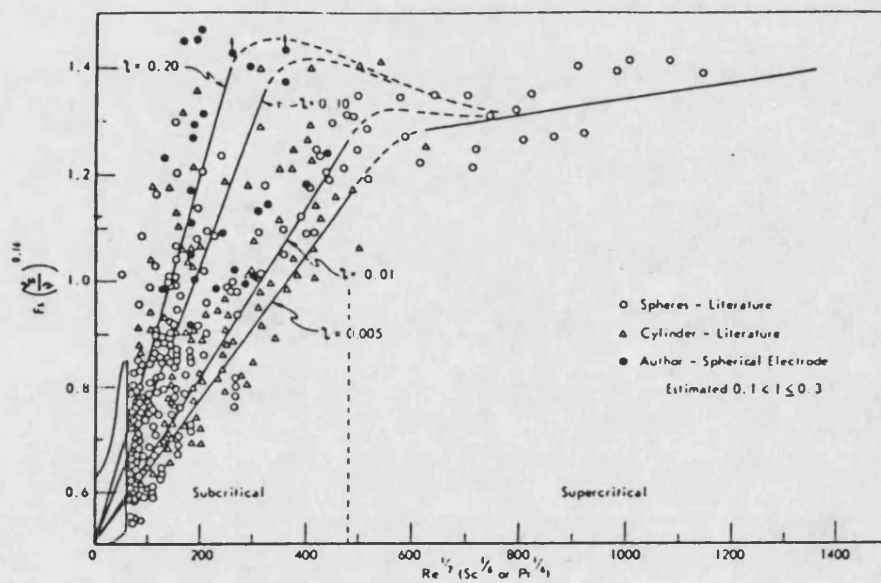


FIGURE 2.6 PLOT OF $Fs \left(\frac{v}{s} \right)^{0.16}$ VERSUS $Re^{\frac{1}{2}} (Sc^{\frac{1}{6}} \text{ or } Pr^{\frac{1}{6}})$
FOR A CLEAN CYLINDRICAL OR SPHERICAL SURFACE⁽²⁶⁾.

$$F_s = \frac{Sh - 2}{Re^{\frac{1}{2}} Sc^{\frac{1}{3}}} \quad 2.26$$

Hence, by assuming a suitable diffusivity ratio, the variation of current with time can be predicted from equation 2.25.

Wolfson and Hartt⁽²⁷⁾ monitored the growth of calcereous deposits on three steel cathodes, each set at a different potential, in a continuous flow sea water system by measuring the current as a function of time for each cathode at three different flow velocities. Their results given in Figures 2.7, 2.8 and 2.9 show the current decreases with time to an asymptote. They also measured the deposit thickness

1. after 182 hours exposure as a function of flow velocity and potential
2. as a function of time

From their results in Figures 2.10 and 2.11 respectively, they concluded that the more positive the potential or the higher the velocity, the thinner the calcereous deposit and the deposit thickness increases linearly with time.

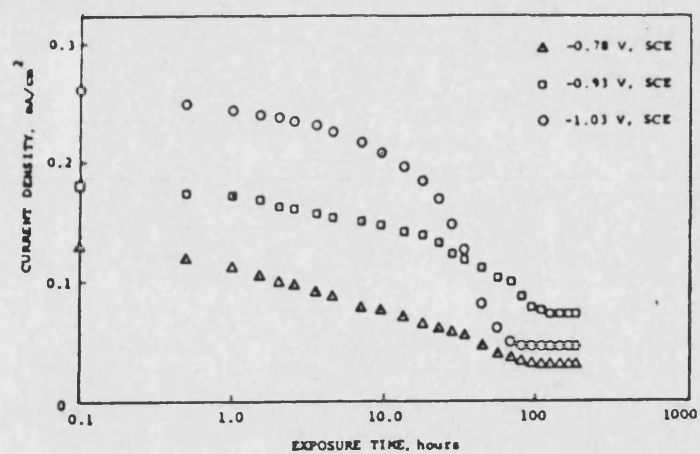


FIGURE 2.7 PLOT OF CURRENT DENSITY VERSUS EXPOSURE TIME FOR THE THREE CATHODIC POTENTIALS AT A FLOW VELOCITY OF 8 cm/s⁽²⁷⁾.

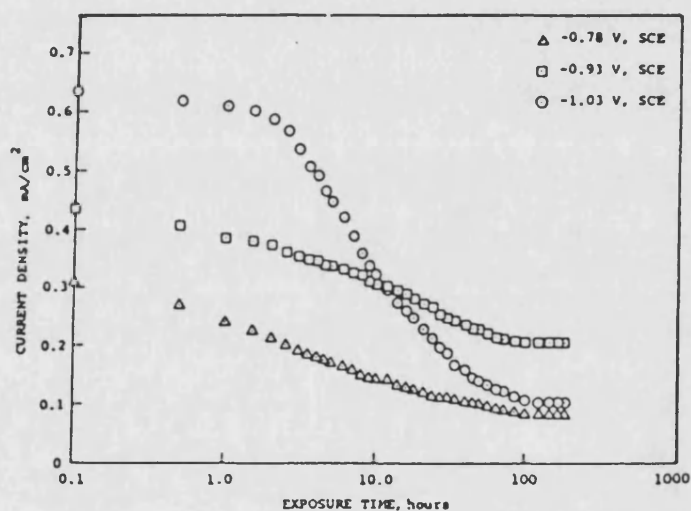


FIGURE 2.8 PLOT OF CURRENT DENSITY VERSUS EXPOSURE TIME FOR THE THREE CATHODIC POTENTIALS AT A FLOW VELOCITY OF 31 cm/s⁽²⁷⁾.

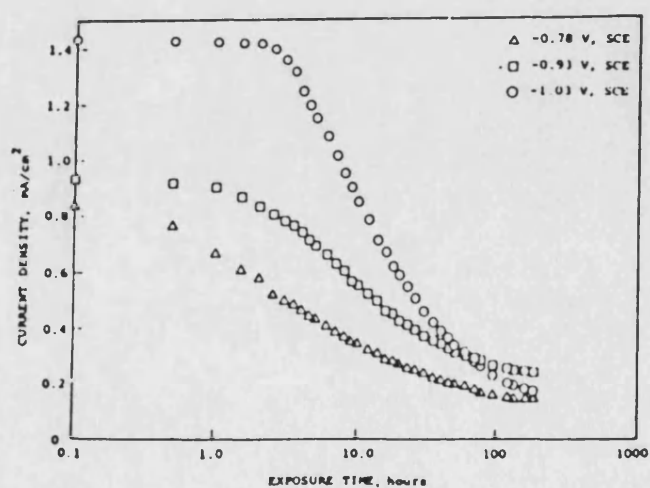


FIGURE 2.9 PLOT OF CURRENT DENSITY VERSUS EXPOSURE TIME FOR THE THREE CATHODIC POTENTIALS AT A FLOW VELOCITY OF 107 cm/s⁽²⁷⁾.

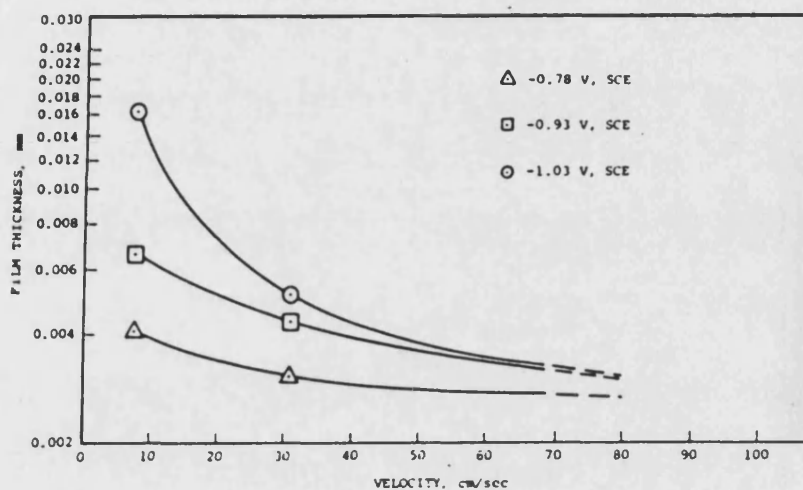


FIGURE 2.10 PLOT OF FILM THICKNESS AFTER 182 HOURS EXPOSURE AS A FUNCTION OF FLOW VELOCITY FOR THE THREE CATHODIC POTENTIALS⁽²⁷⁾.

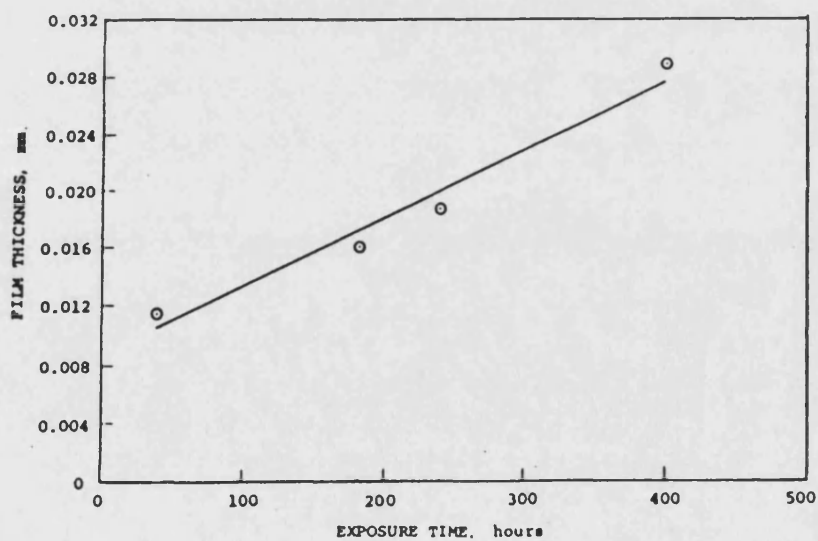


FIGURE 2.11 PLOT OF FILM THICKNESS AS A FUNCTION OF EXPOSURE TIME FOR SPECIMENS TESTED AT A FLOW VELOCITY OF 8 cm/s AND A CATHODE POTENTIAL OF -1.03 V⁽²⁷⁾.

3. EXPERIMENTAL APPARATUS AND PROCEDURE

The apparatus was designed in order to investigate the effect of deposit characteristics on heat transfer and the influence of the deposit interface on fluid flow for a model fouling system by the electrochemical method.

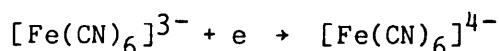
3.1 Model fouling system

The model fouling system used in this study consisted of

1. an electrochemical system
2. a simulated fouling deposit

3.1.1 Electrochemical system

The electrochemical system selected for this study is the cathodic reduction of ferricyanide ions to ferrocyanide ions in a supporting electrolyte of sodium hydroxide at a nickel electrode:



This electrochemical reaction was selected in preference to the cathodic deposition of copper from an acidified copper sulphate solution at a copper electrode for two reasons:

1. it has a longer and more well-defined limiting current plateau
2. the nature of the surface topography remains unchanged throughout the electrochemical reaction

The concentrations used for the electrolytic solution were those found to be suitable by Tagg et al⁽³³²⁾, ie.

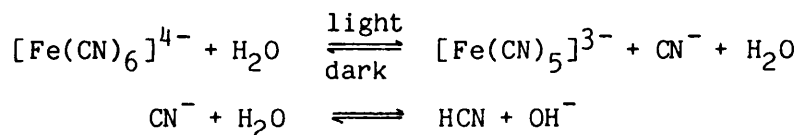
Potassium ferricyanide	0.005M
Potassium ferrocyanide	0.005M
Sodium hydroxide	0.5M

The chemicals were supplied by BDH; potassium ferricyanide and potassium ferrocyanide were of 'Analar' grade while sodium hydroxide was of 'Aristar' grade.

The effect of adverse conditions on the electrolytic solution have been highlighted by several investigators⁽³³³⁻³⁴¹⁾. Such adverse conditions include

1. the photochemical decomposition of the electrolytic solution

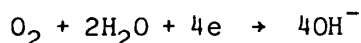
Solutions of potassium ferricyanide and particularly potassium ferrocyanide are known to decompose slowly in light resulting in the formation of free cyanide and hydroxyl ions according to⁽³³³⁻³³⁷⁾:



The free cyanide ions causes the contamination of the electrolytic solution and poisoning of the electrodes. In order to avoid the formation of free cyanide ions, the electrolytic solution must be kept in darkness^(336,337).

2. the exposure of the electrolytic solution to air

The effect of air on the contamination of the electrolytic solution and the electrodes is complex^(338,339). The possible side reaction involving oxygen at the cathode



suggested by Aggerwaal and Talbot⁽³⁴⁰⁾ is unlikely since the discharge potential of this reaction is considerably higher than the normal voltage range over which diffusion controlled conditions exist. However, the presence of dissolved oxygen may lead to the formation of oxide films on electrodes or more likely to the oxidation of potassium ferrocyanide. Other lesser components of air may dissolve in the alkaline solution to form solution contaminants and electrode poisons; eg. hydrogen sulphide is thought to be absorbed by the electrode rendering it 'passive'.

In order to avoid the formation of solution contaminants and electrode poisons, the electrolytic solution must be isolated from air. This is achieved by purging nitrogen through the NaOH solution until all the dissolved gases have been driven off before the addition of $\text{K}_3\text{Fe}(\text{CN})_6$ and $\text{K}_4\text{Fe}(\text{CN})_6$ to the NaOH solution and maintaining this saturated solution under a nitrogen atmosphere at all times⁽³³⁸⁾.

3. the slow oxidation of polymeric materials by the electrolytic solution

The slow oxidation of polymeric materials commonly used in the design of electrochemical rigs by the electrolytic solution will cause the solution to deteriorate gradually with time. In order to overcome the

problem, it is recommended to use a freshly prepared electrolytic solution together with carefully prepared electrodes as often as possible.

4. the inadequate preparation of the electrodes

There is considerable confusion in the literature regarding the required pre-treatment of the electrodes⁽³⁵⁸⁾. Eisenberg et al⁽³³⁷⁾, in their investigation on the chemical polarisation of the electrolytic solution at rotating electrodes, recommended cathodic activation of the electrodes. This consisted of a hydrogen discharge treatment on the electrodes using a current density of 20 mA/cm^2 in 5% NaOH solution for 12-15 minutes. They found that with freshly prepared electrolytic solutions under the exclusion of light and with cathodically treated nickel electrodes, the chemical polarisation is relatively small. In their experiments, some investigators, in particular Sutey and Knudsen⁽³³⁹⁾, found the cathodic activation of the electrodes recommended by Eisenberg et al⁽³³⁷⁾ to be necessary while other investigators, in particular Aggerwaal and Talbot⁽³⁴⁰⁾ and Hubbard and Lightfoot⁽³⁴¹⁾, found it unnecessary.

Berger and Ziai⁽³³⁸⁾ have recently carried out a systematic study in order to clarify the confusing recommendations on cathodic activation of the electrodes. From their results, they found that chemical polarisation at unactivated electrodes became more serious with increasing Re since the error (obtained from the difference in values of I_L at the extremes of the limiting current plateau) was found to vary from 2-3% at $Re_{\text{minimum}} = 4 \times 10^4$ to 9-10% at $Re_{\text{maximum}} = 4 \times 10^5$. However, with cathodically treated electrodes, they found the error at Re_{maximum} was reduced to 1%. These findings explain why some investigators^(340,341) found cathodic activation of the electrodes to be unnecessary since Re_{maximum} in their experiments was generally never above 10^4 at which chemical polarisation becomes significant.

Berger and Ziai⁽³³⁸⁾ also noted that cathodic activation of the electrodes was necessary but not sufficient to achieve the optimum current-potential curve. As shown in Figure 3.1, the optimum current-potential curve is obtained when all the precautions for the elimination of solution contaminants and electrode poisons have been taken.

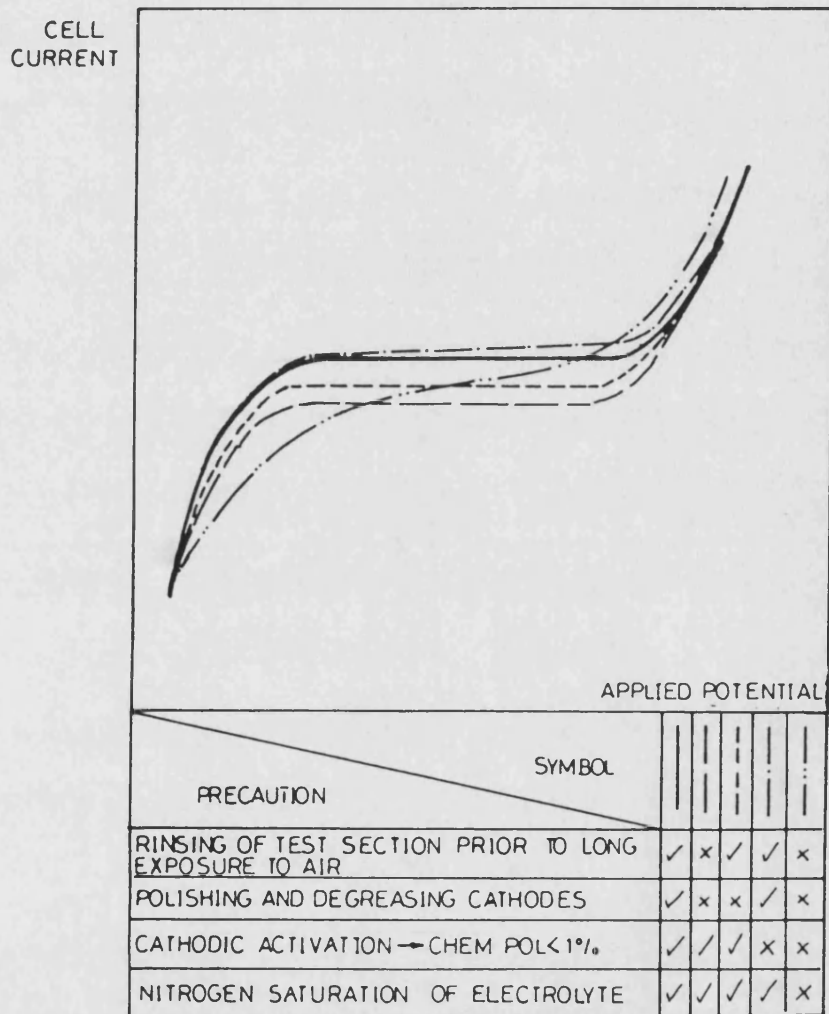


FIGURE 3.1 THE EFFECT OF VARIOUS PRECAUTIONS TAKEN FOR THE $K_3Fe(CN)_6 - K_4Fe(CN)_6 - NaOH$ SYSTEM ON THE CURRENT - POTENTIAL CURVE⁽³³⁸⁾.

In order to avoid any adverse effects due to the inadequate preparation of electrodes, Berger and Ziai⁽³³⁸⁾ recommended that the electrodes (which were already polished) should be buffed with fine emery paper and washed with a degreasing agent such as carbon tetrachloride prior to cathodic activation as prescribed by Eisenberg et al⁽³³⁷⁾.

The physical properties of the electrolytic solution required for use in mass transfer correlations include

1. density
2. kinematic viscosity
3. diffusivity
4. thermal conductivity
5. heat capacity
6. density difference between the electrolytic solution in the bulk and the electrode surface required for the evaluation of Gr_m , $\Delta\rho_h$
7. density difference between the electrolytic solution in the bulk and the electrode surface required for the evaluation of Gr_h , $\Delta\rho_h$

Each of these physical properties will be discussed in turn.

3.1.1.1 Density

Using a hydrometer (Type BS 718 series S50) suspended in a constant temperature bath, the density of the electrolytic solution was measured as a function of temperature. The procedure is outlined in BS 718⁽³⁴²⁾. The data obtained is tabulated in Appendix A1. Using the least squares method, it can be seen from Figure 3.2 that the density over the temperature range 18.0-70.0°C is given by

$$\rho = 1.03052 - 2.142 \times 10^{-4}T - 6.6 \times 10^{-6}T^2 \quad 3.1$$

where ρ = density in g/cm³

T = temperature in °C

The correlation coefficient for equation was found to be 99.9%.

3.1.1.2 Kinematic viscosity

Using a U-tube viscometer (Type BS/U) suspended in a constant temperature bath, the kinematic viscosity of the electrolytic solution was measured as a function of temperature. The procedure is outlined in BS 188⁽³⁴³⁾. The data

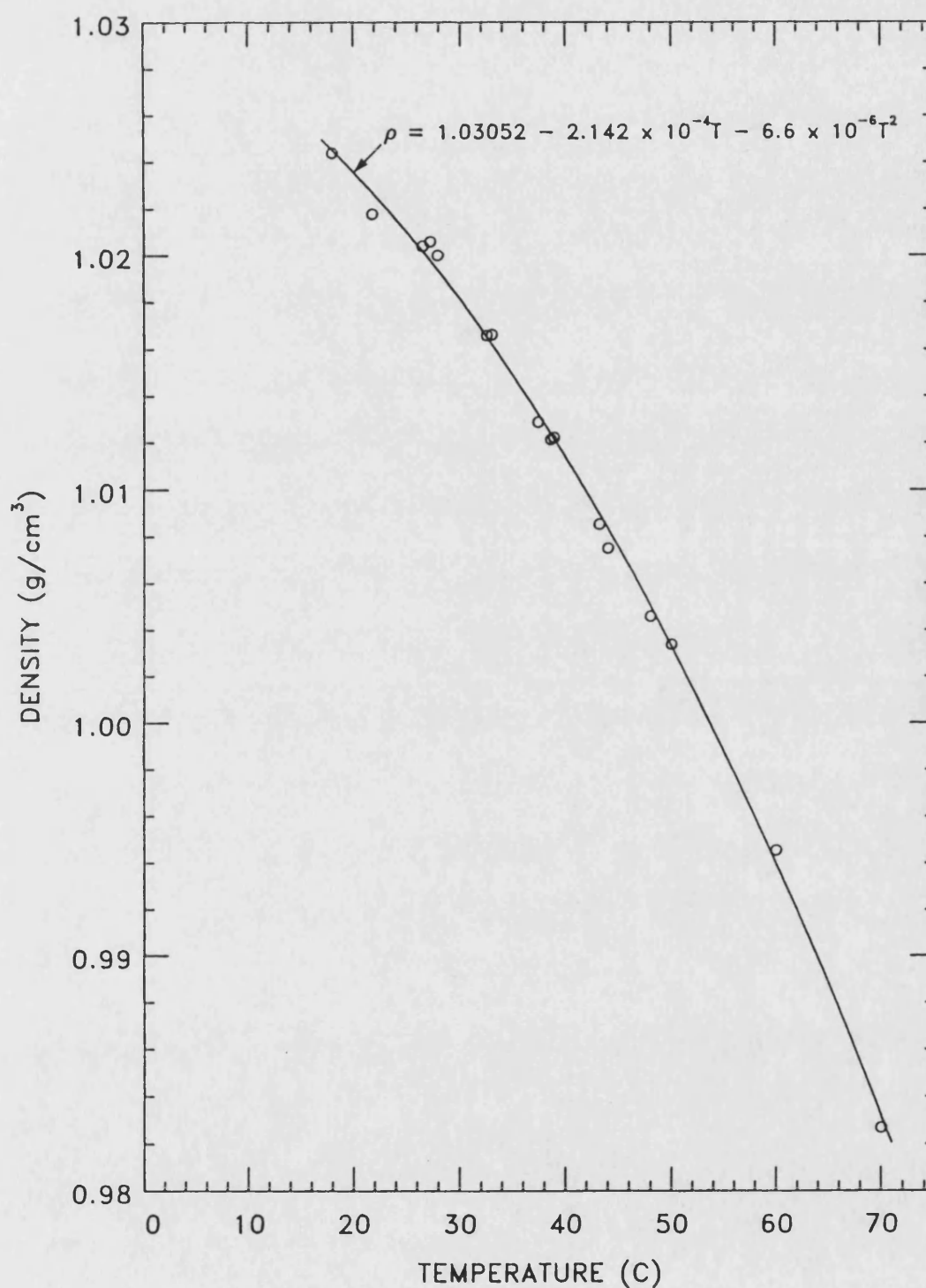


FIGURE 3,2 THE VARIATION OF ELECTROLYTIC SOLUTION DENSITY WITH TEMPERATURE

obtained is tabulated in Appendix A2. Using the least squares method, it can be seen from Figure 3.3 that the kinematic viscosity over the temperature range 18.0-45.0°C is given by

$$\nu = \exp \left[\frac{1868.57}{T} - 6.2926 \right] \quad 3.2$$

where ν = kinematic viscosity in mm²/s

T = temperature in K

The correlation coefficient for equation 3.2 was found to be 99.5%.

3.1.1.3 Diffusivity

In electrochemical mass transfer studies, the diffusivity of the electrolytic solution must be known in order to correlate the results in terms of useful dimensionless numbers such as Sh , Gr_m and Sc . Since the accuracy of the correlation is strongly dependent on the diffusivity of the electrolytic solution, it is necessary to ensure that the correct diffusivity data is used (320).

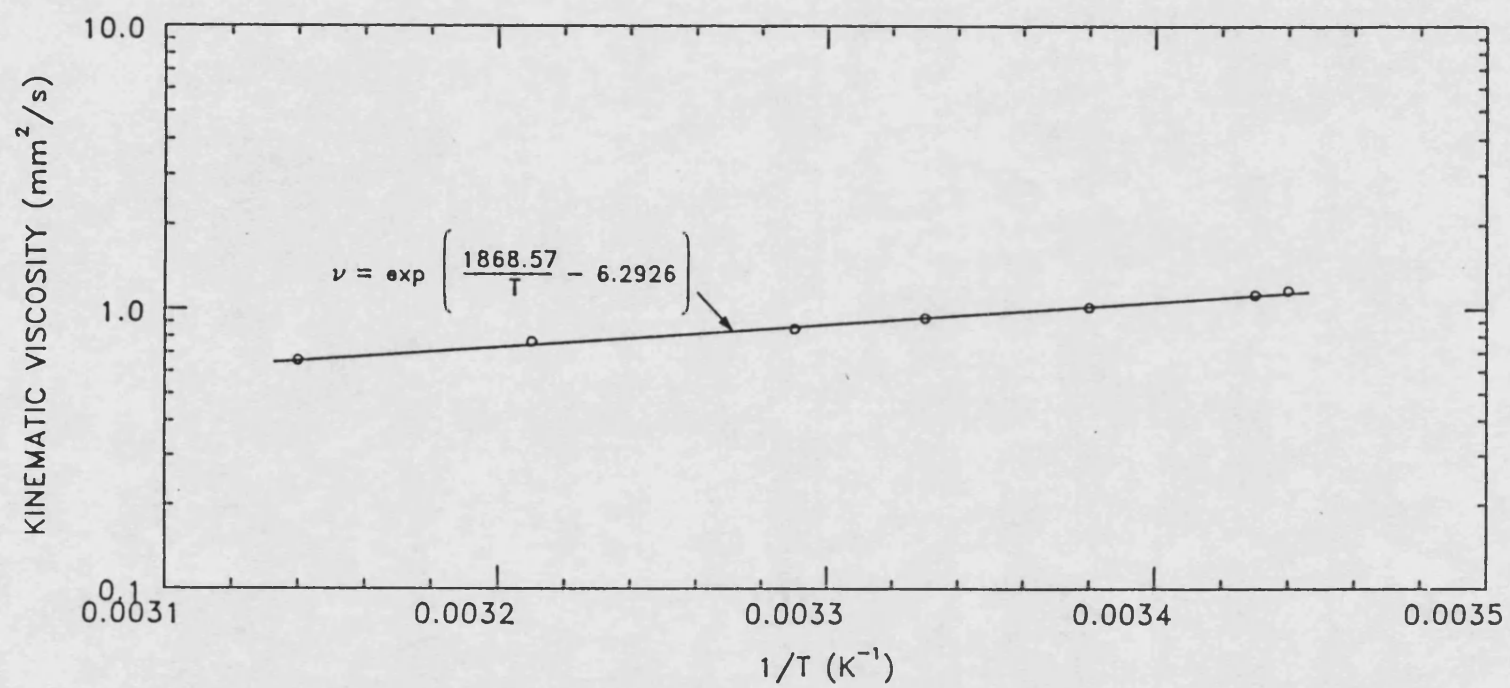
The diffusivity of the electrolytic solution was expressed by the early investigators in terms of either molecular diffusivities which were scarce for multicomponent electrochemical systems or ionic diffusivities which were only known in the limit of infinite dilution according to Nernst-Einstein equation

$$D_j = RTu_j = \frac{RT\lambda_j}{|z_j|F^2} \quad 3.3$$

However, later investigators^(315,344,345) have questioned the use of molecular diffusivity data and ionic diffusivity data at infinite dilution in electrochemical mass transfer correlations. For the diffusivity of the electrolytic solution, they used ionic diffusivities that have been obtained from limiting current measurements of an electrochemical cell where the velocity profile at the electrode is well-defined and known. These ionic diffusivities are effective ionic diffusivities^(321,327) since

1. they reflect a migration contribution that is not always negligible
 2. they contain the effect of variable solution properties near the electrode
- The effective ionic diffusivities appear at first to be applicable only to the particular electrochemical cell in which they were measured. However, it was argued plausibly by Newman⁽³¹⁵⁾ that effective diffusivities determined

FIGURE 3.3 THE VARIATION OF ELECTROLYTIC SOLUTION KINEMATIC VISCOSITY WITH TEMPERATURE



for one particular type of mass transfer may be generally applicable for all situations involving that type of mass transfer provided the same bulk concentration of the electrolytic solution is used. Furthermore, it was also presumed that the effective ionic diffusivities characteristic for free convection electrochemical systems will not be significantly different from that for forced convection electrochemical systems.

Several methods have been used to determine the diffusivity of the ferricyanide ion in a solution of equimolar mixture of potassium ferricyanide and potassium ferrocyanide in excess sodium hydroxide. The details are summarised in Table 3.1. For this study, the results obtained by Bazan and Arvia⁽³⁴⁸⁾ was used. Over the temperature range of 25.0–41.8°C, they found the effective diffusivity is given by

$$\frac{\mu D}{T} = (2.50 \pm 0.17) \times 10^{-10} \quad 3.4$$

where μ = viscosity in g/cm s

D = diffusivity in cm²/s

T = temperature in K

3.1.1.4 Thermal conductivity

For the temperature range 20–100°C, the thermal conductivity of the electrolytic solution can be estimated to within 5% accuracy from

$$k(T) = k(20^\circ) \frac{k_{H_2O}(T)}{k_{H_2O}(20^\circ C)} \quad 3.5$$

in which $k(20^\circ C)$ can be estimated to within 5% accuracy from the equation proposed by Riedel⁽³⁵²⁾ and tested by Vargaftik and Os'minin⁽³⁵³⁾:

$$k(20^\circ C) = k_{H_2O}(20^\circ C) + \sum \sigma_j c_j \quad 3.6$$

where k = thermal conductivity of the electrolytic solution in W/cm K

k_{H_2O} = thermal conductivity of water in W/cm K

c_j = concentration of species j in moles/litre

σ_j = coefficient that is characteristic for species j

Values of σ_j are listed in Table 3.2.

The thermal conductivity of water required in equations 3.5 and 3.6 can be determined from the equation recommended by ESDU⁽³⁵⁷⁾:

TABLE 3.1 VALUES OF $\frac{\mu D}{T}$ FOR THE FERRICYANIDE ION IN A SOLUTION OF EQUIMOLAR MIXTURE OF POTASSIUM FERRICYANIDE AND POTASSIUM FERROCYANIDE IN EXCESS SODIUM HYDROXIDE

SOURCE	CONCENTRATIONS			$\frac{\mu D}{T}$ (g cm/s K)	METHOD ^a
	$K_3Fe(CN)_6$ (M)	$K_4Fe(CN)_6$ (M)	NaOH (M)		
Lin et al ⁽³⁴⁶⁾	0.005 - 0.01	0.0005 - 0.01	0.5	2.67×10^{-10}	LM
Eisenburg et al ⁽³⁴⁷⁾	0.1963	0.1919	2.027	2.50×10^{-10}	CC
Bazán and Arvia ⁽³⁴⁸⁾	0.0016 - 0.0125	0.0016 - 0.0125	~ 0.5	$(2.50 \pm 0.17) \times 10^{-10}$	RDE
	0.0012 - 0.0500	0.0012 - 0.0500	~ 1.0	$(2.52 \pm 0.10) \times 10^{-10}$	
	0.0004 - 0.0980	0.0004 - 0.0980	~ 2.0	$(2.54 \pm 0.13) \times 10^{-10}$	
Gordon et al ⁽³⁴⁹⁾	0.01 - 0.20	0.01 - 0.20	0.0 - 3.5	$([2.34 \pm 0.014I] \pm 0.05) \times 10^{-10}$ ^b	RDE
Van Shaw et al ⁽³⁵⁰⁾	0.0001 - 0.01	0.0001 - 0.01	~ 2.0	2.30×10^{-10}	LFA
Noordsij and Rotte ⁽³⁵¹⁾	0.025	0.025	0.5	2.27×10^{-10}	DS

^a CC Capillary cell
DS Diffusion to a spherical electrode
LFA Laminar flow annular cell
LM Limiting mobility at infinite dilution
RDE Rotating disk electrode

^b I , ionic strength = $\frac{1}{2} \sum c_j z_j^2$

TABLE 3.2 PHYSICAL PROPERTY DATA FOR THE $K_3Fe(CN)_6$ - NaOH SYSTEM AT 25°C (315,354,355,356)

IONIC SPECIES	s_j	z_j	$\bar{\sigma}_j$	λ_j (cm ² /Ω equiv)	D_j (cm ² /s)	a_j (cm ³ /mole)
$Fe(CN)_6^{3-}$	-1	-3	-	100.9	0.896×10^{-5}	167.27
$Fe(CN)_6^{4-}$	1	-4	18.61×10^{-5}	110.5	0.739×10^{-5}	225.91
OH^-	0	-1	20.934×10^{-5}	197.6	5.260×10^{-5}	45.29
Na^+	0	1	0	50.11	1.334×10^{-5}	-6.73
K^+	0	1	-7.560×10^{-5}	73.52	1.957×10^{-5}	0

$$k_{H_2O} = \sqrt{T^*} \left[\sum_{i=0}^3 a_i (T^*)^{-i} \right]^{-1} \exp \left[\rho^* \sum_{j=0}^4 \sum_{k=0}^5 b_{j,k} \left[\frac{1}{T^*} - 1 \right]^j \left[\rho^* - 1 \right]^k \right] \quad 3.7$$

where k_{H_2O} = thermal conductivity of water in W/m K

$$T^* = \text{reduced temperature} = \frac{T}{T_c} \text{ where } T_c = 647.27 \text{ K}$$

$$\rho^* = \text{reduced density} = \frac{\rho}{\rho_c} \text{ where } \rho_c = 317.763 \text{ kg/m}^3$$

The numerical values of the coefficients a_i and $b_{j,k}$ in equation 3.7 are listed in Table 3.3.

The density of water required in equation 3.7 can be determined from the equation recommended by Gibson and Bruges⁽³⁵⁸⁾:

$$\rho^* = \sum_i a_i T_i(z) \quad 3.8$$

$$\text{in which } z = 1 - 2(1 - T^*)^{0.4} \quad 3.9$$

$$\text{where } \rho^* = \text{reduced density} = \frac{\rho}{\rho_c} \text{ where } \rho_c = 317.763 \text{ kg/m}^3$$

$$T^* = \text{reduced temperature} = \frac{T}{T_c} \text{ where } T_c = 347.12 \text{ }^\circ\text{C}$$

The function $T_i(z)$ in equation 3.8 is the Chebyshev polynomial of i th degree with z normalised in the range $-1 \leq z \leq 1$. The first two Chebyshev polynomials are

$$T_0(z) = 1 \quad 3.10$$

$$T_1(z) = z \quad 3.11$$

and the remaining Chebyshev polynomials are calculated using the recurrence relation

$$T_n(z) = 2z T_{n-1}(z) - T_{n-2}(z) \quad 3.12$$

The numerical values of the coefficients a_i in equation 3.8 are listed in Table 3.4.

3.1.1.5 Heat capacity

The heat capacity of the electrolytic solution can be estimated using the Wenner approximation for dilute aqueous electrolytic solutions⁽³⁵⁹⁾ which states

$$c_p = M_{H_2O} \quad 3.13$$

TABLE 3.3 THE COEFFICIENTS OF a_i AND $b_{j,k}$ IN EQUATION 3.7

a_0	=	2.02223
a_1	=	14.11166
a_2	=	5.25597
a_3	=	- 2.01870
b_{00}	=	2.0476004
b_{01}	=	- 1.5962370
b_{02}	=	0.0993949
b_{03}	=	1.3774179
b_{04}	=	- 1.0242464
b_{05}	=	0.2203151
b_{10}	=	7.8791290
b_{11}	=	-10.7813807
b_{12}	=	- 1.2449962
b_{13}	=	8.1477154
b_{14}	=	- 3.7521680
b_{15}	=	0.4418686
b_{20}	=	23.2605736
b_{21}	=	-24.0282944
b_{22}	=	- 7.0974356
b_{23}	=	12.0340912
b_{24}	=	- 3.3303434
b_{25}	=	0.2836892
b_{30}	=	19.5612336
b_{31}	=	- 1.7812867
b_{32}	=	- 7.1641645
b_{33}	=	1.7212905
b_{34}	=	0.0
b_{35}	=	0.0
b_{40}	=	-22.6395931
b_{41}	=	19.4620986
b_{42}	=	- 4.5770117
b_{43}	=	0.2042771
b_{44}	=	0.0
b_{45}	=	0.0

TABLE 3.4 THE COEFFICIENTS OF α_i IN EQUATION 3.8

$$\begin{aligned} \alpha_0 &= 4.332053 \\ \alpha_1 &= -1.107796 \\ \alpha_2 &= -5.275102 \times 10^{-2} \\ \alpha_3 &= 2.173547 \times 10^{-2} \\ \alpha_4 &= -1.754636 \times 10^{-2} \\ \alpha_5 &= 5.125009 \times 10^{-3} \\ \alpha_6 &= -3.765370 \times 10^{-3} \\ \alpha_7 &= 1.123345 \times 10^{-3} \\ \alpha_8 &= -2.458266 \times 10^{-3} \\ \alpha_9 &= -1.425530 \times 10^{-3} \\ \alpha_{10} &= -1.304721 \times 10^{-3} \end{aligned}$$

where c_p = heat capacity of the electrolytic solution in BTU/lb °F

M_{H_2O} = mass fraction of water in the electrolytic solution

The mass fraction of water in the electrolytic solution is given by

$$M_{H_2O} = 1 - (M_{K_3Fe(CN)_6} + M_{K_4Fe(CN)_6} + M_{NaOH}) \quad 3.14$$

$$= 1 - \frac{m_{K_3Fe(CN)_6} + m_{K_4Fe(CN)_6} + m_{NaOH}}{m} \quad 3.15$$

$$= 1 - \frac{m_{K_3Fe(CN)_6} + m_{K_4Fe(CN)_6} + m_{NaOH}}{\rho V} \quad 3.16$$

where M_j = mass fraction of species j in the electrolytic solution

m_j = mass of species j in the electrolytic solution

m = mass of electrolytic solution

ρ = density of electrolytic solution given by equation 3.1

V = volume of electrolytic solution

Since 0.005M $K_3Fe(CN)_6 \equiv 1.6463g K_3Fe(CN)_6$ in $1000cm^3$ solution, 0.005M $K_4Fe(CN)_6 \equiv 2.1120g K_4Fe(CN)_6$ in $1000cm^3$ solution, and 0.5M NaOH $\equiv 20g NaOH$ in $1000cm^3$ solution, then equation 3.16 becomes

$$M_{H_2O} = 1 - \frac{1.6463 + 2.1120 + 20}{1000\rho} = 1 - \frac{0.02376}{\rho} \quad 3.17$$

Substituting equation 3.17 into equation 3.13 yields

$$c_p = 1 - \frac{0.02376}{\rho} \quad 3.18$$

3.1.1.6 $\Delta\rho_m$

The density difference between the electrolytic solution in the bulk and the electrode surface required for the evaluation of Gr_m , $\Delta\rho_m$ can be determined from either the concentration difference of the reacting species between the bulk and the electrode surface through the use of an overall densification coefficient or the concentration difference of different species through the use of ionic/molecular densification coefficients since (310,311,318,319,355,356,360-369).

$$\left[\frac{\Delta \rho}{\rho} \right]_m = \bar{\alpha} \Delta c_R = \sum_j \alpha_j \Delta c_j \quad 3.19$$

where $\bar{\alpha}$ = overall densification coefficient, defined as

$$\bar{\alpha} = \frac{\partial \ln \rho}{\partial c_R} = \frac{1}{\rho} \frac{\partial \rho}{\partial c_R} \quad 3.20$$

α_j = densification coefficient of species j, defined as

$$\alpha_j = \frac{\partial \ln \rho}{\partial c_j} = \frac{1}{\rho} \frac{\partial \rho}{\partial c_j} \quad 3.21$$

Δc_j = concentration difference of species j between the bulk and the electrode surface

Δc_R = concentration difference of limiting reactant R between the bulk and the electrode surface

To date, the only reliable densification coefficient data for the $K_3Fe(CN)_6 - K_4Fe(CN)_6 - NaOH$ system are those of Selman and Newman⁽³⁵⁶⁾. As outlined in Appendix A3, they used the density data obtained by Gordon et al⁽³⁴⁹⁾ and Boeffard⁽³⁷⁰⁾ to evaluate the ionic densification coefficients. These values are tabulated in Table 3.2.

Several methods for the estimation of Δc_j in equation 3.19 have been proposed. Of the various methods outlined in Appendix A4 that have been used to estimate Δc_j for the $K_3Fe(CN)_6 - K_4Fe(CN)_6 - NaOH$ system, the WET method was selected for this study. Hence, Δc_j was estimated from

$$\frac{\Delta c_j}{\Delta c_R} = \left[\frac{s_j - \frac{t_j}{z_j}}{s_R - \frac{t_R}{z_R}} \right] \left[\frac{D_R}{D_j} \right]^{\frac{3}{4}} \quad 3.22$$

where s_j = number of molecules or ions of species j which react at the electrode per one Faraday flowing the electrochemical cell

s_R = number of molecules or ions of limiting reactant R which react at the electrode per one Faraday flowing the electrochemical cell

t_j = transference number of species j, defined as

$$t_j = \frac{|z_j| \lambda_j c_j}{\sum_j |z_j| \lambda_j c_j} \quad 3.23$$

t_R = transference number of limiting reactant R

$\Delta c_R = c_{R_b}$ since $c_{R_s} = 0$ at the limiting condition

The physical properties in equations 3.22 and 3.23 for the $K_3Fe(CN)_6$ - $K_4Fe(CN)_6$ - NaOH system are also tabulated in Table 3.2.

3.1.1.7 $\Delta\rho_h$

The density difference between the electrolytic solution in the bulk and the electrode surface required for the evaluation of Gr_h , $\Delta\rho_h$ can be determined from⁽³⁷¹⁾

$$\left[\frac{\Delta\rho}{\rho} \right]_h = \frac{\rho(T_b) - \rho(T_s)}{\rho(T_s)} \quad 3.24$$

where $\rho(T_s)$ = density of the electrolytic solution at the electrode surface

$\rho(T_b)$ = density of the electrolytic solution in the bulk

3.1.2 Simulated fouling deposit

The simulated fouling deposit used in this study composed of one or more layers of glass spherical particles of known dimensions resting on a flat horizontal nickel cathode. The physical properties of the glass spherical particles supplied as Ballotini from Jencons Ltd are tabulated in Table 3.5.

3.2 Experimental apparatus

The experimental apparatus used in this study is shown schematically in Figure 3.4 and as a photograph in Figure 3.5.

3.2.1 Mixing cell

The main features of the electrolytic mixing cell are shown diagrammatically in Figure 3.6. It consisted of a perspex cylinder, 76mm ID and 150mm high, which was tightened between the Tufnal top plate and the Sindanyo base plate by means of six tie rods. Neoprene gaskets were used to provide a liquid seal between the perspex cylinder and the end plates. To minimise the exposure of the electrolytic solution to light, the transparent surface of the perspex cylinder was covered with an orange celluloid film.

The anode constituted a nickel plate, 58mm diameter and 3.5mm thickness, perforated with 91 holes of 1.7mm diameter and a central hole of 8mm diameter. This was rigidly suspended 90mm from the Tufnal top plate cover. The cathode,

TABLE 3.5 PHYSICAL PROPERTIES OF THE GLASS SPHERICAL PARTICLES⁽³⁷²⁾

GLASS TYPE	d_p average (mm)	ρ_p (kg/m ³)	c_p (J/kg K)	k_p (W/m K)
Lead glass	0.368 ± 0.058	2980	628	0.848
	0.695 ± 0.055			
	0.805 ± 0.130			
	1.290 ± 0.110			
	1.340 ± 0.175			
	1.550 ± 0.150			
	3.000 ± 0.500			
	5.000 ± 0.500			
	7.000 ± 0.500			
Soda glass	10.00 ± 0.50	2400	712	0.952
	12.00 ± 0.50			

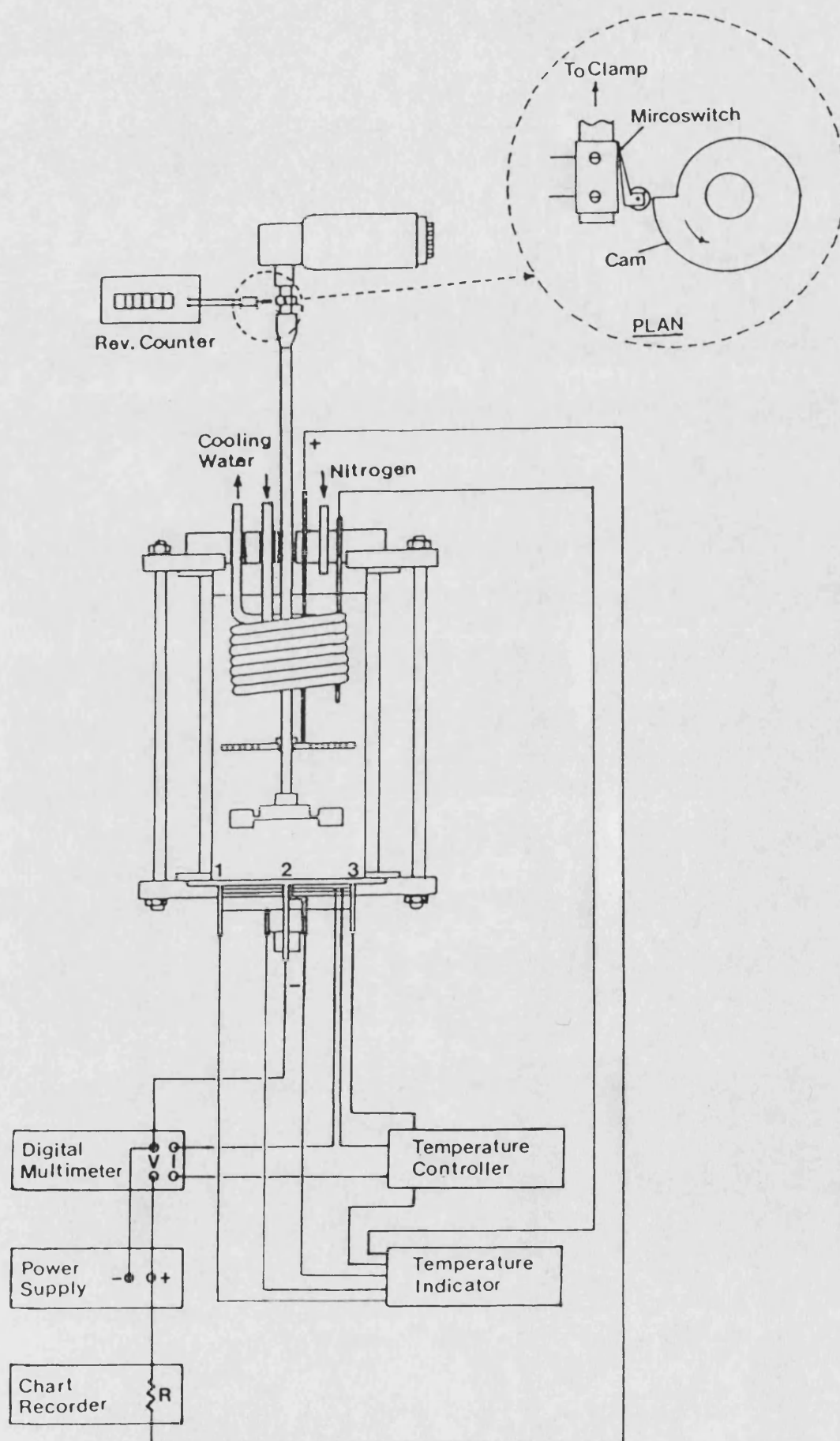


FIGURE 3.4 SCHEMATIC DIAGRAM OF THE EXPERIMENTAL APPARATUS.

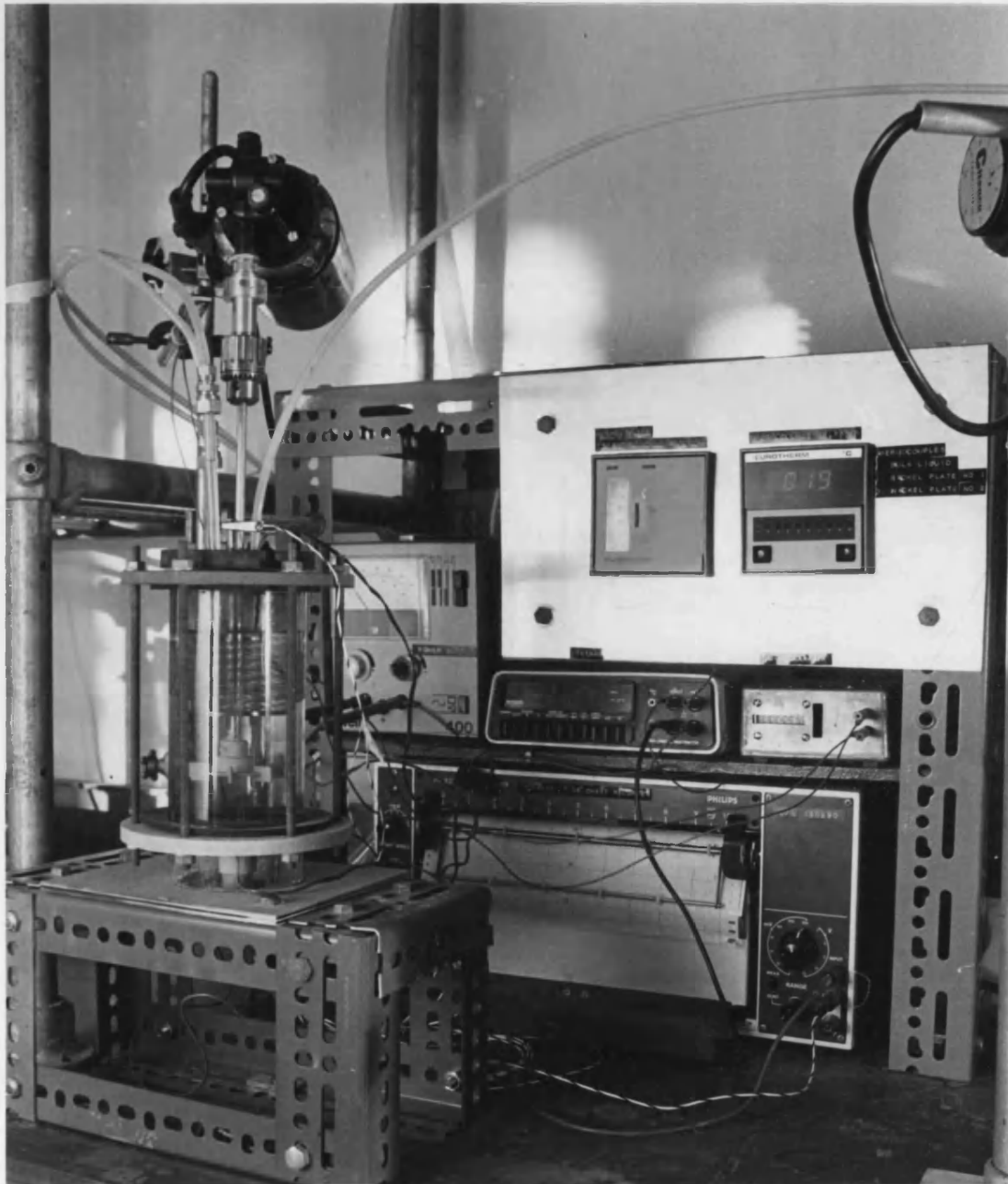


FIGURE 3.5 PHOTOGRAPH OF THE EXPERIMENTAL APPARATUS

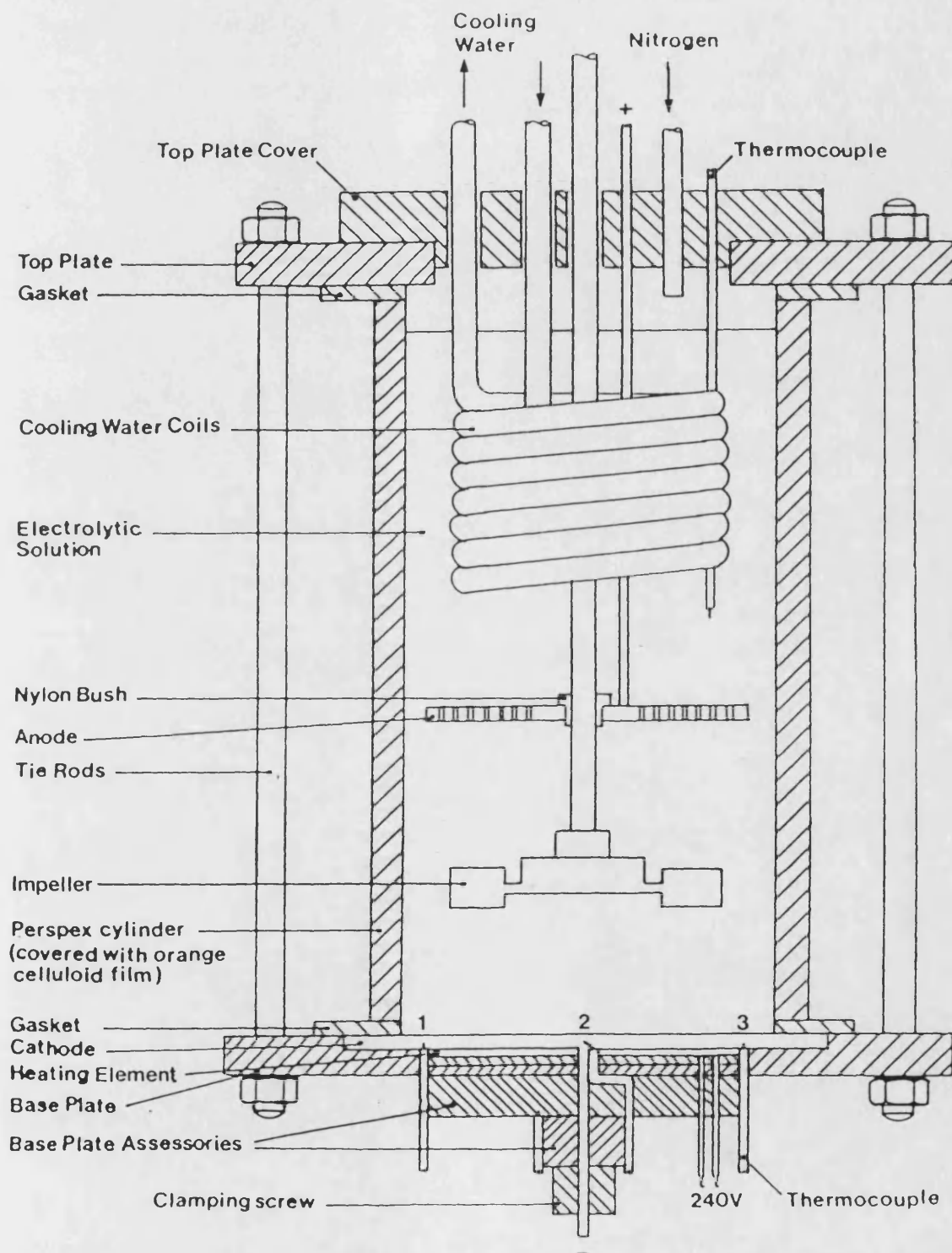


FIGURE 3.6 ELECTROLYTIC MIXING CELL.

a nickel plate of 90mm diameter and 3.5mm thickness, was secured flush with the base plate by means of a clamping screw. The type of nickel selected for the electrodes was Nickel 200. This was supplied by Titanium International Ltd with the following chemical composition:

Ni	99.40%
C	0.06%
Mn	0.25%
Fe	0.15%
S	0.005%
Si	0.05%
Cu	0.05%

Several investigators^(317,319,323,327,332,339,340,371,373-380) have indicated that in order to ensure the electrochemical reaction is cathodically controlled, the surface area of the anode must be larger than that of the cathode. In this study, the ratio of the surface area of the anode to the cathode was 1.55:1.

The electrolytic solution was agitated by a standard 50cm diameter, stainless steel, six flat-bladed, disc-mounted turbine impeller. The impeller was placed centrally in the cell 30mm from the cathode surface via a nylon bush in the anode. The purpose of the nylon bush was to electrically insulate the impeller shaft from the anode. The impeller was driven by a Citenco constant torque motor (Model KQTS supplied by Fisons Scientific Apparatus Ltd) giving a range of output rotational speeds 0-350 rpm. These speeds were measured via a cam - microswitch arrangement shown in Figure 3.4. Each time, the securely clamped roller lever microswitch (Model V4T7YR1 supplied by Burgess Ltd) was tripped by the perspex cam on the stirrer motor shaft, one revolution of the impeller was recorded on a digital counter. The rotational speed of the impeller was obtained by measuring the time taken for the impeller to do one revolution.

The heating of the cathode was effected by means of a 64mm diameter heating element (supplied as a 450W, 240V coffee percolator element from Metway Electrical Industries Ltd) tightly clamped between the cathode and the base plate. The wiring arrangement for the heating element is shown in Figure 3.7. The current flowing through the heating element was recorded by a digital multimeter (Model 7045 supplied by Solartron Electronic Group Ltd). Three

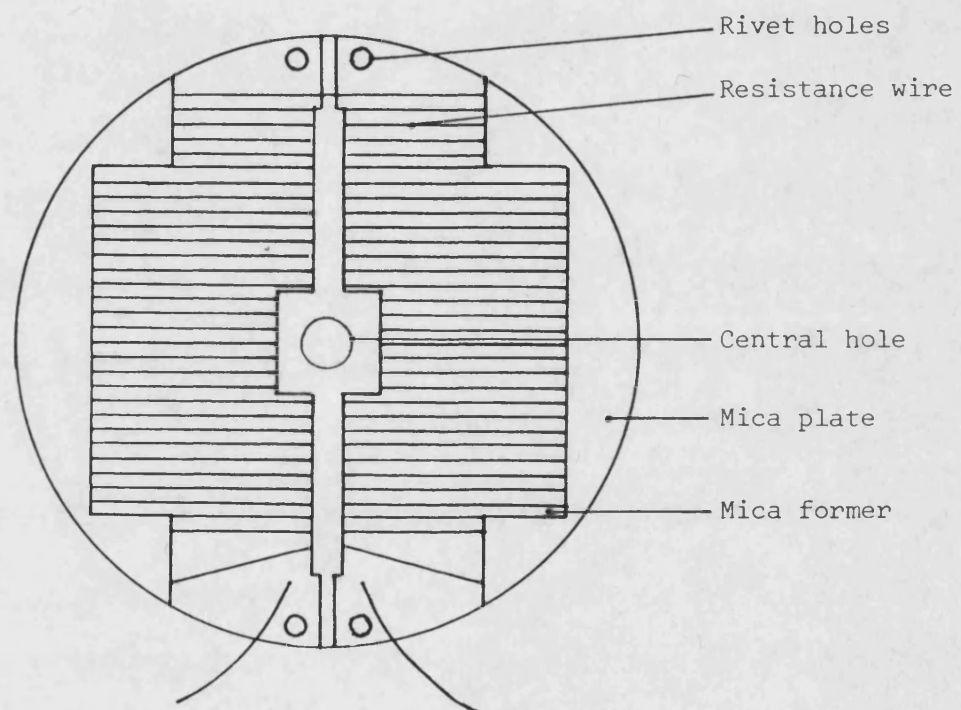


FIGURE 3.7 THE WIRING ARRANGEMENT FOR THE HEATING ELEMENT.

sheathed copper/constantan thermocouples were silver-soldered into notches cut into the base of the cathode at positions shown in Figure 3.4. These thermocouples were connected to a 10 channel temperature indicator (Type 141 supplied by Eurotherm Ltd). The surface temperature of the cathode was controlled by a PID temperature controller (Type 020 supplied by Eurotherm Ltd) via a feedback control loop incorporating the heating element and the thermocouple at position 3 as shown in Figure 3.4.

In order to maintain a temperature difference between the cathode and the bulk solution, the cooling of the electrolytic solution was effected by passing cooling water through a glass coil rigidly suspended from the top plate cover. The temperature of the bulk solution was measured via a sheathed copper/constantan thermocouple connected to the 10 channel temperature indicator. The temperature of the base plate and the ambient temperature were measured via two copper/constantan thermocouples connected to the 10 channel temperature indicator.

To minimise the exposure of the electrolytic solution to air, an air free - nitrogen atmosphere was maintained in the mixing cell.

3.2.2 Electrical circuit

The electrical circuit for the electrolytic mixing cell is shown in Figure 3.4. The potential applied across the cell was provided by a 1A/30V variable output stabilised power supply (Model 400 supplied by Weir Instrumentation Ltd). This applied potential was measured by the Solartron digital multimeter. The current flowing through the cell was measured by a x-θ pen chart recorder (Model PM8202 supplied by Pye Unicam Ltd) via the potential difference across a standard 10Ω resistor.

3.3 Experimental procedure

The experimental procedure can be summarised as follows:

1. Preparation of the electrolytic solution
2. Preparation of the electrodes
3. Assembly of the electrolytic mixing cell
4. Data acquisition

3.3.1 Preparation of the electrolytic solution

The electrolytic solution of the following concentration

Potassium ferricyanide 0.005M

Potassium ferrocyanide 0.005M

Sodium hydroxide 0.5M

was carefully prepared in a 5l volumetric flask. To prevent the degradation of the electrolytic solution in air and light, the solution was transferred to several 1l brown polythene concertina-shaped bottles (Type BGE440 supplied by Fisons Scientific Apparatus Ltd). Before the solution was used for an experiment, the concentration of the solution was checked by titrimetric analysis. The details of titrimetric analysis are given in Appendix A5.

3.3.2 Preparation of the electrodes

Before assembling the electrolytic mixing cell, care was taken to ensure the nickel electrodes were properly cleaned and activated. The electrodes were polished with progressively finer grades of emery paper, washed with detergent, rinsed with distilled water and finally degreased with carbon tetrachloride. The electrodes were then activated in 2M NaOH solution for 5 minutes.

An electron micrograph of 35X magnification taken of a 3mm x 3mm section that was carefully sawn out of the nickel electrode as shown in Figure 3.8 after it was cleaned and activated is given in Figure 3.9. To enable a quantitative assessment to be made of the surface texture characteristics of the cathode, a Talysurf (Model 10 supplied by Rank Taylor Hobson Ltd) was used. The Talysurf uses a stylus in the form of a four-sided 90° diamond pyramid with a slightly rounded tip of 0.0025mm wide bearing on the surface with a force of $1 \times 10^{-3}\text{N}$ to trace the profile of the surface. Eight measurements were conducted along the 10mm lengths designated by the letters A-H in Figure 3.8. The results obtained from the Talysurf traces shown in Figure 3.10 are given in Table 3.6.

It can be concluded from the results given in Table 3.6 that the surface roughness increases radially from the centre of the cathode. A possible explanation for this non-uniformity could be due to the difficulty in the polishing of the cathode surface which was slightly bowed. The bowing of the

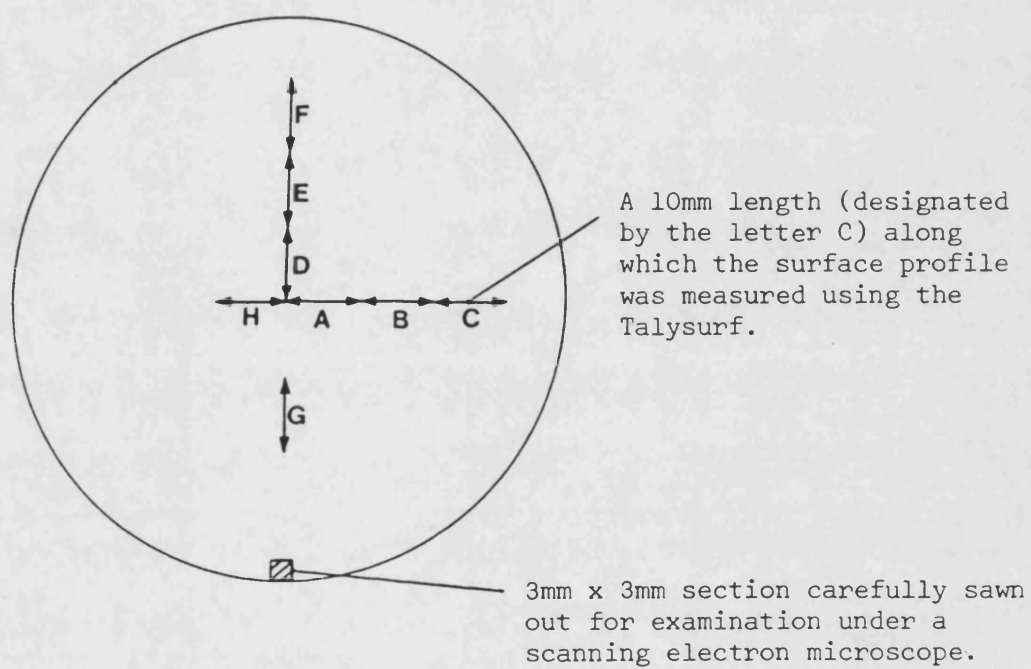
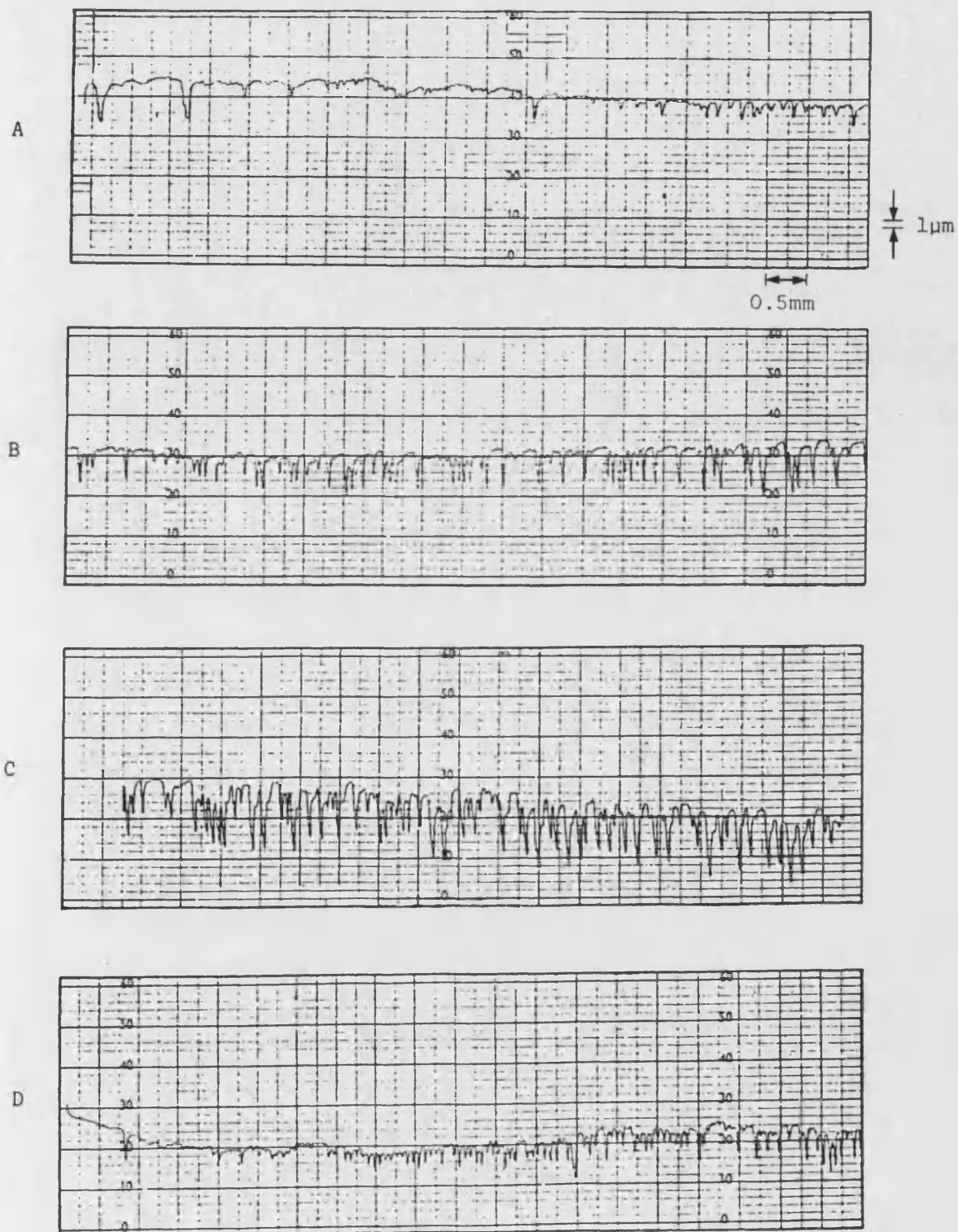


FIGURE 3.8 AREAS OF EXAMINATION ON THE CATHODE FOR THE SCANNING ELECTRON MICROSCOPE AND THE TALYSURF.

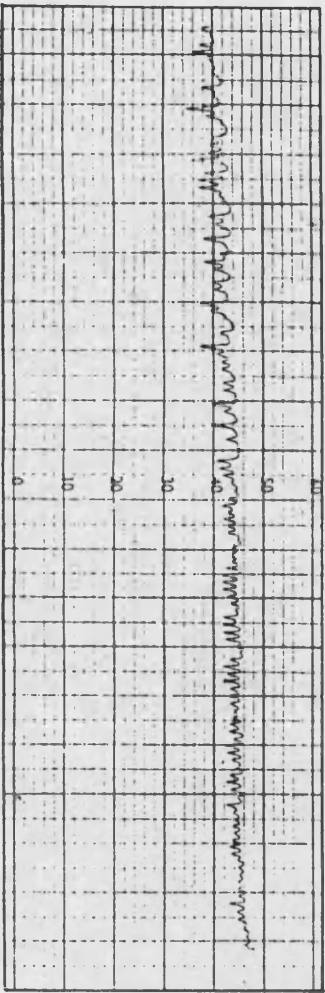


FIGURE 3.9 AN ELECTRON MICROGRAPH OF THE 3MM X 3MM SECTION THAT WAS CAREFULLY SAWN OUT OF THE NICKEL CATHODE AS SHOWN IN FIGURE 3.10 AFTER IT WAS CLEANED AND ACTIVATED

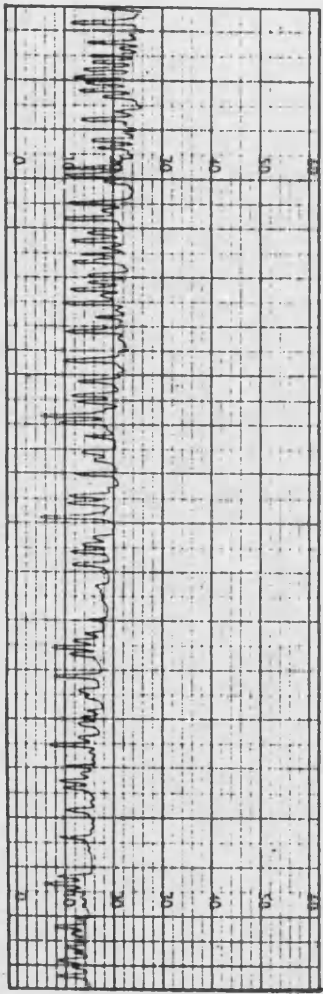
FIGURE 3.10 TALYSURF TRACES ALONG THE 10MM LENGTHS DESIGNATED BY THE LETTERS A - H IN FIGURE 3.8.



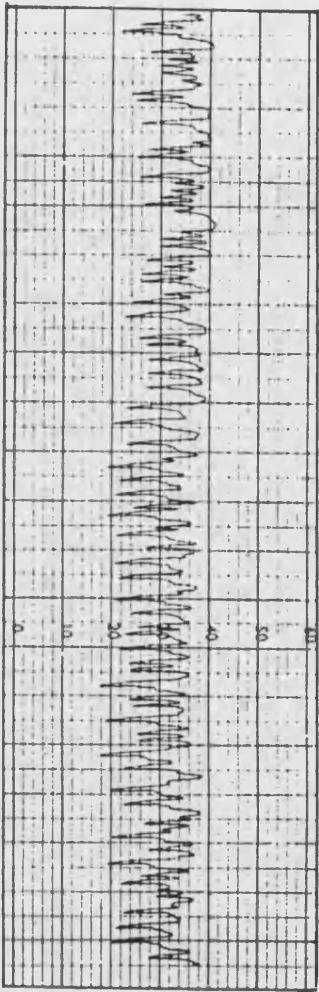
H



G



F



E

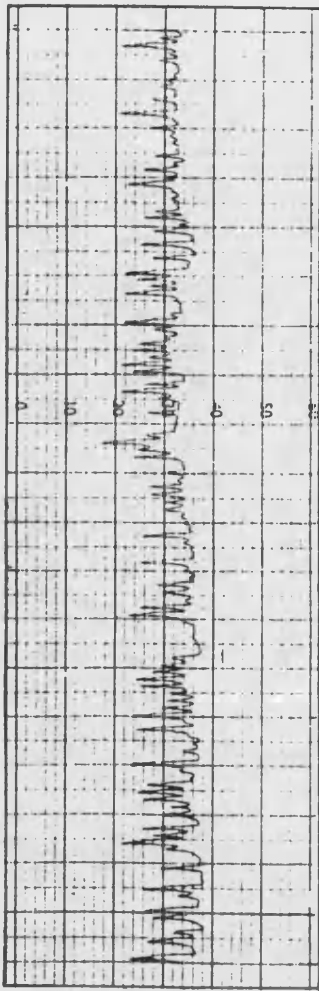
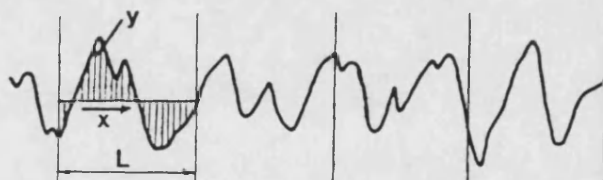


TABLE 3.6 TALYSURF TRACE RESULTS

LENGTH	AVERAGE PEAK TO VALLEY HEIGHT ¹ (μm)	MAXIMUM PEAK TO VALLEY HEIGHT ² (μm)	AVERAGE WAVELENGTH ³ (mm)	Δ_a ⁴
A	0.48	3.3	0.061	0.044
B	1.1	6.2	0.085	0.066
C	1.8	9.4	0.087	0.109
D	0.8	4.6	0.060	0.073
E	1.4	8.3	0.080	0.091
F	2.2	9.5	0.093	0.117
G	1.6	9.2	0.082	0.096
H	0.75	4.7	0.070	0.052

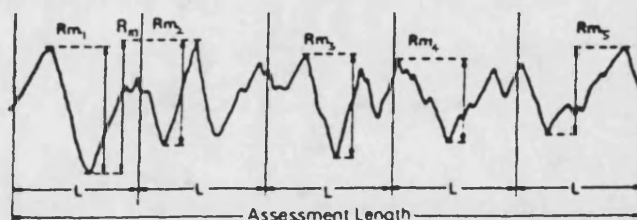
¹ The average peak to valley height, R_a is given by

$$R_a = \frac{1}{L} \int_0^L |y(x)| dx$$



² The maximum peak to valley height, R_m is given by

$$R_m = \frac{1}{5} \sum_{i=1}^{i=5} R_{m_i}$$



³ The average wavelength, λ_a is a measure of the spacings between the local peaks and valleys, taking into account their relative amplitudes and individual spatial frequencies.

⁴ Δ_a is the average of rms value of the slope of the profile throughout its length. From this value, the ratio of the actual profile length to the nominal measured length can be estimated from

$$\frac{\text{Actual}}{\text{Nominal}} \approx 1 + \frac{1}{2}(\Delta_a)^2$$

cathode surface was caused by the heat generated throughout the cathode when the central rod and the thermocouples were silver-soldered into the base of the cathode.

However, an order of magnitude estimate of the surface texture characteristics of the cathode can be obtained by taking the mean of the results given in Table 3.6. Thus, from Table 3.6,

$$(R_a)_{\text{mean}} = 1.27\mu\text{m}$$

$$(R_m)_{\text{mean}} = 6.9\mu\text{m}$$

$$(\lambda_a)_{\text{mean}} = 0.077\text{mm}$$

$$(\Delta_a)_{\text{mean}} = 0.081$$

Using $(\Delta_a)_{\text{mean}} = 0.081$, the mean ratio of actual profile length to the nominal measured length was found to be 1.033. In other words, there will be an error of 0.033% if the diameter of the cathode rather than the actual profile length across the diameter of the cathode is used in the calculations. Due to this small error, the cathode was assumed to be 'smooth'.

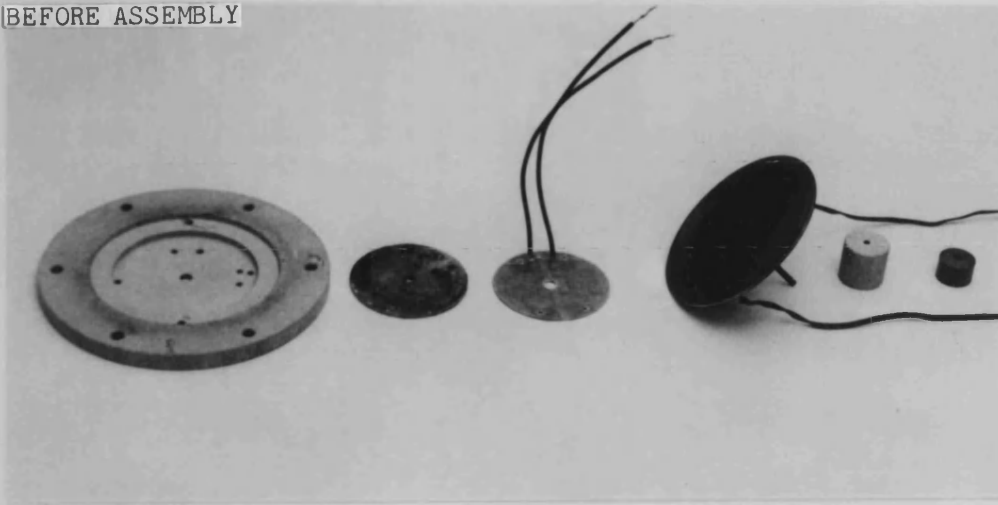
3.3.3 Assembly of the electrolytic mixing cell

The procedure for the assembly of the electrolytic mixing cell was as follows:

After the assembly of the base plate accessories as shown in Figure 3.11, the mixing cell was assembled by tightening the six tie rods which sandwich the perspex cylinder with the neoprene gaskets between the end plates. The mixing cell was then filled with the electrolytic solution that was stored in one of the several 1l brown concertina-shaped bottles to a height of 120mm. If required in the experiment, one or more layers of glass spherical particles of known dimensions was added onto the surface of the cathode. After the assembly of the top plate cover accessories as shown in Figure 3.12, the top plate cover and its accessories were carefully mounted into the mixing cell. It was then ensured that

1. a thermocouple connected to the temperature indicator was inserted into the electrolytic solution
2. The nitrogen line was attached to the mixing cell and flow switched on
3. the impeller was attached to the stirrer motor
4. the cooling water line was connected to the cooling water coil

BEFORE ASSEMBLY



AFTER ASSEMBLY

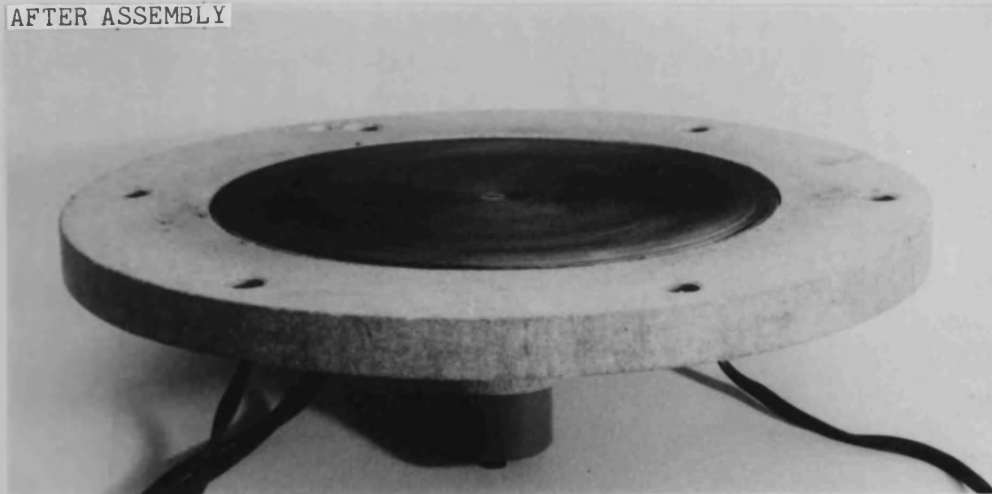
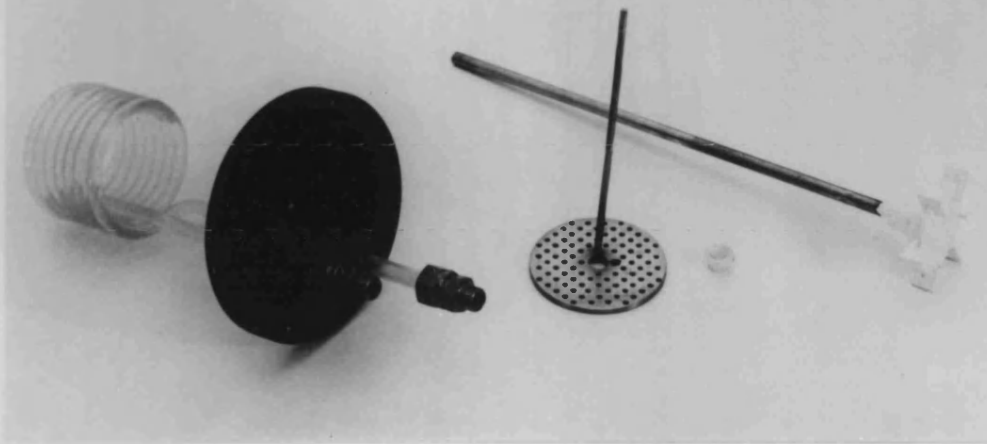


FIGURE 3.11 THE ASSEMBLY OF THE BASE PLATE ACCESSORIES

BEFORE ASSEMBLY



AFTER ASSEMBLY

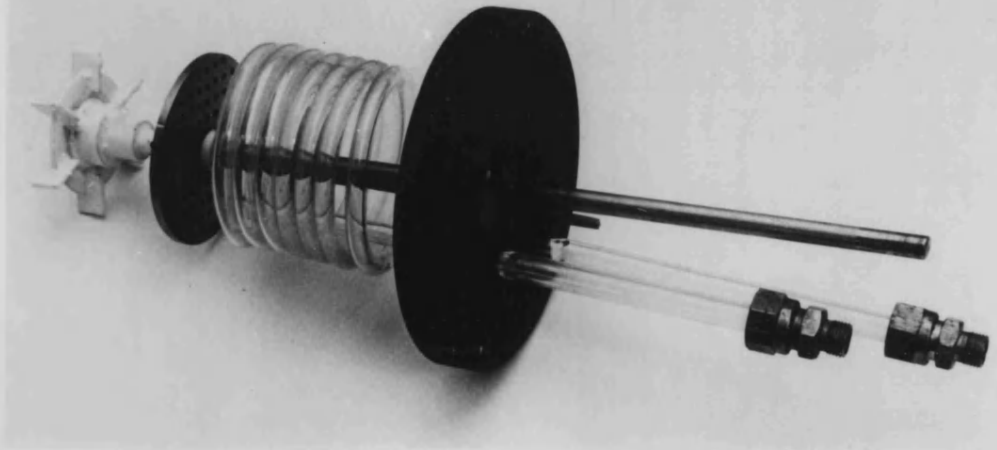


FIGURE 3.12 THE ASSEMBLY OF THE TOP PLATE COVER ACCESSORIES

5. a thermocouple connected to the temperature indicator was inserted into the base plate
6. the wires of the heating element and the thermocouple that was silver-soldered into the base of the cathode at position 3 were connected to the heating circuit
7. all the thermocouples that were silver-soldered into the base of the cathode were connected to the temperature indicator
8. the electrodes were connected to the electrical circuit

3.3.4 Data acquisition

For each of the various experimental conditions studied in the electrolytic mixing cell (see Table 3.7), the following data were determined:

1. the current - potential curve as a function of the impeller rotational speed
2. The limiting current as a function of the impeller rotational speed

3.3.4.1 Determination of the current - potential curve as a function of the impeller rotational speed

For a given impeller rotational speed, the data for the current - potential curve was obtained by deriving the average current from the current - time traces that were recorded at different applied cell potentials over a range of 0-2V. This was repeated for different impeller rotational speeds.

3.3.4.2 Determination of the limiting current as a function of the impeller rotational speed

From the current - potential curves determined in section 3.3.4.1, a potential that corresponds to the limiting current condition for all the curves was selected. By setting the power supply at this potential, the variation of the limiting current with the impeller rotational speed was obtained by deriving the average limiting current from the limiting current - time traces that were recorded at different impeller rotational speeds over a range of 0-350rpm.

In addition to the above data, the following variables necessary for mass transfer calculations, ie

TABLE 3.7 A SUMMARY OF THE VARIOUS EXPERIMENTAL CONDITIONS STUDIED IN THE
ELECTROLYTIC MIXING CELL

		MASS TRANSFER	MASS AND HEAT TRANSFER
<u>Glass spherical particles</u>			
<u>d_p (mm)</u>	<u>n₁</u>		
NONE		✓	✓
0.368	1	✓	
	2	✓	
	3	✓	
0.695	1	✓	
	2	✓	
	3	✓	
	4	✓	
0.805	1	✓	
	2	✓	
	3	✓	
	4	✓	
	5	✓	
	6	✓	
1.290	1	✓	
	2	✓	
	3	✓	
	4	✓	
1.340	1	✓	
	2	✓	
	3	✓	
	4	✓	
	5	✓	
	6	✓	
1.550	1	✓	
	2	✓	
	3	✓	
	4	✓	
	5	✓	
	6	✓	
3.000	1	✓	✓
	2	✓	✓
	3	✓	
	4	✓	
	5	✓	
	6	✓	
	7	✓	
5.000	1	✓	
	2	✓	
	3	✓	
	4	✓	
7.000	1	✓	
	2	✓	
	3	✓	
10.000	1	✓	✓
	2	✓	✓
12.000	1	✓	✓
	2	✓	✓

Bulk solution temperature, T_b

Cathode surface temperatures, T_{s1} , T_{s2} , T_{s3}

and for heat transfer calculations, ie

Bulk solution temperature, T_b

Cathode surface temperatures, T_{s1} , T_{s2} , T_{s3}

Base plate temperature, T_w

Ambient temperature, T_a

Heater current, I_h

were also recorded during the experimental run.

4. EXPERIMENTAL RESULTS AND OBSERVATIONS

The results obtained for the various experimental conditions in the electrolytic mixing cell listed in Table 3.7 are discussed in two main sections:

1. Mass transfer studies
2. Mass and heat transfer studies

4.1 Mass transfer studies

4.1.1 Mass transfer in the electrolytic mixing cell without the presence of glass spherical particles on the cathode

The variation of average current with potential as a function of the impeller rotational speed for the electrolytic mixing cell without the presence of glass spherical particles on the cathode is shown in Figure 4.1. The data used in Figure 4.1 are given in Appendix A6.1. The reproducibility of the current-potential curves in Figure 4.1 was checked by carrying out several determinations of each current-potential curve. As an example, Figure 4.2 illustrates the several determinations of the current-potential curve at an impeller rotational speed of 34.8 ± 2.8 rpm. The data used in Figure 4.2 are given in Appendix A6.2. It was found the current-potential curves in Figure 4.1 are reproducible to within $\pm 5\%$.

It can be seen from Figure 4.1 that the limiting current is attained for all the current-potential curves when the potential is in the range of 0.8 - 1.4 volts. By setting the potential at $\sim 0.9V$, the average limiting current, I_L can be measured as a function of the impeller rotational speed, N . The $I_L - N$ data derived from Figures 4.1 and 4.2 and the $I_L - N$ data derived from several other runs are given in Appendix A6.3.

Since free and forced convection mass transfer can occur in agitated vessels, it is customary to assume^(324,381)

1. free convection mass transfer \gg forced convection mass transfer at very low Re
2. forced convection mass transfer \gg free convection mass transfer at higher Re

FIGURE 4.1 CURRENT-POTENTIAL CURVES AS A FUNCTION OF THE IMPELLER ROTATIONAL SPEED FOR THE ELECTROLYTIC MIXING CELL WITHOUT THE PRESENCE OF GLASS SPHERICAL PARTICLES ON THE CATHODE

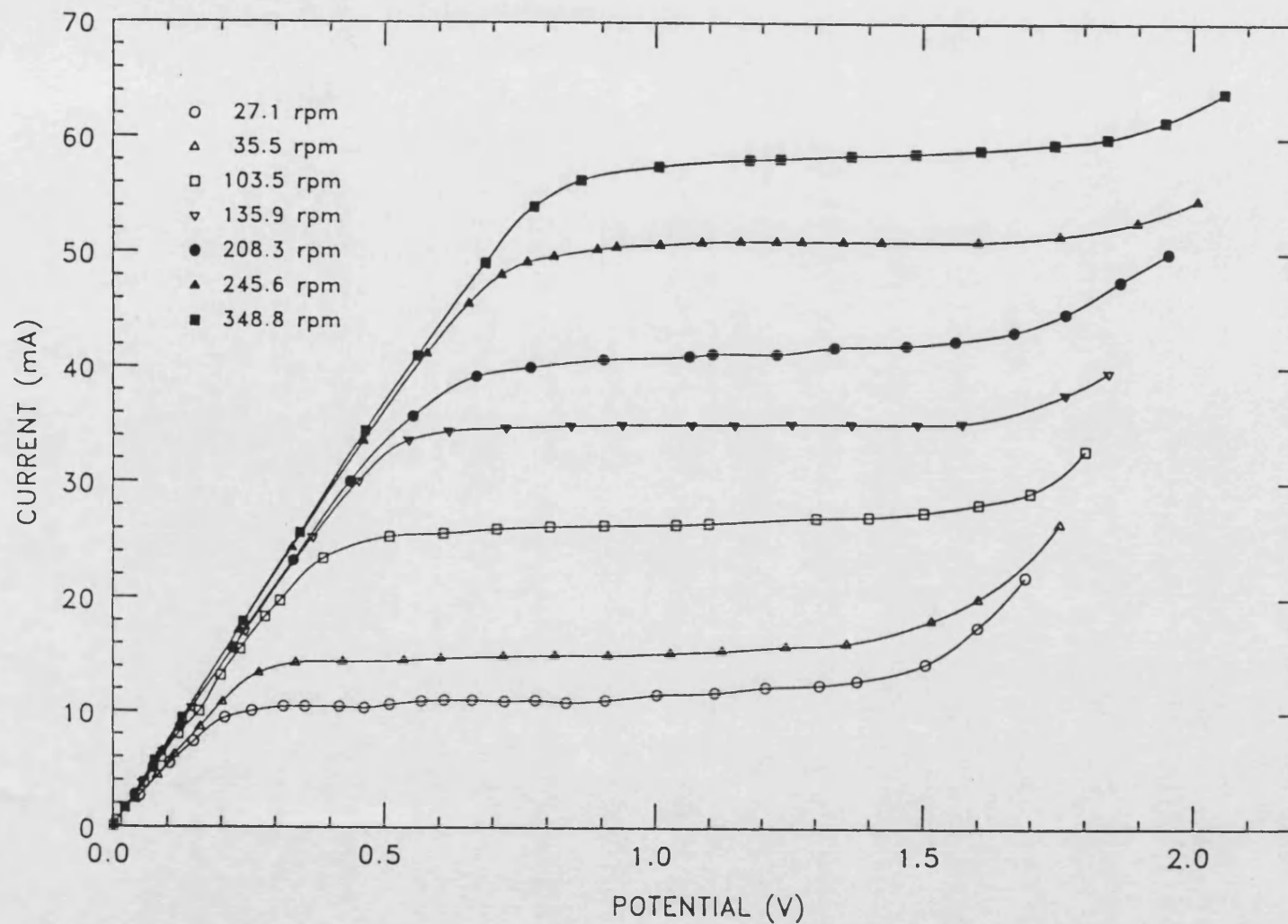
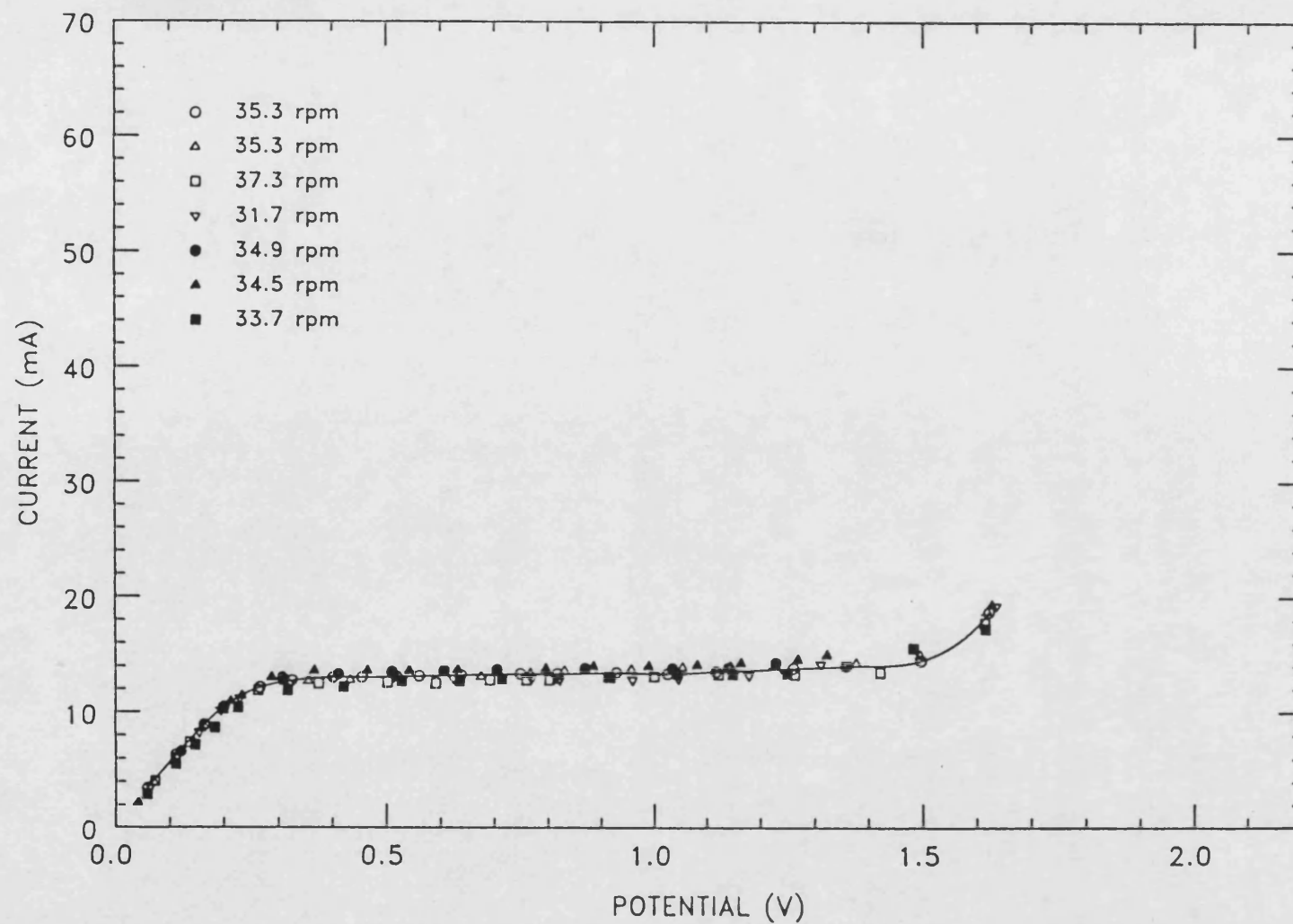


FIGURE 4.2 SEVERAL DETERMINATIONS OF THE CURRENT-POTENTIAL CURVE AT AN IMPELLER ROTATIONAL SPEED OF 34.8 ± 2.8 rpm FOR THE ELECTROLYTIC MIXING CELL WITHOUT THE PRESENCE OF GLASS SPHERICAL PARTICLES ON THE CATHODE



where Re is defined by

$$Re = \frac{d_i^2 N}{\nu} \quad 4.1$$

where d_i = impeller diameter

4.1.1.1 Free convection mass transfer

Free convection mass transfer is usually expressed in terms of

$$Sh = a (Gr_m Sc)^b \quad 4.2$$

where a and b are constants. For cylindrical vessels with horizontal electrodes, Sh , Gr_m and Sc in equation 4.1 are defined by equations 4.3, 4.4 and 2.11 respectively⁽³⁸²⁾

$$Sh = \frac{kd}{D} = \frac{I_L d}{zFADc_b} \quad 4.3$$

$$Gr_m = \frac{gd^3}{\nu^2} \left[\frac{\Delta\rho}{\rho} \right]_m \quad 4.4$$

where d = cathode diameter

For all the I_L-N data where $N = 0$ rpm given in Table A6.3.3, mass transfer in the electrolytic cell was by free convection. By taking Run 1.01 of Table A6.3.3 (ie. $N = 0$ rpm, $I_L = 0.8$ mA, $c_b = 0.005$ M, $T_b = 21^\circ\text{C}$) as an example, the calculation of Sh , Re , Gr_m and Sc carried out by the computer program MASS given in Appendix A7.1 was as follows:

The physical properties of the electrolytic solution required for the dimensionless numbers were calculated at the bulk solution temperature. Hence,

1. the density of the electrolytic solution given by equation 3.1 was found to be

$$\begin{aligned} \rho &= 1.03052 - 2.142 \times 10^{-4}(21) - 6.6 \times 10^{-6}(21)^2 \\ &= 1.0231 \text{ g/cm}^3 \end{aligned}$$

2. the kinematic viscosity of the electrolytic solution given by equation 3.2 was found to be

$$\nu = \exp \frac{1.8710 \times 10^3}{21.0 + 273.15} - 6.3004$$

$$= 1.06215 \text{ mm}^2/\text{s}$$

3. the viscosity of the electrolytic solution given by equation 4.5 was found to be

$$\begin{aligned} \mu &= \nu \times \rho & 4.5 \\ &= 1.06215 \times 10^{-2} \times 1.0231 \\ &= 1.0867 \times 10^{-2} \text{ g/cm s} \end{aligned}$$

4. the diffusivity of the electrolytic solution given by equation 3.4 was found to be

$$\begin{aligned} D &= \frac{2.50 \times 10^{-10} (21.0 + 273.15)}{1.0867 \times 10^{-2}} \\ &= 6.7670 \times 10^{-6} \text{ cm}^2/\text{s} \end{aligned}$$

The transference number for each species in the electrolytic solution required in the evaluation of $\left[\frac{\Delta \rho}{\rho} \right]_m$ was found equation 3.23 to be

$$\begin{aligned} t_{\text{Fe(CN)}_6^{3-}} &= \frac{3(100.9)(0.005 \times 10^{-3})}{3(100.9)(0.005 \times 10^{-3}) + 4(110.5)(0.005 \times 10^{-3}) + 1(197.6)(0.5 \times 10^{-3}) + 1(50.11)(0.5 \times 10^{-3}) + 1(73.52)(0.035 \times 10^{-3})} \\ &= 0.0116 \end{aligned}$$

$$\begin{aligned} t_{\text{Fe(CN)}_6^{4-}} &= \frac{4(110.5)(0.005 \times 10^{-3})}{3(100.9)(0.005 \times 10^{-3}) + 4(110.5)(0.005 \times 10^{-3}) + 1(197.6)(0.5 \times 10^{-3}) + 1(50.11)(0.5 \times 10^{-3}) + 1(73.52)(0.035 \times 10^{-3})} \\ &= 0.0170 \end{aligned}$$

$$\begin{aligned} t_{\text{OH}^-} &= \frac{1(197.6)(0.5 \times 10^{-3})}{3(100.9)(0.005 \times 10^{-3}) + 4(110.5)(0.005 \times 10^{-3}) + 1(197.6)(0.5 \times 10^{-3}) + 1(50.11)(0.5 \times 10^{-3}) + 1(73.52)(0.035 \times 10^{-3})} \\ &= 0.7591 \end{aligned}$$

$$\begin{aligned} t_{\text{Na}^+} &= \frac{1(50.11)(0.5 \times 10^{-3})}{3(100.9)(0.005 \times 10^{-3}) + 4(110.5)(0.005 \times 10^{-3}) + 1(197.6)(0.5 \times 10^{-3}) + 1(50.11)(0.5 \times 10^{-3}) + 1(73.52)(0.035 \times 10^{-3})} \\ &= 0.1925 \end{aligned}$$

$$\begin{aligned} t_{\text{K}^+} &= \frac{1(73.52)(0.035 \times 10^{-3})}{3(100.9)(0.005 \times 10^{-3}) + 4(110.5)(0.005 \times 10^{-3}) + 1(197.6)(0.5 \times 10^{-3}) + 1(50.11)(0.5 \times 10^{-3}) + 1(73.52)(0.035 \times 10^{-3})} \\ &= 0.0198 \end{aligned}$$

The ratio $\left[\frac{\Delta\rho}{\rho}\right]_m$ for the electrolytic solution required in the evaluation of Gr_m was found from equation 3.19 to be

$$\left[\frac{\Delta\rho}{\rho}\right]_m = 167.27\Delta c_{Fe(CN)_6^{3-}} + 225.91\Delta c_{Fe(CN)_6^{4-}} + 45.29\Delta c_{OH^-} - 6.73\Delta c_{Na^+}$$

$$\text{where } \Delta c_{Fe(CN)_6^{3-}} = 5 \times 10^{-6} \text{ mole/cm}^3$$

$$\begin{aligned} \Delta c_{Fe(CN)_6^{4-}} &= \left[\frac{1 + \frac{0.0170}{4}}{-1 + \frac{0.0116}{3}} \right] \left[\frac{0.896 \times 10^{-5}}{0.739 \times 10^{-5}} \right]^{\frac{1}{3}} (0.005 \times 10^{-3}) \\ &= -5.8242 \times 10^{-6} \text{ mole/cm}^3 \end{aligned}$$

$$\begin{aligned} \Delta c_{OH^-} &= \left[\frac{-\frac{0.7591}{(-1)}}{-1 + \frac{0.0116}{3}} \right] \left[\frac{0.896 \times 10^{-5}}{5.260 \times 10^{-5}} \right]^{\frac{1}{3}} (0.005 \times 10^{-3}) \\ &= -1.0103 \times 10^{-6} \text{ mole/cm}^3 \end{aligned}$$

$$\begin{aligned} \Delta c_{Na^+} &= \left[\frac{-\frac{0.1925}{1}}{-1 + \frac{0.0116}{3}} \right] \left[\frac{0.896 \times 10^{-5}}{1.334 \times 10^{-5}} \right]^{\frac{1}{3}} (0.005 \times 10^{-3}) \\ &= 0.7059 \times 10^{-6} \text{ mole/cm}^3 \end{aligned}$$

$$\text{ie. } \left[\frac{\Delta\rho}{\rho}\right]_m = -5.3000 \times 10^{-4}$$

Using the above physical property data, it was found that

1. the Sherwood number defined by equation 4.3 is given by

$$\begin{aligned} Sh &= \frac{0.8 \times 10^{-3} \times 7.6}{1 \times 96487 \times \frac{\pi}{4} (7.6)^2 \times 6.7670 \times 10^{-6} \times 0.005 \times 10^{-3}} \\ &= 41.1 \end{aligned}$$

2. the Reynolds number defined by equation 4.1 is given by

$$\begin{aligned} \text{Re} &= \frac{(5.1)^2 \times \frac{0}{60}}{1.06215 \times 10^{-2}} \\ &= 0 \end{aligned}$$

3. the Grashof number for mass transfer defined by equation 4.4 is given by

$$\begin{aligned} \text{Gr}_m &= \frac{980.655 \times (7.6)^3}{(1.06215 \times 10^{-2})^2} \times |-5.3000 \times 10^{-4}| \\ &= 2.0224 \times 10^6 \end{aligned}$$

4. the Schmidt number defined by equation 2.11 is given by

$$\begin{aligned} \text{Sc} &= \frac{1.06215 \times 10^{-2}}{6.7670 \times 10^{-6}} \\ &= 1569.6 \end{aligned}$$

The derived data obtained from the computer program MASS for all the I_L - N data where $N = 0$ rpm is tabulated in Table A6.3.3.

For free convection mass transfer at horizontal electrodes, several investigators^(318,382-386) have found by experiment that the exponent b in equation 4.2 to be $\frac{1}{4}$ in the laminar regime where $\text{Gr}_m \text{Sc} < 3 \times 10^7$ and $\frac{1}{3}$ in the turbulent regime where $\text{Gr}_m \text{Sc} > 3 \times 10^7$. Since $\text{Gr}_m \text{Sc} > 3 \times 10^7$ in this study, it was reasonable to assume that the exponent b in equation 4.2 is $\frac{1}{3}$. Thus, equation 4.2 can be rewritten as

$$\text{Sh} = a (\text{Gr}_m \text{Sc})^{\frac{1}{3}} \quad 4.6$$

The derived data for all the runs where $N = 0$ rpm given in Table A6.3.3 were plotted in Figure 4.3 as Sh versus $\text{Gr}_m \text{Sc}$ on logarithmic co-ordinates. Due to $\text{Gr}_m \text{Sc}$ being almost identical for each of the runs plotted in Figure 4.3, no attempt was made to evaluate a in equation 4.6. Of the correlations listed in Table 4.1 that have been proposed by various investigators for free convection mass transfer at horizontal electrodes, the correlation proposed by Wragg et al^(382,384,385)

$$\text{Sh} = 0.18 (\text{Gr}_m \text{Sc})^{\frac{1}{3}} \quad 4.7$$

was used for the comparison with the data given in Figure 4.3. This correlation was selected in preference to the other correlations listed in

FIGURE 4.3 A PLOT OF Sh VERSUS $Gr_m Sc$ SHOWING THE COMPARISON BETWEEN THE DATA GIVEN IN TABLE A6.3.3 WHERE $N = 0$ rpm AND WRAGG ET AL'S CORRELATION GIVEN BY EQUATION 4.7

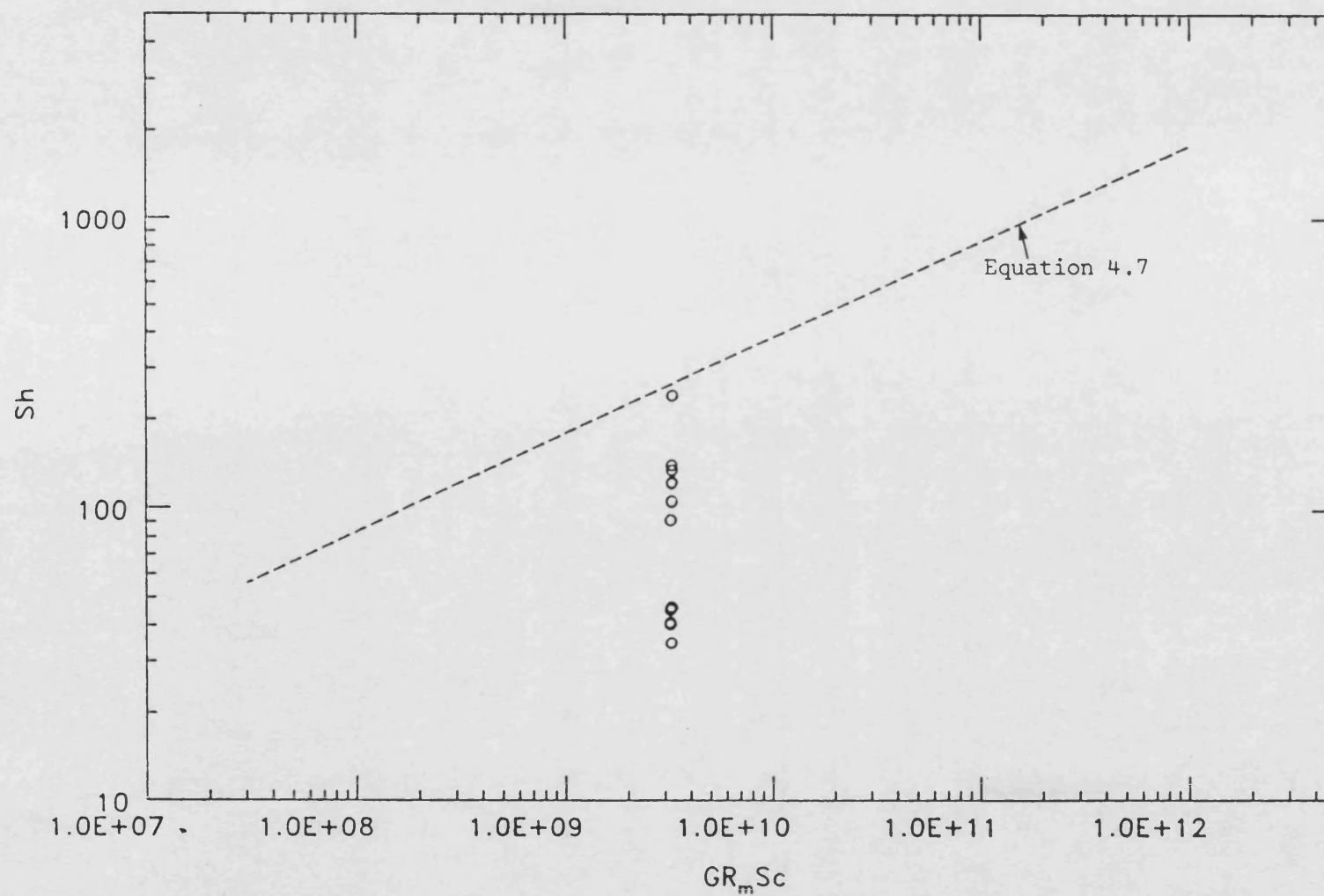


TABLE 4.1 CORRELATIONS FOR FREE CONVECTION MASS TRANSFER AT HORIZONTAL ELECTRODES

REGIME	AUTHOR	ELECTROCHEMICAL SYSTEM	CORRELATION ^a	Gr _m Sc RANGE
LAMINAR	Lloyd and Moran ⁽³⁸³⁾	CuSO ₄ /H ₂ SO ₄	Sh _l = 0.54 (Gr _m Sc) ^{0.25}	2.2 × 10 ⁴ - 8 × 10 ⁶
	Wragg et al ^(382,384,385)	CuSO ₄ /H ₂ SO ₄	Sh _d = 0.72 (Gr _m Sc) ^{0.25}	3 × 10 ⁴ - 3 × 10 ⁷
TURBULENT	Fenech and Tobias ⁽³⁸⁶⁾	CuSO ₄ /H ₂ SO ₄	Sh _{y_{cd}} = 0.19 (Gr _m Sc) ^{0.3333}	1 × 10 ⁸ - 1.4 × 10 ¹²
	Wragg et al ^(382,384,385)	CuSO ₄ /H ₂ SO ₄	Sh _d = 0.18 (Gr _m Sc) ^{0.3333}	3 × 10 ⁷ - 1 × 10 ¹²
	Ravoo ⁽³¹⁸⁾	CuSO ₄ /H ₂ SO ₄	Sh _{y_{fl}} = 0.152 (Gr _m Sc) ^{0.3333}	6 × 10 ⁶ - 5 × 10 ¹²
		K ₃ Fe(CN) ₆ /K ₄ Fe(CN) ₆ /NaOH		
	Lloyd and Moran ⁽³⁸³⁾	CuSO ₄ /H ₂ SO ₄	Sh _l = 0.15 (Gr _m Sc) ^{0.3333}	8 × 10 ⁶ - 1.6 × 10 ⁹

^a The subscript on Sh represents the parameter that was used to represent the characteristic length l in Sh and Gr_m

l = A/p where A = area of cathode surface
p = perimeter of cathode

d = cathode diameter

y_{cd} = vertical distance between the cathode and the horizontal diaphragm

y_{fl} = free liquid distance in the direction normal to the cathode

Table 4.1. since the use of the cathode diameter as the characteristic length in the calculation of Sh and Gr_m for equation 4.7 is identical to that used to calculate Sh and Gr_m in this study. It can be seen from Figure 4.3 that there is little agreement between the data given in Table A6.3.3 and equation 4.7.

4.1.1.2 Forced convection mass transfer

Forced convection mass transfer is usually expressed in the form of Gilliland - Sherwood correlation⁽³⁸⁷⁾

$$Sh = a Re^b Sc^c \quad 4.8$$

where a , b and c are constants. For agitated vessels, Sh , Re and Sc in equation 4.8 are defined by equations 4.3, 4.1 and 2.11 respectively⁽³⁸⁸⁾.

For all the $I_L - N$ data where $N > 0$ rpm given in Appendix A6.3, mass transfer in the electrolytic mixing cell was by forced convection. The calculation of Sh , Re and Sc for this data (see example given in Section 4.1.1.1) was carried out by the computer program MASS given in Appendix A7.1. This derived data is tabulated in Appendix A6.3.

Several investigators have found by experiment that the exponent of Sc in the Gilliland - Sherwood correlation for agitated vessels is $\frac{1}{3}$. This is in agreement with the theoretical prediction of the boundary layer concept of mass transfer⁽³⁸⁸⁾. Thus equation 4.8 can be rewritten as

$$Sh = a Re^b Sc^{\frac{1}{3}} \quad 4.9$$

The values of a and b in equation 4.9 was determined by the least squares method since equation 4.9 can be linearised into

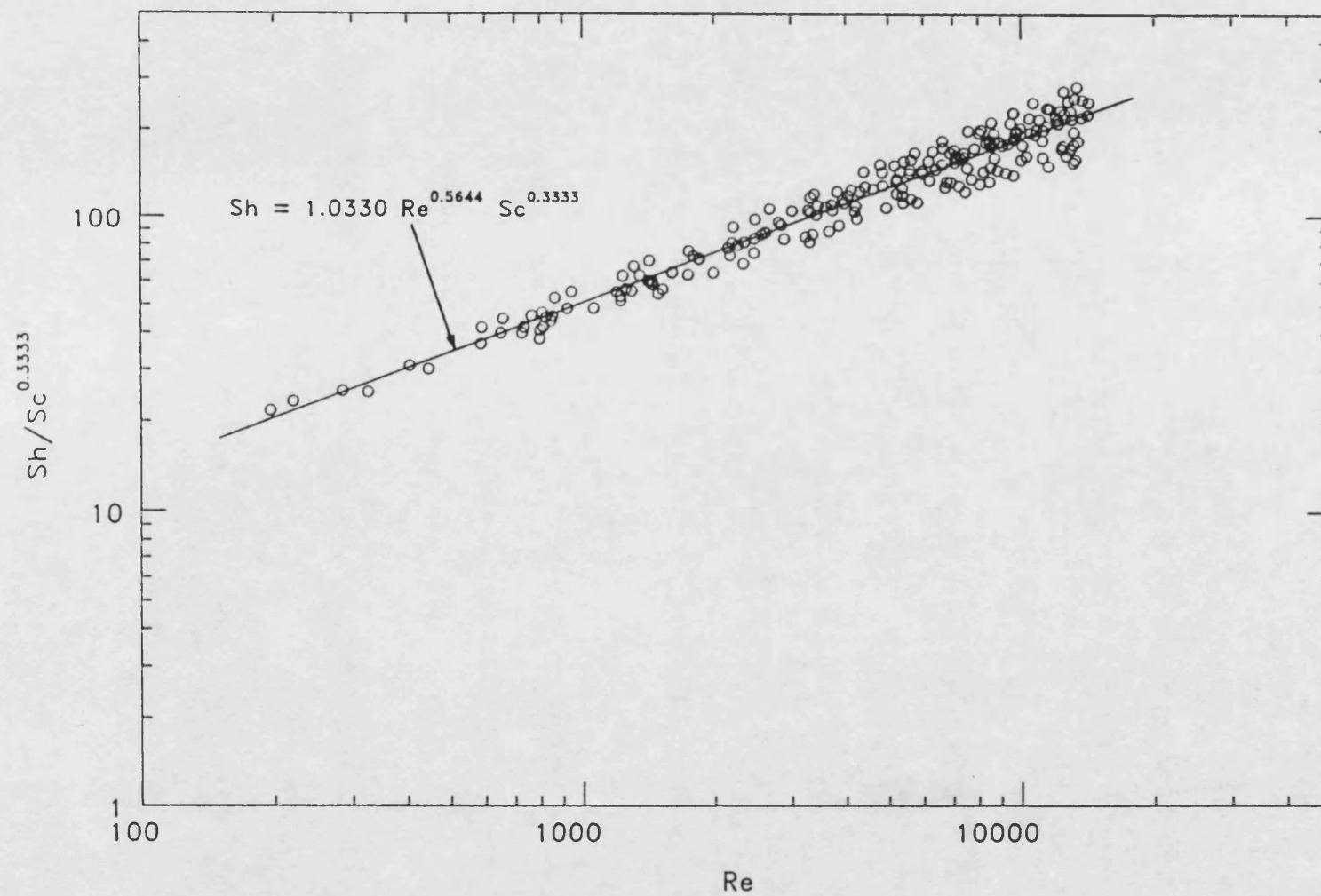
$$\ln \frac{Sh}{Sc^{\frac{1}{3}}} = \ln a + b \ln Re \quad 4.10$$

The derived data for all the runs where $N > 0$ rpm given in Appendix A6.3 were plotted in Figure 4.4 as $Sh/Sc^{\frac{1}{3}}$ versus Re on logarithmic co-ordinates. Using the least squares method, it was found that the 210 data points were correlated by

$$Sh = 1.0330 Re^{0.5644} Sc^{\frac{1}{3}} \quad 4.11$$

with a standard deviation of 0.1236. The correlation coefficient for equation 4.11 was found to be 97.6%.

FIGURE 4.4 A PLOT OF $Sh/Sc^{1/3}$ VERSUS Re FOR THE ELECTROLYTIC MIXING CELL WITHOUT THE PRESENCE OF GLASS SPHERICAL PARTICLES ON THE CATHODE



A summary of the correlations that have been proposed in the literature for forced convection mass transfer in agitated vessels where the impeller is of the turbine type is given in Table 4.2. It can be seen from Figure 4.5 that equation 4.11 is in reasonable agreement with the mass transfer correlations given in Table 4.2. Differences between equation 4.11 and the other mass transfer correlations can be attributed to the differences between the geometrical configuration of the mixing cell used in this study (see Table 4.3) and of the agitated vessels used in the other studies (see Table 4.2).

4.1.2 Mass transfer in the electrolytic mixing cell with the presence of glass spherical particles on the cathode

From the plots of average current with potential as a function of the impeller rotational speed for the electrolytic mixing cell with the presence of one or more layers of glass spherical particles of known dimensions on the cathode, it was found that a limiting current is obtained for each current-potential curve when the potential is the range of 0.8 - 1.4 volts. A typical plot is shown in Figure 4.6. Details of the data used in Figure 4.6 are given in Appendix A6.4.

By setting the potential at -0.9V, the average limiting current can be measured as a function of the impeller rotational speed. As an example, the variation of average limiting current with impeller rotational speed for the electrolytic mixing cell with the presence of 1 layer of 3mm glass spherical particles on the cathode is given in Figure 4.7. Details of the data used in Figure 4.7 are given in Appendix A6.5. Schematic diagrams of this layer at four different impeller rotational speeds are shown in Figure 4.8. From Figures 4.7 and 4.8, it can be seen that there are two regimes, namely

1. the glass spherical particles on the cathode behaving as a fixed bed at $N < N_f$
2. the glass spherical particles on the cathode behaving as a fluidised bed at $N > N_f$

where N_f is the impeller rotational speed at which fluidisation begins to occur. In this study, the I_L-N data for the electrolytic cell with the presence of one or more layers of glass spherical particles of known dimensions on the cathode was normally only obtained for $N < N_f$. This data is given in Appendix A6.6.

TABLE 4.2 CORRELATIONS FOR FORCED CONVECTION MASS TRANSFER IN AGITATED VESSELS

AUTHOR	VESSEL	IMPELLER	VESSEL DIMENSIONS								ELECTROCHEMICAL SYSTEM	CORRELATION	
			d_v (m)	$\frac{d_i}{d_v}$	$\frac{z_l}{d_v}$	$\frac{z_i}{d_v}$	$\frac{w_b}{d_i}$	$\frac{l_b}{d_i}$	n_B	$\frac{w_B}{d_v}$			
Mizushima et al ⁽³⁸⁹⁾	Flat bottomed cylindrical vessel	6 flat-bladed hub-mounted turbine	0.1	0.66	1.04	?	0.3-1.2	?	0	-	CuSO ₄ /H ₂ SO ₄ solution	$Sh = 0.36 Re^{\frac{1}{2}} Sc^{\frac{1}{3}}$	
Lelan and Angelino ^(390,391)	Flat bottomed cylindrical vessel	6 flat-bladed, disc-mounted turbine	0.28	0.22	1.0	0.2-0.8	?	?	0	-	Potassium ferricyanide/ Potassium ferrocyanide/ Sodium hydroxide solution	$Sh = \left\{ 0.990 - 0.290 \left[1 - 2 \frac{z_i}{d_v} + 2 \left[\frac{z_i}{d_v} \right]^2 \right] \right\} Re^{0.59} Sc^{\frac{1}{3}}$	
				0.333									$Sh = \left\{ 0.914 - 0.288 \left[\left[\frac{z_i}{d_v} - 1.02 \right]^2 + \left[\frac{z_i}{d_v} - 0.02 \right]^2 \right] \right\} Re^{0.61} Sc^{\frac{1}{3}}$
				0.475									$Sh = \left\{ 0.632 - 0.212 \left[1 - 2 \frac{z_i}{d_v} + 2 \left[\frac{z_i}{d_v} \right]^2 \right] \right\} Re^{0.65} Sc^{\frac{1}{3}}$
			0.28	0.22	1.0	0.2-0.8	?	?	4	?		$Sh = \left\{ 0.49 - 1.14 \frac{z_i}{d_v} \left[\frac{z_i}{d_v} - 1 \right] \right\} Re^{0.62} Sc^{\frac{1}{3}}$	
				0.333								$Sh = \left\{ 0.41 - 1.14 \frac{z_i}{d_v} \left[\frac{z_i}{d_v} - 1 \right] \right\} Re^{0.65} Sc^{\frac{1}{3}}$	
				0.475								$Sh = \left\{ 0.46 - 1.28 \frac{z_i}{d_v} \left[\frac{z_i}{d_v} - 1 \right] \right\} Re^{0.65} Sc^{\frac{1}{3}}$	

FIGURE 4.5 A PLOT OF $Sh/Sc^{1/3}$ VERSUS Re SHOWING THE COMPARISON BETWEEN EQUATION 4.11 AND THE MASS TRANSFER CORRELATIONS GIVEN IN TABLE 4.2

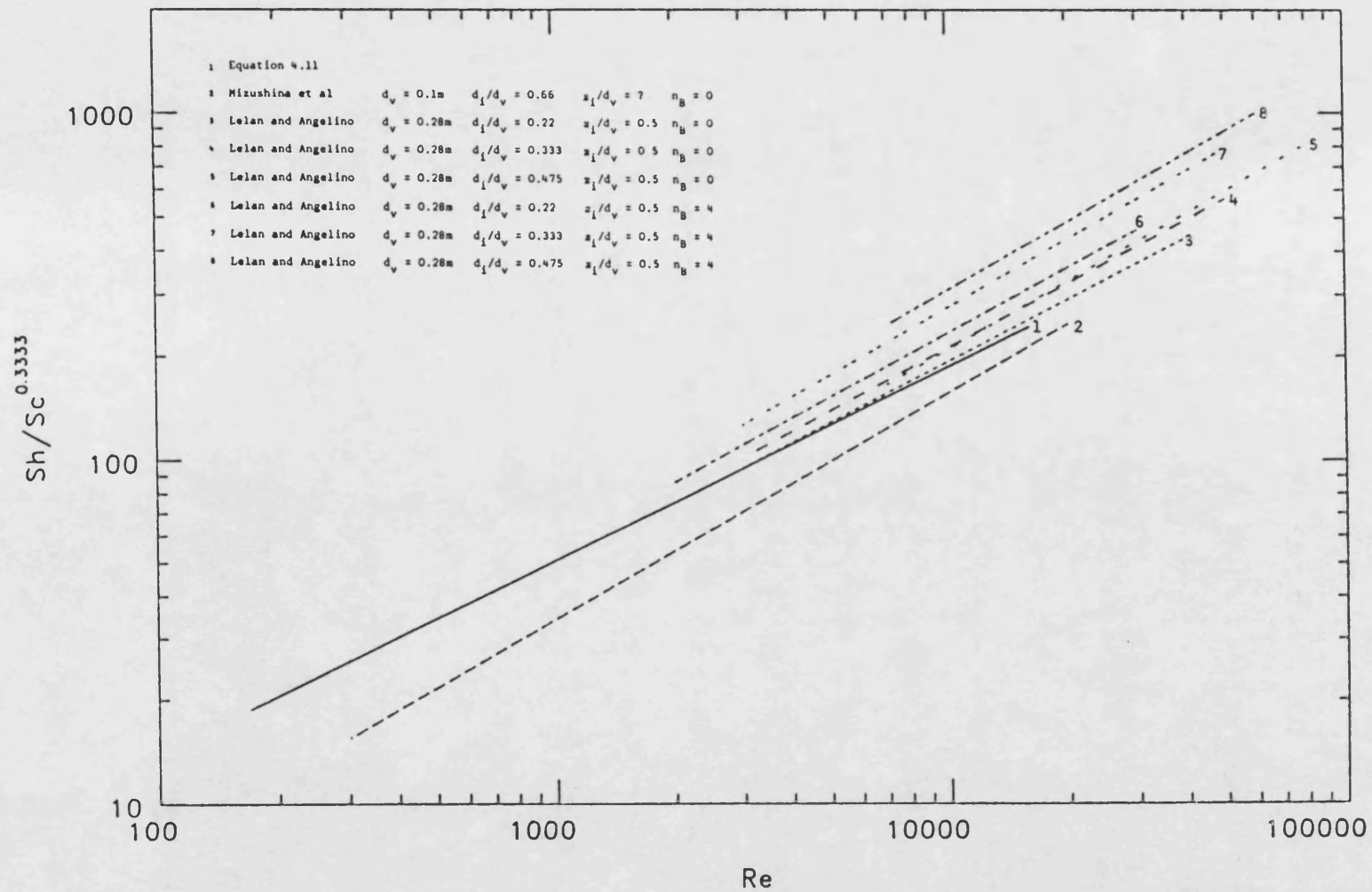


TABLE 4.3 GEOMETRICAL CONFIGURATION OF THE ELECTROLYTIC MIXING
CELL USED IN THIS STUDY

$$d_v = 0.076\text{m}$$

$$\frac{d_i}{d_v} = 0.66$$

$$\frac{z_1}{d_v} = 1.58$$

$$\frac{z_i}{d_v} = 0.39$$

$$\frac{w_b}{d_i} = 0.20$$

$$\frac{l_b}{d_i} = 0.25$$

$$n_B = 0$$

FIGURE 4.6 CURRENT-POTENTIAL CURVES AS A FUNCTION OF THE IMPELLER ROTATIONAL SPEED FOR THE ELECTROLYTIC MIXING CELL WITH THE PRESENCE OF 1 LAYER OF 3MM GLASS SPHERICAL PARTICLES ON THE CATHODE

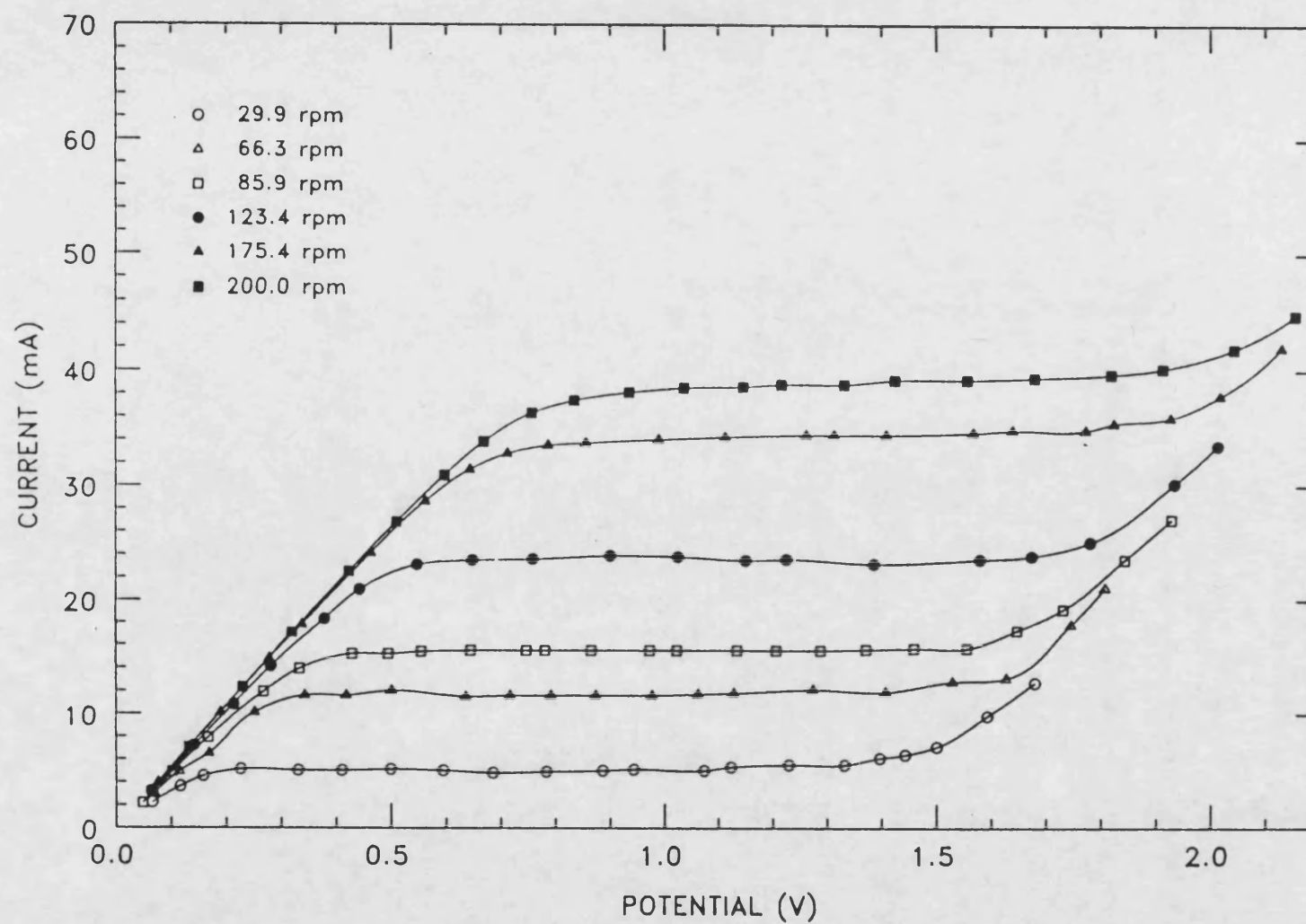
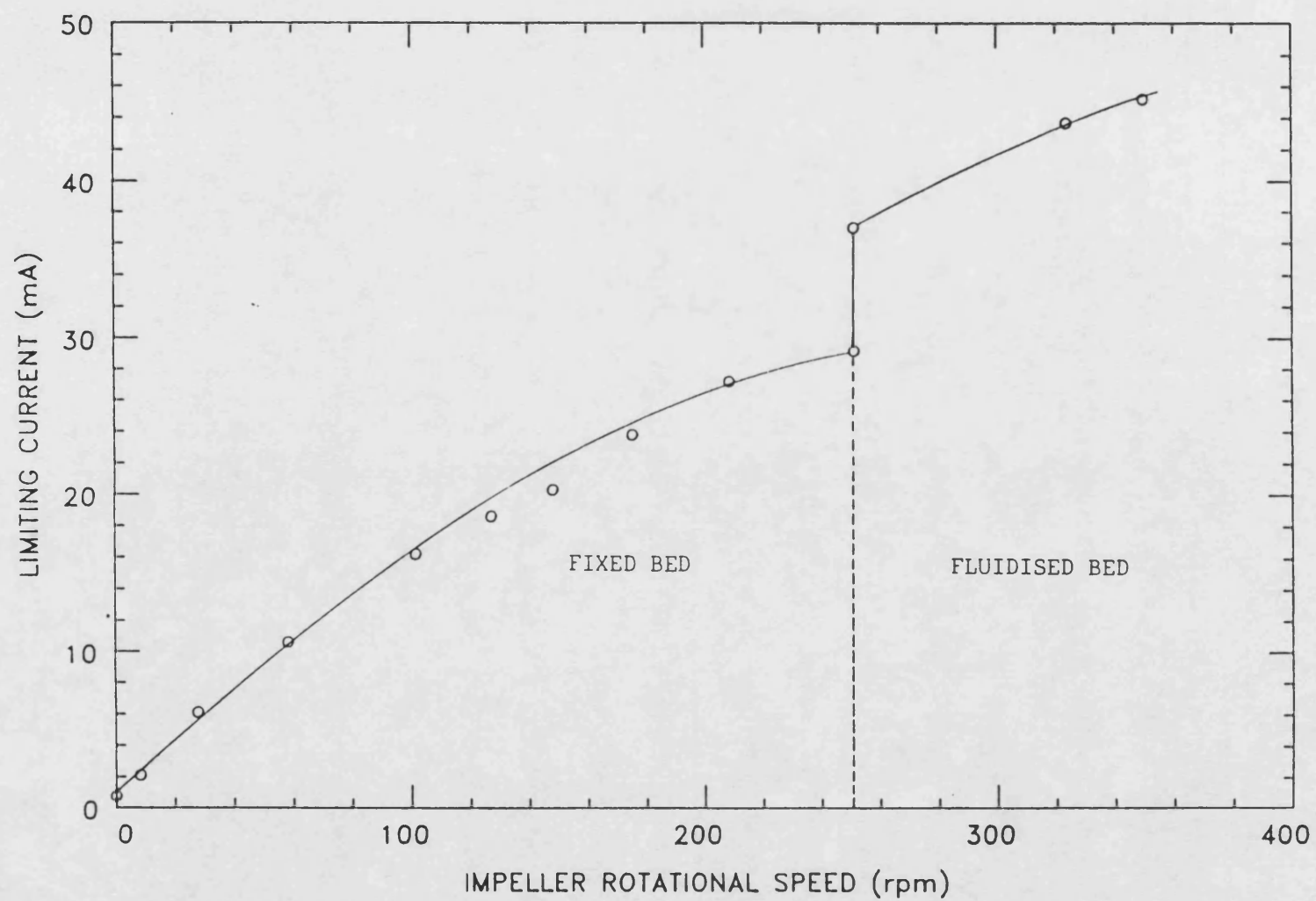


FIGURE 4.7 THE VARIATION OF I_L with N FOR THE ELECTROLYTIC MIXING CELL WITH THE PRESENCE OF 1 LAYER OF 3MM GLASS SPHERICAL PARTICLES



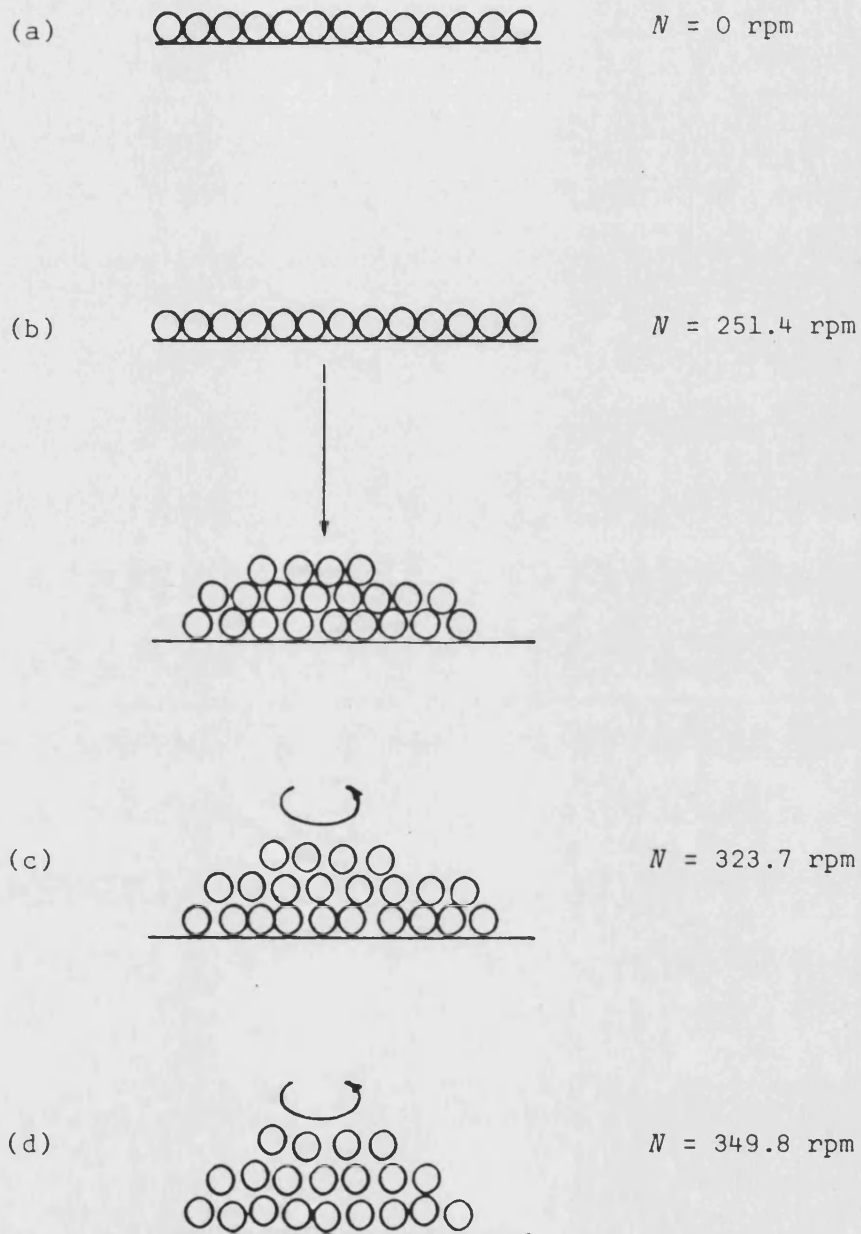


FIGURE 4.8 SCHEMATIC DIAGRAMS OF 1 LAYER OF 3MM GLASS SPHERICAL PARTICLES ON THE CATHODE AT FOUR DIFFERENT IMPELLER ROTATIONAL SPEEDS

For all the I_L - N data where $N > 0$ given in Appendix A6.6, mass transfer in the electrolytic mixing cell with the presence of one or more layers of glass spherical particles of known dimensions on the cathode was by forced convection. Hence, this data was expressed in the form of the Gilliland-Sherwood correlation given by equation 4.8 where Sh , Re and Sc are defined by equations 4.12, 4.1 and 2.11 respectively

$$Sh = \frac{Kd}{D} = \frac{I_L d}{zFADc_b} \quad 4.12$$

where K = overall mass transfer coefficient

The calculation of Sh , Re and Sc (see example given in Section 4.1.1.1) was carried out by the computer program MASS given in Appendix A7.1. This derived data is tabulated in Appendix A6.6

Several investigators have found by experiment that the exponent of Sc in the Gilliland-Sherwood correlation for fixed beds is $\frac{1}{3}$ (327,392). Thus, equation 4.8 can be rewritten in the form of equation 4.9. The values of a and b in equation 4.9 can be determined by the least squares method since equation 4.9 can be linearised into equation 4.10.

The derived data for all the runs where $N > 0$ rpm given in Appendix A6.6 can be plotted as $Sh/Sc^{\frac{1}{3}}$ versus Re on logarithmic co-ordinates. As an example, a plot of $Sh/Sc^{\frac{1}{3}}$ versus Re on logarithmic co-ordinates for the electrolytic mixing cell with the presence of 1 layer of 3mm glass spherical particles on the cathode is given in Figure 4.9. Using the least squares method, the correlations for these plots are listed in Table 4.4 together with the number of data points used for the correlation, the standard deviation and the correlation coefficient.

It was noted from the correlations given in Table 4.4 that for a simulated fouling deposit which constituted of glass spherical particles of a fixed particle diameter, d_p resting on the cathode, the exponent b is reasonably independent of the number of layers which constitute the simulated fouling deposit, n_1 . This is clearly shown in Figure 4.10 where the lower and upper values of b for each d_p is plotted against d_p . The b - d_p data given in Figure 4.10 first increases to a maximum at $d_p \approx 0.8\text{mm}$ and then decreases to an asymptote where b at $d_p > 12\text{mm} \rightarrow b$ at $d_p = 0\text{mm}$. Several attempts have been made to model this data using non-linear least squares analysis. The best

FIGURE 4.9 A PLOT OF $Sh/Sc^{1/3}$ VERSUS Re FOR THE ELECTROLYTIC MIXING CELL WITH THE PRESENCE OF 1 LAYER OF 3MM GLASS SPHERICAL PARTICLES ON THE CATHODE

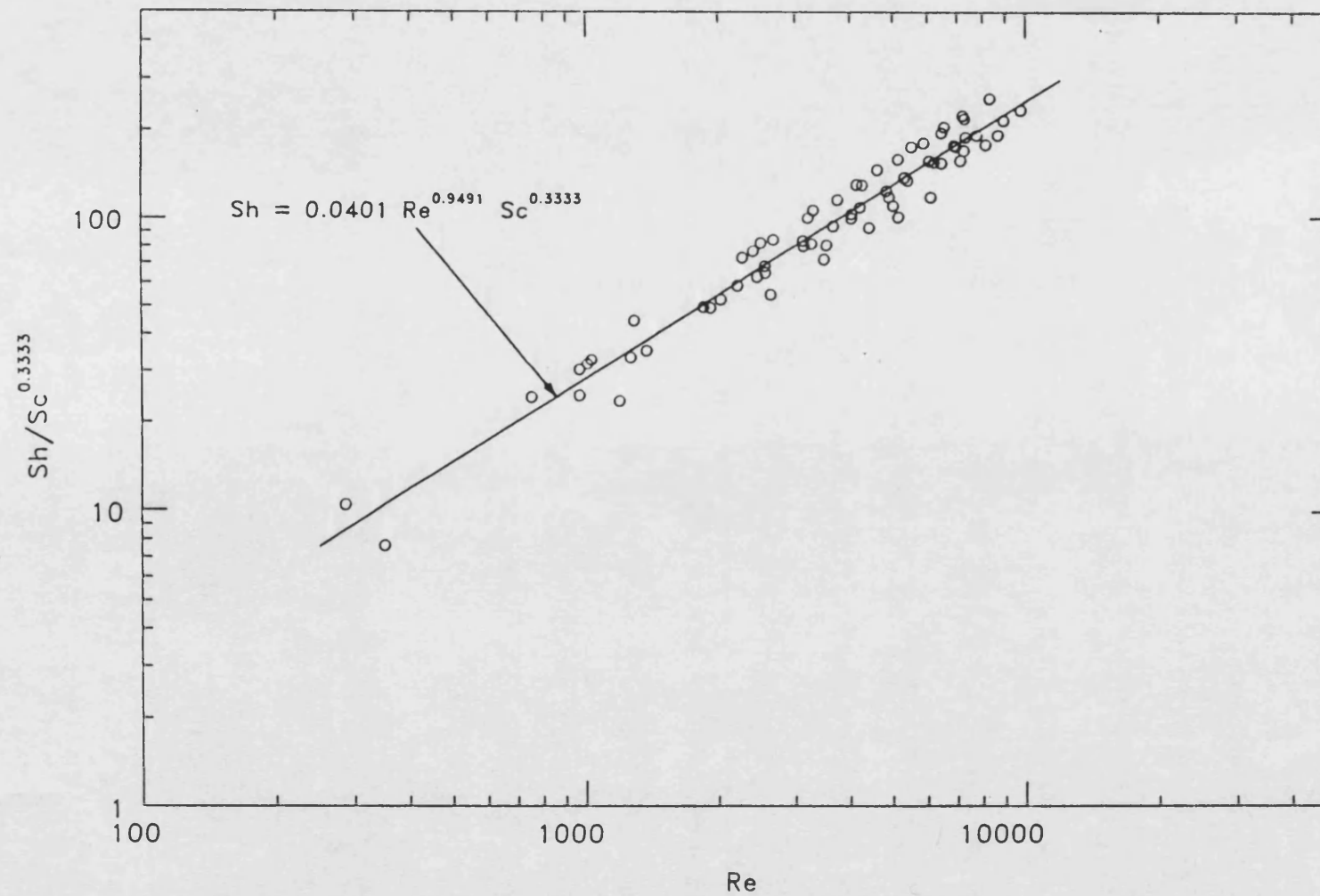
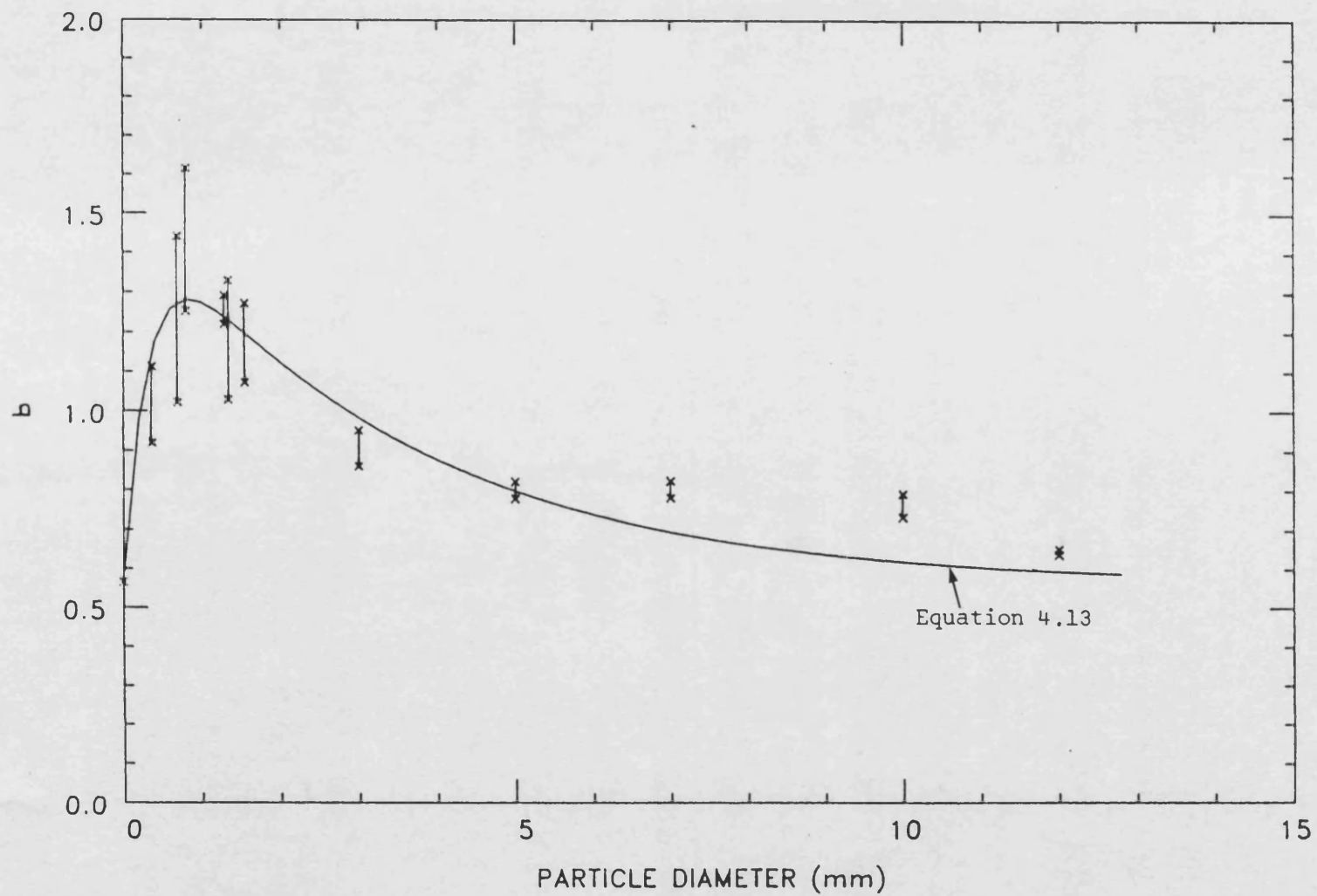


TABLE 4.4 A SUMMARY OF THE MASS TRANSFER CORRELATIONS FOUND FOR THE VARIOUS EXPERIMENTAL CONDITIONS IN THE ELECTROLYTIC MIXING CELL LISTED IN TABLE 3.7

GLASS SPHERICAL PARTICLES d_p (mm)	n_1	NUMBER OF DATA POINTS	CORRELATION			STANDARD DEVIATION	CORRELATION COEFFICIENT
NONE		210	Sh = 1.0330	Re ^{0.5644}	Sc ^{0.3333}	0.1236	97.6%
0.368	1	7	Sh = 0.0288	Re ^{0.9186}	Sc ^{0.3333}	0.0203	99.9%
	2	5	Sh = 0.0053	Re ^{1.0812}	Sc ^{0.3333}	0.0646	99.8%
	3	4	Sh = 0.0037	Re ^{1.1122}	Sc ^{0.3333}	0.0630	99.4%
0.695	1	40	Sh = 0.0059	Re ^{1.1205}	Sc ^{0.3333}	0.0913	99.5%
	2	38	Sh = 0.00041	Re ^{1.4406}	Sc ^{0.3333}	0.2137	97.1%
	3	35	Sh = 0.0087	Re ^{1.0215}	Sc ^{0.3333}	0.1693	97.0%
	4	24	Sh = 0.0024	Re ^{1.1799}	Sc ^{0.3333}	0.1126	98.5%
	5	21	Sh = 0.00054	Re ^{1.3471}	Sc ^{0.3333}	0.1329	98.5%
0.805	1	35	Sh = 0.0025	Re ^{1.2526}	Sc ^{0.3333}	0.1339	98.1%
	2	21	Sh = 0.00041	Re ^{1.4517}	Sc ^{0.3333}	0.0871	99.5%
	3	29	Sh = 0.00018	Re ^{1.4998}	Sc ^{0.3333}	0.1265	99.1%
	4	26	Sh = 0.00018	Re ^{1.4784}	Sc ^{0.3333}	0.0740	99.7%
	5	27	Sh = 0.000058	Re ^{1.6155}	Sc ^{0.3333}	0.1572	98.8%
	6	21	Sh = 0.00028	Re ^{1.4167}	Sc ^{0.3333}	0.0928	99.4%
1.29	1	18	Sh = 0.0026	Re ^{1.2525}	Sc ^{0.3333}	0.0991	99.4%
	2	11	Sh = 0.0015	Re ^{1.2913}	Sc ^{0.3333}	0.1053	99.3%
	3	7	Sh = 0.0016	Re ^{1.2689}	Sc ^{0.3333}	0.0852	99.5%
	4	19	Sh = 0.0023	Re ^{1.2188}	Sc ^{0.3333}	0.1609	98.3%
1.34	1	11	Sh = 0.0163	Re ^{1.0286}	Sc ^{0.3333}	0.0676	99.6%
	2	10	Sh = 0.0019	Re ^{1.2707}	Sc ^{0.3333}	0.0698	99.6%
	3	12	Sh = 0.0018	Re ^{1.2641}	Sc ^{0.3333}	0.0595	99.7%
	4	12	Sh = 0.00084	Re ^{1.3290}	Sc ^{0.3333}	0.1015	99.3%
	5	10	Sh = 0.0020	Re ^{1.2198}	Sc ^{0.3333}	0.0671	99.6%
	6	8	Sh = 0.0024	Re ^{1.1824}	Sc ^{0.3333}	0.0542	99.7%
	7	9	Sh = 0.0023	Re ^{1.1758}	Sc ^{0.3333}	0.0872	99.3%

GLASS SPHERICAL PARTICLES		NUMBER OF DATA POINTS	CORRELATION			STANDARD DEVIATION	CORRELATION COEFFICIENT
d_p (mm)	n_1						
1.55	1	48	Sh = 0.0074	Re ^{1.1402}	Sc ^{0.3333}	0.1664	98.5%
	2	50	Sh = 0.0023	Re ^{1.2722}	Sc ^{0.3333}	0.1160	99.3%
	3	47	Sh = 0.0043	Re ^{1.1812}	Sc ^{0.3333}	0.0855	99.5%
	4	43	Sh = 0.0085	Re ^{1.0959}	Sc ^{0.3333}	0.0900	98.9%
	5	48	Sh = 0.0053	Re ^{1.1474}	Sc ^{0.3333}	0.0456	99.6%
	6	24	Sh = 0.0091	Re ^{1.0727}	Sc ^{0.3333}	0.0489	99.4%
3.0	1	68	Sh = 0.0401	Re ^{0.9491}	Sc ^{0.3333}	0.1488	98.0%
	2	54	Sh = 0.0474	Re ^{0.9224}	Sc ^{0.3333}	0.1394	98.2%
	3	54	Sh = 0.0280	Re ^{0.9516}	Sc ^{0.3333}	0.1450	97.8%
	4	35	Sh = 0.0322	Re ^{0.9230}	Sc ^{0.3333}	0.1446	97.6%
	5	18	Sh = 0.0364	Re ^{0.9125}	Sc ^{0.3333}	0.0536	99.7%
	6	14	Sh = 0.0514	Re ^{0.8603}	Sc ^{0.3333}	0.0423	99.7%
	7	10	Sh = 0.0249	Re ^{0.9297}	Sc ^{0.3333}	0.0732	99.4%
5.0	1	19	Sh = 0.0960	Re ^{0.8210}	Sc ^{0.3333}	0.0687	99.6%
	2	19	Sh = 0.1195	Re ^{0.7782}	Sc ^{0.3333}	0.0480	99.7%
	3	15	Sh = 0.0716	Re ^{0.8222}	Sc ^{0.3333}	0.0450	99.8%
	4	18	Sh = 0.0763	Re ^{0.8011}	Sc ^{0.3333}	0.0372	99.8%
7.0	1	30	Sh = 0.1347	Re ^{0.7857}	Sc ^{0.3333}	0.0881	99.2%
	2	30	Sh = 0.0844	Re ^{0.8242}	Sc ^{0.3333}	0.0704	99.4%
	3	26	Sh = 0.1022	Re ^{0.7813}	Sc ^{0.3333}	0.0573	99.6%
10.0	1	21	Sh = 0.2181	Re ^{0.7329}	Sc ^{0.3333}	0.0945	98.6%
	2	26	Sh = 0.1189	Re ^{0.7923}	Sc ^{0.3333}	0.0435	99.6%
12.0	1	30	Sh = 0.4315	Re ^{0.6372}	Sc ^{0.3333}	0.0636	99.0%
	2	22	Sh = 0.3057	Re ^{0.6514}	Sc ^{0.3333}	0.0986	98.4%

FIGURE 4.10 THE VARIATION OF THE EXPONENT b IN THE GILLILAND-SHERWOOD CORRELATION WITH PARTICLE DIAMETER



model (shown in Figure 4.10) was found to be

$$b = 0.5644 + 1.0081(e^{-0.2924d_p} - e^{-3.1486d_p}) \quad 4.13$$

In general, it was noted from the correlations given in Table 4.4 that for a simulated fouling deposit which constituted of glass spherical particles of a fixed d_p resting on the cathode, the constant a decreases non-linearly with increasing n_1 . This is clearly shown in Figure 4.11 where a is plotted against n_1 for the simulated fouling deposit constituting of 3mm glass spherical particles. Furthermore, it was found from the plots of a - d_p data for $n_1 = 1$, $n_1 = 2$, $n_1 = 3$, $n_1 = 4$, $n_1 = 5$, $n_1 = 6$ and $n_1 = 7$ given respectively in Figures 4.12 - 4.18 that the a - d_p data for each n_1 first decreases to a minimum at $d_p \approx 0.8\text{mm}$ and then increases to an asymptote where a at $d_p > 12\text{mm}$ $\rightarrow a$ at $d_p = 0\text{mm}$. Several attempts have been made to model this data using non-linear least squares analysis. The best model (shown in Figure 4.11 for $d_p = 3\text{mm}$ and in Figures 4.12 - 4.18 for $n_1 = 1$, $n_1 = 2$, $n_1 = 3$, $n_1 = 4$, $n_1 = 5$, $n_1 = 6$ and $n_1 = 7$ respectively) was found to be

$$a = 1.0330 \exp\{-7.7799 n_1^{0.1122} (e^{-0.2672d_p} - e^{-4.0086d_p})\} \quad 4.14$$

4.2 Mass and heat transfer studies

4.2.1 Mass and heat transfer in the electrolytic mixing cell without the presence of glass spherical particles on the cathode

From the plots showing the effect of the cathode surface temperature upon the average current-potential curve at a fixed impeller rotational speed for the electrolytic mixing cell where the temperature difference between the cathode surface and the bulk solution, ΔT is a constant, it was found that a limiting current is obtained for each current-potential curve when the potential is in the range of 0.8 - 1.4 volts. A typical plot is shown in Figure 4.19. Details of the data used in Figure 4.19 is given in Appendix A6.7.

By setting the potential at -0.9V , the average limiting current can be measured as a function of the impeller rotational speed for various ΔT . The I_L - N data obtained from several runs is given in Appendix A6.8.

Since free and forced convection mass and heat transfer can occur in agitated vessels, it is reasonable to assume

FIGURE 4.11 THE VARIATION OF THE EXPONENT a IN THE GILLILAND-SHERWOOD CORRELATION WITH THE NUMBER OF LAYERS OF 3MM GLASS SPHERICAL PARTICLES RESTING ON THE CATHODE

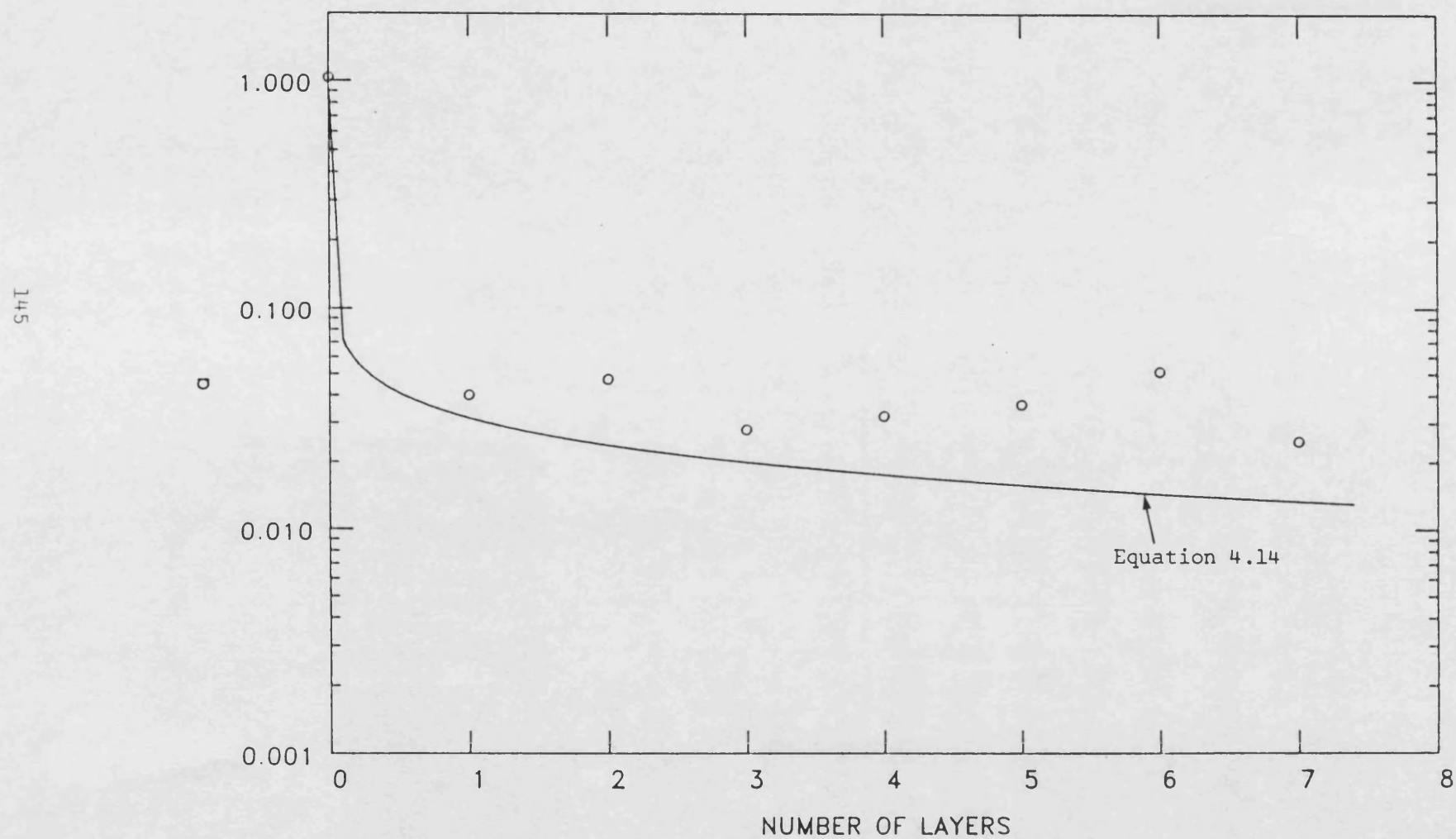


FIGURE 4.12 THE VARIATION OF THE EXPONENT a IN THE GILLILAND-SHERWOOD CORRELATION WITH PARTICLE DIAMETER WHEN $n_1 = 1$

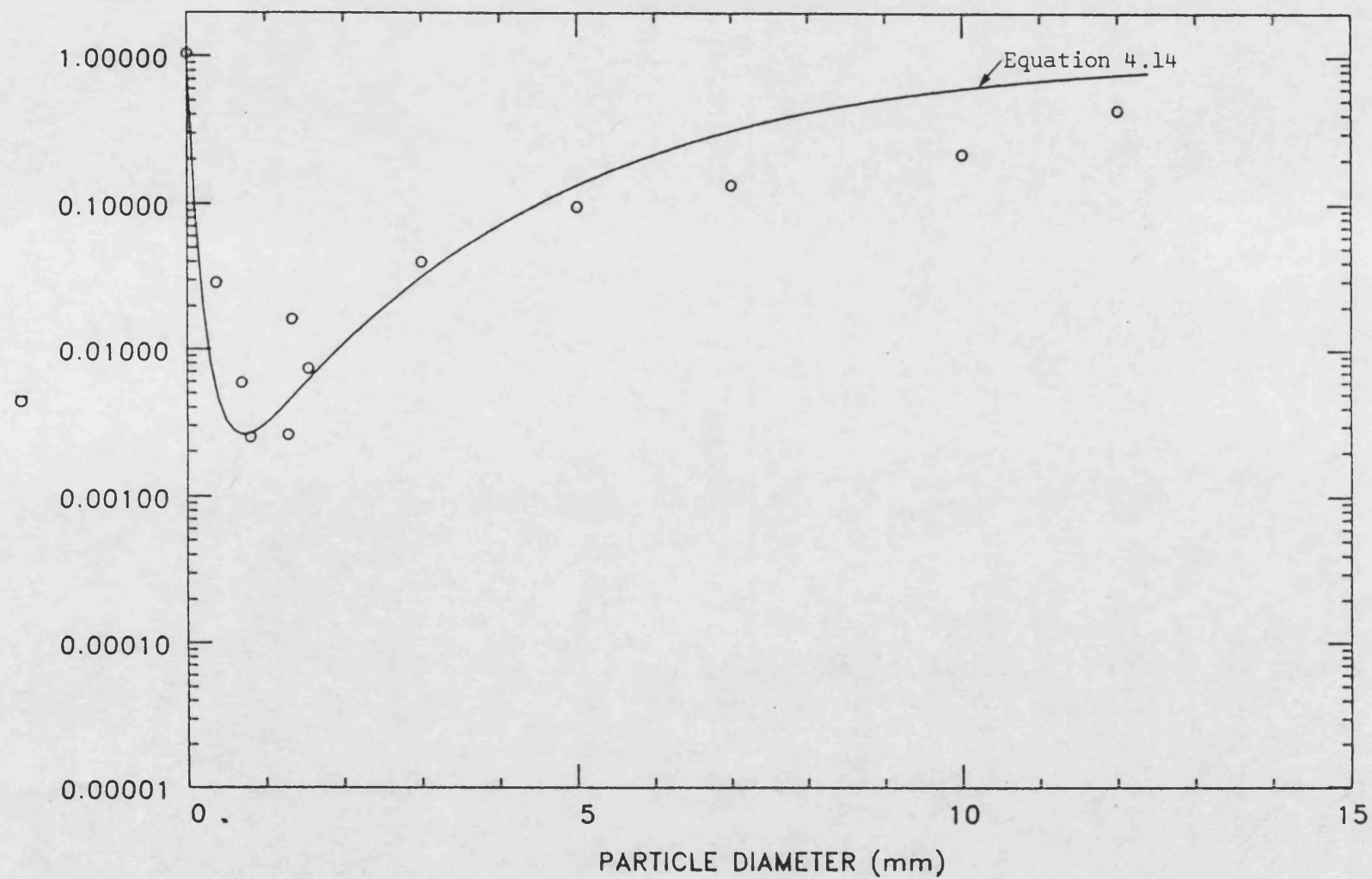


FIGURE 4.13 THE VARIATION OF THE EXPONENT a IN THE GILLILAND-SHERWOOD CORRELATION WITH PARTICLE DIAMETER WHEN $n_1 = 2$

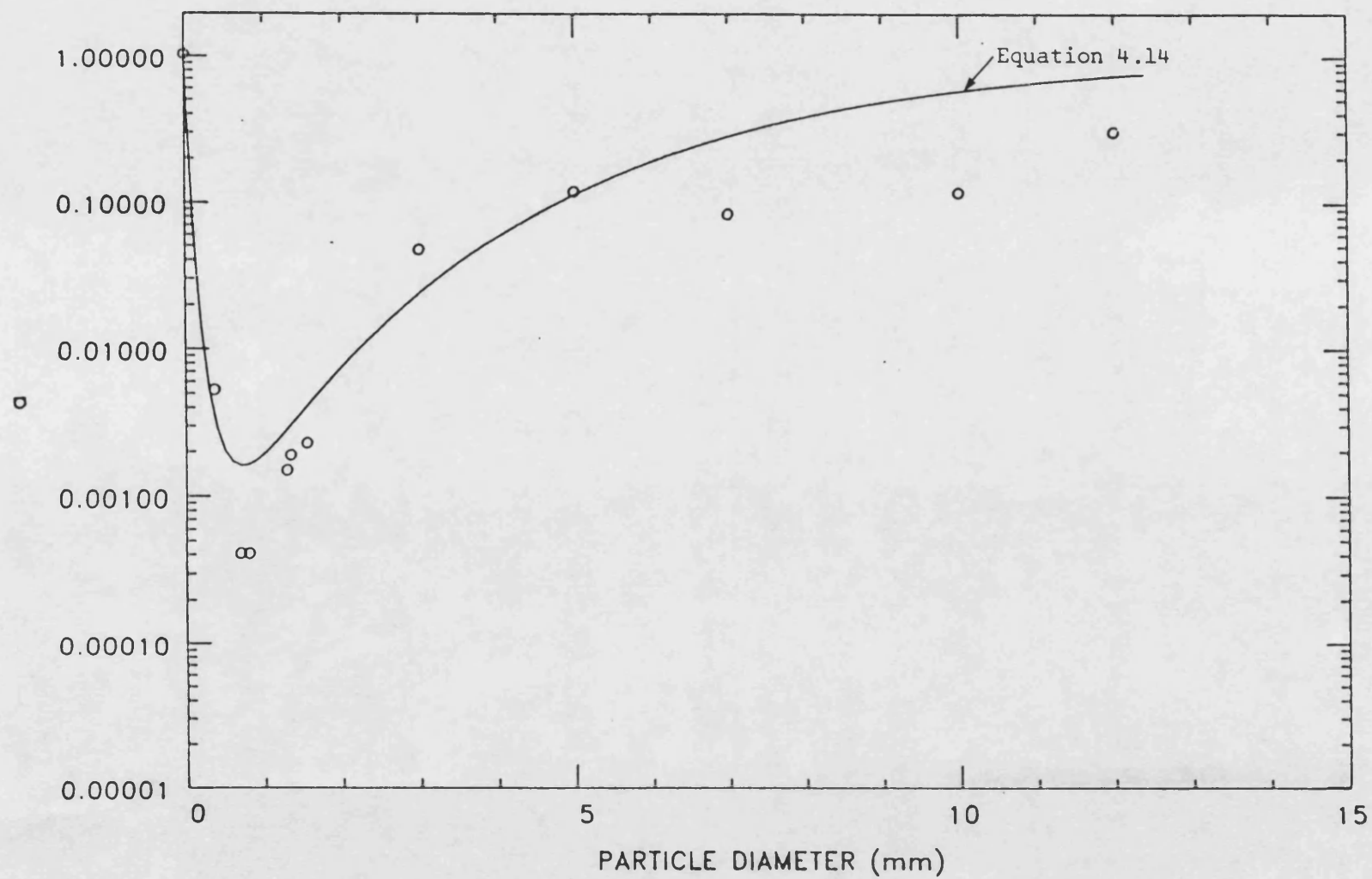


FIGURE 4.14 THE VARIATION OF THE EXPONENT a IN THE GILLILAND-SHERWOOD CORRELATION WITH PARTICLE DIAMETER WHEN $n_1 = 3$

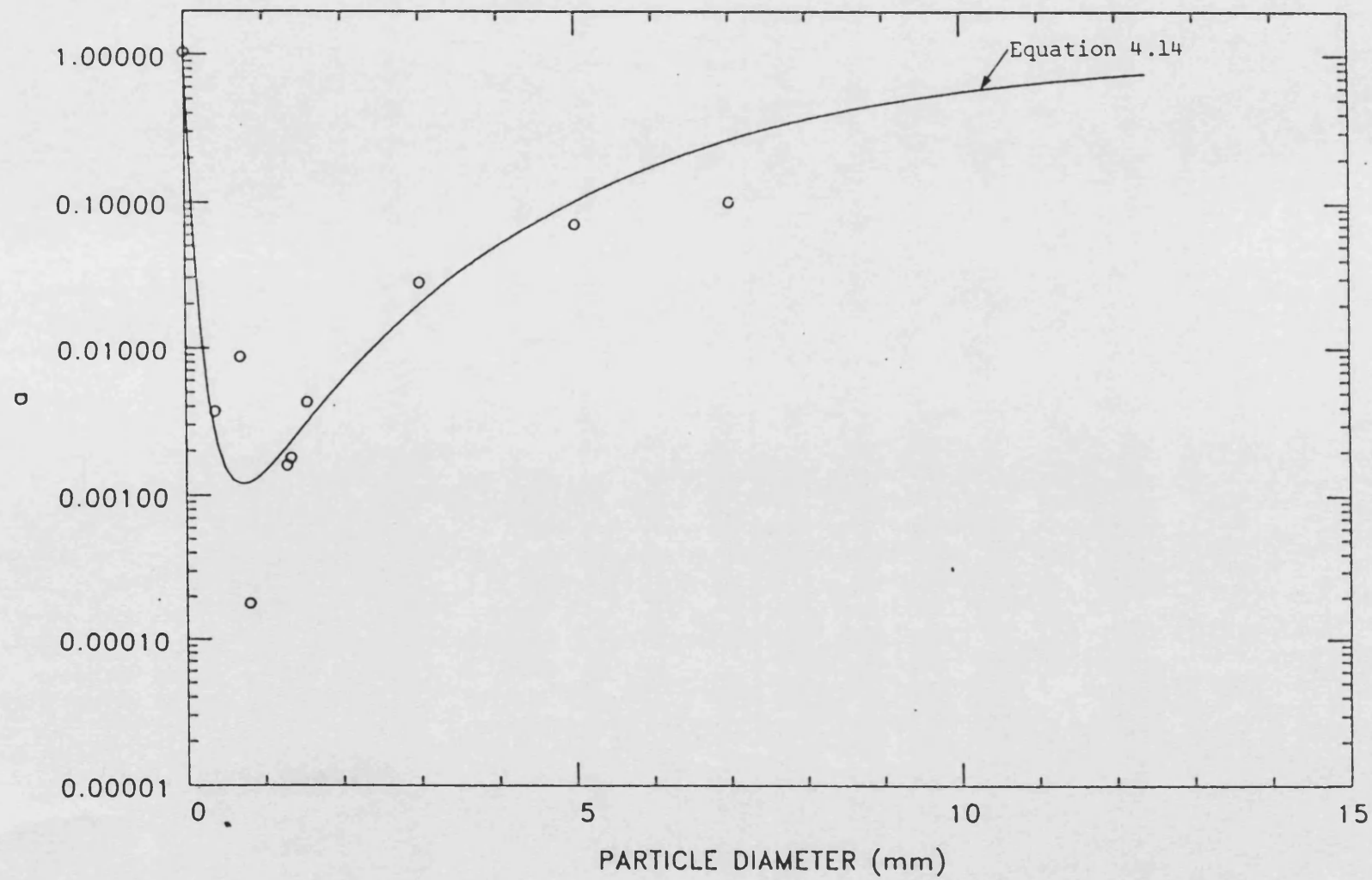


FIGURE 4.15 THE VARIATION OF THE EXPONENT a IN THE GILLILAND-SHERWOOD CORRELATION WITH PARTICLE DIAMETER WHEN $n_1 = 4$

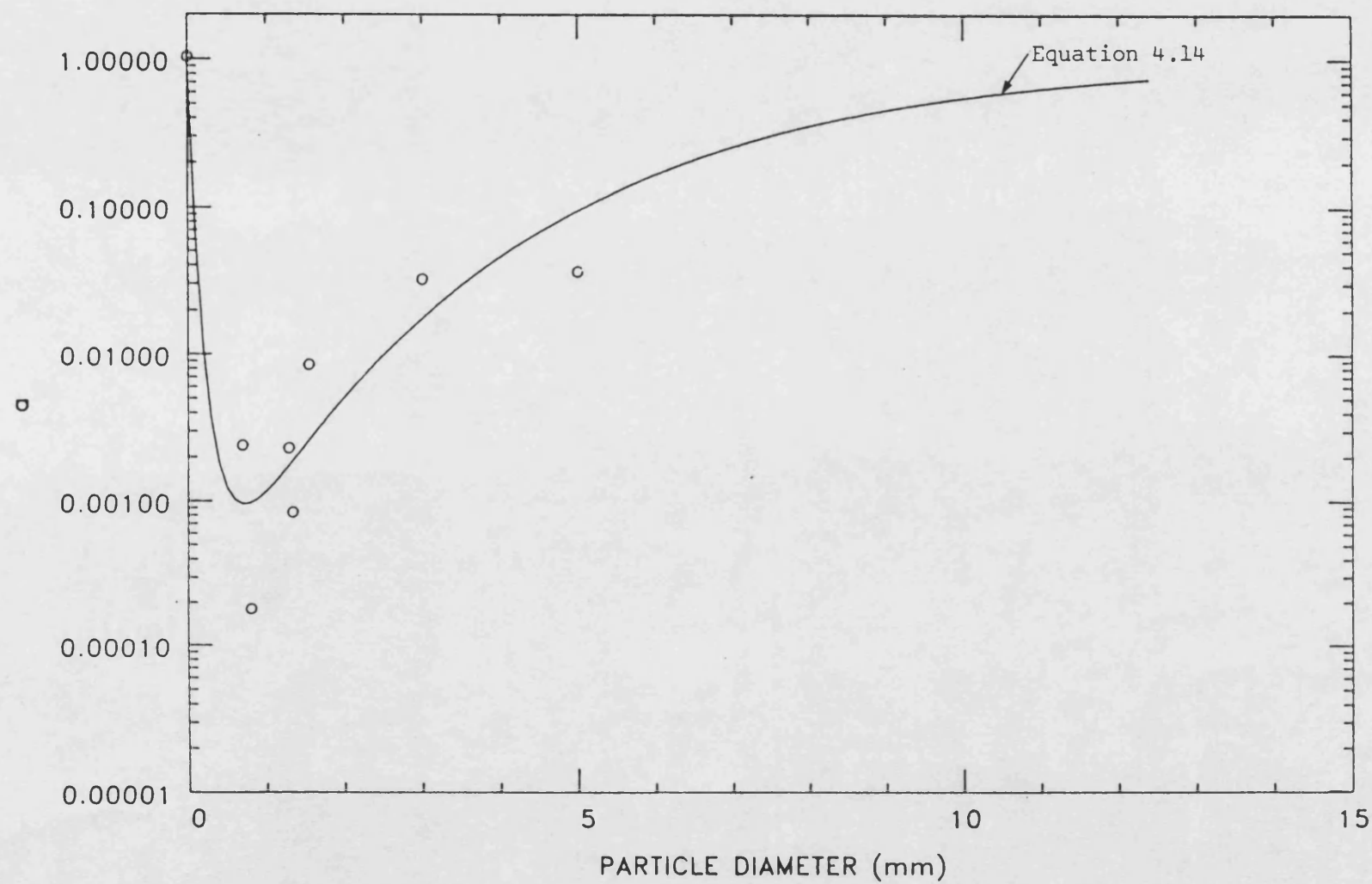


FIGURE 4.16 THE VARIATION OF THE EXPONENT a IN THE GILLILAND-SHERWOOD CORRELATION WITH PARTICLE DIAMETER WHEN $n_1 = 5$

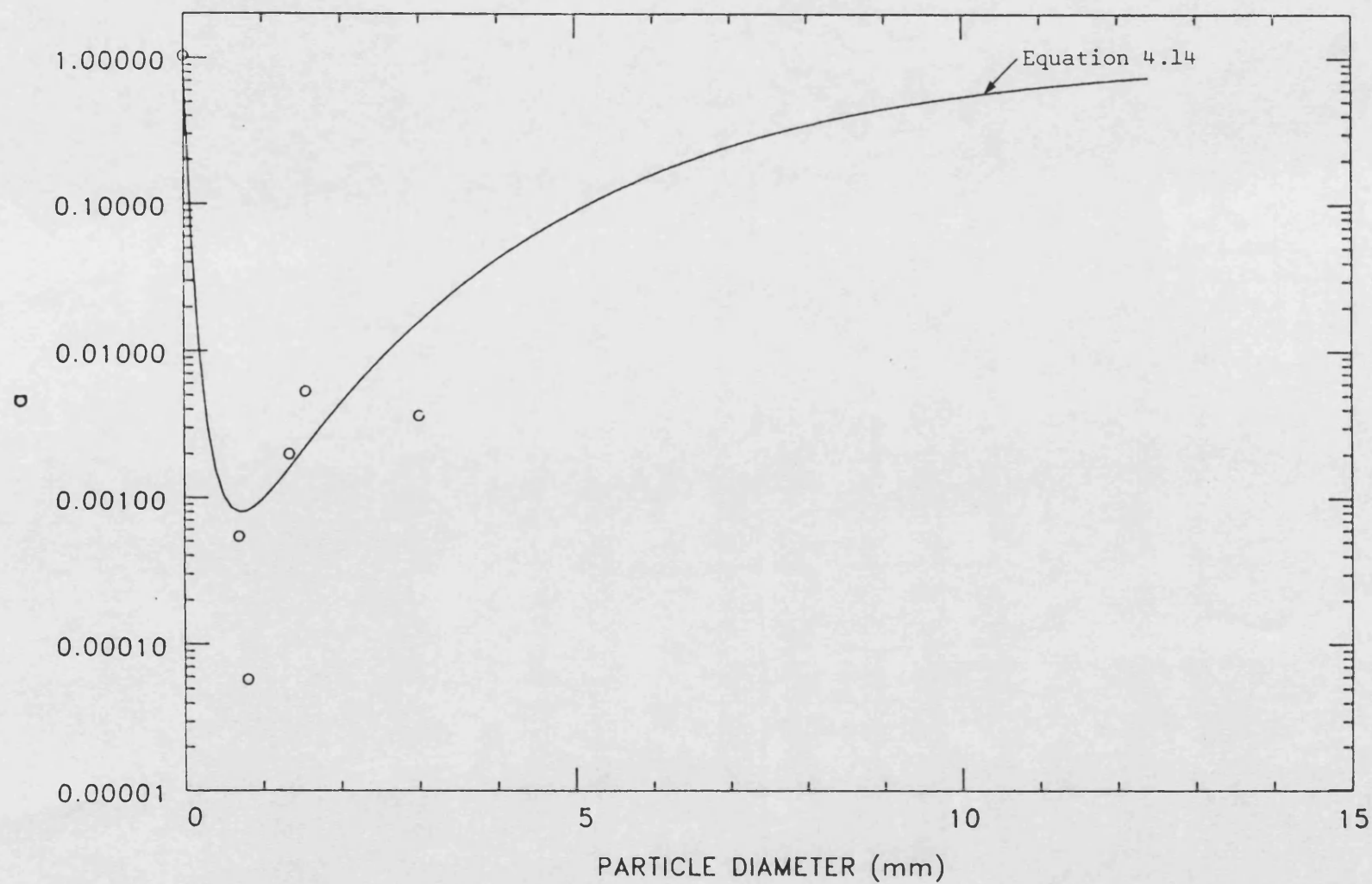


FIGURE 4.17 THE VARIATION OF THE EXPONENT a IN THE GILLILAND-SHERWOOD CORRELATION WITH PARTICLE DIAMETER WHEN $n_1 = 6$

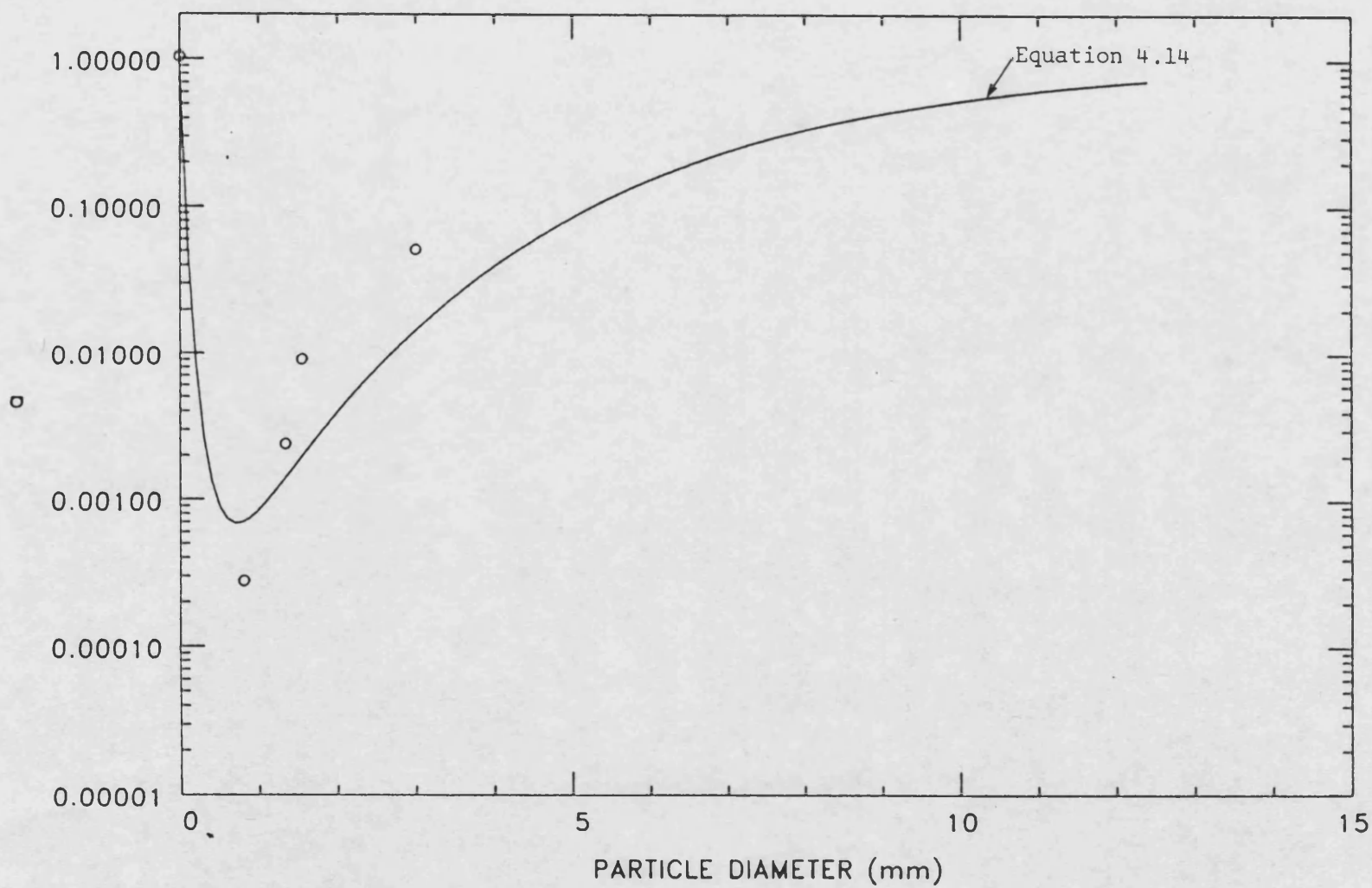


FIGURE 4.18 THE VARIATION OF THE EXPONENT a IN THE GILLILAND-SHERWOOD CORRELATION WITH PARTICLE DIAMETER WHEN $n_1 = 7$

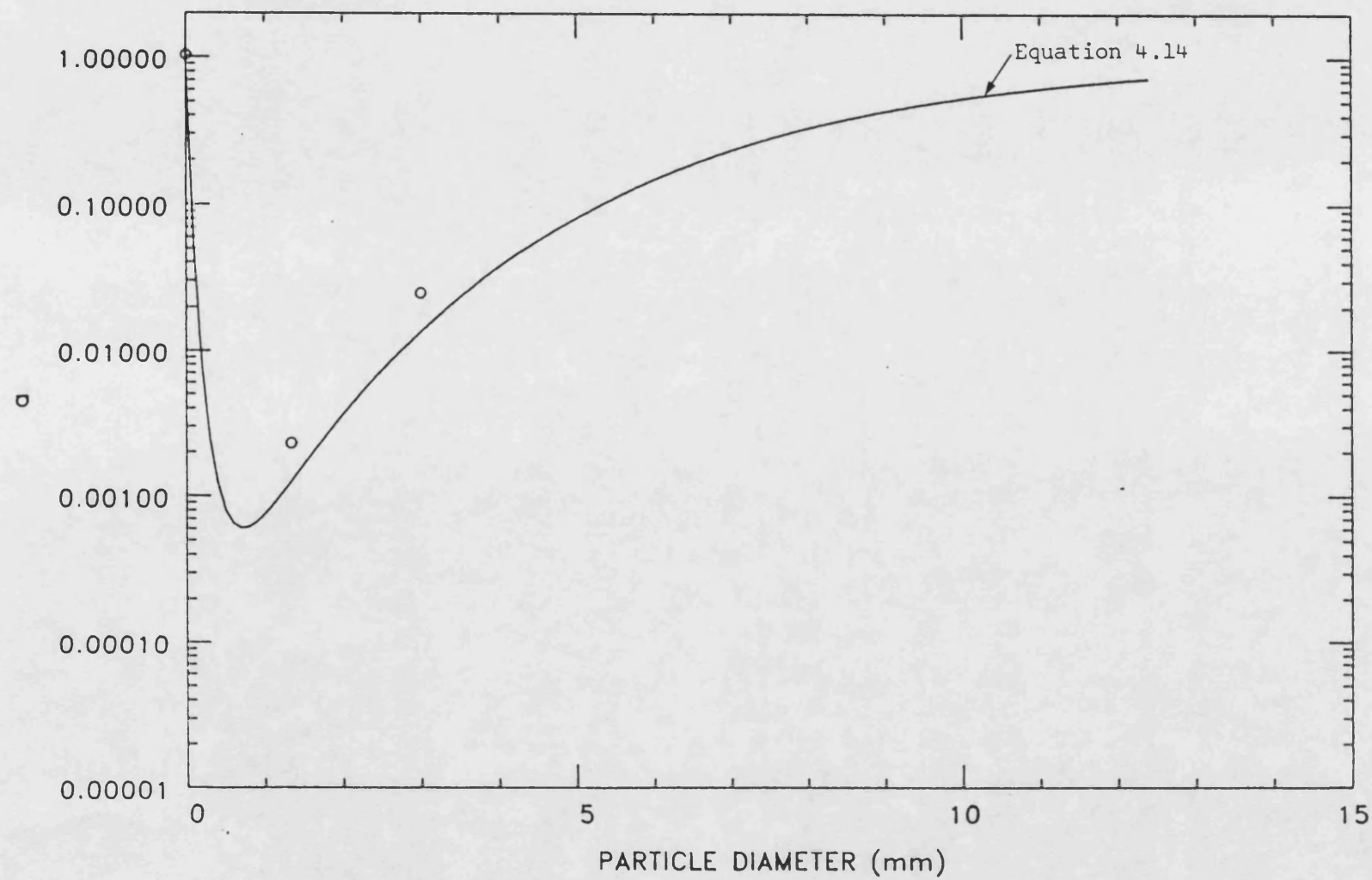
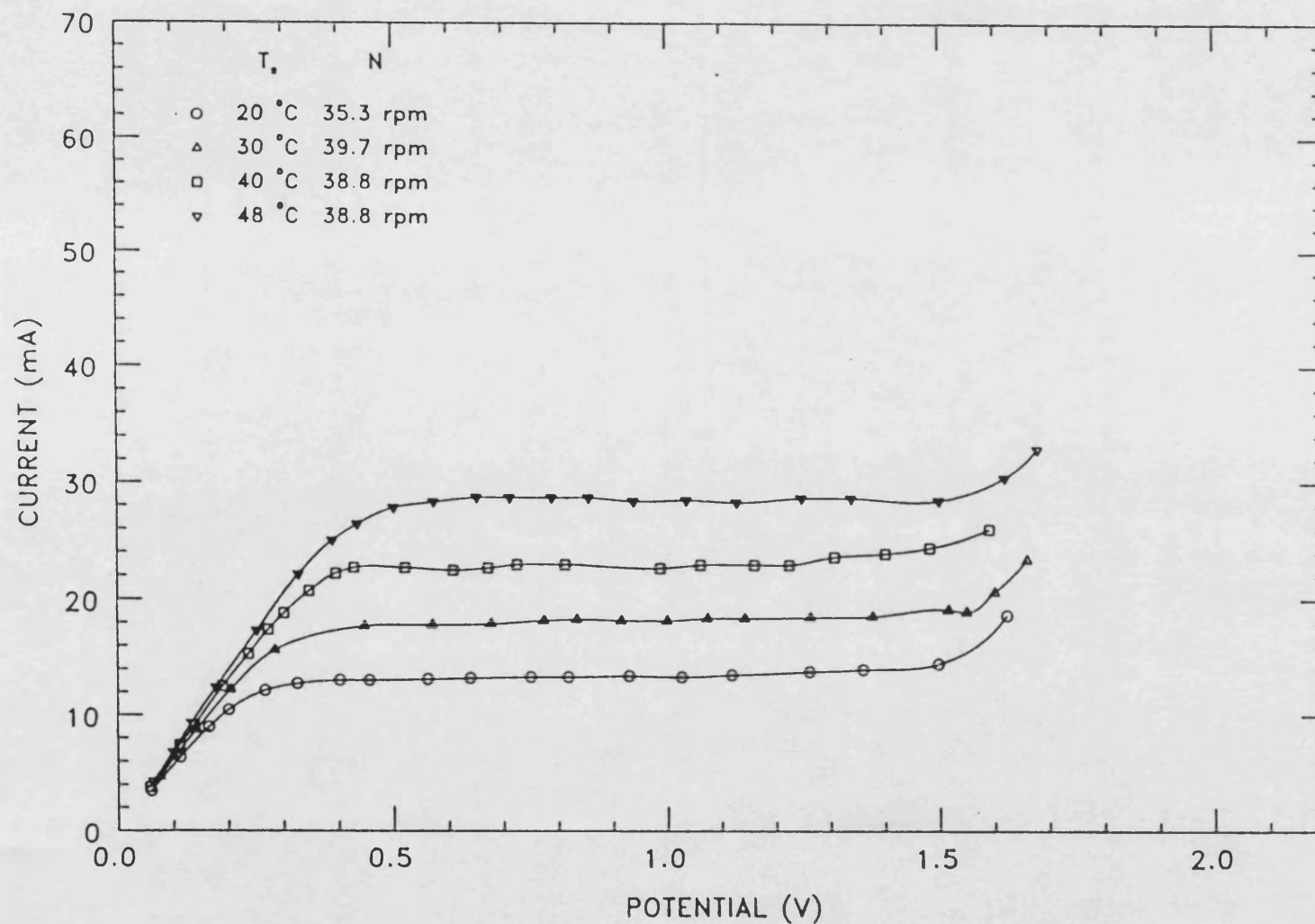


FIGURE 4.19 THE EFFECT OF THE CATHODE SURFACE TEMPERATURE UPON THE CURRENT-POTENTIAL CURVE AT AN IMPELLER
ROTATIONAL SPEED OF 37.5 ± 2.2 rpm FOR THE ELECTROLYTIC MIXING CELL WITHOUT THE PRESENCE OF
GLASS SPHERICAL PARTICLES ON THE CATHODE WHERE $\Delta T = 0$



1. free convection mass and heat transfer >> forced convection mass and heat transfer at very low Re
2. forced convection mass and heat transfer >> free convection mass and heat transfer at higher Re

4.2.1.1 Free convection mass and heat transfer

Simultaneous mass and heat transfer by free convection is usually expressed either in terms of

$$Sh = a (GR_m Sc)^b \quad 4.15$$

where GR_m is the combined Grashof number for mass transfer defined by⁽³⁷¹⁾

$$GR_m = Gr_m + \left[\frac{Sc}{Pr} \right]^{\frac{1}{2}} Gr_h \quad 4.16$$

or

$$Nu = a (GR_h Pr)^b \quad 4.17$$

where GR_h is the combined Grashof number for heat transfer defined by⁽³⁷¹⁾

$$GR_h = Gr_h + \left[\frac{Pr}{Sc} \right]^{\frac{1}{2}} Gr_m \quad 4.18$$

For cylindrical vessels with horizontal electrodes, Sh , Nu , Gr_m , Gr_h , Sc and Pr in equations 4.15 - 4.18 are defined by equations 4.3, 4.19, 4.4, 4.20, 2.11 and 2.16 respectively.

$$Nu = \frac{hd}{k} \quad 4.19$$

$$Gr_h = \frac{gd^3}{\nu^2} \left[\frac{\Delta\rho}{\rho} \right]_h \quad 4.20$$

For all the $I_L - N$ data where $N = 0$ rpm given in Appendix A6.8, simultaneous mass and heat transfer in the electrolytic mixing cell was by free convection. By taking Run 1.01 of Appendix A6.8 (ie. $N = 0$ rpm, $I_L = 3.2$ mA, $c_b = 0.005$ M, $T_b = 16.0^\circ\text{C}$, $T_{s1} = 18.0^\circ\text{C}$, $T_{s2} = 20.7^\circ\text{C}$, $T_{s3} = 18.0^\circ\text{C}$, $T_w = 20.0^\circ\text{C}$, $T_a = 18.0^\circ\text{C}$, $I_h = 0.069$ A, $R_h = 114.5\Omega$) as an example, the calculation of Sh , Nu , Re , Gr_m , Gr_h , Sc and Pr carried out by the computer program MAHE given in Appendix A7.2 was as follows:

The physical properties of the electrolytic solution required for the dimensionless numbers were calculated at the mean film temperature, T_f :

$$T_f = \frac{T_b + T_s}{2} \quad 4.21$$

in which T_s , the mean cathode surface temperature, is defined by

$$T_s = \frac{\int_{r=0}^{r=d/2} T dr}{\int_{r=0}^{r=d/2} dr} \quad 4.22$$

where r is the radial distance from the centre of the cathode.

The temperature profile across the cathode was assumed to be that shown in Figure 4.20 where T between $r = 0$ and $r = \frac{d}{2}$ is given by

$$T = T_{s2} - \left[\frac{T_{s2} - \frac{T_{s1} + T_{s3}}{2}}{\frac{d}{2}} \right] r \quad 4.23$$

Substituting equation 4.23 into equation 4.22 for T and integrating yields

$$T_s = \frac{T_{s2} + \frac{T_{s1} + T_{s3}}{2}}{2} \quad 4.24$$

Substituting equation 4.24 into equation 4.21 for T_s yields

$$T_f = \frac{T_b + \frac{T_{s2} + \frac{T_{s1} + T_{s3}}{2}}{2}}{2} \quad 4.25$$

Hence, from equations 4.24 and 4.25

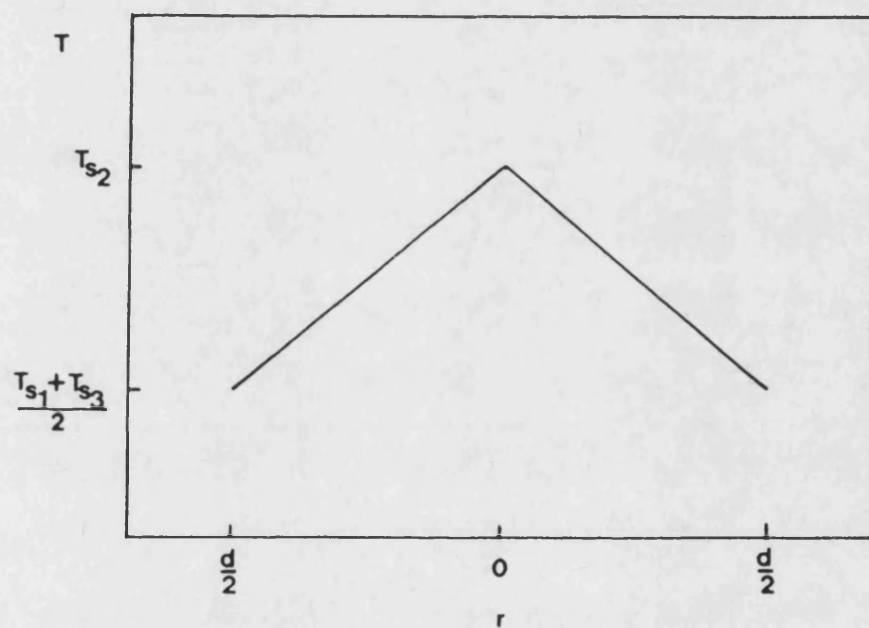
$$T_s = \frac{20.7 + \frac{18.0 + 18.0}{2}}{2} = 19.35^\circ\text{C}$$

$$T_f = \frac{16.0 + \frac{20.7 + \frac{18.0 + 18.0}{2}}{2}}{2} = 17.68^\circ\text{C}$$

Using the method of calculation shown in the example given in Section 4.1.1.1 where T_f was used instead of T_b , it was found that

$$\rho = 1.0247 \text{ g/cm}^3$$

FIGURE 4.20 THE ASSUMED TEMPERATURE PROFILE ACROSS THE CATHODE



$$\begin{aligned}
\nu &= 1.1423 \text{ mm}^2/\text{s} \\
\mu &= 1.1705 \times 10^{-2} \text{ g/cm s} \\
D &= 6.2118 \times 10^{-6} \text{ cm}^2/\text{s} \\
\left[\frac{\Delta \rho}{\rho} \right]_m &= -5.3000 \times 10^{-4}
\end{aligned}$$

The thermal conductivity of the electrolytic solution defined by equation 3.5 was found to be

$$k(17.68^\circ) = k(20^\circ) \frac{k_{\text{H}_2\text{O}}(17.68^\circ\text{C})}{k_{\text{H}_2\text{O}}(20^\circ\text{C})}$$

where $k_{\text{H}_2\text{O}}(20^\circ\text{C})$ was computed from equations 3.7 and 3.8 to be 0.59848 W/m K

$k_{\text{H}_2\text{O}}(17.68^\circ\text{C})$ was computed from equations 3.7 and 3.8 to be 0.59425 W/m K

$k(20^\circ\text{C})$ was found from equation 3.6 to be

$$\begin{aligned}
k(20^\circ\text{C}) &= k_{\text{H}_2\text{O}}(20^\circ\text{C}) + \sigma_{\text{Fe}(\text{CN})_6^{3-}} \text{Fe}(\text{CN})_6^{3-} + \sigma_{\text{Fe}(\text{CN})_6^{4-}} \text{Fe}(\text{CN})_6^{4-} \\
&\quad + \sigma_{\text{OH}^-} \text{OH}^- + \sigma_{\text{Na}^+} \text{Na}^+ + \sigma_{\text{K}^+} \text{K}^+ \\
&\approx 0.5985 \times 10^{-2} + (18.61 \times 10^{-5} \times 0.005) + (18.61 \times 10^{-5} \times 0.005) \\
&\quad + (20.934 \times 10^{-5} \times 0.5) + (0 \times 0.5) + (-7.560 \times 10^{-5} \times 0.035) \\
&\quad \text{assuming } \sigma_{\text{Fe}(\text{CN})_6^{3-}} \approx \sigma_{\text{Fe}(\text{CN})_6^{4-}} \\
&\approx 6.0889 \times 10^{-3} \text{ W/cm K}
\end{aligned}$$

Hence, $k = 6.0899 \times 10^{-3} \text{ W/cm K}$

The heat capacity of the electrolytic solution defined by equation 3.18 was found to be

$$\begin{aligned}
c_p &= 1 - \frac{0.02376}{1.0247} \\
&= 0.9768 \text{ BTU/lb } ^\circ\text{F} \\
&= 4.0870 \text{ J/g K}
\end{aligned}$$

The ratio $\left[\frac{\Delta \rho}{\rho} \right]_h$ for the electrolytic solution required in the evaluation of Gr_h was found from equation 3.24 to be

$$\left[\frac{\Delta \rho}{\rho} \right]_h = \frac{\rho(19.35) - \rho(16.0)}{\rho(19.35)}$$

where $\rho(19.35) = 1.0239 \text{ g/cm}^3$

$\rho(16.0) = 1.0254 \text{ g/cm}^3$

ie.
$$\left[\frac{\Delta \rho}{\rho} \right]_h = \frac{1.0254 - 1.0239}{1.0239} = 1.4650 \times 10^{-3}$$

The heat transfer coefficient, h required for the calculation of Nu is given by

$$h = \frac{q_b}{A(T_s - T_b)} \quad 4.26$$

in which q_b , the heat input into the electrolytic solution, is obtained from an overall heat balance around the nickel cathode (see Figure 4.21):

$$q_b = I_h^2 R_h - q_L \quad 4.27$$

where I_h = heater current

R_h = heater resistance

q_L = total heat loss from the electrolytic mixing cell

The total heat loss from the electrolytic mixing cell is given by

$$q_L = q_{L1} + q_{L2} + q_{L3} + q_{L4} + q_{L5} \quad 4.28$$

where q_{L1} = heat loss through the neoprene gasket

q_{L2} = heat loss through the central nickel rod

q_{L3} = heat loss through the Sindanyo base plate and accessories

q_{L4} = heat loss from the Sindanyo base plate and accessories to air by free convection

q_{L5} = heat loss from the central nickel rod to air by free convection

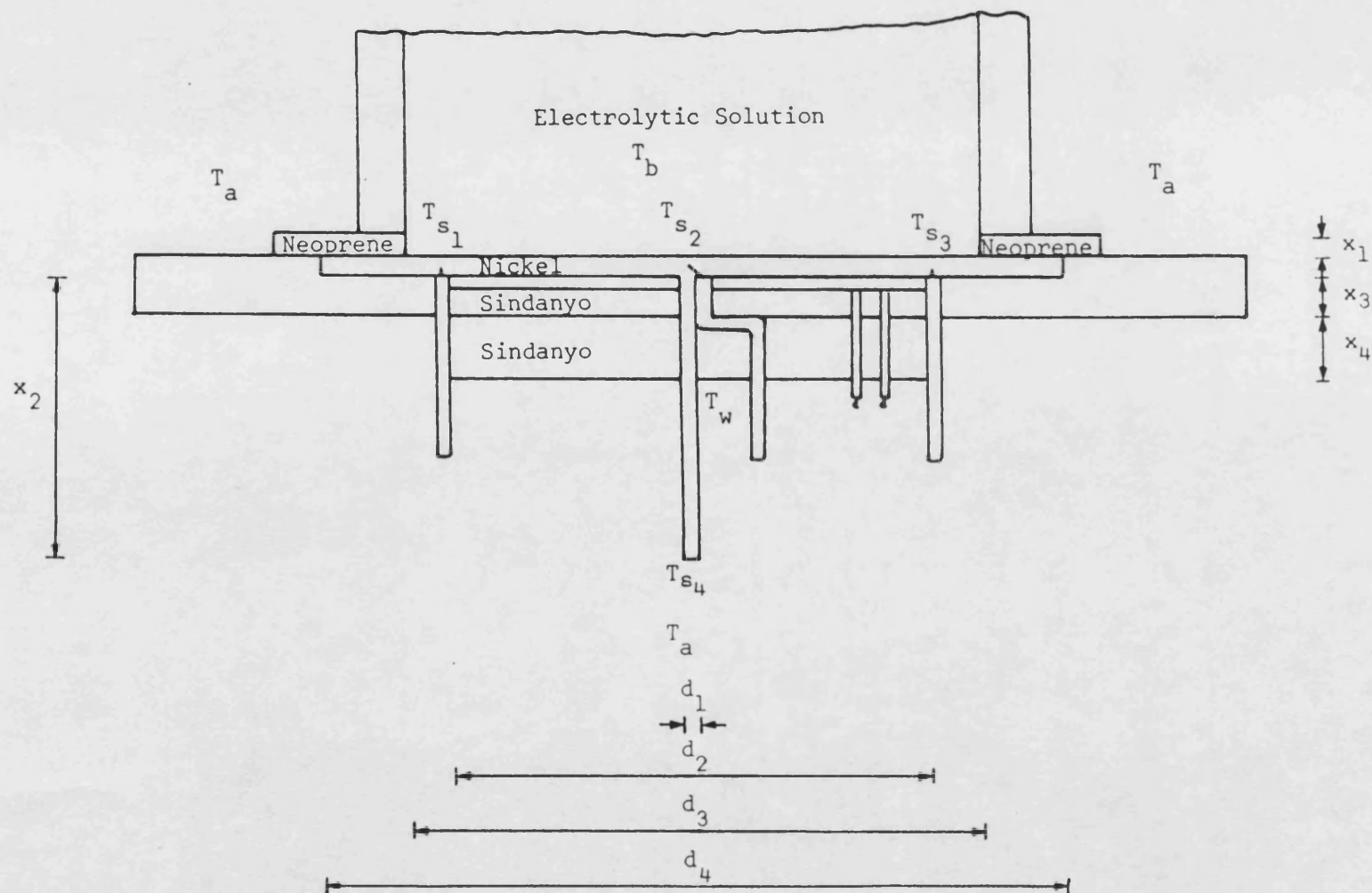
The heat loss through the neoprene gasket is given by

$$q_{L1} = \frac{k_1}{x_1} A_1 \Delta T_1 \quad 4.29$$

where $k_1 = 3.6347 \times 10^{-4} \text{ W/cm K}(393)$

$x_1 = 0.3175 \text{ cm}$

FIGURE 4.21 SCHEMATIC DIAGRAM OF THE BOTTOM HALF OF THE ELECTROLYTIC MIXING CELL



$$A_1 = \frac{\pi}{4}(d_4^2 - d_3^2) = \frac{\pi}{4}(9.0^2 - 7.6^2) = 18.2527 \text{ cm}^2$$

$$\Delta T_1 = \left[\frac{T_{s1} + T_{s3}}{2} + \frac{T_b + T_a}{2} \right] = \left[\frac{18.0 + 18.0}{2} - \frac{16.0 + 16.0}{2} \right] = 1.0^\circ\text{C}$$

Hence, $q_{L1} = 0.0209\text{W}$

The heat loss through the central central rod is given by

$$q_{L2} = \frac{k_2}{x_2} A_2 \Delta T_2 \quad 4.30$$

where $k_2 = 0.60564 \text{ W/cm K}^{(393)}$

$$x_2 = 5.0 \text{ cm}$$

$$A_2 = \frac{\pi}{4}d_1^2 = \frac{\pi}{4}(0.3175)^2 = 0.0792 \text{ cm}^2$$

$$\Delta T_2 = T_{s2} - T_{s4} = 0 \text{ since } T_{s4} = T_{s2}$$

Hence, $q_{L2} = 0\text{W}$

The heat loss through the Sindanyo base plate and accessories is given by

$$q_{L3} = \frac{k_3}{x_3} A_3 \Delta T_3 + \frac{k_3}{x_4} A_4 \Delta T_4 \quad 4.31$$

where $k_3 = 1.0818 \times 10^{-3} \text{ W/cm K}$

$$x_3 = 0.9525 \text{ cm}$$

$$x_4 = 1.0 \text{ cm}$$

$$A_3 = \frac{\pi}{4}(d_4^2 - d_1^2) = \frac{\pi}{4}(9.0^2 - 0.3175^2) = 63.5381 \text{ cm}^2$$

$$A_4 = \frac{\pi}{4}(d_2^2 - d_1^2) = \frac{\pi}{4}(6.4^2 - 0.3175^2) = 32.0907 \text{ cm}^2$$

$$\begin{aligned} \Delta T_3 &= T_{s2} - \left[T_{s2} - \frac{x_3}{x_3 + x_4} (T_{s2} - T_w) \right] \\ &= 20.7 - \left[20.7 - \frac{0.9525}{1.9525} (20.7 - 20.0) \right] \\ &= 0.34^\circ\text{C} \end{aligned}$$

$$\begin{aligned} \Delta T_4 &= \left[T_{s2} - \frac{x_3}{x_3 + x_4} (T_{s2} - T_w) \right] - T_w \\ &= \left[20.7 - \frac{0.9525}{1.9525} (20.7 - 20.0) \right] - 20.0 \end{aligned}$$

$$= 0.36^{\circ}\text{C}$$

$$\text{Hence, } q_{L_3} = 0.0370\text{W}$$

The heat loss from the Sindanyo base plate and accessories to air by free convection is given by

$$q_{L_4} = h_a A_3 \Delta T_5 \quad 4.32$$

$$\begin{aligned} \text{where } h_a &= 1.8657 \left[\frac{T_w - T_a}{d_4} \right]^{0.25} \times 10^{-4} \quad (394) \\ &= 1.8657 \left[\frac{20.0 - 18.0}{9.0} \right]^{0.25} \times 10^{-4} \end{aligned}$$

$$= 1.2810 \times 10^{-4} \text{ W/cm}^2 \text{ K}$$

$$A_3 = \frac{\pi}{4} (d_4^2 - d_1^2) = \frac{\pi}{4} (9.0^2 - 0.3175^2) = 63.5381 \text{ cm}^2$$

$$\Delta T_5 = T_w - T_a = 20.0 - 18.0 = 2.0^{\circ}\text{C}$$

$$\text{Hence, } q_{L_4} = 0.0163\text{W}$$

The heat loss from the central nickel rod to air by free convection is given by

$$q_{L_5} = h_a A_2 \Delta T_6 \quad 4.33$$

$$\begin{aligned} \text{where } h_a &= 1.8657 \left[\frac{T_{s_4} - T_a}{d_1} \right]^{0.25} \times 10^{-4} \quad (394) \\ &= 1.8657 \left[\frac{20.6 - 18.0}{0.3175} \right]^{0.25} \times 10^{-4} \text{ since } T_{s_4} = T_{s_2} \\ &= 3.1562 \times 10^{-4} \text{ W/cm}^2 \text{ K} \end{aligned}$$

$$A_2 = \frac{\pi}{4} d_1^2 = \frac{\pi}{4} (0.3175)^2 = 0.0792 \text{ cm}^2$$

$$\Delta T_6 = T_{s_4} - T_a = 20.7 - 18.0 \text{ since } T_{s_4} = T_{s_2} = 2.7^{\circ}\text{C}$$

$$\text{Hence, } q_{L_5} = 6.7 \times 10^{-5}\text{W}$$

Thus, from equations 4.28, 4.27 and 4.26, it was found that

$$q_L = 0.0209 + 0 + 0.0370 + 0.0163 + 6.7 \times 10^{-5}$$

$$= 0.0743W$$

$$q_D = (0.069)^2 \times 114.5 - 0.0743$$

$$= 0.4688W$$

$$h = \frac{0.4688}{\frac{\pi}{4}(7.6)^2 (19.35 - 16.0)}$$

$$= 3.0845 \times 10^{-3} \text{ W/cm}^2 \text{ K}$$

Using the above physical property and heat transfer data it was found that

1. the Sherwood number defined by equation 4.3 is given by

$$Sh = \frac{3.2 \times 10^{-3} \times 7.6}{1 \times 96487 \times \frac{\pi}{4}(7.6)^2 \times 6.2118 \times 10^{-6} \times 0.005 \times 10^{-3}}$$

$$= 178.9$$

2. the Nusselt number defined by equation 4.19 is given by

$$Nu = \frac{3.0845 \times 10^{-3} \times 7.6}{6.0459 \times 10^{-3}}$$

$$= 3.9$$

3. the Reynolds number defined by equation 4.1 is given by

$$Re = \frac{(5.1)^2 \times \frac{0}{60}}{1.1423 \times 10^{-2}}$$

$$= 0$$

4. the Grashof number for mass transfer defined by equation 4.4 is given by

$$Gr_m = \frac{980.655 \times (7.6)^3}{(1.1423 \times 10^{-2})^2} \times \left| -5.3000 \times 10^{-4} \right|$$

$$= 1.7485 \times 10^6$$

5. the Grashof number for heat transfer defined by equation 4.20 is given by

$$Gr_h = \frac{980.655 \times (7.6)^3}{(1.1423 \times 10^{-2})^2} \times 1.4650 \times 10^{-3}$$

$$= 4.833 \times 10^7$$

6. the Schmidt number defined by equation 2.11 is given by

$$\begin{aligned} Sc &= \frac{1.1423 \times 10^{-2}}{6.2118 \times 10^{-6}} \\ &= 1838.9 \end{aligned}$$

7. the Prandtl number defined by equation 2.16 is given by

$$\begin{aligned} Pr &= \frac{1.1705 \times 10^{-2} \times 4.0870}{6.0459 \times 10^{-3}} \\ &= 7.9 \end{aligned}$$

The derived data obtained from the computer program MAHE for all the $I_L - N$ data where $N = 0$ rpm is tabulated in Appendix A6.8.

Studies in free convection mass and heat transfer at horizontal surfaces is limited in the literature. Wragg and Nasiruddin⁽³⁷¹⁾ used the cathodic deposition of copper from acidified copper sulphate solution to study free convection mass and heat transfer at a heated horizontal copper cathode. They found their results to be well correlated by

$$Sh = 1.75 (GR_m Sc)^{0.227} \quad \text{for } 10^7 < GR_m Sc < 5 \times 10^9 \quad 4.34$$

and

$$Sh = 0.163 (GR_m Sc)^{0.33} \quad \text{for } 5 \times 10^9 < GR_m Sc < 10^{12} \quad 4.35$$

The derived data for all the runs where $N = 0$ rpm given in Appendix A6.8 were plotted in Figure 4.22 as Sh versus $GR_m Sc$ on logarithmic co-ordinates and in Figure 4.23 as Nu versus $GR_h Sc$ on logarithmic co-ordinates. From equations 4.34 and 4.35, it can be concluded that the exponent b in equation 4.15 is approximately $\frac{1}{4}$ when $GR_m Sc < 5 \times 10^9$ and $\frac{1}{3}$ when $GR_m Sc > 5 \times 10^9$.

Since $GR_m Sc > 5 \times 10^9$ in this study, the exponent b in equation 4.15 was assumed to be $\frac{1}{3}$. Using the least squares method, it was found that the 13 data points given in Figure 4.22 were correlated by

$$Sh = 0.0444 (GR_m Sc)^{\frac{1}{3}} \quad 4.36$$

As shown in Figure 4.22, this equation was found to compare poorly with

FIGURE 4.22 A PLOT OF Sh VERSUS $GR_m Sc$ SHOWING THE COMPARISON BETWEEN EQUATION 4.36 OBTAINED FOR ALL RUNS GIVEN IN APPENDIX A6.8 WHERE $N = 0$ rpm AND WRAGG AND NAISRUDDIN'S CORRELATION GIVEN BY EQUATION 4.35

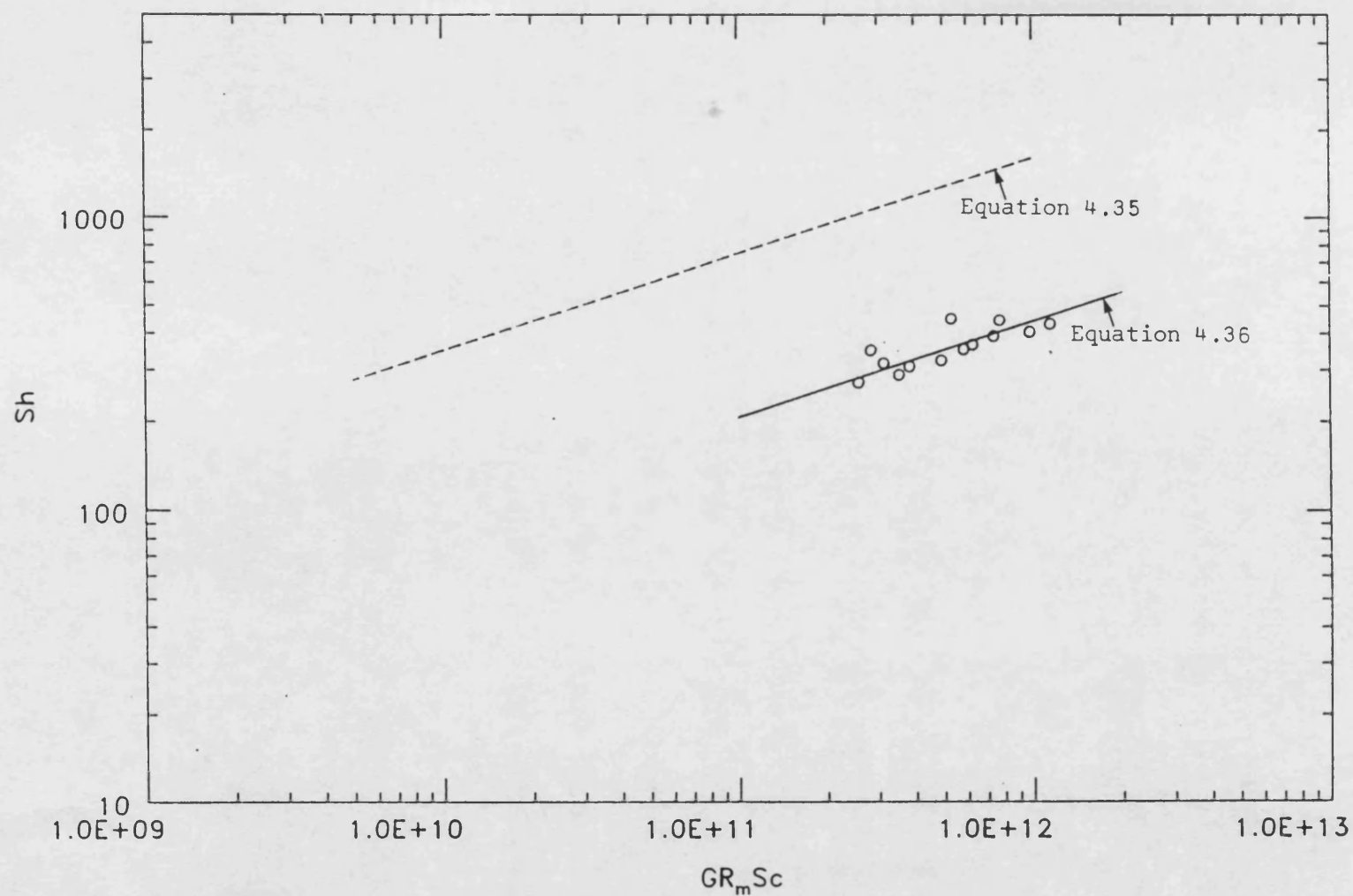
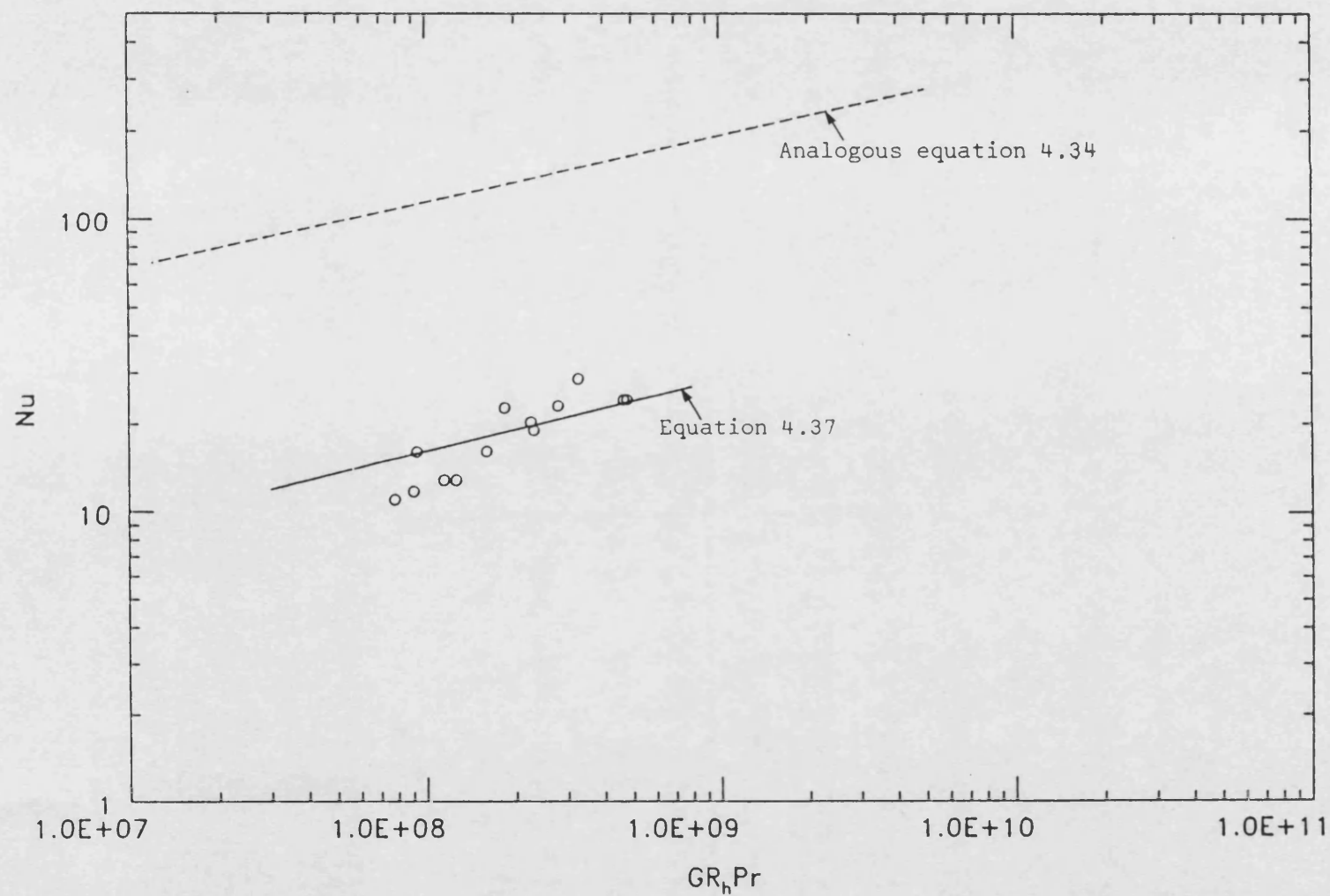


FIGURE 4.23 A PLOT OF Nu VERSUS $Gr_h Pr$ SHOWING THE COMPARISON BETWEEN EQUATION 4.37 OBTAINED FOR ALL RUNS GIVEN IN APPENDIX A6.8 WHERE $N = 0$ rpm AND THE ANALOGOUS EQUATION 4.34



equation 4.35.

Since $GR_h Sc < 5 \times 10^9$ in this study, the exponent b in equation 4.17 was assumed, by analogy with equation 4.15, to be $\frac{1}{4}$. Using the least squares method, it was found that the 13 data points given in Figure 4.23 were correlated by

$$Nu = 0.1609 (GR_h Sc)^{\frac{1}{4}} \quad 4.37$$

As shown in Figure 4.23, this equation was found to compare poorly with the analogous equation 4.34.

4.2.1.2 Forced convection mass and heat transfer

Unlike the correlations for simultaneous mass and heat transfer by free convection which uses GR_m and GR_h instead of Gr_m and Gr_h to take account of both concentration and thermal buoyancy effects, the correlations for simultaneous mass and heat transfer by forced convection are those for mass transfer and heat transfer alone by forced convection where the physical properties for Sh , Nu , Re , Sc and Pr are calculated at T_f .

For agitated vessels, mass transfer by forced convection is usually expressed in the form of the Gilliland-Sherwood correlation⁽³⁸⁷⁾ given by equation 4.8 where Sh , Re and Sc are defined by equations 4.3, 4.1 and 2.11 respectively whereas heat transfer by forced convection is usually expressed in terms of

$$Nu = a Re^b Sc^c \quad 4.38$$

where Nu , Re and Pr are defined by equations 4.19, 4.1 and 2.16 respectively.

For all the $I_L - N$ data where $N > 0$ rpm given in Appendix A6.8, mass and heat transfer in the electrolytic mixing cell was by forced convection. The calculation of Sh , Nu , Re , Sc and Pr for this data (see example given in Section 4.2.1.1) was carried out by the computer program MAHE given in Appendix A7.2. This derived data is tabulated in Appendix A6.8.

Several investigators have found by experiment that the exponent of Sc and Pr in equations 4.8 and 4.38 for agitated vessels is $\frac{1}{3}$. Thus, equations 4.8 and 4.38 can be rewritten in the form of equations 4.9 and 4.39

$$Nu = a Re^b Pr^{\frac{1}{3}} \quad 4.39$$

The values of a and b in equations 4.9 and 4.39 can be determined by the least squares method since equations 4.9 and 4.39 can be linearised into equations 4.40 and 4.40

$$\ln \frac{Nu}{Pr^{\frac{1}{3}}} = \ln a + b \ln Re \quad 4.40$$

The derived data for all the runs where $N > 0$ rpm given in Appendix A6.8 were plotted in Figure 4.24 as $Sh/Sc^{\frac{1}{3}}$ versus Re on logarithmic co-ordinates and in Figure 4.25 as $Nu/Pr^{\frac{1}{3}}$ versus Re on logarithmic co-ordinates. Using the least squares method, it was found that the 89 data points given in Figures 4.24 and 4.25 were correlated by

$$Sh = 2.5244 Re^{0.4205} Sc^{\frac{1}{3}} \quad 4.41$$

$$Nu = 0.4555 Re^{0.4622} Sc^{\frac{1}{3}} \quad 4.42$$

The standard deviation and correlation coefficient for equations 4.41 and 4.42 were found respectively to be 0.1218 and 94.3% and 0.3382 and 74.7%.

It can be seen from Figure 4.26 that equation 4.41 is in some agreement with equation 4.11 that was plotted for forced convection mass transfer in the electrolytic mixing cell. The difference in the two slopes can be possibly be attributed to the errors introduced by the use of T_f to calculate the physical properties in equation 4.41 rather than the use of T_b .

A summary of the correlations that have been proposed in the literature for forced convection heat transfer in agitated vessels where the impeller is of the turbine type is given in Table 4.5. It can be seen from Figure 4.27 that equation 4.42 is in poor agreement with the heat transfer correlations given in Table 4.5. Differences between equation 4.42 and the heat transfer correlations can be attributed to the differences between the geometrical configuration of the mixing cell used in this study (see Table 4.3) and of the agitated vessels used in other studies (see Table 4.5) and possibly the difficulties in estimating q_b required for the calculation of Nu in this study.

It can be seen from the comparison of equations 4.41 and 4.42 that the exponents on Re are similar whereas the constants are different. The difference in the constants can be attributed to $Sc^{\frac{1}{3}}$ being 5-6 times larger than $Pr^{\frac{1}{3}}$ for the electrochemical system used in this study.

FIGURE 4.24 A PLOT OF $Sh/Sc^{1/3}$ VERSUS Re FOR THE ELECTROLYTIC MIXING CELL WITHOUT THE PRESENCE OF GLASS SPHERICAL PARTICLES ON THE HEATED CATHODE

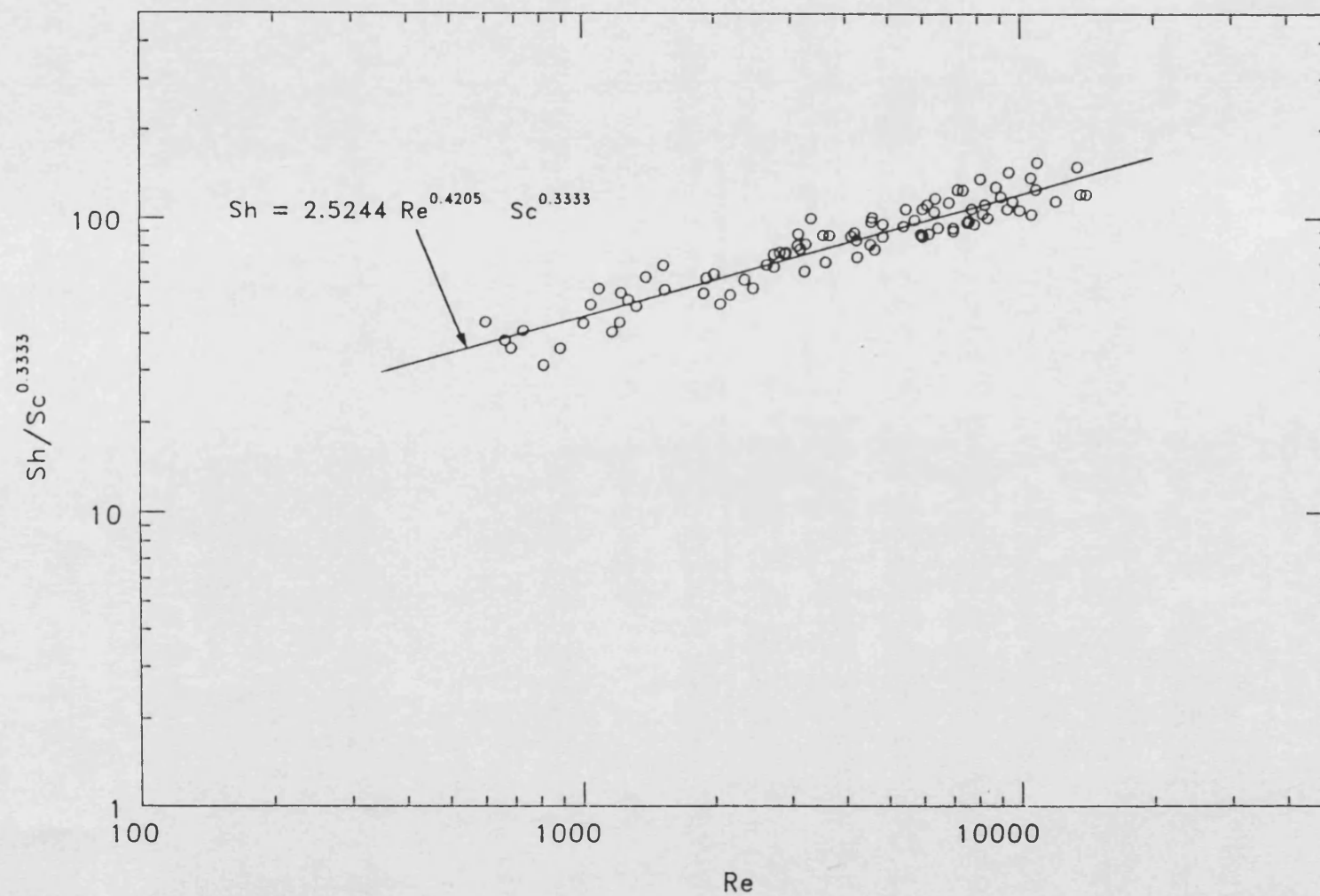


FIGURE 4.25 A PLOT OF $Nu/Pr^{1/3}$ VERSUS Re FOR THE ELECTROLYTIC MIXING CELL WITHOUT THE PRESENCE OF GLASS SPHERICAL PARTICLES ON THE HEATED CATHODE

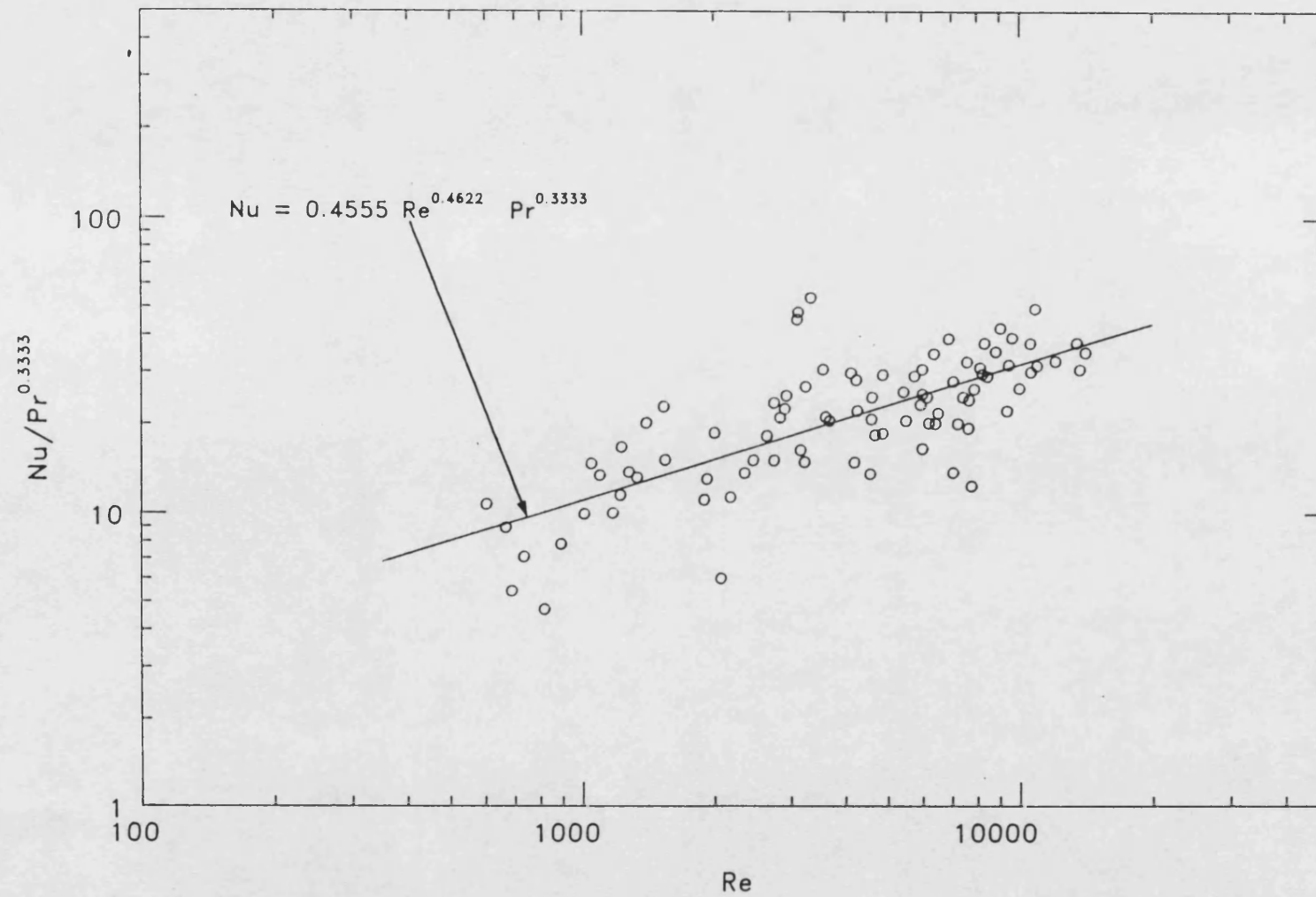


FIGURE 4.26 A PLOT OF $Sh/Sc^{1/3}$ VERSUS Re SHOWING THE COMPARISON BETWEEN EQUATION 4.41 AND EQUATION 4.11

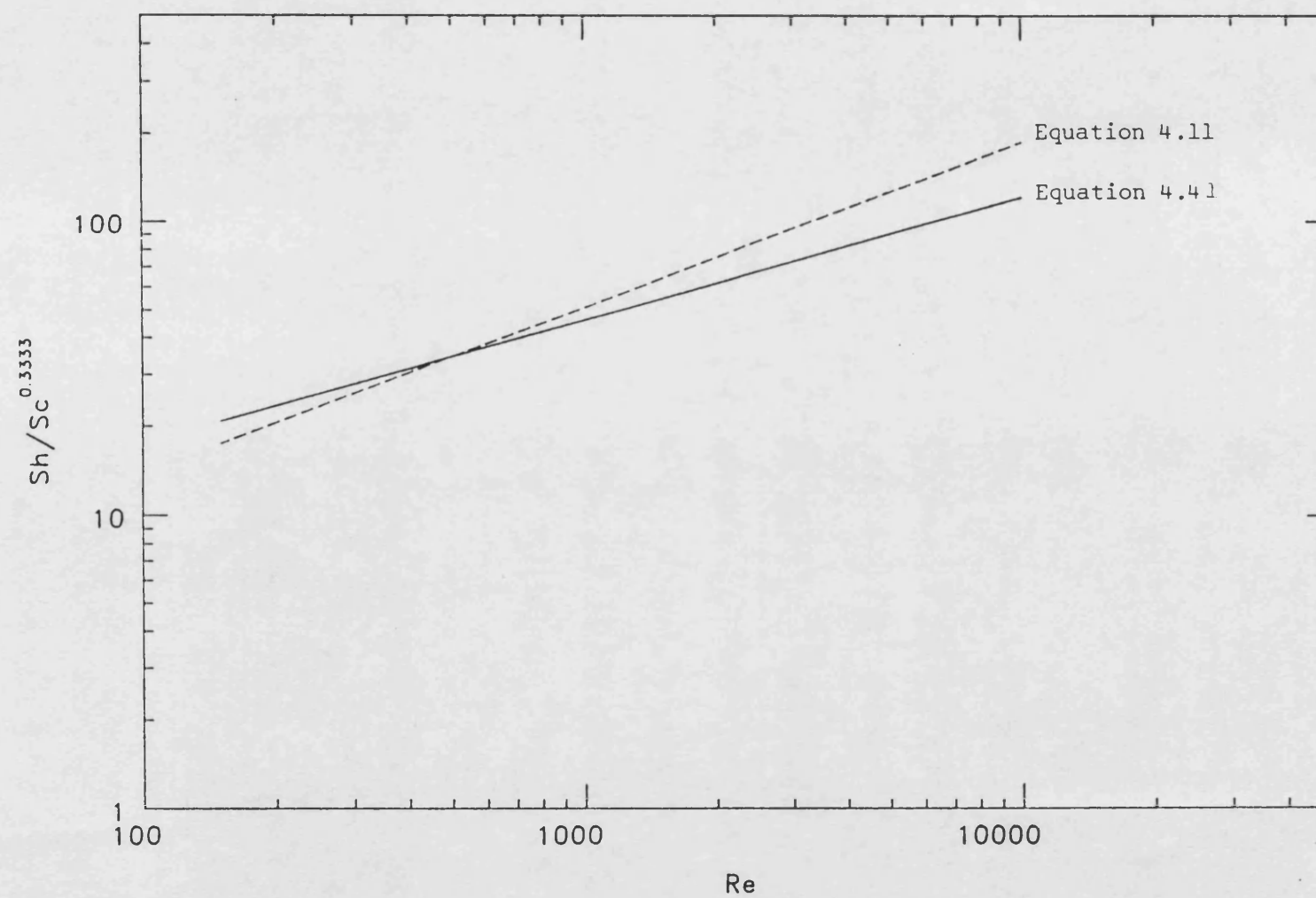
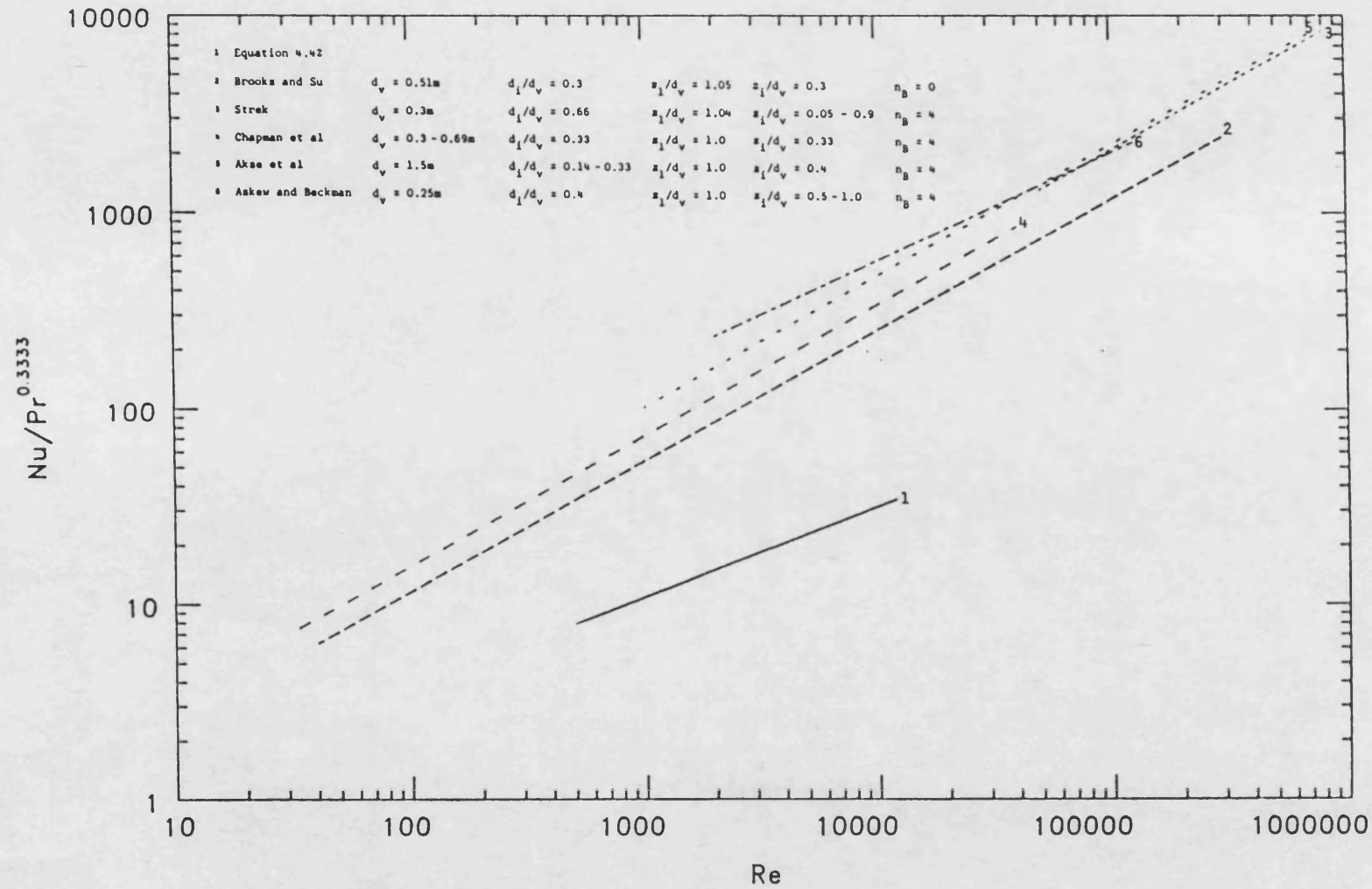


TABLE 4.5 CORRELATIONS FOR HEAT TRANSFER IN AGITATED VESSELS

AUTHOR	VESSEL SCHEME	IMPELLER	VESSEL DIMENSIONS								TEST FLUIDS	CORRELATION	Re	Pr
			d_t (m)	$\frac{d_i}{d_v}$	$\frac{a_1}{d_v}$	$\frac{a_2}{d_v}$	$\frac{w_b}{d_i}$	$\frac{l_b}{d_i}$	n_s	$\frac{w_s}{d_v}$				
Cummings and West (1955)		2 4-bladed, retracting turbines	0.76	0.4	1.0	0.33	0.17	-	0	-	Water Toluene Isopropyl alcohol Ethylene glycol Glycerol Mineral oil	$Nu = a Re^{\frac{1}{2}} Pr^{\frac{1}{3}} V_i^{0.14}$ where $a = 0.68$ (275, 387)	$2 \times 10^3 - 8 \times 10^5$	2-1200
Ackley (1955)		3-bladed, retracting turbine	Not given								Water Heavy viscous organics	$Nu = a Re^{\frac{1}{2}} Pr^{\frac{1}{3}} V_i^{0.14}$ where $a = 0.33$ for glassed steel impeller $a = 0.37$ for alloy impeller	$2 \times 10^3 - 2 \times 10^5$	Not given
Uhl (1957)		6-bladed, 45° pitched turbine	0.6 0.6	0.5 0.5	1.2 1.2	0.17 0.47	0.17 0.17	- -	4 4	0.11 0.11	Linseed Oil	$Nu = 0.44 Re^{\frac{1}{2}} Pr^{\frac{1}{3}} V_i^{0.24}$ $Nu = 0.535 Re^{\frac{1}{2}} Pr^{\frac{1}{3}} V_i^{0.24}$	20-200 20-200	Not given Not given
Kapustin (196)		6-bladed disc turbine	0.3 0.3	0.33 0.33	1.1 1.1	0.11 0.35	0.15 0.15	0.16 0.16	0 0	- -	Mineral oils	$Nu = 1.0 Re^{\frac{1}{2}} Pr^{\frac{1}{3}} V_i^{0.14}$ $Nu = 1.24 Re^{\frac{1}{2}} Pr^{\frac{1}{3}} V_i^{0.14}$	$1 \times 10^2 - 1 \times 10^4$ $1 \times 10^2 - 1 \times 10^5$	300-8500 300-8500
Brooks and Su (199)		6-bladed disc turbine	0.51 0.51	0.3 0.3	1.05 1.05	0.3 0.3	0.21 0.21	0.25 0.25	0 1,2,4	- 0.1	Water Oils Corn syrup	$Nu = 0.54 Re^{\frac{1}{2}} Pr^{\frac{1}{3}} V_i^{0.14}$ $Nu = 0.74 Re^{\frac{1}{2}} Pr^{\frac{1}{3}} V_i^{0.14}$	$40 - 3 \times 10^5$ $300 - 3 \times 10^5$	Not given Not given
Strek (400)		6-bladed disc turbine	0.3	0.17 0.25 0.33 0.42 0.50 0.58 0.66 0.75 0.33	1.04	0.05-0.9	0.2	0.25	4	0.1	Oils Aqueous glycerol solutions	$Nu = 1.01 Re^{\frac{1}{2}} Pr^{\frac{1}{3}} V_i^{0.14} \left[\frac{d_i}{d_v} \right]^{0.13} \left[\frac{a_1}{d_v} \right]^{0.12}$	$5 \times 10^3 - 8 \times 10^5$	1.8 - 105
Chapman, Dallenbach and Holland (401)		6-bladed disc turbine	0.3 0.38 0.46 0.69	0.33	1.0	0.08-0.33	0.2	0.25	4	0.1	Lubricating oils Castor oil	$Nu = 1.15 Re^{0.65} Pr^{\frac{1}{3}} V_i^{0.24} \left[\frac{a_1}{d_v} \right]^{-0.56} \left[\frac{a_2}{d_v} \right]^{-0.4}$	$30 - 4 \times 10^4$	Not given
Akso, Beek, Van Berkel and De Graauw (402)		6-bladed disc turbine	1.5	0.14 0.2 0.33	1.0	0.2-0.7	0.2	0.25	4	0.1	Water	$Nu = 0.81 Re^{0.68} Pr^{\frac{1}{3}} V_i^{0.14} \left\{ \left[\frac{a_1}{d_v} \right]^{\frac{1}{2}} + \left[1 - \frac{a_1}{d_v} \right]^{\frac{1}{2}} \right\}$	$1 \times 10^3 - 7 \times 10^5$	Not given
Aske and Beckman (403)		6-bladed disc turbine	0.25	0.4	1.0	0.5 1.0	?	?	4	0.1	Water Lubricating oils	$Nu = 3.57 Re^{0.55} Pr^{0.30}$	$2 \times 10^3 - 1.25 \times 10^5$	
		6-bladed 45° pitched turbine	0.25	0.4	1.0	0.5 1.0	?	?	4	0.1		$Nu = 2.71 Re^{0.55} Pr^{0.30}$	$5 \times 10^3 - 1.4 \times 10^5$	5 - 2000

FIGURE 4.27 A PLOT OF $Nu/Pr^{1/3}$ VERSUS Re SHOWING THE COMPARISON BETWEEN EQUATION 4.42 AND THE HEAT TRANSFER CORRELATIONS GIVEN IN TABLE 4.5



4.2.2 Mass and heat transfer in the electrolytic mixing cell with the presence of glass spherical particles on the cathode

From the plots showing the effect of the cathode surface temperature upon the average current-potential curve of a fixed impeller rotational speed for the electrolytic mixing cell with the presence of one or more layers of glass spherical particles of known dimensions on the cathode where ΔT is a constant, it was found that a limiting current is obtained for each current-potential curve when the potential is in the range of 0.8-1.4 volts. Hence, by setting the potential at $\sim 0.9V$, the average limiting current can be measured as a function of the impeller rotational speed for various ΔT . In this study, the $I_L - N$ data was obtained for $N < N_f$. This data is given in Appendix A6.9.

For all the $I_L - N$ data where $N > 0$ rpm given in Appendix A6.9, simultaneous mass and heat transfer in the electrolytic mixing cell with the presence of one or more layers of glass spherical particles of known dimensions on the cathode was by forced convection. Hence, this data was expressed in terms of equations 4.8 and 4.39 where Sh , Nu , Re , Sc and Pr , are defined by equations 4.12, 4.43, 4.1, 2.11 and 2.16 respectively.

$$Nu = \frac{h_f d}{k} \quad 4.43$$

where h_f = heat transfer coefficient for the fluid phase

By taking Run 1.02 of Table A6.9.1 (ie. $d_p = 0.3\text{mm}$, $n_1 = 1$, $N = 24.5$ rpm, $I_L = 6.1\text{mA}$, $c_b = 0.005\text{M}$, $T_b = 18.3^\circ\text{C}$, $T_{s1} = 25.3^\circ\text{C}$, $T_{s2} = 32.1^\circ\text{C}$, $T_{s3} = 25.3^\circ\text{C}$, $T_w = 26.9^\circ\text{C}$, $T_a = 16.6^\circ\text{C}$, $I_h = 0.148\text{A}$, $R_h = 114.5\Omega$) as an example, the calculation of Sh , Nu , Re , Sc and Pr carried out by the computer program MAHE given in Appendix A7.2 was as follows:

Using the method of calculation shown in the example given in Section 4.2.1.1, it was found that

$$T_s = 28.7^\circ\text{C}$$

$$T_f = 23.5^\circ\text{C}$$

$$\rho = 1.0219 \text{ g/cm}^3$$

$$\nu = 1.0079 \text{ mm}^2/\text{s}$$

$$\mu = 0.01030 \text{ g/cm s}$$

$$\begin{aligned}
D &= 7.20 \times 10^{-6} \text{ cm}^2/\text{s} \\
k &= 6.164 \times 10^{-3} \text{ W/cm K} \\
c_p &= 4.0867 \text{ J/g K} \\
q_{L_1} &= 0.1629 \text{ W} \\
q_{L_2} &= 0 \text{ W} \\
q_{L_3} &= 0.2755 \text{ W} \\
q_{L_4} &= 0.1255 \text{ W} \\
q_{L_5} &= 0.006 \text{ W} \\
q_L &= 0.5645 \text{ W}
\end{aligned}$$

The heat transfer coefficient for the fluid phase required for the calculation of Nu is given by

$$h_f = \frac{q_f}{A(T_s - T_b)} \quad 4.44$$

in which q_f , the heat input into the fluid phase, is given by

$$q_f = I_h^2 R_h - q_L - q_p \quad 4.45$$

in which q_p , the heat input into the particulate phase, is given by

$$q_p = \frac{k_{eff}(1 - \epsilon)(T_s - T_i)}{x} \quad 4.46$$

where k_{eff} was estimated from Yagi, Kunii and Wakao's correlation for a stagnant porous solid saturated with liquid⁽⁴⁰⁴⁾

$$k_{eff} = \epsilon k_f + (1 - \epsilon)k_p \quad 4.47$$

$\epsilon = 0.39$ for a random packed bed of uniform spherical particles^(405,406)

T_i , the simulated fouling deposit/electrolytic solution interfacial temperature is assumed to be equal to T_f

x , the simulated fouling deposit thickness is estimated from

$$x = d_p(0.933n_1 + 0.067) \quad 4.48$$

The basis of equation 4.48 is outlined in Appendix A8.

Thus from equations 4.47, 4.48, 4.46, 4.45 and 4.44, it was found that

$$\begin{aligned}x &= 0.3(0.933 \times 1 + 0.067) \\&= 0.3\text{cm}\end{aligned}$$

$$\begin{aligned}k_{\text{eff}} &= 0.39(6.164 \times 10^{-3}) + (1 - 0.39)(0.848 \times 10^{-2}) \\&= 7.5768 \times 10^{-3} \text{ W/cm K}\end{aligned}$$

$$\begin{aligned}q_p &= \frac{7.5768 \times 10^{-3} (1 - 0.39) (28.7 - 23.5)}{0.3} \\&= 0.0803\text{W}\end{aligned}$$

$$\begin{aligned}q_f &= (0.148)^2 \times 114.5 - 0.5645 - 0.0803 \\&= 1.8632\text{W}\end{aligned}$$

$$\begin{aligned}h_f &= \frac{1.8632}{\frac{\pi}{4}(7.6)^2 (28.7 - 18.3)} \\&= 3.9492 \times 10^{-3} \text{ W/cm}^2\text{K}\end{aligned}$$

Using the above physical property and heat transfer data, the Nusselt number defined by equation 4.43 was found to be

$$\begin{aligned}\text{Nu} &= \frac{3.9492 \times 10^{-3} \times 7.6}{6.164 \times 10^{-3}} \\&= 4.87\end{aligned}$$

while the other dimensionless groups (see example given in Section 4.2.1.1 for the method of calculation) were found to be

$$\text{Sh} = 293.0$$

$$\text{Re} = 1058.4$$

$$\text{Pr} = 6.8$$

$$\text{Sc} = 1398.9$$

The derived data obtained from the computer program MAHE for all the I_L data is tabulated in Appendix A6.9.

Several investigators have found by experiment that the exponent of Sc and Pr in equations 4.8 and 4.38 for fixed beds is $\frac{1}{3}$ (327,392). Thus, equations 4.8 and 4.38 can be rewritten in the form of equations 4.9 and 4.39. The values of a and b in equations 4.9 and 4.39 can be determined by the least squares method since equations 4.9 and 4.39 can be linearised into equations 4.10 and 4.40.

The derived data for all the runs where $N > 0$ rpm given in Appendix A6.9 can be plotted as $Sh/Sc^{\frac{1}{3}}$ versus Re on logarithmic co-ordinates and $Nu/Pr^{\frac{1}{3}}$ versus Re on logarithmic co-ordinates. As an example, plots of $Sh/Sc^{\frac{1}{3}}$ versus Re on logarithmic co-ordinates and $Nu/Pr^{\frac{1}{3}}$ versus Re on logarithmic co-ordinates for the electrolytic mixing cell with the presence of 1 layer of 3mm glass spherical particles on the heated cathode are respectively given in Figures 4.28 and 4.29. Using the least squares method, the correlations for these plots are listed in Table 4.6 together with the number of data points used for the correlation, the standard deviation and the correlation coefficient.

It was noted from the mass and heat correlations given in Table 4.6 that for a simulated fouling deposit which constituted of glass spherical particles of a fixed d_p resting on the heated cathode, the exponent b is reasonably independent of the number of layers which constitute the simulated fouling deposit, n_1 . This is clearly shown in Figures 4.30 and 4.31 where the lower and upper values of b in equations 4.9 and 4.39 for each d_p are respectively plotted against d_p . It can be suggested from Figures 4.30 and 4.31 that the b - d_p data first increases to a maximum and then decreases to an asymptote where b at $d_p > 12\text{mm} \rightarrow b$ at $d_p = 0\text{mm}$. Due to insufficient data given in Figures 4.30 and 4.31, no attempt was made to model this data.

In general, it was noted from the mass and heat transfer correlations given in Table 4.6 that for a simulated fouling deposit which constituted of glass spherical particles of a fixed d_p resting on the heated cathode, the constant a decreases non-linearly with increasing n_1 . This is clearly shown in Figures 4.32 and 4.33 where a in equations 4.9 and 4.39 are plotted against n_1 for the simulated fouling deposit constituting of 3mm glass spherical particles. Furthermore, it can be suggested from Figures 4.34 and 4.35 where a in equation 4.9 is plotted against d_p for $n_1 = 1$ and $n_1 = 2$ respectively and from Figures 4.36 and 4.37 where a in equation 4.39 is plotted against d_p for

FIGURE 4.28 A PLOT OF $Sh/Sc^{1/3}$ VERSUS Re FOR THE ELECTROLYTIC MIXING CELL WITH THE PRESENCE OF 1 LAYER OF 3MM GLASS PARTICLES ON THE HEATED CATHODE

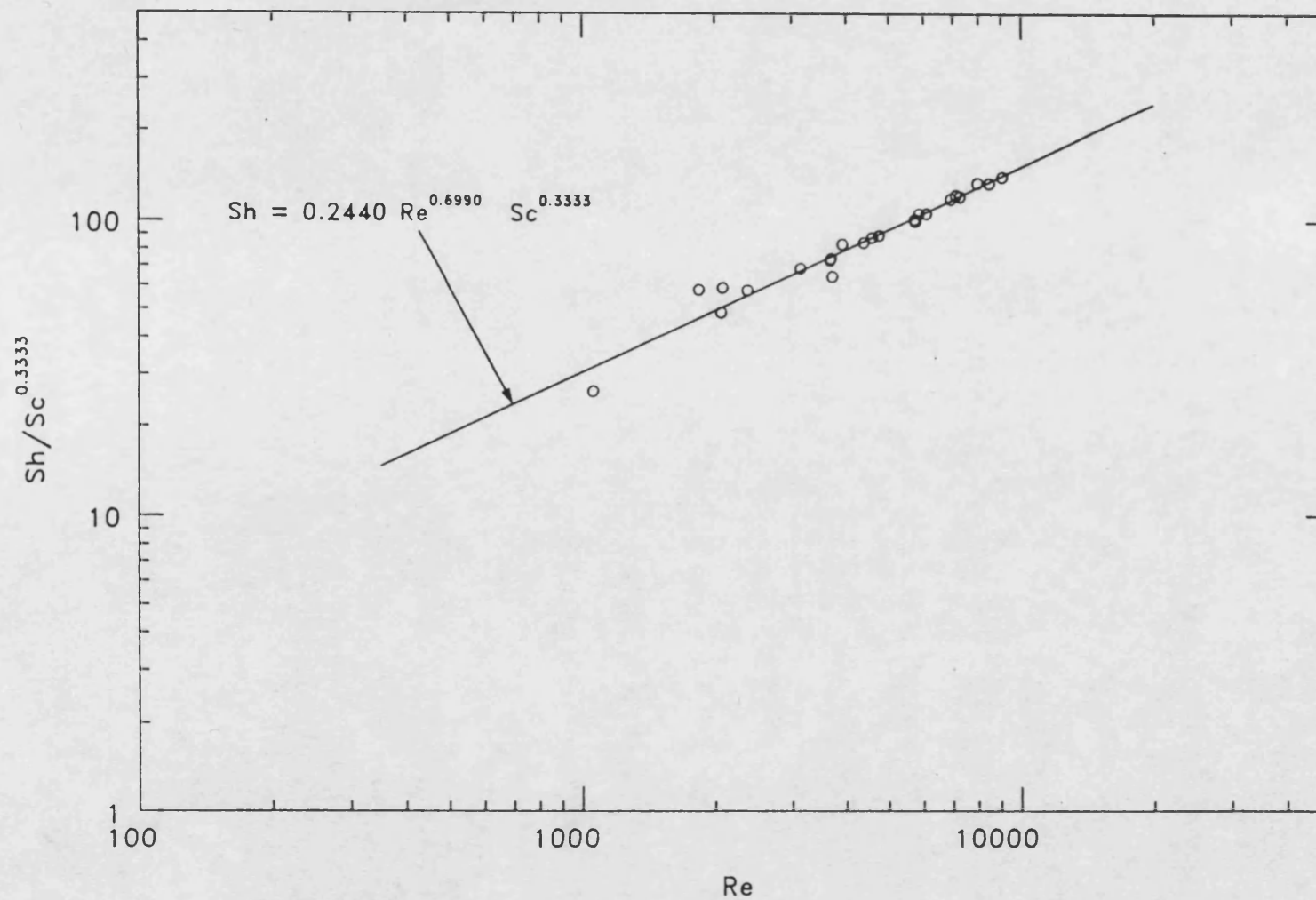


FIGURE 4.29 A PLOT OF $Nu/Pr^{1/3}$ VERSUS Re FOR THE ELECTROLYTIC MIXING CELL WITH THE PRESENCE OF 1 LAYER OF 3MM GLASS SPHERICAL PARTICLES ON THE HEATED CATHODE

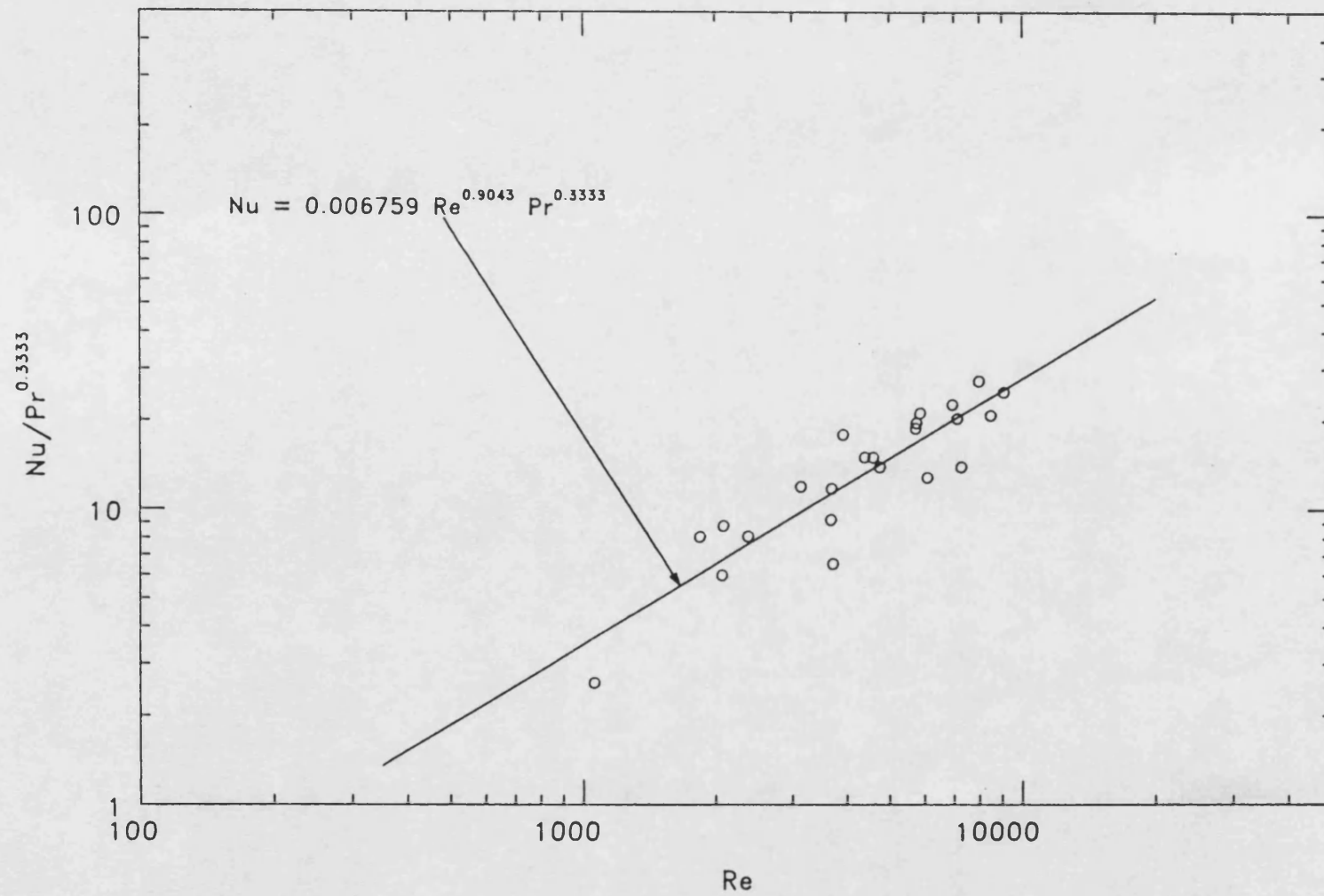


TABLE 4.6 A SUMMARY OF THE MASS AND HEAT TRANSFER CORRELATIONS FOUND FOR THE VARIOUS EXPERIMENTAL CONDITIONS IN THE ELECTROLYTIC MIXING CELL LISTED IN TABLE 3.7

GLASS SPHERICAL PARTICLES		NUMBER OF DATA POINTS	MASS TRANSFER				HEAT TRANSFER			
d_p (mm)	n_1		CORRELATION	STANDARD DEVIATION	CORRELATION COEFFICIENT		CORRELATION	STANDARD DEVIATION	CORRELATION COEFFICIENT	
NONE		89	$Sh = 2.5244 Re^{0.4205} Sc^{0.3333}$	0.1218	94.3%		$Nu = 0.4555 Re^{0.4622} Pr^{0.3333}$	0.3382	74.7%	
3.0	1	23	$Sh = 0.2440 Re^{0.6990} Sc^{0.3333}$	0.0835	97.9%		$Nu = 0.006759 Re^{0.9043} Pr^{0.3333}$	0.2477	90.1%	
	2	7	$Sh = 0.4813 Re^{0.6002} Sc^{0.3333}$	0.1087	93.3%		$Nu = 0.02819 Re^{0.6991} Pr^{0.3333}$	0.1172	94.2%	
7.0	1	17	$Sh = 0.8663 Re^{0.5435} Sc^{0.3333}$	0.0603	98.4%		$Nu = 0.1255 Re^{0.5777} Pr^{0.3333}$	0.2488	82.3%	
	2	13	$Sh = 1.1009 Re^{0.4962} Sc^{0.3333}$	0.0992	96.0%		$Nu = 0.1114 Re^{0.5840} Pr^{0.3333}$	0.2441	85.5%	
12.0	1	25	$Sh = 1.7855 Re^{0.4655} Sc^{0.3333}$	0.1049	95.5%		$Nu = 0.3821 Re^{0.4612} Pr^{0.3333}$	0.2647	78.4%	
	2	19	$Sh = 1.4456 Re^{0.4458} Sc^{0.3333}$	0.0631	97.3%		$Nu = 0.1612 Re^{0.5480} Pr^{0.3333}$	0.2391	80.7%	

FIGURE 4.30 THE VARIATION OF THE EXPONENT b IN EQUATION 4.9 WITH PARTICLE DIAMETER

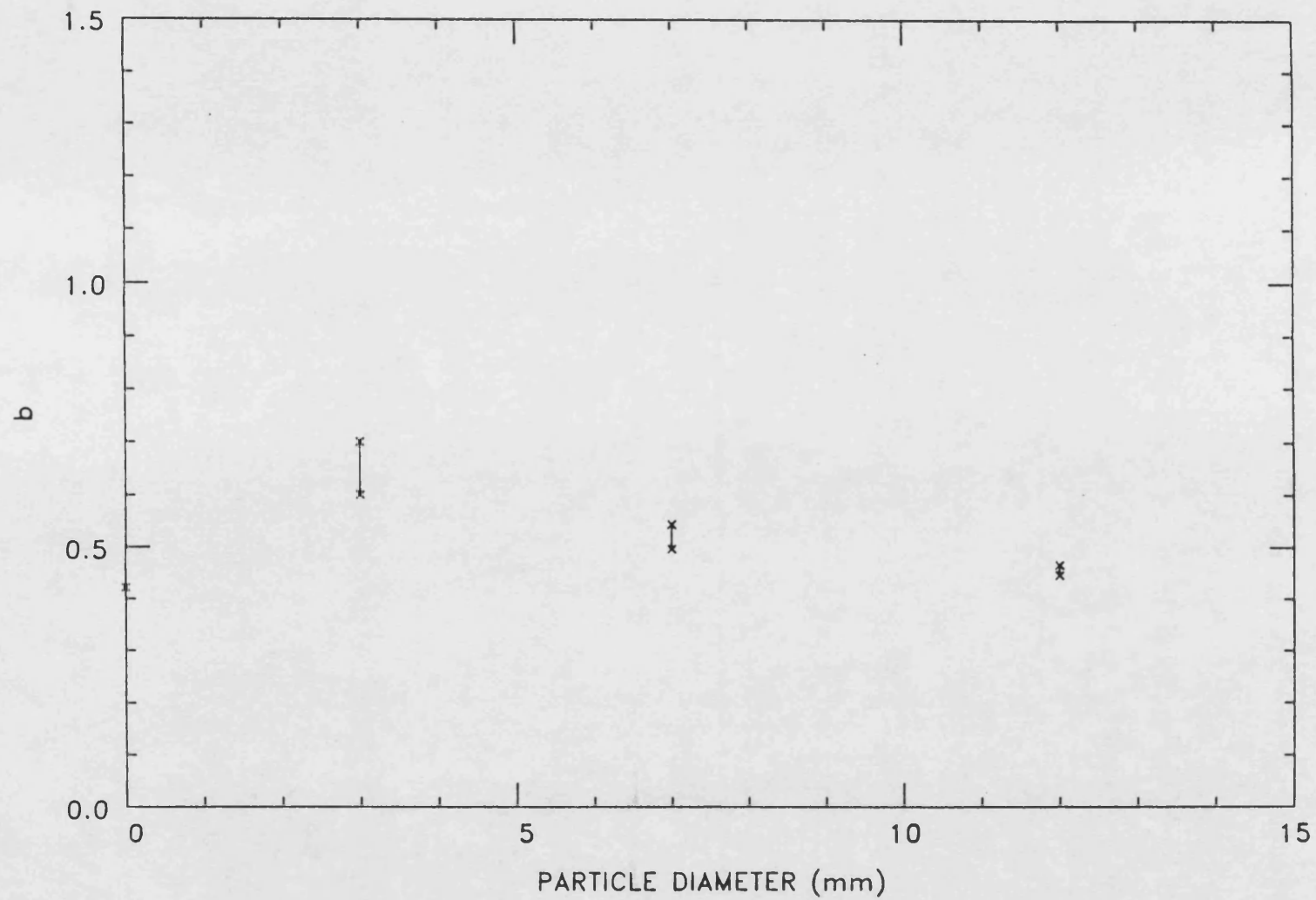


FIGURE 4.31 THE VARIATION OF THE EXPONENT b IN EQUATION 4.39 WITH PARTICLE DIAMETER

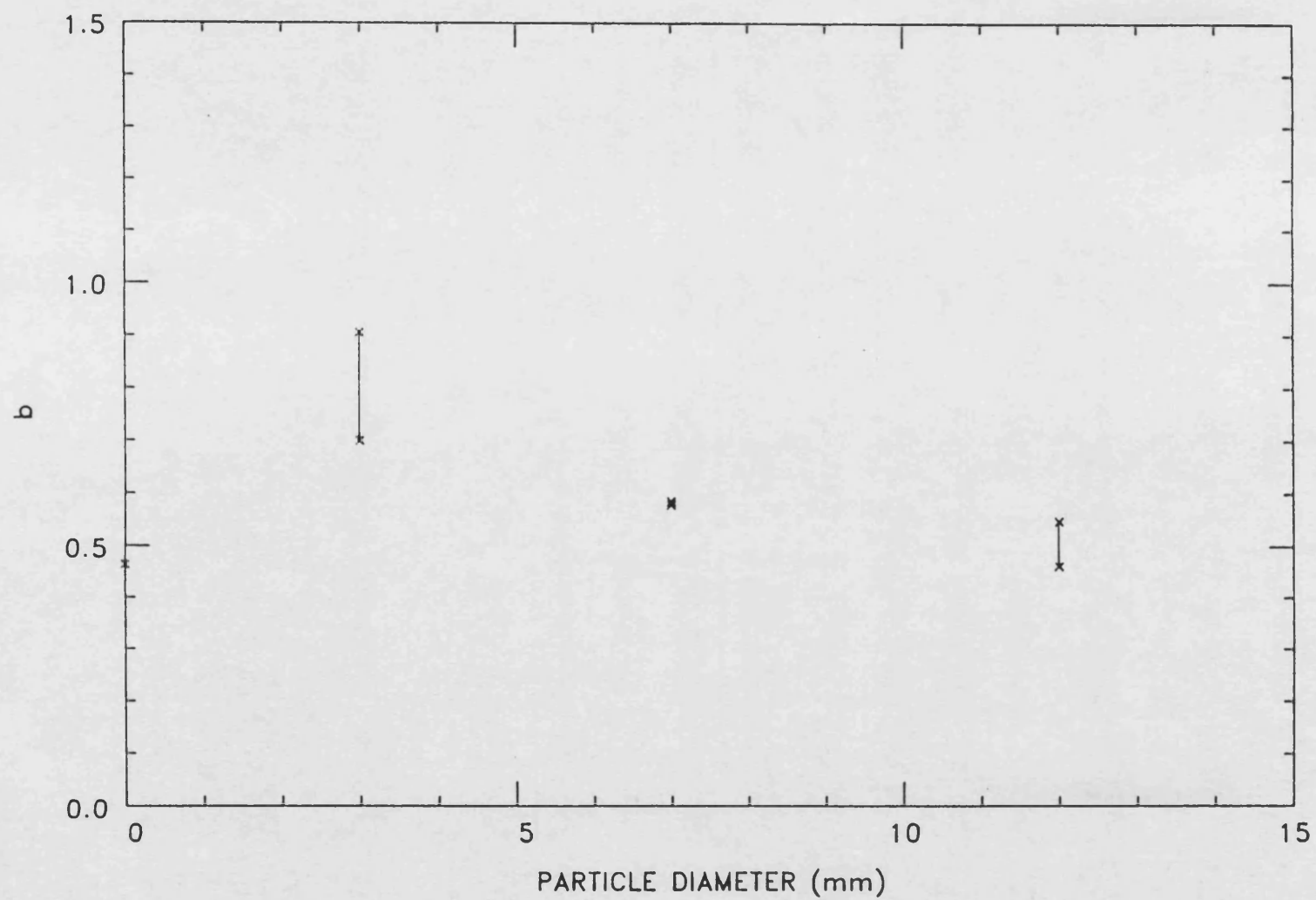


FIGURE 4.32

THE VARIATION OF THE EXPONENT a IN EQUATION 4.9 WITH THE NUMBER OF LAYERS OF 3MM GLASS SPHERICAL PARTICLES RESTING ON THE CATHODE

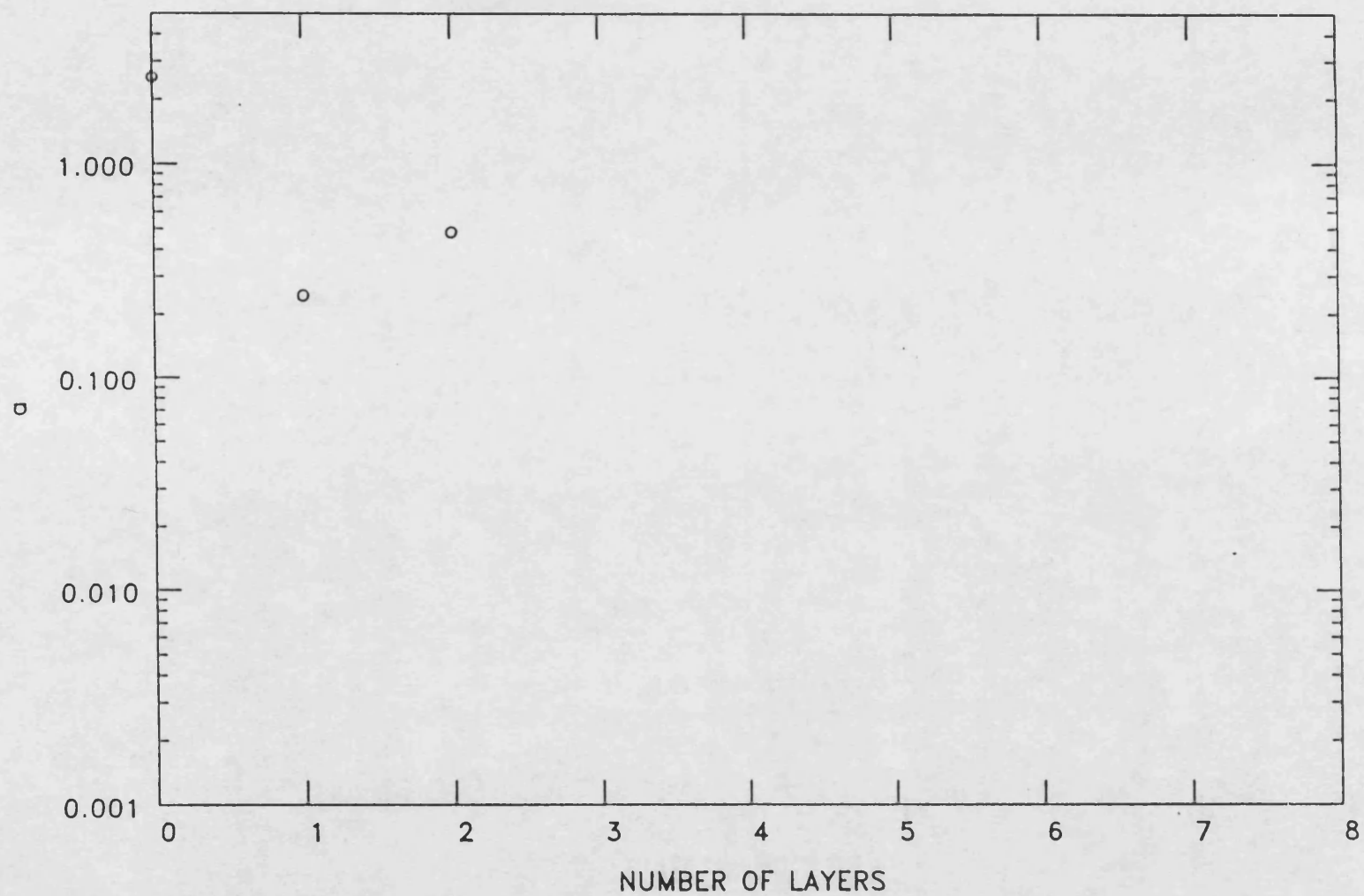


FIGURE 4.33

THE VARIATION OF THE EXPONENT a IN EQUATION 4.39 WITH THE NUMBER OF LAYERS OF 3MM GLASS SPHERICAL PARTICLES RESTING ON THE CATHODE

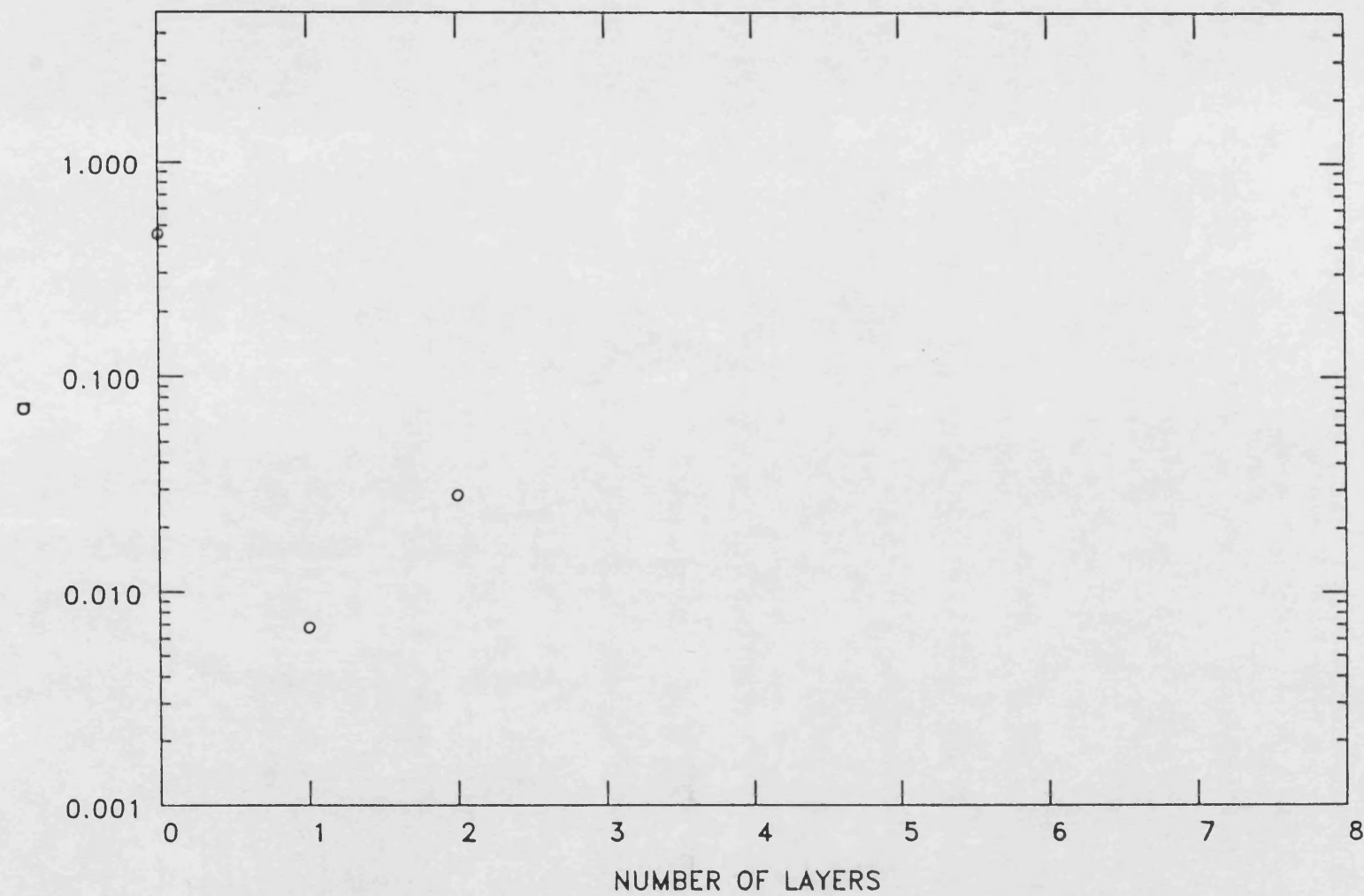


FIGURE 4.34 THE VARIATION OF THE EXPONENT a IN EQUATION 4.9 WITH PARTICLE DIAMETER WHEN $n_1 = 1$

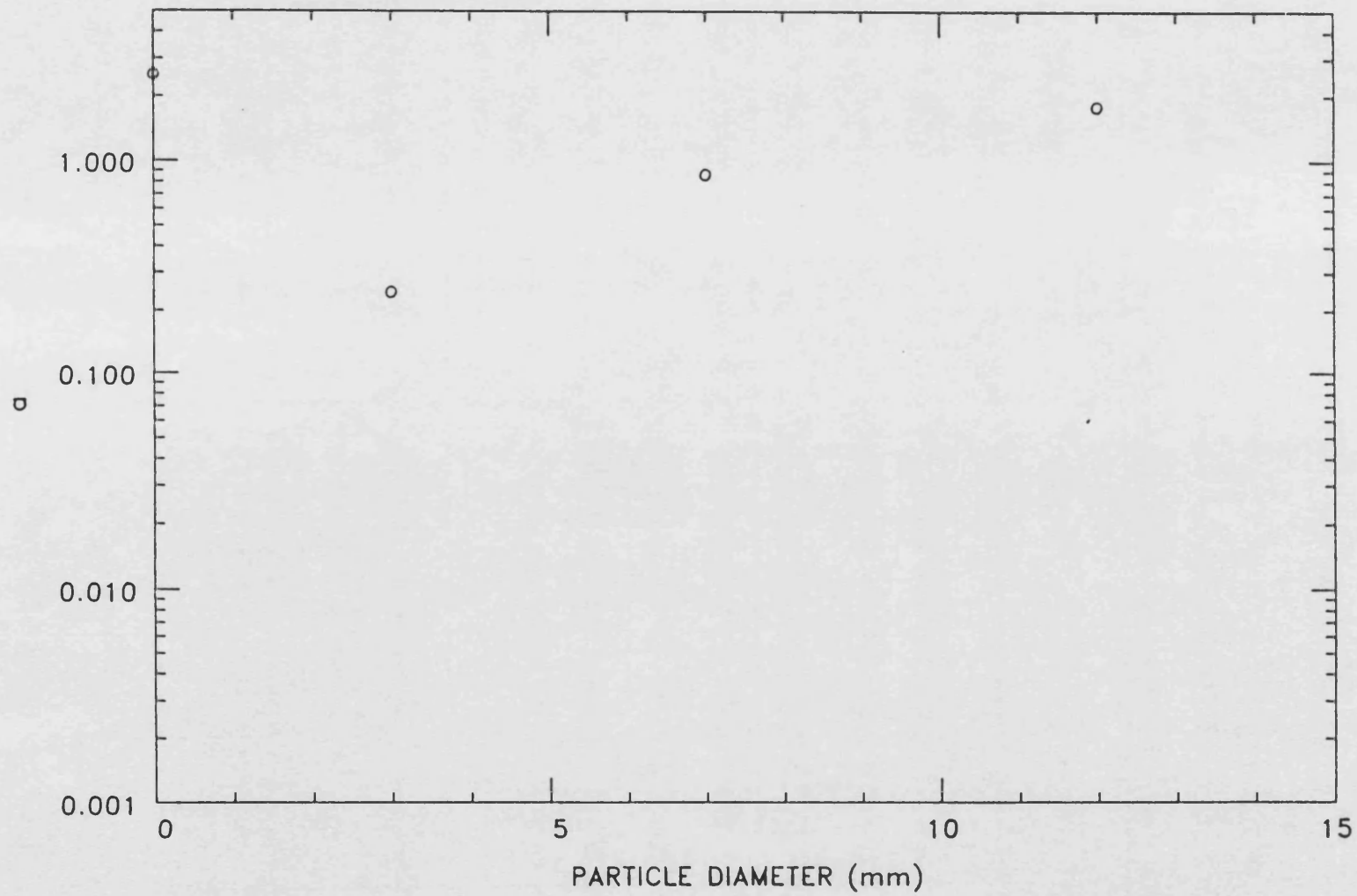


FIGURE 4.35 THE VARIATION OF THE EXPONENT a IN EQUATION 4.9 WITH PARTICLE DIAMETER WHEN $n_1 = 2$

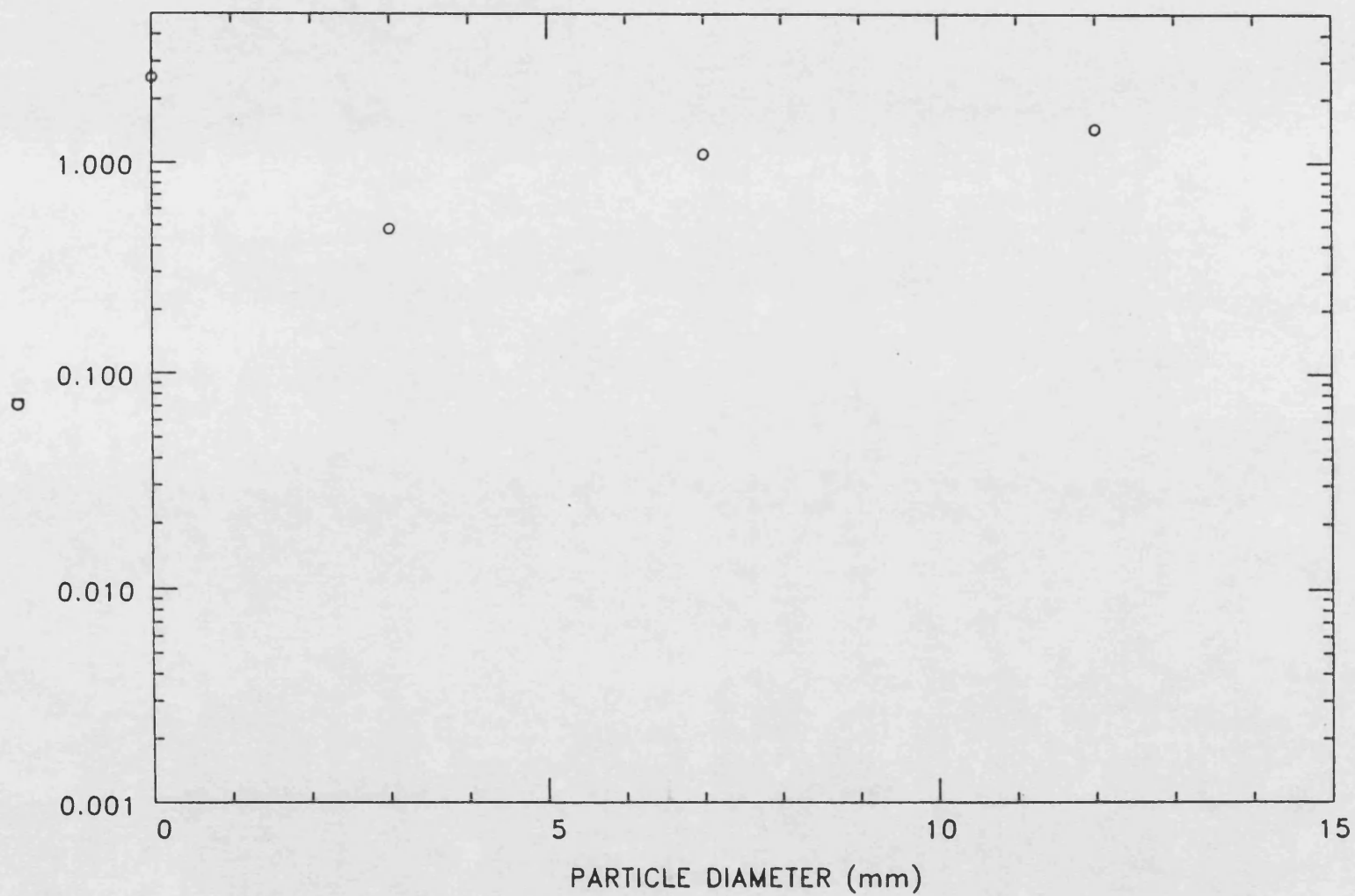


FIGURE 4.36 THE VARIATION OF THE EXPONENT a IN EQUATION 4.39 WITH PARTICLE DIAMETER WHEN $n_1 = 1$

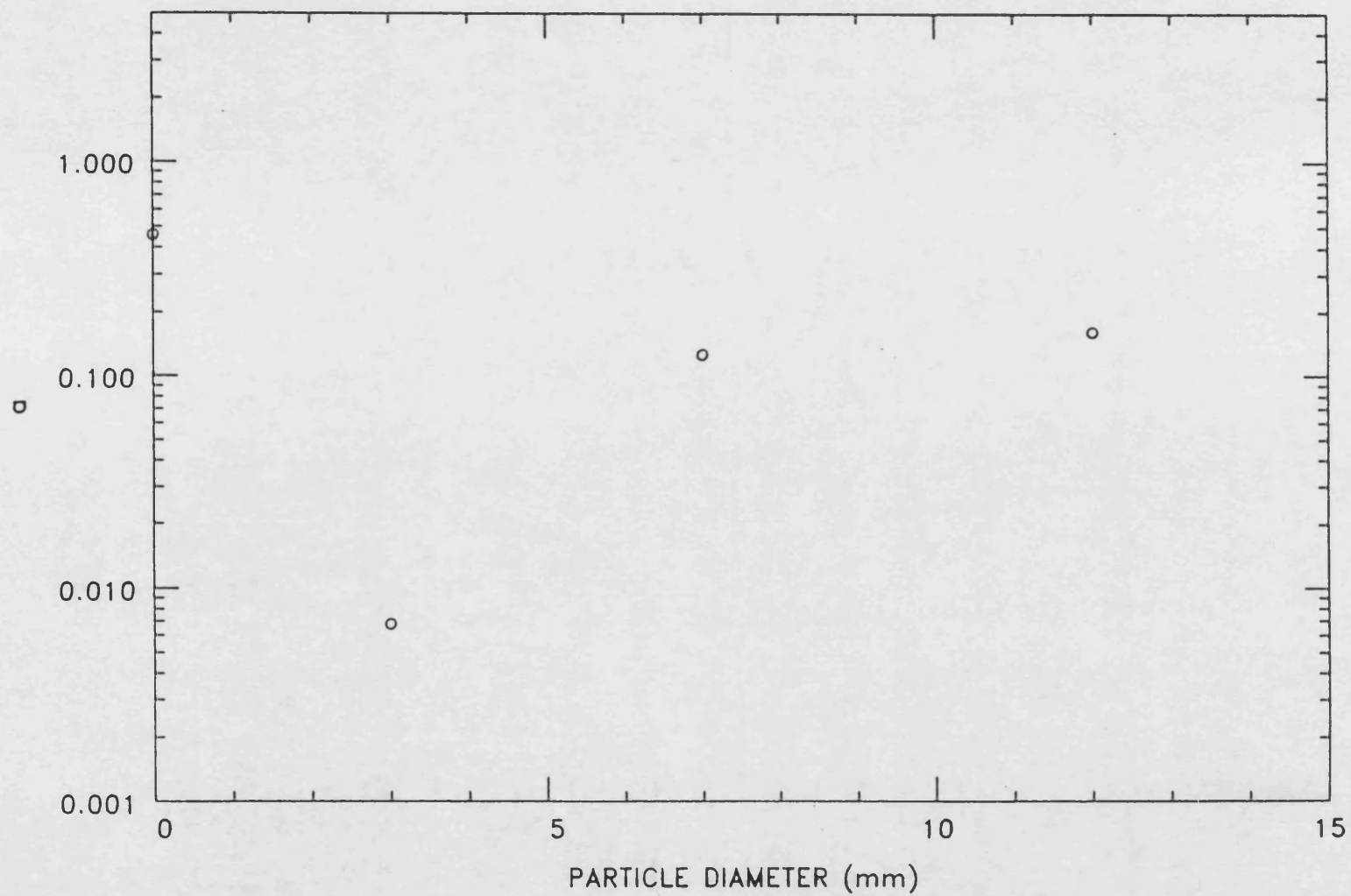
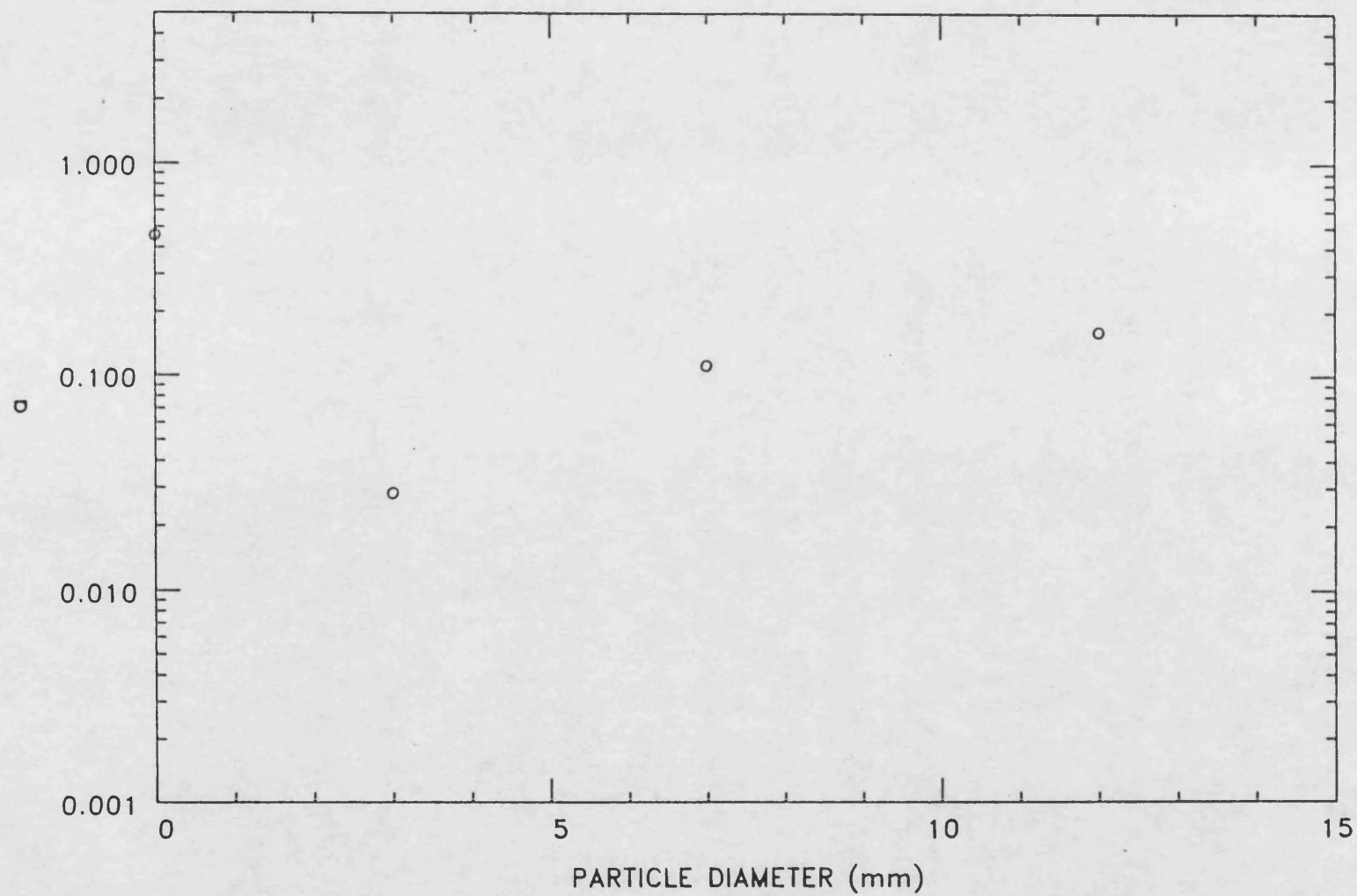


FIGURE 4.37 THE VARIATION OF THE EXPONENT a IN EQUATION 4.39 WITH PARTICLE DIAMETER WHEN $n_1 = 2$

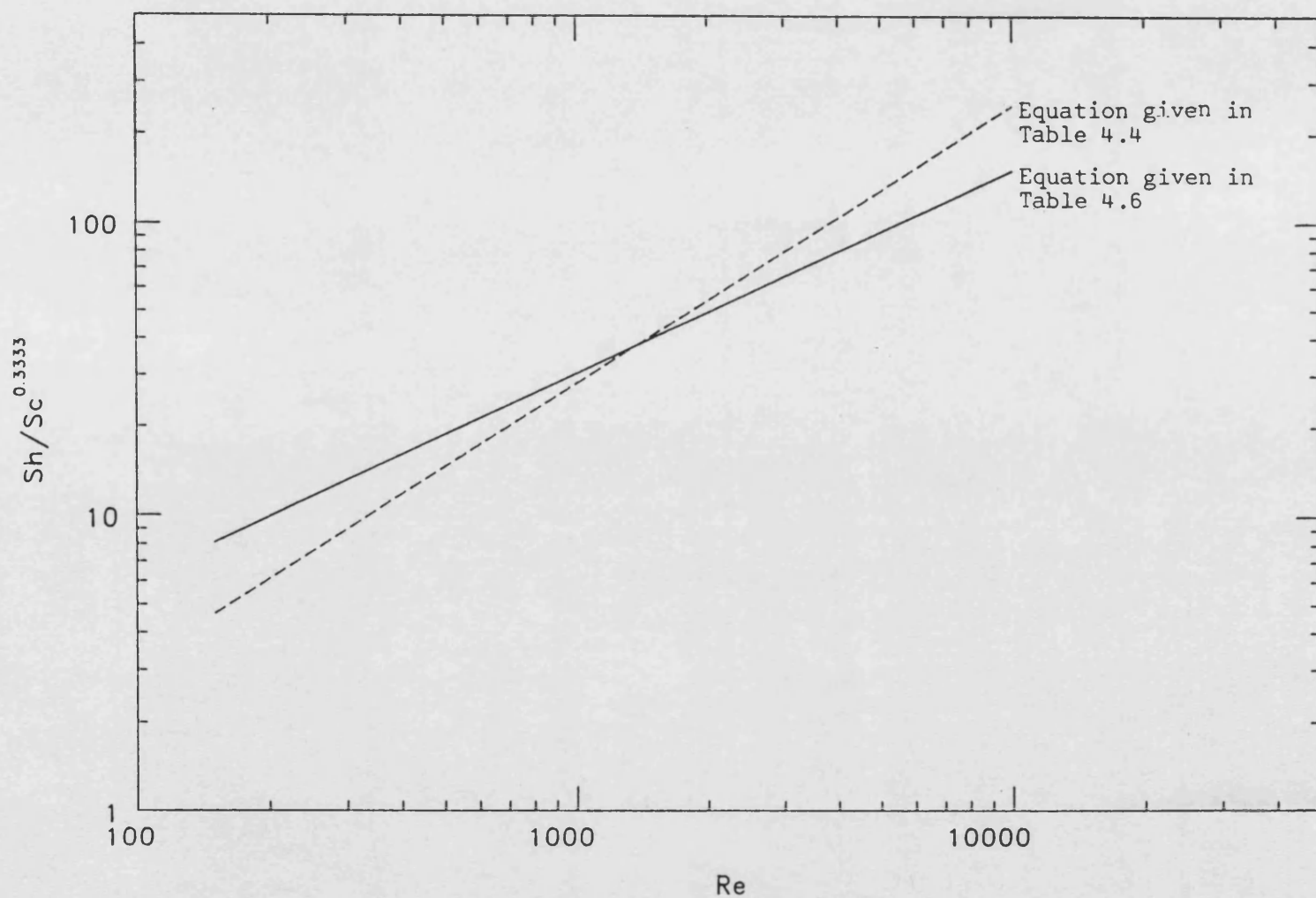


$n_1 = 1$ and $n_1 = 2$ respectively that the $a-d_p$ data for each n_1 first decreases to a minimum and then increases to an asymptote where a at $d_p > 12\text{mm} \rightarrow a$ at $d_p = 0\text{mm}$. Due to insufficient data given in Figures 4.34 - 4.37, no attempt was made to model this data.

It can be seen from the comparison between the mass transfer correlations given in Tables 4.4 and 4.6 that for a given simulated fouling deposit, the values of a given in Table 4.6 are greater than the corresponding values of a given in Table 4.4 whereas the values of b given in Table 4.6 are less than the corresponding values of b given in Table 4.4. However, it was generally found that the mass transfer correlations given in Table 4.6 are in some agreement with those given in Table 4.4. This is clearly shown in the example shown in Figure 4.38. The difference in the two slopes can possibly be attributed to the errors introduced by the use of T_f to calculate the physical properties in the mass transfer correlations given in Table 4.6 rather than the use of T_b .

In general, it can be seen from the comparison between the mass and heat transfer correlations given in Table 4.6 for a given simulated fouling deposit, that the exponent on Re is similar whereas the constants are different. The difference in the constants can be attributed to $Sc^{\frac{1}{3}}$ being 5-6 times larger than $Pr^{\frac{1}{3}}$ for the electrochemical system used in this study.

FIGURE 4.38 A PLOT OF $Sh/Sc^{1/3}$ VERSUS Re SHOWING THE COMPARISON BETWEEN THE EQUATIONS GIVEN IN TABLE 4.6 and 4.4 FOR THE ELECTROLYTIC MIXING CELL WITH THE PRESENCE OF 3MM GLASS SPHERICAL PARTICLES ON THE CATHODE



5. DISCUSSION OF RESULTS

For the electrolytic mixing cell with the presence of glass spherical particles of known dimensions acting as a simulated fouling deposit on the cathode, the transport of the reacting species from the bulk solution to the cathode involves two steps:

1. the diffusion of the reacting species from the bulk solution to the deposit - solution interface
2. the diffusion of the reacting species through the deposit to the cathode

Hence, the rate of transport of the reacting species from the bulk solution to the cathode can be described in terms of the model proposed by Galloway⁽²⁶⁾ for growth of calcereous deposits on cathodic steel surfaces in sea water:

$$N = \frac{I_L}{zFA} = \frac{c_b}{\frac{1}{k} + \frac{x}{D_F}} \quad 5.1$$

in which D_F for a simulated fouling deposit is given by

$$D_F = \frac{\epsilon D}{t} \quad 5.2$$

where ϵ is the tortuosity of the simulated fouling deposit

The tortuosity of the simulated fouling deposit, defined as the ratio of the path length travelled by the reacting species in the simulated fouling deposit to the thickness of the simulated fouling deposit, can be estimated from

$$t = \frac{1.023n_1 - 0.023}{0.933n_1 + 0.067} \quad 5.3$$

The basis of equation 5.3 is given in Appendix A9.

Galloway⁽²⁶⁾ evaluated the mass transfer coefficient for the unfouled surface, k . As fouling proceeded, he assumed that the mass transfer coefficient for the fluid - deposit interface remained equal to k . This assumption may be valid for thin layers of fine deposits in his study. However, in this study, the particle sizes were large and consequently have a significant effect on the mass transfer coefficient. Large particles tend to reduce the resistance to transfer at the fluid - solid interface but on the other hand an increasing number of layers of particles increases the

resistance to transfer through the deposit itself.

In order to avoid the difficulties in accurately evaluating the fluid - deposit mass transfer coefficient required in equations 5.1, the rate of transport of the reacting species from the bulk solution to the cathode can be obtained from equation 5.4 instead of equation 5.1:

$$N = \frac{I_L}{zFA} = \frac{c_b}{\frac{1}{K}} \quad 5.2$$

where K is the overall mass transfer coefficient

Since Re used in this study was in the range of 150 - 20000, it is reasonable to assume the mass transfer in the electrolytic mixing cell was by forced convection. Hence, the mass transfer without and with the presence of a simulated fouling deposit on the cathode were expressed in the form of the Gilliland - Sherwood correlation given by equation 4.9

$$Sh = a Re^b Sc^{\frac{1}{3}} \quad 4.9$$

where a and b for the various experimental conditions in the electrolytic mixing cell listed in Table 3.7 are given by equations 4.14 and 4.13 respectively

$$a = 1.0330 \exp\{-7.7799 n_1^{0.1122} (e^{-0.2672d_p} - e^{-4.0086d_p})\} \quad 4.14$$

$$b = 0.5644 + 1.0081(e^{-0.2924d_p} - e^{-3.1486d_p}) \quad 4.13$$

Since the term $(e^{-0.2924d_p} - e^{-3.1486d_p})$ in equation 4.13 is similar in form to the term $(e^{-0.2672d_p} - e^{-4.0086d_p})$ in equation 4.14, it is suggested that these terms are related in broadly similar manner to the variables which describe the structure of the simulated fouling deposit, namely porosity, tortuosity and roughness.

In order to determine the analogy between the mass and heat transfer, a study of mass and heat transfer in the electrolytic mixing cell without and with the presence of a simulated fouling deposit on the cathode was carried out. Since Re used in this study was again in the range of 150 - 20000, it is reasonable to assume the mass and heat transfer in the electrolytic mixing cell was by forced convection. Hence, the results for mass and heat transfer

in the electrolytic mixing cell without and with the presence of a simulated fouling deposit on the cathode were expressed in terms of equations 4.9 and 4.39

$$Nu = a Re^b Pr^{\frac{1}{3}} \quad 4.39$$

where the values a and b in equations 4.9 and 4.39 are given in Table 4.6 for the various experimental conditions listed in Table 3.7.

In general, it can be seen from the comparison between the mass and heat transfer correlations given in Table 4.6 that the exponents on Re are similar whereas the constants are different. Provided that the exponents on Re are similar, the relationship between the constant a in equation 4.9 (mass transfer correlation) and the constant a in equation 4.39 (heat transfer correlation) is given by

$$\frac{a \text{ in equation 4.9}}{a \text{ in equation 4.39}} = \left[\frac{Sc}{Pr} \right]^{\frac{1}{3}} \quad 5.5$$

This approximation has been derived from the data given in Table 4.6, noting the experimental ranges of Pr and Sc to be:

$$3 < Pr < 8.5 \quad 400 < Sc < 2000$$

Therefore, if the analogy between mass and heat transfer is used to predict heat transfer rates, then the constant a in equation 4.9, which is a function of equipment geometry, should be corrected by an equation of the form of equation 5.5. This conclusion is broadly consistent with that of Berger and Ziai⁽³³⁰⁾.

It is reasonable to conclude that the results obtained for mass and heat transfer without and with the presence of a simulated fouling deposit on the cathode are less reliable than those obtained for mass transfer alone. This is due to the errors introduced into the calculation of physical properties by the use of T_f which is strongly dependent on the accuracy in estimating T_s from the temperature profile across the cathode. This conclusion is reinforced by the observation that the correlations obtained for the mass transfer without the presence of a simulated fouling deposit on the cathode are in far better agreement with the correlations found in the literature than those obtained for mass and heat transfer (compare Figure 4.26 with Figure 4.5). Hence, the correlation for mass transfer is given by equation 4.9

where a and b are given by equations 4.14 and 4.13. The corresponding correlation for heat transfer is given by equation 4.39 where a and b are given by equations 5.5 and 4.13.

The range of d_p found in typical particulate fouling deposits is about $1 - 50\mu\text{m}$ (5,6,47,49-51,100,101,183). This is well within the range of d_p used for the simulated fouling deposit used in this study ($0 - 12000\mu\text{m}$). Taking d_p for an average particulate fouling deposit to be $25\mu\text{m}$, it may be predicted from equations 4.9, 4.13 and 4.14 that

$$\text{Sh} = 1.0330 \exp \left[-0.6901 n_1^{0.1122} \right] \text{Re}^{0.6334} \text{Sc}^{\frac{1}{3}} \quad 5.6$$

ie. $\text{Sh} = 0.5181 \text{Re}^{0.6334} \text{Sc}^{\frac{1}{3}} \quad \text{for } n_1 = 1 \quad 5.7$

$$\text{Sh} = 0.4900 \text{Re}^{0.6334} \text{Sc}^{\frac{1}{3}} \quad \text{for } n_1 = 2 \quad 5.8$$

$$\text{Sh} = 0.4732 \text{Re}^{0.6334} \text{Sc}^{\frac{1}{3}} \quad \text{for } n_1 = 3 \quad 5.9$$

$$\text{Sh} = 0.4613 \text{Re}^{0.6334} \text{Sc}^{\frac{1}{3}} \quad \text{for } n_1 = 4 \quad 5.10$$

$$\text{Sh} = 0.4519 \text{Re}^{0.6334} \text{Sc}^{\frac{1}{3}} \quad \text{for } n_1 = 5 \quad 5.11$$

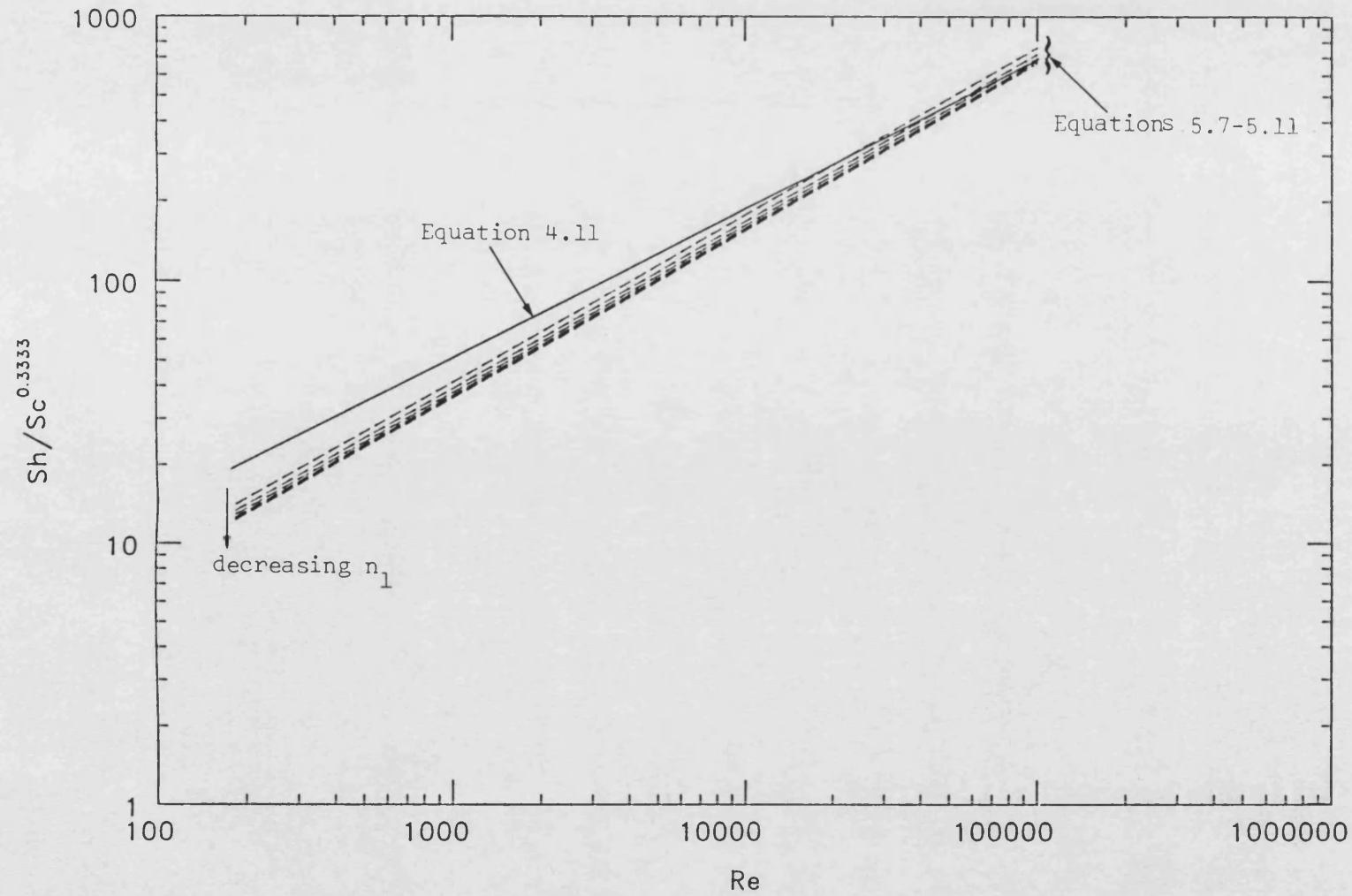
and from equations 4.39, 5.5, 4.14 and 4.13 that

$$\text{Nu} = 1.0330 \left[\frac{\text{Pr}}{\text{Sc}} \right]^{\frac{1}{3}} \exp \left[-0.6901 n_1^{0.1122} \right] \text{Re}^{0.6334} \text{Pr}^{\frac{1}{3}} \quad 5.12$$

Figure 5.1 shows the comparison between equations 5.7 - 5.11 for a surface fouled by 1 to 5 layers of $25\mu\text{m}$ particles and equation 4.11 for an unfouled surface. It is clear that at high Re, the mass transfer coefficient can become greater than that for the unfouled surface. This effect is due to the additional surface roughness caused by the presence of the particles. However, increasing the number of layers inevitably tends to reduce the mass transfer coefficient. At relatively low Re, the deposit thickness has a much greater influence than the additional surface roughness causing the mass transfer coefficient to remain less than that for the unfouled surface.

As the surface of the cathode itself has an average peak to valley height of $1.27\mu\text{m}$ (Section 3.3.2), it is important to establish whether or not the original cathode surface roughness has an effect on these conclusions. Assuming that the average peak to valley height for a simulated fouling deposit is given by $\frac{1}{2}d_p$, then for $d_p = 25\mu\text{m}$ it is predicted from equations 4.9, 4.13 and 4.14 that

FIGURE 5.1 A PLOT OF $Sh/Sc^{1/3}$ VERSUS Re SHOWING THE COMPARISON BETWEEN EQUATIONS 5.7-5.11 FOR A SURFACE FOULED BY 1 TO 5 LAYERS OF $25\mu m$ PARTICLES AND EQUATION 4.11 FOR A CLEAN SURFACE



$$Sh = 1.0330 \exp \left[-0.0724 n_1^{0.1122} \right] Re^{0.5716} Sc^{\frac{1}{3}} \quad 5.13$$

Hence, for $n_1 = 1$

$$Sh = 0.9608 Re^{0.5716} Sc^{\frac{1}{3}} \quad 5.14$$

Figure 5.2 shows the comparison between equation 5.14 for a surface fouled by 1 layer of 2.5 μ m particles and equation 4.11 for an unfouled surface. It is apparent from the similarity between the two curves that the surface roughness of the cathode (which was polished) has little influence on the conclusions.

The negative values of R_F in the fouling curve observed by Bott and Gudmundsson⁽²³⁹⁾ for rippled silica fouling and by Watkinson and Epstein^(100,101) for oil-gas and sand-water fouling were explained by the increase in the heat transfer coefficient which was caused by disturbances in the laminar sublayer as a result of the deposit surface roughness. Further evidence for this phenomenon is provided by the electrochemical analogue, at least for high values of Re . Above the critical Re shown in Figure 5.3A, the mass transfer coefficient is higher than that for an unfouled surface. The fouling curve presented in Figure 5.3B can be explained by the sequence of events shown in Figure 5.3A as the deposit builds up.

FIGURE 5.2 A PLOT OF $Sh/Sc^{1/3}$ VERSUS Re SHOWING THE COMPARISON BETWEEN EQUATION 5.14 FOR A SURFACE FOULED BY 1 LAYER OF $2.5\mu m$ PARTICLES AND EQUATION 4.11 FOR AN UNFOULED SURFACE

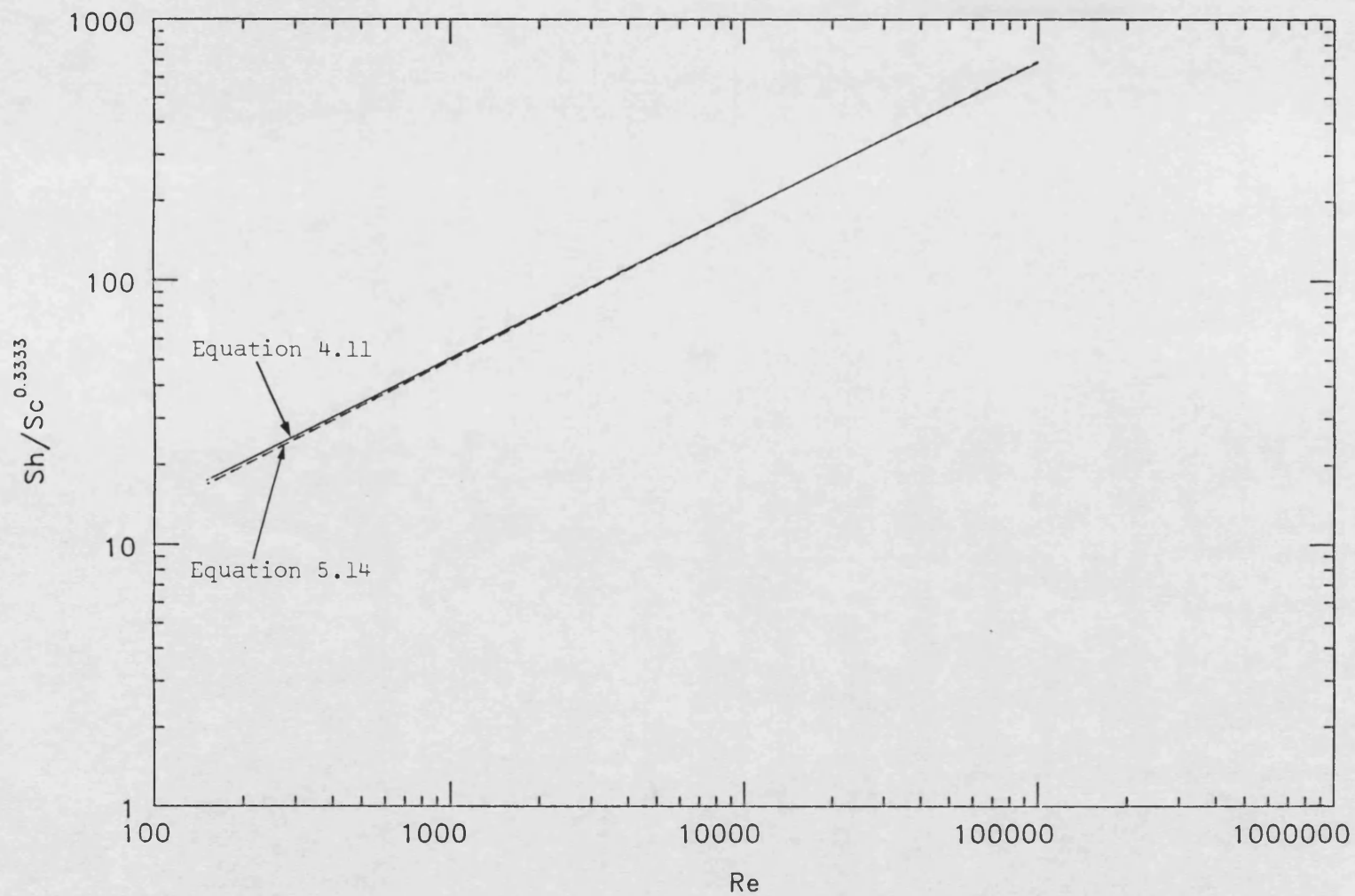
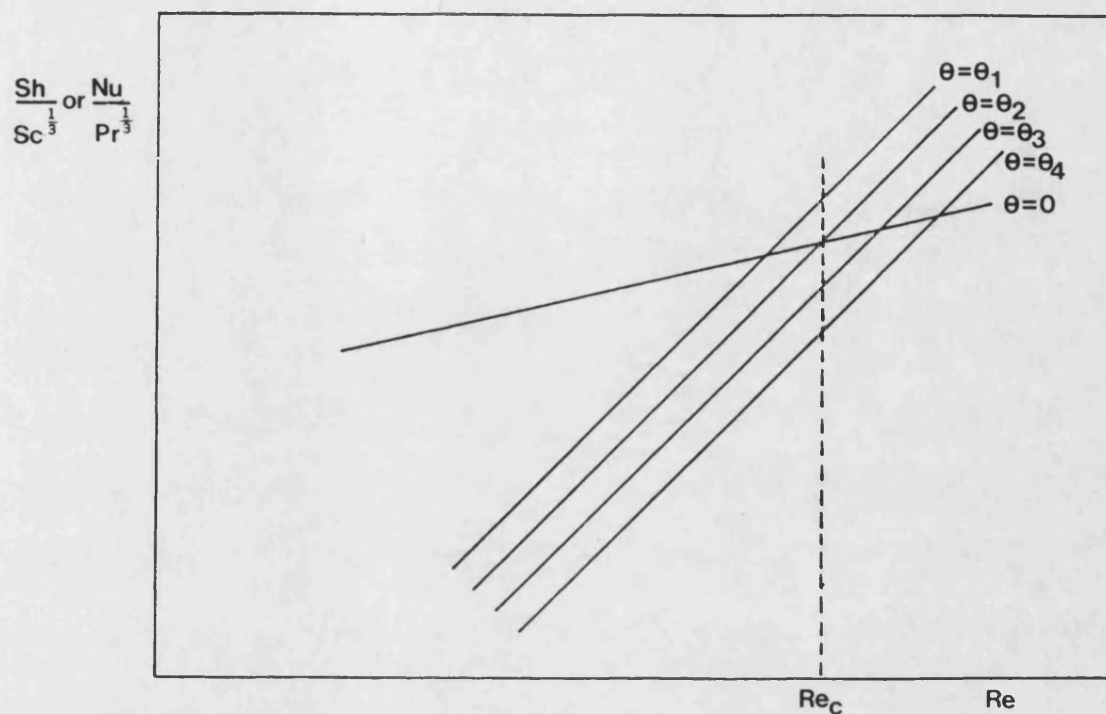
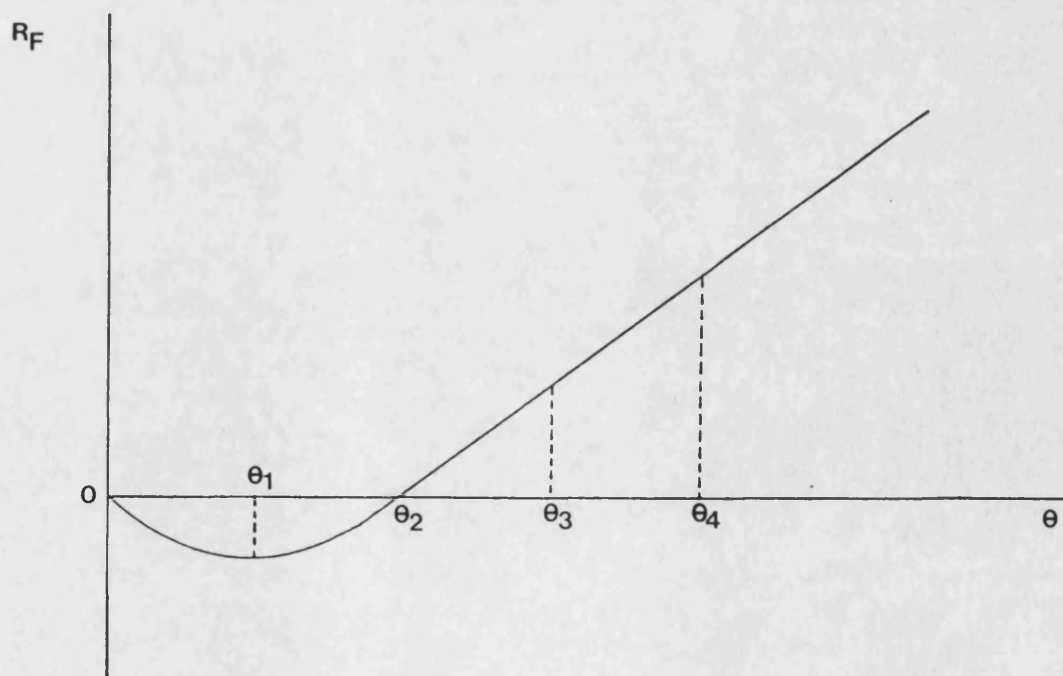


FIGURE 5.3 EXPLANATION OF APPARENT NEGATIVE FOULING RESISTANCES



A. A TYPICAL PLOT OF $Sh/Sc^{1/3}$ or $Nu/Pr^{1/3}$ VERSUS Re AS FOULING PROCEEDS WITH TIME



B. A TYPICAL FOULING CURVE SHOWING APPARENT NEGATIVE VALUES OF R_F

6. CONCLUSIONS

1. The mass transfer in the electrolytic cell without and with the presence of a simulated fouling deposit on the cathode is well described by the Gilliland - Sherwood correlation given by equation 4.9

$$Sh = a Re^b Sc^{\frac{1}{3}} \quad 4.9$$

where a and b for the various experimental conditions listed in Table 3.7 are given by equations 4.14 and 4.13.

$$a = 1.0330 \exp\{-7.7799 n_1^{0.1122} (e^{-0.2672d_p} - e^{-4.0086d_p})\} \quad 4.14$$

$$b = 0.5644 + 1.0081(e^{-0.2924d_p} - e^{-3.1486d_p}) \quad 4.13$$

2. The heat transfer in the electrolytic mixing cell without and with the presence of a simulated fouling deposit on the cathode is given by equation 4.39

$$Nu = a Re^b Pr^{\frac{1}{3}} \quad 4.39$$

where a and b are given by equations 6.1 (obtained from equations 5.5 and 4.14) and 4.13

$$a = 1.0330 \left[\frac{Pr}{Sc} \right]^{\frac{1}{3}} \exp\{-7.7799 n_1^{0.1122} (e^{-0.2672d_p} - e^{-4.0086d_p})\} \quad 6.1$$

$$b = 0.5644 + 1.0081(e^{-0.2924d_p} - e^{-3.1486d_p}) \quad 4.13$$

3. Assuming the analogy between the heat transfer and electrochemical mass transfer, the apparently negative values of R_F observed by Bott and Gudmundsson⁽²³⁹⁾ for rippled silica fouling and Watkinson and Epstein^(100,101) for oil-gas and sand-water fouling can be explained by the effect of deposit surface roughness on heat transfer provided that the Reynolds number is sufficiently high.

REFERENCES

1. Nelson, W.L.
Fouling of heat exchangers.
Part 1: Refiner Nat. Gasoline Manuf., 13(7), 271-276, July 1934.
Part 2: Refiner Nat. Gasoline Manuf., 13(8), 292-298, Aug 1934.
2. Bott, T.R. and Walker, R.A.
Fouling in heat transfer equipment.
Chem. Eng. (London), No 255, 391-395, Nov 1971.
3. Bott, T.R.
Understanding fouling and keep down heat exchanger costs.
Process Eng. (London), 76-81, Nov 1975.
4. Bott, T.R.
Fouling update.
Process Eng. (London), 27-30, Jan 1981.
5. Watkinson, A.P.
Particulate fouling of sensible heat exchangers.
Ph.D. thesis, University of British Columbia, Sept 1968.
6. Gudmundsson, J.S.
Fouling of surfaces.
Ph.D. thesis, University of Birmingham, Aug 1977.
7. Knudsen, J.G.
Fouling of heat exchangers: Are we solving the problem.
Chem. Eng. Prog., 80(2), 63-69, Feb 1984.
8. Sabersky, R.H.
Heat transfer in the seventies.
Int. J. Heat Mass Transfer, 14, 1927-1949, 1971.
9. Thackery, P.A.
The cost of fouling in heat exchange plant.
a. Proc. Conf. on Fouling - Science or Art?, University of Surrey,
Guildford, 27-28 March 1979, pp 1-9.
b. Effluent Water Treat. J., 20(3), 111-115, Mar 1980.
10. Pritchard, A.M.
Heat exchanger fouling in British Industry.
Fouling Prev. Res. Dig., 1(1-4), iv-vi, Dec 1979.
11. Van Nostrand, W.L., Leach, S.H. and Haluska, J.L.
Economic penalties associated with the fouling of refinery heat
transfer equipment.
Proc. Int. Conf. on Fouling of Heat Transfer Equipment, Rensselaer
Polytechnic Institute, Troy, NY, 13-17 August 1979. (E.F.C. Somerscales
and J.G. Knudsen, eds), pp 619-652. London: Hemisphere, 1981.

12. Somerscales, E.F.C.
Introduction and Summary: The fouling of heat transfer equipment.
Proc. Int. Conf. on Fouling of Heat Transfer Equipment, Rensselaer Polytechnic Institute, Troy, NY, 13-17 August 1979. (E.F.C. Somerscales and J.G. Knudsen, eds), pp 1-27. London: Hemisphere, 1981.
13. Bott, T.R.
Fouling in shell and tube heat exchangers.
Proc. Symp. on Advances in Thermal and Mechanical Design of Shell and Tube Heat Exchangers, National Engineering Laboratory, East Kilbride, Nov 1973, NEL Report 590.
14. Suitor, J.W., Marner, W.J. and Ritter, R.B.
The history and status of research in fouling of heat exchangers in cooling water service.
Can. J. Chem. Eng., 55, 374-380, Aug 1977.
15. Epstein, N.
Remarks on fouling of heat transfer surfaces.
Fouling Prev. Res. Dig., 3(2), iv-xii, June 1981.
16. Epstein, N.
Fouling of heat exchangers.
ICHMT Int. Seminar on Advancement in Heat Exchangers, Dubrovnik, Yugoslavia, 7-12 Sept 1981. (J. Taborek, G.F. Hewitt and N. Afgan, eds), pp 795-815. London: Hemisphere, 1983.
17. Epstein, N.
Thinking about heat transfer fouling: a 5 x 5 matrix.
Heat Transfer Engineering, 4(1), 43-56, 1983.
18. Kern, D.Q. and Seaton, R.E.
A theoretical analysis of thermal surface fouling.
Br. Chem. Eng., 4, 258-262, May 1959.
19. Kern, D.Q. and Seaton, R.E.
Surface fouling - How to calculate limits.
Chem. Eng. Prog., 55(6), 71-73, June 1959.
20. Lund, D. and Sandu, C.
State of the art of fouling: Heat transfer surfaces.
Proc. Int. Workshop on Fundamentals and Applications of Surface Phenomena associated with Fouling and Cleaning in Food Processing, Tylosand, Sweden, 6-9 April 1981. (B. Hallstrom, D.B. Lund and Ch. Tragardh, eds), pp 27-56. Sweden: Reprocontralan, 1981.
21. Sandu, C. and Lund, D.
Fouling of heat transfer equipment by food fluids: Computational models.
AIChE Symp. Ser., 78(218), 12-30, 1982.
22. Pinherio, J. de D.R.S.
Fouling of heat transfer surfaces.
In: Heat exchangers: Thermal-Hydraulic Fundamentals and Design (S. Kakac, A.E. Bergles and F. Mayinger, eds), pp 1013-1035. London: Hemisphere, 1981.

23. Characklis, W.G., Bryers, J.D., Trulear, M.G. and Zelter, N.
Biofouling film development and its effects on energy losses: a laboratory study.
Proc. Symp. on Condenser Biofouling Control, Electric Power Research Institute, Atlanta, Georgia, 25-29 March 1979. (J.F. Garey, R.M. Jordan, A.H. Aitken, D.T. Burton and R.H. Gray, eds), pp 49-76. Michigan: Ann Arbor Science, 1980.
24. Characklis, W.G.
Microbial fouling: A process analysis.
Proc. Int. Conf. on Fouling of Heat Transfer Equipment, Rensselaer Polytechnic Institute, Troy, NY, 13-17 August 1979. (E.F.C. Somerscales and J.G. Knudsen, eds), pp 251-291. London: Hemisphere, 1981.
25. Epstein, N.
Fouling of heat exchangers.
Proc. 6th Int. Conf. on Heat Transfer., Toronto, Canada, 7-11 August 1978, Vol 6, pp 235-253. Washington: Hemisphere, 1981.
26. Galloway, T.R.
Heat transfer fouling through growth of calcereous film deposits.
Int. J. Heat Mass Transfer, 16, 443-460, 1973.
27. Wolfson, S.L. and Hartt, W.H.
An initial investigation of calcereous deposits upon cathodic steel surfaces in sea water.
Corrosion (Houston), 37(2), 70-76, Feb 1981.
28. Taborek, J., Aoki, T., Ritter, R.B., Palen, J.W. and Knudsen, J.G.
Fouling: The major unresolved problem in heat transfer.
Chem. Eng. Prog., 68(2), 59-77, Feb 1972.
29. Taborek, J., Aoki, T., Ritter, R.B., Palen, J.W. and Knudsen, J.G.
Predictive methods for fouling behaviour.
Chem. Eng. Prog., 68(7), 69-78, July 1972.
30. Taborek, J., Knudsen, J.G., Aoki, T., Ritter, R.B. and Palen, J.W.
Fouling - The major unresolved problem in heat transfer.
AIChE Symp. Ser., 68(118), 45-49, 1972.
31. Taborek, J. and Ritter, R.B.
Review of fouling studies by HTRI.
Proc. Symp. on Fouling Effects on Heat Transfer Equipment in Power Generation Systems, AIChE 65th Annual Meeting, New York, Nov 1972, Paper 76A, pp 1-11.
32. Hopkins, R.M.
Fouling of heated stainless steel tubes with ferric oxide from flowing water suspensions.
Ph.D. thesis, University of British Columbia, July 1973.
33. Walker, R.A.
Fouling of heat exchanger tubes.
Ph.D. thesis, University of Birmingham, 1972.

34. Gupta, J.P.
Fouling of heat exchanger surfaces.
Chem. Age. India, 29(1), 33-40, 1978.
35. Epstein, N.
Fouling: Technical Aspects.
Proc. Int. Conf. on Fouling of Heat Transfer Equipment, Rensselaer Polytechnic Institute, Troy, NY, 13-17 August 1979. (E.F.C. Somerscales and J.G. Knudsen, eds), pp 31-58. London: Hemisphere, 1981.
36. Knudsen, J.G.
Fouling of heat transfer surfaces: an overview.
Workshop on Modern Development in Marine Condensers, Navel Postgraduate School, Monterey, California, 26-28 March 1980. (P.J. Marto and R.H. Nunn, eds), pp 373-424. London: Hemisphere, 1980.
37. O'Callagan, M.G.
Fouling of heat transfer equipment: Summary Review.
In: Heat Exchangers: Thermal-Hydraulic Fundamentals and Design (S. Kakac, A.E. Bergles and F. Mayinger, eds), pp 1037-1047. London: Hemisphere, 1981.
38. Collier, J.G.
Heat exchanger fouling and corrosion.
In: Heat Exchangers: Thermal-Hydraulic Fundamentals and Design (S. Kakac, A.E. Bergles and F. Mayinger, eds), pp 999-1011. London: Hemisphere, 1981.
39. Knudsen, J.G. and Roy, B.V.
Influence of fouling on heat transfer.
Proc. 7th Int. Conf. on Heat Transfer., Munich, W. Germany, 6-10 Sept 1982, Vol 1, pp 269-287.
40. Cowan, J.C. and Weintritt, D.J.
Water formed scale deposits. Houston: Gulf Publishing Co., 1976.
41. Troup, D.H. and Richardson, J.A.
Scale nucleation on a heat transfer surface and its prevention.
Chem. Eng. Commun., 2(4/5), 167-180, 1978.
42. Bridgwater, J.
Crystallisation Fouling - A review of fundamentals.
Proc. Conf. on Fouling - Science or Art?, University of Surrey, Guildford, 27-28 March 1979, pp 82-91.
43. Bridgwater, J.
Crystallisation Fouling.
Continuing Education Course on Fouling of Heat Exchangers, University of Birmingham, 19-20 March 1981, I.Chem.E. (Spons.), pp 7-14.
44. Loo, C.E.
Deposition and removal of calcium sulphate and calcium carbonate scales.
Ph.D. thesis, Oxford University, 1979.

45. Hasson,D.
Precipitation fouling.
Proc. Int. Conf. on Fouling of Heat Transfer Equipment, Rensselaer Polytechnic Institute, Troy, NY, 13-17 August 1979. (E.F.C.Somerscales and J.G.Knudsen, eds), pp 527-568. London: Hemisphere, 1981.
46. Knudsen,J.G.
Cooling water fouling - a brief review.
'Fouling in Heat Exchange Equipment.' presented at 20th ASME/AIChE Heat Transfer Conf., Milwaukee, Wisconsin, 2-5 August 1981. (J.M.Chenoweth and M.Impagliazzo, eds), pp 29-38. New York: ASME, 1981.
47. Gudmundsson,J.S.
Particulate fouling.
Proc. Int. Conf. on Fouling of Heat Transfer Equipment, Rensselaer Polytechnic Institute, Troy, NY, 13-17 August 1979. (E.F.C.Somerscales and J.G.Knudsen, eds), pp 357-387. London: Hemisphere, 1981.
48. Epstein,N.
Particulate deposition.
Continuing Education Course on Fouling of Heat Exchangers, University of Birmingham, 19-20 March 1981, I.Chem.E. (Spons.), pp 15-22.
49. Newson,I.H.
Studies of particulate deposition from flowing suspension.
Proc. Conf. on Fouling - Science or Art?, University of Surrey, Guildford, 27-28 March 1979. pp 35-81.
50. Newson,I.H., Bott,T.R. and Hussain,C.I.
Studies of magnetite deposition from a flowing suspension.
'Fouling in Heat Exchange equipment.' presented at 20th ASME/AIChE Heat Transfer Conf., Milwaukee, Wisconsin, 2-5 August 1981. (J.M.Chenoweth and M.Impagliazzo, eds), pp 73-81. New York: ASME, 1981.
51. Newson,I.H., Bott,T.R. and Hussain,C.I.
Studies of magnetite deposition from a flowing suspension.
Chem. Eng. Commun., 20(5/6), 335-353, 1983.
52. Taylor,N.K.
Review of available data on the release, transport and deposition of corrosion products in PWR, BWR and SGHWR systems. AERE, Harwell. AERE- 8164, March 1976.
53. Lister,D.H.
Corrosion products in power generating systems.
Proc. Int. Conf. on Fouling of Heat Transfer Equipment, Rensselaer Polytechnic Institute, Troy, NY, 13-17 August 1979. (E.F.C.Somerscales and J.G.Knudsen, eds), pp 135-200. London: Hemisphere, 1981.
54. Kolaczowski,S.T.
Two phase heat transfer and fouling in hydrocarbon vaporizers.
Ph.D. thesis, University of Bath, 1977.

55. Crittenden,B.D.
Chemical reaction fouling.
Continuing Education Course on Fouling of Heat Exchangers, University of Birmingham, 19-20 March 1981, I.Chem.E. (Spons.), pp 34-41.
56. Khater,E.M.H.
Fouling in a hydrocarbon vaporizer.
Ph.D. thesis, University of Bath, 1982.
57. Hout,S.A.
Chemical reaction fouling.
Ph.D. thesis, University of Bath, 1983.
58. Froment,G.F.
Fouling of heat transfer surfaces by coke formation in petrochemical reactors.
Proc. Int. Conf. on Fouling of Heat Transfer Equipment, Rensselaer Polytechnic Institute, Troy, NY, 13-17 August 1979. (E.F.C.Somerscales and J.G.Knudsen, eds), pp 411-435. London: Hemisphere, 1981.
59. Lund,D. and Sandu,C.
Chemical reaction fouling due to foodstuffs.
Proc. Int. Conf. on Fouling of Heat Transfer Equipment, Rensselaer Polytechnic Institute, Troy, NY, 13-17 August 1979. (E.F.C.Somerscales and J.G.Knudsen, eds), pp 437-476. London: Hemisphere, 1981.
60. Dawson,J.L.
Corrosion fouling.
Continuing Education Course on Fouling of Heat Exchangers, University of Birmingham, 19-20 March 1981, I.Chem.E. (Spons.), pp 42-52.
61. Somerscales,E.F.C.
Corrosion fouling.
'Fouling in Heat Exchange Equipment.' presented at 20th ASME/AIChE Heat Transfer Conf., Milwaukee, Wisconsin, 2-5 August 1981. (J.M.Chenoweth and M.Impagliazzo, eds), pp 17-27. New York: ASME, 1981.
62. Bott,T.R.
Biological fouling of heat transfer surfaces.
a. Proc. Conf. on Fouling - Science or Art?, University of Surrey, Guildford, 27-28 March 1979, pp 117-144.
b. Effluent Water Treat. J., 19(9), 453-461, Sept 1979.
63. Characklis,W.G.
Attached microbial growths.
Part 1: Water Res., 7, 1113-1127, 1973.
Part 2: Water Res., 7, 1249-1258, 1973.
64. Kent,C.A.
Biofouling.
Fouling Prev. Res. Dig., 2(1), vi-xi, March 1980.
65. Kent,C.A.
Biological fouling.
Continuing Education Course on Fouling of Heat Exchangers, University of Birmingham, 19-20 March 1981., I.Chem.E. (Spons.), pp 23-33.

66. Thomas,B.M.
The role of algae in the biological fouling of industrial cooling systems.
Fouling Prev. Res. Dig., 2(4), iv-vii, Dec 1980.
67. Bott,T.R. and Gudmundsson,J.S.
Deposition of parrafin wax from flowing systems.
Inst. Pet., IP 77-007, 1976.
68. Bott,T.R.
Fouling due to liquid solidification.
Proc. Int. Conf. on Fouling of Heat Transfer Equipment, Rensselaer Polytechnic Institute, Troy, NY, 13-17 August 1979. (E.F.C.Somerscales and J.G.Knudsen, eds), pp 201-226. London: Hemisphere, 1981.
69. TEMA
Standards of the Tubular Exchangers Manufacturers Association, 6th ed, New York, 1978.
70. Bott,T.R. and Walker,R.A.
Fouling in heat exchanger tubes: some observations.
Proc. Conf. on Heat Transfer and Design and Operation on Heat Exchangers, University of Witwatersrand, Johannesburg, 17-19 April 1974. pp BOTT 1-13.
71. Fischer,P., Suiter,J.W. and Ritter,R.B.
Fouling measurement techniques.
Chem. Eng. Prog., 71(7), 66-72, July 1975.
72. Cousins,L.B. and Pritchard,A.M.
Fouling resistance and the designer.
Fouling Prev. Res. Dig., 2(3), iv-vii, Sept 1980.
73. Crittenden,B.D. and Khater,E.H.
Economic fouling resistance selection.
Proc. Int. Conf. on Fouling of Heat Transfer Equipment, Rensselaer Polytechnic Institute, Troy, NY, 13-17 August 1979. (E.F.C.Somerscales and J.G.Knudsen, eds), pp 645-652. London: Hemisphere, 1981.
74. Badger,W.L. and Othmer,D.F.
Studies in evaporater design - VIII. Optimum cycle for liquids which form scale.
Trans. Am. Inst. Chem. Eng., 16(2), 159-168, 1924.
75. McCabe,W.L.
Economic side of evaporator scale formation.
Chem. Metall. Eng., 33(2), 86-87, Feb 1926.
76. Harker,J.H.
Finding the economic balance in evaporator operation.
Processing, 24(12), 31-32, Dec 1978.

77. Epstein,N.
Optimum evaporator cycles with scale formation.
a. Proc. Int. Conf. on Fouling of Heat Transfer Equipment, Rensselaer Polytechnic Institute, Troy, NY, 13-17 August 1979. (E.F.C.Somerscales and J.G.Knudsen, eds), pp 653-659. London: Hemisphere, 1981.
b. Can. J. Chem. Eng., 57, 659-661, Oct 1979.
78. Ludwig,E.E.
Applied Process Design for Chemical and Petrochemical Plants, Vol 3. Houston: Gulf Publishing Co., 1965.
79. Caplan,F.
Nomograph determines design overall heat transfer coefficient.
Heat. Piping Air. Cond., 46(5), 67-68, May 1974.
80. Cos,M.
Excess exchange surface for fouling.
In: Nomograph handbook, pp 6-7. Houston: Gulf Publishing Co., 1971.
81. Zanker,A.
Predict fouling by nomograph.
Hydrocarbon Process., 57(3), 145-148, March 1978.
82. Ganapathy,V.
Fouling factor estimated quickly.
Oil Gas J., 80(31), 128-129, 1982.
83. Franklin,W.C. and Cocks,R.E.
Determine the resistance that controls heat exchanger cost.
Chem. Eng. (NY), 87(28 July), 93-94, 1980.
84. Franklin,W.C. and Cocks,R.E.
Determining the controlling resistance.
Chem. Eng. (NY), 88(12 Jan), 145, 1981.
85. Meeter,V.V., Krzyzhanovski,R.E., Tchoodhovskaya,I.I., Paulof,I.S., Konopelko,I.N. and Stern,Z.I.
Determination of surface ash and internal pipe deposit heat transfer resistance in steam generator heat transfer calculation.
Proc. 6th Int. Conf. on Heat transfer., Toronto, Canada, 7-11 August 1978, Vol 4, pp 385-390. Washington: Hemisphere, 1981.
86. Knudsen,J.G.
Apparatus and techniques for measurement of fouling of heat transfer equipment.
a. Proc. Symp. on Condenser Biofouling Control, Electric Power Research Institute, Atlanta, Georgia, 25-29 March 1979. (J.F.Garey, R.M.Jordan, A.H.Aitken, D.T.Burton and R.H.Gray eds), pp 143-168. Michigan: Ann Arbor Science, 1980.
b. Proc. Int. Conf. on Fouling of Heat Transfer Equipment, Rensselaer Polytechnic Institute, Troy, NY, 13-17 August 1979. (E.F.C.Somerscales and J.G.Knudsen, eds), pp 57-81. London: Hemisphere, 1981.

87. Merry,H. and Polley,G.T.
Obtaining valid data on fouling resistance.
Proc. Int. Conf. on Fouling of Heat Transfer Equipment, Rensselaer Polytechnic Institute, Troy, NY, 13-17 August 1979. (E.F.C.Somerscales and J.G.Knudsen, eds), pp 83-94. London: Hemisphere, 1981.
88. Merry,H.
Obtaining data.
Continuing Education Course on Fouling of Heat Exchangers, University of Birmingham, 19-20 March 1981, I.Chem.E. (Spons.), pp 19-26.
89. Leach,S.H. and Factor,S.A.
Monitoring fouling in refinery and petrochemical plant heat exchange equipment.
'Fouling in Heat Exchange Equipment.' presented at 20th ASME/AIChE Heat Transfer Conf., Milwaukee, Wisconsin, 2-5 August 1981. (J.M.Chenoweth and M.Impagliazzo, eds), pp 39-43. New York: ASME, 1981.
90. Ritter,R.B., Suitor,J.W. and Cypher,G.A.
Thermal fouling rates of 90:10 copper-nickel and titanium in seawater service.
Proc. Symp. on OTEC Biofouling and Corrosion, Seattle, Washington, 10-12 Oct 1977. (R.H.Gray, ed.), pp 353-365.
91. Noisetani,T., Sato,S., Onda,K., Kashiwada,J. and Kawaguchi,K.
Effect of marine biofouling on the heat transfer performance of titanium condenser tubes.
Proc. Int. Conf. on Fouling of Heat Transfer Equipment, Rensselaer Polytechnic Institute, Troy, NY, 13-17 August 1979. (E.F.C.Somerscales and J.G.Knudsen, eds), pp 345-353. London: Hemisphere, 1981.
92. Kern,D.Q.
Heat exchanger design for fouling service.
Chem. Eng. Prog., 62(7), 51-56, July 1966.
93. Kern,D.Q.
Heat exchanger design for fouling services.
Proc. 3rd Int. Heat Transfer Conf., Chicago, 1966, Vol 1, pp 170-178.
94. Charlesworth, D.H.
The deposition of corrosion products in boiling water systems.
Chem. Eng. Prog. Symp. Ser. 66(104), 21-30, 1970
95. Loo,C.E. and Bridgwater,J.
Theory of thermal stresses and deposit removal.
Proc. Conf. on Progress in the Prevention of Fouling in Industrial Plant, Nottingham University, 1-3 April 1981. pp 154-173.
96. Cleaver,J.W. and Yates,B.
Sub-layer models for the removal and deposition of small particles in turbulent flow.
Proc. 1st. Int. Conf. on Particle Technology., Chicago, August 1973, pp 293-299.

97. Cleaver, J.W. and Yates, B.
Mechanism of detachment of colloidal particles from a flat substrate in a turbulent flow.
J. Coll. Interface Sci., 44(3), 464-474, Sept 1973.
98. Cleaver, J.W. and Yates, B.
A sub layer model for the deposition of particles from a turbulent flow.
Chem. Eng. Sci., 30, 983-992, 1975.
99. Cleaver, J.W. and Yates, B.
The effect of re-entrainment on particle deposition.
Chem. Eng. Sci., 31, 147-151, 1976.
100. Watkinson, A.P. and Epstein, N.
Gas oil fouling in a sensible heat exchanger.
Chem. Eng. Prog. Symp. Ser., 65(92), 84-90, 1969.
101. Watkinson, A.P. and Epstein, N.
Particulate fouling of sensible heat exchangers.
Proc. 4th Int. Heat Transfer Conf., Paris, 1970, (U. Grigull and E. Halne, eds), Vol 1, Paper HE1.6, Amsterdam: Elsevier, 1970.
102. Crittenden, B.D. and Kolaczowski, S.T.
Mass transfer and chemical kinetics in hydrocarbon fouling.
Proc. Conf. on Fouling - Science or Art?, University of Surrey, Guildford, 27-28 March 1979. pp 169-187.
103. Mansfield, G.H.
Some aspects of cooling water treatment.
a. Effluent Water Treatment J., 18(11), 552-556, Nov 1978.
b. Proc. Conf. on Fouling - Science or Art?, University of Surrey, Guildford, 27-28 March 1979. pp 10-13.
104. Mansfield, G.H. and Walters, G.P.
The classification and importance of fouling in heat exchange surfaces in open recirculating cooling water systems.
Proc. Conf. on Progress in the Prevention of Fouling in Industrial Plant, Nottingham University, 1-3 April 1981. pp 40-53.
105. Oberhofer, A.W. and Fulks, K.E.
A cooling water fouling evaluation unit.
Proc. Int. Conf. on Fouling of Heat Transfer Equipment, Rensselaer Polytechnic Institute, Troy, NY, 13-17 August 1979. (E.F.C. Somerscales and J.G. Knudsen, eds), pp 95-109. London: Hemisphere, 1981.
106. Duddridge, J.E.
Some techniques commonly used in the study of biological films.
Proc. Conf. on Progress in the Prevention of Fouling in Industrial Plant, Nottingham University, 1-3 April 1981. pp 54-67.
107. Pritchard, A.M.
Progress in the prevention of fouling in industrial plant - a conference report.
Fouling Prev. Res. Dig., 4(1), iv-vii, March 1982.

108. Crawford, J.D. and Miller, R.M.
Refinery process fouling - effect of trace metals and remedial techniques.
28th Mid Year Meeting of the API Refining Div., Philadelphia, 13 May 1963. In: Division of Refining, 43(III), 106-144, 1963.
109. Nelson, W.L.
Petroleum Refinery Engineering, 4th ed. New York: McGraw-Hill, 1969.
110. McAllister, R.A., Eastman, D.H., Dougharty, N.A. and Hollier, M.
A study of scaling and corrosion in condenser tubes exposed to river water.
Corrosion, 17, 95-104, Dec 1961.
111. Izumi, K., Takahashi, S. and Ikenaga, Y.
Scale prevention by pH control combined with sponge ball cleaning.
Proc. 5th Int. Symp. on Fresh Water from the Sea, 1976. Vol 1, pp 319-328.
112. Castle, J.E. and Epler, D.C.
The development of inorganic and biological fouling layers on copper based alloys.
Fouling Prev. Res. Dig., 3(3), vii-xxii, Sept 1981.
113. Ots, A.A., Pirker, T.A., Sel'g, V.A and Egorov, D.M.
Influence of ash deposits on heat exchange in a furnace.
Therm. Eng. Engl. Transl., 20(9), 2-7, 1973.
114. Charlesworth, D.H.
Fouling in organic cooled systems.
Atomic Energy of Canada Ltd, Ontario. CRCE - 1096, AECL - 1761, April 1963.
115. Styricovich, M.A., Martynova, O.I., Protopopov, V.S. and Lyskov, M.G.
Some aspects of heat exchanger surface fouling due to suspended particle deposition.
ICHMT Int. Seminar on Advancement in Heat Exchangers, Dubrovnik, Yugoslavia, 7-12 Sept 1981. (J. Taborek, G.F. Hewitt and N. Afgan, eds), pp 833-840. London: Hemisphere, 1983.
116. Atkins, G.T.
What to do about high coking rates.
Petro/Chem Eng., 34(4), 20-25, 1962.
117. Backensto, E.B., Prior, J.E. and Porter, B.F.
Reduce heater tube carburization.
Hydrocarbon Process., 45(9), 291-296, Sept 1966.
118. Perera, W.G. and Rafique, K.
Coking in a fired heater.
Chem. Eng. (London), No 306, 107-111, Feb 1976.
119. Crittenden, B.C. and Kolaczowski, S.T.
Energy savings through the accurate estimatin of heat transfer fouling resistances.
In: Energy for Industry (P.W.O'Callagan, ed.), pp 257-266. Oxford: Pergamon, 1979.

120. Silverstein,R.M. and Curtis,S.D.
Cooling water.
Chem. Eng. (NY), 78(9 Aug), 84-94, 1971.
121. Troscinski,E.S. and Watson,R.G.
Controlling deposits in cooling water systems.
Chem. Eng. (NY), 77(9 Mar), 125-132, 1970.
122. Canapary,R.C.
How to control refinery fouling.
Oil Gas J., 59(41), 114-118, 1961.
123. Weinland,B.W., Miller,R.M. and Freedman,A.J.
Reduce refinery fouling.
Mater. Prot., 6, 41-43, Feb 1967.
124. NACE Publication T8170
Process side antifoulants in petroleum refineries.
Mater. Prot., 9(6), 29-33, June 1970.
125. Coggins,J.R.
Blocking of naphtha vaporisers - report of gas industry survey.
The Gas Council, Solihull, E.R.117, 1968.
126. HTFS
Provisional data sheet for fouling deposits.
Fouling Prev. Res. Dig., 2(1), iv-v, 1980.
127. Rankin,B.H. and Adamson,W.L.
Scale formation as related to evaporator surface conditions.
Desalination, 13, 63-87, 1973.
128. Benson,P.R. and Martini,W.R.
Measuring the film forming potentials of liquids.
Ind. Eng. Chem. Prod. Res. Dev., 1(1), 7-10, 1962.
129. Bogdanov,F.F.
Some causes of deposits on heating surfaces which are cooled by
organic coolants.
Therm. Eng. Engl. Transl., 17(1), 64-68, 1970.
130. Scarborough,C.E., Cherrington,D.C., Diener,R. and Golan,L.P.
Coking of crude oil at high heat flux levels.
Chem. Eng. Prog., 75, 41-46, July 1979.
131. Sanders,W.M.
Oxygen utilization by slime organisms in continuous culture.
Int. J. Air Water Pollut., 10(4), 253-276, 1966.
132. Lee,E.J., DeWitt,J.K., Bennett,G.F. and Brockwell,J.L.
Investigation of oxygen transfer to slime as a surface reaction.
Water Res., 10(11), 1011-1017, 1976.

133. Little,B.J. and Lavoie,D.M.
Gulf of Mexico ocean thermal energy conversion biofouling experiment.
Proc. Symp. on Condenser Biofouling Control, Electric Power Research
Institute, Atlanta, Georgia, 25-29 March 1979. (J.F.Garey, R.M.Jordan,
A.H. Aitken, D.T.Burton and R.H.Gray, eds), pp 121-140, Michigan: Ann
Arbor Science, 1980.
134. Ishikawa,H., Suhara,S., Abe,T. and Takahash,T.
Thermal conductivity of scale deposits in supercritical boilers.
Heat Transfer Jpn. Res., 10(1), 23-36, 1981.
135. Rooth,T., Kelen,T. and Arvesen,J.
Deposition of impurities on heat transfer surfaces. The thermal
conductivity of magnetite deposits.
AB Atomenergie, STU-70-386/U317, Sept 1971.
136. Characklis,W.G. and Picologlou,B.F.
Measurement of the formation and destruction of primary biofouling
films.
Proc. Symp. on OTEC Biofouling and Corrosion., Seattle, Washington,
10-12 Oct 1977. (R.H.Gray, ed.), pp 51-61.
137. Bott,T.R. and Pinherio,M.M.V.P.S.
Biological fouling - Velocity and temperature effects.
Can. J. Chem. Eng., 55, 473-474, Aug 1977.
138. Mulchay,M.F.R., Boow,J. and Goard,P.R.C.
Fireside deposits and their effects in a pulverised-fuel fired boiler:
Part I. The radiance emittance and effective thermal conductance of
the deposits.
J. Inst. Fuel, 39, 385-394, 1966.
139. Hoehn,R.C. and Ray,A.D.
Effects of thickness on bacterial film.
J. Water Pollut. Control Fed., 45(11), 2302-2320, 1973.
140. Characklis,W.G.
Biofilm development and destruction.
Symp. on Microbiology power plant thermal effluents., University of
Iowa, 1977.
141. Characklis,W.G.
Biofilm development and destruction.
Electric Power Research Inst., Palo Alto, California, RP 902-1, 1979.
142. Harty,D.W.S. and Bott,T.R.
Deposition and growth of microorganisms on simulated heat transfer
surfaces.
Proc. Int. Conf. on Fouling of Heat Transfer Equipment, Rensselaer
Polytechnic Institute, Troy, NY, 13-17 August 1979. (E.F.C.Somerscales
and J.G.Knudsen, eds), pp 335-344. London: Hemisphere, 1981.
143. Harty,D.W.S.
Microbial fouling of a simulated heat transfer surface.
Ph.D thesis, University of Birmingham, Feb 1980.

144. Sharma,A., Garg,D. and Gupta,J.P.
Solidification fouling of paraffin wax from hydrocarbons.
Letters in Heat and Mass Transfer, 9, 209-219, 1982.
145. Hasson,D. and Zahavi,J.
Mechanism of calcium sulphate scale deposition on heat transfer surfaces.
Ind. Eng. Chem. Fundam., 9(1), 1-10, 1970.
146. Macbeth,R.V., Trenberth,R. and Wood,R.W.
An investigation into the effect of 'crud' deposits on surface temperature, dry-out and pressure drop, with forced convection boiling of water at 69 bar in an annular test section.
AERE, Winfrith, AEEW-R-705, May 1971.
147. Breden,C.R., Charak,I. and Leyse,R.H.
Water chemistry and fuel element scale in EBWR.
Argonne National Laboratory, Illinois, ANL-6136, Nov 1960.
148. Hasson,D., Avriel,M., Resnick,W., Rozenman,T. and Windreich,S.
Mechanism of calcium carbonate scale deposition on heat transfer surfaces.
Ind. Eng. Chem. Fundam., 7(1), 59-65, 1968.
149. Hasson,D.
Scale prevention by annular flow of an immiscible liquid along the walls of a heated tube.
Proc. 6th Int. Heat transfer Conf., Toronto, Canada, 7-11 August 1978, Vol 6, pp 391-396. Washington: Hemisphere, 1981.
150. Burrill,K.A.
Laboratory studies to resolve fouling of heat exchangers and sieve trays in Canadian girdler - sulphide heavy water plants.
Proc. Int. Conf. on Fouling of Heat transfer equipment, Rensselaer Polytechnic Institute, Troy, NY, 13-17 August 1979. (E.F.C.Somerscales and J.G.Knudsen, eds), pp 227-247. London: Hemisphere, 1981.
151. Scott,J.M. and Dawson,D.M.
Crystallisation of calcium carbonate at heated surfaces.
Proc. Conf. on Progress in the Prevention of Fouling in Industrial Plant, Nottingham University, 1-3 April 1981. pp 27-39.
152. Watkinson,A.P.
Water quality effects on fouling from hard waters.
ICHMT Int. Seminar on Advancement in Heat Exchangers, Dubrovnik, Yugoslavia, 7-12 Sept 1981. (J.Taborek, G.F.Hewitt and N.Afgan, eds), pp 835-861, London: Hemisphere, 1983.
153. Hodgson,T.D., Elliot,M.N. and Jordan,T.W.J.
Calcium sulphate scaling in falling film evaporators.
Desalination, 14, 77-91, 1974.
154. Liddle,C.J.
Scale formation in cyclic heat transfer processes.
Dechema Monogr., 65, 109-129, 1971.

155. Goossens,A.G., Dente,M. and Ranzi,E.
Improve steam cracker operation.
Hydrocarbon Process., 57(9), 227-236, Sept 1978.
156. Ryznar,J.W.
A new index for determining amount of calcium carbonate scale formed by a water.
J. Am. Water Works Assoc., 36, 472-483, 1944.
157. Nair,M.K.V. and Misra,B.M.
Electrolytic scale formation in sea water distillation systems.
Desalination, 25, 263-268, 1978.
158. Palen,J.W. and Westwater,J.W.
Heat transfer and fouling rates during pool boiling of calcium sulphate solutions.
Chem. Eng. Prog. Symp. Ser., 62(64), 77-86, 1966.
159. Hedley,A.B., Brown,T.B., and Shuttleworth,A.
Vanadium pentoxide deposition from combustion gases.
ASME Winter Annual Meeting, Chicago, Illinois, 7-11 November 1965, Paper 65-WD/CD-2.
160. Taylor,W.F. and Wallace,T.J.
Kinetics of deposit formation from hydrocarbon fuels at high temperatures - General features of the process.
Ind. Eng. Chem. Prod. Res. Dev., 6(4), 258-262, 1967.
161. Taylor,W.F. and Wallace,T.J.
Kinetics of deposit formation from hydrocarbons - Effect of trace sulphur compounds.
Ind. Eng. Chem. Prod. Res. Dev., 7(3), 198-202, 1968.
162. Taylor,W.F.
Kinetics of deposit formation from hydrocarbons - Fuel composition studies.
Ind. Eng. Chem. Prod. Res. Dev., 8(4), 375-380, 1969.
163. Taylor,W.F.
Kinetics of deposit formation from hydrocarbons - Hetrogeneous and homogeneous metal effects.
J. Appl. Chem., 18, 251-254, 1968.
164. Taylor,W.F.
Kinetics of deposit formation from hydrocarbons - Additive and surface coating effects.
J. Appl. Chem., 19, 222-226, 1969.
165. Taylor,W.F.
Mechanism of deposit formation in wing tanks.
SAE Trans., 77, 2811-2822, 1968.
166. Kinney,C.R. and Del Bel,E.
Pyrolytic behaviour of unsubstituted aromatic hydrocarbons.
Ind. Eng. Chem., 46(3), 548-556, 1954.

167. Shah,Y.T., Stuart,E.B. and Sheth,K.P.
Coke formation during thermal cracking of n-octane.
Ind. Eng. Chem. Proc. Des. Dev., 15(4), 518-524, 1976.
168. Steele,G.L., Brinkmann,D.W. and Whisman,M.L.
Predictive test method for coking and fouling tendency of used lubricating oil.
Proc. Int. Conf. on Fouling of Heat Transfer Equipment, Rensselaer Polytechnic Institute, Troy, NY, 13-17 August 1979. (E.F.C.Somerscales and J.G.Knudsen, eds), pp 483-488, London: Hemisphere, 1981.
169. Frederick,W.J. and Grace,T.M.
Analysis of scaling in a black liquor evaporator.
AIChE Symp. Ser., 184(75), 95-101, 1979.
170. Sondreal,E.A., Gronvold,G.H., Tufte,P.H. and Beckering,W.
Ash fouling studies of low rank Western US coals.
Proc. Int. Conf. on Ash deposits ad Corrosion from Impurities in Combustion Gases, Henniker, New Hampshire, 26 June - 1 July 1977. (R.W.Bryers, ed.), pp 85-111. London: Hemisphere, 1978.
171. Bancroft,A.R.
Equipment for studing fouling in organic coolant systems.
Atomic Energy of Canada Ltd, Ontario, CRCE - 1142, AECL - 1706, March 1963.
172. Bott,T.R. and Gudmundsson,J.S.
Deposition of parrafin wax from kerosene in cooled heat exchanger tubes.
Can. J. Chem. Eng., 55, 381-385, Aug 1977.
173. Sundaram,R.M. and Froment,G.F.
Kinetics of coke deposition in the thermal cracking of propane.
Chem. Eng. Sci., 34, 635-644, 1979.
174. Taylor,W.F.
Deposit formation from deoxygenated hydrocarbons - 1. General features.
Ind. Eng. Chem. Prod. Res. Dev., 13(2), 133-138, 1974.
175. Taylor,W.F.
Deposit formation from deoxygenated hydrocarbons - 2. Effect of trace sulphur compounds.
Ind. Eng. Chem. Prod. Res. Dev., 15(1), 64-68, 1976.
176. Taylor,W.F. and Frankenfeld,J.W.
Deposit formation from deoxygenated hydrocarbons - 3. Effects of trace nitrogen and oxygen compounds.
Ind. Eng. Chem. Prod. Res. Dev., 17(1), 86-90, 1978.
177. Frankenfeld,J.W. and Taylor,W.F.
Deposit formation from deoxygenated hydrocarbons - 4. Studies in pure compound systems.
Ind. Eng. Chem. Prod. Res. Dev., 19(1), 65-70, 1980.

178. Watt,J.J., Evans,A. and Hibbard,R.R.
Fouling characteristics of ASTM jet A fuel when heated to 700F in a simulated heat exchanger tube.
National Aeronautics and Space Administration, NASA TN D - 4958, 1968.
179. Bryers,J.D. and Characklis,W.G.
Measurement of primary biofilm formation.
Proc. Symp. on Condenser Biofouling Control, Electric Power Research Institute, Atlanta, Georgia, 25-29 March 1979. (J.F.Garey, R.M.Jordan, A.H.Aitken, D.T.Burton and R.H.Gray, eds), pp 169-183. Michigan: Ann Arbor Science, 1980.
180. Bryers,J.D. and Characklis,W.G.
Kinetics of initial biofilm formation within a turbulent flow system.
Proc. Int. Conf. on fouling of Heat Transfer Equipment, Rensselaer Polytechnic Institute, Troy, NY, 13-17 August 1981. (E.F.C.Somerscales and J.G.Knudsen, eds), pp 313-333. London: Hemisphere, 1981.
181. Hodgson,T.D. and Smith,S.
The appraisal of additives for scale inhibition during seawater distillation.
Proc. 5th Int. Symp. on Fresh Water from the Sea., 1976, Vol 1, pp 305-318.
182. Langelier,W.F, Caldwell,D.H., Lawrence,W.B. and Spaulding,C.H.
Scale control in sea water distillation equipment.
Ind. Eng. Chem., 42(1), 126-130, 1950.
183. Hopkins,R.M. and Epstein,N.
Fouling of heated stainless steel tubes by a flowing suspension of ferric oxide in water.
Proc. 5th Int. Heat Transfer Conf., Toyko, 1974, Vol 5, pp 180-184.
184. Wynnnyckyj,J.R. and Rhodes,E.
Mechanisms of furnace fouling.
ICHMT Int. Seminar on Advancement in Heat Exchangers, Dubrovnik, Yugoslavia, 7-12 Sept 1981. (J.Taborek, G.F.Hewitt and N.Afgan, eds), pp 817-831. London: Hemisphere, 1983.
185. Corpe,W.A.
Marine microfouling and OTEC heat exchangers.
Proc. Symp. on OTEC Biofouling and Corrosion., Seattle, Washington, 10-12 Oct 1977. (R.H.Gray, ed.), pp 31-44.
186. Corpe,W.A. and Winters,H.
The biology of microfouling of solid surfaces with special reference to power plant heat exchangers.
Proc. Symp. on Condenser Biofouling Control, Electric Power Research Institute, Atlanta, Georgia, 25-29 March 1979. (J.F.Garey, R.M.Jordan, A.H.Aitken, D.T.Burton, and R.H.Gray, eds), pp 29-42. Michigan: Ann Arbor Science, 1980.

187. Marshall,K.C., Stout,R. and Mitchell,R.
Mechanism of the initial events in the sorption of marine bacteria to surfaces.
J.Gen Microbiol., 68, 337-348, 1971.
188. Mitchell,R.
Mechanism of biofilm formation in seawater.
Proc. Symp. on OTEC Biofouling and Corrosion, Seattle, Washington, 10-12 Oct 1977. (R.H.Gray, ed.), pp 45-59.
189. Gerchakov,S.M., Roth,F.J., Sallman,B. and Udey,L.R.
Observation on microfouling applicable to OTEC systems.
Proc. Symp. on OTEC Biofouling and Corrosion, Seattle, Washington, 10-12 Oct 1977. (R.H.Gray, ed.), pp 63-75.
190. Eaton,A., Chamberlin,C. and Cooney,M.
Colonization of CuNi surfaces by microfouling organisms.
Proc. Symp. on Condenser Biofouling Control, Electric Power Research Institute, Atlanta, Georgia, 25-29 March 1979. (J.F.Garey, R.M.Jordan, A.H.Aitken, D.T.Burton and R.H.Gray, eds), pp 105-119. Michigan: Ann Arbor Science, 1980.
191. Thurston,E.F.
Experimental plant for studying methods of controlling scale formation in boilers.
Chem. Ind., No 28, 1238-1243, 10 July 1965.
192. Harris,A. and Marshall,A.
The evaluation of scale control additives.
Proc. Conf. on Progress in the Prevention of Fouling in Industrial Plant, Nottingham University, 1-3 April 1981. pp 174-199.
193. Baier,R.E.
Modification of surfaces to reduce fouling and improve cleaning.
Proc. Int. Workshop on Fundamentals and Applications of Surface Phenomena associated with Fouling and Cleaning in Food Processing, Tysoland, Sweden, 6-9 April 1981. (B.Hallstrom, D.B.Lund and Ch.Tragardh, eds), pp 168-189. Sweden: Reprocontralan, 1981.
194. Nancollas,G.E., Kazmierczak,T.F. and Schuttringer,E.
A controlled composition study of calcium carbonate growth: The influence of scale inhibitors.
Corrosion (Houston), 37(2), 76-81, Feb 1981.
195. Lister,D.H.
The transport of radioactive corrosion products in high temperature water - I. Recirculating Loop Experiments.
Nucl. Sci. Eng., 58, 239-251, 1975.
196. Lister,D.H.
The transport of radioactive corrosion products in high temperature water - II. The activation of isothermal steel surfaces.
Nucl. Sci. Eng., 59, 406-426, 1976.

197. Burrill, K.A.
Corrosion product transport in water-cooled nuclear reactors:
Part III. Boiling water with indirect cycle operation.
Can. J. Chem. Eng., 57, 211-224, Apr 1979.
198. Vranos, A., Marteney, P.J. and Knight, B.A.
Determination of coking rate in jet fuel.
Proc. Int. Conf. on Fouling of Heat transfer equipment, Rensselaer
Polytechnic Institute, Troy, NY, 13-17 August 1979. (E.F.C. Somerscales
and J.G. Knudsen, eds), pp 489-499. London: Hemisphere, 1981.
199. Braun, R.
The nature of petroleum process fouling - results with a practical
instrument.
Mater. Perform., 16(11), 35-41, 1977.
200. Braun, R. and Hausler, R.H.
Contribution to the understanding of fouling phenomena in the
petroleum industry.
Proc. 16th Nat. Heat Transfer Conf., St Louis, Mo, 8-11 August 1976,
76-CSME/CSCHE-23.
201. Hausler, R.H.
New test will show fouling tendency of process streams.
Oil Gas J., 73(23), 56-63, 1973.
202. Hausler, R.H. and Thalmayer, C.E.
Fouling and corrosion in feed effluent exchangers: Discussion of a new
test method.
40th Mid Year Meeting of the API Refining Div., Chicago, May 1975.
Preprint No 06-75, pp 168-184.
203. Bouman, S., Driessan, F.M. and Schmidt, D.G.
Growth of thermoresistant streptococci and deposition of milk
constituents on the plates of heat exchangers during long running
times.
Proc. Int. Workshop on Fundamentals and Applications of Surface
Phenomena associated with Fouling and Cleaning in Food Processing,
Tysoland, Sweden, 6-9 April 1981. (B. Hallstrom, D.B. Lund and
Ch. Tragardh, eds), pp 190-203. Sweden: Reprocontralan, 1981.
204. Baier, R.E., DePalma, V.A., Mayer, A.E., King, R.W. and Fornalik, M.S.
Control of heat exchange surface microfouling by material and process
variations.
'Fouling in Heat Exchange Equipment' presented at 20th ASME/AIChE Heat
Transfer Conf., Milwaukee, Wisconsin, 2-5 August 1981. (J.M. Chenoweth
and M. Impagliazzo, eds), pp 97-103, New York: ASME, 1981.
205. Hodgson, T.D. and Jordan, T.W.J.
Scaling in vertical tube, falling film evaporators.
Proc. 5th Int. Symp. on Fresh Water from the Sea, 1976. Vol 1,
pp 295-303.

206. Lu,C.H. and Fabuss,B.H.
Calcium sulphate scaling in saline water distillation.
Ind. Eng. Chem. Proc. Des. Dev., 7(2), 206-212, 1968.
207. Smith,J.D.
Fuel for supersonic transport - effects of deposits on heat transfer to aviation kerosine.
Ind. Eng. Chem. Proc. Des. Dev., 8(3), 299-308, 1969.
208. Kneil,L., Winter,O. and Stork,K.
Ethylene: Keystone to the Petrochemical Industry, p123. New York: Marcel Dekker, 1980.
209. Hermans,W.F.
Fouling, cleaning and corrosion aspects in tubular heat exchangers for the diary and food industry.
Proc. Int. Workshop on Fundamentals and Applications of Surface Phenomena associated with Fouling and Cleaning in Food Processing, Tylosand, Sweden, 6-9 April 1981. (B.Hallsrom, D.B.Lund and Ch.Tragardh, eds), pp 256-267. Sweden: Reprocontralan, 1981.
210. Haluska,J.L.
Process fouling control by effective antifoulant selection.
Mater. Perform., 15(11), 36-40, 1976.
211. Dugan,C.F., Van Nostrand,W.L. and Haluska,J.L.
How antifoulants reduce the energy consumption of refineries.
Chem. Eng. Prog., 74(5), 53-57, May 1978.
212. Elliott,M.N., Hodgson,T.D. and Harris,A.
Additives for alkaline scale control at temperature above 93°C.
Desalination, 14, 43-55, 1974.
213. Curtis,S.D. and Silverstein,R.M.
Corrosion and fouling control of cooling waters.
Chem. Eng. Prog., 67(7), 39-44, July 1971.
214. Roffman,H.K. and Hoffman,A.
Water that cools but does not pollute.
Chem. Eng. (NY), 83(21 June), 167-174, 1976.
215. Characklis,W.G., Zilver,N., Turakhia,M. and Nimmons,M.J.
Fouling and heat transfer.
'Fouling in Heat Exchange Equipment' presented at 20th ASME/AIChE Heat Transfer Conf., Milwaukee, Wisconsin, 2-5 August 1981. (J.M.Chenoweth and M.Impagliazzo, eds), pp 1-15. New York: ASME, 1981.
216. Hasson,D.
Rate of decrease of heat transfer due to scale deposition.
Dechema Monogr., 47, 233-252, 1962.
217. Hasson,D., Avriel,M. Resnick,W., Rozenman,T. and Windreich,S.
Calcium carbonate scale deposition on heat transfer surfaces.
Desalination, 5, 107-119, 1968.

218. Hasson,D. and Perl,I.
Scale deposition in a laminar falling film system.
Proc Int. Workshop on Fundamentals and Applications of Surface Phenomena associated with Fouling and Cleaning in Food Processing, Tysoland, Sweden, 6-9 April 1981. (B.Hallstrom, D.B.Lund and Ch.Tragardh, eds), pp 236-249. Sweden: Reprocontralan, 1981.
219. Capper,C.B.
Fouling of heat exchangers from cooling water and process materials.
Effluent Water Treat. J., 14(6), 309-314, June 1974.
220. Boow,J. and Goard,P.R.C.
Fireside deposits and their effects in a pulverised-fuel fired boiler: Part III. The influence of the physical characteristics of the deposit on its radiant emittance and effective thermal conductance.
J. Inst. Fuel, 42, 412-419, 1969.
221. Neal,S.B.H.C. and Northover,E.W.
Measuring heat transfer in the boiler furnace.
CEGB Research, 25-34, July 1981.
222. Ivanov,V.P. and Chudnovskaya,I.I.
Investigating some properties of oil ash deposits.
Therm. Eng. Engl. Transl., 16(2), 42-46, 1969.
223. Rassokhim,N.G., Kabonav,L.P., Telvin,S.A. and Tersin,V.A.
Iron oxide deposits on heat transfer surfaces and their removal
Proc. Int. Conf. on High Temperature and High Pressure Electrochemistry in aqueous solutions. University of Surrey, Jan 1973, pp 245-250.
224. Haller,K.H., Lee,R.A. and Slotnik,J.S.
Heat transfer and friction characteristics of porous magnetite layers in once through boilers.
ASME Winter Annual Meeting, Washington DC, 28 Nov - 2 Dec 1971. Paper 71-WA/HT-45.
225. Cohen,P. and Efferding,L.E.
Post-critical heat flux fouling by system corrosion products in a model sodium heated steam generator.
ASME Annual Winter Meeting, NY, Dec 1976. Paper 76-WA/NE-12.
226. Cohen,P.
Water coolant technology of power stations. London: Gordon & Breach Science Publishers, 1969.
227. Cohen,P.
Heat and mass transfer for boiling in porous deposits with chimneys.
AIChE Symp. Ser., 70(138), 71-80, 1974.
228. Parrott,J.E. and Stuckes,A.D.
Thermal conductivity of solids. London: Pion, 1975.
229. BS 1134 : 1972
Assessment of surface texture.

230. Fouad,M.G. and Zatout,A.A.
Mass transfer at rough surfaces.
Electrochim. Acta, 14, 909-919, 1969.
231. Ibl,N., Javet,Ph. and Stahel,F.
Note on the electrodeposits obtained at the limiting current.
Electrochem. Acta, 17, 733-739, 1972.
232. Walker,R.A. and Bott,T.R.
Effect of roughness on heat transfer in exchanger tubes.
Chem. Eng. (London), No 271, 151-156, Mar 1973.
233. Perkins,K.R. and McEligot,D.M.
Roughness of heat transfer surfaces.
Int. J. Heat Mass Transfer, 16, 679-681, 1973.
234. Wiederhold,V.W.
Über den einfluß von rohrablagerungen auf den hydraulischen druckabfall.
Gas Wasserfach, 90, 634-641, 1949.
235. Nordin,S. and Westergren,l.
Practical experiences of prevention of scaling by means of high finish surfaces in evaporator tubes.
Proc. Int. Workshop on Fundamentals and Applications of Surface Phenomena associated with Fouling and Cleaning in Food Processing, Tysoland, Sweden, 6-9 April 1981. (B.Hallstrom, D.B.Lund and Ch.Tragardh, eds), pp 356-364. Sweden: Reprocontralan, 1981.
236. Geßner,W.
Druckverluste in Rohrleitungen und geschlossnen kanälen bei riffelrauigkeit.
Chem. Appar., 84, 329-334, 1960.
237. Schoch,W., Effertz,P. and Richter,R.
Untersuchung über die magnetitbildung in einem überkritischen Benson kessel.
Maschinenschaden, 43, 65-77, 1970.
238. Richter,R., Schoch,W., Schuster,H. and Weihl,H.
Magnetite formation and pressure loss increase in a Benson boiler.
ASME Winter Annual Meeting, Washington DC, 28 Nov - 2 Dec 1971. Paper 71-WA/HT-44.
239. Bott,T.R. and Gudmundsson,J.S.
Rippled silica deposits in heat exchanger tubes.
Proc. 6th Int. Conf. on Heat Transfer., Toronto, Canada, 7-11 August 1978. Vol 4, pp 373-378. Washington: Hemisphere, 1981.
240. Dawson,D.A and Trass,O.
Mass transfer at rough surfaces.
Int. J. Heat Mass Transfer, 15, 1317-1336, 1972.
241. Moody,L.F.
Friction factors for pipe flow.
Trans. ASME, 66, 671-684, Nov 1944.

242. Colebrook,C.F. and White,C.M.
The reduction of carrying capacity of pipes with age.
Inst. Civil Eng., 7, 99-118, 1937.
243. Mahato,B.K. and Shemilt,L.W.
Effect of surface roughness on mass transfer.
Chem. Eng. Sci., 23, 183-185, 1968.
244. Mayo-Abad,O.
Thermal fouling studies: Computations on roughness effects,
modifications of a test loop and tests on a process liquor.
M.A.Sc. thesis, University of British Columbia, Nov 1971.
245. Schubert,H.
Particle adhesion to solid surfaces.
Proc. Int. Workshop on Fundamentals and Applications of Surface
Phenomena associated with Fouling and Cleaning in Food Processing,
Tysoland, Sweden, 6-9 April 1981. (B.Hallstrom, D.B.Lund and Ch.Tragardh,
eds), pp 57-75. Sweden: Reprocontralan, 1981.
246. Krupp,H.
Particle adhesion: Theory and experiment.
Adv. Colloid Interface Sci., 1, 111-239, 1967.
247. Tempel,M.V.D.
Interaction forces between condensed bodies in contact.
Adv. Colloid Interface Sci., 3, 137-159, 1972.
248. Rumpf,H.
Particle adhesion.
In: K.V.S.Sastry, Agglomeration 77, AIME, NY, 1977.
249. Visser,J.
Colloid and other forces in particle adhesion and particle removal (a
review).
Symp. on Deposition and filtration of particles from gases and
liquids., University of Loughborough, 6-8 Sept 1978, pp 121-141.
250. Visser,J.
Adhesion of colloidal particles.
In: Matijevic,E. ed., Surface and Colloid Science, 8, pp 3-84. London:
John Wiley & Sons Ltd, 1967.
251. Parkins,W.E.
Surface film formation in reactor systems.
Atomic Energy of Canada Ltd, Ontario, Report 1265, Paper 9, June 1961.
252. Parkins,W.E.
Surface film formation in heterogeneous and homogeneous reactors.
Nucl. Sci. Eng., 12, 91-105, 1962.
253. Beal,S.K..
Deposition of particles in turbulent flow on channel or pipe walls.
Nucl. Sci. Eng., 40, 1-11, 1970.

254. Beal,S.K.
Correlations for the sticking probability and erosion of particles.
J. Aerosol Sci., 9, 455-461, 1978.
255. Beal,S.K.
Prediction of heat exchanger fouling rates - A fundamental approach.
Proc. Symp. on Fouling Effects on Heat Transfer Equipment in Power
Generation Systems, AIChE 65th Annual Meeting, New York, Nov 1972,
Paper 76C, pp 1-37.
256. Ruckenstein,E. and Preive,D.C.
Rate of deposition of Brownian particles under the action of London
and double-layer forces.
J. Chem. Soc. Faraday Trans. II, 69, 1522-1536, 1973.
257. Spielman,L.A. and Friedlander,S.K.
Role of the electrical double layer in particle deposition by
convective diffusion.
J. Colloid Interface Sci., 46(1), 22-31, Jan 1974.
258. Dahneke,B.
Diffusional deposition of particles.
J. Colloid Interface Sci., 48(3), 520-522, Sept 1974.
259. Prieve,D.C.and Ruckenstein,E.
Effect of London forces upon the role of deposition of Brownian
particles.
AIChE J., 20(6), 1178-1187, 1974.
260. Bowen,B.D., Levine,S. and Epstein,N.
Fine particle deposition in laminar flow through parallel plate and
cylindrical channels.
J. Colloid Interface Sci., 54(3), 375-390, Mar 1976.
261. Prieve,D.C. and Ruckenstein,E.
Role of surface chemistry in particle deposition.
J. Colloid Interface Sci., 60(2), 337-348, June 1977.
262. Bowen,B.D. and Epstein,N.
Fine particle deposition in smooth parallel plate channels.
J. Colloid Interface Sci., 72(1), 81-97, Oct 1979.
263. Ruckenstein,E. and Prieve,D.C.
Role of physicochemical properties in the deposition of hydrosols.
In: J.K.Beddow and T.Melay, Testing and Characterisation of powders and
fine particles, pp 107-135. London: Heyden & Sons Ltd, 1980.
264. Ruckenstein,E. and Kalthod,D.G.
Role of hydrodynamics and physical interaction in the adsorption and
desorption of hydrosols or globular proteins.
Proc. Int. Workshop on Fundamentals and Applications of Surface
Phenomena associated with Fouling and Cleaning in Food Processing,
Tysoland, Sweden, 6-9 April 1981, (B.Hallstrom, D.B.Lund and Ch.Tragardh,
eds), pp 115-147. Sweden: Reprocontralan, 1981.

265. Schmel,C.A.
Particle deposition and re-entrainment in long vertical conduits.
Battelle Northwest Labs, Richland, Washington, BNWL-253-3, May 1966.
266. Schmel,C.A.
Aerosol deposition from turbulent air streams in vertical conduits.
Battelle Northwest Labs, Richland, Washington, BNWL-578, Mar 1968.
267. Schmel,C.A.
Particle deposition velocities and particle concentration profiles
above the deposition surfaces.
Battelle Northwest Labs, Richland, Washington, BNWL-715-3, Vol II, Part
3, 1968.
268. Lips,A. and Jessup,N.E.
Colloidal aspects of bacterial adhesion.
In: Adhesion of microorganisms to surfaces. (D.C.Ellwood, J.Melling and
P.Rutter, eds), pp 5-27. London: Academic Press, 1979.
269. Marshall,K.C.
Bacterial behaviour at solid surfaces - A prelude to microbial
fouling.
Proc. Int. Conf. on Fouling of Heat Transfer Equipment, Rensselaer
Polytechnic Institute, Troy, NY, 13-17 August 1979. (E.F.C.Somerscales
and J.G.Knudsen, eds), pp 305-312. London: Hemisphere, 1981.
270. Rutter,P.R. and Vincent,B.
The adhesion of microorganisms to surfaces: physicochemical aspects.
Microbial adhesion to surfaces. (R.C.W.Berkeley, J.M.Lynch, J.Melling,
P.R.Rutter and B.Vincent, eds), pp 79-92. Chichester: Ellis Horwood,
1980.
271. Tadros,Th.F.
Particle-surface adhesion.
Microbial adhesion to surfaces. (R.C.W.Berkeley, J.M.Lynch, J.Melling,
P.R.Rutter and B.Vincent, eds), pp 93-116. Chichester: Ellis Horwood,
1980.
272. Rutter,P.R.
The physical chemistry of the adhesion of bacteria and other cells.
Cell adhesion and motility. (A.S.G.Curtis and J.D.Pitts, eds),
pp 103-135. Cambridge: CUP, 1980.
273. Norde,W.
The behaviour of biological materials at solid/liquid surfaces:
Physicochemical aspects.
Proc. Int. Workshop on Fundamentals and Applications on Surface
Phenomena associated with Fouling and Cleaning in Food Processing,
Tysoland, Sweden, 6-9 April 1981, (B.Hallstrom, D.B.Lund and Ch.Tragardh,
eds), pp 148-167. Sweden: Reprocontralan, 1981.
274. Duddridge,J.E., Kent,C.A. and Laws,J.F.
Bacterial adhesion to metallic surfaces.
Proc. Conf. on Progress in the Prevention of Fouling in Industrial
Plant, Nottingham University, 1-3 April 1981. pp 137-153.

275. Powell, M.S.
Bacterial motility and adhesion and their relevance to contamination systems.
Ph.D. thesis, University of Cambridge, Oct 1982.
276. Fletcher, M.
Attachment of bacteria to surfaces in aquatic equipment.
Adhesion of microorganisms to surfaces. (D.C. Ellwood, J. Melling and P. Rutter, eds), pp 87-108, London: Academic Press, 1979.
277. Derjaguin, B.V. and Landau, L.
Theory of the stability of strongly charged lyophobic sols and the adhesion of strongly charged particles in solutions of electrolytes.
Acta Physicochem. USSR, 14, 633-662, 1941.
278. Verway, E.J.W. and Overbeek, J.Th.G.
Theory of the stability of lyophobic colloids. Amsterdam: Elsevier, 1948.
279. Fox, H.W. and Zisman, W.A.
The spreading of liquids on low energy surfaces - Modified tetrafluoro-ethylene polymers.
J. Colloid Sci., 7, 109-121, 1952.
280. Fox, H.W. and Zisman, W.A.
The spreading of liquids on low energy surfaces - Hydrocarbon surfaces.
J. Colloid Sci., 7, 428-442, 1952.
281. Zisman, W.A.
Influence of constitution on adhesion.
Ind. Eng. Chem., 55(10), 18-38, 1963.
282. Zisman, W.A.
Relation of the equilibrium contact angle to liquid and solid constitution.
Adv. Chem. Ser., 43, 1-51, 1964.
283. Baier, R.E.
Early events of micro-biofouling of all heat transfer equipment.
Proc. Int. Conf. on Fouling of Heat Transfer Equipment, Rensselaer Polytechnic Institute, Troy, NY, 13-17 August 1979. (E.F.C. Somerscales and J.G. Knudsen, eds), pp 293-304. London: Hemisphere, 1981.
284. Fowler, H.W. and McKay, A.J.
The measurement of microbial adhesion.
Microbial adhesion to surfaces. (R.C.W. Berkeley, J.M. Lynch, J. Melling, P.R. Rutter and B. Vincent, eds), pp 143-161, Chichester, Ellis Horwood, 1980.
285. Masurovsky, E.B. and Jordan, W.K.
Studies on the relative bacterial activity of milk contact surfaces.
J. Dairy Sci., 41(10), 1342-1358, 1958.

286. Kos,D.D. and Tao,L.C.
Effects of polyfluorocarbon coatings on scaling in evaporators with continuous feed CaSO_4 solution.
Ind. Eng. Chem. Prod. Res. Dev., 8(3), 306-309, 1969.
287. Duddridge, J.E., Kent,C.A. and Laws,J.F.
Effects of shear stress on the attachment of *Pseudomonas Fluorescens* to stainless steel under defined flow conditions.
Biotechnol. Bioeng., 24(1) 153-164, 1982.
288. Morse,R.W. and Knudsen,J.G.
Effect of alkalinity on the scaling of simulated cooling tower water.
Can. J. Chem. Eng., 55, 272-278, June 1977.
289. Loucks, C.M. and Groom,C.H.
Chemical cleaning of heat exchange equipment.
Trans. ASME, 71, 831-838, Oct 1949.
290. Creedon,B.
Organic fouling - Chemical vs physical control.
Continuing Education Course on Fouling of Heat Exchangers, University of Birmingham, 19-20 March 1981, I.Chem.E. (Spons.), pp 27-29.
291. Cooper,A., Suitor,J.W. and Usher,J.D.
Cooling water fouling in plate exchngrs.
Proc. 6th Int. Heat Transfer Conf., Toronto, Canada, 7-11 August 1978, Vol 4, pp 403-406, Washington: Hemisphere, 1981.
292. Novak,L
Comparison of the Rhine river and the Oresund sea water fouling and its removal by chlorination.
'Fouling in Heat Exchange Equipment.' presented at 20th ASME/AICHE Heat Transfer Conf., Milwaukee, Wisconsin, 2-5 August 1981. (J.M.Chenoweth and M.Impagliazzo, eds), pp 61-66. New York: ASME, 1981.
293. Puckorious,P.R.
Controlling deposits in cooling water systems.
Mater. Prot. Perform., 11, 19-22, Nov 1972.
294. Watkinson,A.P., Louis,L. and Brent,R.
Scaling of enhanced heat exchanger tubes.
Can. J. Chem. Eng., 52, 558-562, Oct 1974.
295. Watkinson,A.P., and Martinez,O.
Scaling of heat exchanger tubes by calcium carbonate.
J. Heat Transfer, 97, 504-508, Nov 1975.
296. Magaril,R.Z. and Aksenova,E.I.
Study of the mechanism of coke formation in the cracking of petroleum resins.
Int. Chem. Eng., 8(4), 727-729, 1968.
297. Weinland,B.W.
Some new antifouling applications.
Canadian Petroleum, 58-60, March 1967.

298. French, M.A.
Chemical cleaning.
Proc. Conf. on Progress in the Prevention of Fouling in Industrial Plant, Nottingham University, 1-3 April 1981. pp 68-84.
299. Kerst, H.
Influence of inhibitors on corrosion and scale deposition on heat transfer surfaces in fresh water cooling systems.
Mater. Prot., 1, 10-19, Oct 1962.
300. Zuckerman, N.
The Eilat 1,000,000 GPD multistage flash distillation plant operating experience.
Desalination, 4, 167-197, 1968.
301. Skudder, P.J.
The role of sulphydral groups in the formation of proteinaceous deposit from milk on heated surfaces.
Proc. Int. Workshop on Fundamentals and Applications of Surface Phenomena associated with Fouling and Cleaning in Food Processing, Tysoland, Sweden, 6-9 April 1981. (B.Hallstrom, D.B.Lund and Ch.Tragardh, eds), pp 378-386. Sweden: Reprocontralan, 1981.
302. Rodliffe, R.S.
A model for the autoretardation of particulate deposits.
J. Colloid Interface Sci., 76(1), 157-165, July 1980.
303. Kerst, H.
Laboratory investigation of water-side scale and corrosion in the presence of high process side temperatures.
Corrosion, 16, 131-137, Oct 1960.
304. Gazit, E. and Hasson, D.
Scale deposition from an evaporating falling film.
Desalination, 17, 339-351, 1975.
305. Nair, M.K.V. and Misra, B.M.
Electrolytic deposition for scale control in sea water distillation.
Desalination, 27, 59-64, 1978.
306. DePalma, V.A. and Baier, R.E.
Microfouling of metallic and coated metallic flow surfaces in model heat exchange cells.
Proc. Symp. on OTEC Biofouling and Corrosion, Seattle, Washington, 10-12 Oct 1977, (R.H.Gray, ed.), pp 89-106.
307. Tarbuck, L.A. and Wyborn, C.H.E.
Microbial growth and activity in condenser tubes.
Proc. Symp. on Condenser Biofouling Control, Electric Power Research Institute, Atlanta, Georgia, 25-29 March 1979. (J.F.Garey, R.M.Jordan, A.H.Aitken, D.T.Burton and R.H.Gray, eds), pp 85-104, Michigan: Ann Arbor Science, 1980.

308. Levich,B.
The theory of concentration polarisation.
Part I : Acta Physicochim. URSS, 17, 257-307, 1942.
Part II : Acta Physicochim. URSS, 19, 417-432, 1944.
Part III : Acta Physicochim. URSS, 19, 433-438, 1944.
309. Levich,V.G.
Physicochemical hydrodynamics, Englewood Cliffs: Prentice Hall, 1962.
310. Agar,J.N.
Diffusion and convection at electrodes.
Discuss. Faraday Soc., 1, 26-47, 1947.
311. Tobias,C.W., Eisenburg,M. and Wilke,C.R.
Diffusion and convection in electrolysis - a theoretical review.
J. Electrochem. Soc., 99(12), 359C-365C, 1952.
312. Ibl,N.
Probleme des stofftransportes in der angewandten elektrochemie.
Chem. Ing. Tech., 35(5), 353-361, 1963.
313. Newman,J.
Transport processes in electrolytic processes.
Adv. Electrochem. Electrochem. Eng., 5, 87-135, 1967.
314. Newman,J.
Engineering design of electrochemical systems.
Ind. Eng. Chem., 60(4), 12-27, 1968.
315. Newman,J.S.
Electrochemical systems, Englewood Cliffs: Prentice Hall, 1973.
316. Arvia,A.J. and Marchiano,S.L.
Transport phenomena in electrochemical kinetics.
Mod. Aspects Electrochem., No 6, 159-241, 1971.
317. Mizushina,T.
The electrochemical method in transport phenomena.
Adv. Heat Transfer, 7, 87-161, 1971.
318. Ravoo,E.
Mass transfer in electrochemical systems.
Dissertation, Twente Technical University, July 1971.
319. Ravoo,E.
Mass transfer in electrochemical systems with free and forced convection.
Ingenieur (The Hague), 83(8), 11-28, 1971.
320. Selman,J.R.
Measurement and interpretation of limiting currents.
Ph.D. thesis, University of California, June 1971.
321. Selman,J.R.
Technique of mass transfer measurements in electrochemical reactors.
AIChE Symp. Ser., 77(204), 88-102, 1981.

322. Landau,U.
Distribution of mass transfer rates along parallel plane electrodes in forced convection.
Ph.D. thesis, University of California, 1976.
323. Landau,U.
Determination of laminar and turbulent mass transport rates in flow cells by the limiting current technique.
AIChE Symp. Ser., 77(204), 75-87, 1981.
324. Pickett,D.J.
Electrochemical reactor design, Oxford: Elseveir, 1979.
325. Shemilt,L.W.
Principles of electrochemical engineering.
Chemical Engineering Education Development Centre, I.I.T, Madras, 1977.
326. Wragg,A.A.
Applications of the limiting diffusion current technique in chemical engineering.
Chem. Eng. (London), No 316, 39-49, Jan 1977.
327. Selman,J.R. and Tobias,C.W.
Mass transfer measurements by the limiting current technique.
Adv. Chem. Eng., 10, 211-318, 1978.
328. Fahidy,T.Z. and Mohanta,S.
Mass transport in electrochemical systems.
In: Advances in transport processes. (A.S.Mujumdar, eds), Vol 1, pp 83-137. New Dehli: Wiley Eastern Ltd, 1980.
329. Poulson,B.
Electrochemical measurements in flowing solutions.
Corros. Sci., 23(4), 391-430, 1983.
330. Berger,F.P. and Ziai,A.
Problems of electrochemical modelling of heat transfer processes.
I.Chem.E. 11th Annual Research Meeting on Heat Transfer and Catalysis and Catalytic Reactors, University of Bath, 9-10 April 1984, pp 129-134.
331. Fahidy,T.Z.
The chemical engineering approach to some electrochemical processes.
Can. J. Chem. Eng., 51, 521-534, Oct 1973.
332. Tagg,D.J., Patrick,M.A, and Wragg,A.A.
Heat and mass transfer downstream of abrupt nozzle expansions in turbulent flow.
Trans. Inst. Chem. Eng., 57, 176-181, 1979.
333. Matuschek,J.
Ueber den einfluss des sonnenlichtes auf lösungen von rothem blutlaugensalz in wasser.
Part I : Chem. Ztg, 25(38), 411-412, 1901.
Part II: Chem. Ztg, 25(49), 522-523, 1901.

334. Matuschek,J.
Ueber den einfluss des sonnenlichtes auf lösung von gelbem
blutlaugensalz in wasser.
Chem. Ztg, 25(53), 565-566, 1901.
335. Jimori,S.
Bildung von aquopentacyaneisensalz in der wäßrigen lösung von
hexacyaniesenkomplexsalz und sukzessive dissoziation letzteren
salzes.
Z. Anorg. Allg. Chem., 167, 145-172, 1927.
336. Kolthoff,I.M. and Pearson,E.A.
Stability of potassium ferrocyanide solutions.
Ind. Eng. Chem. Anal. Ed., 3(4), 381-382, 1931.
337. Eisenburg,M., Tobias,C.W. and Wilke,C.R.
Ionic mass transfer and concentration polarisation at rotating
electrodes.
J. Electrochem. Soc., 101(6), 306-319, 1954.
338. Berger,F.P. and Ziai,A.
Optimisation of experimental conditions for electrochemical mass
transfer measurements.
Chem. Eng. Res. Des., 61(6), 377-382, Nov 1983.
339. Sutey,A.M. and Knudsen,J.G.
Effect of dissolved oxygen on the redox method for the measurement of
mass transfer coefficients.
Ind. Eng. Chem. Fundam., 6(1), 132-139, 1967.
340. Aggerwaal,J.K. and Talbot,L.
Electrochemical measurements of mass transfer in semi-cylindrical
hollows.
Int. J. Mass Heat Transfer, 22, 61-75, 1979.
341. Hubbard,D.W. and Lightfoot,E.N.
Correlation of mass and heat transfer data for high Schmidt and
Reynolds numbers.
Ind. Eng. Chem. Fundam., 5(3), 370-379, 1966.
342. BS 718 : 1979
Density hydrometers.
343. BS 188 : 1977
Determination of the viscosity of liquids.
344. Arvia,A.J., Bazan,J.C. and Carrozza,J.S.W.
Electrochemical study of the diffusion of cupric ion in aqueous and
aqueous-glycerol solutions containing sulphuric acid.
Electrochim. Acta, 11, 881-889, 1966.
345. Wragg,A.A. and Ross,T.K.
Diffusivity and ionic mass transfer in the cupric sulphate system.
Electrochim. Acta, 13, 2192-2194, 1968.

346. Lin,C.S., Denton,E.B., Gaskill,H.S. and Putnam,G.L.
Diffusion controlled electrode reactions.
Ind. Eng. Chem., 43(9), 2136-2143, 1951.
347. Eisenberg,M., Tobias,C.W. and Wilke,C.R.
Selected physical properties of ternary electrolytes in ionic mass transfer studies.
J. Electrochem. Soc., 103(7), 413-416, 1956.
348. Bazan,J.C. and Arvia,A.J.
The diffusion of ferro and ferricyanide ions in aqueous solutions of sodium hydroxide.
Electrochim. Acta, 10, 1025-1032, 1965.
349. Gordon,S.L., Newman,J.S. and Tobias,C.W.
The role of ionic migration in electrolytic mass transport;
Diffusivities of $[\text{Fe}(\text{CN})_6]^{3-}$ and $[\text{Fe}(\text{CN})_6]^{4-}$ in KOH and NaOH solutions.
Ber. Bunsenges. Phys. Chem., 70, 414-420, 1966.
350. Van Shaw,P., Riess,L.P. and Hanratty,T.J.
Rates of turbulent transfer to a pipe wall in the mass transfer entry region.
AIChE J., 9(3), 362-364, 1963.
351. Noordsij,P. and Rotte,R.W.
Mass transfer coefficients to a rotating and to a vibrating sphere.
Chem. Eng. Sci., 22, 1475-1481, 1967.
352. Riedel,L.
The heat conductivity of aqueous solutions of strong electrolytes.
Chem. Ing. Tech., 23(3), 59-64, 1951.
353. Vargaftik,N.B. and Os'minin,Y.P.
Thermal conductivity of aqueous solutions of salts, acids and alkalis.
Therm. Eng. Engl. Transl., 3(7), 11-15, 1956.
354. Jamieson,D.T. and Tudhope,J.S.
The thermal conductivity of liquids: A survey to 1963. March 1964, NEL Report 137.
355. Selman,J.R. and Newman,J.S.
Migration in supported electrolyte solutions with free convection.
Lawrence Radiation Lab., University of California, Berkeley, UCRL-20322, Jan 1967.
356. Selman,J.R. and Newman,J.
Free convection mass transfer with a supporting electrolyte.
J. Electrochem. Soc., 118(7), 1070-1078, 1971.
357. ESDU 78039
Thermal conductivity of ice, water and steam.

358. Gibson,M.R. and Bruges,E.A.
New equations for the thermodynamic properties of saturated water in both liquid and vapour phases.
J. Mech. Eng. Sci., 9(1), 24-35, 1967.
359. Wenner,R.R.
Thermodynamic calculations, New York: McGraw Hill, 1941.
360. Wagner,C.
The role of natural convection in electrolytic processes.
J. Electrochem. Soc., 95(4), 161-173, 1949.
361. Wilke,C.R., Eisenburg,M. and Tobias,C.W.
Correlation of limiting currents under free convection conditions.
J. Electrochem. Soc., 100(11), 513-523, 1953.
362. Ibl,N.
Theory of steady state limiting current at stationary wire electrodes.
Electrochim. Acta, 1, 3-17, 1959.
363. Ibl,N.
The use of dimensionless groups in electrochemistry.
Electrochem. Acta, 1, 117-129, 1959.
364. Fouad,M.G. and Ibl,N.
Natural convection mass transfer at vertical electrodes under turbulent flow conditions.
Electrochim. Acta, 3, 233-243, 1960.
365. Ibl,N. and Braun,V.
Evaluation of the concentration changes near the electrodes in electrolysis with natural convection.
Chimica, 21, 395-404, 1967.
366. Bohm,U.
The specific densification coefficient for a ternary electrolyte.
An. Asoc. Quim. Argent., 58, 127-131, 1970.
367. Tennant,B.R.
Effect of a supporting electrolyte upon natural convection.
B.S. thesis, University of Illinois, 1974.
368. Taylor,J.L. and Hanratty,T.J.
Influence of natural convection on mass transfer rates for the electrolysis of ferricyanide ions.
Electrochim. Acta, 19, 529-533, 1974.
369. Hiraoka,S., Yamada,I., Takeuchi,H., Ikeno,H., Asano,H., Nomura,S., Sugimoto,H. and Nakamura,H.
Free convection mass transfer in $K_3Fe(CN)_6 - K_4Fe(CN)_6 - KOH$ solution.
J. Chem. Eng. Jpn., 15(2), 98-104, 1982.
370. Boeffard,A.J-L.P.M.
Ionic mass transport by free convection in a redox system.
M.S. thesis, University of California, Jan 1966.

371. Wragg,A.A. and Nasiruddin,A.K.
Ionic mass transfer by free convection with simultaneous heat transfer.
Electrochem. Acta, 18, 619-627, 1973.
372. Wasmund,B. and Smith,J.W.
Wall to fluid heat transfer in liquid fluidised beds.
Can. J. Chem. Eng., 45, 156-165, June 1967.
373. Hanratty,T.J.
The use of electrochemical techniques to study flow fields and mass transfer rates.
Proc. Int. Summer School on Heat and Mass Transfer in Turbulent Boundary Layers, Herceg Novi, September 1968. & Selected Papers and Abstracts of the Int. Seminar on Heat and Mass Transfer in Flows with Separated Regions, Herceg Novi, September 1969. (N.Afgan, Z.Zaric and P.Anastasijevic, eds), pp 919-939. Oxford: Pergamon, 1970.
374. Burdukov,A.P.
Electrochemical techniques of flow studies.
Proc. Int. Summer School on Heat and Mass Transfer in Turbulent Boundary Layers, Herceg Novi, September 1968. & Selected Papers and Abstracts of the Int. Seminar on Heat and Mass Transfer in Flows with Separated Regions, Herceg Novi, September 1969. (N.Afgan, Z.Zaric and P.Anastasijevic, eds), pp 669-675. Oxford: Pergamon, 1970.
375. Ravoo,E., Rotte,J.W. and Sevenstern,F.W.
Theoretical and electrochemical investigation of free convection mass transfer in vertical cylinders.
Chem. Eng. Sci., 25, 1637-1652, 1970.
376. Berger,F.P. and Hau,K.F.L.
Mass transfer in turbulent pipe flow measured by the electrochemical method.
Int. J. Heat Mass Transfer, 20, 1185-1194, 1977.
377. Smith,J.W. and King,D.H.
Electrochemical wall mass transfer in liquid particulate systems.
Can. J. Chem. Eng., 53, 41-47, Feb 1975.
378. Youngquist,G.R.
An entrance region mass transfer experiment.
Chem. Eng. Educ., 20-25, Winter 1979.
379. Hiraoka,S., Yamada,I., Ikeno,H., Asano,H., Nomura,S., Okada,T. and Nakamura,H.
Measurements of diffusivities of ferricyanide and ferrocyanide ions in dilute solution with KOH supporting electrolyte.
J. Chem. Eng. Jpn., 14(5), 345-351, 1981.
380. Man,K.L., Edwards,M.F. and Polley,G.T.
A study of local heat transfer coefficients in agitated vessels.
Inst. Chem. Eng. Symp. Ser. n89 (Proc Symp. on Fluid Mixing II, Bradford University, 3-5 April 1984.) pp 193-207.

381. Uhl,V.W. and Gray,J.B.
Mixing - Theory and Practice, Vol 1. London: Academic Press, 1966.
382. Wragg,A.A.
Free convection mass transfer at horizontal electrodes.
Electrochim. Acta, 13, 2159-2165, 1968.
383. Lloyd,J.R. and Moran,W.R.
Natural convection adjacent to horizontal surface of various planforms.
J. Heat Transfer, 96, 443-477, 1974.
384. Wragg,A.A. and Loomba,R.P.
Free convection flow patterns at horizontal surfaces with ionic mass transfer.
Int. J. Mass Heat Transfer, 13, 439-442, 1970.
385. Patrick,M.A. and Wragg,A.A.
Optical and electrochemical studies of transient free convection mass transfer at horizontal surfaces.
Int. J. Mass Heat Transfer, 18, 1397-1407, 1975.
386. Fenech,E.J. and Tobias,C.W.
Mass transfer by free convection at horizontal electrodes.
Electrochim. Acta, 2, 311-321, 1960.
387. Gilliland,E.R. and Sherwood,T.K.
Diffusion of vapours into air streams.
Ind. Eng. Chem., 26(5), 516-523, 1934.
388. Marangozis,J. and Johnson,A.I.
A correlation of mass transfer data of solid-liquid systems in agitated vessels.
Can. J. Chem. Eng., 40, 231-237, Dec 1962.
389. Mizushina,T., Ito,R., Hiraoka,S., Ibusuki,A. and Sakaguchi,I.
Transport phenomena at the wall of agitated vessels.
J. Chem. Eng. Jpn., 2(1), 89-94, 1969.
390. LeLan,A. and Angelino,H.
Transferts de matiere a la paroi d'une cuve mecaniquement agitee.
Chem. Eng. Sci., 29, 1557-1565, 1974.
391. LeLan,A. and Angelino,H.
Study of the analogy between heat and mass transfer to the wall of a stirred tank.
Int. J. Heat Mass Transfer, 18, 163-167, 1975.
392. Karabelas,A.J., Wegner,T.H. and Hanratty,T.J.
Use of asymptotic relations to correlate mass transfer data in packed beds.
Chem. Eng. Sci., 26, 1581-1589, 1971.
393. Perry,R.H. and Chilton,C.H. eds.
Chemical Engineer's Handbook, 5th ed. London: McGraw-Hill & Kogakusha Ltd, 1973.

394. Coulson, J.M. and Richardson, J.F.
Chemical Engineering, Vol 1. 3rd ed. Oxford: Pergamon Press, 1977.
395. Cummings, G.H. and West, A.S.
Heat Transfer data for kettles with jackets and coils.
Ind. Eng. Chem., 42(11), 2303-2313, 1950.
396. Ackley, E.J.
Film coefficients of heat transfer for agitated process vessels.
Chem. Eng. (NY), 67(22 Aug), 133-140, 1980.
397. Uhl, V.W.
Heat transfer to viscous materials in jacketed agitated vessels.
Chem. Eng. Prog. Symp. Ser., 51(17), 93-108, 1955.
398. Kapustin, A.S.
Investigations of heat exchange in agitated vessels working with viscous liquids.
Int. Chem. Eng., 3(4), 514-518, 1963.
399. Brooks, G. and Su, G-J.
Heat transfer in agitated vessels.
Chem. Eng. Prog., 55(10), 54-57, 1959.
400. Streck, F.
Heat transfer in liquid mixers - Study of a turbine agitator with six flat blades.
Int. Chem. Eng., 3(4), 533-556, 1963.
401. Chapman, F.S., Dallenbach, H. and Holland, F.A.
Heat transfer in baffled, jacketed agitated vessels.
Trans. Inst. Chem. Eng., 42, T398-T406, 1964.
402. Akse, H., Beek, W.J., Van Berkel, F.C.A.A., and De Graauw, J.
The local heat transfer at the wall of a large vessel agitated by turbine impellers.
Chem. Eng. Sci., 22, 135-146, 1967.
403. Askew, W.S. and Beckman, R.B.
Heat and mass transfer in an agitated vessel.
Ind. Eng. Chem. Proc. Des. Dev., 4(3), 311-318, 1965.
404. Yagi, S., Kunii, D. and Wakao, N.
Radially effective thermal conductivities in packed beds.
International Developments in Heat Transfer, ASME, 742-749, 1961.
405. Benenatti, R.F. and Braislow, C.B.
Void fraction distribution in bed of spheres.
AIChE J., 8(3), 351-361, 1962.
406. Ridgeway, K. and Tarbuck, K.J.
Voidage fluctuations in randomly-packed beds of spheres adjacent to a containing wall.
Chem. Eng. Sci., 23, 1147-1155, 1968.

407. Gildseth,W., Habenschuss,A. and Spedding,F.H.
Precision measurements of densities and thermal dilation of water
between 5°C and 80°C.
J. Chem. Eng. Data., 17(4), 402-409, 1972.
408. Kolthoff,I.M., Sandell,E.B., Meehan,E.J. and Bruckenstein,S.
Quantitative chemical analysis, 4th ed. London: Macmillan, 1969.

APPENDICES

APPENDIX A1 ELECTROLYTIC SOLUTION DENSITY DATA

DATE	TEMPERATURE (°C)	RELATIVE DENSITY	DENSITY OF ⁽⁴⁰⁷⁾ WATER (g/cm ³)	DENSITY OF ELECTROLYTIC SOLUTION (g/cm ³)
10.5.82	18.0	1.0258	9.986248	1.02439
	21.8	1.0245	9.973455	1.02178
	27.2	1.0242	9.964886	1.02060
	38.6	1.0195	9.927760	1.01214
	50.0	1.0155	9.880698	1.00338
	60.0	1.0115	9.832330	0.99454
	70.0	1.0050	9.778036	0.98269
11.5.82	27.9	1.0238	9.962926	1.02000
	33.0	1.0220	9.947345	1.01662
	38.9	1.0197	9.926642	1.01222
	44.0	1.0170	9.906610	1.00750
12.5.82	26.5	1.0238	9.966801	1.02040
	32.5	1.0218	9.948971	1.01659
	37.4	1.0198	9.932165	1.01288
	43.2	1.0177	9.909877	1.00853
	48.0	1.0158	9.889606	1.00459

APPENDIX A2

ELECTROLYTIC SOLUTION KINEMATIC VISCOSITY DATA

DATE	TEMPERATURE (°C)	TIME OF EFFLUX (s)	KINEMATIC VISCOSITY ¹ (mm ² /s)
23.4.81	17.8	1827.3	1.1684
	18.1	1765.5	1.1289
	18.1	1760.3	1.1256
	22.5	1590.0	1.0167
	27.0	1451.4	0.9281
24.4.81	30.5	1330.7	0.8509
	38.5	1193.5	0.7632
	45.0	1023.2	0.6543

¹

The kinematic viscosity was computed from

$$\nu = 0.0006398 \theta_E$$

where ν = kinematic viscosity in mm/s

θ_E = time of efflux in s.

The value of 0.0006398 was obtained from the calibration of the viscometer using fresh distilled water at 20°C .

APPENDIX A3 THE BASIS OF THE IONIC DENSIFICATION COEFFICIENTS EVALUATED BY SELMAN AND NEWMAN⁽³⁵⁶⁾ FOR THE $K_3Fe(CN)_6 - K_4Fe(CN)_6 - KOH/NaOH$ SYSTEM.

Using 23 density data points in the range $0.01 \leq c \leq 2.0M$ equimolar $K_3Fe(CN)_6$ and $K_4Fe(CN)_6$ and $0 \leq c_{KOH} \leq 2.0M$ measured at $25^\circ C$ by Gordon et al⁽³⁴⁹⁾, Selman and Newman⁽³⁵⁶⁾ computed the following equation:

$$\rho = 0.99946 + 0.19648 c_{redox} + 0.045266 c_{KOH} \quad A3.1$$

where ρ = density in g/cm^3

with a standard error of 0.0011. They differentiated equation A3.1 with respect to $(c_{K_3Fe(CN)_6} + c_{K_4Fe(CN)_6})$ and c_{KOH} to yield

$$\frac{\partial \rho}{\partial c_{redox}} = 0.19648 \quad A3.2$$

$$\frac{\partial \rho}{\partial c_{KOH}} = 0.045266 \quad A3.3$$

Using equation 3.6, they evaluated the following densification coefficients

$$\alpha_{redox} = \frac{0.19648}{0.99946} = 0.19659 \quad A3.4$$

$$\alpha_{KOH} = \frac{0.045266}{0.99946} = 0.04529 \quad A3.5$$

Using 32 density data points in the range $0.01 \leq c_{K_3Fe(CN)_6} \leq 0.2M$, $0.05 \leq c_{K_4Fe(CN)_6} \leq 0.4M$ and $1.0 \leq c_{NaOH} \leq 2.0M$ measured at $25^\circ C$ by Boeffard⁽³⁶⁴⁾, Selman and Newman⁽³⁵⁶⁾ computed the following equation:

$$\rho = 0.996821 + 0.1768 c_{K_3Fe(CN)_6} + 0.023182 c_{K_4Fe(CN)_6} + 0.044374 c_{NaOH} \quad A3.6$$

where ρ = density in g/cm^3

with a standard error of 0.0004. They differentiated equation A3.6 with respect to $c_{K_3Fe(CN)_6}$ and $c_{K_4Fe(CN)_6}$ to yield

$$\frac{\partial \rho}{\partial c_{K_3Fe(CN)_6}} = 0.17618 \quad A3.7$$

$$\frac{\partial \rho}{\partial c_{K_4Fe(CN)_6}} = 0.23182 \quad A3.8$$

From equations A3.6, A3.7 and A3.8, they computed the following ratio

$$\frac{\alpha_{K_3Fe(CN)_6}}{\alpha_{K_4Fe(CN)_6}} = 0.7404 \quad A3.9$$

Noting $\alpha_{redox} = \frac{\alpha_{K_3Fe(CN)_6} + \alpha_{K_4Fe(CN)_6}}{2}$, they solved equations A3.4 and A3.9 to obtain the following densification coefficients

$$\alpha_{K_3Fe(CN)_6} = 0.16727 \quad A3.10$$

$$\alpha_{K_4Fe(CN)_6} = 0.22591 \quad A3.11$$

Based on density data in the range $0.01 \leq c \leq 0.20M$ equimolar $K_3Fe(CN)_6$ and $K_4Fe(CN)_6$ and $0 \leq c_{NaOH} \leq 2.0M$ measured at $25^\circ C$ by Gordon et al⁽³⁴⁹⁾, Selman and Newman⁽³⁵⁸⁾ computed the following equation:

$$\rho = 1.000116 + 0.19356 c_{redox} + 0.038535 c_{NaOH} \quad A3.12$$

where ρ = density in g/cm^3

with a standard error of 0.0013. They differentiated equation A3.12 with respect to c_{NaOH} to yield

$$\frac{\partial \rho}{\partial c_{NaOH}} = 0.038535 \quad A3.13$$

Using equation 3.6, they evaluated the densification coefficient for NaOH

$$\alpha_{NaOH} = \frac{0.038535}{0.99946} = 0.03856 \quad A3.14$$

By setting α_{K^+} to zero, Selman and Newman⁽³⁵⁶⁾ obtained $\alpha_{[Fe(CN)_6]^{3-}}$ from equation A3.10, $\alpha_{[Fe(CN)_6]^{4-}}$ from equation A3.11, α_{OH^-} from equation A3.5 and α_{Na^+} from equations A3.5 and A3.14. These ionic densification coefficients are given in Table 3.2.

APPENDIX A4 THE VARIOUS METHODS THAT HAVE BEEN USED TO ESTIMATE Δc_j FOR THE

$K_3Fe(CN)_6 - K_4Fe(CN)_6 - KOH/NaOH$ SYSTEM

The various methods that have been used to estimate Δc_j for the $K_3Fe(CN)_6 - K_4Fe(CN)_6 - KOH/NaOH$ system include

1. APPROXIMATE METHODS

(a) The WET method

The method developed by Wilke, Eisenburg and Tobias⁽³⁶¹⁾ for the estimation of Δc_j in binary electrolytes was generalised by Ibl and Braun⁽³⁶⁵⁾. The method is based on the assumption that the flux of species j , $\frac{s_j i}{F}$ can be represented as the sum of an amount due to convection and diffusion, N_j and an amount to migration, $\frac{it_j}{Fz_j}$

$$N_j = k_j \Delta c_j = \frac{i}{F} \left[s_j - \frac{t_j}{z_j} \right] \quad A4.1$$

where s_j = number of molecules or ions of species j which react at the electrode per one Faraday flowing through the electrochemical cell (negative when the species is consumed and positive when the species is produced)

t_j = transference number of species j , defined by

$$t_j = \frac{|z_j| \lambda_j c_j}{\sum_j |z_j| \lambda_j c_j} \quad 3.23$$

As it can be assumed that the mass transfer correlation for electrochemical systems with free convection is of the form⁽³⁶¹⁾

$$Sh = a(Gr_m Sc)^{\frac{1}{4}} \quad A4.2$$

it can be deduced from equations A4.1 and A4.2 that Δc_j is given by

$$\Delta c_j = \frac{i}{aF} \left[s_j - \frac{t_j}{z_j} \right] \left[\frac{D_j^3 g}{\nu l} \left[\frac{\Delta \rho}{\rho} \right]_m \right]^{\frac{1}{4}} \quad A4.3$$

Similarly, for the limiting reactant, R

$$\Delta c_R = \frac{i}{aF} \left[s_R - \frac{t_R}{z_R} \right] \left[\frac{D_R^3}{v} \frac{g}{l} \left[\frac{\Delta \rho}{\rho} \right]_m \right]^{\frac{1}{4}} \quad A4.4$$

Dividing equation A4.3 by equation A4.4 yields

$$\frac{\Delta c_j}{\Delta c_R} = \frac{\left[s_j - \frac{t_j}{z_j} \right]}{\left[s_R - \frac{t_R}{z_R} \right]} \left[\frac{D_R}{D_j} \right]^{\frac{3}{4}} \quad 3.22$$

(b) The Wagner method

The method developed by Wagner⁽³⁶⁰⁾ for the estimation of Δc_j in binary electrolytes was generalised by Ibl and Braun⁽³⁶⁵⁾. For an electrolytic solution at rest, the flux of species j at $y = 0$ is given by

$$N_j = \frac{s_{ji}}{F} = \left[-D_j \frac{\partial c_j}{\partial y} - z_j u_j F c_j \frac{\partial \Phi}{\partial y} \right] \Big|_{y=0} \quad A4.5$$

since from equation 3.3

$$u_j = \frac{D_j}{RT} \quad A4.6$$

equation A4.5 can be rewritten as

$$\frac{s_{ji}}{F} = \left[-D_j \frac{\partial c_j}{\partial y} - \frac{z_j D_j F c_j}{RT} \frac{\partial \Phi}{\partial y} \right] \Big|_{y=0} \quad A4.7$$

Upon multiplying equation A4.7 throughout by $\frac{z_j}{D_j}$ for each species of the electrolytic solution and adding all these equations, the sum of the terms involving $\frac{\partial c_j}{\partial y}$ vanishes due to the electroneutrality condition

$$\sum_j z_j c_j = 0 \quad A4.8$$

Thus, the potential gradient at $y = 0$ is given by

$$\frac{\partial \Phi}{\partial y} \Big|_{y=0} = - \frac{iRT}{F^2} \frac{\sum_j \frac{z_j s_j}{D_j}}{\sum_j c_j z_j^2} \Big|_{y=0} \quad A4.9$$

Substituting equation A4.9 into equation A4.7 yields

$$\left. \frac{\partial c_j}{\partial y} \right|_{y=0} = -\frac{i}{F} \left[\frac{s_j}{D_j} - z_j c_j \frac{\sum \frac{z_j s_j}{D_j}}{\sum c_j z_j^2} \right] \bigg|_{y=0} \quad \text{A4.10}$$

The concentration profile across the diffusion layer was assumed to be of the form

$$(c_{jb} - c_j) = (c_{jb} - c_{js}) \left[1 - \frac{y}{\delta_j} \right]^2 \quad \text{A4.11}$$

where δ_j = thickness of the diffusion layer.

Differentiating equation A4.11 with respect to y yields

$$\left. \frac{\partial c_j}{\partial y} \right|_{y=0} = \frac{2}{\delta_j} (c_{jb} - c_{js}) = \frac{2}{\delta_j} \Delta c_j \quad \text{A4.12}$$

Since $\delta_j = D_j$, equation A4.12 can be rewritten as

$$\left. \frac{\partial c_j}{\partial y} \right|_{y=0} = \frac{2}{D_j^{1/4}} \Delta c_j \quad \text{A4.13}$$

Substituting equation A4.13 into equation A4.10 to yield

$$\Delta c_j = -\frac{i}{2F} \left[\frac{s_j}{D_j^{3/4}} - z_j c_j D_j^{1/4} \frac{\sum \frac{z_j s_j}{D_j}}{\sum c_j z_j^2} \right] \bigg|_{y=0} \quad \text{A4.14}$$

For the case of the limiting reactant R, equation A4.14 reduces to

$$\Delta c_R = -\frac{is_R}{2FD_R^{3/4}} \quad \text{A4.15}$$

since $c_R = 0$ at $y = 0$. Dividing equation A4.14 by equation A4.15 yields

$$\frac{\Delta c_j}{\Delta c_R} = \frac{s_j}{s_R} \left[\frac{D_R}{D_j} \right]^{3/4} - \left[\frac{z_j c_j D_j^{1/4} D_R^{3/4}}{s_j} \frac{\sum \frac{z_j s_j}{D_j}}{\sum c_j z_j^2} \right] \bigg|_{y=0} \quad \text{A4.16}$$

2. EXACT METHODS

The governing equations of free convection mass transfer in electrolytic solutions at the vicinity of the vertical flat plate electrode surface are^(355,356)

(i) the equation of continuity

$$\frac{\partial v_x}{\partial x} + \frac{\partial v_y}{\partial y} = 0 \quad A4.17$$

(ii) the equation of motion

$$v_x \frac{\partial v_x}{\partial x} + v_y \frac{\partial v_y}{\partial y} = \nu \frac{\partial^2 v_x}{\partial y^2} + g \sum_j \alpha_j \Delta c_j \quad A4.18$$

(iii) the mass balance for species j

$$v_x \frac{\partial c_j}{\partial x} + v_y \frac{\partial c_j}{\partial y} = D_j \frac{\partial^2 c_j}{\partial y^2} + z_j u_j F \frac{\partial}{\partial y} \left[c_j \frac{\partial \phi}{\partial y} \right] \quad A4.19$$

(iv) the electroneutrality equation

$$\sum_j z_j c_j = 0 \quad A4.8$$

where x is the distance from the edge along the electrode surface

y is the normal distance from the electrode surface.

Denoting the limiting reactant with subscript R, the boundary conditions are

$$\text{At } y = 0 ; \quad v_x = v_y = 0 \quad A4.20$$

$$c_R = c_{R_s} \quad A4.21$$

$$D_j \frac{\partial c_j}{\partial y} + z_j u_j F c_j \frac{\partial \phi}{\partial y} = \frac{s_j}{s_R} \left[D_R \frac{\partial c_R}{\partial y} + z_R u_R F c_R \frac{\partial \phi}{\partial y} \right] \quad A4.22$$

$$\text{At } y = \infty ; \quad v_x = 0 \quad \text{A4.23}$$

$$c_j = c_{jb} \quad \text{A4.24}$$

(a) The Selman and Newman method

In their analysis, Selman and Newman^(355,356) made the following assumptions:

1. At high Sc , the inertial terms in equation A4.18 are negligible within the diffusion layer. Hence equation A4.18 becomes

$$v \frac{\partial^2 v_x}{\partial y^2} + g \sum_j \alpha_j \Delta c_j = 0 \quad \text{A4.25}$$

2. u_j is defined by equation A4.6

Using the similarity transformation

$$\zeta = y \left[\frac{3g\alpha_R \Delta c_R}{4\nu D_{RX}} \right]^{\frac{1}{4}} \quad \text{A4.26}$$

$$\Gamma = \frac{4}{3} D_{RX} \left[\frac{3g\alpha_R \Delta c_R}{4\nu D_{RX}} \right]^{\frac{1}{4}} f(\zeta) \quad \text{A4.27}$$

where Γ is the stream function defined so that the equation of continuity is satisfied identically

$$v_x = \frac{\partial \Gamma}{\partial y} ; \quad v_y = - \frac{\partial \Gamma}{\partial x} \quad \text{A4.28}$$

and the dimensionless variables

$$T(\zeta) = \frac{F\phi}{RT} \quad \text{A4.29}$$

$$c_j(\zeta) = \frac{c_j}{\Delta c_R} \quad \text{A4.30}$$

Selman and Newman^(355,356) expressed the governing equations given by equations A4.8, A4.17, A4.19 and A4.25 as

$$f''' + \sum_j \frac{\alpha_j}{\alpha_R} (C_j - C_{j_b}) = 0 \quad \text{A4.31}$$

$$\frac{D_j}{D_R} [C_j'' + z_j (C_j T')'] + f C_j' = 0 \quad \text{A4.32}$$

$$\sum_j z_j C_j = 0 \quad \text{A4.33}$$

and the boundary conditions given by equations A4.20 - A4.24 as

$$\text{At } \zeta = 0 ; \quad f = f' = 0 \quad \text{A4.34}$$

$$C_R = C_{R_s} \quad \text{A4.35}$$

$$C_j' + z_j C_j T' = \frac{s_j D_R}{s_R D_j} [C_R' + z_R C_{RT}'] \quad \text{A4.36}$$

$$\text{At } \zeta = \infty ; \quad f' = 0 \quad \text{A4.37}$$

$$C_j = C_{j_b} \quad \text{A4.38}$$

where the primes denote differentiation with respect to ζ .

By solving the set of coupled, non-linear differential equations given by equations A4.31 - A4.33 with the boundary conditions given by equations A4.34 - A4.38, the concentration profiles for each ionic species can be obtained. The solution procedure used by Selman and Newman^(355,356) is outlined as follows:

By linearising about a trial solution, the set of coupled, non-linear differential equations are reduced to a set of coupled, linear differential equations. This set of equations when represented in finite difference form will give coupled, tridiagonal matrices which can be solved numerically. This

solution is then used as the trial solution to obtain a second approximation and the calculation procedure is repeated until the desired accuracy is achieved.

In the evaluation of the concentration profiles for each ionic species in the $K_3Fe(CN)_6 - K_4Fe(CN)_6 - KOH/NaOH$ system, Selman and Newman^(355,356) used

1. 150 mesh points with a mesh width of the ζ scale of 0.08
2. ionic diffusivity data at infinite dilution given in Table 3.2
3. ionic densification coefficient data given in Table 3.2

Defining the concentration ratio for the cathodic reaction, r_c and the concentration ratio for the anodic reaction, r_a as

$$r_c = 1 - r_a = \frac{c_{Fe(CN)_6^{3-}}}{c_{Fe(CN)_6^{3-}} + c_{Fe(CN)_6^{4-}}} \quad A4.39$$

and the concentration ratio for the supporting electrolyte, r as

$$r = \frac{c_{OH^-}}{c_{K^+} + c_{Na^+}} \quad A4.40$$

Selman and Newman^(355,356) presented their results in the form of a plot of $\frac{\Delta c_j}{\Delta c_R}$ against r as a function of r_c and r_a . The plot reproduced in Figure A4.1 is the case for $r_c = r_a = 0.5$.

(b) The Hiraoka method

In their analysis, Hiraoka et al⁽³⁶⁹⁾ assumed u_j is given by equation A4.6.

Using the similarity transformation

$$\eta = y \left[\frac{g \bar{\alpha} \Delta c_R}{\nu D_R x} \right]^{\frac{1}{4}} \quad A4.41$$

$$\Lambda = D_R x \left[\frac{g \bar{\alpha} \Delta c_R}{\nu D_R x} \right]^{\frac{1}{4}} f(\eta) \quad A4.42$$

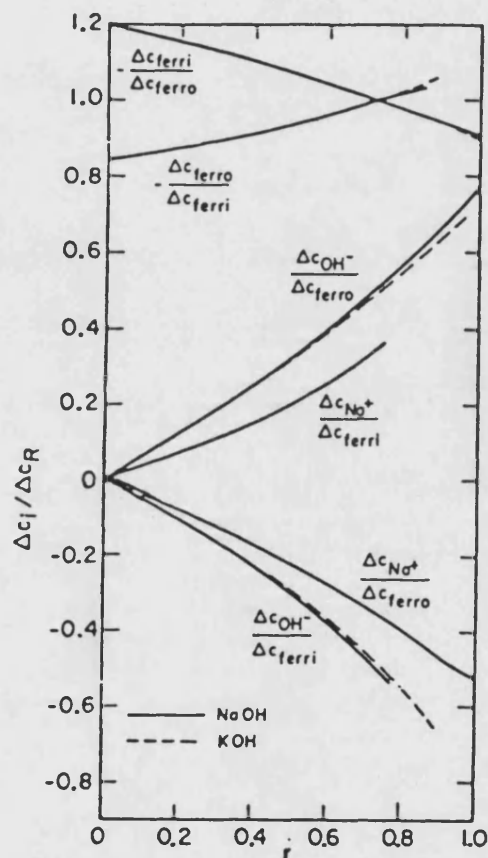


FIGURE A4.1 PLOT OF $\frac{\Delta c_j}{\Delta c_R}$ VERSUS r FOR $K_3Fe(CN)_6 - K_4Fe(CN)_6 -$
 NaOH/KOH SYSTEM WHERE $r_c = r_a = 0.5$ (355,356).

where Λ is the stream function defined so that the equation of continuity is satisfied identically:

$$v_x = \frac{\partial \Lambda}{\partial y} ; \quad v_y = - \frac{\partial \Lambda}{\partial x} \quad A4.43$$

and the dimensionless variables

$$T(\eta) = \frac{F\phi}{RT} \quad A4.44$$

$$C_j(\eta) = \frac{c_j}{\Delta c_R} \quad A4.45$$

Hiraoka et al⁽³⁶⁹⁾ expressed the governing equations given by equations A4.8, A4.17 - A4.19 as

$$f''' + \frac{3}{4} \left[\frac{1}{Sc} \right] f f'' - \frac{1}{2} \left[\frac{1}{Sc} \right] f f'^2 + \frac{1}{\alpha} \sum_j \alpha_j (C_j - C_{jb}) = 0 \quad A4.46$$

$$\frac{4D_j}{3D_R} \left[C_j'' + z_j (C_j T')' \right] + f C_j' = 0 \quad A4.47$$

$$\sum_j z_j C_j = 0 \quad A4.48$$

and the boundary conditions give by equations A4.20 - A4.24 as

$$\text{At } \eta = 0 ; \quad f = f' = 0 \quad A4.49$$

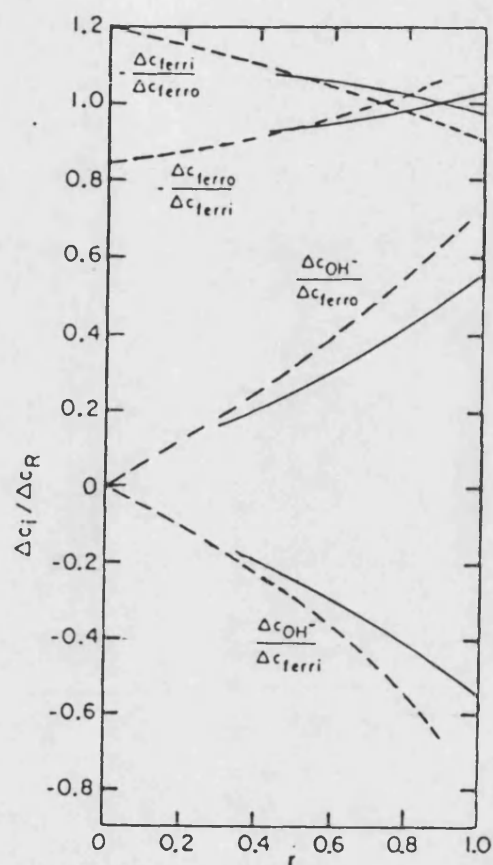
$$C_R = C_{R_S} \quad A4.50$$

$$C_j' + z_j C_j T' = \frac{s_j D_R}{s_R D_j} \left[C_R' + z_R C_R T' \right] \quad A4.51$$

$$\text{At } \eta = \infty ; \quad f' = 0 \quad A4.52$$

$$C_j = C_{jb} \quad A4.53$$

where the primes denote differentiation with respect to η .



----- Selman and Newman^(355,356)
 ————— Hiroaka et al⁽³⁶³⁾

FIGURE A4.2 PLOT OF $\frac{\Delta c_i}{\Delta c_R}$ VERSUS r FOR $K_3Fe(CN)_6 - K_4Fe(CN)_6 -$

KOH SYSTEM WHERE $r_c = r_a = 0.5$.

By solving the set of coupled, non-linear differential equations given by equations A4.46 - A4.48 with the boundary conditions given by equations A4.49 - A4.53 the concentration profiles of each ionic species can be obtained.

Hiraoka et al⁽³⁶⁹⁾ used the solution procedure similar to that used by Selman and Newman^(355,356) to evaluate the concentration profiles for each ionic species in the $K_3Fe(CN)_6$ - $K_4Fe(CN)_6$ - KOH system. In these calculations, Hiraoka et al⁽³⁶⁹⁾

1. used their own experimental diffusivity data (see Table A4.1)
2. used their own ionic densification coefficient data (see Table A4.2)
3. calculated the term $\sum_j \alpha_j \Delta C_j$ in equation A4.46 from the following equation:

$$\sum_j \alpha_j \Delta C_j = \alpha_{K_3Fe(CN)_6} \Delta C_{K_3Fe(CN)_6} + \alpha_{K_4Fe(CN)_6} \Delta C_{K_4Fe(CN)_6} + \alpha_{KOH} \Delta C_{KOH} \quad A4.54$$

assuming that the addition rule holds for α_j :

$$\alpha_{K_3Fe(CN)_6} = 3\alpha_{K^+} + \alpha_{Fe(CN)_6^{3-}} \quad A4.55$$

$$\alpha_{K_4Fe(CN)_6} = 4\alpha_{K^+} + \alpha_{Fe(CN)_6^{4-}} \quad A4.56$$

$$\alpha_{KOH} = \alpha_{K^+} + \alpha_{OH^-} \quad A4.57$$

4. obtained $\bar{\alpha}$ by iteration since $\bar{\alpha}$ cannot be evaluated directly from the physical properties of the electrolytic solution due to the dependency of $\bar{\alpha}$ on all ionic concentration profiles in the boundary layer (see equation 3.19)

In the same manner as that of Selman and Newman^(355,356), Hiraoka et al⁽³⁶⁹⁾ presented the results in the form of a plot of $\frac{\Delta c_j}{\Delta c_R}$ against r as a function of r_c and r_a . The plot reproduced in Figure A4.2 is for the case $r_c = r_a = 0.5$.

It can be seen from Figure A4.2 that the results obtained by Hiraoka et al⁽³⁶⁹⁾ are almost coincident with those of Selman and Newman^(355,356).

TABLE A4.1 DIFFUSIVITY RATIO DATA

DIFFUSIVITY RATIO	Hiraoka et al ⁽³⁶⁹⁾	Selman and Newman ^(355,356)
$\frac{D_{\text{Fe(CN)}_6^{4-}}}{D_{\text{Fe(CN)}_6^{3-}}}$	$\frac{2.23 - 0.065I^a}{2.25 + 0.044I}$	0.82
$\frac{D_{\text{OH}^-}}{D_{\text{Fe(CN)}_6^{3-}}}$	4.8	5.9
$\frac{D_{\text{K}^+}}{D_{\text{Fe(CN)}_6^{3-}}}$	3.7	2.2

a

$$I = \frac{1}{2} \sum_j z_j^2$$

TABLE A4.2 DENSIFICATION COEFFICIENT DATA

DENSIFICATION COEFFICIENT (cm ³ /mole)	Hiraoka et al ^(36,9)	Selman and Newman ^(355,356)
$\alpha_{K_3Fe(CN)_6}$	0.1532	0.16727
$\alpha_{K_4Fe(CN)_6}$	0.2086	0.22591
α_{KOH}	0.0463	0.04520

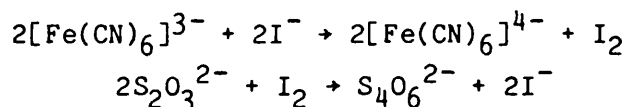
Hiraoka et al⁽³⁶⁹⁾ attributed this very slight difference in the two results to the difference in the physical properties of the electrolytic solution (see Tables A4.1 and A4.2). Since it can be seen from the Figure A4.1 that the results for the $K_3Fe(CN)_6 - K_4Fe(CN)_6 - KOH$ system are similar to those for the $K_3Fe(CN)_6 - K_4Fe(CN)_6 - NaOH$ system, it is reasonable to assume that the results obtained by Hiraoka et al⁽³⁶⁹⁾ in Figure A4.2 for $K_3Fe(CN)_6 - K_4Fe(CN)_6 - KOH$ system could be used for the $K_3Fe(CN)_6 - K_4Fe(CN)_6 - NaOH$ system.

APPENDIX A5 TITRIMETRIC ANALYSIS FOR THE ELECTROLYTIC SOLUTION

1. The determination of the ferricyanide ion concentration by titration with standard 0.1N sodium thiosulphate solution⁽⁴⁰⁸⁾

Reaction

The ferricyanide ion reacts with potassium iodide in an acidified medium, liberating iodine which can be titrated with sodium thiosulphate solution:



The reaction between the ferricyanide ion and potassium iodide is slow but becomes rapid in the presence of zinc sulphate.

Procedure

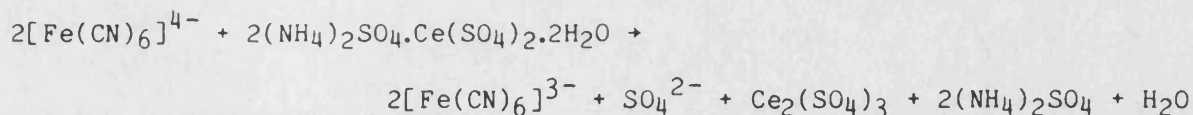
1. Pipette 25cm³ of the electrolytic solution under test into a glass stoppered flask.
2. Add 2g of potassium iodide and 2cm³ of 4N hydrochloric acid and stopper the flask.
3. Mix well and allow the flask to stand for one minute.
4. Add 10cm³ of 30% zinc sulphate solution.
5. Titrate the solution containing the gelatinous precipitate with standard 0.1N sodium thiosulphate solution has a pale yellow colour.
6. Add 5cm³ of starch solution and continue the titration slowly until the solution is colourless.
7. Compute the concentration of $[\text{Fe}(\text{CN})_6]^{3-}$ from

$$\text{Normality of } [\text{Fe}(\text{CN})_6]^{3-} = \frac{\text{Normality of } \text{S}_2\text{O}_3^{2-} \times \text{Volume of } \text{S}_2\text{O}_3^{2-}}{\text{Volume of } [\text{Fe}(\text{CN})_6]^{3-}}$$

2. The determination of the ferrocyanide ion by titration with standard 0.1N ammonium cerium (IV) sulphate solution⁽⁴⁰⁸⁾

Reaction

The ferricyanide ion reacts with ammonium cerium (IV) sulphate according to



Procedure

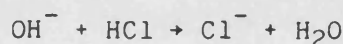
1. Pipette 25cm³ of the electrolytic solution under test into a conical flask.
2. Add 20cm³ of 1:5 sulphuric acid and one drop of ferroin indicator.
3. Titrate the solution with standard 0.1N ammonium cerium (IV) sulphate solution until the colour changes sharply from orange to yellow
4. Compute the concentration of $[\text{Fe}(\text{CN})_6]^{4-}$ from

$$\text{Normality of } [\text{Fe}(\text{CN})_6]^{4-} = \frac{\text{Normality of } 2(\text{NH}_4)_2\text{SO}_4 \cdot \text{Ce}(\text{SO}_4)_2 \cdot 2\text{H}_2\text{O} \times \text{volume of } 2(\text{NH}_4)_2\text{SO}_4 \cdot \text{Ce}(\text{SO}_4)_2 \cdot 2\text{H}_2\text{O}}{\text{volume of } [\text{Fe}(\text{CN})_6]^{3-}}$$

3. The determination of the hydroxyl ion concentration by titration with standard 1N hydrochloric acid⁽⁴⁰⁸⁾

Reaction

The hydroxyl ion reacts with the hydrochloric acid according to



Procedure

1. Pipette 25cm³ of the electrolytic solution under test into a conical flask.
2. Add a few drops of phenolphthalien.
3. Titrate the solution with standard 1N hydrochloric acid until the colour changes sharply from red to colourless.
4. Compute the concentration of OH^- from

$$\text{Normality of } \text{OH}^- = \frac{\text{Normality of HCl} \times \text{Volume of HCl}}{\text{Volume of OH}^-}$$

APPENDIX A.6

EXPERIMENTAL DATA

APPENDIX A6.1

CURRENT-POTENTIAL DATA AS A FUNCTION OF THE IMPELLER ROTATIONAL SPEED FOR THE ELECTROLYTIC MIXING CELL WITHOUT THE PRESENCE OF GLASS SPHERICAL PARTICLES ON THE CATHODE.

DATE 15-1-81

BATCH Batch 1 of 0.005M Potassium Ferricyanide/0.005M
Potassium Ferrocyanide/0.5M Sodium Hydroxide
solution prepared on 15-1-81

Run No 1.01

Stirrer Speed = 27.1 rpm

Solution Temperature = 19.0 C

Potential (V)	Current (mA)
0.0590	2.6
0.1040	5.4
0.1480	7.3
0.2060	9.4
0.2560	10.0
0.3140	10.4
0.3530	10.4
0.4160	10.4
0.4620	10.3
0.5090	10.6
0.5670	10.9
0.6090	11.0
0.6610	11.0
0.7210	10.9
0.7780	11.0
0.8340	10.8
0.9060	11.0
1.0020	11.5
1.1100	11.7
1.2060	12.2
1.3070	12.4
1.3770	12.8
1.5040	14.3
1.6000	17.5
1.6900	21.9
1.7580	25.5
1.8440	29.8

DATE 16-1-81

BATCH Batch 1 of 0.005M Potassium Ferricyanide/0.005M
Potassium Ferrocyanide/0.5M Sodium Hydroxide
solution prepared on 15-1-81

Run No 1.02

Stirrer Speed = 103.5 rpm

Solution Temperature = 19.0 C

Potential (V)	Current (mA)
0.0070	0.5
0.0570	3.8
0.0880	5.9
0.1200	8.0
0.1590	10.0
0.1990	13.2
0.2350	15.5
0.2810	18.3
0.3080	19.7
0.3870	23.4
0.5090	25.3
0.6080	25.6
0.7070	26.0
0.8050	26.2
0.9040	26.3
1.0380	26.4
1.0440	26.5
1.0990	26.5
1.2030	26.9
1.3010	27.0
1.3990	27.1
1.5010	27.5
1.6020	28.2
1.7000	29.2
1.8010	32.8
1.9050	39.0
2.0100	46.0

DATE 24-1-81
 BATCH Batch 2 of 0.005M Potassium Ferricyanide/0.005M
 Potassium Ferrocyanide/0.5M Sodium Hydroxide
 solution prepared on 15-1-81

Run No 1.03
 Stirrer Speed = 348.8 rpm
 Solution Temperature = 21.0 C

Potential (V)	Current (mA)
0.0010	0.1
0.0220	1.6
0.0760	5.7
0.1270	0.9
0.2400	17.9
0.3440	25.6
0.4640	34.4
0.5600	41.0
0.6860	49.1
0.7760	54.0
0.8620	56.3
1.0060	57.5
1.1760	58.1
1.2340	58.2
1.3670	58.5
1.4870	58.7
1.6070	59.0
1.7460	59.5
1.8430	60.0
1.9500	61.5
2.0580	64.0

DATE 5-2-81
 BATCH Batch 4 of 0.005M Potassium Ferricyanide/0.005M
 Potassium Ferrocyanide/0.5M Sodium Hydroxide
 solution prepared on 15-1-81

Run No 2.01
 Stirrer Speed = 208.3 rpm
 Solution Temperature = 21.0 C

Potential (V)	Current (mA)
0.0400	2.8
0.0730	5.1
0.1230	8.6
0.2210	15.6
0.3320	23.2
0.4360	30.0
0.5520	35.7
0.6690	39.2
0.7690	40.0
0.9030	40.7
1.0630	41.0
1.1060	41.2
1.2270	41.2
1.3350	41.8
1.4690	42.0
1.5590	42.4
1.6690	43.2
1.7650	44.8
1.8660	47.6
1.9550	50.0
2.0480	54.0

DATE 24-9-81
 BATCH Batch 1 of 0.005M Potassium Ferricyanide/0.005M
 Potassium Ferrocyanide/0.5M Sodium Hydroxide
 solution prepared on 24-9-81

Run No 3.01
 Stirrer Speed = 33.5 rpm
 Solution Temperature = 19.0 C

Potential (V)	Current (mA)
0.0417	2.3
0.0819	4.4
0.1124	6.2
0.1598	8.6
0.2014	10.8
0.2685	13.4
0.3356	14.3
0.4221	14.4
0.5345	14.5
0.6029	14.7
0.7185	14.9
0.8136	15.0
0.9108	15.0
1.0268	15.2
1.1234	15.4
1.2439	15.8
1.3575	16.1
1.5144	18.1
1.6004	20.0
1.7534	26.5
1.9318	33.7

DATE 24-9-81
 BATCH Batch 1 of 0.005M Potassium Ferricyanide/0.005M
 Potassium Ferrocyanide/0.5M Sodium Hydroxide
 solution prepared on 24-9-81

Run No 3.02
 Stirrer Speed = 135.9 rpm
 Solution Temperature = 20.0 C

Potential (V)	Current (mA)
0.0531	3.8
0.0908	6.5
0.1454	10.3
0.2440	17.0
0.3675	25.2
0.4521	30.0
0.5440	33.6
0.6179	34.4
0.7241	34.7
0.8430	34.9
0.9370	35.0
1.0670	35.0
1.1471	35.0
1.2547	35.1
1.3665	35.1
1.4891	35.1
1.5710	35.2
1.7647	37.7
1.8437	39.6
1.9786	42.9

DATE 24-9-81
 BATCH Batch 1 of 0.005M Potassium Ferricyanide/0.005M
 Potassium Ferrocyanide/0.5M Sodium Hydroxide
 solution prepared on 24-9-81

Run No 0.03
 Stirrer Speed = 245.6 rpm
 Solution Temperature = 19.0 C

Potential (V)	Current (mA)
0.0888	6.6
0.2310	17.1
0.3294	24.3
0.4610	33.5
0.5770	41.2
0.6547	45.6
0.7155	48.1
0.7629	49.2
0.8116	49.7
0.8912	50.3
0.9268	50.5
1.0078	50.7
1.0854	50.9
1.1583	51.0
1.2264	51.0
1.2739	51.0
1.3511	51.0
1.4224	51.0
1.6009	51.0
1.7540	51.5
1.8971	52.7
2.0080	52.7
2.1210	60.0
2.2280	66.5
2.3610	75.5
2.4470	81.2

APPENDIX A6.2 REPRODUCIBILITY DATA FOR THE CURRENT-POTENTIAL CURVE DETERMINED AT AN IMPELLER ROTATIONAL SPEED OF 34.8 ± 2.8 rpm IN THE ELECTROLYTIC MIXING CELL WITHOUT THE PRESENCE OF GLASS SPHERICAL PARTICLES ON THE CATHODE.

DATE 13-1-81
 BATCH Batch 1 of 0.005M Potassium Ferricyanide/0.005M
 Potassium Ferrocyanide/0.5M Sodium Hydroxide
 solution prepared on 9-12-80

Run No 1.01
 Stirrer Speed = 35.3 rpm
 Solution Temperature = 21.0 C

Potential (V)	Current (mA)
0.0590	3.4
0.1114	6.3
0.1640	8.9
0.2000	10.4
0.2658	12.1
0.3243	12.7
0.4013	13.0
0.4553	13.0
0.5606	13.1
0.6381	13.2
0.7484	13.3
0.8172	13.3
0.9283	13.4
1.0247	13.3
1.1175	13.5
1.2602	13.8
1.3584	14.0
1.4961	14.5
1.6214	18.7

DATE 13-1-81
 BATCH Batch 1 of 0.005M Potassium Ferricyanide/0.005M
 Potassium Ferrocyanide/0.5M Sodium Hydroxide
 solution prepared on 9-12-80

Run No 1.02
 Stirrer Speed = 35.3 rpm
 Solution Temperature = 21.0 C

Potential (V)	Current (mA)
0.0692	4.0
0.1189	6.7
0.1618	8.8
0.2320	11.4
0.3096	12.6
0.3546	12.7
0.4323	12.8
0.5231	13.1
0.6746	13.1
0.7660	13.4
0.8301	13.6
0.9560	13.7
1.0526	13.9
1.1437	14.0
1.2256	14.1
1.3758	14.3
1.4939	15.0
1.6172	18.8

DATE 14-1-81
 BATCH Batch 1 of 0.005M Potassium Ferricyanide/0.005M
 Potassium Ferrocyanide/0.5M Sodium Hydroxide
 solution prepared on 9-12-80

Run No 1.03
 Stirrer Speed = 37.3 rpm
 Solution Temperature = 21.0 C

Potential (V)	Current (mA)
0.0723	4.1
0.1368	7.4
0.1985	10.3
0.2622	11.9
0.3741	12.5
0.5019	12.6
0.5912	12.5
0.6914	12.8
0.7593	12.8
0.8023	12.8
0.9130	13.1
0.9995	13.1
1.1218	13.3
1.2627	13.3
1.4203	13.5
1.6137	17.8

DATE 26-1-81
 BATCH Batch 2 of 0.005M Potassium Ferricyanide/0.005M
 Potassium Ferrocyanide/0.5M Sodium Hydroxide
 solution prepared on 9-12-80

Run No 2.01
 Stirrer Speed = 31.7 rpm
 Solution Temperature = 21.0 C

Potential (V)	Current (mA)
0.0633	3.5
0.1136	6.2
0.1539	8.3
0.1939	10.1
0.2285	11.2
0.3250	12.9
0.4020	12.9
0.5131	13.0
0.6227	12.9
0.7680	12.9
0.8212	12.8
0.9581	12.8
1.0445	12.9
1.1779	13.2
1.2442	13.4
1.3104	14.2
1.6340	19.3

DATE 2-2-81
 BATCH Batch 2 of 0.005M Potassium Ferricyanide/0.005M
 Potassium Ferrocyanide/0.5M Sodium Hydroxide
 solution prepared on 9-12-80

Run No 3.01
 Stirrer Speed = 34.9 rpm
 Solution Temperature = 20.5 C

Potential (V)	Current (mA)
0.1202	6.6
0.2007	10.4
0.3071	13.0
0.4110	13.3
0.5104	13.5
0.6066	13.6
0.7047	13.7
0.8690	13.8
1.0333	13.8
1.1407	13.9
1.2279	14.3

DATE 20-3-81
 BATCH Batch 1 of 0.005M Potassium Ferricyanide/0.005M
 Potassium Ferrocyanide/0.5M Sodium Hydroxide
 solution prepared on 16-3-81

Run No 4.01
 Stirrer Speed = 34.5 rpm
 Solution Temperature = 19.0 C

Potential (V)	Current (mA)
0.0408	2.2
0.1047	5.8
0.1583	8.6
0.2116	10.9
0.2860	13.0
0.3657	13.6
0.4647	13.6
0.5416	13.6
0.6312	13.7
0.7062	13.7
0.7951	13.8
0.8844	14.0
0.9888	14.0
1.0806	14.1
1.1631	14.3
1.2681	14.6
1.3219	15.0
1.6262	19.4

DATE 27-4-81
BATCH Batch 1 of 0.005M Potassium Ferricyanide/0.005M
Potassium Ferrocyanide/0.5M Sodium Hydroxide
solution prepared on 22-4-81

Run No 5.01
Stirrer Speed = 33.7 rpm
Solution Temperature = 16.0 C

Potential (V)	Current (mA)
0.0578	2.9
0.1107	5.6
0.1467	7.2
0.1832	8.6
0.2254	10.4
0.3165	11.9
0.4203	12.2
0.5280	12.7
0.6355	12.7
0.7136	12.9
0.8161	12.9
0.9168	13.0
1.0417	13.3
1.1481	13.3
1.2485	13.4
1.3580	14.1
1.4815	15.6
1.6147	17.3

APPENDIX A6.3 MASS TRANSFER DATA FOR THE ELECTROLYTIC MIXING CELL WITHOUT THE PRESENCE OF GLASS SPHERICAL PARTICLES ON THE CATHODE.

TABLE A6.3.1 I_L - N DATA DERIVED FROM FIGURE 4.1

Run No	Potential (volts)	Stirrer Speed (rpm)	Limiting Current (mA)	Solution Temp. (C)	Ferricyanide Concentration (mol/cm ³)	Density (g/cm ³)	Viscosity (g/cm s)	Diffusivity (cm ² /s)	Sh	Re	Sc
1.01	0.8340	27.1	10.8	19.0	0.500E-05	1.0241	0.01136	0.643E-05	583.5	1058.9	1725.8
1.02	0.9040	103.5	26.3	19.0	0.500E-05	1.0241	0.01136	0.643E-05	1420.8	4044.2	1725.8
1.03	0.8620	348.8	56.3	21.0	0.500E-05	1.0231	0.01087	0.677E-05	2889.4	14235.6	1569.6
2.01	0.9030	208.3	40.7	21.0	0.500E-05	1.0231	0.01087	0.677E-05	2088.8	8501.4	1569.6
3.01	0.9108	33.5	15.0	19.0	0.500E-05	1.0241	0.01136	0.643E-05	810.4	1309.0	1725.8
3.02	0.9370	135.9	35.0	20.0	0.500E-05	1.0236	0.01111	0.660E-05	1842.8	5427.4	1645.6
3.03	1.2739	245.6	51.0	19.0	0.500E-05	1.0241	0.01136	0.643E-05	2755.2	9596.6	1725.8

TABLE A6.3.2 I_L-N DATA DERIVED FROM FIGURE 4.2

Run No	Potential (volts)	Stirrer Speed (rpm)	Limiting Current (mA)	Solution Temp. (C)	Ferricyanide Concentration (mol/cm ³)	Density (g/cm ³)	Viscosity (g/cm s)	Diffusivity (cm ² /s)	Sh	Re	Sc
1.01	0.8172	35.3	13.3	21.0	0.500E-05	1.0231	0.01087	0.677E-05	682.6	1440.7	1569.6
1.02	0.8301	35.3	13.6	21.0	0.500E-05	1.0231	0.01087	0.677E-05	698.0	1440.7	1569.6
1.03	0.8023	37.3	12.8	21.0	0.500E-05	1.0231	0.01087	0.677E-05	656.9	1522.3	1569.6
2.01	0.9581	31.7	12.8	21.0	0.507E-05	1.0231	0.01087	0.677E-05	647.9	1293.8	1569.6
3.01	0.8690	34.9	13.8	20.5	0.507E-05	1.0234	0.01099	0.668E-05	707.4	1409.0	1607.1
4.01	0.8844	34.5	14.0	19.0	0.500E-05	1.0241	0.01136	0.643E-05	756.3	1348.1	1725.8
5.01	0.8161	33.7	12.9	16.0	0.477E-05	1.0254	0.01216	0.595E-05	789.8	1232.1	1994.1

TABLE A6.3.3 I_L - N DATA OBTAINED FROM SEVERAL RUNS

DATE 23-1-81
 BATCH Batch 4 of 0.005M Potassium Ferricyanide/0.005M
 Potassium Ferrocyanide/0.5M Sodium Hydroxide
 solution prepared on 15-1-81

Potential = 1.0000 V
 Solution Temperature = 21.0 C
 Ferricyanide concentration = $0.500E-05$ mol/cm³
 Density = 1.0231 g/cm³
 Viscosity = 0.010867 g/cm s
 Diffusivity = $0.6767E-05$ cm²/s

DATE 28-1-81
 BATCH Batch 2 of 0.005M Potassium Ferricyanide/0.005M
 Potassium Ferrocyanide/0.5M Sodium Hydroxide
 solution prepared on 9-12-80

Potential = 0.9574 V
 Solution Temperature = 21.0 C
 Ferricyanide concentration = $0.507E-05$ mol/cm³
 Density = 1.0231 g/cm³
 Viscosity = 0.010867 g/cm s
 Diffusivity = $0.6767E-05$ cm²/s

Run No	Stirrer Speed (rpm)	Limiting Current (mA)	Sh	Re	Gr	Sc
1.01	0.0	0.8	41.1	0.0	0.20224E+07	1569.6
1.02	9.9	7.0	359.2	404.1		1569.6
1.03	18.0	9.5	487.5	734.6		1569.6
1.04	22.6	11.0	564.5	922.4		1569.6
1.05	43.9	16.6	851.9	1791.7		1569.6
1.06	64.1	20.0	1026.3	2616.1		1569.6
1.07	68.8	21.7	1113.6	2807.9		1569.6
1.08	84.0	24.8	1272.7	3428.3		1569.6
1.09	108.3	28.8	1477.9	4420.1		1569.6
1.10	128.0	30.7	1575.4	5224.1		1569.6
1.11	151.1	35.4	1816.6	6166.9		1569.6
1.12	182.0	37.8	1939.8	7428.0		1569.6
1.13	172.9	38.7	1986.0	7056.6		1569.6
1.14	213.0	41.3	2119.4	8693.2		1569.6
1.15	212.8	44.0	2257.9	8685.0		1569.6
1.16	240.0	44.8	2299.0	9795.2		1569.6
1.17	270.3	49.3	2529.9	11031.8		1569.6
1.18	256.4	49.8	2555.6	10464.5		1569.6
1.19	300.8	52.8	2709.5	12276.6		1569.6
1.20	285.7	53.5	2745.5	11660.3		1569.6
1.21	314.1	56.9	2919.9	12819.4		1569.6
1.22	338.0	57.5	2950.7	13794.8		1569.6

Run No	Stirrer Speed (rpm)	Limiting Current (mA)	Sh	Re	Gr	Sc
2.01	0.0	0.9	45.5	0.0	0.20224E+07	1569.6
2.02	20.2	10.4	526.3	824.4		1569.6
2.03	45.3	16.4	830.0	1848.8		1569.6
2.04	69.7	21.5	1088.1	2844.7		1569.6
2.05	90.7	25.3	1289.4	3701.8		1569.6
2.06	113.0	28.7	1452.5	4611.9		1569.6
2.07	146.1	33.3	1685.3	5962.8		1569.6
2.08	174.2	36.7	1857.3	7109.6		1569.6
2.09	209.7	40.3	2039.5	8558.5		1569.6
2.10	238.1	43.0	2176.2	9717.6		1569.6
2.11	266.1	46.0	2328.0	10860.4		1569.6
2.12	298.5	48.5	2454.5	12182.7		1569.6
2.13	347.5	51.7	2616.5	14182.6		1569.6

DATE 23-1-81
 BATCH Batch 2 of 0.005M Potassium Ferricyanide/0.005M
 Potassium Ferrocyanide/0.5M Sodium Hydroxide
 solution prepared on 15-1-81

Potential = 0.9640 V
 Solution Temperature = 21.0 C
 Ferricyanide concentration = 0.507E-05 mol/cm³
 Density = 1.0231 g/cm³
 Viscosity = 0.010867 g/cm s
 Diffusivity = 0.6767E-05 cm²/s

Run No	Stirrer Speed (rpm)	Limiting Current (mA)	Sh	Re	Gr	Sc
3.01	0.0	0.8	40.5	0.0	0.20224E+07	1569.6
3.02	4.8	5.0	253.0	195.9		1569.6
3.03	20.9	10.5	531.4	853.0		1569.6
3.04	52.6	17.9	905.9	2146.8		1569.6
3.05	87.9	24.9	1260.2	3587.5		1569.6
3.06	118.8	29.5	1492.9	4848.6		1569.6
3.07	162.2	35.0	1771.3	6619.9		1569.6
3.08	236.2	42.7	2161.0	9640.1		1569.6
3.09	258.0	45.0	2277.4	10529.8		1569.6
3.10	298.5	48.2	2439.3	12182.7		1569.6
3.11	320.0	50.0	2530.4	13060.2		1569.6

DATE 16-2-81
 BATCH Batch 3 of 0.005M Potassium Ferricyanide/0.005M
 Potassium Ferrocyanide/0.5M Sodium Hydroxide
 solution prepared on 9-12-80

Potential = 0.9511 V
 Solution Temperature = 21.0 C
 Ferricyanide concentration = 0.500E-05 mol/cm³
 Density = 1.0231 g/cm³
 Viscosity = 0.010867 g/cm s
 Diffusivity = 0.6767E-05 cm²/s

Run No	Stirrer Speed (rpm)	Limiting Current (mA)	Sh	Re	Sc
4.01	5.4	5.3	272.0	220.4	1569.6
4.02	39.2	14.6	749.2	1599.9	1569.6
4.03	64.2	19.9	1021.2	2620.2	1569.6
4.04	96.3	26.0	1334.2	3930.3	1569.6
4.05	130.2	32.5	1667.8	5313.9	1569.6
4.06	192.2	39.2	2011.6	7844.3	1569.6
4.07	238.0	44.3	2273.3	9713.5	1569.6
4.08	297.0	49.0	2514.5	12121.5	1569.6

DATE 8-4-81
 BATCH Batch 2 of 0.005M Potassium Ferricyanide/0.005M
 Potassium Ferrocyanide/0.5M Sodium Hydroxide
 solution prepared on 16-3-81

Potential = 1.0038 V
 Solution Temperature = 18.0 C
 Ferricyanide concentration = $0.500\text{E-}05$ mol/cm³
 Density = 1.0245 g/cm³
 Viscosity = 0.011619 g/cm s
 Diffusivity = $0.6264\text{E-}05$ cm²/s

Run No	Stirrer Speed (rpm)	Limiting Current (mA)	Sh	Re	Sc
5.01	38.9	12.0	665.2	1486.9	1810.4
5.02	60.9	15.2	842.6	2327.8	1810.4
5.03	86.3	18.0	997.8	3298.7	1810.4
5.04	110.8	21.7	1202.9	4235.2	1810.4
5.05	129.4	23.7	1313.8	4946.2	1810.4
5.06	147.1	25.4	1408.0	5622.7	1810.4
5.07	175.9	27.9	1546.6	6723.6	1810.4
5.08	202.0	29.8	1651.9	7721.2	1810.4
5.09	231.4	32.0	1773.9	8845.0	1810.4
5.10	293.2	35.4	1962.4	11207.3	1810.4
5.11	338.9	37.8	2095.4	12954.1	1810.4

DATE 9-4-81
 BATCH Batch 2 of 0.005M Potassium Ferricyanide/0.005M
 Potassium Ferrocyanide/0.5M Sodium Hydroxide
 solution prepared on 16-3-81

Potential = 1.0045 V
 Solution Temperature = 19.0 C
 Ferricyanide concentration = $0.500\text{E-}05$ mol/cm³
 Density = 1.0241 g/cm³
 Viscosity = 0.011361 g/cm s
 Diffusivity = $0.6429\text{E-}05$ cm²/s

Run No	Stirrer Speed (rpm)	Limiting Current (mA)	Sh	Re	Sc
6.01	20.4	8.5	459.2	797.1	1725.8
6.02	31.2	11.9	642.8	1219.1	1725.8
6.03	50.9	14.3	772.5	1988.9	1725.8
6.04	85.7	19.3	1042.6	3348.6	1725.8
6.05	138.2	24.9	1345.1	5400.0	1725.8
6.06	185.1	28.5	1539.5	7232.6	1725.8
6.07	236.3	31.7	1712.4	9233.2	1725.8
6.08	324.3	36.3	1960.9	12671.7	1725.8

DATE 28-4-81
 BATCH Batch 1 of 0.005M Potassium Ferricyanide/0.005M
 Potassium Ferrocyanide/0.5M Sodium Hydroxide
 solution prepared on 22-4-81

Potential = 0.8580 V
 Solution Temperature = 18.0 C
 Ferricyanide concentration = 0.477E-05 mol/cm³
 Density = 1.0245 g/cm³
 Viscosity = 0.011619 g/cm s
 Diffusivity = 0.6264E-05 cm²/s

Run No	Stirrer Speed (rpm)	Limiting Current (mA)	Sh	Re	Gr	Sc
7.01	0.0	0.6	34.9	0.0	0.17739E+07	1810.4
7.02	45.5	13.3	772.8	1739.2		1810.4
7.03	75.5	17.6	1022.7	2885.9		1810.4
7.04	110.1	22.9	1330.7	4208.5		1810.4
7.05	140.8	24.9	1446.9	5381.9		1810.4
7.06	181.0	27.7	1609.6	6918.5		1810.4
7.07	215.0	30.2	1754.8	8218.2		1810.4
7.08	262.0	33.2	1929.2	10014.7		1810.4
7.09	324.3	36.2	2103.5	12396.0		1810.4
7.10	344.8	37.4	2173.2	13179.6		1810.4

DATE 29-4-81
 BATCH Batch 1 of 0.005M Potassium Ferricyanide/0.005M
 Potassium Ferrocyanide/0.5M Sodium Hydroxide
 solution prepared on 22-4-81

Potential = 0.8373 V
 Solution Temperature = 18.0 C
 Ferricyanide concentration = 0.477E-05 mol/cm³
 Density = 1.0245 g/cm³
 Viscosity = 0.011619 g/cm s
 Diffusivity = 0.6264E-05 cm²/s

Run No	Stirrer Speed (rpm)	Limiting Current (mA)	Sh	Re	Sc
8.01	95.5	18.7	1086.6	3650.4	1810.4
8.02	195.5	25.7	1493.4	7472.8	1810.4
8.03	343.8	32.4	1882.7	13141.4	1810.4

DATE 29-4-81
 BATCH Batch 2 of 0.005M Potassium Ferricyanide/0.005M
 Potassium Ferrocyanide/0.5M Sodium Hydroxide
 solution prepared on 22-4-81

Potential = 0.8373 V
 Solution Temperature = 17.5 C
 Ferricyanide concentration = $0.477\text{E-}05$ mol/cm³
 Density = 1.0247 g/cm³
 Viscosity = 0.011751 g/cm s
 Diffusivity = $0.6184\text{E-}05$ cm²/s

Run No	Stirrer Speed (rpm)	Limiting Current (mA)	Sh	Re	Sc
9.01	21.5	8.8	518.0	812.8	1854.5
9.02	65.2	15.7	924.2	2464.8	1854.5
9.03	85.4	17.8	1047.8	3228.4	1854.5
9.04	101.9	19.5	1147.9	3852.2	1854.5
9.05	153.8	23.5	1383.4	5814.2	1854.5
9.06	213.3	27.2	1601.2	8063.5	1854.5
9.07	224.3	27.7	1630.6	8479.4	1854.5
9.08	254.2	29.2	1718.9	9609.7	1854.5
9.09	305.3	31.4	1848.4	11541.5	1854.5
9.10	351.9	33.0	1942.6	13303.1	1854.5

DATE 30-4-81
 BATCH Batch 3 of 0.005M Potassium Ferricyanide/0.005M
 Potassium Ferrocyanide/0.5M Sodium Hydroxide
 solution prepared on 22-4-81

Potential = 0.8362 V
 Solution Temperature = 19.0 C
 Ferricyanide concentration = $0.477\text{E-}05$ mol/cm³
 Density = 1.0241 g/cm³
 Viscosity = 0.011361 g/cm s
 Diffusivity = $0.6429\text{E-}05$ cm²/s

Run No	Stirrer Speed (rpm)	Limiting Current (mA)	Sh	Re	Sc
10.01	15.0	7.8	441.7	586.1	1725.8
10.02	32.1	12.0	679.5	1254.3	1725.8
10.03	60.0	17.3	979.6	2344.4	1725.8
10.04	101.3	23.7	1342.0	3958.2	1725.8
10.05	133.3	28.1	1591.1	5208.6	1725.8
10.06	181.0	32.8	1857.2	7072.4	1725.8
10.07	239.2	38.0	2151.7	9346.5	1725.8
10.08	288.5	42.3	2395.2	11272.9	1725.8
10.09	352.9	46.8	2650.0	13789.2	1725.8

DATE 5-5-81
 BATCH Batch 4 of 0.005M Potassium Ferricyanide/0.005M
 Potassium Ferrocyanide/0.5M Sodium Hydroxide
 solution prepared on 22-4-81

Potential = 0.8382 V
 Solution Temperature = 16.5 C
 Ferricyanide concentration = 0.477E-05 mol/cm³
 Density = 1.0252 g/cm³
 Viscosity = 0.012020 g/cm s
 Diffusivity = 0.6024E-05 cm²/s

Run No	Stirrer Speed (rpm)	Limiting Current (mA)	Sh	Re	Gr	Sc
11.01	0.0	1.7	102.7	0.0	0.16597E+07	1946.3
11.02	8.8	5.2	314.2	325.4		1946.3
11.03	22.9	9.1	549.9	846.7		1946.3
11.04	33.0	10.7	646.5	1220.1		1946.3
11.05	61.2	16.5	997.0	2262.7		1946.3
11.06	100.8	21.8	1317.2	3726.9		1946.3
11.07	141.2	24.9	1504.5	5220.6		1946.3
11.08	167.6	27.7	1673.7	6196.6		1946.3
11.09	204.1	30.6	1849.0	7546.2		1946.3
11.10	235.5	33.2	2006.1	8707.1		1946.3
11.11	272.7	36.7	2217.5	10082.5		1946.3
11.12	303.0	38.1	2302.1	11202.8		1946.3
11.13	357.1	40.7	2459.2	13203.0		1946.3

DATE 12-5-81
 BATCH Batch 5 of 0.005M Potassium Ferricyanide/0.005M
 Potassium Ferrocyanide/0.5M Sodium Hydroxide
 solution prepared on 22-4-81

Potential = 0.8385 V
 Solution Temperature = 16.0 C
 Ferricyanide concentration = 0.477E-05 mol/cm³
 Density = 1.0254 g/cm³
 Viscosity = 0.012158 g/cm s
 Diffusivity = 0.5946E-05 cm²/s

Run No	Stirrer Speed (rpm)	Limiting Current (mA)	Sh	Re	Gr	Sc
12.01	0.0	2.0	122.4	0.0	0.16230E+07	1994.1
12.02	12.2	6.2	379.6	446.1		1994.1
12.03	20.9	9.4	575.5	764.1		1994.1
12.04	32.7	11.4	697.9	1195.6		1994.1
12.05	60.0	16.7	1022.4	2193.7		1994.1
12.06	90.7	21.3	1304.0	3316.2		1994.1
12.07	117.6	25.2	1542.8	4299.7		1994.1
12.08	152.8	29.2	1787.6	5586.7		1994.1
12.09	194.4	33.5	2050.9	7107.7		1994.1
12.10	228.1	37.2	2277.4	8339.8		1994.1
12.11	266.7	40.7	2491.7	9751.1		1994.1
12.12	328.5	45.5	2785.5	12010.7		1994.1
12.13	355.0	47.7	2920.2	12979.6		1994.1

DATE 19-5-81
 BATCH Batch 6 of 0.005M Potassium Ferricyanide/0.005M
 Potassium Ferrocyanide/0.5M Sodium Hydroxide
 solution prepared on 22-4-81

Potential = 0.8377 V
 Solution Temperature = 18.0 C
 Ferricyanide concentration = 0.477E-05 mol/cm³
 Density = 1.0245 g/cm³
 Viscosity = 0.011619 g/cm s
 Diffusivity = 0.6264E-05 cm²/s

DATE 26-5-81
 BATCH Batch 7 of 0.005M Potassium Ferricyanide/0.005M
 Potassium Ferrocyanide/0.5M Sodium Hydroxide
 solution prepared on 22-4-81

Potential = 0.8385 V
 Solution Temperature = 16.0 C
 Ferricyanide concentration = 0.477E-05 mol/cm³
 Density = 1.0254 g/cm³
 Viscosity = 0.012158 g/cm s
 Diffusivity = 0.5946E-05 cm²/s

Run No	Stirrer Speed (rpm)	Limiting Current (mA)	Sh	Re	Gr	Sc
13.01	0.0	0.8	46.5	0.0	0.17739E+07	1810.4
13.02	20.9	8.6	499.7	798.9		1810.4
13.03	67.0	18.2	1057.5	2561.0		1810.4
13.04	109.6	21.9	1272.5	4189.3		1810.4
13.05	140.8	24.8	1441.1	5381.9		1810.4
13.06	177.3	27.8	1615.4	6777.1		1810.4
13.07	223.0	31.2	1812.9	8523.9		1810.4
13.08	269.0	34.1	1981.5	10282.2		1810.4
13.09	326.1	37.1	2155.8	12464.8		1810.4
13.10	352.9	38.4	2231.3	13489.2		1810.4

Run No	Stirrer Speed (rpm)	Limiting Current (mA)	Sh	Re	Gr	Sc
14.01	0.0	2.2	134.7	0.0	0.16230E+07	1994.1
14.02	16.1	8.6	526.5	588.7		1994.1
14.03	50.4	14.8	906.1	1842.7		1994.1
14.04	89.6	21.7	1328.5	3276.0		1994.1
14.05	112.5	25.5	1561.1	4113.2		1994.1
14.06	153.1	30.0	1836.6	5597.7		1994.1
14.07	189.1	34.3	2099.9	6913.9		1994.1
14.08	231.7	38.0	2326.4	8471.4		1994.1
14.09	272.7	41.7	2552.9	9970.5		1994.1
14.10	343.5	46.7	2859.0	12559.1		1994.1

DATE 27-5-81
 BATCH Batch 1 of 0.005M Potassium Ferricyanide/0.005M
 Potassium Ferrocyanide/0.5M Sodium Hydroxide
 solution prepared on 27-5-81

Potential = 0.8331 V
 Solution Temperature = 20.0 C
 Ferricyanide concentration = $0.487E-05$ mol/cm³
 Density = 1.0236 g/cm³
 Viscosity = 0.011111 g/cm s
 Diffusivity = $0.6596E-05$ cm²/s

Run No	Stirrer Speed (rpm)	Limiting Current (mA)	Sh	Re	Gr	Sc
15.01	0.0	1.7	91.9	0.0	0.19365E+07	1645.6
15.02	18.2	8.7	470.2	726.9		1645.6
15.03	54.3	16.1	870.2	2168.6		1645.6
15.04	85.7	22.2	1199.9	3422.6		1645.6
15.05	134.5	27.5	1486.4	5371.5		1645.6
15.06	160.4	32.0	1729.7	6405.9		1645.6
15.07	182.9	34.7	1875.6	7304.5		1645.6
15.08	227.3	38.7	2091.8	9077.7		1645.6
15.09	270.3	42.2	2281.0	10795.0		1645.6
15.10	342.9	48.1	2599.9	13694.4		1645.6

DATE 3-6-81
 BATCH Batch 2 of 0.005M Potassium Ferricyanide/0.005M
 Potassium Ferrocyanide/0.5M Sodium Hydroxide
 solution prepared on 27-5-81

Potential = 0.8393 V
 Solution Temperature = 17.0 C
 Ferricyanide concentration = $0.497E-05$ mol/cm³
 Density = 1.0250 g/cm³
 Viscosity = 0.011885 g/cm s
 Diffusivity = $0.6104E-05$ cm²/s

Run No	Stirrer Speed (rpm)	Limiting Current (mA)	Sh	Re	Gr	Sc
16.01	0.0	2.4	137.4	0.0	0.16970E+07	1899.7
16.02	17.6	9.7	555.2	658.0		1899.7
16.03	38.0	13.1	749.8	1420.7		1899.7
16.04	66.1	18.2	1041.8	2471.3		1899.7
16.05	106.4	24.2	1385.2	3977.9		1899.7
16.06	159.6	30.7	1757.2	5966.9		1899.7
16.07	198.7	34.9	1997.6	7428.7		1899.7
16.08	240.0	39.3	2249.5	8972.8		1899.7
16.09	306.1	44.7	2558.6	11444.1		1899.7
16.10	337.1	47.2	2701.7	12603.1		1899.7

DATE 23-7-81
 BATCH Batch 6 of 0.005M Potassium Ferricyanide/0.005M
 Potassium Ferrocyanide/0.5M Sodium Hydroxide
 solution prepared on 27-5-81

Potential = 0.8352 V
 Solution Temperature = 17.0 C
 Ferricyanide concentration = 0.497E-05 mol/cm³
 Density = 1.0250 g/cm³
 Viscosity = 0.011885 g/cm s
 Diffusivity = 0.6104E-05 cm²/s

DATE 25-9-81
 BATCH Batch 1 of 0.005M Potassium Ferricyanide/0.005M
 Potassium Ferrocyanide/0.5M Sodium Hydroxide
 solution prepared on 24-9-81

Potential = 1.0026 V
 Solution Temperature = 16.5 C
 Ferricyanide concentration = 0.500E-05 mol/cm³
 Density = 1.0252 g/cm³
 Viscosity = 0.012020 g/cm s
 Diffusivity = 0.6024E-05 cm²/s

Run No	Stirrer Speed (rpm)	Limiting Current (mA)	Sh	Re	Gr	Sc
17.01	0.0	2.1	120.2	0.0	0.16970E+07	1899.7
17.02	17.4	8.7	498.0	650.5		1899.7
17.03	21.6	10.2	583.8	807.6		1899.7
17.04	46.7	16.5	944.4	1746.0		1899.7
17.05	66.3	21.2	1213.5	2478.7		1899.7
17.06	80.5	22.7	1299.3	3009.6		1899.7
17.07	102.1	26.5	1516.8	3817.2		1899.7
17.08	138.2	32.7	1871.7	5166.8		1899.7
17.09	178.0	37.6	2152.2	6654.8		1899.7
17.10	215.0	42.3	2421.2	8038.1		1899.7
17.11	253.2	45.8	2621.6	9466.3		1899.7
17.12	354.3	55.5	3176.8	13246.1		1899.7

Run No	Stirrer Speed (rpm)	Limiting Current (mA)	Sh	Re	Gr	Sc
18.01	0.0	0.8	46.1	0.0	0.16597E+07	1946.3
18.02	7.7	5.5	317.0	284.7		1946.3
18.03	25.5	12.0	691.7	942.8		1946.3
18.04	38.4	15.3	882.0	1419.8		1946.3
18.05	72.4	23.1	1331.6	2676.8		1946.3
18.06	89.6	25.3	1458.4	3312.8		1946.3
18.07	118.8	31.1	1792.7	4392.4		1946.3
18.08	129.6	33.0	1902.3	4791.7		1946.3
18.09	155.4	36.2	2086.7	5745.6		1946.3
18.10	179.6	39.7	2288.5	6640.3		1946.3
18.11	205.5	43.0	2478.7	7597.9		1946.3
18.12	231.9	46.1	2657.4	8574.0		1946.3
18.13	260.8	49.5	2853.4	9642.5		1946.3
18.14	288.5	53.8	3101.3	10666.7		1946.3
18.15	338.4	59.0	3401.0	12511.6		1946.3
18.16	362.5	61.0	3516.3	13402.6		1946.3

DATE 6-11-81
 BATCH Batch 2 of 0.005M Potassium Ferricyanide/0.005M
 Potassium Ferrocyanide/0.5M Sodium Hydroxide
 solution prepared on 24-9-81

Potential = 0.9928 V
 Solution Temperature = 14.0 C
 Ferricyanide concentration = 0.298E-05 mol/cm³
 Density = 1.0262 g/cm³
 Viscosity = 0.012728 g/cm s
 Diffusivity = 0.5640E-05 cm²/s

Run No	Stirrer Speed (rpm)	Limiting Current (mA)	Sh	Re	Gr	Sc
19.01	0.0	2.3	237.6	0.0	0.14831E+07	2199.1
19.02	24.7	6.6	681.8	863.3		2199.1
19.03	63.2	11.6	1198.4	2208.9		2199.1
19.04	96.8	15.1	1560.0	3383.2		2199.1
19.05	138.5	18.0	1859.6	4840.7		2199.1
19.06	161.1	19.9	2055.8	5630.6		2199.1
19.07	180.7	21.3	2200.5	6315.6		2199.1
19.08	232.6	25.2	2603.4	8129.6		2199.1
19.09	298.5	27.7	2861.6	10432.9		2199.1
19.10	328.8	30.0	3099.3	11491.9		2199.1

APPENDIX A6.4 CURRENT-POTENTIAL DATA AS A FUNCTION OF THE IMPELLER ROTATIONAL SPEED FOR THE ELECTROLYTIC MIXING
CELL WITH THE PRESENCE OF 1 LAYER OF 3MM GLASS SPHERICAL PARTICLES ON THE CATHODE

DATE 19-5-82
BATCH Batch 2 of 0.005M Potassium Ferricyanide/0.005M
Potassium Ferrocyanide/0.5M Sodium Hydroxide
solution prepared on 23-4-82

Run No 1.01
Stirrer Speed = 29.9 rpm
Solution Temperature = 20.0 C

Potential (V)	Current (mA)
0.0659	2.2
0.1156	3.6
0.1586	4.5
0.2264	5.1
0.3305	5.0
0.4100	5.0
0.4993	5.1
0.5947	5.0
0.6853	4.8
0.7831	4.9
0.8861	5.0
0.9433	5.1
1.0730	5.0
1.1231	5.3
1.2291	5.5
1.3315	5.5
1.3966	6.1
1.4428	6.4
1.5001	7.1
1.5724	9.8
1.6795	12.7

DATE 19-5-82
BATCH Batch 2 of 0.005M Potassium Ferricyanide/0.005M
Potassium Ferrocyanide/0.5M Sodium Hydroxide
solution prepared on 23-4-82

Run No 1.02
Stirrer Speed = 66.3 rpm
Solution Temperature = 20.0 C

Potential (V)	Current (mA)
0.0697	3.0
0.1146	4.9
0.1683	6.5
0.2513	10.1
0.3423	11.6
0.4180	11.6
0.5004	12.0
0.6353	11.5
0.7160	11.6
0.7911	11.6
0.8729	11.6
0.9762	11.6
1.0608	11.7
1.1278	11.8
1.2727	12.1
1.4065	11.9
1.5283	12.8
1.6263	13.1
1.7451	17.8
1.8072	21.1

DATE 20-5-82
 BATCH Batch 2 of 0.005M Potassium Ferricyanide/0.005M
 Potassium Ferrocyanide/0.5M Sodium Hydroxide
 solution prepared on 23-4-82

Run No 1.03
 Stirrer Speed = 85.9 rpm
 Solution Temperature = 21.0 C

Potential (V)	Current (mA)
0.0484	2.2
0.1021	4.9
0.1672	7.9
0.2677	11.9
0.3333	13.9
0.4293	15.2
0.4950	15.2
0.5550	15.4
0.6447	15.5
0.7468	15.5
0.7812	15.5
0.8657	15.5
0.9727	15.5
1.0228	15.5
1.1340	15.5
1.2057	15.5
1.2874	15.5
1.3711	15.6
1.4587	15.7
1.5552	15.7
1.6469	17.3
1.7312	19.2
1.8434	23.6
1.9289	27.1

DATE 20-5-82
 BATCH Batch 2 of 0.005M Potassium Ferricyanide/0.005M
 Potassium Ferrocyanide/0.5M Sodium Hydroxide
 solution prepared on 23-4-82

Run No 1.04
 Stirrer Speed = 123.4 rpm
 Solution Temperature = 21.0 C

Potential (V)	Current (mA)
0.0639	3.2
0.1413	7.2
0.2132	10.8
0.2814	14.1
0.3784	18.3
0.4425	20.9
0.5470	23.1
0.6480	23.5
0.7583	23.6
0.9001	23.9
1.0248	23.8
1.1500	23.5
1.2246	23.6
1.3856	23.2
1.5790	23.6
1.6738	23.9
1.7802	25.1
1.9340	30.2
2.0130	33.5

DATE 21-5-82
 BATCH Batch 2 of 0.005M Potassium Ferricyanide/0.005M
 Potassium Ferrocyanide/0.5M Sodium Hydroxide
 solution prepared on 23-4-82

Run No 1.05
 Stirrer Speed = 175.4 rpm
 Solution Temperature = 21.0 C

Potential (V)	Current (mA)
0.0753	4.0
0.1326	7.1
0.1889	10.1
0.2784	14.8
0.3373	17.8
0.4632	24.1
0.5617	28.6
0.6431	31.4
0.7122	32.8
0.7863	33.5
0.8558	33.7
0.9890	34.0
1.1121	34.2
1.2613	34.4
1.3125	34.4
1.4085	34.4
1.5670	34.6
1.6389	34.8
1.7721	34.8
1.8232	35.4
1.9267	35.9
2.0170	37.8
2.1290	42.0

DATE 21-5-82
 BATCH Batch 2 of 0.005M Potassium Ferricyanide/0.005M
 Potassium Ferrocyanide/0.5M Sodium Hydroxide
 solution prepared on 23-4-82

Run No 1.06
 Stirrer Speed = 200.0 rpm
 Solution Temperature = 21.0 C

Potential (V)	Current (mA)
0.0633	3.3
0.1315	7.1
0.2296	12.3
0.3196	17.1
0.4231	22.5
0.5098	26.8
0.5969	30.9
0.6690	33.8
0.7568	36.3
0.8344	37.4
0.9353	38.1
1.0360	38.5
1.1451	38.6
1.2156	38.8
1.3313	38.8
1.4242	39.2
1.5562	39.2
1.6792	39.4
1.8189	39.7
1.9129	40.2
2.0430	41.9
2.1540	44.8
2.2530	48.5
2.3850	52.9
2.4650	54.3

APPENDIX A6.5 I_L - N DATA FOR THE ELECTROLYTIC MIXING CELL WITH THE
 PRESENCE OF 1 LAYER OF 3MM GLASS SPHERICAL PARTICLES
 ON THE CATHODE

DATE 29-4-81

BATCH Batch 2 of 0.005M Potassium Ferricyanide/0.005M Potassium
 Ferrocyanide/0.5M Sodium Hydroxide solution prepared
 on 22-4-81

Potential = 0.8410 V

Solution Temperature = 14.0 C

Ferricyanide concentration = 4.77×10^{-6} mol/cm³

I_L	N
0.7	0
2.1	8.2
6.1	27.7
10.6	58.3
16.2	101.5
18.7	127.1
20.3	148.1
23.8	175.3
27.2	208.6
29.2	251.4
37.0	251.4
43.7	323.7
45.2	349.8

APPENDIX A6.6 MASS TRANSFER DATA FOR THE ELECTROLYTIC MIXING CELL WITH THE PRESENCE OF ONE OR MORE LAYERS OF GLASS SPHERICAL PARTICLES ON THE CATHODE

TABLE A6.6.1.1 I_L - N DATA FOR THE ELECTROLYTIC MIXING CELL WITH THE PRESENCE OF 1 LAYER OF 0.368MM GLASS SPHERICAL PARTICLES ON THE CATHODE

DATE 3-6-81
 BATCH Batch 2 of 0.005M Potassium Ferricyanide/0.005M Potassium Ferrocyanide/0.5M Sodium Hydroxide solution prepared on 27-5-81

Potential = 0.8434 V
 Solution Temperature = 16.0 C
 Ferricyanide concentration = 0.497E-05 mol/cm³
 Density = 1.0254 g/cm³
 Viscosity = 0.012158 g/cm s
 Diffusivity = 0.5946E-05 cm²/s

Run No	Stirrer Speed (rpm)	Limiting Current (mA)	Sh	Re	Sc
1.01	0.0	1.3	76.4	0.0	1994.1
1.02	12.0	1.6	95.2	438.7	1994.1
1.03	20.5	2.8	163.9	749.5	1994.1
1.04	33.1	4.1	242.1	1210.2	1994.1
1.05	59.7	7.1	420.1	2182.8	1994.1
1.06	67.0	7.9	467.1	2449.7	1994.1
1.07	89.6	10.6	622.8	3276.0	1994.1
1.08	107.8	12.3	722.7	3941.4	1994.1

TABLE A6.6.1.2 I_L - N DATA FOR THE ELECTROLYTIC MIXING CELL WITH THE PRESENCE OF 2 LAYERS OF 0.368MM GLASS SPHERICAL PARTICLES ON THE CATHODE

DATE 3-6-81
 BATCH Batch 2 of 0.005M Potassium Ferricyanide/0.005M Potassium Ferrocyanide/0.5M Sodium Hydroxide solution prepared on 27-5-81

Potential = 0.8444 V
 Solution Temperature = 18.0 C
 Ferricyanide concentration = 0.497E-05 mol/cm³
 Density = 1.0245 g/cm³
 Viscosity = 0.011619 g/cm s
 Diffusivity = 0.6264E-05 cm²/s

Run No	Stirrer Speed (rpm)	Limiting Current (mA)	Sh	Re	Sc
1.01	0.0	0.8	44.6	0.0	1810.4
1.02	15.3	1.2	65.8	584.8	1810.4
1.03	39.5	2.9	164.5	1509.8	1810.4
1.04	74.5	6.0	334.6	2847.7	1810.4
1.05	90.0	7.7	429.4	3440.2	1810.4
1.06	106.5	9.8	549.3	4070.9	1810.4

TABLE A6.6.1.3 I_L - N DATA FOR THE ELECTROLYTIC MIXING
CELL WITH THE PRESENCE OF 3 LAYERS OF
0.368MM GLASS SPHERICAL PARTICLES ON
THE CATHODE

DATE 3-8-81
BATCH Batch 2 of 0.005M Potassium Ferricyanide/0.005M
Potassium Ferrocyanide/0.5M Sodium Hydroxide
solution prepared on 27-5-81

Potential = 0.8450 V
Solution Temperature = 19.0 C
Ferricyanide concentration = $0.497E-05$ mol/cm³
Density = 1.0241 g/cm³
Viscosity = 0.011361 g/cm s
Diffusivity = $0.6429E-05$ cm²/s

Run No	Stirrer Speed (rpm)	Limiting Current (mA)	Sh	Re	Sc
1.01	0.0	0.8	44.6	0.0	1725.8
1.02	34.5	2.5	138.6	1348.1	1725.8
1.03	60.0	4.2	231.0	2344.4	1725.8
1.04	71.4	5.5	301.6	2789.9	1725.8
1.05	92.7	7.7	419.5	3622.2	1725.8

TABLE A6.6.2.1 I_L - N DATA FOR THE ELECTROLYTIC MIXING CELL WITH THE PRESENCE OF 1 LAYER OF 0.695MM GLASS
SPHERICAL PARTICLES ON THE CATHODE

DATE 26-5-81
BATCH Batch 7 of 0.005M Potassium Ferricyanide/0.005M
Potassium Ferrocyanide/0.5M Sodium Hydroxide
solution prepared on 22-4-81

Potential = 0.8383 V
Solution Temperature = 16.5 C
Ferricyanide concentration = $0.477E-05$ mol/cm³
Density = 1.0252 g/cm³
Viscosity = 0.012020 g/cm s
Diffusivity = $0.6024E-05$ cm²/s

Run No	Stirrer Speed (rpm)	Limiting Current (mA)	Sh	Re	Sc
1.01	0.0	0.7	42.3	0.0	1946.3
1.02	12.7	1.4	84.6	469.6	1946.3
1.03	23.7	2.4	145.0	876.3	1946.3
1.04	34.1	3.6	217.5	1260.8	1946.3
1.05	59.5	6.5	392.8	2199.9	1946.3
1.06	63.5	7.7	468.3	2347.8	1946.3
1.07	76.9	9.7	589.1	2843.2	1946.3
1.08	97.8	12.9	779.5	3615.9	1946.3
1.09	123.7	15.0	966.8	4573.5	1946.3

DATE 27-5-81
BATCH Batch 1 of 0.005M Potassium Ferricyanide/0.005M
Potassium Ferrocyanide/0.5M Sodium Hydroxide
solution prepared on 22-4-81

Potential = 0.8387 V
Solution Temperature = 18.0 C
Ferricyanide concentration = $0.487E-05$ mol/cm³
Density = 1.0245 g/cm³
Viscosity = 0.011619 g/cm s
Diffusivity = $0.6264E-05$ cm²/s

Run No	Stirrer Speed (rpm)	Limiting Current (mA)	Sh	Re	Sc
2.01	0.0	0.7	41.0	0.0	1810.4
2.02	9.7	1.0	56.9	370.8	1810.4
2.03	28.6	2.8	159.4	1093.2	1810.4
2.04	42.3	5.5	315.9	1616.9	1810.4
2.05	67.4	9.0	515.1	2576.3	1810.4
2.06	85.5	11.3	643.1	3268.1	1810.4
2.07	97.1	13.1	745.6	3711.5	1810.4

DATE 28-5-81
 BATCH Batch 1 of 0.005M Potassium Ferricyanide/0.005M
 Potassium Ferrocyanide/0.5M Sodium Hydroxide
 solution prepared on 22-4-81

Potential = 0.8330 V
 Solution Temperature = 20.0 °C
 Ferricyanide concentration = $0.487\text{E-}05$ mol/cm³
 Density = 1.0236 g/cm³
 Viscosity = 0.011111 g/cm s
 Diffusivity = $0.6596\text{E-}05$ cm²/s

Run No	Stirrer Speed (rpm)	Limiting Current (mA)	Sh	Re	Sc
3.01	0.0	0.6	32.4	0.0	1645.6
3.02	8.8	1.1	57.8	351.4	1645.6
3.03	24.0	2.2	120.0	958.5	1645.6
3.04	35.7	4.0	216.2	1425.8	1645.6
3.05	70.6	9.0	486.5	2819.6	1645.6
3.06	91.8	11.7	632.4	3666.2	1645.6
3.07	108.3	14.5	783.7	4325.2	1645.6
3.08	131.6	17.5	945.9	5255.7	1645.6

DATE 28-1-82
 BATCH Batch 4 of 0.005M Potassium Ferricyanide/0.005M
 Potassium Ferrocyanide/0.5M Sodium Hydroxide
 solution prepared on 16-11-82

Potential = 1.0028 V
 Solution Temperature = 19.0 °C
 Ferricyanide concentration = $0.467\text{E-}05$ mol/cm³
 Density = 1.0241 g/cm³
 Viscosity = 0.011361 g/cm s
 Diffusivity = $0.6429\text{E-}05$ cm²/s

Run No	Stirrer Speed (rpm)	Limiting Current (mA)	Sh	Re	Sc
4.01	0.0	0.8	47.4	0.0	1725.8
4.02	12.6	1.3	75.8	492.3	1725.8
4.03	16.1	1.7	101.2	629.1	1725.8
4.04	32.2	3.4	199.5	1258.2	1725.8
4.05	50.0	5.7	332.6	1953.7	1725.8
4.06	68.2	8.1	468.5	2664.9	1725.8
4.07	81.1	10.3	595.7	3168.9	1725.8
4.08	91.5	11.5	665.1	3575.3	1725.8
4.09	99.3	12.5	722.9	3880.1	1725.8
4.10	101.7	12.8	740.3	3973.8	1725.8
4.11	117.3	14.2	821.3	4583.4	1725.8
4.12	120.0	15.1	873.3	4688.9	1725.8

DATE 28-1-82
 BATCH Batch 4 of 0.005M Potassium Ferricyanide/0.005M
 Potassium Ferrocyanide/0.5M Sodium Hydroxide
 solution prepared on 16-11-82

Potential = 1.0123 V
 Solution Temperature = 19.0 C
 Ferricyanide concentration = $0.467\text{E-}05$ mol/cm³
 Density = 1.0241 g/cm³
 Viscosity = 0.011361 g/cm s
 Diffusivity = $0.6429\text{E-}05$ cm²/s

Run No	Stirrer Speed (rpm)	Limiting Current (mA)	Sh	Re	Sc
5.01	0.0	0.7	43.4	0.0	1725.8
5.02	12.5	1.1	63.6	488.4	1725.8
5.03	50.8	6.3	365.5	1985.0	1725.8
5.04	56.3	7.4	430.9	2199.9	1725.8
5.05	66.7	8.7	503.2	2606.2	1725.8
5.06	84.5	12.3	711.4	3301.8	1725.8
5.07	92.3	14.0	809.7	3606.5	1725.8
5.08	100.8	14.8	856.0	3938.7	1725.8
5.09	115.4	16.9	977.4	4509.1	1725.8

TABLE A6.6.2.2 I_L-N DATA FOR THE ELECTROLYTIC MIXING CELL WITH THE PRESENCE OF 2 LAYERS OF 0.695MM GLASS
SPHERICAL PARTICLES ON THE CATHODE

DATE 28-5-81
BATCH Batch 1 of 0.005M Potassium Ferricyanide/0.005M
Potassium Ferrocyanide/0.5M Sodium Hydroxide
solution prepared on 27-5-81

Potential = 0.8407 V
Solution Temperature = 21.0 C
Ferricyanide concentration = $0.487E-05$ mol/cm³
Density = 1.0231 g/cm³
Viscosity = 0.010867 g/cm s
Diffusivity = $0.6767E-05$ cm²/s

Run No	Stirrer Speed (rpm)	Limiting Current (mA)	Sh	Re	Sc
1.01	0.0	0.4	21.1	0.0	1569.6
1.02	10.9	0.5	26.3	444.9	1569.6
1.03	21.9	1.3	71.1	893.8	1569.6
1.04	39.7	2.7	144.9	1620.3	1569.6
1.05	55.1	5.3	281.9	2289.6	1569.6
1.06	85.7	8.8	466.3	3497.7	1569.6

DATE 29-5-81
BATCH Batch 1 of 0.005M Potassium Ferricyanide/0.005M
Potassium Ferrocyanide/0.5M Sodium Hydroxide
solution prepared on 27-5-81

Potential = 0.8319 V
Solution Temperature = 20.0 C
Ferricyanide concentration = $0.487E-05$ mol/cm³
Density = 1.0236 g/cm³
Viscosity = 0.011111 g/cm s
Diffusivity = $0.6596E-05$ cm²/s

Run No	Stirrer Speed (rpm)	Limiting Current (mA)	Sh	Re	Sc
2.01	0.0	0.5	25.9	0.0	1645.6
2.02	16.0	0.7	37.8	639.0	1645.6
2.03	22.9	1.3	70.3	914.6	1645.6
2.04	55.6	4.7	254.0	2220.5	1645.6
2.05	71.4	7.0	378.4	2851.5	1645.6
2.06	90.9	9.4	510.8	3630.3	1645.6
2.07	104.5	11.3	610.8	4173.4	1645.6

DATE 20-1-82
 BATCH Batch 4 of 0.005M Potassium Ferricyanide/0.005M
 Potassium Ferrocyanide/0.5M Sodium Hydroxide
 solution prepared on 16-11-81

Potential = 1.0069 V
 Solution Temperature = 20.0 C
 Ferricyanide concentration = $0.467\text{E-}05$ mol/cm³
 Density = 1.0236 g/cm³
 Viscosity = 0.011111 g/cm s
 Diffusivity = $0.6596\text{E-}05$ cm²/s

Run No	Stirrer Speed (rpm)	Limiting Current (mA)	Sh	Re	Sc
3.01	0.0	0.2	9.6	0.0	1645.6
3.02	48.2	7.7	434.0	1925.0	1645.6
3.03	59.0	9.2	521.4	2356.3	1645.6
3.04	80.0	13.1	738.4	3195.0	1645.6
3.05	96.0	14.9	839.9	3834.0	1645.6
3.06	109.1	16.9	952.6	4357.1	1645.6

DATE 20-1-82
 BATCH Batch 4 of 0.005M Potassium Ferricyanide/0.005M
 Potassium Ferrocyanide/0.5M Sodium Hydroxide
 solution prepared on 16-11-81

Potential = 1.0074 V
 Solution Temperature = 21.0 C
 Ferricyanide concentration = $0.467\text{E-}05$ mol/cm³
 Density = 1.0231 g/cm³
 Viscosity = 0.010867 g/cm s
 Diffusivity = $0.6767\text{E-}05$ cm²/s

Run No	Stirrer Speed (rpm)	Limiting Current (mA)	Sh	Re	Sc
4.01	0.0	1.4	76.9	0.0	1569.6
4.02	24.7	2.5	137.4	1008.1	1569.6
4.03	49.2	5.5	304.9	2008.0	1569.6
4.04	60.0	6.9	381.9	2448.8	1569.6
4.05	61.8	7.8	428.6	2522.3	1569.6
4.06	72.0	9.7	535.7	2938.5	1569.6
4.07	82.4	11.2	615.4	3363.0	1569.6
4.08	86.7	11.8	648.3	3538.5	1569.6
4.09	100.6	13.3	730.7	4105.8	1569.6
4.10	112.7	15.0	824.1	4599.6	1569.6

DATE 20-1-82
 BATCH Batch 4 of 0.005M Potassium Ferricyanide/0.005M
 Potassium Ferrocyanide/0.5M Sodium Hydroxide
 solution prepared on 16-11-81

Potential = 1.0078 V
 Solution Temperature = 21.0 C
 Ferricyanide concentration = $0.467\text{E-}05$ mol/cm³
 Density = 1.0231 g/cm³
 Viscosity = 0.010867 g/cm s
 Diffusivity = $0.6767\text{E-}05$ cm²/s

Run No	Stirrer Speed (rpm)	Limiting Current (mA)	Sh	Re	Sc
5.01	0.0	1.4	75.3	0.0	1569.6
5.02	60.0	6.4	351.6	2448.8	1569.6
5.03	64.2	7.4	409.3	2620.2	1569.6
5.04	72.7	8.7	476.9	2967.1	1569.6
5.05	96.0	12.3	675.8	3918.1	1569.6
5.06	110.0	13.9	763.7	4489.4	1569.6

DATE 22-1-82
 BATCH Batch 4 of 0.005M Potassium Ferricyanide/0.005M
 Potassium Ferrocyanide/0.5M Sodium Hydroxide
 solution prepared on 16-11-81

Potential = 1.0078 V
 Solution Temperature = 17.0 C
 Ferricyanide concentration = $0.467\text{E-}05$ mol/cm³
 Density = 1.0250 g/cm³
 Viscosity = 0.011885 g/cm s
 Diffusivity = $0.6104\text{E-}05$ cm²/s

Run No	Stirrer Speed (rpm)	Limiting Current (mA)	Sh	Re	Sc
6.01	0.0	1.4	84.1	0.0	1899.7
6.02	22.4	2.1	127.9	837.5	1899.7
6.03	34.3	3.1	188.8	1282.4	1899.7
6.04	54.5	5.4	328.9	2037.6	1899.7
6.05	70.6	7.3	444.7	2639.5	1899.7
6.06	82.7	8.8	539.1	3091.9	1899.7
6.07	101.1	11.8	718.8	3779.8	1899.7
6.08	108.1	12.6	767.5	4041.5	1899.7
6.09	121.0	15.3	932.0	4523.8	1899.7

TABLE A6.6.2.3 I_L - N DATA FOR THE ELECTROLYTIC MIXING CELL WITH THE PRESENCE OF 3 LAYERS OF 0.695MM GLASS
SPHERICAL PARTICLES ON THE CATHODE

DATE 29-5-81
BATCH Batch 1 of 0.005M Potassium Ferricyanide/0.005M
Potassium Ferrocyanide/0.5M Sodium Hydroxide
solution prepared on 27-5-81

Potential = 0.8390 V
Solution Temperature = 21.0 C
Ferricyanide concentration = $0.487E-05$ mol/cm³
Density = 1.0231 g/cm³
Viscosity = 0.010867 g/cm s
Diffusivity = $0.6767E-05$ cm²/s

Run No	Stirrer Speed (rpm)	Limiting Current (mA)	Sh	Re	Sc
1.01	0.0	0.4	21.1	0.0	1569.6
1.02	35.7	1.9	102.7	1457.0	1569.6
1.03	62.5	4.8	251.3	2550.8	1569.6
1.04	68.2	6.7	358.6	2783.5	1569.6
1.05	90.9	8.9	468.9	3709.9	1569.6

DATE 22-1-82
BATCH Batch 4 of 0.005M Potassium Ferricyanide/0.005M
Potassium Ferrocyanide/0.5M Sodium Hydroxide
solution prepared on 16-11-81

Potential = 1.0031 V
Solution Temperature = 15.0 C
Ferricyanide concentration = $0.467E-05$ mol/cm³
Density = 1.0258 g/cm³
Viscosity = 0.012439 g/cm s
Diffusivity = $0.5791E-05$ cm²/s

Run No	Stirrer Speed (rpm)	Limiting Current (mA)	Sh	Re	Sc
2.01	0.0	1.2	78.3	0.0	2093.8
2.02	17.8	1.5	96.9	636.4	2093.8
2.03	31.4	2.1	135.5	1122.6	2093.8
2.04	51.3	3.7	238.2	1834.0	2093.8
2.05	67.4	5.3	340.3	2409.6	2093.8
2.06	70.2	5.7	365.9	2509.7	2093.8

DATE 25-1-82
 BATCH Batch 4 of 0.005M Potassium Ferricyanide/0.005M
 Potassium Ferrocyanide/0.5M Sodium Hydroxide
 solution prepared on 16-11-81

Potential = 1.0014 V
 Solution Temperature = 20.0 C
 Ferricyanide concentration = $0.467\text{E-}05$ mol/cm³
 Density = 1.0236 g/cm³
 Viscosity = 0.011111 g/cm s
 Diffusivity = $0.6596\text{E-}05$ cm²/s

Run No	Stirrer Speed (rpm)	Limiting Current (mA)	Sh	Re	Sc
3.01	0.0	1.2	70.5	0.0	1645.6
3.02	10.4	1.2	70.5	415.3	1645.6
3.03	22.7	1.7	98.6	906.6	1645.6
3.04	48.0	3.6	202.9	1917.0	1645.6
3.05	62.5	5.3	298.7	2496.1	1645.6
3.06	70.6	6.2	349.5	2819.6	1645.6
3.07	78.4	7.2	405.8	3131.1	1645.6
3.08	93.8	8.2	465.0	3746.1	1645.6
3.09	106.5	10.9	614.4	4253.3	1645.6

DATE 25-1-82
 BATCH Batch 4 of 0.005M Potassium Ferricyanide/0.005M
 Potassium Ferrocyanide/0.5M Sodium Hydroxide
 solution prepared on 16-11-81

Potential = 1.0070 V
 Solution Temperature = 20.0 C
 Ferricyanide concentration = $0.467\text{E-}05$ mol/cm³
 Density = 1.0236 g/cm³
 Viscosity = 0.011111 g/cm s
 Diffusivity = $0.6596\text{E-}05$ cm²/s

Run No	Stirrer Speed (rpm)	Limiting Current (mA)	Sh	Re	Sc
4.01	0.0	1.0	59.2	0.0	1645.6
4.02	9.2	1.1	60.3	367.4	1645.6
4.03	20.3	1.7	94.7	810.7	1645.6
4.04	28.8	2.1	117.2	1150.2	1645.6
4.05	45.5	3.6	202.9	1817.1	1645.6
4.06	65.2	5.4	307.2	2603.9	1645.6
4.07	69.8	6.3	353.4	2787.6	1645.6
4.08	81.1	7.4	416.0	3238.9	1645.6
4.09	88.9	7.9	445.3	3550.4	1645.6
4.10	95.2	9.1	512.9	3802.0	1645.6
4.11	102.3	9.5	538.3	4085.6	1645.6

DATE 25-1-82
 BATCH Batch 4 of 0.005M Potassium Ferricyanide/0.005M
 Potassium Ferrocyanide/0.5M Sodium Hydroxide
 solution prepared on 16-11-81

Potential = 1.0070 V
 Solution Temperature = 16.0 C
 Ferricyanide concentration = $0.467\text{E-}05$ mol/cm³
 Density = 1.0254 g/cm³
 Viscosity = 0.012158 g/cm s
 Diffusivity = $0.5946\text{E-}05$ cm²/s

Run No	Stirrer Speed (rpm)	Limiting Current (mA)	Sh	Re	Sc
5.01	0.0	0.5	32.5	0.0	1994.1
5.02	20.4	1.0	63.8	745.9	1994.1
5.03	34.5	2.1	131.3	1261.4	1994.1
5.04	49.4	3.6	225.1	1806.2	1994.1
5.05	62.5	4.7	297.0	2285.1	1994.1
5.06	64.9	5.1	318.9	2372.9	1994.1
5.07	80.0	6.8	428.3	2925.0	1994.1
5.08	102.6	8.1	506.5	3751.3	1994.1
5.09	106.2	9.0	562.8	3882.9	1994.1

TABLE A6.6.2.4 I_L - N DATA FOR THE ELECTROLYTIC MIXING CELL WITH THE PRESENCE OF 4 LAYERS OF 0.695MM GLASS
SPHERICAL PARTICLES ON THE CATHODE

DATE 30-1-82
BATCH Batch 4 of 0.005M Potassium Ferricyanide/0.005M
Potassium Ferrocyanide/0.5M Sodium Hydroxide
solution prepared on 16-11-81

Potential = 1.0070 V
Solution Temperature = 16.0 C
Ferricyanide concentration = $0.467E-05$ mol/cm³
Density = 1.0254 g/cm³
Viscosity = 0.012158 g/cm s
Diffusivity = $0.5946E-05$ cm²/s

Run No	Stirrer Speed (rpm)	Limiting Current (mA)	Sh	Re	Sc
1.01	0.0	1.0	62.5	0.0	1994.1
1.02	62.2	4.5	281.4	2274.2	1994.1
1.03	67.8	5.4	338.3	2478.9	1994.1
1.04	85.7	6.7	422.1	3133.4	1994.1
1.05	93.0	7.8	487.7	3400.3	1994.1
1.06	102.9	8.6	537.8	3762.2	1994.1
1.07	111.1	9.2	574.0	4062.1	1994.1

DATE 30-1-82
BATCH Batch 4 of 0.005M Potassium Ferricyanide/0.005M
Potassium Ferrocyanide/0.5M Sodium Hydroxide
solution prepared on 16-11-81

Potential = 0.9960 V
Solution Temperature = 16.0 C
Ferricyanide concentration = $0.467E-05$ mol/cm³
Density = 1.0254 g/cm³
Viscosity = 0.012158 g/cm s
Diffusivity = $0.5946E-05$ cm²/s

Run No	Stirrer Speed (rpm)	Limiting Current (mA)	Sh	Re	Sc
2.01	0.0	1.0	62.5	0.0	1994.1
2.02	18.6	1.3	78.8	680.1	1994.1
2.03	33.0	1.9	121.9	1206.6	1994.1
2.04	41.8	2.6	163.8	1528.3	1994.1
2.05	54.1	3.7	231.4	1978.0	1994.1
2.06	66.7	5.2	325.2	2438.7	1994.1
2.07	71.9	5.9	372.1	2628.8	1994.1
2.08	87.6	6.9	431.5	3202.8	1994.1
2.09	96.8	7.7	482.7	3539.2	1994.1
2.10	102.9	8.3	519.0	3762.2	1994.1
2.11	112.1	9.3	582.8	4098.6	1994.1

DATE 1-2-82
 BATCH Batch 4 of 0.005M Potassium Ferricyanide/0.005M
 Potassium Ferrocyanide/0.5M Sodium Hydroxide
 solution prepared on 16-11-81

Potential = 0.9960 V
 Solution Temperature = 21.0 C
 Ferricyanide concentration = $0.467\text{E-}05$ mol/cm³
 Density = 1.0231 g/cm³
 Viscosity = 0.010867 g/cm s
 Diffusivity = $0.6767\text{E-}05$ cm²/s

Run No	Stirrer Speed (rpm)	Limiting Current (mA)	Sh	Re	Sc
3.01	0.0	1.0	54.9	0.0	1569.6
3.02	16.3	1.1	63.2	665.3	1569.6
3.03	23.5	1.4	76.9	959.1	1569.6
3.04	46.0	2.9	162.1	1959.0	1569.6
3.05	61.8	4.6	255.5	2522.3	1569.6
3.06	71.0	5.4	299.4	2897.7	1569.6
3.07	84.5	7.0	387.3	3448.7	1569.6
3.08	96.7	8.3	456.0	3946.6	1569.6
3.09	107.8	8.4	464.3	4399.7	1569.6

TABLE A6.6.2.5

I_L - N DATA FOR THE ELECTROLYTIC MIXING CELL WITH THE PRESENCE OF 5 LAYERS OF 0.695MM GLASS
SPHERICAL PARTICLES ON THE CATHODE

DATE 3-2-82

BATCH Batch 4 of 0.005M Potassium Ferricyanide/0.005M
Potassium Ferrocyanide/0.5M Sodium Hydroxide
solution prepared on 16-11-81

Potential = 1.0050 V

Solution Temperature = 20.0 C

Ferricyanide concentration = $0.467E-05$ mol/cm³Density = 1.0236 g/cm³

Viscosity = 0.011111 g/cm s

Diffusivity = $0.6596E-05$ cm²/s

Run No	Stirrer Speed (rpm)	Limiting Current (mA)	Sh	Re	Sc
1.01	0.0	0.5	28.2	0.0	1645.6
1.02	10.8	0.5	28.2	431.3	1645.6
1.03	27.3	1.3	73.3	1090.3	1645.6
1.04	48.8	3.0	169.1	1948.9	1645.6
1.05	61.8	4.1	231.1	2468.1	1645.6
1.06	75.0	5.3	298.7	2995.3	1645.6
1.07	85.7	6.5	369.2	3422.6	1645.6
1.08	96.3	7.5	422.7	3845.9	1645.6
1.09	107.1	8.4	473.5	4277.3	1645.6

DATE 3-2-82

BATCH Batch 4 of 0.005M Potassium Ferricyanide/0.005M
Potassium Ferrocyanide/0.5M Sodium Hydroxide
solution prepared on 16-11-81

Potential = 1.0122 V

Solution Temperature = 20.0 C

Ferricyanide concentration = $0.467E-05$ mol/cm³Density = 1.0236 g/cm³

Viscosity = 0.011111 g/cm s

Diffusivity = $0.6596E-05$ cm²/s

Run No	Stirrer Speed (rpm)	Limiting Current (mA)	Sh	Re	Sc
2.01	0.0	0.4	23.7	0.0	1645.6
2.02	57.1	4.5	256.5	2280.4	1645.6
2.03	69.0	5.5	312.8	2755.7	1645.6
2.04	75.9	6.3	354.0	3031.2	1645.6
2.05	81.8	6.8	386.1	3266.9	1645.6
2.06	87.4	7.6	431.2	3490.5	1645.6
2.07	109.8	8.6	484.8	4235.1	1645.6

DATE 5-2-82
 BATCH Batch 4 of 0.005M Potassium Ferricyanide/0.005M
 Potassium Ferrocyanide/0.5M Sodium Hydroxide
 solution prepared on 16-11-81

Potential = 0.9939 V
 Solution Temperature = 20.0 C
 Ferricyanide concentration = $0.467\text{E-}05$ mol/cm³
 Density = 1.0236 g/cm³
 Viscosity = 0.011111 g/cm s
 Diffusivity = $0.6596\text{E-}05$ cm²/s

Run No	Stirrer Speed (rpm)	Limiting Current (mA)	Sh	Re	Sc
3.01	0.0	0.3	18.0	0.0	1645.6
3.02	28.6	1.0	56.4	1142.2	1645.6
3.03	39.2	2.1	117.2	1565.5	1645.6
3.04	69.8	4.6	262.1	2787.6	1645.6
3.05	72.2	5.0	281.8	2883.5	1645.6
3.06	83.3	6.0	341.0	3326.8	1645.6
3.07	84.9	6.3	355.1	3390.7	1645.6
3.08	73.8	6.9	391.7	3746.1	1645.6

TABLE A6.6.3.1 I_L-N DATA FOR THE ELECTROLYTIC MIXING CELL WITH THE PRESENCE OF 1 LAYER OF 0.805MM GLASS
SPHERICAL PARTICLES ON THE CATHODE

DATE 9-12-81
BATCH Batch 3 of 0.005M Potassium Ferricyanide/0.005M
Potassium Ferrocyanide/0.5M Sodium Hydroxide
solution prepared on 16-11-81

Potential = 0.9916 V
Solution Temperature = 14.0 C
Ferricyanide concentration = $0.477E-05$ mol/cm³
Density = 1.0262 g/cm³
Viscosity = 0.012728 g/cm s
Diffusivity = $0.5640E-05$ cm²/s

Run No	Stirrer Speed (rpm)	Limiting Current (mA)	Sh	Re	Sc
1.01	0.0	0.6	36.8	0.0	2199.1
1.02	25.0	2.6	169.1	873.8	2199.1
1.03	47.6	5.9	380.8	1663.7	2199.1
1.04	48.4	5.9	380.8	1691.6	2199.1
1.05	58.8	7.7	497.0	2055.1	2199.1
1.06	65.9	8.6	555.1	2303.3	2199.1
1.07	65.9	9.4	606.7	2303.3	2199.1
1.08	71.4	9.7	626.0	2495.5	2199.1
1.09	80.0	11.0	709.9	2796.1	2199.1
1.10	82.2	11.4	735.8	2873.0	2199.1
1.11	83.9	11.6	748.7	2932.4	2199.1
1.12	81.6	11.8	761.6	2852.0	2199.1
1.13	89.6	13.2	851.9	3131.6	2199.1
1.14	98.9	13.5	871.3	3456.6	2199.1
1.15	101.7	15.0	968.1	3554.5	2199.1
1.16	114.5	15.9	1026.2	4001.9	2199.1

DATE 9-12-81
BATCH Batch 3 of 0.005M Potassium Ferricyanide/0.005M
Potassium Ferrocyanide/0.5M Sodium Hydroxide
solution prepared on 16-11-81

Potential = 0.9915 V
Solution Temperature = 14.0 C
Ferricyanide concentration = $0.477E-05$ mol/cm³
Density = 1.0262 g/cm³
Viscosity = 0.012728 g/cm s
Diffusivity = $0.5640E-05$ cm²/s

Run No	Stirrer Speed (rpm)	Limiting Current (mA)	Sh	Re	Sc
2.01	16.8	1.8	116.2	587.2	2199.1
2.02	18.8	2.0	129.1	657.1	2199.1
2.03	33.0	3.5	225.9	1153.4	2199.1
2.04	46.9	5.2	335.6	1639.2	2199.1
2.05	61.2	7.7	497.0	2139.0	2199.1
2.06	69.8	9.2	593.8	2439.6	2199.1
2.07	78.9	10.8	697.0	2757.6	2199.1
2.08	72.3	11.3	729.3	2527.0	2199.1
2.09	91.4	12.7	819.7	3194.5	2199.1
2.10	96.3	13.3	858.4	3365.8	2199.1
2.11	103.4	14.3	922.9	3613.9	2199.1
2.12	105.9	14.9	961.7	3701.3	2199.1
2.13	108.4	15.0	968.1	3788.7	2199.1
2.14	125.9	17.0	1097.2	4400.3	2199.1

DATE 26-5-82
 BATCH Batch 3 of 0.005M Potassium Ferricyanide/0.005M
 Potassium Ferrocyanide/0.5M Sodium Hydroxide
 solution prepared on 23-4-82

Potential = 1.0217 V
 Solution Temperature = 21.0 C
 Ferricyanide concentration = $0.477\text{E-}05$ mol/cm³
 Density = 1.0331 g/cm³
 Viscosity = 0.010867 d/cm s
 Diffusivity = $0.6767\text{E-}05$ cm²/s

Run No	Stirrer Speed (rpm)	Limiting Current (mA)	Sh	Re	Sc
3.01	0.0	0.9	25.7	0.0	1569.6
3.02	18.8	1.3	71.0	767.3	1569.6
3.03	28.8	3.5	188.3	1175.4	1569.6
3.04	43.8	5.4	293.2	1787.6	1569.6
3.05	53.5	7.8	405.8	2265.1	1569.6
3.06	72.7	10.2	548.7	2967.1	1569.6
3.07	90.9	12.8	668.5	3709.9	1569.6

TABLE A6.6.3.2 I_L-N DATA FOR THE ELECTROLYTIC MIXING CELL WITH THE PRESENCE OF 2 LAYERS OF 0.805MM GLASS

SPHERICAL PARTICLES ON THE CATHODE

DATE 26-5-82
 BATCH Batch 3 of 0.005M Potassium Ferricyanide/0.005M Potassium Ferrocyanide/0.5M Sodium Hydroxide solution prepared on 23-4-82

Potential = 1.0269 V
 Solution Temperature = 21.5 C
 Ferricyanide concentration = $0.477E-05$ mol/cm³
 Density = 1.0229 g/cm³
 Viscosity = 0.010748 g/cm s
 Diffusivity = $0.6854E-05$ cm²/s

Run No	Stirrer Speed (rpm)	Limiting Current (mA)	Sh	Re	Sc
1.01	0.0	0.3	16.4	0.0	1533.1
1.02	15.7	0.7	37.6	647.7	1533.1
1.03	24.7	1.8	98.3	1019.0	1533.1
1.04	54.5	5.0	265.6	2248.5	1533.1
1.05	62.0	6.1	321.9	2557.9	1533.1
1.06	72.3	7.3	390.4	2982.8	1533.1
1.07	85.3	9.2	490.2	3519.1	1533.1
1.08	102.3	11.2	594.8	4220.5	1533.1

DATE 26-5-82
 BATCH Batch 3 of 0.005M Potassium Ferricyanide/0.005M Potassium Ferrocyanide/0.5M Sodium Hydroxide solution prepared on 23-4-82

Potential = 1.0270 V
 Solution Temperature = 21.5 C
 Ferricyanide concentration = $0.477E-05$ mol/cm³
 Density = 1.0229 g/cm³
 Viscosity = 0.010748 g/cm s
 Diffusivity = $0.6854E-05$ cm²/s

Run No	Stirrer Speed (rpm)	Limiting Current (mA)	Sh	Re	Sc
2.01	0.0	0.4	20.4	0.0	1533.1
2.02	20.8	1.4	73.3	858.1	1533.1
2.03	50.8	4.4	234.7	2095.8	1533.1
2.04	71.8	7.0	371.8	2962.2	1533.1
2.05	77.9	8.8	470.0	3213.8	1533.1

DATE 27-5-82
 BATCH Batch 3 of 0.005M Potassium Ferricyanide/0.005M
 Potassium Ferrocyanide/0.5M Sodium Hydroxide
 solution prepared on 23-4-82

Potential = 1.02/2 V
 Solution Temperature = 20.0 C
 Ferricyanide concentration = $0.477\text{E-}05$ mol/cm³
 Density = 1.0336 g/cm³
 Viscosity = 0.01111 g/cm s
 Diffusivity = $0.6596\text{E-}05$ cm²/s

Run No	Stirrer Speed (rpm)	Limiting Current (mA)	Sh	Re	Sc
3.01	9.0	0.3	17.0	0.0	1645.6
3.02	16.2	0.8	42.4	647.0	1645.6
3.03	30.9	2.2	120.9	1234.1	1645.6
3.04	40.8	3.0	165.6	1629.4	1645.6
3.05	46.9	4.7	259.9	1873.0	1645.6
3.06	57.7	5.2	288.6	2304.4	1645.6
3.07	69.8	6.9	381.9	2787.6	1645.6
3.08	75.9	7.1	394.6	3031.2	1645.6
3.09	88.2	9.5	522.0	3522.5	1645.6
3.10	101.7	11.0	607.0	4061.6	1645.6
3.11	111.1	11.9	656.7	4437.0	1645.6

TABLE A6.6.3.3 I_L-N DATA FOR THE ELECTROLYTIC MIXING CELL WITH THE PRESENCE OF 3 LAYERS OF 0.805MM GLASS
SPHERICAL PARTICLES ON THE CATHODE

DATE 27-5-82
BATCH Batch 3 of 0.005M Potassium Ferricyanide/0.005M
Potassium Ferrocyanide/0.5M Sodium Hydroxide
solution prepared on 23-4-82

Potential = 1.0250 V
Solution Temperature = 21.5 C
Ferricyanide concentration = $0.477E-05$ mol/cm³
Density = 1.0229 g/cm³
Viscosity = 0.010748 g/cm s
Diffusivity = $0.6854E-05$ cm²/s

Run No	Stirrer Speed (rpm)	Limiting Current (mA)	Sh	Re	Sc
1.01	0.0	0.2	12.3	0.0	1533.1
1.02	14.0	0.5	25.3	577.6	1533.1
1.03	24.8	1.4	75.4	1023.1	1533.1
1.04	53.6	4.6	245.4	2211.3	1533.1
1.05	75.0	7.1	376.0	3094.2	1533.1
1.06	85.7	8.6	455.7	3535.6	1533.1
1.07	89.6	9.3	494.5	3696.5	1533.1
1.08	111.1	11.3	600.2	4583.5	1533.1

DATE 27-5-82
BATCH Batch 3 of 0.005M Potassium Ferricyanide/0.005M
Potassium Ferrocyanide/0.5M Sodium Hydroxide
solution prepared on 23-4-82

Potential = 1.0316 V
Solution Temperature = 22.0 C
Ferricyanide concentration = $0.477E-05$ mol/cm³
Density = 1.0226 g/cm³
Viscosity = 0.010630 g/cm s
Diffusivity = $0.6941E-05$ cm²/s

Run No	Stirrer Speed (rpm)	Limiting Current (mA)	Sh	Re	Sc
2.01	0.0	0.3	16.2	0.0	1497.6
2.02	16.4	1.0	54.5	683.9	1497.6
2.03	33.9	2.1	112.7	1413.7	1497.6
2.04	38.7	2.7	142.1	1613.9	1497.6
2.05	55.6	4.8	254.3	2318.6	1497.6
2.06	67.4	6.1	320.9	2810.7	1497.6
2.07	75.5	7.3	385.4	3148.5	1497.6
2.08	94.5	9.5	496.1	3940.9	1497.6
2.09	108.7	11.2	587.3	4533.0	1497.6

DATE 27-5-82
 BATCH Batch 3 of 0.005M Potassium Ferricyanide/0.005M
 Potassium Ferrocyanide/0.5M Sodium Hydroxide
 solution prepared on 23-4-82

Potential = 1.0310 V
 Solution Temperature = 22.0 C
 Ferricyanide concentration = 0.477E-05 mol/cm³
 Density = 1.0226 g/cm³
 Viscosity = 0.010650 g/cm s
 Diffusivity = 0.6941E-05 cm²/s

Run No	Stirrer Speed (rpm)	Limiting Current (mA)	Sh	Re	Sc
3.01	0.0	0.3	14.1	0.0	1497.6
3.02	26.5	1.1	56.6	1105.1	1497.6
3.03	44.8	3.4	177.2	1868.3	1497.6
3.04	66.7	6.5	338.8	2781.5	1497.6
3.05	72.3	7.3	383.3	3015.1	1497.6

DATE 28-5-82
 BATCH Batch 3 of 0.005M Potassium Ferricyanide/0.005M
 Potassium Ferrocyanide/0.5M Sodium Hydroxide
 solution prepared on 23-4-82

Potential = 1.0310 V
 Solution Temperature = 20.0 C
 Ferricyanide concentration = 0.477E-05 mol/cm³
 Density = 1.0236 g/cm³
 Viscosity = 0.011111 g/cm s
 Diffusivity = 0.6596E-05 cm²/s

Run No	Stirrer Speed (rpm)	Limiting Current (mA)	Sh	Re	Sc
4.01	0.0	0.2	13.6	0.0	1645.6
4.02	25.2	1.3	72.3	1006.4	1645.6
4.03	58.8	4.6	255.0	2348.3	1645.6
4.04	71.4	6.3	346.0	2851.5	1645.6
4.05	87.0	8.2	454.2	3474.5	1645.6

DATE 1-6-82
 BATCH Batch 3 of 0.005M Potassium Ferricyanide/0.005M
 Potassium Ferrocyanide/0.5M Sodium Hydroxide
 solution prepared on 23-4-82

Potential = 1.0218 V
 Solution Temperature = 21.0 C
 Ferricyanide concentration = $0.477\text{E-}05$ mol/cm³
 Density = 1.0231 g/cm³
 Viscosity = 0.010867 g/cm s
 Diffusivity = $0.6767\text{E-}05$ cm²/s

Run No	Stirrer Speed (rpm)	Limiting Current (mA)	Sh	Re	Sc
5.01	0.0	0.3	14.5	0.0	1569.6
5.02	14.0	0.4	22.8	571.4	1569.6
5.03	28.6	1.6	85.0	1167.3	1569.6
5.04	63.2	4.8	260.9	2579.4	1569.6
5.05	75.0	6.6	353.9	3061.0	1569.6
5.06	96.0	8.6	463.7	3918.1	1569.6
5.07	106.2	9.9	533.6	4334.4	1569.6

TABLE A6.6.3.4 I_L-N DATA FOR THE ELECTROLYTIC MIXING CELL WITH THE PRESENCE OF 4 LAYERS OF 0.805MM GLASS
SPHERICAL PARTICLES ON THE CATHODE

DATE 1-6-82
BATCH Batch 3 of 0.005M Potassium Ferricyanide/0.005M
Potassium Ferrocyanide/0.5M Sodium Hydroxide
solution prepared on 23-4-82

Potential = 1.0299 V
Solution Temperature = 22.0 C
Ferricyanide concentration = $0.477E-05$ mol/cm³
Density = 1.0226 g/cm³
Viscosity = 0.010630 g/cm s
Diffusivity = $0.6941E-05$ cm²/s

Run No	Stirrer Speed (rpm)	Limiting Current (mA)	Sh	Re	Sc
1.01	0.0	0.2	12.1	0.0	1497.6
1.02	27.3	1.3	70.8	1138.5	1497.6
1.03	51.3	3.6	191.4	2137.3	1497.6
1.04	68.2	5.6	296.3	2844.1	1497.6
1.05	77.5	6.5	343.0	3315.3	1497.6
1.06	96.0	8.6	452.0	4003.4	1497.6
1.07	108.1	9.9	520.2	4508.0	1497.6
1.08	111.1	10.2	534.9	4633.1	1497.6

DATE 1-6-82
BATCH Batch 3 of 0.005M Potassium Ferricyanide/0.005M
Potassium Ferrocyanide/0.5M Sodium Hydroxide
solution prepared on 23-4-82

Potential = 1.0299 V
Solution Temperature = 22.0 C
Ferricyanide concentration = $0.477E-05$ mol/cm³
Density = 1.0226 g/cm³
Viscosity = 0.010630 g/cm s
Diffusivity = $0.6941E-05$ cm²/s

Run No	Stirrer Speed (rpm)	Limiting Current (mA)	Sh	Re	Sc
2.01	0.0	0.2	10.1	0.0	1497.6
2.02	41.4	2.5	131.1	1726.5	1497.6
2.03	69.8	5.7	298.4	2910.8	1497.6
2.04	75.5	6.3	330.9	3148.5	1497.6
2.05	90.2	7.1	373.4	3761.5	1497.6
2.06	99.2	8.6	449.9	4136.9	1497.6
2.07	117.6	9.7	508.1	4904.2	1497.6

DATE 1-5-82
 BATCH Batch 3 of 0.005M Potassium Ferricyanide/0.005M
 Potassium Ferrocyanide/0.5M Sodium Hydroxide
 solution prepared on 23-4-82

Potential = 1.0310 V
 Solution Temperature = 23.0 C
 Ferricyanide concentration = $0.477\text{E-}05$ mol/cm³
 Density = 1.0221 g/cm³
 Viscosity = 0.010400 g/cm s
 Diffusivity = $0.7119\text{E-}05$ cm²/s

Run No	Stirrer Speed (rpm)	Limiting Current (mA)	Sh	Re	Sc
3.01	0.0	0.3	15.7	0.0	1429.3
3.02	15.4	0.6	29.5	656.1	1429.3
3.03	27.0	1.5	74.7	1150.3	1429.3
3.04	61.2	4.6	236.2	2607.4	1429.3
3.05	71.4	6.0	306.8	3042.0	1429.3
3.06	85.7	7.3	375.8	3651.2	1429.3
3.07	94.5	8.7	444.3	4026.1	1429.3

DATE 2-6-82
 BATCH Batch 3 of 0.005M Potassium Ferricyanide/0.005M
 Potassium Ferrocyanide/0.5M Sodium Hydroxide
 solution prepared on 23-4-82

Potential = 1.0238 V
 Solution Temperature = 22.5 C
 Ferricyanide concentration = $0.477\text{E-}05$ mol/cm³
 Density = 1.0224 g/cm³
 Viscosity = 0.010514 g/cm s
 Diffusivity = $0.7030\text{E-}05$ cm²/s

Run No	Stirrer Speed (rpm)	Limiting Current (mA)	Sh	Re	Sc
4.01	0.0	0.2	12.7	0.0	1463.0
4.02	13.8	0.4	20.7	581.7	1463.0
4.03	24.2	1.2	61.6	1020.1	1463.0
4.04	46.5	3.1	163.1	1960.1	1463.0
4.05	72.3	6.0	308.6	3047.6	1463.0
4.06	90.2	8.1	418.4	3802.1	1463.0
4.07	99.2	8.8	454.1	4181.4	1463.0
4.08	105.9	9.4	485.7	4463.9	1463.0

TABLE A6.6.4.5

I_L - N DATA FOR THE ELECTROLYTIC MIXING CELL WITH THE PRESENCE OF 5 LAYERS OF 0.805MM. GLASS
SPHERICAL PARTICLES ON THE CATHODE

DATE 2-6-82
BATCH Batch 3 of 0.005M Potassium Ferricyanide/0.005M
Potassium Ferrocyanide/0.5M Sodium Hydroxide
solution prepared on 23-4-82

Potential = 1.0236 V
Solution temperature = 23.0 C
Ferricyanide concentration = $0.477E-05$ mol/cm³
Density = 1.0221 g/cm³
Viscosity = 0.010400 g/cm s
Diffusivity = $0.7119E-05$ cm²/s

Run No	Stirrer Speed (rpm)	Limiting Current (mA)	Sh	Re	Sc
1.01	0.0	0.2	11.8	0.0	1429.3
1.02	25.6	1.6	82.8	1090.7	1429.3
1.03	57.1	4.6	237.8	2432.7	1429.3
1.04	75.4	6.3	320.6	3212.4	1429.3
1.05	86.5	7.3	373.8	3429.7	1429.3

DATE 2-6-82
BATCH Batch 3 of 0.005M Potassium Ferricyanide/0.005M
Potassium Ferrocyanide/0.5M Sodium Hydroxide
solution prepared on 23-4-82

Potential = 1.0328 V
Solution temperature = 24.0 C
Ferricyanide concentration = $0.477E-05$ mol/cm³
Density = 1.0216 g/cm³
Viscosity = 0.010176 g/cm s
Diffusivity = $0.7300E-05$ cm²/s

Run No	Stirrer Speed (rpm)	Limiting Current (mA)	Sh	Re	Sc
2.01	0.0	0.3	13.4	0.0	1364.4
2.02	14.1	0.4	19.2	613.6	1364.4
2.03	34.9	2.2	109.2	1518.8	1364.4
2.04	55.0	4.0	201.4	2393.6	1364.4
2.05	64.5	5.3	264.8	2807.0	1364.4
2.06	72.7	6.0	299.2	3163.9	1364.4
2.07	82.2	7.1	355.0	3577.3	1364.4
2.08	90.9	8.3	414.3	3956.0	1364.4
2.09	109.1	9.8	491.1	4748.0	1364.4

DATE 3-6-82
 BATCH Batch 3 of 0.005M Potassium Ferricyanide/0.005M
 Potassium Ferrocyanide/0.5M Sodium Hydroxide
 solution prepared on 23-4-82

Potential = 1.0229 V
 Solution Temperature = 22.5 C
 Ferricyanide concentration = $0.477\text{E-}05$ mol/cm³
 Density = 1.0224 g/cm³
 Viscosity = 0.010514 g/cm s
 Diffusivity = $0.7030\text{E-}05$ cm²/s

Run No	Stirrer Speed (rpm)	Limiting Current (mA)	Sh	Re	Sc
3.01	0.0	0.3	15.9	0.0	1463.0
3.02	20.8	0.5	27.9	876.8	1463.0
3.03	28.7	1.3	65.8	1209.8	1463.0
3.04	51.7	3.4	175.0	2179.2	1463.0
3.05	67.4	4.9	254.8	2841.0	1463.0
3.06	80.0	6.2	320.5	3372.1	1463.0
3.07	91.6	7.6	392.5	3861.1	1463.0
3.08	105.3	8.6	446.4	4438.6	1463.0
3.09	107.1	9.1	473.8	4514.4	1463.0

DATE 3-6-82
 BATCH Batch 3 of 0.005M Potassium Ferricyanide/0.005M
 Potassium Ferrocyanide/0.5M Sodium Hydroxide
 solution prepared on 23-4-82

Potential = 1.0274 V
 Solution Temperature = 24.0 C
 Ferricyanide concentration = $0.477\text{E-}05$ mol/cm³
 Density = 1.0216 g/cm³
 Viscosity = 0.010176 g/cm s
 Diffusivity = $0.7300\text{E-}05$ cm²/s

Run No	Stirrer Speed (rpm)	Limiting Current (mA)	Sh	Re	Sc
4.01	0.0	0.2	7.7	0.0	1364.4
4.02	14.5	0.3	15.4	631.0	1364.4
4.03	30.3	1.5	74.8	1318.7	1364.4
4.04	36.6	2.1	103.7	1592.8	1364.4
4.05	65.2	5.1	253.3	2837.5	1364.4
4.06	73.1	5.8	291.7	3181.3	1364.4
4.07	78.9	6.6	330.1	3433.7	1364.4
4.08	102.6	8.7	433.3	4465.1	1364.4

TABLE A6.6.3.6

I_L - W DATA FOR THE ELECTROLYTIC MIXING CELL WITH THE PRESENCE OF 6 LAYERS OF 0.805MM GLASS
SPHERICAL PARTICLES ON THE CATHODE

DATE 4-6-82

BATCH Batch 3 of 0.005M Potassium Ferricyanide/0.005M
Potassium Ferrocyanide/0.5M Sodium Hydroxide
solution prepared on 23-4-82

Potential = 1.0242 V

Solution Temperature = 22.0 C

Ferricyanide concentration = $0.477E-05$ mol/cm³Density = 1.0226 g/cm³

Viscosity = 0.010630 g/cm s

Diffusivity = $0.6941E-05$ cm²/s

Run No	Stirrer Speed (rpm)	Limiting Current (mA)	Sh	Re	Sc
1.01	0.0	0.3	16.2	0.0	1497.6
1.02	12.4	0.4	20.2	517.1	1497.6
1.03	21.9	1.1	58.7	913.3	1497.6
1.04	30.8	1.5	78.7	1284.4	1497.6
1.05	37.5	2.1	111.2	1563.8	1497.6
1.06	56.6	4.0	207.7	2360.3	1497.6
1.07	69.8	5.4	281.6	2910.8	1497.6
1.08	73.2	5.8	306.8	3052.6	1497.6
1.09	90.9	7.3	383.3	3790.7	1497.6
1.10	96.8	7.9	415.3	4036.8	1497.6
1.11	107.1	9.0	474.1	4466.3	1497.6

DATE 4-6-82

BATCH Batch 3 of 0.005M Potassium Ferricyanide/0.005M
Potassium Ferrocyanide/0.5M Sodium Hydroxide
solution prepared on 23-4-82

Potential = 1.0281 V

Solution Temperature = 23.0 C

Ferricyanide concentration = $0.477E-05$ mol/cm³Density = 1.0221 g/cm³

Viscosity = 0.010400 g/cm s

Diffusivity = $0.7119E-05$ cm²/s

Run No	Stirrer Speed (rpm)	Limiting Current (mA)	Sh	Re	Sc
2.01	0.0	0.3	13.8	0.0	1429.3
2.02	24.8	1.1	55.2	1056.6	1429.3
2.03	53.1	3.9	200.4	2262.3	1429.3
2.04	69.0	5.3	273.6	2939.7	1429.3
2.05	89.6	7.6	389.6	3817.4	1429.3
2.06	101.7	8.5	432.6	4332.9	1429.3

DATE 4-6-82

BATCH Batch 3 of 0.005M Potassium Ferricyanide/0.005M
Potassium Ferrocyanide/0.5M Sodium Hydroxide
solution prepared on 23-4-82

Potential = 1.0301 V

Solution Temperature = 24.0 C

Ferricyanide concentration = $0.477\text{E-}05$ mol/cm³

Density = 1.0216 g/cm³

Viscosity = 0.010176 g/cm s

Diffusivity = $0.7300\text{E-}05$ cm²/s

Run No	Stirrer Speed (rpm)	Limiting Current (mA)	Sh	Re	Sc
3.01	0.0	0.3	15.4	0.0	1364.4
3.02	30.6	1.6	78.8	1331.7	1364.4
3.03	55.6	4.4	219.4	2419.7	1364.4
3.04	71.4	6.0	297.2	3107.3	1364.4
3.05	81.1	6.6	330.1	3529.5	1364.4
3.06	95.2	7.9	394.9	4143.1	1364.4
3.07	114.3	8.6	427.8	4974.3	1364.4

TABLE A6.6.4.1 I_L - N DATA FOR THE ELECTROLYTIC MIXING CELL WITH THE PRESENCE OF 1 LAYER OF 1.29MM GLASS
SPHERICAL PARTICLES ON THE CATHODE

DATE 12-5-81
BATCH Batch 5 of 0.005M Potassium Ferricyanide/0.005M
Potassium Ferrocyanide/0.5M Sodium Hydroxide
solution prepared on 22-4-81

Potential = 0.835 V
Solution Temperature = 19.5 C
Ferricyanide concentration = $0.477E-05$ mol/cm³
Density = 1.0233 g/cm³
Viscosity = 0.011033 g/cm s
Diffusivity = $0.6512E-05$ cm²/s

Run No	Stirrer Speed (rpm)	Limiting Current (mA)	Sh	Re	Sc
1.01	0.0	0.2	11.2	0.0	1685.1
1.02	14.7	1.3	72.7	580.7	1685.1
1.03	26.7	3.7	209.6	1054.8	1685.1
1.04	39.9	6.2	346.6	1576.2	1685.1
1.05	61.1	10.3	575.8	2413.7	1685.1
1.06	74.2	13.0	726.7	2931.2	1685.1
1.07	82.1	14.8	827.3	3243.3	1685.1
1.08	90.1	16.4	916.7	3559.3	1685.1
1.09	103.1	18.5	1034.1	4072.9	1685.1
1.10	123.5	21.3	1190.6	4878.7	1685.1

DATE 13-5-81
BATCH Batch 5 of 0.005M Potassium Ferricyanide/0.005M
Potassium Ferrocyanide/0.5M Sodium Hydroxide
solution prepared on 22-4-81

Potential = 0.8347 V
Solution Temperature = 18.5 C
Ferricyanide concentration = $0.477E-05$ mol/cm³
Density = 1.0243 g/cm³
Viscosity = 0.011489 g/cm s
Diffusivity = $0.6346E-05$ cm²/s

Run No	Stirrer Speed (rpm)	Limiting Current (mA)	Sh	Re	Sc
2.01	0.0	0.2	13.8	0.0	1767.5
2.02	12.8	1.2	67.7	494.7	1767.5
2.03	22.7	2.8	163.5	877.3	1767.5
2.04	48.0	7.0	401.5	1855.1	1767.5
2.05	68.4	11.1	636.7	2643.5	1767.5
2.06	76.4	12.5	717.0	2952.7	1767.5
2.07	89.6	14.9	854.7	3462.8	1767.5
2.08	104.4	17.3	992.3	4034.8	1767.5
2.09	123.5	19.6	1124.2	4773.0	1767.5
2.10	139.5	21.5	1233.2	5391.3	1767.5

TABLE A6.6.4.2 I_L-N DATA FOR THE ELECTROLYTIC MIXING CELL WITH THE PRESENCE OF 2 LAYERS OF 1.29MM GLASS SPHERICAL PARTICLES ON THE CATHODE.

DATE 13-5-81
BATCH Batch 5 of 0.005M Potassium Ferricyanide/0.005M Potassium Ferrocyanide/0.5M Sodium Hydroxide solution prepared on 22-4-81

Potential = 0.8381 V
Solution Temperature = 20.0 C
Ferricyanide concentration = 0.477E-05 mol/cm³
Density = 1.0236 g/cm³
Viscosity = 0.011111 g/cm s
Diffusivity = 0.6596E-05 cm²/s

Run No	Stirrer Speed (rpm)	Limiting Current (mA)	Sh	Re	Sc
1.01	0.0	0.1	8.3	0.0	1645.6
1.02	17.9	1.2	67.3	714.9	1645.6
1.03	25.6	2.7	149.0	1022.4	1645.6
1.04	41.7	4.7	262.1	1665.4	1645.6
1.05	55.0	7.3	402.8	2196.5	1645.6
1.06	69.4	9.2	507.7	2771.6	1645.6
1.07	77.9	10.8	576.0	3111.1	1645.6
1.08	89.3	12.1	667.7	3566.4	1645.6
1.09	103.6	14.6	805.7	4137.5	1645.6
1.10	114.5	15.9	877.4	4572.8	1645.6
1.11	120.2	16.8	927.1	4800.4	1645.6
1.12	153.5	22.0	1214.1	6130.3	1645.6

TABLE A6.6.4.3 I_L-N DATA FOR THE ELECTROLYTIC MIXING CELL WITH THE PRESENCE OF 3 LAYERS OF 1.29MM GLASS SPHERICAL PARTICLES ON THE CATHODE

DATE 13-5-81
BATCH Batch 5 of 0.005M Potassium Ferricyanide/0.005M Potassium Ferrocyanide/0.5M Sodium Hydroxide solution prepared on 22-4-81

Potential = 0.8277 V
Solution Temperature = 22.0 C
Ferricyanide concentration = 0.477E-05 mol/cm³
Density = 1.0226 g/cm³
Viscosity = 0.010630 g/cm s
Diffusivity = 0.6941E-05 cm²/s

Run No	Stirrer Speed (rpm)	Limiting Current (mA)	Sh	Re	Sc
1.01	0.0	0.1	7.9	0.0	1497.6
1.02	23.1	2.0	103.3	963.3	1497.6
1.03	56.3	7.1	375.0	2347.8	1497.6
1.04	80.5	10.9	571.6	3357.0	1497.6
1.05	92.3	12.5	655.5	3849.1	1497.6
1.06	102.6	14.5	760.4	4278.6	1497.6
1.07	115.9	17.0	891.5	4833.3	1497.6
1.08	152.1	20.3	1064.5	6342.9	1497.6

TABLE A6.6.4.4 I_L-N DATA FOR THE ELECTROLYTIC MIXING CELL WITH THE PRESENCE OF 4 LAYERS OF 1.29MM GLASS
SPHERICAL PARTICLES ON THE CATHODE

DATE 13-5-81
BATCH Batch 5 of 0.005M Potassium Ferricyanide/0.005M
Potassium Ferrocyanide/0.5M Sodium Hydroxide
solution prepared on 22-4-81

Potential = 0.8375 V
Solution Temperature = 21.5 C
Ferricyanide concentration = $0.477E-05$ mol/cm³
Density = 1.0229 g/cm³
Viscosity = 0.010748 g/cm s
Diffusivity = $0.6854E-05$ cm²/s

Run No	Stirrer Speed (rpm)	Limiting Current (mA)	Sh	Re	Sc
1.01	0.0	0.2	10.6	0.0	1533.1
1.02	15.2	0.9	47.8	627.1	1533.1
1.03	58.8	7.7	409.0	2425.9	1533.1
1.04	116.5	15.8	839.2	4806.3	1533.1
1.05	131.0	18.0	956.0	5404.5	1533.1
1.06	161.8	21.3	1131.3	6675.2	1533.1

DATE 14-5-81
BATCH Batch 5 of 0.005M Potassium Ferricyanide/0.005M
Potassium Ferrocyanide/0.5M Sodium Hydroxide
solution prepared on 22-4-81

Potential = 0.8330 V
Solution Temperature = 18.0 C
Ferricyanide concentration = $0.477E-05$ mol/cm³
Density = 1.0245 g/cm³
Viscosity = 0.011619 g/cm s
Diffusivity = $0.6264E-05$ cm²/s

Run No	Stirrer Speed (rpm)	Limiting Current (mA)	Sh	Re	Sc
2.01	0.0	0.2	11.6	0.0	1810.4
2.02	27.3	2.9	168.5	1043.5	1810.4
2.03	40.5	4.5	264.4	1548.1	1810.4
2.04	59.1	6.4	371.9	2259.0	1810.4
2.05	71.4	8.0	467.8	2729.2	1810.4
2.06	90.6	10.3	598.5	3463.1	1810.4
2.07	103.1	12.1	703.1	3940.9	1810.4
2.08	115.2	13.2	767.0	4403.4	1810.4
2.09	125.5	14.8	860.0	4797.1	1810.4
2.10	146.0	16.5	958.8	5580.7	1810.4

DATE 14-5-81
 BATCH Batch 5 of 0.005M Potassium Ferricyanide/0.005M
 Potassium Ferrocyanide/0.5M Sodium Hydroxide
 solution prepared on 22-4-81

Potential = 0.8329 V
 Solution Temperature = 15.0 C
 Ferricyanide concentration = $0.477\text{E-}05$ mol/cm³
 Density = 1.0258 g/cm³
 Viscosity = 0.012437 g/cm s
 Diffusivity = $0.5791\text{E-}05$ cm²/s

Run No	Stirrer Speed (rpm)	Limiting Current (mA)	Sh	Re	Sc
3.01	0.0	0.3	18.9	0.0	2093.8
3.02	18.5	1.5	94.3	661.4	2093.8
3.03	38.0	2.3	144.6	1358.5	2093.8
3.04	68.2	5.5	348.8	2438.2	2093.8
3.05	89.6	7.5	474.5	3203.2	2093.8
3.06	113.9	9.9	625.4	4072.0	2093.8

TABLE A6.6.5.1 I_L-N DATA FOR THE ELECTROLYTIC MIXING CELL WITH THE PRESENCE OF 1 LAYER OF 1.34MM GLASS SPHERICAL PARTICLES ON THE CATHODE

DATE 30-1-81
BATCH Batch 3 of 0.005M Potassium Ferricyanide/0.005M Potassium Ferrocyanide/0.5M Sodium Hydroxide solution prepared on 15-1-81

Potential = 1.0000 V
Solution Temperature = 20.0 C
Ferricyanide concentration = 0.500E-05 mol/cm³
Density = 1.0236 g/cm³
Viscosity = 0.011111 g/cm s
Diffusivity = 0.6596E-05 cm²/s

Run No	Stirrer Speed (rpm)	Limiting Current (mA)	Sh	Re	Sc
1.01	0.0	0.5	26.3	0.0	1645.6
1.02	15.8	2.7	142.1	631.0	1645.6
1.03	25.2	4.7	250.1	1006.4	1645.6
1.04	36.2	5.9	310.6	1445.7	1645.6
1.05	47.5	8.4	442.2	1877.0	1645.6
1.06	60.2	10.9	573.8	2404.2	1645.6
1.07	65.4	14.0	737.0	2611.9	1645.6
1.08	87.7	16.2	852.9	3502.5	1645.6
1.09	100.3	18.6	979.2	4005.7	1645.6
1.10	114.4	21.0	1105.6	4568.8	1645.6
1.11	128.0	23.3	1226.7	5111.9	1645.6
1.12	143.0	25.8	1358.3	5711.0	1645.6

TABLE A6.6.5.2 I_L-N DATA FOR THE ELECTROLYTIC MIXING CELL WITH THE PRESENCE OF 2 LAYERS OF 1.34MM GLASS SPHERICAL PARTICLES ON THE CATHODE

DATE 8-2-81
BATCH Batch 4 of 0.005M Potassium Ferricyanide/0.005M Potassium Ferrocyanide/0.5M Sodium Hydroxide solution prepared on 15-1-81

Potential = 1.0000 V
Solution Temperature = 20.0 C
Ferricyanide concentration = 0.500E-05 mol/cm³
Density = 1.0236 g/cm³
Viscosity = 0.011111 g/cm s
Diffusivity = 0.6596E-05 cm²/s

Run No	Stirrer Speed (rpm)	Limiting Current (mA)	Sh	Re	Sc
1.01	0.0	0.3	18.4	0.0	1645.6
1.02	20.4	1.9	100.0	814.7	1645.6
1.03	38.0	5.0	263.2	1517.6	1645.6
1.04	47.1	6.6	350.1	1881.0	1645.6
1.05	59.1	8.9	468.6	2360.3	1645.6
1.06	74.3	11.6	610.7	2967.3	1645.6
1.07	80.3	12.8	673.9	3205.9	1645.6
1.08	98.8	16.0	842.3	3945.8	1645.6
1.09	116.3	18.8	989.8	4644.7	1645.6
1.10	127.9	21.4	1126.6	5108.0	1645.6
1.11	139.2	23.0	1210.9	5559.2	1645.6

TABLE A6.6.5.3 I_L-N DATA FOR THE ELECTROLYTIC MIXING
CELL WITH THE PRESENCE OF 3 LAYERS OF
1.34MM GLASS SPHERICAL PARTICLES ON
THE CATHODE

DATE 6-2-81
BATCH Batch 4 of 0.005M Potassium Ferricyanide/0.005M
Potassium Ferrocyanide/0.5M Sodium Hydroxide
solution prepared on 15-1-81

Potential = 1.0000 V
Solution temperature = 20.0 C
Ferricyanide concentration = 0.500E-05 mol/cm³
Density = 1.0236 g/cm³
Viscosity = 0.011111 g/cm s
Diffusivity = 0.6596E-05 cm²/s

Run No	Stirrer Speed (rpm)	Limiting Current (mA)	Sh	Re	Sc
1.01	0.0	0.2	10.5	0.0	1645.6
1.02	20.0	1.7	89.5	798.7	1645.6
1.03	32.8	3.3	176.4	1309.9	1645.6
1.04	44.3	5.2	276.4	1769.2	1645.6
1.05	62.0	8.2	431.7	2476.1	1645.6
1.06	69.4	9.5	500.1	2771.6	1645.6
1.07	76.6	10.6	558.1	3059.2	1645.6
1.08	83.3	11.7	616.0	3326.8	1645.6
1.09	89.8	12.7	668.6	3586.3	1645.6
1.10	104.3	14.8	779.2	4165.4	1645.6
1.11	114.9	16.1	847.6	4588.8	1645.6
1.12	125.0	17.6	926.6	4992.1	1645.6
1.13	140.8	20.0	1052.9	5623.1	1645.6

TABLE A6.6.5.4 I_L-N DATA FOR THE ELECTROLYTIC MIXING
CELL WITH THE PRESENCE OF 4 LAYERS OF
1.34MM GLASS SPHERICAL PARTICLES ON
THE CATHODE

DATE 9-2-81
BATCH Batch 4 of 0.005M Potassium Ferricyanide/0.005M
Potassium Ferrocyanide/0.5M Sodium Hydroxide
solution prepared on 15-1-81

Potential = 1.0000 V
Solution temperature = 20.0 C
Ferricyanide concentration = 0.500E-05 mol/cm³
Density = 1.0236 g/cm³
Viscosity = 0.011111 g/cm s
Diffusivity = 0.6596E-05 cm²/s

Run No	Stirrer Speed (rpm)	Limiting Current (mA)	Sh	Re	Sc
1.01	0.0	0.3	15.8	0.0	1645.6
1.02	18.3	1.0	52.6	730.8	1645.6
1.03	31.7	2.5	131.6	1266.0	1645.6
1.04	38.1	3.3	176.4	1521.6	1645.6
1.05	47.1	5.0	264.8	1881.0	1645.6
1.06	61.6	6.5	344.8	2460.1	1645.6
1.07	73.6	8.0	423.8	2939.4	1645.6
1.08	85.7	9.9	523.8	3422.6	1645.6
1.09	92.0	10.4	547.5	3674.2	1645.6
1.10	105.3	12.3	647.6	4205.4	1645.6
1.11	114.7	13.2	694.9	4580.8	1645.6
1.12	125.5	14.3	752.8	5012.1	1645.6
1.13	142.2	16.3	858.1	5679.1	1645.6

TABLE A6.6.5.5 I_L - N DATA FOR THE ELECTROLYTIC MIXING
CELL WITH THE PRESENCE OF 5 LAYERS OF
1.34MM GLASS SPHERICAL PARTICLES ON
THE CATHODE

DATE 10-2-81
BATCH Batch 4 of 0.005M Potassium Ferricyanide/0.005M
Potassium Ferrocyanide/0.5M Sodium Hydroxide
solution prepared on 15-1-81

Potential = 1.0000 V
Solution Temperature = 19.5 C
Ferricyanide concentration = 0.500E-05 mol/cm³
Density = 1.0238 g/cm³
Viscosity = 0.011235 g/cm s
Diffusivity = 0.6512E-05 cm²/s

Run No	Stirrer Speed (rpm)	Limiting Current (mA)	Sh	Re	Sc
1.01	0.0	0.3	16.0	0.0	1685.1
1.02	20.9	1.4	77.3	825.6	1685.1
1.03	31.1	2.5	133.3	1228.6	1685.1
1.04	44.1	4.2	224.0	1742.1	1685.1
1.05	61.9	6.4	341.3	2445.3	1685.1
1.06	70.2	7.4	394.6	2773.2	1685.1
1.07	77.2	8.1	431.9	3049.7	1685.1
1.08	88.6	9.5	506.6	3500.1	1685.1
1.09	105.6	11.3	602.6	4171.6	1685.1
1.10	127.1	13.7	730.6	5021.0	1685.1
1.11	144.6	15.2	810.6	5712.3	1685.1

TABLE A6.6.5.6 I_L - N DATA FOR THE ELECTROLYTIC MIXING
CELL WITH THE PRESENCE OF 6 LAYERS OF
1.34MM GLASS SPHERICAL PARTICLES ON
THE CATHODE

DATE 10-2-81
BATCH Batch 4 of 0.005M Potassium Ferricyanide/0.005M
Potassium Ferrocyanide/0.5M Sodium Hydroxide
solution prepared on 15-1-81

Potential = 1.0000 V
Solution Temperature = 19.5 C
Ferricyanide concentration = 0.500E-05 mol/cm³
Density = 1.0238 g/cm³
Viscosity = 0.011235 g/cm s
Diffusivity = 0.6512E-05 cm²/s

Run No	Stirrer Speed (rpm)	Limiting Current (mA)	Sh	Re	Sc
1.01	0.0	0.3	16.0	0.0	1685.1
1.02	27.3	1.9	101.3	1078.5	1685.1
1.03	42.6	3.5	186.6	1682.9	1685.1
1.04	68.0	6.2	330.6	2686.3	1685.1
1.05	80.0	7.6	405.3	3160.3	1685.1
1.06	92.0	8.8	469.3	3634.4	1685.1
1.07	104.3	10.1	538.6	4120.3	1685.1
1.08	125.0	11.9	634.6	4938.0	1685.1
1.09	141.8	13.1	698.6	5601.7	1685.1

TABLE A6.6.5.7 I_L - N DATA FOR THE ELECTROLYTIC MIXING
CELL WITH THE PRESENCE OF 7 LAYERS OF
1.34MM GLASS SPHERICAL PARTICLES ON
THE CATHODE

DATE 10-2-81
BATCH Batch 4 of 0.005M Potassium Ferricyanide/0.005M
Potassium Ferrocyanide/0.5M Sodium Hydroxide
solution prepared on 15-1-81

Potential = 1.0000 V
Solution Temperature = 20.0 C
Ferricyanide concentration = $0.500E-05$ mol/cm³
Density = 1.0236 g/cm³
Viscosity = 0.011111 g/cm s
Diffusivity = $0.6595E-05$ cm²/s

Run No	Stirrer Speed (rpm)	Limiting Current (mA)	Sh	Re	Sc
1.01	0.0	0.2	10.5	0.0	1645.6
1.02	25.8	1.5	81.6	1030.4	1645.6
1.03	36.6	3.1	163.2	1461.7	1645.6
1.04	63.4	5.4	286.9	2532.0	1645.6
1.05	74.3	6.5	343.3	2979.3	1645.6
1.06	87.7	7.8	413.3	3502.5	1645.6
1.07	98.5	8.9	469.1	3933.8	1645.6
1.08	115.4	10.5	552.8	4608.7	1645.6
1.09	130.4	11.8	621.2	5207.8	1645.6
1.10	144.9	12.6	663.3	5786.7	1645.6

TABLE A6.6.6.1 I_L-N DATA FOR THE ELECTROLYTIC MIXING CELL WITH THE PRESENCE OF 1 LAYER OF 1.55MM GLASS
SPHERICAL PARTICLES ON THE CATHODE

DATE 19-5-81
BATCH Batch 6 of 0.005M Potassium Ferricyanide/0.005M
Potassium Ferrocyanide/0.5M Sodium Hydroxide
solution prepared on 22-4-81

Potential = 0.8378 V
Solution Temperature = 18.0 C
Ferricyanide concentration = $0.477E-05$ mol/cm³
Density = 1.0245 g/cm³
Viscosity = 0.011619 g/cm s
Diffusivity = $0.6264E-05$ cm²/s

Run No	Stirrer Speed (rpm)	Limiting Current (mA)	Sh	Re	Sc
1.01	0.0	0.3	15.7	0.0	1810.4
1.02	22.0	2.9	169.7	840.9	1810.4
1.03	35.9	5.5	319.6	1372.2	1810.4
1.04	58.2	9.5	554.9	2224.6	1810.4
1.05	86.9	14.1	819.3	3321.7	1810.4
1.06	113.2	17.5	1016.9	4326.9	1810.4
1.07	143.4	21.4	1243.5	5481.3	1810.4

DATE 17-11-81
BATCH Batch 1 of 0.005M Potassium Ferricyanide/0.005M
Potassium Ferrocyanide/0.5M Sodium Hydroxide
solution prepared on 16-11-81

Potential = 0.9847 V
Solution Temperature = 14.7 C
Ferricyanide concentration = $0.477E-05$ mol/cm³
Density = 1.0259 g/cm³
Viscosity = 0.012525 g/cm s
Diffusivity = $0.5746E-05$ cm²/s

Run No	Stirrer Speed (rpm)	Limiting Current (mA)	Sh	Re	Sc
2.01	0.0	0.7	41.8	0.0	2124.8
2.02	12.2	1.4	86.2	433.2	2124.8
2.03	22.5	3.7	236.9	799.0	2124.8
2.04	45.3	8.3	525.8	1608.6	2124.8
2.05	51.9	9.7	614.5	1842.9	2124.8
2.06	68.9	12.6	798.3	2446.6	2124.8
2.07	84.9	15.9	1007.3	3014.7	2124.8
2.08	98.9	18.5	1172.1	3511.9	2124.8
2.09	139.5	23.4	1482.5	4953.5	2124.8
2.10	174.9	35.0	2217.4	6210.5	2124.8

DATE 17-11-81
 BATCH Batch 1 of 0.005M Potassium Ferricyanide/0.005M
 Potassium Ferrocyanide/0.5M Sodium Hydroxide
 solution prepared on 16-11-81

Potential = 0.9946 V
 Solution Temperature = 17.5 C
 Ferricyanide concentration = $0.477\text{E-}05$ mol/cm³
 Density = 1.0247 g/cm³
 Viscosity = 0.011751 g/cm s
 Diffusivity = $0.6184\text{E-}05$ cm²/s

Run No	Stirrer Speed (rpm)	Limiting Current (mA)	Sh	Re	Sc
3.01	0.0	0.6	38.3	0.0	1854.5
3.02	8.8	0.8	45.9	332.7	1854.5
3.03	16.0	3.4	200.1	604.9	1854.5
3.04	23.8	4.4	262.0	899.7	1854.5
3.05	26.2	5.0	294.3	990.5	1854.5
3.06	29.1	5.3	314.9	1100.1	1854.5
3.07	62.8	12.5	735.8	2374.1	1854.5
3.08	73.2	14.5	853.6	2767.2	1854.5
3.09	92.0	16.3	959.5	3477.9	1854.5
3.10	100.0	19.8	1165.6	3780.4	1854.5
3.11	107.1	21.1	1242.1	4048.8	1854.5
3.12	131.6	24.2	1424.6	4975.0	1854.5

DATE 17-11-81
 BATCH Batch 1 of 0.005M Potassium Ferricyanide/0.005M
 Potassium Ferrocyanide/0.5M Sodium Hydroxide
 solution prepared on 16-11-81

Potential = 0.9965 V
 Solution Temperature = 18.0 C
 Ferricyanide concentration = $0.477\text{E-}05$ mol/cm³
 Density = 1.0245 g/cm³
 Viscosity = 0.011619 g/cm s
 Diffusivity = $0.6264\text{E-}05$ cm²/s

Run No	Stirrer Speed (rpm)	Limiting Current (mA)	Sh	Re	Sc
4.01	0.0	0.6	34.9	0.0	1810.4
4.02	10.5	1.0	58.1	401.4	1810.4
4.03	24.3	4.1	238.2	928.8	1810.4
4.04	41.4	8.1	470.7	1582.5	1810.4
4.05	68.2	13.1	761.2	2606.9	1810.4
4.06	82.2	15.6	906.5	3142.0	1810.4
4.07	131.9	22.0	1278.4	5041.7	1810.4
4.08	139.5	25.0	1452.7	5332.2	1810.4

DATE 18-11-81
 BATCH Batch 1 of 0.005M Potassium Ferricyanide/0.005M
 Potassium Ferrocyanide/0.5M Sodium Hydroxide
 solution prepared on 16-11-81

Potential = 0.9916 V
 Solution Temperature = 18.0 C
 Ferricyanide concentration = 0.477E-05 mol/cm³
 Density = 1.0245 g/cm³
 Viscosity = 0.011619 g/cm s
 Diffusivity = 0.6264E-05 cm²/s

Run No	Stirrer Speed (rpm)	Limiting Current (mA)	Sh	Re	Sc
5.01	0.0	0.6	34.9	0.0	1810.4
5.02	7.8	0.7	41.8	298.1	1810.4
5.03	20.2	2.9	169.7	772.1	1810.4
5.04	28.0	4.5	264.4	1070.3	1810.4
5.05	40.2	7.2	418.4	1536.6	1810.4
5.06	44.1	7.9	459.0	1685.7	1810.4
5.07	56.6	10.3	598.5	2163.5	1810.4
5.08	68.2	12.5	726.3	2606.9	1810.4
5.09	75.9	14.0	813.5	2901.2	1810.4
5.10	96.0	17.0	987.8	3669.5	1810.4
5.11	104.4	18.2	1057.5	3990.6	1810.4
5.12	110.0	19.7	1144.7	4204.6	1810.4
5.13	115.4	20.5	1191.2	4411.0	1810.4
5.14	134.1	22.7	1319.0	5125.8	1810.4
5.15	142.2	24.3	1412.0	5435.4	1810.4
5.16	145.5	25.2	1464.3	5561.6	1810.4

TABLE A6.6.6.2 I_L - N DATA FOR THE ELECTROLYTIC MIXING CELL WITH THE PRESENCE OF 2 LAYERS OF 1.55MM GLASS

SPHERICAL PARTICLES ON THE CATHODE.

DATE 19-5-81
BATCH Batch 6 of 0.005M Potassium Ferricyanide/0.005M Potassium Ferrocyanide/0.5M Sodium Hydroxide solution prepared on 22-4-81

Potential = 0.8370 V
Solution Temperature = 17.0 C
Ferricyanide concentration = 0.477E-05 mol/cm³
Density = 1.0250 g/cm³
Viscosity = 0.011885 g/cm s
Diffusivity = 0.6104E-05 cm²/s

Run No	Stirrer Speed (rpm)	Limiting Current (mA)	Sh	Re	Sc
1.01	0.0	0.3	20.9	0.0	1899.7
1.02	15.4	2.0	122.3	575.8	1899.7
1.03	36.4	4.5	268.4	1360.9	1899.7
1.04	60.6	8.0	477.1	2265.6	1899.7
1.05	90.9	12.9	769.3	3398.4	1899.7
1.06	101.1	15.9	948.3	3779.8	1899.7

DATE 21-5-81
BATCH Batch 6 of 0.005M Potassium Ferricyanide/0.005M Potassium Ferrocyanide/0.5M Sodium Hydroxide solution prepared on 22-4-81

Potential = 0.8321 V
Solution Temperature = 18.0 C
Ferricyanide concentration = 0.477E-05 mol/cm³
Density = 1.0245 g/cm³
Viscosity = 0.011619 g/cm s
Diffusivity = 0.6264E-05 cm²/s

Run No	Stirrer Speed (rpm)	Limiting Current (mA)	Sh	Re	Sc
2.01	0.0	0.5	29.1	0.0	1810.4
2.02	10.7	0.8	46.5	409.0	1810.4
2.03	20.9	2.4	140.6	798.9	1810.4
2.04	33.9	4.6	270.2	1295.8	1810.4
2.05	57.1	8.4	491.0	2182.6	1810.4
2.06	66.3	10.5	610.1	2534.2	1810.4
2.07	71.4	11.4	662.4	2729.2	1810.4
2.08	89.6	14.1	819.3	3424.9	1810.4
2.09	112.5	18.2	1057.5	4300.2	1810.4
2.10	125.9	20.2	1173.8	4812.4	1810.4

DATE 18-11-81
 BATCH Batch 1 of 0.005M Potassium Ferricyanide/0.005M
 Potassium Ferrocyanide/0.5M Sodium Hydroxide
 solution prepared on 16-11-81

Potential = 0.9952 V
 Solution Temperature = 19.0 C
 Ferricyanide concentration = $0.477\text{E-}05$ mol/cm³
 Density = 1.0241 g/cm³
 Viscosity = 0.011361 g/cm s
 Diffusivity = $0.6429\text{E-}05$ cm²/s

Run No	Stirrer Speed (rpm)	Limiting Current (mA)	Sh	Re	Sc
3.01	0.0	0.3	19.8	0.0	1725.8
3.02	8.4	0.7	39.6	328.2	1725.8
3.03	33.0	4.8	271.8	1289.4	1725.8
3.04	51.3	8.7	492.6	2004.5	1725.8
3.05	62.5	10.8	611.5	2442.1	1725.8
3.06	75.0	13.4	758.7	2930.6	1725.8
3.07	93.0	15.5	877.7	3633.9	1725.8
3.08	111.1	19.2	1087.2	4341.1	1725.8
3.09	125.9	20.3	1149.4	4919.4	1725.8

DATE 19-11-81
 BATCH Batch 1 of 0.005M Potassium Ferricyanide/0.005M
 Potassium Ferrocyanide/0.5M Sodium Hydroxide
 solution prepared on 16-11-81

Potential = 0.9927 V
 Solution Temperature = 17.0 C
 Ferricyanide concentration = $0.477\text{E-}05$ mol/cm³
 Density = 1.0250 g/cm³
 Viscosity = 0.011885 g/cm s
 Diffusivity = $0.6104\text{E-}05$ cm²/s

Run No	Stirrer Speed (rpm)	Limiting Current (mA)	Sh	Re	Sc
4.01	0.0	0.3	17.9	0.0	1899.7
4.02	20.3	2.1	126.4	758.9	1899.7
4.03	27.7	3.9	231.4	1035.6	1899.7
4.04	57.1	9.6	575.5	2134.8	1899.7
4.05	67.4	11.0	656.0	2519.9	1899.7
4.06	79.5	13.5	805.1	2972.2	1899.7
4.07	89.6	15.3	912.5	3349.8	1899.7
4.08	108.1	17.7	1055.6	4041.5	1899.7

DATE 19-11-81
 BATCH Batch 1 of 0.005M Potassium Ferricyanide/0.005M
 Potassium Ferrocyanide/0.5M Sodium Hydroxide
 solution prepared on 16-11-81

Potential = 0.9965 V
 Solution Temperature = 18.0 C
 Ferricyanide concentration = $0.477\text{E-}05$ mol/cm³
 Density = 1.0245 g/cm³
 Viscosity = 0.011619 g/cm s
 Diffusivity = $0.6264\text{E-}05$ cm²/s

Run No	Stirrer Speed (rpm)	Limiting Current (mA)	Sh	Re	Sc
5.01	0.0	0.3	15.7	0.0	1810.4
5.02	14.4	1.2	72.6	550.4	1810.4
5.03	30.9	4.5	262.6	1181.1	1810.4
5.04	60.0	9.4	549.1	2293.4	1810.4
5.05	62.8	10.1	586.9	2400.5	1810.4
5.06	65.2	10.6	615.9	2492.2	1810.4
5.07	73.6	12.3	714.7	2813.3	1810.4
5.08	83.3	13.7	796.1	3184.1	1810.4
5.09	93.8	15.3	889.0	3585.4	1810.4
5.10	112.7	18.2	1057.5	4307.8	1810.4
5.11	119.4	19.7	1144.7	4563.9	1810.4

DATE 19-11-81
 BATCH Batch 1 of 0.005M Potassium Ferricyanide/0.005M
 Potassium Ferrocyanide/0.5M Sodium Hydroxide
 solution prepared on 16-11-81

Potential = 0.9971 V
 Solution Temperature = 18.0 C
 Ferricyanide concentration = $0.477\text{E-}05$ mol/cm³
 Density = 1.0245 g/cm³
 Viscosity = 0.011619 g/cm s
 Diffusivity = $0.6264\text{E-}05$ cm²/s

Run No	Stirrer Speed (rpm)	Limiting Current (mA)	Sh	Re	Sc
6.01	0.0	0.4	20.9	0.0	1810.4
6.02	7.3	0.4	25.6	279.0	1810.4
6.03	17.4	1.8	107.5	665.1	1810.4
6.04	42.3	6.6	383.5	1616.9	1810.4
6.05	55.0	9.3	540.4	2102.3	1810.4
6.06	65.2	10.8	627.6	2492.2	1810.4
6.07	75.0	12.7	738.0	2866.8	1810.4
6.08	83.9	14.6	848.4	3207.0	1810.4
6.09	99.4	17.1	993.6	3799.5	1810.4
6.10	115.4	19.5	1133.1	4411.0	1810.4
6.11	124.3	20.7	1202.8	4751.2	1810.4
6.12	133.3	21.5	1249.3	5095.3	1810.4

TABLE A6.6.6.3 I_L - N DATA FOR THE ELECTROLYTIC MIXING CELL WITH THE PRESENCE OF 3 LAYERS OF 1.55MM GLASS
SPHERICAL PARTICLES ON THE CATHODE

DATE 21-5-81
BATCH Batch 6 of 0.005M Potassium Ferricyanide/0.005M
Potassium Ferrocyanide/0.5M Sodium Hydroxide
solution prepared on 22-4-81

Potential = 0.8373 V
Solution Temperature = 19.0 C
Ferricyanide concentration = $0.477E-05$ mol/cm³
Density = 1.0241 g/cm³
Viscosity = 0.011361 g/cm s
Diffusivity = $0.6429E-05$ cm²/s

Run No	Stirrer Speed (rpm)	Limiting Current (mA)	Sh	Re	Sc
1.01	0.0	0.3	17.0	0.0	1725.8
1.02	25.3	2.7	152.9	988.6	1725.8
1.03	35.7	4.1	235.0	1394.9	1725.8
1.04	68.2	9.2	523.8	2664.9	1725.8
1.05	86.3	12.1	685.1	3372.1	1725.8
1.06	92.8	13.3	753.1	3626.1	1725.8
1.07	104.0	14.7	832.4	4063.7	1725.8
1.08	124.1	18.0	1019.2	4849.1	1725.8

DATE 1-12-81
BATCH Batch 2 of 0.005M Potassium Ferricyanide/0.005M
Potassium Ferrocyanide/0.5M Sodium Hydroxide
solution prepared on 16-11-81

Potential = 0.9920 V
Solution Temperature = 18.0 C
Ferricyanide concentration = $0.477E-05$ mol/cm³
Density = 1.0245 g/cm³
Viscosity = 0.011619 g/cm s
Diffusivity = $0.6264E-05$ cm²/s

Run No	Stirrer Speed (rpm)	Limiting Current (mA)	Sh	Re	Sc
2.01	0.0	0.3	20.3	0.0	1810.4
2.02	27.8	3.6	209.2	1062.6	1810.4
2.03	49.0	7.1	415.5	1873.0	1810.4
2.04	58.8	9.0	521.2	2247.6	1810.4
2.05	69.8	11.5	668.2	2668.0	1810.4
2.06	84.5	13.3	772.8	3229.9	1810.4
2.07	102.2	16.0	929.7	3906.5	1810.4
2.08	119.0	18.3	1063.4	4548.6	1810.4
2.09	138.7	21.1	1226.1	5301.7	1810.4

DATE 1-12-81
 BATCH Batch 2 of 0.005M Potassium Ferricyanide/0.005M
 Potassium Ferrocyanide/0.5M Sodium Hydroxide
 solution prepared on 16-11-81

Potential = 0.9992 V
 Solution Temperature = 18.0 C
 Ferricyanide concentration = $0.477\text{E-}05$ mol/cm³
 Density = 1.0245 g/cm³
 Viscosity = 0.011619 g/cm s
 Diffusivity = $0.6264\text{E-}05$ cm²/s

Run No	Stirrer Speed (rpm)	Limiting Current (mA)	Sh	Re	Sc
3.01	0.0	0.3	19.2	0.0	1810.4
3.02	13.3	1.5	90.1	508.4	1810.4
3.03	23.8	3.0	174.3	909.7	1810.4
3.04	29.4	3.5	203.4	1123.8	1810.4
3.05	52.2	7.6	441.6	1995.3	1810.4
3.06	59.4	9.4	549.1	2270.5	1810.4
3.07	75.3	12.0	697.3	2878.3	1810.4
3.08	88.2	14.4	836.7	3371.4	1810.4
3.09	99.4	15.7	912.3	3799.5	1810.4
3.10	124.6	19.3	1121.5	4762.7	1810.4

DATE 2-12-81
 BATCH Batch 2 of 0.005M Potassium Ferricyanide/0.005M
 Potassium Ferrocyanide/0.5M Sodium Hydroxide
 solution prepared on 16-11-81

Potential = 0.9916 V
 Solution Temperature = 14.0 C
 Ferricyanide concentration = $0.477\text{E-}05$ mol/cm³
 Density = 1.0262 g/cm³
 Viscosity = 0.012728 g/cm s
 Diffusivity = $0.5640\text{E-}05$ cm²/s

Run No	Stirrer Speed (rpm)	Limiting Current (mA)	Sh	Re	Sc
4.01	0.0	0.4	24.5	0.0	2199.1
4.02	9.3	0.8	49.7	325.0	2199.1
4.03	16.4	1.4	93.6	573.2	2199.1
4.04	28.8	3.0	196.8	1006.6	2199.1
4.05	53.6	7.0	450.5	1873.4	2199.1
4.06	62.5	8.3	538.9	2184.4	2199.1
4.07	70.6	9.8	635.7	2467.5	2199.1
4.08	75.9	11.2	722.9	2652.8	2199.1
4.09	92.3	12.8	826.1	3226.0	2199.1
4.10	101.1	14.1	910.0	3533.5	2199.1
4.11	107.8	14.8	955.2	3767.7	2199.1
4.12	113.7	15.5	1000.4	3973.9	2199.1
4.13	121.8	16.7	1077.8	4257.0	2199.1
4.14	138.2	18.3	1181.1	4830.2	2199.1
4.15	131.6	18.9	1219.8	4599.5	2199.1
4.16	147.0	19.9	1284.4	5137.8	2199.1

DATE 2-12-81
 BATCH Batch 2 of 0.005M Potassium Ferricyanide/0.005M
 Potassium Ferrocyanide/0.5M Sodium Hydroxide
 solution prepared on 16-11-81

Potential = 0.9950 V
 Solution Temperature = 14.0 C
 Ferricyanide concentration = $0.477\text{E-}05$ mol/cm³
 Density = 1.0262 g/cm³
 Viscosity = 0.012728 g/cm s
 Diffusivity = $0.5640\text{E-}05$ cm²/s

Run No	Stirrer Speed (rpm)	Limiting Current (mA)	Sh	Re	Sc
5.01	0.0	0.3	16.8	0.0	2199.1
5.02	13.9	1.1	71.0	485.8	2199.1
5.03	20.0	2.1	138.8	699.0	2199.1
5.04	37.5	4.3	279.5	1310.7	2199.1
5.05	60.0	8.4	545.4	2097.1	2199.1
5.06	77.9	10.8	697.0	2722.7	2199.1
5.07	106.2	14.0	903.6	3711.8	2199.1
5.08	117.6	16.4	1058.5	4110.2	2199.1
5.09	134.5	18.6	1200.5	4700.9	2199.1

TABLE A6.6.6.4 I_L - N DATA FOR THE ELECTROLYTIC MIXING CELL WITH THE PRESENCE OF 4 LAYERS OF 1.55MM GLASS
SPHERICAL PARTICLES ON THE CATHODE

DATE 21-5-81
BATCH Batch 6 of 0.005M Potassium Ferricyanide/0.005M
Potassium Ferrocyanide/0.5M Sodium Hydroxide
solution prepared on 22-4-81

Potential = 0.8389 V
Solution Temperature = 20.0 C
Ferricyanide concentration = $0.477E-05$ mol/cm³
Density = 1.0236 g/cm³
Viscosity = 0.011111 g/cm s
Diffusivity = $0.6596E-05$ cm²/s

Run No	Stirrer Speed (rpm)	Limiting Current (mA)	Sh	Re	Sc
1.01	0.0	0.4	22.1	0.0	1645.6
1.02	12.4	1.4	77.3	495.2	1645.6
1.03	31.7	6.6	365.3	2064.7	1645.6
1.04	61.2	8.7	480.1	2444.1	1645.6
1.05	85.1	12.0	662.2	3398.6	1645.6
1.06	106.5	15.3	844.3	4253.3	1645.6
1.07	116.1	16.2	894.0	4636.7	1645.6

DATE 2-12-81
BATCH Batch 2 of 0.005M Potassium Ferricyanide/0.005M
Potassium Ferrocyanide/0.5M Sodium Hydroxide
solution prepared on 16-11-81

Potential = 0.9960 V
Solution Temperature = 18.0 C
Ferricyanide concentration = $0.477E-05$ mol/cm³
Density = 1.0245 g/cm³
Viscosity = 0.011619 g/cm s
Diffusivity = $0.6264E-05$ cm²/s

Run No	Stirrer Speed (rpm)	Limiting Current (mA)	Sh	Re	Sc
2.01	0.0	0.3	16.3	0.0	1810.4
2.02	47.6	7.6	441.6	1819.5	1810.4
2.03	63.5	9.8	569.4	2427.2	1810.4
2.04	81.1	13.0	755.4	3100.0	1810.4
2.05	85.1	13.8	801.9	3252.9	1810.4
2.06	94.2	15.1	877.4	3600.7	1810.4
2.07	100.4	15.9	923.9	3837.7	1810.4
2.08	104.9	16.6	964.6	4009.7	1810.4
2.09	112.4	17.8	1034.3	4296.4	1810.4
2.10	119.0	18.9	1098.2	4548.6	1810.4

DATE 2-12-81
 BATCH Batch 2 of 0.005M Potassium Ferricyanide/0.005M
 Potassium Ferrocyanide/0.5M Sodium Hydroxide
 solution prepared on 16-11-81

Potential = 0.9960 V
 Solution Temperature = 19.0 C
 Ferricyanide concentration = $0.477\text{E-}05$ mol/cm³
 Density = 1.0241 g/cm³
 Viscosity = 0.011361 g/cm s
 Diffusivity = $0.6429\text{E-}05$ cm²/s

Run No	Stirrer Speed (rpm)	Limiting Current (mA)	Sh	Re	Sc
3.01	60.0	10.7	605.9	2344.4	1725.8
3.02	70.5	11.1	628.5	2754.7	1725.8
3.03	84.2	13.6	770.1	3290.0	1725.8
3.04	89.1	14.4	815.4	3481.5	1725.8
3.05	101.4	16.5	934.3	3962.1	1725.8
3.06	106.4	16.7	945.6	4157.5	1725.8
3.07	115.5	17.7	1002.2	4513.1	1725.8

DATE 2-12-81
 BATCH Batch 2 of 0.005M Potassium Ferricyanide/0.005M
 Potassium Ferrocyanide/0.5M Sodium Hydroxide
 solution prepared on 16-11-81

Potential = 0.9960 V
 Solution Temperature = 19.0 C
 Ferricyanide concentration = $0.477\text{E-}05$ mol/cm³
 Density = 1.0241 g/cm³
 Viscosity = 0.011361 g/cm s
 Diffusivity = $0.6429\text{E-}05$ cm²/s

Run No	Stirrer Speed (rpm)	Limiting Current (mA)	Sh	Re	Sc
4.01	88.9	14.3	809.7	3473.7	1725.8
4.02	89.6	14.6	826.7	3501.0	1725.8
4.03	94.7	15.0	849.3	3700.3	1725.8
4.04	100.4	16.3	923.0	3923.0	1725.8
4.05	107.5	17.2	973.9	4200.5	1725.8
4.06	115.4	18.2	1030.5	4509.1	1725.8
4.07	119.5	18.8	1064.5	4669.3	1725.8
4.08	124.1	19.2	1087.2	4849.1	1725.8

DATE 2-12-81
 BATCH Batch 2 of 0.005M Potassium Ferricyanide/0.005M
 Potassium Ferrocyanide/0.5M Sodium Hydroxide
 solution prepared on 16-11-81

Potential = 0.9960 V
 Solution Temperature = 19.0 C
 Ferricyanide concentration = $0.477\text{E-}05$ mol/cm³
 Density = 1.0241 g/cm³
 Viscosity = 0.011361 g/cm s
 Diffusivity = $0.6429\text{E-}05$ cm²/s

Run No	Stirrer Speed (rpm)	Limiting Current (mA)	Sh	Re	Sc
5.01	56.6	9.3	526.6	2211.6	1725.8
5.02	72.7	12.0	679.5	2840.7	1725.8
5.03	91.4	14.6	826.7	3571.4	1725.8
5.04	109.7	17.2	973.9	4286.4	1725.8

DATE 2-12-81
 BATCH Batch 2 of 0.005M Potassium Ferricyanide/0.005M
 Potassium Ferrocyanide/0.5M Sodium Hydroxide
 solution prepared on 16-11-81

Potential = 0.9960 V
 Solution Temperature = 20.0 C
 Ferricyanide concentration = $0.477\text{E-}05$ mol/cm³
 Density = 1.0236 g/cm³
 Viscosity = 0.011111 g/cm s
 Diffusivity = $0.6596\text{E-}05$ cm²/s

Run No	Stirrer Speed (rpm)	Limiting Current (mA)	Sh	Re	Sc
6.01	9.5	1.3	71.7	379.4	1645.6
6.02	28.5	3.4	187.6	1138.2	1645.6
6.03	60.6	9.6	529.8	2420.2	1645.6
6.04	74.1	11.7	645.7	2959.3	1645.6
6.05	90.0	14.5	800.2	3594.3	1645.6
6.06	95.2	15.6	860.9	3802.0	1645.6
6.07	112.1	17.8	982.3	4476.9	1645.6
6.08	127.6	19.2	1059.5	5096.0	1645.6
6.09	153.2	20.5	1131.3	6118.4	1645.6

TABLE A6.6.6.5 I_L - N DATA FOR THE ELECTROLYTIC MIXING CELL WITH THE PRESENCE OF 5 LAYERS OF 1.55MM GLASS
SPHERICAL PARTICLES ON THE CATHODE

DATE 3-12-81
BATCH Batch 2 of 0.005M Potassium Ferricyanide/0.005M Potassium Ferrocyanide/0.5M Sodium Hydroxide solution prepared on 16-11-81

Potential = 0.9910 V
Solution Temperature = 19.0 C
Ferricyanide concentration = 0.477E-05 mol/cm³
Density = 1.0241 g/cm³
Viscosity = 0.011361 g/cm s
Diffusivity = 0.6429E-05 cm²/s

Run No	Stirrer Speed (rpm)	Limiting Current (mA)	Sh	Re	Sc
1.01	0.0	0.3	17.0	0.0	1725.8
1.02	14.2	1.5	86.1	554.9	1725.8
1.03	23.8	2.5	141.6	930.0	1725.8
1.04	38.0	5.0	283.1	1484.8	1725.8
1.05	50.8	7.2	410.5	1985.0	1725.8
1.06	61.9	9.2	520.9	2418.7	1725.8
1.07	68.2	10.3	583.2	2664.9	1725.8
1.08	77.9	11.8	648.2	3043.9	1725.8
1.09	82.6	12.5	707.8	3227.5	1725.8
1.10	94.2	14.1	798.4	3680.8	1725.8
1.11	102.9	15.4	872.0	4020.7	1725.8
1.12	110.0	16.7	945.6	4298.1	1725.8
1.13	119.0	17.5	990.9	4649.8	1725.8
1.14	123.5	17.7	1002.2	4825.6	1725.8
1.15	129.9	19.2	1087.2	5075.7	1725.8

DATE 3-12-81
BATCH Batch 2 of 0.005M Potassium Ferricyanide/0.005M Potassium Ferrocyanide/0.5M Sodium Hydroxide solution prepared on 16-11-81

Potential = 0.9910 V
Solution Temperature = 19.0 C
Ferricyanide concentration = 0.477E-05 mol/cm³
Density = 1.0241 g/cm³
Viscosity = 0.011361 g/cm s
Diffusivity = 0.6429E-05 cm²/s

Run No	Stirrer Speed (rpm)	Limiting Current (mA)	Sh	Re	Sc
2.01	75.5	11.7	662.5	2950.1	1725.8
2.02	89.1	13.6	770.1	3481.5	1725.8
2.03	106.0	15.7	889.0	4141.8	1725.8
2.04	114.9	17.3	979.6	4489.6	1725.8
2.05	120.5	18.1	1024.9	4708.4	1725.8
2.06	125.6	18.8	1064.5	4907.7	1725.8

DATE 3-12-81
 BATCH Batch 2 of 0.005M Potassium Ferricyanide/0.005M
 Potassium Ferrocyanide/0.5M Sodium Hydroxide
 solution prepared on 16-11-81

Potential = 0.9910 V
 Solution Temperature = 19.0 C
 Ferricyanide concentration = $0.477\text{E-}05$ mol/cm³
 Density = 1.0241 g/cm³
 Viscosity = 0.011361 g/cm s
 Diffusivity = $0.6429\text{E-}05$ cm²/s

Run No	Stirrer Speed (rpm)	Limiting Current (mA)	Sh	Re	Sc
3.01	27.4	3.1	175.5	1070.6	1725.8
3.02	56.3	8.0	453.0	2199.9	1725.8
3.03	69.8	10.4	588.9	2727.4	1725.8
3.04	77.2	11.7	662.5	3016.5	1725.8
3.05	91.8	12.9	730.4	3587.0	1725.8
3.06	97.3	14.9	843.7	3801.9	1725.8
3.07	104.0	15.6	883.3	4063.7	1725.8
3.08	107.8	16.4	928.6	4212.2	1725.8
3.09	115.4	17.3	979.6	4509.1	1725.8
3.10	118.4	17.7	1002.2	4626.4	1725.8
3.11	128.6	18.4	1041.9	5024.9	1725.8

DATE 3-12-81
 BATCH Batch 2 of 0.005M Potassium Ferricyanide/0.005M
 Potassium Ferrocyanide/0.5M Sodium Hydroxide
 solution prepared on 16-11-81

Potential = 0.9910 V
 Solution Temperature = 20.0 C
 Ferricyanide concentration = $0.477\text{E-}05$ mol/cm³
 Density = 1.0236 g/cm³
 Viscosity = 0.011111 g/cm s
 Diffusivity = $0.6596\text{E-}05$ cm²/s

Run No	Stirrer Speed (rpm)	Limiting Current (mA)	Sh	Re	Sc
4.01	48.8	7.0	386.3	1948.9	1645.6
4.02	70.0	10.5	579.4	2795.6	1645.6
4.03	75.6	11.5	634.6	3019.2	1645.6
4.04	84.9	12.9	711.9	3390.7	1645.6
4.05	85.7	13.0	717.4	3422.6	1645.6
4.06	88.2	13.5	745.0	3522.5	1645.6
4.07	90.5	13.6	750.5	3614.3	1645.6
4.08	97.3	15.1	833.3	3885.9	1645.6
4.09	97.8	14.9	822.3	3905.8	1645.6
4.10	98.9	15.4	849.8	3949.8	1645.6
4.11	103.4	15.9	877.4	4129.5	1645.6
4.12	107.1	16.6	916.1	4277.3	1645.6
4.13	109.1	16.6	916.1	4357.1	1645.6
4.14	110.4	17.1	943.7	4409.1	1645.6
4.15	116.1	17.8	982.3	4636.7	1645.6
4.16	120.8	17.9	987.8	4824.4	1645.6
4.17	125.9	18.7	1032.0	5028.1	1645.6

TABLE A6.6.6.6 I_L - N DATA FOR THE ELECTROLYTIC MIXING CELL WITH THE PRESENCE OF 6 LAYERS OF 1.55MM GLASS

SPHERICAL PARTICLES ON THE CATHODE

DATE 8-12-81
 BATCH Batch 2 of 0.005M Potassium Ferricyanide/0.005M
 Potassium Ferrocyanide/0.5M Sodium Hydroxide
 solution prepared on 16-11-81

Potential = 0.9924 V
 Solution Temperature = 19.0 C
 Ferricyanide concentration = $0.477E-05$ mol/cm³
 Density = 1.0241 g/cm³
 Viscosity = 0.011361 g/cm s
 Diffusivity = $0.6429E-05$ cm²/s

Run No	Stirrer Speed (rpm)	Limiting Current (mA)	Sh	Re	Sc
1.01	0.0	0.3	17.0	0.0	1725.8
1.02	26.8	2.9	164.2	1047.2	1725.8
1.03	54.5	7.3	413.3	2129.5	1725.8
1.04	56.1	7.5	424.7	2192.1	1725.8
1.05	62.5	8.6	487.0	2442.1	1725.8
1.06	74.1	10.8	611.5	2895.4	1725.8
1.07	90.9	13.0	736.1	3551.8	1725.8
1.08	100.8	13.8	781.4	3938.7	1725.8
1.09	104.3	14.3	809.7	4075.4	1725.8
1.10	114.6	15.7	889.0	4477.9	1725.8
1.11	122.4	16.9	956.9	4782.7	1725.8
1.12	128.3	17.3	979.6	5013.2	1725.8
1.13	134.5	18.1	1024.9	5255.5	1725.8

DATE 8-12-81
 BATCH Batch 2 of 0.005M Potassium Ferricyanide/0.005M
 Potassium Ferrocyanide/0.5M Sodium Hydroxide
 solution prepared on 16-11-81

Potential = 0.9924 V
 Solution Temperature = 19.0 C
 Ferricyanide concentration = $0.477E-05$ mol/cm³
 Density = 1.0241 g/cm³
 Viscosity = 0.011361 g/cm s
 Diffusivity = $0.6429E-05$ cm²/s

Run No	Stirrer Speed (rpm)	Limiting Current (mA)	Sh	Re	Sc
2.01	53.1	7.4	419.0	2074.8	1725.8
2.02	60.0	8.0	453.0	2344.4	1725.8
2.03	67.4	9.1	515.3	2633.6	1725.8
2.04	71.4	9.9	560.6	2789.9	1725.8
2.05	81.6	11.3	639.8	3188.4	1725.8
2.06	96.8	13.5	764.4	3782.4	1725.8
2.07	108.1	14.8	838.0	4223.9	1725.8
2.08	112.1	15.7	889.0	4380.2	1725.8
2.09	113.5	15.7	889.0	4434.9	1725.8
2.10	119.2	16.3	923.0	4657.6	1725.8
2.11	135.1	19.3	1092.8	5278.9	1725.8
2.12	138.5	17.5	990.9	5411.8	1725.8

TABLE A6.6.7.1.1 I_L-N DATA FOR THE ELECTROLYTIC MIXING CELL WITH THE PRESENCE OF 1 LAYER OF 3MM GLASS
SPHERICAL PARTICLES ON THE CATHODE DERIVED FROM FIGURE 4.6

Run No	Potential (volts)	Stirrer Speed (rpm)	Limiting Current (mA)	Solution Temp. (C)	Ferricyanide Concentration (mol/cm ³)	Density (g/cm ³)	Viscosity (g/cm s)	Diffusivity (cm ² /s)	Sh	Re	Sc
1.01	1.0730	29.9	5.0	20.0	0.477E-05	1.0236	0.01111	0.660E-05	278.2	1194.1	1645.6
1.02	1.0608	66.3	11.7	20.0	0.477E-05	1.0236	0.01111	0.660E-05	645.7	2647.8	1645.6
1.03	1.0228	85.9	15.5	21.0	0.477E-05	1.0231	0.01087	0.677E-05	833.8	3505.8	1569.6
1.04	1.0248	123.4	23.8	21.0	0.477E-05	1.0231	0.01087	0.677E-05	1280.4	5036.3	1569.6
1.05	0.9890	175.4	34.0	21.0	0.477E-05	1.0231	0.01087	0.677E-05	1829.1	7158.6	1569.6
1.06	1.0360	200.0	38.5	21.0	0.477E-05	1.0231	0.01087	0.677E-05	2071.2	8162.6	1569.6

TABLE A6.6.7.1.2 I_L - N DATA FOR THE ELECTROLYTIC MIXING CELL WITH THE PRESENCE OF 1 LAYER OF 3MM GLASS
SPHERICAL PARTICLES ON THE CATHODE 'OBTAINED' FROM SEVERAL RUNS

DATE 19-2-81
BATCH Batch 5 of 0.005M Potassium Ferricyanide/0.005M
Potassium Ferrocyanide/0.5M Sodium Hydroxide
solution prepared on 15-1-81

Potential = 1.0000 V
Solution Temperature = 19.5 C
Ferricyanide concentration = 0.500E-05 mol/cm³
Density = 1.0238 g/cm³
Viscosity = 0.011035 g/cm s
Diffusivity = 0.6512E-05 cm²/s

Run No	Stirrer Speed (rpm)	Limiting Current (mA)	Sh	Re	Sc
1.01	0.0	0.3	18.7	0.0	1685.1
1.02	24.5	5.5	293.3	967.8	1685.1
1.03	34.9	7.8	418.6	1378.7	1685.1
1.04	48.9	11.0	586.6	1927.8	1685.1
1.05	62.5	14.0	746.6	2469.0	1685.1
1.06	79.7	17.8	949.2	3148.5	1685.1
1.07	95.2	20.9	1114.5	3681.8	1685.1
1.08	107.1	24.3	1295.8	4230.9	1685.1
1.09	123.0	27.7	1477.2	4859.0	1685.1
1.10	135.1	30.7	1637.1	5337.0	1685.1
1.11	153.6	35.0	1866.4	6075.7	1685.1
1.12	175.4	39.5	2106.4	6929.0	1685.1
1.13	186.1	42.2	2250.4	7351.7	1685.1

DATE 27-4-81
BATCH Batch 2 of 0.005M Potassium Ferricyanide/0.005M
Potassium Ferrocyanide/0.5M Sodium Hydroxide
solution prepared on 22-4-81

Potential = 0.8410 V
Solution Temperature = 14.0 C
Ferricyanide concentration = 0.477E-05 mol/cm³
Density = 1.0262 g/cm³
Viscosity = 0.012728 g/cm s
Diffusivity = 0.5640E-05 cm²/s

Run No	Stirrer Speed (rpm)	Limiting Current (mA)	Sh	Re	Sc
2.01	0.0	0.7	47.8	0.0	2199.1
2.02	8.2	2.1	135.5	286.6	2199.1
2.03	27.7	6.1	393.7	968.1	2199.1
2.04	58.3	10.6	684.1	2037.6	2199.1
2.05	101.5	16.2	1045.6	3547.5	2199.1
2.06	127.1	18.7	1204.3	4442.3	2199.1
2.07	148.1	20.3	1310.2	5176.2	2199.1
2.08	175.3	23.8	1536.1	6126.9	2199.1

DATE 5-5-81
 BATCH Batch 4 of 0.005M Potassium Ferricyanide/0.005M
 Potassium Ferrocyanide/0.5M Sodium Hydroxide
 solution prepared on 22-4-81

Potential = 0.8413 V
 Solution Temperature = 16.0 C
 Ferricyanide concentration = $0.477\text{E-}05$ mol/cm³
 Density = 1.0254 g/cm³
 Viscosity = 0.012158 g/cm s
 Diffusivity = $0.5946\text{E-}05$ cm²/s

Run No	Stirrer Speed (rpm)	Limiting Current (mA)	Sh	Re	Sc
3.01	0.0	0.4	24.5	0.0	1994.1
3.02	9.6	1.6	96.1	351.0	1994.1
3.03	34.7	6.8	419.4	1268.7	1994.1
3.04	50.8	10.2	624.5	1857.4	1994.1
3.05	70.4	13.3	814.2	2574.0	1994.1
3.06	89.6	16.7	1022.4	3276.0	1994.1
3.07	110.7	20.5	1255.0	4047.4	1994.1
3.08	134.8	24.3	1487.7	4928.6	1994.1
3.09	148.5	27.7	1695.8	5429.5	1994.1
3.10	177.3	31.7	1940.7	6482.5	1994.1
3.11	199.3	35.0	2142.7	7286.8	1994.1
3.12	238.0	39.5	2418.2	8701.8	1994.1

DATE 24-7-81
 BATCH Batch 6 of 0.005M Potassium Ferricyanide/0.005M
 Potassium Ferrocyanide/0.5M Sodium Hydroxide
 solution prepared on 27-5-81

Potential = 0.8414 V
 Solution Temperature = 14.0 C
 Ferricyanide concentration = $0.497\text{E-}05$ mol/cm³
 Density = 1.0262 g/cm³
 Viscosity = 0.012728 g/cm s
 Diffusivity = $0.5640\text{E-}05$ cm²/s

Run No	Stirrer Speed (rpm)	Limiting Current (mA)	Sh	Re	Sc
4.01	0.0	0.2	14.1	0.0	2199.1
4.02	63.6	12.3	761.9	2222.9	2199.1
4.03	73.5	14.3	885.8	2568.9	2199.1
4.04	89.7	17.5	1084.0	3135.1	2199.1
4.05	115.8	21.7	1344.2	4047.3	2199.1
4.06	153.1	29.0	1796.4	5351.0	2199.1
4.07	178.6	32.6	2019.4	6242.2	2199.1
4.08	200.0	36.8	2279.5	6990.2	2199.1
4.09	223.0	40.3	2496.3	7794.1	2199.1
4.10	256.4	45.4	2812.2	8961.4	2199.1
4.11	280.4	49.3	3053.8	9800.2	2199.1

DATE 25-9-81
 BATCH Batch 1 of 0.005M Potassium Ferricyanide/0.005M
 Potassium Ferrocyanide/0.5M Sodium Hydroxide
 solution prepared on 24-9-81

Potential = 1.0010 V
 Solution temperature = 18.0 C
 Ferricyanide concentration = 0.500E-05 mol/cm³
 Density = 1.0245 g/cm³
 Viscosity = 0.011619 g/cm s
 Diffusivity = 0.6264E-05 cm²/s

Run No	Stirrer Speed (rpm)	Limiting Current (mA)	Sh	Re	Sc
5.01	0.0	0.5	26.6	0.0	1810.4
5.02	19.7	5.3	296.6	753.0	1810.4
5.03	27.0	7.2	399.1	1032.0	1810.4
5.04	59.7	16.0	886.9	2282.0	1810.4
5.05	65.7	18.0	997.8	2511.3	1810.4
5.06	86.5	23.4	1297.2	3306.4	1810.4
5.07	108.7	28.7	1591.0	4154.9	1810.4
5.08	121.3	32.2	1785.0	4636.6	1810.4
5.09	144.9	38.5	2134.2	5538.6	1810.4
5.10	171.9	45.1	2500.1	6570.7	1810.4
5.11	189.3	49.4	2738.4	7235.8	1810.4
5.12	217.9	56.5	3132.0	8329.0	1810.4

DATE 28-9-81
 BATCH Batch 1 of 0.005M Potassium Ferricyanide/0.005M
 Potassium Ferrocyanide/0.5M Sodium Hydroxide
 solution prepared on 24-9-81

Potential = 0.9965 V
 Solution temperature = 17.0 C
 Ferricyanide concentration = 0.500E-05 mol/cm³
 Density = 1.0250 g/cm³
 Viscosity = 0.011885 g/cm s
 Diffusivity = 0.6104E-05 cm²/s

Run No	Stirrer Speed (rpm)	Limiting Current (mA)	Sh	Re	Sc
6.01	0.0	0.4	22.8	0.0	1899.7
6.02	27.0	6.9	392.6	1009.4	1899.7
6.03	34.5	9.7	551.9	1289.8	1899.7
6.04	64.6	16.7	950.2	2415.2	1899.7
6.05	71.8	18.3	1041.2	2684.4	1899.7
6.06	86.1	21.8	1240.3	3219.0	1899.7
6.07	100.5	25.2	1433.8	3757.4	1899.7
6.08	114.4	28.3	1610.1	4277.0	1899.7
6.09	138.2	34.6	1968.6	5166.8	1899.7
6.10	157.9	39.3	2236.0	5903.4	1899.7
6.11	173.4	42.6	2423.8	6482.9	1899.7
6.12	195.4	47.7	2713.9	7305.4	1899.7

TABLE A6.6.7.2 I_L-N DATA FOR THE ELECTROLYTIC MIXING CELL WITH THE PRESENCE OF 2 LAYERS OF 3MM GLASS
SPHERICAL PARTICLES ON THE CATHODE.

DATE 18-2-81
BATCH Batch 5 of 0.005M Potassium Ferricyanide/0.005M
Potassium Ferrocyanide/0.5M Sodium Hydroxide
solution prepared on 15-1-81

Potential = 1.0000 V
Solution Temperature = 19.5 C
Ferricyanide concentration = 0.500E-05 mol/cm³
Density = 1.0238 g/cm³
Viscosity = 0.011235 g/cm s
Diffusivity = 0.6512E-05 cm²/s

Run No	Stirrer Speed (rpm)	Limiting Current (mA)	Sh	Re	Sc
1.01	0.0	0.3	16.0	0.0	1685.1
1.02	26.5	5.5	293.3	1046.9	1685.1
1.03	34.3	7.1	378.6	1355.0	1685.1
1.04	44.8	9.5	506.6	1769.8	1685.1
1.05	61.4	12.7	677.3	2425.5	1685.1
1.06	76.4	15.6	831.9	3018.1	1685.1
1.07	94.3	19.2	1023.9	3725.2	1685.1
1.08	110.5	22.0	1173.2	4365.2	1685.1
1.09	119.3	23.8	1269.2	4712.8	1685.1
1.10	133.0	26.4	1407.8	5254.0	1685.1
1.11	152.7	30.5	1626.5	6032.3	1685.1
1.12	157.9	32.1	1711.8	6237.7	1685.1
1.13	168.5	35.6	1898.4	6656.4	1685.1
1.14	177.0	36.0	1919.8	6992.2	1685.1
1.15	188.1	37.8	2015.8	7430.7	1685.1

DATE 5-5-81
BATCH Batch 4 of 0.005M Potassium Ferricyanide/0.005M
Potassium Ferrocyanide/0.5M Sodium Hydroxide
solution prepared on 22-4-81

Potential = 0.8421 V
Solution Temperature = 17.0 C
Ferricyanide concentration = 0.477E-05 mol/cm³
Density = 1.0250 g/cm³
Viscosity = 0.011885 g/cm s
Diffusivity = 0.6104E-05 cm²/s

Run No	Stirrer Speed (rpm)	Limiting Current (mA)	Sh	Re	Sc
2.01	0.0	0.3	18.5	0.0	1899.7
2.02	20.4	4.0	236.8	762.7	1899.7
2.03	60.0	10.6	632.2	2243.2	1899.7
2.04	75.0	12.9	769.3	2804.0	1899.7
2.05	107.6	18.9	1127.2	4022.8	1899.7
2.06	145.2	24.2	1443.3	5428.5	1899.7
2.07	158.7	26.3	1568.5	5933.3	1899.7
2.08	179.6	29.8	1777.2	6714.6	1899.7
2.09	212.0	35.1	2093.3	7926.0	1899.7
2.10	223.9	37.5	2236.5	8370.9	1899.7

DATE 28-7-81
 BATCH Batch 6 of 0.005M Potassium Ferricyanide/0.005M
 Potassium Ferrocyanide/0.5M Sodium Hydroxide
 solution prepared on 27-5-81

Potential = 0.8362 V
 Solution Temperature = 16.0 C
 Ferricyanide concentration = $0.497\text{E-}05$ mol/cm³
 Density = 1.0254 g/cm³
 Viscosity = 0.012158 g/cm s
 Diffusivity = $0.5946\text{E-}05$ cm²/s

Run No	Stirrer Speed (rpm)	Limiting Current (mA)	Sh	Re	Sc
3.01	0.0	0.3	17.0	0.0	1994.1
3.02	33.3	6.4	374.9	1217.5	1994.1
3.03	55.5	10.4	611.1	2029.2	1994.1
3.04	94.7	15.9	934.2	3462.4	1994.1
3.05	150.0	23.6	1386.7	5484.3	1994.1
3.06	169.0	25.8	1515.9	6179.0	1994.1
3.07	192.3	29.7	1745.1	7030.9	1994.1
3.08	216.6	33.0	1939.0	7919.4	1994.1

DATE 28-9-81
 BATCH Batch 1 of 0.005M Potassium Ferricyanide/0.005M
 Potassium Ferrocyanide/0.5M Sodium Hydroxide
 solution prepared on 24-9-81

Potential = 0.9965 V
 Solution Temperature = 16.5 C
 Ferricyanide concentration = $0.500\text{E-}05$ mol/cm³
 Density = 1.0252 g/cm³
 Viscosity = 0.012020 g/cm s
 Diffusivity = $0.6024\text{E-}05$ cm²/s

Run No	Stirrer Speed (rpm)	Limiting Current (mA)	Sh	Re	Sc
4.01	0.0	0.3	18.4	0.0	1946.3
4.02	18.1	5.1	294.0	669.2	1946.3
4.03	34.0	9.2	533.2	1257.1	1946.3
4.04	58.5	15.1	870.4	2162.9	1946.3
4.05	103.4	25.7	1481.5	3823.0	1946.3
4.06	127.4	31.5	1815.8	4710.3	1946.3
4.07	145.9	35.7	2057.9	5394.3	1946.3
4.08	167.1	41.0	2363.4	6178.2	1946.3
4.09	192.9	46.5	2680.5	7132.1	1946.3

DATE 1-10-81
 BATCH Batch 1 of 0.005M Potassium Ferricyanide/0.005M
 Potassium Ferrocyanide/0.5M Sodium Hydroxide
 solution prepared on 24-9-81

Potential = 0.9975 V
 Solution Temperature = 21.0 C
 Ferricyanide concentration = 0.500E-05 mol/cm³
 Density = 1.0231 g/cm³
 Viscosity = 0.010867 g/cm s
 Diffusivity = 0.6767E-05 cm²/s

Run No	Stirrer Speed (rpm)	Limiting Current (mA)	Sh	Re	Sc
5.01	0.0	0.4	19.5	0.0	1569.6
5.02	60.5	16.0	821.1	2469.2	1569.6
5.03	100.3	25.9	1329.1	4093.6	1569.6
5.04	126.3	32.0	1642.1	5154.7	1569.6
5.05	153.5	38.0	1950.0	6264.8	1569.6
5.06	182.9	45.7	2345.2	7464.7	1569.6
5.07	198.6	50.2	2576.1	8105.5	1569.6

DATE 2-10-81
 BATCH Batch 1 of 0.005M Potassium Ferricyanide/0.005M
 Potassium Ferrocyanide/0.5M Sodium Hydroxide
 solution prepared on 24-9-81

Potential = 0.9983 V
 Solution Temperature = 15.0 C
 Ferricyanide concentration = 0.500E-05 mol/cm³
 Density = 1.0258 g/cm³
 Viscosity = 0.012439 g/cm s
 Diffusivity = 0.5791E-05 cm²/s

Run No	Stirrer Speed (rpm)	Limiting Current (mA)	Sh	Re	Sc
6.01	0.0	0.4	22.8	0.0	2093.8
6.02	7.3	1.7	104.9	261.0	2093.8
6.03	26.2	5.7	341.8	936.7	2093.8
6.04	35.2	7.9	473.7	1258.4	2093.8
6.05	49.4	10.5	629.6	1766.1	2093.8
6.06	65.2	13.7	821.5	2330.9	2093.8
6.07	99.8	20.0	1199.3	3567.9	2093.8
6.08	117.6	23.7	1421.1	4204.2	2093.8
6.09	149.2	31.6	1894.8	5333.9	2093.8
6.10	160.0	34.2	2050.7	5720.0	2093.8
6.11	186.9	40.5	2428.5	6681.7	2093.8

TABLE A6.6.7.3 I_L-N DATA FOR THE ELECTROLYTIC MIXING CELL WITH THE PRESENCE OF 3 LAYERS OF 3MM GLASS
SPHERICAL PARTICLES ON THE CATHODE

DATE 18-2-81
BATCH Batch 5 of 0.005M Potassium Ferricyanide/0.005M
Potassium Ferrocyanide/0.5M Sodium Hydroxide
solution prepared on 15-1-81

Potential = 1.0000 V
Solution temperature = 19.5 C
Ferricyanide concentration = 0.500E-05 mol/cm³
Density = 1.0238 g/cm³
Viscosity = 0.011235 g/cm s
Diffusivity = 0.6512E-05 cm²/s

Run No	Stirrer Speed (rpm)	Limiting Current (mA)	Sh	Re	Sc
1.01	0.0	0.3	16.0	0.0	1685.1
1.02	24.8	4.7	253.3	979.7	1685.1
1.03	35.4	6.9	368.0	1398.4	1685.1
1.04	50.6	9.6	514.6	1998.9	1685.1
1.05	63.3	12.0	639.9	2500.6	1685.1
1.06	78.2	14.8	789.2	3089.2	1685.1
1.07	90.5	16.8	895.9	3579.1	1685.1
1.08	100.7	18.5	986.5	3978.1	1685.1
1.09	109.1	19.8	1055.9	4309.9	1685.1
1.10	124.5	22.5	1199.9	4918.2	1685.1
1.11	133.3	23.8	1269.2	5265.9	1685.1
1.12	143.5	25.7	1370.5	5668.8	1685.1
1.13	158.2	28.3	1509.2	6249.5	1685.1
1.14	169.5	30.7	1637.1	6695.9	1685.1
1.15	180.4	32.4	1727.8	7126.5	1685.1

DATE 3-3-81
BATCH Batch 4 of 0.005M Potassium Ferricyanide/0.005M
Potassium Ferrocyanide/0.5M Sodium Hydroxide
solution prepared on 22-4-81

Potential = 0.8429 V
Solution temperature = 19.0 C
Ferricyanide concentration = 0.477E-05 mol/cm³
Density = 1.0241 g/cm³
Viscosity = 0.011361 g/cm s
Diffusivity = 0.6429E-05 cm²/s

Run No	Stirrer Speed (rpm)	Limiting Current (mA)	Sh	Re	Sc
2.01	0.0	0.3	17.0	0.0	1725.8
2.02	14.6	1.8	103.1	570.5	1725.8
2.03	24.8	5.1	291.6	969.0	1725.8
2.04	45.5	8.3	470.0	1777.9	1725.8
2.05	74.1	13.4	758.7	2895.4	1725.8
2.06	92.3	16.5	934.3	3606.5	1725.8
2.07	133.3	22.2	1257.0	5208.6	1725.8
2.08	159.8	25.2	1426.9	6244.0	1725.8
2.09	174.7	28.6	1619.4	6826.2	1725.8
2.10	201.7	32.4	1834.6	7881.2	1725.8

DATE 6-5-81
 BATCH Batch 4 of 0.005M Potassium Ferricyanide/0.005M
 Potassium Ferrocyanide/0.5M Sodium Hydroxide
 solution prepared on 22-4-81

Potential = 0.8353 V
 Solution Temperature = 17.0 C
 Ferricyanide concentration = $0.477\text{E-}05$ mol/cm³
 Density = 1.0250 g/cm³
 Viscosity = 0.011885 g/cm s
 Diffusivity = $0.6104\text{E-}05$ cm²/s

Run No	Stirrer Speed (rpm)	Limiting Current (mA)	Sh	Re	Sc
3.01	0.0	0.3	20.9	0.0	1899.7
3.02	14.7	2.4	144.3	549.6	1899.7
3.03	51.8	8.9	530.8	1936.6	1899.7
3.04	80.5	13.4	799.2	3009.6	1899.7
3.05	114.5	18.0	1073.5	4280.8	1899.7
3.06	142.2	21.7	1294.2	5316.4	1899.7
3.07	164.8	25.0	1491.0	6151.3	1899.7
3.08	186.3	29.3	1747.4	6965.1	1899.7

DATE 30-7-81
 BATCH Batch 6 of 0.005M Potassium Ferricyanide/0.005M
 Potassium Ferrocyanide/0.5M Sodium Hydroxide
 solution prepared on 27-5-81

Potential = 0.8428 V
 Solution Temperature = 17.0 C
 Ferricyanide concentration = $0.497\text{E-}05$ mol/cm³
 Density = 1.0250 g/cm³
 Viscosity = 0.011885 g/cm s
 Diffusivity = $0.6104\text{E-}05$ cm²/s

Run No	Stirrer Speed (rpm)	Limiting Current (mA)	Sh	Re	Sc
4.01	0.0	0.5	31.5	0.0	1899.7
4.02	21.6	4.1	237.5	807.6	1899.7
4.03	48.1	8.4	480.8	1798.3	1899.7
4.04	87.4	14.1	807.1	3267.6	1899.7
4.05	113.9	17.3	990.2	4258.3	1899.7
4.06	152.9	23.0	1316.5	5716.4	1899.7
4.07	175.4	25.8	1476.8	6557.6	1899.7
4.08	191.7	28.6	1637.0	7167.0	1899.7
4.09	209.8	31.1	1780.1	7843.7	1899.7

DATE 12-10-81
 BATCH Batch 1 of 0.005M Potassium Ferricyanide/0.005M
 Potassium Ferrocyanide/0.5M Sodium Hydroxide
 solution prepared on 24-9-81

Potential = 1.0007 V
 Solution Temperature = 16.0 C
 Ferricyanide concentration = 0.500E-05 mol/cm³
 Density = 1.0254 g/cm³
 Viscosity = 0.012158 g/cm s
 Diffusivity = 0.5946E-05 cm²/s

Run No	Stirrer Speed (rpm)	Limiting Current (mA)	Sh	Re	Sc
S.01	0.0	0.2	11.7	0.0	1994.1
S.02	24.1	3.4	201.5	881.1	1994.1
S.03	35.3	5.0	294.9	1290.6	1994.1
S.04	74.1	9.3	546.1	2709.3	1994.1
S.05	91.9	10.8	630.8	3360.1	1994.1
S.06	106.8	12.8	747.6	3904.8	1994.1
S.07	131.0	15.7	917.0	4789.6	1994.1
S.08	150.0	17.9	1045.4	5484.3	1994.1
S.09	166.2	20.5	1197.3	6076.6	1994.1
S.10	176.5	21.7	1267.4	6453.2	1994.1

DATE 14-10-81
 BATCH Batch 1 of 0.005M Potassium Ferricyanide/0.005M
 Potassium Ferrocyanide/0.5M Sodium Hydroxide
 solution prepared on 24-9-81

Potential = 1.0064 V
 Solution Temperature = 17.5 C
 Ferricyanide concentration = 0.500E-05 mol/cm³
 Density = 1.0247 g/cm³
 Viscosity = 0.011751 g/cm s
 Diffusivity = 0.6184E-05 cm²/s

Run No	Stirrer Speed (rpm)	Limiting Current (mA)	Sh	Re	Sc
6.01	0.0	0.2	11.2	0.0	1854.5
6.02	34.9	4.7	266.8	1319.3	1854.5
6.03	64.5	8.2	463.3	2438.3	1854.5
6.04	73.1	9.1	513.9	2763.5	1854.5
6.05	104.0	12.5	702.0	3931.6	1854.5
6.06	123.5	14.9	836.8	4668.8	1854.5
6.07	150.7	18.9	1061.4	5697.0	1854.5
6.08	180.7	22.1	1241.1	6831.1	1854.5

TABLE A6.6.7.4

I_L-N DATA FOR THE ELECTROLYTIC MIXING CELL WITH THE PRESENCE OF 4 LAYERS OF 3MM GLASS

SPHERICAL PARTICLES ON THE CATHODE

DATE 19-2-81

BATCH Batch 5 of 0.005M Potassium Ferricyanide/0.005M
Potassium Ferrocyanide/0.5M Sodium Hydroxide
solution prepared on 15-1-81

Potential = 1.0000 V

Solution Temperature = 19.0 C

Ferricyanide concentration = 0.500E-05 mol/cm³Density = 1.0241 g/cm³

Viscosity = 0.011361 g/cm s

Diffusivity = 0.6429E-05 cm²/s

Run No	Stirrer Speed (rpm)	Limiting Current (mA)	Sh	Re	Sc
1.01	0.0	0.2	13.5	0.0	1725.8
1.02	18.4	3.1	167.5	719.0	1725.8
1.03	36.7	6.5	351.1	1434.0	1725.8
1.04	52.7	9.1	494.3	2059.2	1725.8
1.05	70.8	12.1	653.6	2766.4	1725.8
1.06	81.1	13.7	740.1	3168.9	1725.8
1.07	95.4	15.8	853.5	3727.7	1725.8
1.08	114.7	18.2	983.1	4481.8	1725.8
1.09	133.3	21.0	1134.4	5208.6	1725.8
1.10	144.6	22.5	1215.4	5650.1	1725.8
1.11	153.1	23.8	1285.6	5982.2	1725.8
1.12	162.2	25.1	1355.9	6337.6	1725.8
1.13	172.4	26.6	1436.9	6736.4	1725.8
1.14	180.2	28.6	1544.9	7041.1	1725.8

DATE 6-5-81

BATCH Batch 4 of 0.005M Potassium Ferricyanide/0.005M
Potassium Ferrocyanide/0.5M Sodium Hydroxide
solution prepared on 22-4-81

Potential = 0.8386 V

Solution Temperature = 19.0 C

Ferricyanide concentration = 0.477E-05 mol/cm³Density = 1.0241 g/cm³

Viscosity = 0.011361 g/cm s

Diffusivity = 0.6429E-05 cm²/s

Run No	Stirrer Speed (rpm)	Limiting Current (mA)	Sh	Re	Sc
2.01	0.0	0.2	11.3	0.0	1725.8
2.02	17.9	3.1	178.4	699.4	1725.8
2.03	55.7	9.7	550.4	2176.4	1725.8
2.04	63.5	10.6	600.2	2481.2	1725.8
2.05	102.3	16.3	923.0	3997.3	1725.8
2.06	127.9	20.1	1138.1	4997.6	1725.8
2.07	157.9	23.9	1353.3	6169.8	1725.8
2.08	184.2	28.0	1585.4	7197.4	1725.8
2.09	205.1	31.6	1789.3	8014.1	1725.8

DATE 5-6-81
 BATCH Batch 6 of 0.005M Potassium Ferricyanide/0.005M
 Potassium Ferrocyanide/0.5M Sodium Hydroxide
 solution prepared on 27-5-81

Potential = 0.8425 V
 Solution Temperature = 15.0 C
 Ferricyanide concentration = $0.497\text{E-}05$ mol/cm³
 Density = 1.0258 g/cm³
 Viscosity = 0.012439 g/cm s
 Diffusivity = $0.5791\text{E-}05$ cm²/s

Run No	Stirrer Speed (rpm)	Limiting Current (mA)	Sh	Re	Sc
3.01	0.0	0.4	27.1	0.0	2093.8
3.02	17.2	2.6	159.9	614.9	2093.8
3.03	37.8	5.1	310.7	1351.4	2093.8
3.04	63.8	7.7	465.7	2280.9	2093.8
3.05	74.8	8.9	537.5	2674.1	2093.8
3.06	95.5	10.8	651.5	3414.2	2093.8
3.07	138.7	12.5	754.1	4958.6	2093.8
3.08	140.8	14.9	898.8	5033.6	2093.8
3.09	161.3	16.8	1013.5	5766.5	2093.8
3.10	162.6	18.6	1122.0	5813.0	2093.8
3.11	200.0	21.5	1297.0	7150.1	2093.8

DATE 16-10-81
 BATCH Batch 1 of 0.005M Potassium Ferricyanide/0.005M
 Potassium Ferrocyanide/0.5M Sodium Hydroxide
 solution prepared on 24-9-81

Potential = 1.0094 V
 Solution Temperature = 18.0 C
 Ferricyanide concentration = $0.500\text{E-}05$ mol/cm³
 Density = 1.0245 g/cm³
 Viscosity = 0.011619 g/cm s
 Diffusivity = $0.6264\text{E-}05$ cm²/s

Run No	Stirrer Speed (rpm)	Limiting Current (mA)	Sh	Re	Sc
4.01	0.0	0.2	11.1	0.0	1810.4
4.02	58.2	7.2	401.9	2224.6	1810.4
4.03	70.6	8.5	471.2	2698.6	1810.4
4.04	80.5	9.3	518.3	3077.0	1810.4
4.05	87.8	10.0	554.3	3356.1	1810.4

TABLE A6.6.7.5 I_L-N DATA FOR THE ELECTROLYTIC MIXING CELL WITH THE PRESENCE OF 5 LAYERS OF 3MM GLASS

SPHERICAL PARTICLES ON THE CATHODE

DATE 19-2-81
 BATCH Batch 3 of 0.005M Potassium Ferricyanide/0.005M Potassium Ferrocyanide/0.5M Sodium Hydroxide solution prepared on 15-1-81

Potential = 1.0000 V
 Solution Temperature = 19.0 C
 Ferricyanide concentration = $0.500E-05$ mol/cm³
 Density = 1.0241 g/cm³
 Viscosity = 0.011361 g/cm s
 Diffusivity = $0.6429E-05$ cm²/s

Run No	Stirrer Speed (rpm)	Limiting Current (mA)	Sh	Re	Sc
1.01	0.0	0.3	18.9	0.0	1725.8
1.02	23.8	3.9	209.6	930.0	1725.8
1.03	32.6	5.3	285.2	1273.8	1725.8
1.04	41.2	6.7	361.9	1609.9	1725.8
1.05	53.3	8.5	459.2	2082.6	1725.8
1.06	75.4	11.7	632.0	2946.2	1725.8
1.07	86.2	13.3	718.4	3368.2	1725.8
1.08	105.8	15.7	848.1	4134.0	1725.8
1.09	126.1	18.0	972.3	4927.2	1725.8
1.10	147.1	20.5	1107.4	5747.9	1725.8
1.11	167.1	23.2	1253.2	6529.3	1725.8
1.12	187.5	25.7	1386.3	7326.4	1725.8

DATE 6-5-81
 BATCH Batch 4 of 0.005M Potassium Ferricyanide/0.005M Potassium Ferrocyanide/0.5M Sodium Hydroxide solution prepared on 22-4-81

Potential = 0.8399 V
 Solution Temperature = 19.0 C
 Ferricyanide concentration = $0.477E-05$ mol/cm³
 Density = 1.0241 g/cm³
 Viscosity = 0.011361 g/cm s
 Diffusivity = $0.6429E-05$ cm²/s

Run No	Stirrer Speed (rpm)	Limiting Current (mA)	Sh	Re	Sc
2.01	0.0	0.4	21.0	0.0	1725.8
2.02	20.8	3.6	203.8	812.7	1725.8
2.03	58.8	9.9	560.6	2297.6	1725.8
2.04	84.9	13.9	767.1	3317.4	1725.8
2.05	113.7	17.5	990.9	4442.7	1725.8
2.06	150.7	22.1	1251.4	5868.5	1725.8
2.07	180.7	25.7	1455.2	7060.7	1725.8
2.08	196.9	27.7	1568.5	7693.7	1725.8

TABLE A6.6.7.6 I_L-N DATA FOR THE ELECTROLYTIC MIXING CELL WITH THE PRESENCE OF 6 LAYERS OF 3MM GLASS
SPHERICAL PARTICLES ON THE CATHODE

DATE 19-2-81
BATCH Batch 5 of 0.005M Potassium Ferricyanide/0.005M
Potassium Ferrocyanide/0.5M Sodium Hydroxide
solution prepared on 15-1-81

Potential = 1.0000 V
Solution Temperature = 19.0 C
Ferricyanide concentration = $0.500E-05$ mol/cm³
Density = 1.0241 g/cm³
Viscosity = 0.011361 g/cm s
Diffusivity = $0.6429E-05$ cm²/s

Run No	Stirrer Speed (rpm)	Limiting Current (mA)	Sh	Re	Sc
1.01	0.0	0.3	16.2	0.0	1725.8
1.02	24.1	3.9	209.1	941.7	1725.8
1.03	48.6	7.2	391.6	1899.0	1725.8
1.04	65.6	9.5	515.9	2563.3	1725.8
1.05	87.1	12.3	664.4	3403.4	1725.8
1.06	106.4	14.7	794.1	4157.5	1725.8
1.07	121.7	16.3	880.5	4755.3	1725.8
1.08	137.0	18.2	983.1	5353.1	1725.8
1.09	156.3	20.1	1085.8	6107.3	1725.8
1.10	168.1	21.6	1166.8	6568.4	1725.8
1.11	179.6	23.1	1247.8	7017.7	1725.8

DATE 6-5-81
BATCH Batch 4 of 0.005M Potassium Ferricyanide/0.005M
Potassium Ferrocyanide/0.5M Sodium Hydroxide
solution prepared on 22-4-81

Potential = 1.0000 V
Solution Temperature = 18.0 C
Ferricyanide concentration = $0.477E-05$ mol/cm³
Density = 1.0245 g/cm³
Viscosity = 0.011619 g/cm s
Diffusivity = $0.6264E-05$ cm²/s

Run No	Stirrer Speed (rpm)	Limiting Current (mA)	Sh	Re	Sc
2.01	0.0	0.3	17.4	0.0	1810.4
2.02	21.7	3.7	217.9	829.5	1810.4
2.03	57.7	8.5	493.9	2205.5	1810.4
2.04	118.6	16.0	929.7	4533.4	1810.4
2.05	164.0	21.0	1220.2	6268.7	1810.4

TABLE A6.6.7.7 I_L - N DATA FOR THE ELECTROLYTIC MIXING CELL WITH THE PRESENCE OF 7 LAYERS OF 3MM GLASS
SPHERICAL PARTICLES ON THE CATHODE

DATE 19-2-81
BATCH Batch 5 of 0.005M Potassium Ferricyanide/0.005M
Potassium Ferrocyanide/0.5M Sodium Hydroxide
solution prepared on 15-1-81

Potential = 1.0000 V
Solution Temperature = 19.0 C
Ferricyanide concentration = 0.500E-05 mol/cm³
Density = 1.0241 g/cm³
Viscosity = 0.011361 g/cm s
Diffusivity = 0.6429E-05 cm²/s

Run No	Stirrer Speed (rpm)	Limiting Current (mA)	Sh	Re	Sc
1.01	0.0	0.3	16.2	0.0	1725.8
1.02	18.7	2.3	124.2	730.7	1725.8
1.03	41.5	5.5	297.1	1621.6	1725.8
1.04	59.3	7.7	418.6	2317.1	1725.8
1.05	73.0	9.4	507.8	2852.4	1725.8
1.06	80.6	11.4	615.8	3149.4	1725.8
1.07	108.9	13.1	707.6	4255.2	1725.8
1.08	127.1	14.9	804.9	4966.3	1725.8
1.09	141.2	16.0	864.3	5517.3	1725.8
1.10	156.3	17.4	939.9	6107.3	1725.8
1.11	174.9	19.1	1031.8	6834.1	1725.8

TABLE A6.6.8.1 I_L - N DATA FOR THE ELECTROLYTIC MIXING
CELL WITH THE PRESENCE OF 1 LAYER OF
5MM GLASS SPHERICAL PARTICLES ON THE
CATHODE.

DATE 16-8-82
BATCH Batch 6 of 0.005M Potassium Ferricyanide/0.005M
Potassium Ferrocyanide/0.5M Sodium Hydroxide
solution prepared on 23-6-82

Potential = 1.0131 V
Solution Temperature = 18.0 C
Ferricyanide concentration = 0.500E-05 mol/cm³
Density = 1.0245 g/cm³
Viscosity = 0.011319 g/cm s
Diffusivity = 0.6264E-05 cm²/s

Run No	Stirrer Speed (rpm)	Limiting Current (mA)	Sh	Re	Sc
1.01	0.0	0.5	26.4	0.0	1810.4
1.02	15.0	3.2	179.6	573.4	1810.4
1.03	15.3	4.1	228.4	584.8	1810.4
1.04	28.6	7.1	392.5	1100.9	1810.4
1.05	34.1	10.8	598.7	2067.9	1810.4
1.06	63.5	12.8	709.6	2427.2	1810.4
1.07	76.4	15.1	837.1	2920.3	1810.4
1.08	91.6	18.1	1003.4	3501.3	1810.4
1.09	106.2	19.8	1097.6	4059.4	1810.4
1.10	116.1	21.8	1208.5	4437.8	1810.4
1.11	120.8	23.6	1308.2	4617.5	1810.4
1.12	133.3	25.6	1419.1	5095.3	1810.4
1.13	161.1	27.8	1541.1	6157.9	1810.4
1.14	177.8	29.8	1651.9	6796.2	1810.4
1.15	192.0	31.5	1746.2	7339.0	1810.4
1.16	212.4	33.3	1846.0	8118.8	1810.4
1.17	225.6	35.0	1940.2	8623.3	1810.4
1.18	248.3	36.8	2040.0	9491.0	1810.4
1.19	262.8	38.6	2139.8	10045.3	1810.4
1.20	297.5	40.9	2267.3	11371.6	1810.4

TABLE A6.6.8.2 I_L - N DATA FOR THE ELECTROLYTIC MIXING
CELL WITH THE PRESENCE OF 2 LAYERS OF
5MM GLASS SPHERICAL PARTICLES ON THE
CATHODE

DATE 16-8-82
BATCH Batch 6 of 0.005M Potassium Ferricyanide/0.005M
Potassium Ferrocyanide/0.5M Sodium Hydroxide
solution prepared on 23-6-82

Potential = 1.0131 V
Solution Temperature = 19.5 C
Ferricyanide concentration = 0.500E-05 mol/cm³
Density = 1.0238 g/cm³
Viscosity = 0.011235 g/cm s
Diffusivity = 0.6512E-05 cm²/s

Run No	Stirrer Speed (rpm)	Limiting Current (mA)	Sh	Re	Sc
1.01	0.0	0.5	27.5	0.0	1685.1
1.02	16.7	4.5	237.8	659.7	1685.1
1.03	32.1	6.5	346.6	1268.1	1685.1
1.04	64.5	10.7	570.6	2548.0	1685.1
1.05	74.5	12.8	682.6	2943.0	1685.1
1.06	88.9	15.8	842.6	3511.9	1685.1
1.07	127.6	20.5	1093.2	5040.7	1685.1
1.08	134.1	21.8	1162.5	5297.5	1685.1
1.09	147.8	23.6	1258.5	5838.7	1685.1
1.10	163.0	25.2	1343.8	6439.1	1685.1
1.11	170.5	26.9	1434.5	6735.4	1685.1
1.12	187.5	28.7	1530.5	7407.0	1685.1
1.13	198.7	29.4	1567.8	7849.4	1685.1
1.14	211.3	30.5	1626.5	8347.2	1685.1
1.15	229.0	31.9	1701.1	9046.4	1685.1
1.16	232.5	32.9	1754.5	9184.7	1685.1
1.17	254.2	33.6	1791.8	10041.9	1685.1
1.18	262.5	34.1	1818.5	10369.8	1685.1
1.19	269.2	35.0	1866.4	10634.5	1685.1
1.20	280.0	35.8	1909.1	11061.1	1685.1

TABLE A6.6.8.3 I_L-N DATA FOR THE ELECTROLYTIC MIXING
CELL WITH THE PRESENCE OF 3 LAYERS OF
5MM GLASS SPHERICAL PARTICLES ON THE
CATHODE.

DATE 17-8-82
BATCH Batch 6 of 0.005M Potassium Ferricyanide/0.005M
Potassium Ferrocyanide/0.5M Sodium Hydroxide
solution prepared on 23-6-82

Potential = 1.0131 V
Solution Temperature = 15.0 C
Ferricyanide concentration = 0.500E-05 mol/cm³
Density = 1.0258 g/cm³
Viscosity = 0.012439 g/cm s
Diffusivity = 0.5791E-05 cm²/s

Run No	Stirrer Speed (rpm)	Limiting Current (mA)	Sh	Re	Sc
1.01	0.0	1.0	57.7	0.0	2093.8
1.02	12.7	2.1	128.9	454.0	2093.8
1.03	33.3	5.6	337.0	1190.5	2093.8
1.04	51.3	7.6	456.9	1834.0	2093.8
1.05	76.9	10.1	605.6	2749.2	2093.8
1.06	88.9	11.5	689.6	3178.2	2093.8
1.07	100.0	12.7	761.5	3575.0	2093.8
1.08	116.5	14.6	875.5	4164.9	2093.8
1.09	140.0	17.2	1031.4	5005.0	2093.8
1.10	153.8	18.6	1115.3	5498.4	2093.8
1.11	163.6	19.5	1169.3	5848.7	2093.8
1.12	168.5	20.5	1229.2	6023.9	2093.8
1.13	192.3	22.1	1325.2	6874.8	2093.8
1.14	223.9	23.6	1415.1	8004.5	2093.8
1.15	240.0	25.2	1511.1	8580.1	2093.8
1.16	252.1	25.8	1547.0	9012.6	2093.8

TABLE A6.6.8.4 I_L-N DATA FOR THE ELECTROLYTIC MIXING
CELL WITH THE PRESENCE OF 4 LAYERS OF
5MM GLASS SPHERICAL PARTICLES ON THE
CATHODE

DATE 18-8-82
BATCH Batch 6 of 0.005M Potassium Ferricyanide/0.005M
Potassium Ferrocyanide/0.5M Sodium Hydroxide
solution prepared on 23-6-82

Potential = 1.0135 V
Solution Temperature = 17.5 C
Ferricyanide concentration = 0.500E-05 mol/cm³
Density = 1.0247 g/cm³
Viscosity = 0.011751 g/cm s
Diffusivity = 0.6184E-05 cm²/s

Run No	Stirrer Speed (rpm)	Limiting Current (mA)	Sh	Re	Sc
1.01	0.0	0.5	26.8	0.0	1854.5
1.02	30.0	5.1	287.5	1134.1	1854.5
1.03	55.2	7.6	427.9	2086.8	1854.5
1.04	72.7	9.5	531.3	2748.3	1854.5
1.05	86.3	10.7	600.9	3262.5	1854.5
1.06	93.7	11.8	662.7	3542.2	1854.5
1.07	117.6	13.3	746.9	4445.7	1854.5

DATE 18-8-82
 BATCH Batch 6 of 0.005M Potassium Ferricvanide/0.005M
 Potassium Ferrocyanide/0.5M Sodium Hydroxide
 solution prepared on 23-6-82

Potential = 1.0131 V
 Solution Temperature = 18.0 C
 Ferricvanide concentration = 0.500E-05 mol/cm³
 Density = 1.0240 g/cm³
 Viscosity = 0.011619 g/cm s
 Diffusivity = 0.6264E-05 cm²/s

Run No	Stirrer Speed (rpm)	Limiting Current (mA)	Sh	Re	Sc
2.01	0.0	0.3	19.2	0.0	1810.4
2.02	16.1	2.8	153.6	615.4	1810.4
2.03	44.8	6.2	343.1	1712.4	1810.4
2.04	58.3	8.1	447.9	2228.5	1810.4
2.05	85.7	10.8	598.7	3275.8	1810.4
2.06	102.6	13.0	720.6	3921.6	1810.4
2.07	116.5	14.1	781.6	4453.1	1810.4
2.08	134.8	16.3	903.6	5152.6	1810.4
2.09	152.9	18.2	1008.9	5844.4	1810.4
2.10	186.0	20.9	1158.6	7109.7	1810.4
2.11	205.1	22.5	1247.3	7839.7	1810.4
2.12	230.8	23.6	1308.2	8822.1	1810.4
2.13	242.4	24.4	1352.6	9265.5	1810.4

TABLE A6.6.9.1 I_L - N DATA FOR THE ELECTROLYTIC MIXING CELL WITH THE PRESENCE OF 1 LAYER of 7MM GLASS
SPHERICAL PARTICLES ON THE CATHODE

DATE 12-8-82
BATCH Batch 5 of 0.005M Potassium Ferricyanide/0.005M
Potassium Ferrocyanide/0.5M Sodium Hydroxide
solution prepared on 23-6-82

Potential = 1.0220 V
Solution Temperature = 20.0 C
Ferricyanide concentration = $0.500E-05$ mol/cm³
Density = 1.0236 g/cm³
Viscosity = 0.011111 g/cm s
Diffusivity = $0.6596E-05$ cm²/s

Run No	Stirrer Speed (rpm)	Limiting Current (mA)	Sh	Re	Sc
1.01	0.0	0.7	36.4	0.0	1645.6
1.02	20.9	5.5	287.4	834.7	1645.6
1.03	59.6	15.3	805.5	2380.3	1645.6
1.04	88.9	19.6	1031.9	3550.4	1645.6
1.05	102.6	22.5	1184.5	4097.5	1645.6
1.06	124.1	26.8	1410.9	4956.2	1645.6
1.07	141.7	28.8	1516.2	5659.1	1645.6
1.08	165.5	31.7	1668.9	6609.6	1645.6
1.09	184.0	34.7	1826.8	7348.4	1645.6
1.10	214.3	37.3	1963.7	8558.5	1645.6
1.11	238.4	44.6	2348.0	9521.0	1645.6
1.12	278.1	43.3	2279.6	11106.5	1645.6
1.13	320.9	46.3	2437.5	12815.8	1645.6
1.14	346.8	47.7	2511.2	13850.2	1645.6

DATE 12-8-82
BATCH Batch 5 of 0.005M Potassium Ferricyanide/0.005M
Potassium Ferrocyanide/0.5M Sodium Hydroxide
solution prepared on 23-6-82

Potential = 1.0220 V
Solution Temperature = 20.0 C
Ferricyanide concentration = $0.500E-05$ mol/cm³
Density = 1.0236 g/cm³
Viscosity = 0.011111 g/cm s
Diffusivity = $0.6596E-05$ cm²/s

Run No	Stirrer Speed (rpm)	Limiting Current (mA)	Sh	Re	Sc
2.01	0.0	0.5	28.3	0.0	1645.6
2.02	13.3	3.5	182.2	531.2	1645.6
2.03	25.9	6.3	332.2	1034.4	1645.6
2.04	40.0	9.9	522.3	1597.5	1645.6
2.05	60.0	14.2	747.6	2396.2	1645.6
2.06	69.0	15.9	837.1	2755.7	1645.6
2.07	81.1	18.8	989.8	3238.9	1645.6
2.08	100.8	22.7	1195.1	4025.7	1645.6
2.09	126.8	26.8	1410.9	5064.0	1645.6
2.10	147.5	28.9	1521.5	5890.7	1645.6
2.11	175.2	32.7	1721.5	6997.0	1645.6
2.12	188.9	35.2	1853.2	7544.1	1645.6
2.13	230.8	38.6	2032.2	9217.5	1645.6
2.14	245.9	40.4	2126.9	9820.5	1645.6
2.15	276.5	42.7	2248.0	11042.6	1645.6
2.16	298.5	44.5	2342.8	11921.2	1645.6
2.17	324.3	46.6	2453.3	12951.6	1645.6
2.18	361.4	47.6	2506.0	14433.3	1645.6

TABLE A6.6.9.2 I_L-N DATA FOR THE ELECTROLYTIC MIXING CELL WITH THE PRESENCE OF 2 LAYERS OF 7MM GLASS

SPHERICAL PARTICLES ON THE CATHODE.

DATE 12-8-82
 BATCH Batch 5 of 0.005M Potassium Ferricyanide/0.005M
 Potassium Ferrocyanide/0.5M Sodium Hydroxide
 solution prepared on 23-6-82

Potential = 1.0235 V
 Solution Temperature = 20.0 C
 Ferricyanide concentration = $0.500E-05$ mol/cm³
 Density = 1.0236 g/cm³
 Viscosity = 0.011111 g/cm s
 Diffusivity = $0.6596E-05$ cm²/s

Run No	Stirrer Speed (rpm)	Limiting Current (mA)	Sh	Re	Sc
1.01	0.0	0.6	33.2	0.0	1645.6
1.02	11.8	2.6	135.8	471.3	1645.6
1.03	31.1	6.9	362.2	1242.0	1645.6
1.04	53.1	10.9	573.8	2120.7	1645.6
1.05	63.1	13.5	710.7	2520.0	1645.6
1.06	96.0	18.8	989.8	3834.0	1645.6
1.07	113.2	21.0	1105.6	4520.9	1645.6
1.08	121.6	22.5	1184.5	4856.4	1645.6
1.09	132.4	23.2	1221.4	5287.7	1645.6
1.10	138.5	24.8	1305.6	5531.3	1645.6
1.11	156.5	26.5	1395.1	6250.2	1645.6
1.12	173.9	28.2	1484.6	6945.1	1645.6
1.13	184.6	30.2	1589.9	7372.4	1645.6
1.14	196.1	31.2	1642.6	7831.7	1645.6
1.15	215.8	33.2	1747.9	8618.4	1645.6
1.16	243.9	34.5	1816.3	9740.7	1645.6
1.17	260.9	36.6	1926.9	10419.6	1645.6
1.18	297.0	38.6	2032.2	11861.3	1645.6

DATE 13-8-82
 BATCH Batch 5 of 0.005M Potassium Ferricyanide/0.005M
 Potassium Ferrocyanide/0.5M Sodium Hydroxide
 solution prepared on 23-6-82

Potential = 1.0176 V
 Solution Temperature = 18.5 C
 Ferricyanide concentration = $0.500E-05$ mol/cm³
 Density = 1.0243 g/cm³
 Viscosity = 0.011489 g/cm s
 Diffusivity = $0.6346E-05$ cm²/s

Run No	Stirrer Speed (rpm)	Limiting Current (mA)	Sh	Re	Sc
2.01	0.0	0.5	29.4	0.0	1767.5
2.02	30.0	5.5	303.2	1159.4	1767.5
2.03	46.2	8.9	488.1	1785.5	1767.5
2.04	71.4	13.3	727.8	2759.4	1767.5
2.05	103.4	17.9	979.5	3996.1	1767.5
2.06	112.1	18.8	1028.7	4332.4	1767.5
2.07	141.2	22.7	1242.2	5457.0	1767.5
2.08	151.3	24.0	1313.3	5847.4	1767.5
2.09	172.4	26.5	1450.1	6662.8	1767.5
2.10	177.5	27.1	1482.9	6859.9	1767.5
2.11	206.9	29.7	1625.2	7996.2	1767.5
2.12	223.9	32.3	1767.5	8653.2	1767.5
2.13	286.7	35.2	1926.2	11080.2	1767.5
2.14	303.0	38.5	2106.7	11710.2	1767.5

TABLE A6.6.9.3 I_L-N DATA FOR THE ELECTROLYTIC MIXING CELL WITH THE PRESENCE OF 3 LAYERS OF 7MM GLASS
SPHERICAL PARTICLES ON THE CATHODE:

DATE 13-8-82
BATCH Batch 5 of 0.005M Potassium Ferricyanide/0.005M
Potassium Ferrocyanide/0.5M Sodium Hydroxide
solution prepared on 23-6-82

Potential = 1.0175 V
Solution Temperature = 18.5 C
Ferricyanide concentration = 0.500E-05 mol/cm³
Density = 1.0243 g/cm³
Viscosity = 0.011489 g/cm s
Diffusivity = 0.6346E-05 cm²/s

Run No	Stirrer Speed (rpm)	Limiting Current (mA)	Sh	Re	Sc
1.01	0.0	0.4	21.1	0.0	1767.5
1.02	11.5	2.2	123.1	444.4	1767.5
1.03	31.6	6.1	336.5	1221.3	1767.5
1.04	55.0	9.1	496.9	2125.6	1767.5
1.05	83.3	12.9	705.9	3219.3	1767.5
1.06	98.9	14.8	809.9	3822.2	1767.5
1.07	116.1	16.8	919.3	4487.0	1767.5
1.08	129.5	19.0	1039.7	5004.8	1767.5
1.09	157.9	21.6	1171.0	6102.4	1767.5
1.10	196.7	24.6	1346.1	7601.9	1767.5
1.11	214.3	26.4	1444.6	8282.1	1767.5
1.12	243.9	28.8	1576.0	9426.1	1767.5
1.13	274.0	30.5	1669.0	10589.4	1767.5
1.14	298.5	31.1	1701.8	11536.3	1767.5

DATE 13-8-82
BATCH Batch 5 of 0.005M Potassium Ferricyanide/0.005M
Potassium Ferrocyanide/0.5M Sodium Hydroxide
solution prepared on 23-6-82

Potential = 1.0176 V
Solution Temperature = 19.0 C
Ferricyanide concentration = 0.500E-05 mol/cm³
Density = 1.0241 g/cm³
Viscosity = 0.011361 g/cm s
Diffusivity = 0.6429E-05 cm²/s

Run No	Stirrer Speed (rpm)	Limiting Current (mA)	Sh	Re	Sc
2.01	0.0	0.7	35.3	0.0	1725.8
2.02	18.5	4.1	222.6	722.9	1725.8
2.03	33.1	6.0	326.3	1293.4	1725.8
2.04	61.2	9.8	527.8	2391.3	1725.8
2.04	80.0	12.5	675.2	3125.9	1725.8
2.05	88.2	13.3	718.4	3446.3	1725.8
2.07	107.1	14.3	772.5	4184.8	1725.8
2.08	123.7	17.9	966.9	4833.5	1725.8
2.09	136.4	19.5	1053.4	5329.7	1725.8
2.10	171.4	22.8	1231.6	6697.3	1725.8
2.11	200.0	24.8	1339.7	7814.0	1725.8
2.12	219.4	26.4	1426.1	8572.8	1725.8
2.13	256.4	29.0	1566.5	10018.6	1725.8
2.14	285.7	29.6	1598.9	11163.5	1725.8

TABLE A6.6.10.1 I_L-N DATA FOR THE ELECTROLYTIC MIXING CELL WITH THE PRESENCE OF 1 LAYER OF 10MM GLASS
SPHERICAL PARTICLES ON THE CATHODE

DATE 11-8-82
BATCH Batch 4 of 0.005M Potassium Ferricyanide/0.005M
Potassium Ferrocyanide/0.5M Sodium Hydroxide
solution prepared on 23-6-82

Potential = 1.0141 V
Solution Temperature = 21.0 C
Ferricyanide concentration = 0.500E-05 mol/cm³
Density = 1.0231 g/cm³
Viscosity = 0.010867 g/cm s
Diffusivity = 0.6767E-05 cm²/s

Run No	Stirrer Speed (rpm)	Limiting Current (mA)	Sh	Re	Sc
1.01	0.0	0.7	33.6	0.0	1569.6
1.02	25.0	7.8	402.8	1020.3	1569.6
1.03	37.3	11.8	605.5	1522.3	1569.6
1.04	66.6	19.1	980.2	2718.2	1569.6
1.05	101.7	25.2	1293.2	4150.7	1569.6
1.06	122.4	29.5	1513.9	4995.5	1569.6
1.07	147.5	32.7	1678.1	6019.9	1569.6

DATE 11-8-82
BATCH Batch 4 of 0.005M Potassium Ferricyanide/0.005M
Potassium Ferrocyanide/0.5M Sodium Hydroxide
solution prepared on 23-6-82

Potential = 1.0141 V
Solution Temperature = 20.0 C
Ferricyanide concentration = 0.500E-05 mol/cm³
Density = 1.0236 g/cm³
Viscosity = 0.011111 g/cm s
Diffusivity = 0.6596E-05 cm²/s

Run No	Stirrer Speed (rpm)	Limiting Current (mA)	Sh	Re	Sc
2.01	0.0	0.4	22.7	0.0	1645.6
2.02	19.7	5.5	287.4	786.8	1645.6
2.03	27.3	7.3	384.8	1090.3	1645.6
2.04	51.3	12.4	652.8	2048.8	1645.6
2.05	72.3	17.1	900.3	2887.5	1645.6
2.06	88.2	20.4	1074.0	3522.5	1645.6
2.07	109.0	23.2	1221.4	4353.1	1645.6
2.08	128.6	25.5	1342.5	5135.9	1645.6
2.09	152.7	29.1	1532.0	6098.4	1645.6
2.10	172.4	31.7	1668.9	6885.2	1645.6
2.11	198.7	34.2	1800.5	7935.5	1645.6
2.12	227.3	37.5	1974.2	9077.7	1645.6
2.13	236.2	38.5	2026.9	9433.1	1645.6
2.14	270.3	40.8	2148.0	10795.0	1645.6
2.15	297.0	43.5	2290.1	11861.3	1645.6
2.16	335.0	46.3	2437.5	13378.9	1645.6

TABLE A6.6.10.2 I_L-N DATA FOR THE ELECTROLYTIC MIXING CELL WITH THE PRESENCE OF 2 LAYERS OF 10MM GLASS
SPHERICAL PARTICLES ON THE CATHODE.

DATE 11-8-82
BATCH Batch 4 of 0.005M Potassium Ferricyanide/0.005M
Potassium Ferrocyanide/0.5M Sodium Hydroxide
solution prepared on 23-6-82

Potential = 1.0141 V
Solution Temperature = 20.0 C
Ferricyanide concentration = 0.500E-05 mol/cm³
Density = 1.0236 g/cm³
Viscosity = 0.011111 g/cm s
Diffusivity = 0.6596E-05 cm²/s

Run No	Stirrer Speed (rpm)	Limiting Current (mA)	Sh	Re	Sc
1.01	0.0	0.4	22.3	0.0	1645.6
1.02	33.7	7.5	392.7	1345.9	1645.6
1.03	65.2	14.7	773.9	2603.9	1645.6
1.04	86.9	16.7	879.2	3470.5	1645.6
1.05	98.4	19.0	1000.3	3929.8	1645.6
1.06	114.6	21.3	1121.4	4576.8	1645.6
1.07	141.2	25.2	1326.7	5639.1	1645.6
1.08	154.6	27.1	1426.7	6174.3	1645.6
1.09	162.2	29.2	1537.3	6477.8	1645.6
1.10	187.5	31.3	1647.8	7488.2	1645.6
1.11	209.8	34.0	1790.0	8378.8	1645.6
1.12	244.9	37.2	1958.4	9780.6	1645.6
1.13	284.6	40.6	2137.4	11366.1	1645.6

DATE 11-8-82
BATCH Batch 4 of 0.005M Potassium Ferricyanide/0.005M
Potassium Ferrocyanide/0.5M Sodium Hydroxide
solution prepared on 23-6-82

Potential = 1.0141 V
Solution Temperature = 20.5 C
Ferricyanide concentration = 0.500E-05 mol/cm³
Density = 1.0234 g/cm³
Viscosity = 0.010988 g/cm s
Diffusivity = 0.6681E-05 cm²/s

Run No	Stirrer Speed (rpm)	Limiting Current (mA)	Sh	Re	Sc
2.01	0.0	0.7	38.0	0.0	1607.1
2.02	26.0	6.2	321.7	1049.7	1607.1
2.03	47.2	10.5	545.8	1905.6	1607.1
2.04	61.8	14.8	769.3	2495.1	1607.1
2.05	99.2	19.5	1013.5	4005.0	1607.1
2.06	109.1	21.3	1107.1	4404.7	1607.1
2.07	132.3	23.5	1221.4	5341.4	1607.1
2.08	145.6	25.6	1330.6	5878.4	1607.1
2.09	163.9	28.2	1465.7	6617.2	1607.1
2.10	167.9	30.5	1585.3	6778.7	1607.1
2.11	192.3	32.7	1699.6	7763.8	1607.1
2.12	211.3	34.8	1808.8	8530.9	1607.1
2.13	214.3	35.8	1860.8	8652.0	1607.1
2.14	230.8	36.9	1917.9	9318.2	1607.1
2.15	252.1	39.2	2037.5	10178.2	1607.1

TABLE A6.6.11.1 I_L-N DATA FOR THE ELECTROLYTIC MIXING CELL WITH THE PRESENCE OF 1 LAYER OF 12MM GLASS
SPHERICAL PARTICLES ON THE CATHODE.

DATE 5-8-81
BATCH Batch 3 of 0.005M Potassium Ferricyanide/0.005M
Potassium Ferrocyanide/0.5M Sodium Hydroxide
solution prepared on 23-6-81

Potential = 1.0092 V
Solution Temperature = 19.0 C
Ferricyanide concentration = 0.500E-05 mol/cm³
Density = 1.0241 g/cm³
Viscosity = 0.011361 g/cm s
Diffusivity = 0.6429E-05 cm²/s

Run No	Stirrer Speed (rpm)	Limiting Current (mA)	Sh	Re	Sc
1.01	0.0	1.1	62.1	0.0	1725.8
1.02	15.8	5.0	267.9	617.4	1725.8
1.03	29.6	8.3	448.9	1156.6	1725.8
1.04	36.1	9.3	505.1	1410.6	1725.8
1.05	60.3	14.3	772.5	2356.2	1725.8
1.06	72.6	16.7	902.1	2836.8	1725.8
1.07	78.3	17.2	929.1	3059.5	1725.8
1.08	95.5	19.8	1069.6	3731.6	1725.8
1.09	112.5	21.5	1161.4	4395.8	1725.8
1.10	125.0	23.3	1258.6	4884.3	1725.8
1.11	149.9	24.7	1334.3	5857.2	1725.8
1.12	153.1	25.8	1393.7	5982.2	1725.8
1.13	176.5	27.1	1463.9	6896.6	1725.8
1.14	191.1	28.1	1517.9	7467.1	1725.8
1.15	195.4	28.8	1555.7	7635.1	1725.8
1.16	260.9	31.5	1701.6	10194.4	1725.8

DATE 5-8-81
BATCH Batch 3 of 0.005M Potassium Ferricyanide/0.005M
Potassium Ferrocyanide/0.5M Sodium Hydroxide
solution prepared on 23-6-81

Potential = 1.0092 V
Solution Temperature = 18.0 C
Ferricyanide concentration = 0.500E-05 mol/cm³
Density = 1.0245 g/cm³
Viscosity = 0.011619 g/cm s
Diffusivity = 0.6264E-05 cm²/s

Run No	Stirrer Speed (rpm)	Limiting Current (mA)	Sh	Re	Sc
2.01	0.0	1.0	53.3	0.0	1810.4
2.02	26.5	7.5	415.8	1012.9	1810.4
2.03	54.1	12.4	687.4	2067.9	1810.4
2.04	75.9	15.8	875.9	2901.2	1810.4
2.05	87.6	16.9	936.8	3348.4	1810.4
2.06	106.2	19.8	1097.6	4059.4	1810.4
2.07	109.1	20.0	1108.7	4170.2	1810.4
2.08	125.0	21.2	1175.2	4778.0	1810.4
2.09	133.3	22.1	1225.1	5095.3	1810.4
2.10	142.3	22.8	1263.9	5439.3	1810.4
2.11	162.2	23.9	1324.9	6199.9	1810.4
2.12	168.5	25.0	1385.9	6440.7	1810.4
2.13	193.5	26.3	1457.9	7396.3	1810.4
2.14	215.6	27.5	1524.4	8241.1	1810.4
2.15	238.1	28.7	1591.0	9101.1	1810.4
2.16	260.9	29.8	1651.9	9972.6	1810.4

TABLE A6.6.11.2 I_L-N DATA FOR THE ELECTROLYTIC MIXING CELL WITH THE PRESENCE OF 2 LAYERS OF 12MM GLASS
SPHERICAL PARTICLES ON THE CATHODE

DATE 5-8-81
BATCH Batch 5 of 0.005M Potassium Ferricyanide/0.005M
Potassium Ferrocyanide/0.5M Sodium Hydroxide
solution prepared on 23-6-81

Potential = 1.0092 V
Solution Temperature = 20.0 C
Ferricyanide concentration = 0.500E-05 mol/cm³
Density = 1.0236 g/cm³
Viscosity = 0.011111 g/cm s
Diffusivity = 0.6596E-05 cm²/s

Run No	Stirrer Speed (rpm)	Limiting Current (mA)	Sh	Re	Sc
1.01	0.0	1.6	85.3	0.0	1645.6
1.02	10.5	3.9	206.4	419.3	1645.6
1.03	33.3	7.0	368.5	1329.9	1645.6
1.04	65.2	12.4	652.8	2603.9	1645.6
1.05	77.4	14.4	758.1	3091.1	1645.6
1.06	87.6	15.5	816.0	3498.5	1645.6
1.07	102.3	17.1	900.3	4085.6	1645.6
1.08	113.9	18.9	995.0	4548.8	1645.6
1.09	145.5	21.3	1121.4	5810.8	1645.6
1.10	171.4	23.3	1226.7	6845.2	1645.6
1.11	194.6	24.9	1310.9	7771.8	1645.6
1.12	215.8	26.0	1368.8	8618.4	1645.6
1.13	250.0	26.9	1416.2	9984.3	1645.6
1.14	290.0	29.0	1526.7	11581.8	1645.6

DATE 6-8-81
BATCH Batch 5 of 0.005M Potassium Ferricyanide/0.005M
Potassium Ferrocyanide/0.5M Sodium Hydroxide
solution prepared on 23-6-81

Potential = 1.0092 V
Solution Temperature = 21.0 C
Ferricyanide concentration = 0.500E-05 mol/cm³
Density = 1.0231 g/cm³
Viscosity = 0.010867 g/cm s
Diffusivity = 0.6767E-05 cm²/s

Run No	Stirrer Speed (rpm)	Limiting Current (mA)	Sh	Re	Sc
2.01	0.0	0.6	30.8	0.0	1569.6
2.02	26.5	5.6	289.9	1081.5	1569.6
2.03	37.0	6.9	356.1	1510.1	1569.6
2.04	66.7	11.4	585.0	2722.2	1569.6
2.05	85.1	13.2	677.4	3473.2	1569.6
2.06	98.4	14.5	744.1	4016.0	1569.6
2.07	103.4	16.6	851.9	4220.1	1569.6
2.08	144.9	18.3	939.1	5913.8	1569.6
2.09	176.5	20.2	1036.6	7203.5	1569.6
2.10	208.3	21.8	1118.7	8501.4	1569.6

APPENDIX A6.7 THE EFFECT OF THE CATHODE SURFACE TEMPERATURE UPON THE CURRENT-POTENTIAL DATA AT AN IMPELLER
ROTATIONAL SPEED OF 37.5 ± 2.2 rpm FOR THE ELECTROLYTIC MIXING CELL WITHOUT THE PRESENCE OF
GLASS SPHERICAL PARTICLES ON THE CATHODE WHERE $\Delta T = 0$

DATE 13-1-81
BATCH Batch 1 of 0.005M Potassium Ferricyanide/0.005M
Potassium Ferrocyanide/0.5M Sodium Hydroxide
solution prepared on 9-12-80

Run No 1.01
Stirrer Speed = 35.3 rpm
Solution Temperature = 21.0 C
Cathode Surface Temperature = 21.0 C

Potential (V)	Current (mA)
0.0590	3.4
0.1114	6.3
0.1640	8.9
0.2000	10.4
0.2658	12.1
0.3243	12.7
0.4013	13.0
0.4553	13.0
0.5606	13.1
0.6381	13.2
0.7484	13.3
0.8172	13.3
0.9283	13.4
1.0247	13.3
1.1175	13.5
1.2602	13.8
1.3584	14.0
1.4961	14.5
1.6214	18.7

DATE 26-2-81
BATCH Batch 3 of 0.005M Potassium Ferricyanide/0.005M
Potassium Ferrocyanide/0.5M Sodium Hydroxide
solution prepared on 9-12-80

Run No 1.01
Stirrer Speed = 39.7 rpm
Solution Temperature = 30.0 C
Cathode Surface Temperature = 30.0 C

Potential (V)	Current (mA)
0.0753	4.7
0.1058	6.6
0.1421	8.7
0.2044	12.2
0.2845	15.6
0.4472	17.7
0.5701	17.8
0.6767	17.9
0.7735	18.2
0.8337	18.3
0.9151	18.2
0.9991	18.2
1.0735	18.4
1.1424	18.4
1.2624	18.5
1.3767	18.6
1.5155	19.2
1.5485	19.0
1.5997	20.7
1.6592	23.5

DATE 26-2-81
 BATCH Batch 3 of 0.005M Potassium Ferricyanide/0.005M
 Potassium Ferrocyanide/0.5M Sodium Hydroxide
 solution prepared on 9-12-80

Run No 1.01
 Stirrer Speed = 38.8 rpm
 Solution Temperature = 40.0 C
 Cathode Surface Temperature = 40.0 C

Potential (V)	Current (mA)
0.0574	3.8
0.1115	7.4
0.1380	9.1
0.1895	12.5
0.2370	15.3
0.2729	17.4
0.3014	18.8
0.3470	20.7
0.3957	22.2
0.4289	22.7
0.5220	22.7
0.6091	22.5
0.6723	22.7
0.7256	23.0
0.8132	23.0
0.9873	22.7
1.0614	23.0
1.1609	23.0
1.2251	23.0
1.3081	23.7
1.4012	24.0
1.4823	24.5
1.5911	26.1

DATE 26-2-81
 BATCH Batch 3 of 0.005M Potassium Ferricyanide/0.005M
 Potassium Ferrocyanide/0.5M Sodium Hydroxide
 solution prepared on 9-12-80

Run No 1.01
 Stirrer Speed = 38.8 rpm
 Solution Temperature = 48.0 C
 Cathode Surface Temperature = 48.0 C

Potential (V)	Current (mA)
0.0629	4.3
0.0985	6.8
0.1327	9.3
0.1775	12.4
0.2520	17.3
0.3277	22.1
0.3895	25.0
0.4351	26.4
0.5011	27.8
0.5733	28.3
0.6514	28.7
0.7119	28.7
0.7884	28.7
0.8560	28.7
0.9382	28.4
1.0354	28.5
1.1285	28.3
1.2476	28.7
1.3387	28.7
1.4987	28.5
1.6187	30.5
1.6785	33.0

APPENDIX A6.8 MASS AND HEAT TRANSFER DATA FOR THE ELECTROLYTIC MIXING CELL WITHOUT THE PRESENCE OF GLASS SPHERICAL PARTICLES ON THE HEATED CATHODE

DATE 27-4-82

BATCH Batch 1 of 0.005M Potassium Ferricyanide/ 0.005M Potassium Ferrocyanide/ 0.5M Sodium Hydroxide solution prepared on 23-4-82

Run No	V (volts)	N (rpm)	I _l (mA)	C _b (mol/cm ³)	T _b (C)	T _{s1} (C)	T _{s2} (C)	T _{s3} (C)	T _w (C)	T _a (C)	I _h (A)	Q (J/s)	Q _L (J/s)	Q _b (J/s)
1.01	0.8398	0.0	3.2	0.500D-05	16.0	18.0	20.7	18.0	20.0	18.0	0.069	0.55	0.07	0.47
1.02	0.8398	0.0	4.0	0.500D-05	16.0	19.3	22.7	19.0	22.0	18.0	0.104	1.24	0.12	1.12
1.03	0.8398	0.0	5.2	0.500D-05	17.0	21.5	26.4	21.0	23.0	18.0	0.155	2.75	0.32	2.44
1.04	0.8398	0.0	6.2	0.500D-05	18.0	23.5	29.6	23.0	28.0	18.0	0.197	4.44	0.32	4.12
1.05	0.8398	0.0	8.1	0.500D-05	19.0	27.0	37.7	26.0	31.0	18.0	0.302	10.44	0.70	9.74

Run No	k (W/cm K)	p (g/cm ³)	u (g/cm s)	cp (J/g K)	D (cm ² /s)	Nu	Sh	Re	Grh	Grm	Pr	Sc
1.01	0.6046D-02	1.0247	0.01170	4.0870	0.621D-05	3.9	178.9	0.0	0.483D+07	0.175D+07	7.9	1838.9
1.02	0.6061D-02	1.0243	0.01149	4.0869	0.634D-05	6.2	219.0	0.0	0.762D+07	0.181D+07	7.7	1768.6
1.03	0.6098D-02	1.0234	0.01099	4.0869	0.668D-05	9.6	270.5	0.0	0.123D+08	0.198D+07	7.4	1609.0
1.04	0.6130D-02	1.0225	0.01057	4.0868	0.699D-05	13.2	308.0	0.0	0.172D+08	0.214D+07	7.0	1478.4
1.05	0.6191D-02	1.0207	0.00981	4.0866	0.761D-05	19.7	369.5	0.0	0.338D+08	0.247D+07	6.5	1263.2

DATE 27-4-82

BATCH Batch 1 of 0.005M Potassium Ferricyanide/ 0.005M Potassium Ferrocyanide/ 0.5M Sodium Hydroxide solution prepared on 23-4-82

Run No	V (volts)	N (rpm)	I _l (mA)	C _b (mol/cm ³)	T _b (C)	T _{s1} (C)	T _{s2} (C)	T _{s3} (C)	T _w (C)	T _a (C)	I _h (A)	Q (J/s)	Q _L (J/s)	Q _b (J/s)
2.01	0.8398	0.0	3.5	0.500D-05	15.0	17.0	19.9	17.0	19.0	19.5	0.072	0.60	0.05	0.55
2.02	0.8398	0.0	5.2	0.500D-05	17.0	19.8	26.4	19.0	21.0	19.5	0.155	2.74	0.33	2.42

Run No	k (W/cm K)	p (g/cm ³)	u (g/cm s)	cp (J/g K)	D (cm ² /s)	Nu	Sh	Re	Grh	Grm	Pr	Sc
2.01	0.6028D-02	1.0251	0.01196	4.0870	0.606D-05	4.4	198.3	0.0	0.466D+07	0.168D+07	8.1	1924.4
2.02	0.6089D-02	1.0236	0.01110	4.0869	0.660D-05	11.0	271.1	0.0	0.104D+08	0.194D+07	7.5	1643.4

DATE 28-4-82

BATCH Batch 1 of 0.005M Potassium Ferricyanide/ 0.005M Potassium Ferrocyanide/ 0.5M Sodium Hydroxide solution prepared on 23-4-82

Run No	V (volts)	N (rpm)	I _L (mA)	C _b (mol/cm ³)	T _b (C)	T _{s1} (C)	T _{s2} (C)	T _{s3} (C)	T _w (C)	T _a (C)	I _h (A)	Q (J/s)	Q _L (J/s)	Q _b (J/s)
3.01	0.8398	0.0	3.8	0.500D-05	17.0	18.0	22.6	18.0	19.0	20.0	0.085	0.82	0.19	0.63
3.02	0.8398	0.0	5.8	0.500D-05	18.0	23.0	29.2	22.0	25.0	20.0	0.191	4.16	0.36	3.80
3.03	0.8398	0.0	8.1	0.500D-05	21.0	28.0	39.5	26.0	33.0	20.0	0.300	10.30	0.67	9.63
3.04	0.8398	0.0	10.9	0.500D-05	24.0	32.5	56.0	30.0	41.0	20.0	0.417	19.91	1.32	18.59

Run No	k (W/cm K)	p (g/cm ³)	u (g/cm s)	cp (J/g K)	D (cm ² /s)	Nu	Sh	Re	Grh	Grm	Pr	Sc
3.01	0.6064D-02	1.0242	0.01145	4.0869	0.637D-05	5.2	207.5	0.0	0.515D+07	0.183D+07	7.7	1754.1
3.02	0.6127D-02	1.0226	0.01062	4.0868	0.695D-05	12.8	288.2	0.0	0.161D+08	0.212D+07	7.1	1493.2
3.03	0.6221D-02	1.0197	0.00946	4.0865	0.794D-05	20.3	353.2	0.0	0.362D+08	0.265D+07	6.2	1168.5
3.04	0.6334D-02	1.0155	0.00822	4.0861	0.935D-05	24.3	405.9	0.0	0.878D+08	0.348D+07	5.3	866.0

DATE 28-4-82

BATCH Batch 1 of 0.005M Potassium Ferricyanide/ 0.005M Potassium Ferrocyanide/ 0.5M Sodium Hydroxide solution prepared on 23-4-82

Run No	V (volts)	N (rpm)	I _L (mA)	C _b (mol/cm ³)	T _b (°C)	T _{s1} (°C)	T _{s2} (°C)	T _{s3} (°C)	T _w (°C)	T _a (°C)	I _h (A)	Q (J/s)	Q _L (J/s)	Q _b (J/s)
4.01	0.8322	21.2	6.9	0.500D-05	17.0	18.5	21.2	18.0	19.0	20.6	0.095	1.03	0.12	0.91
4.02	0.8322	21.2	8.2	0.500D-05	19.0	22.0	30.0	21.0	21.0	20.6	0.192	4.22	0.52	3.70
4.03	0.8322	21.2	10.6	0.500D-05	21.0	29.0	41.3	30.0	39.0	20.6	0.300	10.31	0.55	9.75
4.04	0.8322	21.2	14.5	0.500D-05	23.0	31.0	52.4	30.0	39.0	20.6	0.393	17.68	1.16	16.52
4.05	0.8322	21.2	14.8	0.500D-05	26.0	35.0	66.1	33.0	43.0	20.6	0.493	27.83	1.80	26.03
4.06	0.8322	21.2	17.8	0.500D-05	29.0	40.5	82.8	38.0	53.0	20.6	0.611	42.75	2.44	40.30
4.07	0.8322	21.2	20.4	0.500D-05	31.0	43.5	95.9	41.0	59.0	20.6	0.700	56.10	2.98	53.12

Run No	k (W/cm K)	p (g/cm ³)	u (g/cm s)	cp (J/g K)	D (cm ² /s)	Nu	Sh	Re	Grh	Grm	Pr	Sc
4.01	0.6060D-02	1.0243	0.01151	4.0869	0.633D-05	8.9	379.6	817.9			7.8	1774.4
4.02	0.6134D-02	1.0224	0.01052	4.0868	0.703D-05	14.4	402.8	893.5			7.0	1463.4
4.03	0.6233D-02	1.0193	0.00933	4.0865	0.807D-05	18.5	456.5	1004.5			6.1	1133.1
4.04	0.6305D-02	1.0167	0.00853	4.0862	0.896D-05	23.5	560.7	1095.7			5.5	936.6
4.05	0.6399D-02	1.0127	0.00756	4.0858	0.103D-04	27.8	500.5	1231.2			4.8	724.7
4.06	0.6501D-02	1.0072	0.00658	4.0853	0.121D-04	31.8	512.2	1406.6			4.1	540.0
4.07	0.6566D-02	1.0030	0.00598	4.0849	0.135D-04	35.0	523.7	1540.7			3.7	441.3

DATE 29-4-82

BATCH Batch 1 of 0.005M Potassium Ferricyanide/ 0.005M Potassium Ferrocyanide/ 0.5M Sodium Hydroxide solution prepared on 23-4-82

Run No	V (volts)	N (rpm)	I _L (mA)	C _b (mol/cm ³)	T _b (C)	T _{s1} (C)	T _{s2} (C)	T _{s3} (C)	T _w (C)	T _a (C)	I _h (A)	Q (J/s)	Q _L (J/s)	Q _b (J/s)
5.01	0.8322	56.6	11.0	0.500D-05	15.0	16.0	17.8	16.0	17.0	20.6	0.087	0.86	0.04	0.82
5.02	0.8322	56.6	12.1	0.500D-05	16.0	17.5	24.1	17.0	20.0	20.6	0.187	3.99	0.21	3.78
5.03	0.8322	56.6	14.1	0.500D-05	17.0	21.5	31.9	21.0	27.0	20.6	0.290	9.63	0.38	9.24
5.04	0.8322	56.6	16.7	0.500D-05	20.0	26.0	43.8	25.0	34.0	20.6	0.409	19.15	0.82	18.34
5.05	0.8322	56.6	19.0	0.500D-05	21.0	29.0	52.4	28.0	41.0	20.6	0.500	28.63	1.07	27.55

Run No	k (W/cm K)	p (g/cm ³)	u (g/cm s)	cp (J/g K)	D (cm ² /s)	Nu	Sh	Re	Grh	Grm	Pr	Sc
5.01	0.6014D-02	1.0254	0.01217	4.0871	0.594D-05	11.9	643.1	2067.6			8.3	1998.0
5.02	0.6059D-02	1.0243	0.01151	4.0870	0.633D-05	21.7	662.5	2182.8			7.8	1775.7
5.03	0.6123D-02	1.0227	0.01067	4.0868	0.691D-05	26.1	707.1	2352.4			7.1	1508.7
5.04	0.6222D-02	1.0197	0.00945	4.0865	0.796D-05	33.1	728.6	2648.5			6.2	1164.5
5.05	0.6280D-02	1.0176	0.00879	4.0863	0.864D-05	37.3	763.5	2839.0			5.7	1000.1

DATE 29-4-82

BATCH Batch 1 of 0.005M Potassium Ferricyanide/ 0.005M Potassium Ferrocyanide/ 0.5M Sodium Hydroxide solution prepared on 23-4-82

Run No	V (volts)	N (rpm)	I _l (mA)	C _b (mol/cm ³)	T _b (C)	T _{s1} (C)	T _{s2} (C)	T _{s3} (C)	T _w (C)	T _a (C)	I _h (A)	Q (J/s)	Q _L (J/s)	Q _b (J/s)
6.01	0.8322	55.5	19.2	0.500D-05	23.0	30.0	56.4	29.0	45.0	20.6	0.521	31.08	1.15	29.93
6.02	0.8322	55.5	21.8	0.500D-05	26.0	34.0	69.2	32.0	52.0	20.6	0.628	45.16	1.65	43.51
6.03	0.8322	55.5	24.4	0.500D-05	28.0	37.0	81.5	35.0	57.0	20.6	0.734	61.69	2.18	59.51

Run No	k (W/cm K)	p (g/cm ³)	u (g/cm s)	cp (J/g K)	D (cm ² /s)	Nu	Sh	Re	Grh	Grm	Pr	Sc
6.01	0.6317D-02	1.0162	0.00839	4.0862	0.912D-05	39.3	732.1	2912.7			5.4	905.6
6.02	0.6407D-02	1.0123	0.00748	4.0858	0.104D-04	44.4	725.0	3256.3			4.8	708.6
6.03	0.6477D-02	1.0086	0.00680	4.0854	0.116D-04	49.2	727.2	3568.1			4.3	579.1

DATE 29-4-82

BATCH Batch 1 of 0.005M Potassium Ferricyanide/ 0.005M Potassium Ferrocyanide/ 0.5M Sodium Hydroxide solution prepared on 23-4-82

Run No	V (volts)	N (rpm)	I _L (mA)	C _b (mol/cm ³)	T _b (C)	T _{s1} (C)	T _{s2} (C)	T _{s3} (C)	T _w (C)	T _a (C)	I _h (A)	Q (J/s)	Q _L (J/s)	Q _b (J/s)
7.01	0.8322	119.2	17.9	0.500D-05	16.0	17.5	22.6	17.0	21.0	20.6	0.185	3.94	0.07	3.87
7.02	0.8322	119.2	19.6	0.500D-05	18.0	19.0	28.9	19.0	24.0	20.6	0.267	8.16	0.28	7.88
7.03	0.8322	119.2	22.4	0.500D-05	21.0	22.5	40.3	22.0	32.0	20.6	0.406	18.87	0.62	18.25
7.04	0.8322	119.2	24.2	0.500D-05	22.0	24.5	47.5	24.0	39.0	20.6	0.497	28.28	0.78	27.50
7.05	0.8322	119.2	27.1	0.500D-05	25.0	27.5	58.9	27.0	45.0	20.6	0.611	42.75	1.21	41.54
7.06	0.8322	119.2	30.2	0.500D-05	27.0	30.0	68.3	29.0	52.0	20.6	0.706	57.07	1.51	55.56

Run No	k (W/cm K)	p (g/cm ³)	u (g/cm s)	cp (J/g K)	D (cm ² /s)	Nu	Sh	Re	Grh	Grm	Pr	Sc
7.01	0.6052D-02	1.0245	0.01161	4.0870	0.627D-05	26.5	992.9	4558.7			7.8	1808.3
7.02	0.6107D-02	1.0231	0.01087	4.0868	0.676D-05	36.4	1007.4	4861.6			7.3	1571.9
7.03	0.6200D-02	1.0204	0.00970	4.0866	0.771D-05	47.3	1007.7	5434.4			6.4	1232.7
7.04	0.6249D-02	1.0188	0.00914	4.0864	0.826D-05	52.6	1018.4	5758.2			6.0	1086.1
7.05	0.6333D-02	1.0155	0.00822	4.0861	0.934D-05	60.4	1006.8	6380.6			5.3	867.1
7.06	0.6396D-02	1.0128	0.00759	4.0858	0.103D-04	65.6	1021.0	6898.1			4.8	730.4

DATE 29-4-82

BATCH Batch 1 of 0.005M Potassium Ferricyanide/ 0.005M Potassium Ferrocyanide/ 0.5M Sodium Hydroxide solution prepared on 23-4-82

Run No	V (volts)	N (rpm)	I _l (mA)	C _b (mol/cm ³)	T _b (C)	T _{s1} (C)	T _{s2} (C)	T _{s3} (C)	T _w (C)	T _a (C)	I _h (A)	Q (J/s)	Q _L (J/s)	Q _b (J/s)
8.01	0.8322	155.2	19.1	0.500D-05	17.0	17.0	22.6	17.0	19.0	20.6	0.175	3.49	0.17	3.32
8.02	0.8322	155.2	21.3	0.500D-05	19.0	20.0	30.8	20.0	26.0	20.6	0.298	10.17	0.31	9.85
8.03	0.8322	155.2	21.5	0.500D-05	21.0	22.5	39.6	22.0	33.0	20.6	0.415	19.72	0.54	19.18
8.04	0.8322	155.2	23.8	0.500D-05	23.0	25.0	47.4	24.0	38.0	20.6	0.507	29.43	0.81	28.62
8.05	0.8322	155.2	28.7	0.500D-05	26.0	27.5	57.0	27.0	44.0	20.6	0.602	41.50	1.13	40.37
8.06	0.8322	155.2	31.7	0.500D-05	28.0	30.5	67.2	30.0	53.0	20.6	0.715	58.54	1.41	57.12

Run No	k (W/cm K)	p (g/cm ³)	u (g/cm s)	cp (J/g K)	D (cm ² /s)	Nu	Sh	Re	Grh	Grm	Pr	Sc
8.01	0.6060D-02	1.0243	0.01151	4.0870	0.633D-05	32.5	1046.3	5986.5			7.8	1774.9
8.02	0.6129D-02	1.0225	0.01058	4.0868	0.698D-05	42.1	1060.7	6499.4			7.1	1483.9
8.03	0.6197D-02	1.0205	0.00974	4.0866	0.768D-05	51.7	974.3	7047.3			6.4	1243.6
8.04	0.6259D-02	1.0184	0.00903	4.0864	0.839D-05	57.9	987.6	7590.5			5.9	1057.0
8.05	0.6333D-02	1.0155	0.00822	4.0861	0.934D-05	65.8	1066.5	8309.7			5.3	866.6
8.06	0.6401D-02	1.0125	0.00754	4.0858	0.103D-04	71.7	1064.7	9040.4			4.8	719.9

DATE 5-5-82

BATCH Batch 1 of 0.005M Potassium Ferricyanide/ 0.005M Potassium Ferrocyanide/ 0.5M Sodium Hydroxide solution prepared on 23-4-82

Run No	V (volts)	N (rpm)	I _L (mA)	C _b (mol/cm ³)	T _b (C)	T _{s1} (C)	T _{s2} (C)	T _{s3} (C)	T _w (C)	T _a (C)	I _h (A)	Q (J/s)	Q _L (J/s)	Q _b (J/s)
9.01	0.8319	192.3	20.0	0.500D-05	14.0	16.0	20.0	16.0	18.0	17.3	0.190	4.14	0.12	4.02
9.02	0.8319	192.3	21.8	0.500D-05	17.0	17.5	28.0	17.0	25.0	17.3	0.295	9.96	0.25	9.71
9.03	0.8319	192.3	24.0	0.500D-05	19.0	19.5	35.2	19.0	31.0	17.3	0.391	17.50	0.43	17.08
9.04	0.8319	192.3	28.5	0.500D-05	23.0	24.5	52.1	24.0	45.0	17.3	0.600	41.22	0.90	40.32
9.05	0.8319	192.3	33.1	0.500D-05	26.0	27.5	68.2	26.0	60.0	17.3	0.787	70.92	1.31	69.61

Run No	k (W/cm K)	p (g/cm ³)	u (g/cm s)	cp (J/g K)	D (cm ² /s)	Nu	Sh	Re	Grh	Grm	Pr	Sc
9.01	0.6015D-02	1.0254	0.01216	4.0871	0.595D-05	28.0	1168.1	7031.1			8.3	1994.0
9.02	0.6086D-02	1.0237	0.01114	4.0869	0.657D-05	46.6	1150.0	7657.9			7.5	1655.9
9.03	0.6146D-02	1.0220	0.01036	4.0867	0.715D-05	55.9	1165.9	8221.6			6.9	1418.4
9.04	0.6277D-02	1.0178	0.00883	4.0863	0.860D-05	70.3	1149.5	9605.3			5.8	1009.3
9.05	0.6378D-02	1.0136	0.00776	4.0859	0.998D-05	83.6	1150.5	10882.3			5.0	767.3

DATE 23-8-82

BATCH Batch 7 of 0.005M Potassium Ferricyanide/ 0.005M Potassium Ferrocyanide/ 0.5M Sodium Hydroxide solution prepared on 23-5-82

Run No	V (volts)	N (rpm)	I1 (mA)	Cb (mol/cm ³)	Tb (C)	Ts1 (C)	Ts2 (C)	Ts3 (C)	Tw (C)	Ta (C)	Ih (A)	Q (J/s)	QL (J/s)	Qb (J/s)
10.01	1.0116	0.0	7.0	0.500D-05	19.0	22.0	29.0	22.0	24.0	17.2	0.192	4.22	0.42	3.80
10.02	1.0116	18.1	9.3	0.500D-05	17.0	20.5	28.0	21.0	23.5	17.2	0.189	4.09	0.38	3.71
10.03	1.0116	49.2	13.9	0.500D-05	17.0	18.0	24.0	18.0	22.0	17.2	0.185	3.92	0.17	3.75
10.04	1.0116	70.6	16.7	0.500D-05	17.0	18.0	23.0	18.0	22.0	17.2	0.185	3.92	0.12	3.80
10.05	1.0116	107.8	19.8	0.500D-05	17.0	19.0	22.0	19.0	21.0	17.2	0.184	3.88	0.13	3.75
10.06	1.0116	119.2	21.5	0.500D-05	17.0	17.0	22.0	17.0	21.0	17.2	0.183	3.83	0.09	3.75
10.07	1.0116	142.9	23.8	0.500D-05	17.0	17.0	22.0	17.0	21.0	17.2	0.182	3.79	0.09	3.71
10.08	1.0116	166.7	25.9	0.500D-05	17.0	17.0	22.0	17.0	20.0	17.2	0.181	3.76	0.13	3.63
10.09	1.0116	187.5	27.7	0.500D-05	17.0	17.0	22.0	17.0	20.0	17.2	0.181	3.76	0.13	3.63

Run No	k (W/cm K)	p (g/cm ³)	u (g/cm s)	cp (J/g K)	D (cm ² /s)	Nu	Sh	Re	Grh	Grm	Pr	Sc
10.01	0.6130D-02	1.0225	0.01057	4.0868	0.699D-05	16.0	349.9	0.0	0.130D+08	0.213D+07	7.0	1480.2
10.02	0.6100D-02	1.0233	0.01096	4.0869	0.670D-05	14.1	482.2	732.7			7.3	1597.6
10.03	0.6070D-02	1.0241	0.01136	4.0869	0.643D-05	25.8	752.1	1922.4			7.6	1725.8
10.04	0.6066D-02	1.0242	0.01143	4.0869	0.639D-05	30.0	907.5	2743.5			7.7	1746.5
10.05	0.6066D-02	1.0242	0.01143	4.0869	0.639D-05	29.6	1074.8	4189.1			7.7	1746.5
10.06	0.6057D-02	1.0244	0.01155	4.0870	0.631D-05	41.5	1186.3	4581.5			7.8	1788.8
10.07	0.6057D-02	1.0244	0.01155	4.0870	0.631D-05	41.0	1313.3	5492.4			7.8	1788.8
10.08	0.6057D-02	1.0244	0.01155	4.0870	0.631D-05	40.1	1427.7	6407.2			7.8	1788.8
10.09	0.6057D-02	1.0244	0.01155	4.0870	0.631D-05	40.1	1525.2	7206.6			7.8	1788.8

DATE 23-8-82

BATCH Batch 7 of 0.005M Potassium Ferricyanide/ 0.005M Potassium Ferrocyanide/ 0.5M Sodium Hydroxide solution prepared on 23-5-82

Run No	V (volts)	N (rpm)	I _L (mA)	C _b (mol/cm ³)	T _b (C)	T _{s1} (C)	T _{s2} (C)	T _{s3} (C)	T _w (C)	T _a (C)	I _h (A)	Q (J/s)	Q _L (J/s)	Q _b (J/s)
11.01	1.0189	0.0	9.5	0.500D-05	18.0	23.0	37.0	23.0	21.0	18.3	0.310	11.00	0.97	10.03
11.02	1.0189	13.0	10.6	0.500D-05	21.0	26.0	40.0	26.0	30.0	18.3	0.290	9.63	0.81	8.82
11.03	1.0189	28.2	12.5	0.500D-05	21.0	24.0	37.0	24.0	29.0	18.3	0.291	9.70	0.65	9.05
11.04	1.0189	34.5	13.5	0.500D-05	21.0	23.0	36.0	23.0	29.0	18.3	0.288	9.50	0.57	8.92
11.05	1.0189	47.0	15.5	0.500D-05	20.0	22.0	34.0	22.0	27.5	18.3	0.286	9.37	0.51	8.85
11.06	1.0189	72.8	18.3	0.500D-05	20.0	21.0	34.0	21.0	27.0	18.3	0.282	9.11	0.51	8.59
11.07	1.0189	86.2	20.2	0.500D-05	20.0	21.0	31.0	21.0	26.0	18.3	0.281	9.04	0.39	8.65
11.08	1.0189	109.1	23.2	0.500D-05	20.0	20.0	30.0	20.0	25.0	18.3	0.281	9.04	0.36	8.68
11.09	1.0189	147.2	25.6	0.500D-05	19.5	20.0	29.0	20.0	24.5	18.3	0.281	9.04	0.33	8.71
11.10	1.0189	179.6	28.5	0.500D-05	19.0	20.0	28.0	20.0	24.5	18.3	0.281	9.04	0.28	8.76
11.11	1.0189	198.7	30.9	0.500D-05	19.0	19.0	27.0	19.0	23.0	18.3	0.282	9.11	0.27	8.84
11.12	1.0189	230.8	32.6	0.500D-05	19.0	19.0	27.0	19.0	23.0	18.3	0.285	9.30	0.27	9.03
11.13	1.0189	267.8	35.2	0.500D-05	19.0	19.0	27.0	19.0	23.0	18.3	0.284	9.24	0.27	8.97

Run No	k (W/cm K)	p (g/cm ³)	u (g/cm s)	cp (J/g K)	D (cm ² /s)	Nu	Sh	Re	Grh	Grm	Pr	Sc
11.01	0.6161D-02	1.0216	0.01018	4.0867	0.730D-05	22.7	450.1	0.0	0.272D+08	0.230D+07	6.7	1364.4
11.02	0.6214D-02	1.0199	0.00954	4.0865	0.787D-05	19.8	468.7	602.5			6.3	1189.1
11.03	0.6192D-02	1.0206	0.00980	4.0866	0.763D-05	25.8	570.9	1273.4			6.5	1258.9
11.04	0.6184D-02	1.0209	0.00990	4.0866	0.753D-05	28.4	620.6	1541.6			6.5	1288.1
11.05	0.6161D-02	1.0216	0.01018	4.0867	0.730D-05	30.1	735.5	2045.4			6.7	1364.4
11.06	0.6157D-02	1.0217	0.01023	4.0867	0.725D-05	31.2	876.3	3151.5			6.8	1380.3
11.07	0.6143D-02	1.0221	0.01040	4.0867	0.712D-05	39.3	986.8	3672.5			6.9	1429.3
11.08	0.6134D-02	1.0224	0.01051	4.0868	0.703D-05	47.4	1147.6	4598.8			7.0	1463.0
11.09	0.6125D-02	1.0226	0.01063	4.0868	0.694D-05	47.7	1281.5	6138.6			7.1	1497.6
11.10	0.6116D-02	1.0229	0.01075	4.0868	0.685D-05	48.0	1446.0	7409.6			7.2	1533.1
11.11	0.6107D-02	1.0231	0.01087	4.0868	0.677D-05	60.6	1586.9	8109.6			7.3	1569.6
11.12	0.6107D-02	1.0231	0.01087	4.0868	0.677D-05	62.0	1673.7	9419.7			7.3	1569.6
11.13	0.6107D-02	1.0231	0.01087	4.0868	0.677D-05	61.5	1807.9	10929.8			7.3	1569.6

DATE 24-8-82

BATCH Batch 7 of 0.005M Potassium Ferricyanide/ 0.005M Potassium Ferrocyanide/ 0.5M Sodium Hydroxide solution prepared on 23-5-82

Run No	V (volts)	N (rpm)	I _L (mA)	C _b (mol/cm ³)	T _b (C)	T _{s1} (C)	T _{s2} (C)	T _{s3} (C)	T _w (C)	T _a (C)	I _h (A)	Q (J/s)	Q _L (J/s)	Q _b (J/s)
12.01	1.0189	0.0	10.9	0.500D-05	22.0	27.0	50.0	27.0	33.0	18.3	0.407	18.97	1.24	17.72
12.02	1.0189	21.0	12.6	0.500D-05	22.0	28.0	50.0	28.0	33.0	18.3	0.398	18.14	1.26	16.87
12.03	1.0189	43.2	15.5	0.500D-05	20.5	23.0	44.0	23.0	32.0	18.3	0.392	17.59	0.89	16.70
12.04	1.0189	96.8	19.7	0.500D-05	20.0	20.0	37.0	20.0	29.0	18.3	0.389	17.33	0.57	16.75
12.05	1.0189	94.5	20.3	0.500D-05	20.0	20.0	36.0	20.0	28.0	18.3	0.388	17.24	0.56	16.68
12.06	1.0189	114.3	22.1	0.500D-05	19.0	19.0	35.0	19.0	27.0	18.3	0.386	17.06	0.53	16.53
12.07	1.0189	144.5	24.7	0.500D-05	18.0	18.0	33.0	18.0	27.0	18.3	0.382	16.71	0.42	16.29
12.08	1.0189	214.3	29.1	0.500D-05	18.0	18.0	31.0	18.0	26.0	18.3	0.381	16.62	0.35	16.27
12.09	1.0189	258.7	31.2	0.500D-05	18.0	18.0	30.0	18.0	26.0	18.3	0.378	16.36	0.30	16.06
12.10	1.0189	329.7	34.0	0.500D-05	18.0	18.0	30.0	18.0	25.0	18.3	0.379	16.45	0.34	16.11

Run No	k (W/cm K)	p (g/cm ³)	u (g/cm s)	cp (J/g K)	D (cm ² /s)	Nu	Sh	Re	Grh	Grm	Pr	Sc
12.01	0.6270D-02	1.0180	0.00891	4.0863	0.852D-05	28.7	445.4	0.0	0.562D+08	0.298D+07	5.8	1027.4
12.02	0.6274D-02	1.0178	0.00886	4.0863	0.857D-05	26.5	511.3	1045.8			5.8	1016.0
12.03	0.6214D-02	1.0199	0.00954	4.0865	0.787D-05	34.6	686.0	2002.2			6.3	1189.1
12.04	0.6166D-02	1.0214	0.01012	4.0867	0.735D-05	53.5	930.9	4235.1			6.7	1348.8
12.05	0.6161D-02	1.0216	0.01018	4.0867	0.730D-05	56.7	966.0	4112.6			6.7	1364.4
12.06	0.6143D-02	1.0221	0.01040	4.0867	0.712D-05	56.3	1076.9	4869.7			6.9	1429.3
12.07	0.6121D-02	1.0227	0.01069	4.0868	0.690D-05	59.5	1243.2	5993.7			7.1	1515.2
12.08	0.6112D-02	1.0230	0.01081	4.0868	0.681D-05	68.6	1482.7	8793.6			7.2	1551.2
12.09	0.6107D-02	1.0231	0.01087	4.0868	0.677D-05	73.4	1598.7	10558.4			7.3	1569.6
12.10	0.6107D-02	1.0231	0.01087	4.0868	0.677D-05	73.7	1744.8	13456.1			7.3	1569.6

DATE 24-8-82

BATCH Batch 7 of 0.005M Potassium Ferricyanide/ 0.005M Potassium Ferrocyanide/ 0.5M Sodium Hydroxide solution prepared on 23-5-82

Run No	V (volts)	N (rpm)	I _l (mA)	C _b (mol/cm ³)	T _b (C)	T _{s1} (C)	T _{s2} (C)	T _{s3} (C)	T _w (C)	T _a (C)	I _h (A)	Q (J/s)	Q _L (J/s)	Q _b (J/s)
13.01	1.0140	69.8	15.2	0.500D-05	18.0	18.0	23.0	18.0	19.0	18.3	0.197	4.44	0.21	4.23
13.02	1.0140	69.8	17.5	0.500D-05	19.0	22.0	29.0	22.0	23.0	18.3	0.322	11.87	0.44	11.44
13.03	1.0140	69.8	19.0	0.500D-05	22.0	22.0	34.0	22.0	25.0	18.3	0.413	19.53	0.59	18.94
13.04	1.0140	69.8	20.9	0.500D-05	21.0	23.0	36.0	23.0	26.0	18.3	0.504	29.08	0.69	28.40
13.05	1.0140	69.8	24.4	0.500D-05	22.0	25.0	45.0	25.0	31.0	18.3	0.653	48.82	1.01	47.82

Run No	k (W/cm K)	p (g/cm ³)	u (g/cm s)	cp (J/g K)	D (cm ² /s)	Nu	Sh	Re	Grh	Grm	Pr	Sc
13.01	0.6075D-02	1.0240	0.01130	4.0869	0.647D-05	46.7	817.5	2742.3			7.6	1705.3
13.02	0.6130D-02	1.0225	0.01057	4.0868	0.699D-05	48.1	868.1	2926.5			7.0	1460.2
13.03	0.6179D-02	1.0210	0.00996	4.0866	0.749D-05	85.6	881.5	3102.5			6.6	1302.9
13.04	0.6184D-02	1.0209	0.00990	4.0866	0.753D-05	90.5	964.7	3118.9			6.5	1288.1
13.05	0.6240D-02	1.0191	0.00924	4.0864	0.816D-05	98.7	1037.6	3336.9			6.1	1111.1

DATE 26-8-82

BATCH Batch 7 of 0.005M Potassium Ferricyanide/ 0.005M Potassium Ferrocyanide/ 0.5M Sodium Hydroxide solution prepared on 23-5-82

Run No	V (volts)	N (rpm)	I _l (mA)	C _b (mol/cm ³)	T _b (C)	T _{s1} (C)	T _{s2} (C)	T _{s3} (C)	T _w (C)	T _a (C)	I _h (A)	Q (J/s)	Q _L (J/s)	Q _b (J/s)
14.01	1.0129	0.0	5.8	0.500D-05	14.7	18.1	26.4	18.1	21.4	17.5	0.176	3.55	0.34	3.20
14.02	1.0129	18.4	7.8	0.500D-05	13.1	17.7	24.1	17.7	21.9	17.5	0.169	3.27	0.21	3.06
14.03	1.0129	52.6	11.9	0.500D-05	13.4	14.4	20.0	14.4	19.2	17.5	0.165	3.11	0.03	3.07

Run No	k (W/cm K)	p (g/cm ³)	u (g/cm s)	cp (J/g K)	D (cm ² /s)	Nu	Sh	Re	Grh	Grm	Pr	Sc
14.01	0.6061D-02	1.0243	0.01150	4.0869	0.634D-05	11.7	315.9	0.0	0.116D+08	0.181D+07	7.8	1769.6
14.02	0.6033D-02	1.0250	0.01188	4.0870	0.610D-05	10.9	442.0	687.9			8.1	1899.7
14.03	0.6001D-02	1.0257	0.01235	4.0871	0.584D-05	22.6	709.3	1893.2			8.4	2063.3

DATE 27-8-82

BATCH Batch 7 of 0.005M Potassium Ferricyanide/ 0.005M Potassium Ferrocyanide/ 0.5M Sodium Hydroxide solution prepared on 23-5-82

Run No	V (volts)	N (rpm)	I _L (mA)	C _b (mol/cm ³)	T _b (C)	T _{s1} (C)	T _{s2} (C)	T _{s3} (C)	T _w (C)	T _a (C)	I _h (A)	Q (J/s)	Q _L (J/s)	Q _b (J/s)
15.01	1.0132	0.0	7.2	0.500D-05	14.0	20.4	25.2	20.4	21.9	16.7	0.162	3.00	0.33	2.67
15.02	1.0132	5.8	11.7	0.500D-05	14.3	18.0	24.0	18.0	22.0	16.7	0.156	2.80	0.21	2.59
15.03	1.0132	214.3	23.2	0.500D-05	14.0	15.0	18.9	15.0	19.0	16.7	0.153	2.68	0.01	2.68

Run No	k (W/cm K)	p (g/cm ³)	u (g/cm s)	cp (J/g K)	D (cm ² /s)	Nu	Sh	Re	Grh	Grm	Pr	Sc
15.01	0.6059D-02	1.0243	0.01152	4.0870	0.633D-05	8.4	396.7	0.0	0.134D+08	0.181D+07	7.8	1776.0
15.02	0.6045D-02	1.0247	0.01171	4.0870	0.621D-05	10.7	654.1	220.0			7.9	1841.1
15.03	0.6005D-02	1.0256	0.01230	4.0871	0.586D-05	25.3	1375.6	7743.6			8.4	2045.7

DATE 30-8-82

BATCH Batch 7 of 0.005M Potassium Ferricyanide/ 0.005M Potassium Ferrocyanide/ 0.5M Sodium Hydroxide solution prepared on 23-5-82

Run No	V (volts)	N (rpm)	I _l (mA)	C _b (mol/cm ³)	T _b (C)	T _{s1} (C)	T _{s2} (C)	T _{s3} (C)	T _w (C)	T _a (C)	I _h (A)	Q (J/s)	Q _L (J/s)	Q _b (J/s)
16.01	1.0114	0.0	6.5	0.500D-05	16.3	21.9	33.4	21.9	25.8	16.9	0.252	7.27	0.62	6.65
16.02	1.0114	28.3	9.3	0.500D-05	17.1	20.8	31.3	20.8	26.8	16.9	0.243	6.76	0.44	6.32
16.03	1.0114	51.7	12.1	0.500D-05	16.1	18.2	27.7	18.2	25.7	16.9	0.241	6.65	0.25	6.40
16.04	1.0114	83.3	14.6	0.500D-05	15.6	17.1	25.8	17.1	25.1	16.9	0.237	6.43	0.15	6.28
16.05	1.0114	122.4	17.2	0.500D-05	15.6	16.2	24.2	16.2	24.0	16.9	0.233	6.22	0.09	6.13
16.06	1.0114	157.9	19.3	0.500D-05	15.6	15.9	22.5	15.9	23.0	16.9	0.231	6.11	0.03	6.08
16.07	1.0114	204.1	21.4	0.500D-05	14.8	15.5	22.6	15.5	22.3	16.9	0.230	6.06	0.07	5.99
16.08	1.0114	250.0	23.5	0.500D-05	15.1	15.6	22.0	15.6	22.3	16.9	0.229	6.03	0.03	6.00

Run No	k (W/cm K)	p (g/cm ³)	u (g/cm s)	cp (J/g K)	D (cm ² /s)	Nu	Sh	Re	Grh	Grm	Pr	Sc
16.01	0.6125D-02	1.0226	0.01064	4.0868	0.694D-05	16.0	323.5	0.0	0.223D+08	0.211D+07	7.1	1499.3
16.02	0.6118D-02	1.0228	0.01073	4.0868	0.687D-05	19.3	470.7	1169.4			7.2	1527.7
16.03	0.6080D-02	1.0238	0.01123	4.0869	0.652D-05	25.8	643.6	2043.5			7.5	1683.1
16.04	0.6062D-02	1.0243	0.01148	4.0869	0.635D-05	29.7	799.2	3221.1			7.7	1765.4
16.05	0.6050D-02	1.0246	0.01165	4.0870	0.625D-05	36.9	957.7	4668.3			7.9	1819.1
16.06	0.6041D-02	1.0248	0.01178	4.0870	0.617D-05	46.8	1087.1	5956.0			8.0	1863.4
16.07	0.6032D-02	1.0250	0.01190	4.0870	0.609D-05	39.2	1219.1	7617.9			8.1	1906.6
16.08	0.6032D-02	1.0250	0.01190	4.0870	0.610D-05	45.0	1336.6	9336.3			8.1	1904.3

DATE 30-8-82

BATCH Batch 7 of 0.005M Potassium Ferricyanide/ 0.005M Potassium Ferrocyanide/ 0.5M Sodium Hydroxide solution prepared on 23-5-82

Run No	V (volts)	N (rpm)	I _l (mA)	C _b (mol/cm ³)	T _b (C)	T _{s1} (C)	T _{s2} (C)	T _{s3} (C)	T _w (C)	T _a (C)	I _h (A)	Q (J/s)	Q _L (J/s)	Q _b (J/s)
17.01	1.0160	0.0	8.8	0.500D-05	18.7	24.4	45.4	24.4	33.3	16.1	0.361	14.92	1.03	13.89
17.02	1.0160	14.9	9.0	0.500D-05	15.2	26.1	44.8	26.1	35.0	16.1	0.343	13.47	1.01	12.46
17.03	1.0160	27.3	10.4	0.500D-05	17.7	23.5	41.7	23.5	33.3	16.1	0.333	12.70	0.82	11.87
17.04	1.0160	59.4	13.2	0.500D-05	16.3	19.3	34.7	19.3	29.9	16.1	0.323	11.95	0.50	11.44
17.05	1.0160	106.1	16.6	0.500D-05	16.5	17.0	30.7	17.0	28.3	16.1	0.323	11.95	0.30	11.65
17.06	1.0160	160.0	19.6	0.500D-05	14.4	16.5	28.9	16.5	27.5	16.1	0.328	12.32	0.24	12.07
17.07	1.0160	202.0	21.2	0.500D-05	15.6	16.8	27.1	16.8	27.8	16.1	0.326	12.17	0.13	12.04
17.08	1.0160	256.0	23.7	0.500D-05	15.6	16.8	27.1	16.8	27.3	16.1	0.327	12.24	0.15	12.09
17.09	1.0160	355.0	26.8	0.500D-05	15.6	16.1	26.1	16.1	27.3	16.1	0.327	12.24	0.08	12.16

Run No	k (W/cm K)	p (g/cm ³)	u (g/cm s)	cp (J/g K)	D (cm ² /s)	Nu	Sh	Re	Grh	Grm	Pr	Sc
17.01	0.6211D-02	1.0200	0.00958	4.0865	0.783D-05	23.1	392.5	0.0	0.442D+08	0.259D+07	6.3	1200.0
17.02	0.6185D-02	1.0209	0.00989	4.0866	0.755D-05	16.7	414.2	666.8			6.5	1283.6
17.03	0.6182D-02	1.0210	0.00993	4.0866	0.751D-05	21.6	480.0	1217.3			6.6	1294.0
17.04	0.6119D-02	1.0228	0.01071	4.0868	0.688D-05	29.3	667.8	2458.5			7.2	1522.4
17.05	0.6092D-02	1.0235	0.01107	4.0869	0.663D-05	43.6	870.8	4253.5			7.4	1632.0
17.06	0.6062D-02	1.0243	0.01148	4.0869	0.635D-05	40.2	1072.0	6190.4			7.7	1763.3
17.07	0.6066D-02	1.0242	0.01142	4.0869	0.639D-05	52.4	1149.4	7854.1			7.7	1744.4
17.08	0.6066D-02	1.0242	0.01142	4.0869	0.639D-05	52.6	1287.3	9953.7			7.7	1744.4
17.09	0.6058D-02	1.0244	0.01153	4.0870	0.632D-05	61.1	1470.5	13674.6			7.8	1780.3

DATE 1-9-82

BATCH Batch 7 of 0.005M Potassium Ferricyanide/ 0.005M Potassium Ferrocyanide/ 0.5M Sodium Hydroxide solution prepared on 23-5-82

Run No	V (volts)	N (rpm)	I _L (mA)	C _b (mol/cm ³)	T _b (C)	T _{s1} (C)	T _{s2} (C)	T _{s3} (C)	T _w (C)	T _a (C)	I _h (A)	Q (J/s)	Q _L (J/s)	Q _b (J/s)
18.01	1.0143	0.0	10.5	0.500D-05	17.7	27.5	56.8	27.5	42.9	16.5	0.454	23.60	1.37	22.23
18.02	1.0143	27.3	12.3	0.500D-05	17.7	27.5	54.6	27.5	42.9	16.5	0.440	22.17	1.25	20.92
18.03	1.0143	82.7	16.5	0.500D-05	16.8	19.5	42.9	19.5	37.8	16.5	0.438	21.97	0.64	21.32
18.04	1.0143	144.0	20.1	0.500D-05	15.9	17.7	38.1	17.7	36.8	16.5	0.437	21.87	0.40	21.47
18.05	1.0143	206.9	22.8	0.500D-05	15.8	16.5	35.5	16.5	34.7	16.5	0.432	21.37	0.31	21.06
18.06	1.0143	260.9	23.4	0.500D-05	15.8	16.7	34.7	16.7	35.2	16.5	0.433	21.47	0.25	21.22
18.07	1.0143	300.0	25.8	0.500D-05	15.7	16.3	33.1	16.3	33.1	16.5	0.431	21.27	0.23	21.04
18.08	1.0143	352.9	27.2	0.500D-05	15.7	15.8	32.6	15.8	33.5	16.5	0.433	21.47	0.18	21.28

Run No	k (W/cm K)	p (g/cm ³)	u (g/cm s)	cp (J/g K)	D (cm ² /s)	Nu	Sh	Re	Grh	Grm	Pr	Sc
18.01	0.6264D-02	1.0182	0.00897	4.0864	0.845D-05	24.3	433.1	0.0	0.819D+08	0.294D+07	5.8	1042.4
18.02	0.6255D-02	1.0185	0.00907	4.0864	0.834D-05	24.0	512.7	1328.7			5.9	1068.3
18.03	0.6161D-02	1.0216	0.01018	4.0867	0.730D-05	40.3	786.7	3599.1			6.7	1364.4
18.04	0.6124D-02	1.0227	0.01065	4.0868	0.692D-05	48.9	1007.0	5992.2			7.1	1504.6
18.05	0.6105D-02	1.0232	0.01089	4.0868	0.675D-05	56.7	1171.4	8426.0			7.3	1577.0
18.06	0.6103D-02	1.0232	0.01093	4.0868	0.672D-05	58.8	1207.7	10590.7			7.3	1588.2
18.07	0.6093D-02	1.0235	0.01106	4.0869	0.663D-05	64.3	1353.7	12033.4			7.4	1630.1
18.08	0.6088D-02	1.0236	0.01112	4.0869	0.659D-05	68.9	1431.4	14078.5			7.5	1649.5

APPENDIX A6.9 MASS AND HEAT TRANSFER DATA FOR THE ELECTROLYTIC MIXING CELL WITH THE PRESENCE OF ONE OR MORE LAYERS OF GLASS SPHERICAL PARTICLES ON THE HEATED CATHODE

TABLE A6.9.1.1 I_L - N DATA FOR THE ELECTROLYTIC MIXING CELL WITH THE PRESENCE OF 1 LAYER OF 3MM GLASS SPHERICAL PARTICLES ON THE HEATED CATHODE

DATE 6-9-82

BATCH Batch 1 of 0.005M Potassium Ferricyanide/ 0.005M Potassium Ferrocyanide/ 0.5M Sodium Hydroxide solution prepared on 6-9-82

Run No	V (volts)	N (rpm)	I _L (mA)	C _b (mol/cm ³)	T _b (C)	T _{s1} (C)	T _{s2} (C)	T _{s3} (C)	T _w (C)	T _a (C)	I _h (A)	Q (J/s)	Q _L +Q _p (J/s)	Q _f (J/s)
1.01	1.0121	0.0	4.3	0.500D-05	18.8	25.9	33.1	25.9	27.1	16.6	0.164	3.08	0.70	2.38
1.02	1.0121	24.6	6.1	0.500D-05	18.3	25.3	32.1	25.3	26.9	16.6	0.148	2.52	0.64	1.87
1.03	1.0121	51.3	11.0	0.500D-05	17.8	20.4	26.1	20.4	25.1	16.6	0.149	2.55	0.26	2.29
1.04	1.0121	94.2	14.5	0.500D-05	16.9	19.4	24.4	19.4	24.3	16.6	0.148	2.50	0.18	2.32
1.05	1.0121	94.5	16.3	0.500D-05	17.0	18.0	23.1	18.0	22.7	16.6	0.147	2.47	0.14	2.33
1.06	1.0121	122.4	19.8	0.500D-05	17.5	17.8	22.1	17.8	22.7	16.6	0.148	2.50	0.07	2.44
1.07	1.0121	157.9	23.5	0.500D-05	17.1	17.4	22.0	17.4	21.4	16.6	0.147	2.46	0.11	2.35
1.08	1.0121	188.7	26.8	0.500D-05	17.1	17.9	21.2	17.9	21.9	16.6	0.147	2.46	0.06	2.40

Run No	k (W/cm K)	p (g/cm ³)	u (g/cm s)	cp (J/g K)	D (cm ² /s)	Nu	Sh	Re	Grh	Grm	Pr	Sc
1.01	0.6164D-02	1.0215	0.01015	4.0867	0.732D-05	6.0	204.3	0.0	0.245D+08	0.231D+07	6.7	1356.6
1.02	0.6152D-02	1.0219	0.01030	4.0867	0.720D-05	4.9	293.0	1058.4			6.8	1398.9
1.03	0.6098D-02	1.0233	0.01098	4.0869	0.668D-05	11.6	571.6	2071.7			7.4	1606.1
1.04	0.6078D-02	1.0239	0.01126	4.0869	0.649D-05	12.8	773.4	3712.1			7.6	1694.2
1.05	0.6066D-02	1.0242	0.01142	4.0869	0.639D-05	18.1	886.0	3674.3			7.7	1744.4
1.06	0.6065D-02	1.0242	0.01143	4.0869	0.638D-05	27.5	1079.7	4753.9			7.7	1748.6
1.07	0.6060D-02	1.0243	0.01151	4.0869	0.633D-05	25.4	1290.5	6092.4			7.8	1773.9
1.08	0.6058D-02	1.0244	0.01153	4.0870	0.632D-05	27.6	1470.5	7268.7			7.8	1780.3

DATE 7-9-82

BATCH Batch 1 of 0.005M Potassium Ferricyanide/ 0.005M Potassium Ferrocyanide/ 0.5M Sodium Hydroxide solution prepared on 6-9-82

Run No	V (volts)	N (rpm)	I _L (mA)	C _b (mol/cm ³)	T _b (C)	T _{s1} (C)	T _{s2} (C)	T _{s3} (C)	T _w (C)	T _a (C)	I _h (A)	Q (J/s)	Q _L +Q _p (J/s)	Q _f (J/s)
2.01	1.0116	0.0	9.6	0.500D-05	23.9	33.8	48.6	33.8	35.6	16.3	0.260	7.74	1.39	6.35
2.02	1.0116	12.0	10.0	0.500D-05	21.4	31.9	46.4	31.9	35.0	16.3	0.246	6.93	1.28	5.65
2.03	1.0116	53.3	13.7	0.500D-05	19.8	23.9	37.4	23.9	32.9	16.3	0.243	6.76	0.68	6.09
2.04	1.0116	85.7	17.3	0.500D-05	19.8	21.7	32.6	21.7	28.6	16.3	0.240	6.60	0.51	6.09
2.05	1.0116	109.1	20.2	0.500D-05	19.5	20.8	29.8	20.8	26.4	16.3	0.238	6.49	0.41	6.08
2.06	1.0116	138.7	22.8	0.500D-05	19.5	19.8	28.3	19.8	26.6	16.3	0.239	6.54	0.29	6.25

Run No	k (W/cm K)	p (g/cm ³)	u (g/cm s)	cp (J/g K)	D (cm ² /s)	Nu	Sh	Re	Grh	Grm	Pr	Sc
2.01	0.6308D-02	1.0165	0.00849	4.0862	0.901D-05	9.8	370.7	0.0	0.679D+08	0.327D+07	5.5	927.0
2.02	0.6270D-02	1.0180	0.00891	4.0863	0.851D-05	8.5	407.9	594.4			5.8	1028.0
2.03	0.6183D-02	1.0209	0.00992	4.0866	0.752D-05	15.1	632.1	2379.1			6.6	1291.0
2.04	0.6152D-02	1.0219	0.01030	4.0867	0.720D-05	22.3	834.5	3687.4			6.8	1398.9
2.05	0.6132D-02	1.0224	0.01054	4.0868	0.701D-05	28.8	1002.2	4587.7			7.0	1470.7
2.06	0.6121D-02	1.0227	0.01069	4.0868	0.690D-05	37.8	1149.9	5754.6			7.1	1514.3

DATE 26-9-82

BATCH Batch 3 of 0.005M Potassium Ferricyanide/ 0.005M Potassium Ferrocyanide/ 0.5M Sodium Hydroxide solution prepared on 6-9-82

Run No	V (volts)	N (rpm)	Il (mA)	Cb (mol/cm ³)	Tb (C)	Ts1 (C)	Ts2 (C)	Ts3 (C)	Tw (C)	Ta (C)	Ih (A)	Q (J/s)	QL+Qp (J/s)	Qf (J/s)
3.01	1.0180	0.0	11.7	0.500D-05	21.0	29.8	50.8	29.8	37.1	15.6	0.345	13.63	1.35	12.28
3.02	1.0180	35.7	12.5	0.500D-05	18.3	25.1	47.5	25.1	37.1	15.6	0.334	12.77	1.10	11.67
3.03	1.0180	103.8	18.9	0.500D-05	16.3	19.3	34.1	19.3	32.4	15.6	0.324	12.02	0.43	11.59
3.04	1.0180	140.6	22.1	0.500D-05	16.3	17.5	31.0	17.5	31.0	15.6	0.324	12.02	0.27	11.75
3.05	1.0180	189.9	24.7	0.500D-05	16.3	17.8	35.3	17.8	29.3	15.6	0.322	11.87	0.57	11.30
3.06	1.0180	234.4	26.8	0.500D-05	15.3	17.0	34.1	17.0	28.1	15.6	0.315	11.36	0.55	10.82

Run No	k (W/cm K)	p (g/cm ³)	u (g/cm s)	cp (J/g K)	D (cm ² /s)	Nu	Sh	Re	Grh	Grm	Pr	Sc
3.01	0.6277D-02	1.0178	0.00883	4.0863	0.860D-05	17.0	472.2	0.0	0.675D+08	0.303D+07	5.8	1009.3
3.02	0.6219D-02	1.0198	0.00948	4.0865	0.792D-05	17.4	546.3	1664.5			6.2	1173.7
3.03	0.6116D-02	1.0229	0.01075	4.0868	0.685D-05	30.6	959.1	4281.2			7.2	1534.0
3.04	0.6094D-02	1.0235	0.01104	4.0869	0.664D-05	40.6	1154.1	5648.8			7.4	1624.3
3.05	0.6115D-02	1.0229	0.01077	4.0868	0.684D-05	30.2	1253.5	7821.9			7.2	1538.5
3.06	0.6097D-02	1.0234	0.01101	4.0869	0.667D-05	29.0	1394.0	9448.2			7.4	1612.8

DATE 8-9-82

BATCH Batch 1 of 0.005M Potassium Ferricyanide/ 0.005M Potassium Ferrocyanide/ 0.5M Sodium Hydroxide solution prepared on 6-9-82

Run No	V (volts)	N (rpm)	I _L (mA)	C _b (mol/cm ³)	T _b (C)	T _{s1} (C)	T _{s2} (C)	T _{s3} (C)	T _w (C)	T _a (C)	I _h (A)	Q (J/s)	Q _L +Q _p (J/s)	Q _f (J/s)
4.01	1.0212	0.0	14.0	0.500D-05	19.8	36.1	62.1	36.1	43.3	16.9	0.390	17.42	2.01	15.41
4.02	1.0212	35.5	14.8	0.500D-05	18.9	32.9	59.6	32.9	44.5	16.9	0.379	16.45	1.76	14.68
4.03	1.0212	68.2	16.5	0.500D-05	17.3	24.4	47.7	24.4	38.6	16.9	0.379	16.45	1.10	15.34
4.04	1.0212	102.6	19.6	0.500D-05	15.8	19.8	41.3	19.8	36.7	16.9	0.376	16.19	0.71	15.47
4.05	1.0212	138.5	23.3	0.500D-05	15.8	17.8	37.1	17.8	33.8	16.9	0.374	16.02	0.53	15.48
4.06	1.0212	179.1	27.5	0.500D-05	14.3	16.3	34.3	16.3	31.4	16.9	0.378	16.36	0.45	15.92
4.07	1.0212	214.3	30.0	0.500D-05	14.3	15.4	34.3	15.4	31.4	16.9	0.375	16.10	0.42	15.68

Run No	k (W/cm K)	p (g/cm ³)	u (g/cm s)	cp (J/g K)	D (cm ² /s)	Nu	Sh	Re	Grh	Grm	Pr	Sc
4.01	0.6339D-02	1.0153	0.00817	4.0861	0.941D-05	13.9	516.4	0.0	0.130D+09	0.353D+07	5.3	854.5
4.02	0.6308D-02	1.0165	0.00849	4.0862	0.900D-05	14.2	569.6	1842.9			5.5	927.5
4.03	0.6209D-02	1.0201	0.00961	4.0865	0.780D-05	22.1	736.0	3139.6			6.3	1206.8
4.04	0.6146D-02	1.0220	0.01036	4.0867	0.715D-05	28.6	952.9	4386.4			6.9	1418.5
4.05	0.6119D-02	1.0228	0.01072	4.0868	0.688D-05	36.3	1174.9	5730.9			7.2	1523.2
4.06	0.6085D-02	1.0237	0.01116	4.0869	0.656D-05	39.8	1453.2	7121.6			7.5	1661.3
4.07	0.6081D-02	1.0238	0.01122	4.0869	0.652D-05	40.9	1596.7	8479.6			7.5	1679.1

TABLE A6.9.1.2 I_L-N DATA FOR THE ELECTROLYTIC MIXING CELL WITH THE PRESENCE OF 2 LAYERS OF 3MM GLASS
SPHERICAL PARTICLES ON THE HEATED CATHODE

DATE 9-9-82

BATCH Batch 1 of 0.005M Potassium Ferricyanide/ 0.005M Potassium Ferrocyanide/ 0.5M Sodium Hydroxide solution prepared on 6-9-82

Run No	V (volts)	N (rpm)	I _L (mA)	Cb (mol/cm ³)	Tb (C)	Ts1 (C)	Ts2 (C)	Ts3 (C)	Tw (C)	Ta (C)	Ih (A)	Q (J/s)	QL+Qp (J/s)	Qf (J/s)
1.01	1.0125	0.0	4.5	0.500D-05	17.3	28.6	35.7	28.6	25.9	16.5	0.165	3.12	0.94	2.18
1.02	1.0125	61.2	10.3	0.500D-05	15.8	18.3	25.6	18.3	24.7	16.5	0.158	2.86	0.21	2.64
1.03	1.0125	87.6	12.7	0.500D-05	15.8	17.8	22.7	17.8	22.7	16.5	0.152	2.65	0.12	2.53
1.04	1.0125	121.2	15.2	0.500D-05	15.3	16.3	21.5	16.3	22.0	16.5	0.149	2.54	0.05	2.49
1.05	1.0125	159.3	18.8	0.500D-05	15.5	15.8	20.3	15.8	20.3	16.5	0.148	2.51	0.04	2.47
1.06	1.0125	209.8	22.7	0.500D-05	14.8	15.0	19.9	15.0	20.4	16.5	0.148	2.51	0.01	2.50

Run No	k (W/cm K)	p (g/cm ³)	u (g/cm s)	cp (J/g K)	D (cm ² /s)	Nu	Sh	Re	Grh	Grm	Pr	Sc
1.01	0.6174D-02	1.0212	0.01002	4.0867	0.743D-05	4.0	208.5	0.0	0.352D+08	0.237D+07	6.6	1320.3
1.02	0.6068D-02	1.0241	0.01139	4.0869	0.641D-05	11.9	558.6	2384.8			7.7	1736.1
1.03	0.6052D-02	1.0245	0.01161	4.0870	0.627D-05	15.7	703.1	3350.3			7.8	1808.2
1.04	0.6035D-02	1.0249	0.01186	4.0870	0.612D-05	19.2	859.9	4541.3			8.0	1890.6
1.05	0.6029D-02	1.0251	0.01195	4.0870	0.607D-05	27.1	1078.9	5924.3			8.1	1921.7
1.06	0.6017D-02	1.0254	0.01212	4.0870	0.597D-05	26.2	1321.0	7692.2			8.2	1982.0

DATE 16-9-82

BATCH Batch 1 of 0.005M Potassium Ferricyanide/ 0.005M Potassium Ferrocyanide/ 0.5M Sodium Hydroxide solution prepared on 6-9-82

Run No	V (volts)	N (rpm)	I _L (mA)	C _b (mol/cm ³)	T _b (°C)	T _{s1} (°C)	T _{s2} (°C)	T _{s3} (°C)	T _w (°C)	T _a (°C)	I _h (A)	Q (J/s)	Q _L +Q _p (J/s)	Q _f (J/s)
2.01	1.0095	0.0	8.8	0.500D-05	19.0	35.0	50.4	35.0	38.1	16.3	0.264	7.98	1.43	6.55
2.02	1.0095	26.4	10.9	0.500D-05	17.0	31.4	48.6	31.4	36.4	16.3	0.255	7.45	1.34	6.10
2.03	1.0095	61.2	14.0	0.500D-05	15.3	21.2	35.7	21.2	29.5	16.3	0.247	6.99	0.67	6.32
2.04	1.0095	105.8	18.1	0.500D-05	15.3	17.3	29.5	17.3	27.8	16.3	0.246	6.93	0.30	6.63

Run No	k (W/cm K)	p (g/cm ³)	u (g/cm s)	cp (J/g K)	D (cm ² /s)	Nu	Sh	Re	Gr _h	Gr _m	Pr	Sc
2.01	0.6280D-02	1.0176	0.00880	4.0863	0.864D-05	7.4	355.5	0.0	0.841D+08	0.305D+07	5.7	1000.3
2.02	0.6240D-02	1.0190	0.00924	4.0864	0.816D-05	7.1	464.7	1262.4			6.0	1110.5
2.03	0.6123D-02	1.0227	0.01066	4.0868	0.692D-05	13.1	702.6	2545.3			7.1	1506.4
2.04	0.6077D-02	1.0239	0.01127	4.0869	0.649D-05	22.6	967.7	4165.8			7.6	1697.2

TABLE A6.9.2.1 I_L-N DATA FOR THE ELECTROLYTIC MIXING CELL WITH THE PRESENCE OF 1 LAYER OF 7MM GLASS
SPHERICAL PARTICLES ON THE HEATED CATHODE

DATE 26-9-82

BATCH Batch 3 of 0.005M Potassium Ferricyanide/ 0.005M Potassium Ferrocyanide/ 0.5M Sodium Hydroxide solution prepared on 6-9-82

Run No	V (volts)	N (rpm)	I _L (mA)	Cb (mol/cm ³)	Tb (C)	Ts1 (C)	Ts2 (C)	Ts3 (C)	Tw (C)	Ta (C)	Ih (A)	Q (J/s)	QL+Qp (J/s)	Qf (J/s)
1.01	1.0180	0.0	6.3	0.500D-05	17.3	22.2	28.8	22.2	24.4	15.6	0.165	3.14	0.48	2.65
1.02	1.0180	37.5	9.2	0.500D-05	15.5	17.5	24.1	17.5	24.1	15.6	0.162	3.01	0.16	2.86
1.03	1.0180	70.6	13.2	0.500D-05	14.5	15.8	20.3	15.8	19.3	15.6	0.155	2.74	0.11	2.63
1.04	1.0180	116.9	17.5	0.500D-05	14.5	15.5	19.8	15.5	19.8	15.6	0.151	2.63	0.06	2.57

Run No	k (W/cm K)	p (g/cm ³)	u (g/cm s)	cp (J/g K)	D (cm ² /s)	Nu	Sh	Re	Grh	Grm	Pr	Sc
1.01	0.6114D-02	1.0229	0.01077	4.0868	0.684D-05	8.9	320.4	0.0	0.155D+08	0.206D+07	7.2	1540.3
1.02	0.6055D-02	1.0245	0.01158	4.0870	0.629D-05	15.0	505.6	1437.8			7.8	1798.5
1.03	0.6020D-02	1.0253	0.01209	4.0870	0.599D-05	20.7	767.4	2596.5			8.2	1968.8
1.04	0.6016D-02	1.0254	0.01214	4.0870	0.596D-05	22.9	1018.2	4280.1			8.2	1988.0

DATE 27-9-82

BATCH Batch 3 of 0.005M Potassium Ferricyanide/ 0.005M Potassium Ferrocyanide/ 0.5M Sodium Hydroxide solution prepared on 6-9-82

Run No	V (volts)	N (rpm)	I _l (mA)	C _b (mol/cm ³)	T _b (C)	T _{s1} (C)	T _{s2} (C)	T _{s3} (C)	T _w (C)	T _a (C)	I _h (A)	Q (J/s)	Q _L +Q _p (J/s)	Q _f (J/s)
2.01	1.0180	0.0	10.9	0.500D-05	20.0	30.0	48.8	30.0	37.4	16.7	0.306	10.76	1.22	9.54
2.02	1.0180	46.9	12.5	0.500D-05	17.5	24.0	41.4	25.5	34.3	16.7	0.307	10.79	0.82	9.97
2.03	1.0180	70.6	15.5	0.500D-05	17.5	20.8	36.2	20.8	32.6	16.7	0.308	10.86	0.52	10.34
2.04	1.0180	111.1	19.4	0.500D-05	16.3	19.5	32.4	19.5	31.2	16.7	0.307	10.79	0.35	10.44
2.05	1.0180	159.3	22.8	0.500D-05	16.3	17.5	29.3	17.5	29.3	16.7	0.308	10.86	0.21	10.65

Run No	k (W/cm K)	p (g/cm ³)	u (g/cm s)	cp (J/g K)	D (cm ² /s)	Nu	Sh	Re	Grh	Grm	Pr	Sc
2.01	0.6261D-02	1.0183	0.00901	4.0864	0.840D-05	13.2	451.4	0.0	0.639D+08	0.291D+07	5.9	1052.9
2.02	0.6181D-02	1.0210	0.00994	4.0866	0.750D-05	17.8	576.7	2089.0			6.6	1297.0
2.03	0.6143D-02	1.0221	0.01040	4.0867	0.712D-05	25.7	758.2	3007.1			6.9	1430.1
2.04	0.6109D-02	1.0231	0.01084	4.0868	0.679D-05	29.7	991.6	4546.6			7.2	1560.4
2.05	0.6086D-02	1.0237	0.01115	4.0869	0.657D-05	41.3	1207.4	6341.2			7.5	1657.4

DATE 27-9-82

BATCH Batch 3 of 0.005M Potassium Ferricyanide/ 0.005M Potassium Ferrocyanide/ 0.5M Sodium Hydroxide solution prepared on 6-9-82

Run No	V (volts)	N (rpm)	I _L (mA)	C _b (mol/cm ³)	T _b (C)	T _{s1} (C)	T _{s2} (C)	T _{s3} (C)	T _w (C)	T _a (C)	I _h (A)	Q (J/s)	Q _L +Q _p (J/s)	Q _f (J/s)
3.01	1.0180	0.0	11.7	0.500D-05	21.0	29.8	50.8	29.8	37.1	15.6	0.345	13.63	1.28	12.35
3.02	1.0180	35.7	12.5	0.500D-05	18.3	25.1	47.5	25.1	37.1	15.6	0.334	12.77	1.04	11.73
3.03	1.0180	103.8	18.9	0.500D-05	16.3	19.3	34.1	19.3	32.4	15.6	0.324	12.02	0.39	11.63
3.04	1.0180	140.6	22.1	0.500D-05	16.3	17.5	31.0	17.5	31.0	15.6	0.324	12.02	0.24	11.78
3.05	1.0180	189.9	24.7	0.500D-05	16.3	17.8	35.3	17.8	29.3	15.6	0.322	11.87	0.54	11.33
3.06	1.0180	234.4	26.8	0.500D-05	15.3	17.0	34.1	17.0	28.1	15.6	0.315	11.36	0.51	10.85

Run No	k (W/cm K)	p (g/cm ³)	u (g/cm s)	cp (J/g K)	D (cm ² /s)	Nu	Sh	Re	Grh	Grm	Pr	Sc
3.01	0.6277D-02	1.0178	0.00883	4.0863	0.860D-05	17.1	472.2	0.0	0.675D+08	0.303D+07	5.8	1009.3
3.02	0.6219D-02	1.0198	0.00948	4.0865	0.792D-05	17.5	546.3	1664.5			6.2	1173.7
3.03	0.6116D-02	1.0229	0.01075	4.0868	0.685D-05	30.7	959.1	4281.2			7.2	1534.0
3.04	0.6094D-02	1.0235	0.01104	4.0869	0.664D-05	40.7	1154.1	5648.8			7.4	1624.3
3.05	0.6115D-02	1.0229	0.01077	4.0868	0.684D-05	30.3	1253.5	7821.9			7.2	1538.5
3.06	0.6097D-02	1.0234	0.01101	4.0869	0.667D-05	29.1	1394.0	9448.2			7.4	1612.8

DATE 29-9-82

BATCH Batch 3 of 0.005M Potassium Ferricyanide/ 0.005M Potassium Ferrocyanide/ 0.5M Sodium Hydroxide solution prepared on 6-9-82

Run No	V (volts)	N (rpm)	I _l (mA)	C _b (mol/cm ³)	T _b (C)	T _{s1} (C)	T _{s2} (C)	T _{s3} (C)	T _w (C)	T _a (C)	I _h (A)	Q (J/s)	Q _L +Q _p (J/s)	Q _f (J/s)
4.01	1.0180	0.0	14.6	0.500D-05	23.9	34.1	64.6	34.1	50.1	15.6	0.441	22.27	1.73	20.54
4.02	1.0180	54.5	16.3	0.500D-05	20.3	25.2	54.8	25.3	46.6	15.6	0.440	22.17	1.15	21.02
4.03	1.0180	129.0	21.8	0.500D-05	19.3	20.8	43.9	20.8	42.3	15.6	0.441	22.27	0.61	21.65
4.04	1.0180	155.2	24.2	0.500D-05	18.3	19.8	39.0	19.8	39.0	15.6	0.437	21.87	0.45	21.42
4.05	1.0180	152.4	28.5	0.500D-05	18.5	18.8	39.5	18.8	39.5	15.6	0.435	21.67	0.43	21.23
4.06	1.0180	267.9	30.2	0.500D-05	18.1	18.8	36.9	18.8	36.9	15.6	0.437	21.87	0.39	21.48

Run No	k (W/cm K)	p (g/cm ³)	u (g/cm s)	cp (J/g K)	D (cm ² /s)	Nu	Sh	Re	Grh	Grm	Pr	Sc
4.01	0.6373D-02	1.0138	0.00781	4.0859	0.991D-05	21.2	512.0	0.0	0.128D+09	0.384D+07	5.0	777.5
4.02	0.6268D-02	1.0181	0.00893	4.0864	0.849D-05	28.5	667.2	2692.8			5.8	1033.7
4.03	0.6193D-02	1.0206	0.00979	4.0866	0.763D-05	44.9	994.2	5828.0			6.5	1257.4
4.04	0.6158D-02	1.0217	0.01021	4.0867	0.727D-05	52.3	1157.7	6729.3			6.8	1375.5
4.05	0.6158D-02	1.0217	0.01022	4.0867	0.727D-05	54.4	1360.2	6608.3			6.8	1376.3
4.06	0.6143D-02	1.0221	0.01041	4.0867	0.711D-05	60.2	1476.0	11404.6			6.9	1431.8

TABLE A6.9.2.2 I_L - N DATA FOR THE ELECTROLYTIC MIXING CELL WITH THE PRESENCE OF 2 LAYERS OF 7MM GLASS
SPHERICAL PARTICLES ON THE HEATED CATHODE

DATE 29-9-82

BATCH Batch 3 of 0.005M Potassium Ferricyanide/ 0.005M Potassium Ferrocyanide/ 0.5M Sodium Hydroxide solution prepared on 6-9-82

Run No	V (volts)	N (rpm)	I _L (mA)	C _b (mol/cm ³)	T _b (C)	T _{s1} (C)	T _{s2} (C)	T _{s3} (C)	T _w (C)	T _a (C)	I _h (A)	Q (J/s)	Q _L +Q _p (J/s)	Q _f (J/s)
1.01	1.0170	0.0	6.5	0.500D-05	15.6	24.9	32.2	24.9	25.1	16.1	0.183	3.83	0.69	3.14
1.02	1.0170	63.2	9.7	0.500D-05	15.5	17.3	24.2	17.3	22.7	16.1	0.172	3.38	0.19	3.18
1.03	1.0170	112.5	14.2	0.500D-05	14.8	15.3	21.2	15.3	20.5	16.1	0.166	3.14	0.08	3.06

Run No	k (W/cm K)	p (g/cm ³)	u (g/cm s)	cp (J/g K)	D (cm ² /s)	Nu	Sh	Re	Grh	Grm	Pr	Sc
1.01	0.6127D-02	1.0226	0.01061	4.0868	0.696D-05	6.7	322.4	0.0	0.256D+08	0.212D+07	7.1	1490.6
1.02	0.6054D-02	1.0245	0.01159	4.0870	0.628D-05	16.8	535.5	2422.4			7.8	1799.6
1.03	0.6024D-02	1.0252	0.01201	4.0870	0.603D-05	24.6	819.8	4161.8			8.1	1943.9
1.07	0.6004D-02	1.0256	0.01231	4.0871	0.586D-05	46.1	1445.4	11520.8			8.4	2049.5

DATE 1-10-82

BATCH Batch 3 of 0.005M Potassium Ferricyanide/ 0.005M Potassium Ferrocyanide/ 0.5M Sodium Hydroxide solution prepared on 6-9-82

Run No	V (volts)	N (rpm)	I1 (mA)	Cb (mol/cm ³)	Tb (C)	Ts1 (C)	Ts2 (C)	Ts3 (C)	Tw (C)	Ta (C)	Ih (A)	Q (J/s)	QL+Qp (J/s)	Qf (J/s)
2.01	1.0170	0.0	7.7	0.500D-05	21.7	31.2	47.3	31.2	37.6	19.1	0.287	9.43	1.03	8.40
2.02	1.0170	20.9	9.8	0.500D-05	20.0	29.3	45.4	29.3	36.4	19.1	0.274	8.60	0.96	7.64
2.03	1.0170	61.2	11.3	0.500D-05	18.3	21.5	36.7	21.5	32.4	19.1	0.271	8.41	0.48	7.93
2.04	1.0170	100.0	16.2	0.500D-05	17.8	19.3	31.2	19.3	28.8	19.1	0.272	8.47	0.27	8.20
2.05	1.0170	144.6	19.6	0.500D-05	17.8	19.0	28.1	19.0	28.1	19.1	0.268	8.22	0.13	8.10
2.06	1.0170	191.5	22.1	0.500D-05	17.5	18.8	26.9	18.8	28.1	19.1	0.268	8.22	0.06	8.16
2.07	1.0170	241.9	23.8	0.500D-05	16.8	17.8	25.6	17.8	27.6	19.1	0.268	8.22	0.00	8.22

Run No	k (W/cm K)	p (g/cm ³)	u (g/cm s)	cp (J/g K)	D (cm ² /s)	Nu	Sh	Re	Grh	Grm	Pr	Sc
2.01	0.6273D-02	1.0179	0.00887	4.0863	0.856D-05	12.8	312.1	0.0	0.605D+08	0.301D+07	5.8	1017.7
2.02	0.6243D-02	1.0189	0.00920	4.0864	0.820D-05	11.8	417.1	1003.0			6.0	1101.8
2.03	0.6156D-02	1.0217	0.01025	4.0867	0.724D-05	19.9	542.3	2645.1			6.8	1385.1
2.04	0.6117D-02	1.0229	0.01074	4.0868	0.686D-05	30.2	818.2	4126.7			7.2	1532.2
2.05	0.6101D-02	1.0233	0.01095	4.0868	0.671D-05	38.7	1015.0	5860.2			7.3	1593.9
2.06	0.6092D-02	1.0235	0.01107	4.0869	0.662D-05	42.2	1157.4	7675.0			7.4	1633.0
2.07	0.6075D-02	1.0239	0.01129	4.0869	0.647D-05	46.0	1279.4	9506.5			7.6	1704.3

DATE 1-10-82

BATCH Batch 3 of 0.005M Potassium Ferricyanide/ 0.005M Potassium Ferrocyanide/ 0.5M Sodium Hydroxide solution prepared on 6-9-82

Run No	V (volts)	N (rpm)	I _l (mA)	C _b (mol/cm ³)	T _b (C)	T _{s1} (C)	T _{s2} (C)	T _{s3} (C)	T _w (C)	T _a (C)	I _h (A)	Q (J/s)	Q _{L+Qp} (J/s)	Q _f (J/s)
3.01	1.0170	0.0	12.7	0.500D-05	23.2	34.8	58.6	34.8	46.1	18.9	0.407	18.97	1.42	17.55
3.02	1.0170	58.8	13.6	0.500D-05	20.3	25.1	48.2	25.1	41.1	18.9	0.389	17.33	0.85	16.47
3.03	1.0170	100.0	17.2	0.500D-05	19.3	23.4	42.5	23.4	39.3	18.9	0.386	17.06	0.58	16.48
3.04	1.0170	160.0	20.5	0.500D-05	19.3	20.8	55.8	20.8	35.0	18.9	0.371	15.76	1.39	14.37
3.05	1.0170	209.3	23.1	0.500D-05	18.5	19.5	34.1	19.5	34.1	18.9	0.368	15.51	0.24	15.27
3.06	1.0170	203.4	24.9	0.500D-05	18.5	19.8	32.9	19.8	34.1	18.9	0.370	15.68	0.18	15.50

Run No	k (W/cm K)	p (g/cm ³)	u (g/cm s)	cp (J/g K)	D (cm ² /s)	Nu	Sh	Re	Grh	Grm	Pr	Sc
3.01	0.6347D-02	1.0150	0.00808	4.0861	0.953D-05	19.7	462.5	0.0	0.107D+09	0.360D+07	5.2	835.7
3.02	0.6239D-02	1.0191	0.00925	4.0864	0.815D-05	26.9	579.9	2808.8			6.1	1113.0
3.03	0.6199D-02	1.0204	0.00972	4.0866	0.770D-05	32.4	774.1	4549.8			6.4	1238.2
3.04	0.6245D-02	1.0189	0.00919	4.0864	0.821D-05	20.3	868.4	7690.3			6.0	1098.1
3.05	0.6137D-02	1.0223	0.01048	4.0868	0.706D-05	50.2	1135.7	8850.7			7.0	1452.8
3.06	0.6133D-02	1.0224	0.01053	4.0868	0.701D-05	54.1	1233.9	8557.6			7.0	1469.0

TABLE A6.9.3.1

I_L -N DATA FOR THE ELECTROLYTIC MIXING CELL WITH THE PRESENCE OF 1 LAYER of 12MM GLASS
SPHERICAL PARTICLES ON THE HEATED CATHODE

DATE 16-9-82

BATCH Batch 2 of 0.005M Potassium Ferricyanide/ 0.005M Potassium Ferrocyanide/ 0.5M Sodium Hydroxide solution prepared on 6-9-82

Run No	V (volts)	N (rpm)	I _L (mA)	C _b (mol/cm ³)	T _b (C)	T _{s1} (C)	T _{s2} (C)	T _{s3} (C)	T _w (C)	T _a (C)	I _h (A)	Q (J/s)	Q _L +Q _p (J/s)	Q _f (J/s)
1.01	1.0136	0.0	6.8	0.500D-05	18.3	23.2	29.5	23.2	19.8	19.4	0.162	2.99	0.63	2.36
1.02	1.0136	27.1	8.8	0.500D-05	19.3	21.2	26.9	21.2	20.0	19.4	0.158	2.84	0.42	2.42
1.03	1.0136	43.9	11.8	0.500D-05	17.5	19.0	24.7	19.0	19.0	19.4	0.154	2.73	0.32	2.40
1.04	1.0136	97.6	19.8	0.500D-05	18.0	17.8	22.2	17.8	19.8	19.4	0.152	2.64	0.12	2.52
1.05	1.0136	130.4	22.5	0.500D-05	18.3	18.8	22.2	18.8	19.8	19.4	0.151	2.62	0.13	2.49
1.06	1.0136	171.4	26.3	0.500D-05	17.8	19.0	22.2	19.0	19.0	19.4	0.147	2.48	0.19	2.29
1.07	1.0136	222.2	29.2	0.500D-05	17.3	18.3	21.5	18.3	20.0	19.4	0.151	2.60	0.09	2.51

Run No	k (W/cm K)	p (g/cm ³)	u (g/cm s)	cp (J/g K)	D (cm ² /s)	Nu	Sh	Re	Grh	Grm	Pr	Sc
1.01	0.6131D-02	1.0225	0.01056	4.0868	0.699D-05	8.0	338.0	0.0	0.163D+08	0.214D+07	7.0	1476.7
1.02	0.6119D-02	1.0228	0.01071	4.0868	0.688D-05	13.8	446.5	1121.7			7.2	1522.4
1.03	0.6083D-02	1.0238	0.01119	4.0869	0.654D-05	15.2	628.9	1742.8			7.5	1671.2
1.04	0.6070D-02	1.0241	0.01136	4.0869	0.643D-05	34.8	1067.9	3813.6			7.6	1725.8
1.05	0.6077D-02	1.0239	0.01127	4.0869	0.649D-05	30.8	1202.1	5135.9			7.6	1696.2
1.06	0.6074D-02	1.0240	0.01131	4.0869	0.646D-05	22.6	1413.8	6726.7			7.6	1709.4
1.07	0.6063D-02	1.0243	0.01147	4.0869	0.636D-05	27.0	1595.9	8604.0			7.7	1760.1

DATE 16-9-82

BATCH Batch 2 of 0.005M Potassium Ferricyanide/ 0.005M Potassium Ferrocyanide/ 0.5M Sodium Hydroxide solution prepared on 6-9-82

Run No	V (volts)	N (rpm)	I1 (mA)	Cb (mol/cm ³)	Tb (C)	Ts1 (C)	Ts2 (C)	Ts3 (C)	Tw (C)	Ta (C)	Ih (A)	Q (J/s)	QL+Qp (J/s)	Qf (J/s)
2.01	1.0248	0.0	11.2	0.500D-05	24.7	30.3	47.7	30.3	21.2	17.6	0.313	11.22	1.66	9.56
2.02	1.0248	13.6	12.5	0.500D-05	22.0	28.6	45.5	28.6	19.8	17.6	0.312	11.15	1.60	9.55
2.03	1.0248	75.0	19.3	0.500D-05	20.8	22.7	36.7	22.7	20.3	17.6	0.309	10.93	0.99	9.94
2.04	1.0248	106.2	23.4	0.500D-05	21.0	23.2	34.1	23.2	20.3	17.6	0.306	10.72	0.86	9.87
2.05	1.0248	147.1	26.4	0.500D-05	19.8	20.5	31.4	20.5	20.3	17.6	0.306	10.72	0.67	10.05
2.06	1.0248	179.6	28.8	0.500D-05	20.3	20.3	31.0	20.3	20.3	17.6	0.309	10.93	0.63	10.30
2.07	1.0248	219.0	30.8	0.500D-05	21.0	22.2	31.9	22.2	22.2	17.6	0.309	10.93	0.63	10.30

Run No	k (W/cm K)	p (g/cm ³)	u (g/cm s)	cp (J/g K)	D (cm ² /s)	Nu	Sh	Re	Grh	Grm	Pr	Sc
2.01	0.6296D-02	1.0170	0.00862	4.0863	0.885D-05	17.8	437.7	0.0	0.537D+08	0.318D+07	5.6	957.5
2.02	0.6258D-02	1.0184	0.00904	4.0864	0.837D-05	17.0	517.2	664.0			5.9	1061.2
2.03	0.6183D-02	1.0209	0.00991	4.0866	0.753D-05	30.1	890.7	3349.5			6.5	1289.5
2.04	0.6176D-02	1.0211	0.01000	4.0866	0.745D-05	35.0	1089.6	4703.1			6.6	1313.5
2.05	0.6141D-02	1.0222	0.01043	4.0867	0.709D-05	44.1	1291.5	6248.8			6.9	1438.4
2.06	0.6142D-02	1.0221	0.01041	4.0867	0.711D-05	52.3	1405.6	7641.6			6.9	1433.4
2.07	0.6162D-02	1.0216	0.01017	4.0867	0.730D-05	46.3	1466.4	9535.9			6.7	1362.9

DATE 17-9-82

BATCH Batch 2 of 0.005M Potassium Ferricyanide/ 0.005M Potassium Ferrocyanide/ 0.5M Sodium Hydroxide solution prepared on 6-9-82

Run No	V (volts)	N (rpm)	I _l (mA)	C _b (mol/cm ³)	T _b (C)	T _{s1} (C)	T _{s2} (C)	T _{s3} (C)	T _w (C)	T _a (C)	I _h (A)	Q (J/s)	Q _L +Q _p (J/s)	Q _f (J/s)
3.01	1.0140	0.0	10.2	0.500D-05	21.5	28.6	47.6	28.6	21.0	17.6	0.330	12.47	1.67	10.80
3.02	1.0140	30.6	11.7	0.500D-05	19.0	25.1	42.3	25.1	21.0	17.6	0.320	11.72	1.33	10.39
3.03	1.0140	61.5	15.2	0.500D-05	17.8	20.3	35.9	20.3	20.3	17.6	0.314	11.29	0.93	10.36
3.04	1.0140	84.5	18.2	0.500D-05	17.5	19.0	32.4	19.0	20.3	17.6	0.311	11.07	0.71	10.36
3.05	1.0140	133.3	21.5	0.500D-05	17.0	17.8	29.3	17.8	21.7	17.6	0.309	10.93	0.47	10.47
3.06	1.0140	170.4	24.1	0.500D-05	16.3	17.0	27.6	17.0	22.5	17.6	0.309	10.93	0.33	10.60
3.07	1.0140	205.5	25.5	0.500D-05	16.5	17.8	26.9	17.8	22.5	17.6	0.307	10.79	0.31	10.48
3.08	1.0140	217.4	26.3	0.500D-05	16.8	18.3	25.9	18.3	21.7	17.6	0.306	10.72	0.30	10.43

Run No	k (W/cm K)	p (g/cm ³)	u (g/cm s)	cp (J/g K)	D (cm ² /s)	Nu	Sh	Re	Grh	Grm	Pr	Sc
3.01	0.6262D-02	1.0183	0.00899	4.0864	0.843D-05	17.4	421.6	0.0	0.551D+08	0.293D+07	5.9	1047.6
3.02	0.6203D-02	1.0203	0.00967	4.0866	0.774D-05	19.1	524.6	1399.2			6.4	1224.8
3.03	0.6142D-02	1.0221	0.01041	4.0867	0.711D-05	27.5	744.1	2616.7			6.9	1433.4
3.04	0.6118D-02	1.0228	0.01072	4.0868	0.687D-05	34.6	921.4	3493.7			7.2	1525.9
3.05	0.6094D-02	1.0235	0.01104	4.0869	0.664D-05	43.9	1126.0	5355.6			7.4	1624.3
3.06	0.6076D-02	1.0239	0.01129	4.0869	0.648D-05	48.7	1290.6	6702.1			7.6	1701.3
3.07	0.6078D-02	1.0239	0.01125	4.0869	0.650D-05	49.4	1364.5	8104.8			7.6	1691.2
3.08	0.6079D-02	1.0239	0.01125	4.0869	0.650D-05	54.5	1405.2	8576.4			7.6	1690.2

DATE 20-9-82

BATCH Batch 2 of 0.005M Potassium Ferricyanide/ 0.005M Potassium Ferrocyanide/ 0.5M Sodium Hydroxide solution prepared on 6-9-82

Run No	V (volts)	N (rpm)	I _L (mA)	C _b (mol/cm ³)	T _b (C)	T _{s1} (C)	T _{s2} (C)	T _{s3} (C)	T _w (C)	T _a (C)	I _h (A)	Q (J/s)	Q _{L+Qp} (J/s)	Q _f (J/s)
4.01	1.0130	0.0	11.8	0.500D-05	22.0	31.2	59.4	31.2	40.4	16.8	0.444	22.57	1.66	20.91
4.02	1.0130	36.6	13.3	0.500D-05	22.2	27.6	56.5	27.6	42.5	16.8	0.437	21.87	1.35	20.52
4.03	1.0130	73.6	17.1	0.500D-05	19.3	22.0	45.2	22.0	38.8	16.8	0.431	21.27	0.78	20.49
4.04	1.0130	101.7	19.4	0.500D-05	17.5	19.8	40.4	19.8	36.4	16.8	0.428	20.97	0.58	20.40
4.05	1.0130	130.4	21.2	0.500D-05	17.5	18.8	37.9	18.8	35.5	16.8	0.430	21.17	0.45	20.72
4.06	1.0130	160.6	22.8	0.500D-05	17.0	18.5	36.2	18.5	34.1	16.8	0.424	20.58	0.41	20.18
4.07	1.0130	200.0	24.6	0.500D-05	17.0	18.3	34.6	18.3	34.1	16.8	0.422	20.39	0.31	20.08

Run No	k (W/cm K)	p (g/cm ³)	u (g/cm s)	cp (J/g K)	D (cm ² /s)	Nu	Sh	Re	Grh	Grm	Pr	Sc
4.01	0.6326D-02	1.0158	0.00830	4.0861	0.924D-05	23.7	442.2	0.0	0.984D+08	0.342D+07	5.4	883.8
4.02	0.6301D-02	1.0168	0.00857	4.0862	0.891D-05	27.5	518.7	1883.4			5.6	945.5
4.03	0.6204D-02	1.0203	0.00966	4.0866	0.775D-05	38.6	764.7	3370.6			6.4	1220.6
4.04	0.6158D-02	1.0217	0.01022	4.0867	0.726D-05	44.1	927.0	4406.1			6.8	1377.9
4.05	0.6142D-02	1.0222	0.01042	4.0867	0.710D-05	52.3	1034.5	5543.8			6.9	1435.9
4.06	0.6129D-02	1.0225	0.01059	4.0868	0.697D-05	53.3	1137.9	6722.6			7.1	1485.4
4.07	0.6120D-02	1.0228	0.01070	4.0868	0.689D-05	58.5	1240.9	8286.8			7.1	1518.8

TABLE A6.9.3.2 I_L-N DATA FOR THE ELECTROLYTIC MIXING CELL WITH THE PRESENCE OF 2 LAYERS OF 12MM GLASS
SPHERICAL PARTICLES ON THE HEATED CATHODE

DATE 21-9-82

BATCH Batch 2 of 0.005M Potassium Ferricyanide/ 0.005M Potassium Ferrocyanide/ 0.5M Sodium Hydroxide solution prepared on 6-9-82

Run No	V (volts)	N (rpm)	I _L (mA)	C _b (mol/cm ³)	T _b (C)	T _{s1} (C)	T _{s2} (C)	T _{s3} (C)	T _w (C)	T _a (C)	I _h (A)	Q (J/s)	Q _L +Q _p (J/s)	Q _f (J/s)
1.01	1.0119	0.0	5.5	0.500D-05	17.8	28.0	28.1	28.0	24.3	16.3	0.149	2.54	0.53	2.01
1.02	1.0119	59.4	8.5	0.500D-05	16.0	17.3	23.2	17.3	21.7	16.3	0.147	2.48	0.16	2.32
1.03	1.0119	106.2	11.8	0.500D-05	15.3	16.8	20.3	16.8	19.5	16.3	0.141	2.28	0.09	2.18
1.04	1.0119	176.5	15.5	0.500D-05	15.5	15.5	19.3	15.5	19.4	16.3	0.140	2.25	0.01	2.24
1.05	1.0119	233.0	18.1	0.500D-05	15.5	14.8	19.4	14.8	19.4	16.3	0.141	2.26	0.01	2.26

Run No	k (W/cm K)	p (g/cm ³)	u (g/cm s)	cp (J/g K)	D (cm ² /s)	Nu	Sh	Re	Grh	Grm	Pr	Sc
1.01	0.6142D-02	1.0221	0.01042	4.0867	0.711D-05	5.3	270.7	0.0	0.215D+08	0.220D+07	6.9	1434.3
1.02	0.6054D-02	1.0245	0.01159	4.0870	0.628D-05	15.1	471.8	2276.8			7.8	1799.6
1.03	0.6032D-02	1.0250	0.01191	4.0870	0.609D-05	18.8	675.5	3962.8			8.1	1907.8
1.04	0.6023D-02	1.0252	0.01204	4.0870	0.601D-05	33.2	892.7	6516.6			8.2	1952.2
1.05	0.6020D-02	1.0253	0.01207	4.0870	0.599D-05	38.6	1047.2	8578.7			8.2	1964.1

DATE 21-9-82

BATCH Batch 2 of 0.005M Potassium Ferricyanide/ 0.005M Potassium Ferrocyanide/ 0.5M Sodium Hydroxide solution prepared on 6-9-82

Run No	V (volts)	N (rpm)	I _L (mA)	C _b (mol/cm ³)	T _b (C)	T _{s1} (C)	T _{s2} (C)	T _{s3} (C)	T _w (C)	T _a (C)	I _h (A)	Q (J/s)	Q _L +Q _p (J/s)	Q _f (J/s)
2.01	1.0174	0.0	8.1	0.500D-05	19.5	25.4	38.8	25.4	30.0	17.5	0.267	8.16	0.79	7.38
2.02	1.0174	25.9	8.5	0.500D-05	18.5	25.1	38.3	25.1	31.2	17.5	0.262	7.86	0.72	7.14
2.03	1.0174	77.5	11.3	0.500D-05	16.5	18.5	30.5	18.5	27.1	17.5	0.256	7.50	0.34	7.17
2.04	1.0174	128.3	14.6	0.500D-05	16.3	17.8	27.4	17.8	25.4	17.5	0.250	7.16	0.22	6.94
2.05	1.0174	157.9	16.3	0.500D-05	17.3	17.8	25.4	17.8	24.9	17.5	0.248	7.04	0.12	6.92
2.06	1.0174	229.0	18.8	0.500D-05	16.0	18.0	24.9	18.0	24.9	17.5	0.248	7.04	0.12	6.93

Run No	k (W/cm K)	p (g/cm ³)	u (g/cm s)	cp (J/g K)	D (cm ² /s)	Nu	Sh	Re	Grh	Grm	Pr	Sc
2.01	0.6193D-02	1.0206	0.00979	4.0866	0.764D-05	15.8	367.3	0.0	0.322D+08	0.248D+07	6.5	1256.0
2.02	0.6181D-02	1.0210	0.00993	4.0866	0.751D-05	14.6	391.5	1154.0			6.6	1296.2
2.03	0.6098D-02	1.0234	0.01099	4.0869	0.668D-05	24.6	587.7	3128.9			7.4	1607.1
2.04	0.6079D-02	1.0239	0.01125	4.0869	0.650D-05	30.5	780.6	5061.4			7.6	1690.2
2.05	0.6079D-02	1.0239	0.01125	4.0869	0.650D-05	44.3	870.8	6230.9			7.6	1689.2
2.06	0.6065D-02	1.0242	0.01143	4.0869	0.638D-05	35.1	1021.1	8894.1			7.7	1748.6

DATE 22-9-82

BATCH Batch 2 of 0.005M Potassium Ferricyanide/ 0.005M Potassium Ferrocyanide/ 0.5M Sodium Hydroxide solution prepared on 6-9-82

Run No	V (volts)	N (rpm)	I _L (mA)	C _b (mol/cm ³)	T _b (C)	T _{s1} (C)	T _{s2} (C)	T _{s3} (C)	T _w (C)	T _a (C)	I _h (A)	Q (J/s)	Q _L +Q _p (J/s)	Q _f (J/s)
3.01	1.0180	0.0	8.8	0.500D-05	21.0	28.8	49.7	28.8	34.6	17.0	0.395	17.86	1.27	16.59
3.02	1.0180	22.0	10.3	0.500D-05	19.3	26.6	47.9	26.6	36.2	17.0	0.395	17.86	1.09	16.77
3.03	1.0180	75.0	12.3	0.500D-05	18.5	21.0	39.9	21.0	32.4	17.0	0.395	17.86	0.69	17.17
3.04	1.0180	125.0	15.1	0.500D-05	16.0	19.0	35.5	19.0	31.7	17.0	0.395	17.86	0.46	17.40
3.05	1.0180	203.8	16.6	0.500D-05	16.5	17.8	33.4	17.8	28.3	17.0	0.395	17.86	0.44	17.42
3.06	1.0180	220.0	18.2	0.500D-05	16.5	17.3	31.0	17.3	28.3	17.0	0.341	13.31	0.31	13.01
3.07	1.0180	230.8	19.2	0.500D-05	15.8	17.3	30.7	17.3	28.3	17.0	0.342	13.39	0.30	13.10
3.08	1.0180	262.0	20.0	0.500D-05	15.8	17.0	28.8	17.0	27.1	17.0	0.332	12.62	0.23	12.39

Run No	k (W/cm K)	p (g/cm ³)	u (g/cm s)	cp (J/g K)	D (cm ² /s)	Nu	Sh	Re	Grh	Grm	Pr	Sc
3.01	0.6268D-02	1.0181	0.00893	4.0864	0.849D-05	24.3	358.7	0.0	0.617D+08	0.297D+07	5.8	1033.1
3.02	0.6236D-02	1.0192	0.00929	4.0865	0.811D-05	25.0	441.3	1046.3			6.1	1123.7
3.03	0.6170D-02	1.0213	0.01007	4.0867	0.739D-05	38.9	578.3	3297.8			6.7	1334.1
3.04	0.6119D-02	1.0228	0.01072	4.0868	0.688D-05	42.4	761.5	5170.9			7.2	1524.1
3.05	0.6108D-02	1.0231	0.01086	4.0868	0.677D-05	52.7	851.8	8324.5			7.3	1566.8
3.06	0.6095D-02	1.0234	0.01103	4.0869	0.665D-05	46.7	947.8	8848.5			7.4	1620.5
3.07	0.6087D-02	1.0236	0.01114	4.0869	0.658D-05	44.0	1015.0	9197.4			7.5	1653.4
3.08	0.6077D-02	1.0239	0.01127	4.0869	0.649D-05	46.1	1070.7	10316.2			7.6	1697.2

DATE 22-9-82

BATCH Batch 2 of 0.005M Potassium Ferricyanide/ 0.005M Potassium Ferrocyanide/ 0.5M Sodium Hydroxide solution prepared on 6-9-82

Run No	V (volts)	N (rpm)	I _L (mA)	C _b (mol/cm ³)	T _b (C)	T _{s1} (C)	T _{s2} (C)	T _{s3} (C)	T _w (C)	T _a (C)	I _h (A)	Q (J/s)	Q _L +Q _p (J/s)	Q _f (J/s)
4.01	1.0180	0.0	12.8	0.500D-05	23.7	31.4	61.3	31.4	42.3	17.2	0.484	26.82	1.65	25.17
4.02	1.0180	63.8	14.4	0.500D-05	19.3	25.9	55.0	25.9	42.3	17.2	0.469	25.19	1.24	23.94
4.03	1.0180	96.0	15.9	0.500D-05	18.5	22.5	49.3	22.5	39.5	17.2	0.463	24.55	0.97	23.58
4.04	1.0180	150.0	18.1	0.500D-05	19.0	20.8	44.5	20.8	37.9	17.2	0.457	23.91	0.72	23.19
4.05	1.0180	208.3	20.2	0.500D-05	18.3	20.3	41.6	20.3	36.9	17.2	0.458	24.02	0.60	23.42

Run No	k (W/cm K)	p (g/cm ³)	u (g/cm s)	cp (J/g K)	D (cm ² /s)	Nu	Sh	Re	Grh	Grm	Pr	Sc
4.01	0.6348D-02	1.0149	0.00807	4.0860	0.955D-05	29.3	467.2	0.0	0.104D+09	0.361D+07	5.2	832.5
4.02	0.6263D-02	1.0182	0.00898	4.0864	0.843D-05	30.2	592.3	3135.5			5.9	1045.9
4.03	0.6218D-02	1.0198	0.00950	4.0865	0.790D-05	36.5	699.5	4467.8			6.2	1178.4
4.04	0.6193D-02	1.0206	0.00979	4.0866	0.764D-05	46.0	821.9	6782.0			6.5	1255.3
4.05	0.6172D-02	1.0213	0.01005	4.0867	0.741D-05	50.3	948.6	9176.1			6.7	1328.7

APPENDIX A7 PROGRAM LISTINGS

APPENDIX A7.1 A LISTING OF THE PROGRAM 'MASS'

```

      REAL IL,KV,L,N
      DIMENSION RN(50),IL(50),N(50),SH(50),RE(50),GR(50),SC(50)
10  READ (1,*) RN(1),VO,T,CB,M
      DO20J=1,M,1
      READ (1,*) N(J),IL(J)
20  CONTINUE
      L=7.6
      DI=5.1
      A=3.1415927*L**2.0/4.0
      Z=1.0
      F=96487.0
      G=980.665
      P=1.03052-2.142E-04*T-6.6E-06*T**2
      KV=0.01*EXP((1.8710E03/(T+273.15))-6.3004)
      V=KV*P
      D=(2.50E-10*(T+273.15))/V
      CALL DENDIF(DPP)
      DO30J=1,M,1
      RN(J+1)=RN(J)+0.01
      SH(J)=((IL(J)/1000.0)*L)/(F*A*CB*Z*D)
      RE(J)=((N(J)/60)*DI**2.0)/KV
      GR(J)=(G*L**3.0/KV**2.0)*ABS(DPP)
      SC(J)=KV/D
30  CONTINUE
      WRITE(2,100)
      WRITE(2,200) VO,T,CB,P,V,D
      WRITE(2,600)
      WRITE(2,300)
      WRITE(2,600)
      DO50J=1,M,1
      IF(RE(J).GT.0.0) GOTO40
      WRITE(2,400) RN(J),N(J),IL(J),SH(J),RE(J),GR(J),SC(J)
      GOTO50
40  WRITE(2,500) RN(J),N(J),IL(J),SH(J),RE(J),SC(J)
50  CONTINUE
      WRITE(2,600)
100 FORMAT(///3X,'DATE 6-11-81',/3X,'BATCH Batch 2 of 0.005M',
&' Potassium Ferricyanide/0.005M',/10X,'Potassium Ferrocyanide/',
&'0.5M Sodium Hydroxide',/10X,'solution prepared on 24-9-81'/)
200 FORMAT(3X,'Potential = ',F6.4,1X,'V',/
&3X,'Solution Temperature = ',F4.1,1X,'C',/
&3X,'Ferricyanide concentration = ',E9.3,1X,'mol/cm3',/
&3X,'Density = ',F6.4,1X,'g/cm3',/
&3X,'Viscosity = ',F8.6,1X,'g/cm s',/
&3X,'Diffusivity = ',E10.4,1X,'cm2/s',/)
300 FORMAT(5X,'Run',5X,'Stirrer',3X,'Limiting',5X,'Sh',9X,'Re',11X,
&'Gr',10X,'Sc',/5X,'No',7X,'Speed',4X,'Current',/,14X,'(rpm)',
&6X,'(mA)')
400 FORMAT(4X,F5.2,5X,F5.1,6X,F4.1,5X,F6.1,4X,F7.1,4X,E11.5,4X,F6.1)
500 FORMAT(4X,F5.2,5X,F5.1,6X,F4.1,5X,F6.1,4X,F7.1,19X,F6.1)
600 FORMAT(3X,75(1H-))
      STOP
      END

```

C

```

      SUBROUTINE DENDIF(DPP)
      DIMENSION L(5),C(5),S(5),Z(5),D(5),A(5),T(5),CD(5)
      REAL L
      S(1)=-1.0
      S(2)=1.0
      S(3)=0.0

```

```

S(4)=0.0
S(5)=0.0
Z(1)=-3.0
Z(2)=-4.0
Z(3)=-1.0
Z(4)=1.0
Z(5)=1.0
L(1)=100.9
L(2)=110.5
L(3)=197.6
L(4)=50.11
L(5)=73.52
D(1)=0.896E-05
D(2)=0.739E-05
D(3)=5.26E-05
D(4)=1.334E-05
D(5)=1.957E-05
A(1)=167.27
A(2)=225.91
A(3)=45.29
A(4)=-6.73
A(5)=0.0
C(1)=0.005E-03
C(2)=0.005E-03
C(3)=0.5E-03
C(4)=0.5E-03
C(5)=0.035E-03
DO10J=1,5,1
T(J)=ABS(Z(J))*L(J)*C(J)
10 CONTINUE
TT=T(1)+T(2)+T(3)+T(4)+T(5)
DO20J=1,5,1
T(J)=T(J)/TT
CD(J)=(S(J)-(T(J)/Z(J)))/(S(1)-(T(1)/Z(1)))*((D(1)/D(J))**0.75)
CD(J)=CD(J)*C(1)
20 CONTINUE
DPP =A(1)*CD(1)+A(2)*CD(2)+A(3)*CD(3)+A(4)*CD(4)+A(5)*CD(5)
RETURN
END

```

```

      IMPLICIT REAL*8 (A-H,O-Z)
      REAL*8 IH,IL,K,KEFF,KP,KV,KW,KW1,L,N,NL,NU
      DIMENSION RN(100),TA(100),TB(100),TS1(100),TS2(100),TS3(100)
      DIMENSION TW(100),TS(100),TF(100),IH(100),IL(100),N(100)
      DIMENSION Q(100),Q1(100),Q2(100),Q3(100),Q4(100),Q5(100)
      DIMENSION QP(100),QL(100),QB(100),HB(100)
      DIMENSION K(100),P(100),V(100),DP(100),D(100),CP(100)
      DIMENSION KEFF(100)
      DIMENSION NU(100),SH(100),RE(100),GRM(100),GRH(100)
      DIMENSION PR(100),SC(100)
10  READ(1,*) RN(1),VO,RES,CB,RH,M,PD,NL,KP
      DO20J=1,M,1
      READ(1,*) IL(J),TB(J),TS1(J),TS2(J),TS3(J),TW(J),TA(J),IH(J),N(J)
20  CONTINUE
      L=7.6
      DI=5.1
      A=3.1415927*L**2.0/4.0
      Z=1.0
      F=96487.0
      G=980.665
      X=(PD/10.0)*(0.933*NL+0.067)
      DO50J=1,M,1
      RN(J+1)=RN(J)+0.01
      IL(J)=IL(J)*10./RES
      TS1(J)=(TS1(J)+TS3(J))/2.0
      TS(J)=(TS1(J)+TS2(J))/2.0
      TF(J)=(TB(J)+TS(J))/2.0
      TR=20.0
      CALL DENSIT(TR,PW1)
      CALL THCOND(TR,PW1,KW1)
      CALL DENSIT(TF(J),PW)
      CALL THCOND(TF(J),PW,KW)
      K(J)=0.60889E-02*(KW/KW1)
      KV=0.01*DEXP((1.8710E03/(TF(J)+273.15))-6.3004)
      P(J)=1.03052-2.142D-04*TF(J)-6.6D-06*TF(J)**2.0
      V(J)=KV*P(J)
      P1=1.03052-2.142D-04*TB(J)-6.6D-06*TB(J)**2.0
      P2=1.03052-2.142D-04*TS(J)-6.6D-06*TS(J)**2.0
      DP(J)=(P1-P2)/P2
      D(J)=(2.50E-10*(TF(J)+273.15))/V(J)
      CP(J)=4.184*(1.0-(0.02376/P(J)))
      CALL DENDIF(DPP)
      KEFF(J)=0.39*K(J)+0.61*KP
      Q(J)=IH(J)**2.0*RH
      Q1(J)=0.02089*(TS1(J)-((TB(J)+TA(J))*0.5))
      Q2(J)=0.0
      Q3(J)=0.0529839*(TS2(J)-TW(J))
      Q4(J)=6.84408E-03*(TW(J)-TA(J))**1.25
      Q5(J)=1.96848E-05*(TS2(J)-TA(J))**1.25
      IF(X.LE.0.0)GOTO30
      QP(J)=0.61*KEFF(J)*(TS(J)-TF(J))/X
      GOTO40
30  QP(J)=0.0
40  QL(J)=Q1(J)+Q2(J)+Q3(J)+Q4(J)+Q5(J)
      QB(J)=Q(J)-QL(J)-QP(J)
      HB(J)=QB(J)/((TS(J)-TB(J))*A)
      NU(J)=HB(J)*L/K(J)
      SH(J)=(IL(J)/1000)*L/(F*A*CB*Z*D(J))
      RE(J)=((N(J)/60.0)*DI**2.0)/KV
      SC(J)=V(J)/(P(J)*D(J))

```



```

PR(J)=V(J)*CP(J)/K(J)
GRM(J)=(G*DABS(DPP)*L**3.0)/(KV**2.0)
GRH(J)=(G*DP(J)*L**3.0)/(KV**2.0)
50 CONTINUE
WRITE(2,100)
WRITE(2,800)
WRITE(3,800)
IF(X.GT.0.0)GOTO60
WRITE(2,200)
GOTO70
60 WRITE(2,300)
70 WRITE(3,400)
WRITE(2,800)
WRITE(3,800)
DO90J=1,M,1
WRITE(2,500) RN(J),VO,N(J),IL(J),CB,TB(J),TS1(J),TS2(J),TS3(J),
&TW(J),TA(J),IH(J),Q(J),QL(J),QB(J)
IF(RE(J).LE.0.0) GOTO80
WRITE(3,600) RN(J),K(J),P(J),V(J),CP(J),D(J),NU(J),SH(J),RE(J),
&PR(J),SC(J)
GOTO90
80 WRITE(3,600) RN(J),K(J),P(J),V(J),CP(J),D(J),NU(J),SH(J),RE(J),
&GRH(J),GRM(J),PR(J),SC(J)
90 CONTINUE
WRITE(2,800)
WRITE(3,800)
100 FORMAT(///1X,'DATE 1-10-82',/1X,'BATCH Batch 3 of 0.005M',
&' Potassium Ferricyanide/ 0.005M Potassium Ferrocyanide/ 0.5M',
&' Sodium Hydroxide solution prepared on 6-9-82'//)
200 FORMAT(1H ,1X,'Run No',6X,'V',8X,'N',7X,'I1',8X,'Cb',9X,'Tb',
&6X,'Ts1',5X,'Ts2',5X,'Ts3',5X,'Tw',6X,'Ta',6X,'Ih',
&8X,'Q',7X,'QL',7X,'Qb',
&/,11X,'(volts)',3X,'(rpm)',4X,'(mA)',4X,'(mol/cm3)',
&5X,'(C)',5X,'(C)',5X,'(C)',5X,'(C)',5X,'(C)',5X,'(C)',
&5X,'(A)',5X,'(J/s)',3X,'(J/s)',4X,'(J/s)')
300 FORMAT(1H ,1X,'Run No',6X,'V',8X,'N',7X,'I1',8X,'Cb',9X,'Tb',
&6X,'Ts1',5X,'Ts2',5X,'Ts3',5X,'Tw',6X,'Ta',6X,'Ih',
&8X,'Q',5X,'QL+Qp',6X,'Qf',
&/,11X,'(volts)',3X,'(rpm)',4X,'(mA)',4X,'(mol/cm3)',
&5X,'(C)',5X,'(C)',5X,'(C)',5X,'(C)',5X,'(C)',5X,'(C)',
&5X,'(A)',5X,'(J/s)',3X,'(J/s)',4X,'(J/s)')
400 FORMAT(1H ,1X,'Run No',6X,'k',11X,'p',8X,'u',8X,'cp',9X,'D',
&10X,'Nu',7X,'Sh',8X,'Re',8X,'Grh',9X,'Grm',8X,'Pr',6X,'Sc',/11X,
&'(W/cm K)',4X,'(g/cm3)',2X,'(g/cm s)',2X,'(J/g K)',3X,
&'(cm2/s)')
500 FORMAT(2X,F5.2,4X,F6.4,4X,F5.1,4X,F4.1,4X,E9.3,4X,F4.1,
&4X,F4.1,4X,F4.1,4X,F4.1,4X,F4.1,4X,F5.3,4X,F5.2,4X,
&F4.2,4X,F5.2)
600 FORMAT(2X,F5.2,3X,E10.4,3X,F6.4,3X,F7.5,3X,F6.4,3X,E9.3,4X,
&F6.1,3X,F6.1,3X,F7.1,27X,F5.1,3X,F6.1)
700 FORMAT(2X,F5.2,3X,E10.4,3X,F6.4,3X,F7.5,3X,F6.4,3X,E9.3,4X,
&F6.1,3X,F6.1,3X,F7.1,3X,E9.3,3X,E9.3,3X,F5.1,3X,F6.1)
800 FORMAT(132(1H-))
STOP
END

```

C

```

SUBROUTINE DENSIT(T,P)
IMPLICIT REAL*8 (A-H,O-Z)
DIMENSION B(20),TT(20),S(20)
TC=374.12

```

```

VC=0.00317
TR=T/TC
R=1.0-(2.0*(1.-TR)**0.4)
TT(1)=1
TT(2)=R
DO10J=3,11,1
TT(J)=2.*R*TT(J-1)-TT(J-2)
10 CONTINUE
SUM=0.0
B(1)=4.332053
B(2)=-1.107796
B(3)=-5.275102E-02
B(4)=2.173547E-02
B(5)=-1.754636E-02
B(6)=5.125009E-03
B(7)=-3.765370E-03
B(8)=1.123345E-03
B(9)=-2.458266E-03
B(10)=-1.425500E-03
B(11)=-1.304721E-03
S(1)=B(1)*TT(1)/2.0
SUM=SUM+S(1)
DO20J=2,11,1
S(J)=B(J)*TT(J)
SUM=SUM+S(J)
20 CONTINUE
V=VC/SUM
P=1/V
RETURN
END

```

C

```

SUBROUTINE THCOND(T,P,KW)
IMPLICIT REAL*8 (A-H,O-Z)
REAL*8 KO,KW
DOUBLE PRECISION B(5,6),S1(5,6)
DIMENSION A(5),S(5)
T=T+273.15
TC=647.27
PC=317.763
TR=T/TC
PR=P/PC
SUM=0.0
A(1)=2.0223
A(2)=14.11166
A(3)=5.25597
A(4)=-2.01870
DO10K=1,4,1
S(K)=(A(K)*(TR**(1-K)))
SUM=SUM+S(K)
10 CONTINUE
KO=DSQRT(TR)/(SUM)
B(1,1)=2.0476004D0
B(2,1)=7.879129D0
B(3,1)=23.2605736D0
B(4,1)=19.5612336D0
B(5,1)=-22.6395931D0
B(1,2)=-1.5962370D0
B(2,2)=-10.7813807D0
B(3,2)=-24.0282944D0
B(4,2)=-1.7812867D0

```

```

B(5,2)=19.4620986D0
B(1,3)=0.0993949D0
B(2,3)=-1.2449962D0
B(3,3)=-7.09743566D0
B(4,3)=-7.1641645D0
B(5,3)=-4.5770117D0
B(1,4)=1.3774179D0
B(2,4)=8.1477154D0
B(3,4)=12.0340912D0
B(4,4)=1.7212905D0
B(5,4)=0.2042771D0
B(1,5)=-1.0242464D0
B(2,5)=-3.7521680D0
B(3,5)=-3.3303434D0
B(4,5)=0.0D0
B(5,5)=0.0D0
B(1,6)=0.2203151D0
B(2,6)=0.4418686D0
B(3,6)=0.2836892D0
B(4,6)=0.0D0
B(5,6)=0.0D0
SUM1=0.0
DO20I=1,5,1
DO20J=1,6,1
S1(I,J)=B(I,J)*((1-TR)/TR)**(I-1)*(PR-1)**(J-1)
SUM1=SUM1+S1(I,J)
20 CONTINUE
T=T-273.15
KW=KO*DEXP(PR*SUM1)
RETURN
END

```

C

```

SUBROUTINE DENDIF(DPP)
DIMENSION L(5),C(5),S(5),Z(5),D(5),A(5),T(5),CD(5)
REAL L
S(1)=-1.0
S(2)=1.0
S(3)=0.0
S(4)=0.0
S(5)=0.0
Z(1)=-3.0
Z(2)=-4.0
Z(3)=-1.0
Z(4)=1.0
Z(5)=1.0
L(1)=100.9
L(2)=110.5
L(3)=197.6
L(4)=50.11
L(5)=73.52
D(1)=0.896E-05
D(2)=0.739E-05
D(3)=5.26E-05
D(4)=1.334E-05
D(5)=1.957E-05
A(1)=167.27
A(2)=225.91
A(3)=45.29
A(4)=-6.73
A(5)=0.0

```

```

C(1)=0.005E-03
C(2)=0.005E-03
C(3)=0.5E-03
C(4)=0.5E-03
C(5)=0.035E-03
DO10J=1,5,1
T(J)=ABS(Z(J))*L(J)*C(J)
10 CONTINUE
TT=T(1)+T(2)+T(3)+T(4)+T(5)
DO20J=1,5,1
T(J)=T(J)/TT
CD(J)=(S(J)-(T(J)/Z(J)))/(S(1)-(T(1)/Z(1)))*((D(1)/D(J))**0.75)
CD(J)=CD(J)*C(1)
20 CONTINUE
DPP =A(1)*CD(1)+A(2)*CD(2)+A(3)*CD(3)+A(4)*CD(4)+A(5)*CD(5)
RETURN
END

```

APPENDIX A8 THE BASIS OF THE EQUATION FOR THE SIMULATED FOULING DEPOSIT THICKNESS

The simulated fouling deposit consisted of one or more layers of glass spherical particles of a fixed d_p randomly packed on the cathode. As Ridgeway and Tarbuck⁽⁴⁰⁶⁾ have stated that

"In a random packed bed of spherical particles formed in a container with smooth walls, the layer of spherical particles nearest to the wall tends to be highly ordered, with most of the spherical particles touching the wall. The next layer builds up on the surface of the first layer in a less ordered fashion. The third, fourth and successive layers become less and less ordered until a fully randomised arrangement is achieved in regions far removed from the wall and the term 'layer' ceases to be applicable at all"

it is reasonable to assume that the first layer of a random packed bed of spherical particles is closely packed and the last layer of a random packed bed of spherical particles is openly packed. Hence, the thickness of a random packed bed of spherical particles, x can be assumed to be the mean of the thickness of a close packed bed of spherical particles, x_{close} and the thickness of an open packed bed of spherical particles, x_{open} :

$$x = 0.5(x_{\text{close}} + x_{\text{open}}) \quad \text{A8.1}$$

From Figure A8.1, it was found that x_{close} is given by

$$x_{\text{close}} = d_p \{1 + \sqrt{0.75(n_1 - 1)}\} \quad \text{A8.2}$$

and x_{open} is given by

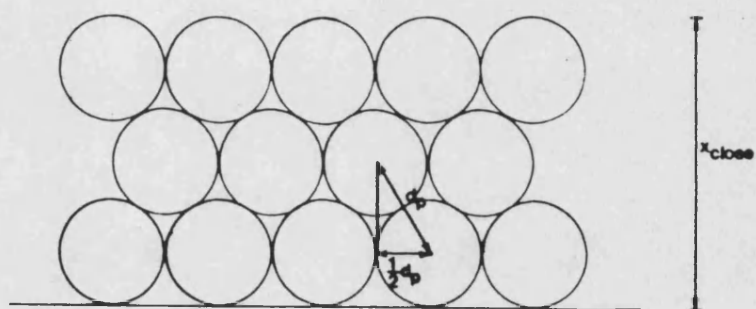
$$x_{\text{open}} = d_p n_1 \quad \text{A8.3}$$

Substituting equations A8.2 and A8.3 for x_{close} and x_{open} in equation A8.1 yields

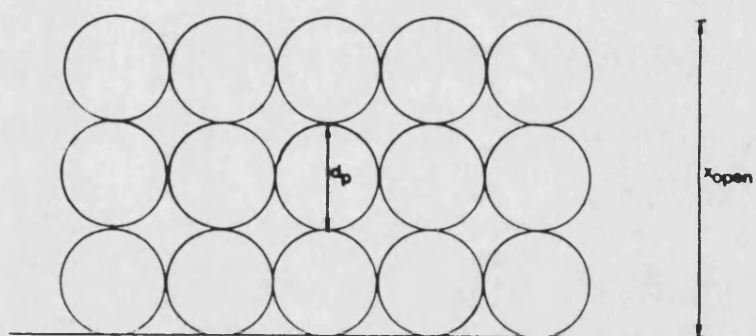
$$x = d_p (0.933n_1 + 0.067) \quad \text{4.49}$$

It was generally found that the values of x obtained from equation 4.49 are in agreement with the measured values of x to within $\pm 2.5\%$.

FIGURE A8.1 PACKING ARRANGEMENTS OF GLASS SPHERICAL PARTICLES
ON THE CATHODE



(a) CLOSE PACKING ARRANGEMENT



(b) OPEN PACKING ARRANGEMENT

APPENDIX A9 THE BASIS OF THE EQUATION FOR THE TORTUOSITY OF THE SIMULATED FOULING DEPOSIT

As the simulated fouling deposit consisted of one or more layers of glass spherical particles of a fixed d_p randomly packed on the cathode, it is reasonable to assume that the first layer of a random packed bed of spherical particles is closely packed and the last layer of a random packed bed of spherical particles is openly packed. Hence, the path length of a random packed bed of spherical particles, l' can be assumed to be the mean of the path length of a close packed bed of spherical particles, l'_{close} and the path length of an open packed bed of spherical particles, l'_{open} :

$$l' = 0.5(l'_{close} + l'_{open}) \quad A9.1$$

From Figure A9.1, it was found that l'_{close} is given by

$$l'_{close} = d_p \left\{ 1 + \frac{\pi}{3}(n_1 - 1) \right\} \quad A9.2$$

and l'_{open} is given by

$$l'_{open} = d_p n_1 \quad A9.3$$

Substituting equations A9.2 and A9.3 for l'_{close} and l'_{open} in equation A9.1 yields

$$l' = d_p (1.023n_1 - 0.023) \quad A9.4$$

The tortuosity of the fouling deposit is defined as the ratio of the path length travelled by the reacting species in the simulated fouling deposit to the thickness of the simulated fouling deposit:

$$t = \frac{l'}{x} \quad A9.5$$

Hence, substituting equations A9.4 and 4.49 for l' and x in equation A9.5 yields

$$t = \frac{1.023n_1 - 0.023}{0.933n_1 + 0.067} \quad 5.3$$

ie.

$$t = 1 \quad \text{for } n_1 = 1$$

$$t = 1.047 \quad \text{for } n_1 = 2$$

$$t = 1.063 \quad \text{for } n_1 = 3$$

$$t = 1.071 \quad \text{for } n_1 = 4$$

$$t = 1.076 \quad \text{for } n_1 = 5$$

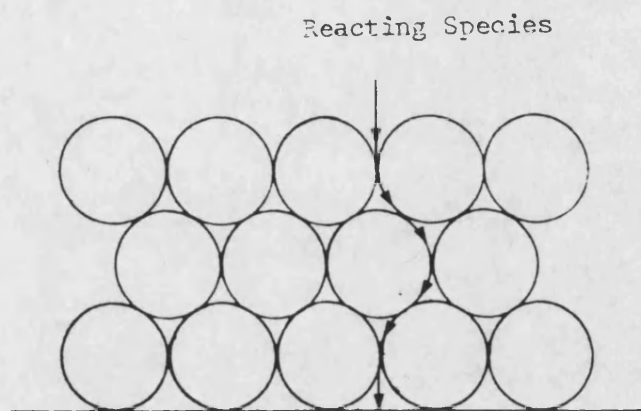
$$t = 1.079 \quad \text{for } n_1 = 6$$

$$t = 1.082 \quad \text{for } n_1 = 7$$

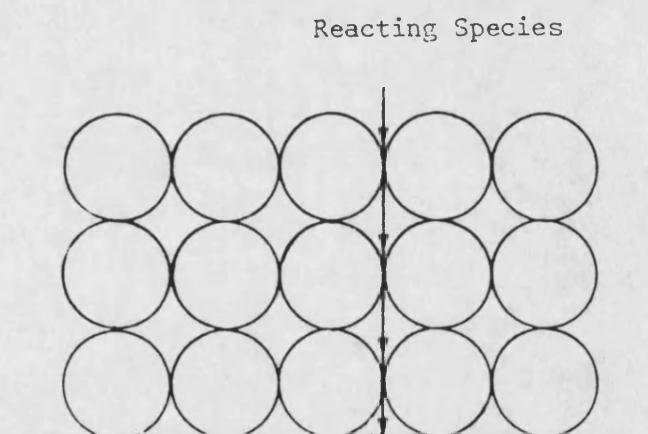
The tortuosity, t is independent of d_p .

FIGURE A9.1

THE PATH OF REACTING SPECIES THROUGH THE
DIFFERENT PACKING ARRANGEMENTS OF GLASS
SPHERICAL PARTICLES ON THE CATHODE FROM
THE BULK SOLUTION TO THE CATHODE



(a) CLOSE PACKING ARRANGEMENT



(b) OPEN PACKING ARRANGEMENT